

*“Do not fear your enemies –  
at worst, they can kill you.  
Do not fear friends –  
at worst, they may betray you.  
Fear those who do not care –  
they neither kill nor betray, but betrayal and murder exist  
because of their silent consent.”*

Bruno Jasiński

*Be less curious about people and more curious about ideas.*

Marie Skłodowska-Curie

*RNA pol II, is a stripper, is exciting plenty of genes.*

Enrico Ne

To my parents, family and friends.

And to Madonna



**Solving a BAF'ling problem.**

**Pharmacological reversal of HIV-1 latency.**

Een BAF-probleem oplossen.

Farmacologische omkering van de latentie  
van HIV-1

**Thesis**

to obtain the degree of Doctor from the  
Erasmus University Rotterdam  
by command of the  
rector magnificus

**Prof.dr. R.C.M.E. Engels**

and in accordance with the decision of the Doctorate Board. The  
public defence shall be held on

Wednesday 4 December 2019 at 13:30 hrs

by

**Mateusz Łukasz Stoszko**

born in Kowary (Poland)

**Erasmus University Rotterdam**

The Erasmus University logo, featuring a stylized, handwritten-style script of the word "Erasmus" in a dark color.

**Doctoral Committee:**

**Promotor:** Prof. dr. C.P. Verrijzer

**Other members:** Dr. D. ten Berge  
Prof. dr. R. Fodde  
Dr. M. Nijnhuis

**Co-promotor:** Dr. T. Mahmoudi



## Table of contents

### Chapter 1 General introduction

- I. Molecular Mechanisms Controlling HIV Transcription and Latency –  
Implications for Therapeutic Viral Reactivation  
*Advances in Molecular Retrovirology, Shailendra K. Saxena,*  
*IntechOpen, doi: 10.5772/61948*
- II. A broad drug arsenal to attack a strenuous latent HIV reservoir  
*Current Opinion in Virology 2019. 38, 37–53. doi.org/10.1016/J.COVIRO.2019.06.001*
- III. Scope of the thesis

### Chapter 2 Small Molecule Inhibitors of BAF; A Promising Family of Compounds in HIV-1 Latency Reversal

*EBioMedicine 2016, 1–14. doi: 10.1016/j.ebiom.2015.11.047*

### Chapter 3 Small Molecule Targeting of Specific BAF (mSWI/SNF) Complexes for HIV Latency Reversal

*Cell Chemical Biology 2018; 25(12):1443-1455.e14. doi: 10.1016/j.chembiol.2018.08.004.*

### Chapter 4 A New Quinoline BRD4 Inhibitor Targets a Distinct Latent HIV-1 Reservoir for Reactivation from Other “Shock” Drugs

*Journal of Virology 2018; 92(10). pii: e02056-17. doi: 10.1128/JVI.02056-17*

### Chapter 5 Gliotoxin, identified from a screen of *Aspergillus fumigatus* metabolites, reverses HIV-1 latency via release of P-TEFb

*Nature microbiology- submitted*

### Summary with discussion

### Curriculum vitae

### Portfolio

### Acknowledgements



# Chapter 1

## General introduction

I.

### **Molecular Mechanisms Controlling HIV Transcription and Latency – Implications for Therapeutic Viral Reactivation.**

Michael D. Röling, **Mateusz Stoszko** and Tokameh Mahmoudi

Published:

Advances in Molecular Retrovirology (2016). InTech, Editor: S. K. Saxena. (pp. 45–105)



---

# Molecular Mechanisms Controlling HIV Transcription and Latency – Implications for Therapeutic Viral Reactivation

---

Michael D. Röling, Mateusz Stoszko and Tokameh Mahmoudi

Additional information is available at the end of the chapter

<http://dx.doi.org/10.5772/61948>

---

## Abstract

Persistence of transcriptionally silent replication competent HIV-1 is a major barrier to clearance of the virus from patients; current combinatorial antiretroviral therapies are successful in abrogating active viral replication, but are unable to eradicate latent HIV-1. A “shock and kill” strategy has been proposed as a curative approach in which latent virus is activated and infected cells are removed by immune clearance, while new rounds of infection are prevented by antiretroviral therapy. Much effort has been put toward understanding the molecular mechanisms maintaining HIV latency and the nature of reservoirs, to provide novel therapeutic targets. This has led to the development of latency reversal agents (LRAs), some of which are undergoing clinical trials. Targeting multiple mechanisms underlying HIV latency via a combination of LRAs is likely to result in more potent activation of the latent reservoir. Therefore, novel as well as synergistic combinations of therapeutic molecules are required to accomplish more potent latency reversal.

**Keywords:** HIV-1 latency, Latency reversal agents (LRAs), Combinatorial antiretroviral therapy

---

## 1. Introduction

Human immunodeficiency virus-1 (HIV-1) is a lentivirus, a subgroup of Retroviridae. Like all retroviruses, HIV-1 virions consist of an RNA genome with viral proteins encapsulated in a viral envelope. The viral proteins execute key steps to establish a productive infection by stably integrating into the host genome. Unlike most retroviruses, HIV-1 can also directly infect nondividing cells. HIV-1 preferably infects a subset of T-lymphocytes (CD4<sup>+</sup> T-cells) that play a crucial role in the immune response. HIV-1 infection causes exhaustion and ultimately

depletion of the host immune system, a syndrome termed acquired immuno-deficiency syndrome (AIDS). HIV-1 came into prominence with the outbreak of the AIDS epidemic in the 1980s. Major steps have been taken toward treating this viral infection. In particular, combinatorial antiretroviral therapy (cART) successfully abrogated HIV-1 replication. Thus, for compliant patients with access to cART, HIV infection has become a chronic rather than a lethal disease. However, cessation of antiretroviral therapy results in viral rebound in infected patients, even after years of cART. This is because in a small fraction of infected cells, HIV persists in a latent but replication-competent state. Latent HIV is unaffected by cART, but infection can rebound upon cART interruption. Therefore, HIV latency is the main challenge in developing a curative therapy for HIV.

The quest for an HIV-1 cure involves the development of either a sterilizing or a functional cure. A sterilizing cure would require complete removal of replication competent viral genetic material from the infected patient and thus the stable depletion of latently HIV-infected cells. A functional cure, on the other hand, requires the patient's immune system to suppress HIV-1 replication life-long in the absence of cART without disease progression, loss of CD4<sup>+</sup> T cells and HIV transmission. The functional cure does not aim to eradicate the virus entirely from the patient. Both the sterilizing and functional cure strategies are currently the subject of major research efforts.

## 2. Clinical picture of HIV

The AIDS epidemic in the 1980s led to the identification of HIV as the causative agent. AIDS is a condition in which depletion of CD4<sup>+</sup> T-cells overtime leads to the loss of the host immune system's ability to fight infections and cancers, eventually leading to death. As HIV was identified as the causative agent, cure efforts focused on disrupting the viral lifecycle. In the early 1990s, the first antiretroviral therapies – monotherapies – had limited success as they resulted in rebound of viremia due to the appearance of resistant viral strains. Resistant HIV required novel therapeutic strategies. Therefore, a combination of anti-retrovirals, targeting distinct steps of the viral life cycle was developed, so-called combinatorial antiretroviral therapy (cART). cART has proven to be extremely successful in lowering the amount of viral RNA in plasma below the limits of detection by standard laboratory techniques. Unfortunately, the therapy does not eradicate the virus as cessation of medication causes re-emergence of viral replication [1–3]. Thus, a fraction of the virus escapes the effects of cART. The source for this recurring viral replication is a small pool of latently infected cells that harbor integrated proviruses which, while silent, are not recognized by either the immune system nor are they subject to cART. Moreover, HIV can persist in the presence of cART in certain anatomical sites if drug penetrance is incomplete.

According to the World Health Organization (WHO), the number of HIV-infected individuals worldwide in late 2014 was estimated to be approximately 37 million [4]. The vast majority of infected people live in sub-Saharan Africa, where access to appropriate diagnostic centers and cART is limited. Estimates put new infections at 5,600 a day in 2014.

## **2.1. HIV-1 replication cycle and state-of-the-art antiretroviral therapy**

HIV-1, as all viruses, is a parasite of the host cell and hijacks key cellular processes to establish a productive infection. To produce new virions, the virus goes through a viral replication cycle. HIV's replication cycle consists of entering the cell by docking at the cell surface receptor CD4 and co-receptors CCR5/CXCR4 and fusing to the cell, un-packaging of the genome, reverse transcription of the viral RNA genome into double-stranded DNA, which is the main component of the pre-integration complex, followed by integration of the double-stranded DNA genome into the host genome, transcription of the provirus, translation of viral proteins, and ultimately virion biogenesis followed by budding from host cell and maturation. Modern cART targets most steps in the HIV viral replication cycle (Figure 1). There are currently 28 approved agents for the treatment of HIV infection [5]. They fall into six mechanistic major classes, which act at different stages in the HIV replication cycle:

1. Fusion inhibitors: enfuvirtide (ENF, T-20), the only currently available fusion inhibitor, binds to the gp41 receptor site, preventing the fusion of the virus with the target cell.
2. C-C chemokine receptor type 5 (CCR5) antagonists: maraviroc (MVC) is currently the only available CCR5 antagonist. This drug is an entry inhibitor, specifically blocking the human chemokine receptor CCR5.
3. Nucleoside (nucleotide) reverse transcriptase inhibitors (NRTIs) block the addition of nucleosides to the DNA chain during reverse transcription of RNA.
4. Non-nucleoside reverse transcriptase inhibitors (NNRTIs) bind to and inhibit the enzyme reverse transcriptase (RT), preventing conversion of viral RNA to DNA during infection.
5. Integrase inhibitors (INIs): raltegravir (RAL), elvitegravir (EVG) and dolutegravir (DTG) are the only currently available drugs in this class. They target the HIV enzyme integrase (IN) that is required for insertion of viral genetic material into human DNA.
6. Protease inhibitors (PIs) bind to the catalytic site of HIV aspartic protease, blocking the processing of viral proteins (eg. Saquinavir).

These antivirals comprise the various current cART regimens that are used in the clinic. cART has proven to be extremely successful in suppressing viral replication in compliant patients. In fact, it has been argued that the theoretical potential of cART has already been reached [6]. Therefore, in the developed world with access to medication, HIV has become a chronic and not a lethal disease.

## **2.2. The burden of lifelong cART**

Implementation of cART has provided long-term suppression of viral replication, improving the life expectancy and life quality of infected patients. Unfortunately, the economic burden of cART is debilitating. According to the Centers for Disease Control and Prevention (CDC), lifetime costs of treating HIV infection is estimated to be \$379,668 per infected individual in the United States [7].

Moreover, patients on cART overtime can experience several side effects of cART such as: cardiovascular diseases (e.g., myocardial infarction); non-AIDS cancers (e.g., anal cancer, liver cancer, Hodgkin's disease); liver, kidney, and bone disease as well as neurologic complications, such as dementia [8]. Interestingly, most of these conditions are associated with the ageing process. Hence, it is thought, that HIV infection controlled by cART accelerates ageing. And importantly, HIV persists in a latent state that is not targeted by cART, rendering cART a therapeutic management of the disease as opposed to a curative treatment. Thus, there is much need to develop a curative therapy for HIV.

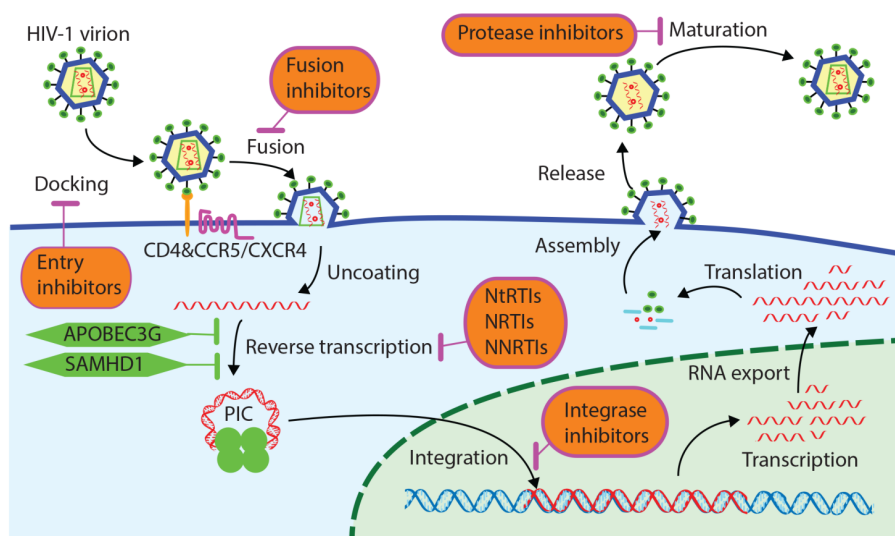


**Figure 1.** The viral replication cycle can be targeted pharmacologically at different stages

### 2.3. Clinical latency

The first step in finding a cure for HIV-1 infection is to identify the main source of cells that carry silenced, replication-competent HIV-1. Therefore, it is critical to define which cells or anatomical compartments constitute a reservoir of latent but replication-competent HIV-infected cells.

HIV-1 infects cells expressing the cell surface CD4 receptor and either of the co-receptors CCR5 or CXCR4. These cells include T helper cells, monocytes, macrophages, and dendritic cells. *In vivo*, HIV infects mostly activated CD4<sup>+</sup> T-cells as quiescent and resting CD4<sup>+</sup> T-cells are less permissive to infection due to low expression of CD4 and CCR5, and minimal metabolism [9–12]. The low metabolism is characterized by low levels of available dNTPs for reverse transcription and lack of energy sources [13–17]. Additionally, the cortical actin barrier in resting cells is thought to inhibit virus entry, reverse transcription and nuclear import [18,19]. However, the biggest pool of latently infected cells comprises resting memory CD4<sup>+</sup> T-cells.



It is thought that these latent infections are predominantly generated while activated infected cells revert back to a resting memory state [20–22]. During this process, as the genome of the (partially) activated cell condenses and is silenced in transition to a memory state, so does the HIV genome [14,15]. There is also evidence for direct infection of resting cells by HIV, resulting in the generation of a latent infection [23]. Studying these cells in patients is challenging as the frequency of latently infected cells in suppressed patients is very low, estimated to be 1 latent cell per 1 million of uninfected cells [24,25]. Due to the long half-life of a latently infected resting memory CD4<sup>+</sup> T-cells (estimated at 44 months), cART would take over 70 years in order to eradicate HIV from the infected patient [6,26,27].

Naive T-cells are also found to be latently infected; however, the frequency of such cells is even smaller than resting memory cells [28]. Interestingly, the naive T-cell reservoir may increase over time in suppressed individuals due to high proliferation of these cells compared to resting memory cells [29].

HIV is found also in cells of monocyte/macrophage lineage such as macrophages in brain and lung sections of infected individuals on anti-retroviral therapy [30,31]. However, proviral transcription occurs in these cells at low levels; therefore, it is debatable whether these cells are part of the latent reservoir [32,33].

Among the anatomical compartments affected by HIV-1, the central nervous system (CNS) and gut-associated lymphoid tissues (GALT) are two major sites [34–36]. The source of infection in the CNS is most likely infected monocytes, which are able to cross the blood–brain barrier as the virus itself cannot [37–39]. Approximately 5–10 times more HIV-1 RNA can be obtained from GALT than from blood cells in patients receiving cART [40,41], potentially indicative of lower penetrance of cART in cells within this anatomical site. However, the contribution of these compartments to rebound of viremia after cART cessation remains controversial [42,43].

#### **2.4. Clinical proof-of-concepts for HIV-1 eradication**

Thus far, only one patient, the so-called Berlin patient, was cured from HIV-1 after receiving treatment for acute myeloid leukemia [44,45]. HIV eradication in this patient was accomplished after several rounds of radio- and chemotherapy, total body irradiation, and two hematopoietic stem cell (HSC) transplantations from a donor bearing homozygous thirty-two base pair deletion in the CCR5 co-receptor gene (CCR5 $\Delta$ 32) were performed. The mutant CCR5 impedes viral entry of R5 tropic viruses in the first phase of the infection [46–49]. It is estimated that between 1% and 15% of the European Caucasian population harbor this mutation, while it occurs less frequently in African and Asian populations [47, 48]. In this patient, cART was ceased a day before the first transplant and after 7 years, no viremia or other indications of viral replication have been detectable [52].

Following the success of the case of the “Berlin patient”, two HIV-1-positive patients, the “Boston patients”, received HSCs transplants after developing Hodgkin’s lymphoma [53]. Both patients carried heterozygous CCR5 $\Delta$ 32 mutation. While still under cART regimen, no viral production was observed which led to cessation of therapy. Unfortunately, after several

months, strong viral rebound occurred in these patients. Follow-up analysis pointed to the likely presence of a small refractory source of cells, which is thought to have seeded the viral rebound; phylogenetic studies revealed that only a few latent proviruses contributed to the viral rebound [53]. Several other similar studies have been conducted with infected patients suffering from either leukemias or lymphomas who received autologous or allogenic HSC transplantation alongside cART as a strategy to deplete the latent pool of cells. However, in most of these studies, viral rebound was detected following therapy interruption [54].

In another case, the Mississippi baby, an infant presumably infected *in utero*, received cART 30 h after birth. As newborns do not have resting memory CD4<sup>+</sup> T-cells, it was reasoned that cART will prevent establishment of the latent reservoir – the main impediment in eradication strategies. One month after therapy, viremia reached undetectable levels and cART was stopped after 18 months. Unfortunately, 2 years post therapy interruption, rebound of viremia was detected (52, <http://www.niaid.nih.gov/news/newsreleases/2014/pages/mississippibaby-hiv.aspx>).

The immune system of rare “elite controllers” maintains low HIV-1 plasma levels, without the need of medication for many years. Although the capability of these patient to control viral replication is not completely understood, their circulating myeloid dendritic cells and CD8<sup>+</sup> T-cells are more effective in depletion of infected CD4 T-cells [56–61]. Interestingly, the ANRS VISCONTI cohort showed that cessation of long-term cART, started during the acute phase of HIV-1 infection, resulted in post-treatment control (PST) of infection. Fourteen of the studied individuals were able to keep or even further reduce the viral reservoir. Furthermore, these individuals were able to maintain long-lasting, low level of viremia [62]. Recently, a perinatally infected baby displayed more than 11 years of HIV-1 remission. At 3 months of age, plasma HIV-RNA reached  $2.1 \times 10^6$  copies/ml, and cART was administered for about 5–6 years. At 6.8 years of age, no HIV-1 RNA was detectable and cART was discontinued. After more than 12 years, plasma viremia still remains undetectable [63]. Therefore, this case provides the first evidence that early initiated, long-term cART can result in stable and durable HIV-1 remission.

Data from the Berlin and Boston patients provided a rationale for the creation of HIV-resistant cells. Since the CCR5 $\Delta$ 32 homozygous mutation is not lethal and not associated with abnormal immune functions [52], many approaches to silence the CCR5 gene have been or are under investigation [64–67]. These studies all employ genome editing technologies such as transcription activator-like effector nuclease (TALEN), clustered regularly interspaced short palindromic repeats (CRISPRs) or zinc-finger nucleases (ZNFs), which target the genome with high specificity and introduce deletions in the sequence of interest, in this case in the DNA sequence of CCR5 or/and CXCR4 co-receptors [64,65,68]. The rationale for this approach is based on the notion that cells bearing mutated CCR5 protein are not permissive to infection with R5 HIV-1 viruses, while cells with a mutated CXCR4 are resistant to C4 viruses. The double knock-out of both CCR5 and CXCR4 would allow resistance to infection regardless of viral tropism. However, the safety of such an approach remains to be elucidated. Uninfected HSCs isolated from infected individuals are engineered with either technology and then transfused back into patients. The ZNF approach targeting CCR5 has shown some promising results, although the sizes of cohorts used have been small. Gene-modified cells persisted in

patients over 9 months, and cells seemed to expand and undergo trafficking to other tissues [66]. An increase in CD4+ T-cell counts was observed in all individuals. Importantly HIV-1 DNA in the blood decreased. The encouraging outcome of this study has resulted in phase II clinical trials.

Another gene therapy-based approach is the introduction of HIV-1 expression-dependent suicide genes encoding either toxic or pro-apoptotic proteins such as members of the Bcl-2 protein family. Constructs that are responsive to Tat and Rev viral proteins were tested [69]. While obtaining encouraging results, activity of such suicide genes only affects cells that are actively producing viruses, thus the latent pool of cells would still be unaffected.

Despite many attempts at HIV-1 cure, thus far only two cases, the "Berlin patient" and the early treated infant have resulted in eradication [44,45,63]. Due to safety and economic issues associated with transplantation and gene therapy approaches, broad use of such a therapeutic approach is not feasible for HIV cure. Moreover, the gene therapy approach provides a functional rather than sterilizing cure. Nevertheless, all these studies provided valuable insights into the biology of the latent reservoirs. They constitute a proof-of-concept for HIV-1 cure. Moreover, it seems that immediate initiation of cART contributes to restricting the establishment of the latent pool.

These studies highlight the need for more robust, cheaper, and feasible treatments in order to achieve HIV-1 eradication among all infected individuals. In 2004, the concept of so-called "shock and kill" or "kick and kill" therapy was proposed [70–72]. The aim is to specifically reactivate proviruses in latently infected cells ("shock") and eliminate the infected cells via viral cytopathic effects or/and render the cells susceptible to immune clearance ("kill"). New rounds of infection would be prevented by cART. "Shock and kill" therapy relies on the identification of potent and specific latency reversal agents (LRAs) alongside induction of an effective immune response against the reactivated latent pool of cells. The LRAs currently under investigation do not result in sufficient reactivation of latent HIV *in vivo*. Therefore, novel molecules that specifically reactivate latent HIV-1 are urgently needed.

### **3. Model systems and assays to detect and study HIV-1**

To study the complex nature of HIV-1 latency, reliable model systems are required that recapitulate the nature and dynamics of the latent reservoir *in vivo*. Several cell lines of lymphocytic or monocytic lineage, primary-cell models, as well as animal models, are used to study HIV latency [73].

#### **3.1. Cell lines**

Immortalized cell lines of T-cell and monocytic origin are cost-effective and easy to use in the study of latent HIV. They allow fast read-outs in large scale for mechanistic molecular characterization of HIV gene expression. Therefore, cell lines are an attractive platform for screening and mechanistic characterization of LRAs. To generate a latent cell line, cells must

first be latently infected with a HIV derived virus. Several different HIV derived viruses are used ranging from full length to minimal virus and can make use of a wide range of reporter constructs (e.g. GFP or luciferase). The viral Tat/TAR axis is of vital importance for the transcriptional regulation of HIV and can be included or excluded from the viral construct used. Latent infection of relevant cell lines derived from T-cells or monocytic lineage, depending on reservoir of interest generate cell lines that can be used to study the molecular mechanisms of HIV latency [74–78].

Ach-2 and U1 cells are characterized by low expression of HIV-1, which can be strongly upregulated upon TNF $\alpha$  or mitogens stimulation [74,79]. However, in these cell lines, latency results from mutations in Tat protein (U1 cell-line) or in RNA stem loop TAR (Ach-2) [76,77]. Therefore, these cell lines do not represent complexity of latency found *in vivo*, however, they do allow Tat/TAR-independent HIV-1 reactivation investigation.

A more appropriate system to study latency are J-Lat cell lines derived from Jurkat cells of T-lymphocytic origin [78, 80,81]. These cells have integrated replication-competent full-length or minimal proviral constructs with an intact promoter and Tat-TAR axis, a GFP reporter gene replaces the *Nef* sequence in full-length proviruses or is located downstream of *Tat* in minimal proviruses [78].

These cell lines have been extremely useful to delineate the molecular requirements of HIV transcription activation and silencing. Although useful for molecular analysis and screening platforms, the cell line model systems of HIV latency also present some limitations; first, clonal cell lines are derived from a single integration event, and therefore do not reflect the diverse distribution of integration sites in the host chromatin [82,83]. Consistently, results vary depending on the cell lines used, indicating possible clonal cell line effects [84]. Due to the above mentioned limitations and the considerable difference between cell line models and primary cells in terms of proliferative capacity, genomic stability and mechanisms involved in establishing and maintaining latency, generally latency models based on primary cells are preferable.

### 3.2. Primary cells

To more closely resemble infection *in vivo* and validate putative LRAs more accurately, several primary cell models have been developed. Depending on the cell status at infection, these models can be divided into two groups.

The first group relies on purification of CD4<sup>+</sup> T-cells from healthy donors, that are then activated and subsequently infected. Depending on the method, CD4<sup>+</sup>T-cells are purified and stimulated with a-CD3/IL-2 [85], a-CD3/aCD-28 [86], a-CD3/aCD-28/IL-2 [87], or Ag-MDDC (antigen-loaded monocyte-derived dendritic cells; [88]), and infected with virus. Productively infected cells die due to virus-induced apoptosis or become latent by reverting back to a resting state. To limit infection to only one replication cycle, replication-defective viruses or antiretroviral drugs are also used. The rationale for these systems rely on the notion that a portion of activated, infected CD4<sup>+</sup> T-cells transition to a quiescent state, shutting down general transcription and slowing down metabolism, resulting in latency [6,25,28,89–91]. Depending

on the method used, different populations of latently infected cells are generated for use in reactivation studies. In the methods suggested by Sahu and Marini central memory T ( $T_{CM}$ ) cells remain in culture, in Yang's protocol mainly effector memory T ( $T_{EM}$ ) cells are produced, in Bosque and Planelles's method cells phenotype resembles central memory-like ( $T_{CM}$ ). The main disadvantage of these methods is the time needed to obtain results, which varies from 1 to 4 months. Furthermore, they are labor-intensive and technically challenging.

The second group uses direct infection of resting memory CD4+ T-cells, which immediately after integration become latent. Cells are infected after purification and can be used after several days for reactivation studies [90, 91]. Stimulation of CCR7, CXCR3, or CCR6 receptors increases the susceptibility of resting memory CD4+ T-cells to infection without T-cell activation. In the methods of Swiggard and Lassen, central memory T ( $T_{CM}$ ) and effector memory T ( $T_{EM}$ ) cells are the source of latent HIV-1; in Saleh's method naïve resting memory T-cells, in addition to  $T_{CM}$  and  $T_{EM}$  cells, constitute the latent pool. The main advantage of these methods is the time needed to evaluate the potency of putative LRA, as results can be obtained within one week.

Depending on the protocol used, the amounts of cells that become latent differ from as little as 1% to up to 40%. In models where cells are activated, on average more latently infected cells are generated. Using these models, we can quantify the level of reactivation of HIV-1 in a reliable manner by measuring the production of the viral protein p24 by enzyme-linked immunosorbent assay (ELISA) or quantification of viral transcription by quantitative RT-PCR, or by detection of GFP/luciferase in case of reporter-based constructs.

A novel detection method distinguishes uninfected, productively infected, and latently infected cells using a dual reporter system. A modified HIV-1 derived genome containing GFP as a reporter of viral transcriptional activity and mCherry under an EF1a promoter as a reporter of infection (latent or productive) allows easy isolation of the different cell populations [23].

Ultimately, the golden standard for testing activity of LRAs are primary cells from infected individuals under cART obtained by leukaphoresis, a process in which white blood cells are specifically isolated while other blood components are reverted back to the patients' circulatory system. The isolated cells are uninfected, latently infected, and infected with defective viruses. Large amounts of CD4+ T-cells are required and isolated from patients for testing LRAs.

The development of primary cell models greatly improved the quest for LRAs, yet results differ between each model system [84]. No *in vitro* models completely recapitulate the full range of latent cells *in vivo*; instead, only a small sub-fraction of latently infected cells is represented. Hence, the validation process of putative LRAs requires testing on cells derived from infected individuals [93].

### 3.3. Animal models of HIV-1 infection

The number of animal models available to study latency is limited. The toxicity of putative LRAs can be assessed with use of mouse and non-human primate (NHP) models [94]. Two mouse models have been developed and used in HIV latency studies: the humanized SCID

(SCID-hu) mouse, transplanted with human thymus and liver fragments, and the humanized blood, liver, and thymus (BLT) mouse which has a human immune system with full mucosal immunity [95–97]. Unfortunately, SCID-hu mice do not express human proteins involved in the viral replication cycle; therefore, the study of HIV-1 in these mice is restricted to events taking place within organs of human origin in this model. In addition, HIV-1 is not responsive to cART in these animals. BLT mice are a better model of HIV-1 infection, as they produce resting memory CD4<sup>+</sup> T-cells of human origin. However, some components of cART do not repress replication in BLT mice [34].

NHP models employ the Simian immunodeficiency virus (SIV) infection in rhesus and pig tailed macaques to recapitulate HIV-1 infection in humans [98,99]. NHP models allow the monitoring of the spread of infection. Moreover, infection in this model can be controlled by antiretroviral therapy. NHP models are helpful in studying the first stages of latency establishment, as investigating this part of HIV-1 infection is extremely challenging in patients, as the pool of latently infected cells is established early during infection [100]. One caveat to the use of SIV-based NHP models of HIV latency is that the viral 5'LTR or promoter of SIV is considerably different in sequence from HIV-1 [101] and therefore latent SIV response to LRAs, which is a direct consequence of promoter-mediated transcription activation may vary substantially from latent HIV-1. In addition, animal models are far more expensive than cell-based systems. Nor do they fully reflect human infection or metabolism. Finally, ethical concerns are inherent to the use of NHP models of HIV latency.

### 3.4. Detection of the latent reservoir

The study of latent HIV infection requires accurate measurement of the size of the latent reservoir and the extent of reactivation following LRA treatment. Depending on the experimental aim, different detection methods can be employed. These methods generally rely on PCR, protein quantification, or reporter detection.

The quantitative viral outgrowth assay (QVOA) is a well-established method to estimate the latent pool. The assay relies on the use of serial dilutions of cells obtained from an infected individual in co-culture with uninfected cells that are permissive to infection. Viral proteins are detected by ELISA. Unfortunately, QVOA is time-consuming, costly, and might generate false-negative results as not all replication-competent proviruses are reactivated, and thus not detected [83].

The HIV reservoir can be approximated by detecting the number of viral DNA copies present in the cells. The recently introduced digital droplet PCR (ddPCR) improves on classic and nested qRT-PCR by simultaneously amplifying thousands of nanoliter reactions in combination with very sensitive detection system based on flow cytometry [94,102,103]. ddPCR is therefore superior to nested qRT-PCR in its ability to resolve rare events such as latent HIV-1. Although PCR based methods provide increased sensitivity for the detection of viral genetic material, these approaches also detect defective proviruses, which results in false-positive results.



Another recent PCR-based method for reservoir detection evades false positive results from defective proviruses. The *Tat/rev* induced limiting diluting assay (TILDA) relies on PCR amplification of multiply spliced RNA (msRNA) of *tat/rev* transcripts that are present in productively infected cells and absent in latent infection [104]. Small amounts of cells isolated from patients are divided into two equal parts and distributed in limiting dilution. One half is left unstimulated while the other is activated with PMA/Ionomycin. After 12 hours, cells are lysed and subjected to ultrasensitive nested RT-PCR. By employing statistical modeling, the frequency of cells that are expressing msRNA in both groups is estimated and based on the unstimulated group a threshold of activation can be set. Using the TILDA assay, the size of the reservoir is estimated at 24 cells per million, which is more than measured by QVOA but less than measured by PCR methods [24,83,104]. The assay more accurately estimates the true size of the latent reservoir, is highly sensitive, reproducible, fast, relatively inexpensive, and requires only 10 mL of patients' blood. However, a limitation on the TILDA assay is that it detects the presence of viral transcripts but not the production or release of infectious viral particles; therefore, it may still overestimate the true size of the reservoir, yet to a smaller extent than other PCR-based methods. Additionally, signal detection relies on amplification of highly variable region of the HIV-1 DNA; therefore, detection of all subspecies of HIV-1 might be challenging and require extra optimization steps.

Unfortunately, all current methods to detect latent HIV-1 have limitations. First, the pool of latently infected cells in patients is extremely low, resulting in a high noise-to-signal ratio. Furthermore, defective or hyper-mutated proviruses are detectable by PCR-based techniques, yet irrelevant for eradication strategies. Moreover, not all replication-competent proviruses are inducible in the first round of treatment, yet get reactivated upon subsequent rounds of stimulation [83]. Thus, assays to measure latency reversal are overestimating – in the case of PCR-based methods – or underestimating – in the case of QVOA – the latent pool. This poses a main problem in measuring efficiency of the reactivation of HIV-1. A captivating approach employing the use of a biomarker (e.g., gene), which responds to treatment in the same way as HIV-1, would allow more easily quantifiable assessments as to whether latent HIV in patient cells would be responsive to a particular treatment.

## 4. Molecular mechanisms of latency

Although replication-competent, latent HIV is transcriptionally silenced but susceptible to reactivation upon certain stimuli. Following integration into the host genome, transcription from the HIV genome is controlled by key cellular host factors, and subject to host cell gene regulation similar to endogenous genes. Since viral transcription initiation, elongation, and termination are tightly regulated by host proteins, HIV is also widely used as a model system to study gene regulation.

### 4.1. Host antiretroviral mechanisms thwart infection

Host defense mechanisms impede HIV-1 infection. Upon entering the cell, HIV's RNA genome is reverse transcribed into double-stranded DNA (dsDNA). This process requires freely

available deoxynucleotide triphosphates (dNTPs). By limiting the pool of freely available dNTPs, the nucleotide scavenger SAMHD1 restricts viral replication in non-cycling myeloid cells and quiescent CD4<sup>+</sup> T-cells [105–108]. Additionally, SAMHD1 has 3′–5′ exonucleases (RNase) activity that specifically cleaves single-stranded RNA [109,110]. Interestingly, Vpx, encoded by HIV-2 and Simian immunodeficiency virus, is an accessory protein packaged into the virion, which induces SAMHD1 degradation [111].

Additionally, APOBEC3G limits viral replication by catalyzing the deamination of cytidine to uridine in the viral single-stranded DNA (ssDNA) genome during reverse transcription [112]. Interestingly, APOBEC3G is inactive in memory CD4<sup>+</sup>T-cells, which helps to explain why this cell type is more permissive to HIV-1 infection. Therefore, activated CD4<sup>+</sup> T-cells are the main target cell type of HIV infection and of the main source of the latent reservoir.

#### **4.2. Integration of HIV into the host genome required by host factors**

The reverse-transcribed viral DNA genome is incorporated in the pre-integration complex (PIC). The PIC is imported into the nucleus. Host factors identified so far that affect viral integration are lens epithelium-derived growth factor (LEDGF/p75/PSIP1) and hepatoma-derived growth factor related protein 2 (HRP- 2/ HDGFRP2), through an integrase binding domain. In the absence of LEDGF, provirus integration is decreased 10-fold and HIV's pattern of integration is altered [113–115]. Simultaneous LEDGF and HRP-2 knockdown further decreases viral replication [116]. Nevertheless, knockdown of both factors does not completely abolish HIV-1 integration, indicating that IN alone and/or in cooperation with other host factors can still integrate the viral genome [117]. PIC nuclear import stimulates export to the cytoplasm of INI-1 and PML, disrupting this effect greatly improves integration efficiency [118–120]. Upon knockdown of transportin-3/TNPO3 and nuclear pore protein RanBP2/Nup35 HIV-1 integrates randomly [121]. Therefore, nuclear import affects the site of integration with a preference for open chromatin.

#### **4.3. Pre-integration vs post-integration latency**

Two states of latency can be defined based on the integration state of HIV: pre-integration latency and post-integration latency. Defects in integration or in a prior phase of the viral replication cycle (e.g., incomplete reverse transcription) might result in unintegrated viral DNA. The half-life of the linear pre-integration complex is approximately 1 day [122]. The linear unintegrated viral DNA can also be circularized, resulting in slightly extended half-life of the virus [123]. In quiescent cells, the pre-integrated virus can reside near the centromere for weeks [124]. Unintegrated virus can replicate, albeit very inefficiently [125]. The half-life of both forms of unintegrated virus is too short and replication inefficient to serve as the source required for the long-term persistence of latent HIV making pre-integration latency less clinically relevant.

Post-integration latency occurs when the HIV virus is stably integrated into the host genome, but a productive infection is not achieved. The site of integration and the abundance of transcription factors are crucial for determining whether an infection will be latent or produc-



tive. The site of integration will determine the chromatin environment (such as histone modifications), relative position to other genes (intronic insertion vs gene desert) and position within the nucleus of the provirus.

#### **4.4. Integration biases**

The site of integration greatly determines the transcriptional activity of the provirus. HIV preferentially integrates into active genes both in patient material and transformed cell lines [82,126–128]. Moreover, HIV-1 integrates in regions of genome that are in close proximity to nuclear envelope [129]. Latent integrations are in or close to aliphoid repeat elements in heterochromatin, whereas productive integrations avoid insertion in or near heterochromatin [78]. Integration is associated with transcription-inducing histone modifications (i.e., H3 & H4 acetylation and H3K4 methylation) but not transcription-inhibiting modifications (i.e., H3K27 trimethylation and DNA CpG methylation) [130]. A comparison of integration sites in resting and activated CD4+ T-cells showed that in both cell types HIV integrates in active genes. However, in activated cells, insertions were enriched for gene dense, CpG island-rich and high G/C-content regions [131]. Latency in infected Jurkat cell lines correlated with integrations in gene deserts, centromeric heterochromatin, and highly expressed cellular genes [128]. Within the nucleus, HIV-1 is located mostly in decondensed chromatin at the nuclear periphery, while it disfavors heterochromatic regions [132]. Interestingly, latent proviruses were found to interact with a pericentromeric region of chromosome 12 in quiescent cells [133]. In a study of viremic progressors and viremic controllers, integration was enriched into, or in close proximity to, Alu repeats, local hotspots, and silent regions of the genome [134]. In addition, close proximity of the provirus to PML bodies is associated with latency, an association that is lost upon reactivation [135].

#### **4.5. Integration relative to host genes affects transcriptional state of the provirus**

Sense and antisense integration relative to host genes can greatly affect the transcriptional state of HIV. Integration in sense orientation can lead to promoter occlusion, whereas integration in antisense orientation can lead to collision of the transcriptional machinery. Promoter occlusion occurs when the transcriptional machinery is depleted from the viral promoter by a dominant host promoter that is transcribed and negatively affects proviral expression.

Indeed, chimeric transcripts of the host gene and in sense viral integrations were observed [136,137]. Additionally, Han et al. compared the effect of sense and antisense insertions of HIV relative to the active HPRT gene [138]. In this setting, sense integration enhanced viral expression whereas antisense integration (transcriptional collision) led to suppression. Sense integrations were shown to be modestly preferred in latent cells, a preference that was not present in productively infected cells [139]. Transcriptional interference and transcriptional collision are examples of host genes interference with viral expression. On the other hand, reactivation of HIV may lead to suppression of host gene expression [136]. Indeed, in a cell model with a latent integration into the HMBOX1 gene, the host gene was repressed upon viral reactivation [140].

#### 4.6. Viral transcription starts at the 5'LTR

The provirus is flanked by a 5' and 3' long terminal repeats (LTRs). While transcription can be initiated from both LTRs, the 5' LTR is dominant and serves as the HIV promoter, although 3' transcription is activated when the 5' LTR is defective [141]. Transcriptional interference has been proposed as the mechanism by which the 5' LTR exerts its dominance over the 3' [142]. Interestingly, low-level antisense transcription takes place at the 3' LTR, a mechanism by which latency can be maintained [143–147]. Sense transcription results in at least 40 coding transcripts due to alternative splicing of the HIV-1 genome [148]. Finally, both LTRs also act as a source of negative sense transcription, which could potentially affect the expression of neighboring genes [149,150].

#### 4.7. The 5' LTR contains numerous putative transcription factor binding sites

HIV-1 encodes a potent trans-activating protein – Tat – that drives viral expression during productive infection. However, initially, before sufficient levels of Tat are expressed, the provirus relies on host factors to initiate transcription. The 5' LTR contains three regions – U3, R, and U5 (Figure 2) [151]. The R region, immediately next to the transcription start site (TSS), contains the trans-activation response (TAR) element, an important regulator of HIV expression. The U3 region contains the core promoter (nucleotides –78 to –1 upstream of TSS), a core enhancer (nucleotides –105 to –79), and a modulator region (nucleotides –454 to –104) [152,153]. The core promoter contains three Sp1 binding sites in tandem, a TATA box, and an initiator element at the transcription start site. The core enhancer contains two NF-κB-binding sites. The modulator region – so-called because early experiments with deletion upstream of the LTR caused increased activity of the LTR – was shown by later experiments to contain binding sites for both repressive and activating factors including nuclear factor of activated T-cells NFAT, STAT5, NF-κB p65/p50 heterodimers, lymphocyte enhancer factor (LEF-1), CCAAT/enhancer binding protein (C/EBP) factors, AP-1, and activating transcription factor/cyclic AMP response element binding (ATF/CREB) factors (Figure 2) [152,154–162]. It is well established that these transcription factors have binding sites within HIV-1 sequence. Moreover, they are strong activators of HIV-1 transcription of which NF-κB is considered the most critical [163–166]. In addition to the presence of these sites, bioinformatic tools indicate that this region of the HIV LTR contains a tightly clustered distribution of multiple transcription factor consensus binding elements [167].

#### 4.8. Positive host factors bind to the 5' LTR

Initial transcription of HIV-1 is entirely dependent on host factors. Nuclear factor kappa-light-chain-enhancer of activated B cells (NF-κB) is a hetero dimer comprised of p50 and p65 subunits involved in T-cell activation. NF-κB acts as a transcription factor and is a potent activator of HIV-1 transcription initiation and elongation. It interacts and functions cooperatively with numerous proteins. Independent of Tat, NF-κB can reactivate HIV to high expression levels [168]. Mutated NF-κB-binding sites on the LTR inhibit basal transcription and Tat transactivation [169]. NF-κB, Sp1, and other factors (LEF-1, Ets1, and TFE-3) bind to sites near NF-κB sites and synergistically activate HIV transcription, even in the presence of repressive

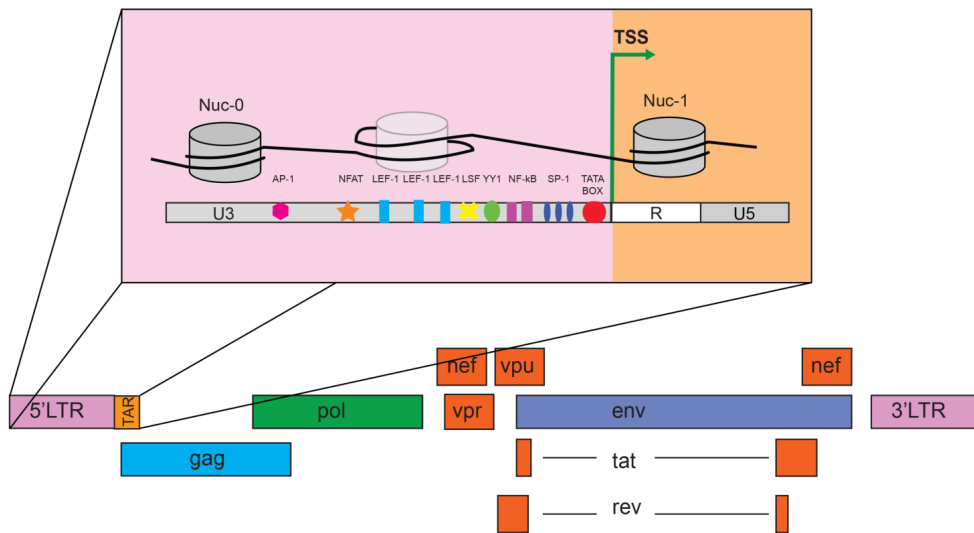


**Figure 2.** The genome of HIV-1

chromatin structures [170,171]. NF-kB and AP-1, a heterodimer of proteins from the c-Fos, c-Jun, ATF, and JDP families, cooperatively trans-activated LTR activity through the ERK1/ERK2 mitogen-activated protein kinase (MAPK) pathway [161]. Acetylation of Lys310 in NF-kB p65 subunit is an activating mark that is removed by NAD<sup>+</sup>-dependent protein deacetylases SIRT1 and SIRT2 [172]. Tat positively affects NF-kB by inhibiting SIRT1 and stimulating degradation of IκB, a protein that sequesters NF-kB in the cytoplasm [169,173]. The viral nucleocapsid (NC) protein enhances NF-kB-mediated activity by interacting with the LTR [174]. p65 recruits THIIH which is part of the preinitiation complex and its subunit CDK7 with kinase activity activates CDK9, resulting in increased HIV transcription [175,176]. The cell surface receptor OX40, bound by its ligand gp34, activates transcription from 5' LTR, in a manner dependent on the presence of NF-kB-binding sites on the LTR [177]. The transcription factor E2F-1, a regulator of S-phase gene expression, inhibits LTR transcription through the recruitment of p50 at the NF-kB-binding sites on the LTR [178].

Members of the SV40-promoter (Sp) specific transcription factor family regulate LTR activity. Sp1 and Sp4 are activators of HIV-1 [179]. Expression of Sp transcription factors changes during monocytic maturation, suggesting differences in susceptibility to LTR activation during differentiation [180].

Nuclear factor of activated T-cells (NFAT) can induce LTR activity in T-cells [155]. NFAT recruits HATs through CBP/p300, which results in reactivation of HIV-1 transcription [181]. The Janus kinase (JAK)/signal transducers and activators of transcription (STAT5) can stimulate or inhibit HIV transcription. STAT5 binds to its binding sites in the U3 enhancer region on the LTR where it promotes transcription [156]. In response to a broad range of cytokines (e.g., IL-2, IL-7, IL-15) and granulocyte-macrophage colony-stimulating factor (GM-

CSF) JAK-mediated phosphorylation of a C-terminal tyrosine residue activates STAT5A and STAT5B. Homodimers or heterodimers of activated STAT5A and STAT5B translocate to the nucleus to stimulate HIV expression [182,183]. Interestingly, STAT5 $\Delta$ , an isoform of STAT5 truncated on the C-terminus, acts as a repressor of LTR activity [184]. Indeed, in the promonocytic cell line U1 high levels of STAT5 $\Delta$  are present. Upon stimulation with GM-CSF, STAT5 $\Delta$  blocks RNAPII from binding to LTR U3 region, inhibiting activity of HIV promoter [185]. STAT5 $\Delta$  promotes p50 homodimers binding to the LTR, contributing to latency maintenance [186].

In monocytes and macrophages, CCAAT/enhancer binding protein (C/EBP) factors are crucial for activation of HIV-1 [160,187–189]. C/EBP, a member of the bZIP superfamily, contains a DNA-binding domain and a leucine zipper for homo- and heterodimerizations. Similar to Sp-1, levels of C/EBP vary during myeloid development [190]. Interestingly, the HIV-1 LTR contains several C/EBP binding sites [159].

Some studies employing mutagenesis of binding sites for activator protein-1 (AP-1) within proviral genome showed that AP-1 transcription factor is the crucial activator of proviral transcription, as proviruses with altered AP-1-binding sites were less prone to reactivation even if treated with strong activator such as phorbol 12-myristate 13-acetate – PMA [191]. Furthermore, the latent pool was bigger in cells infected with a virus carrying a deletion in AP-1 sites, implicating that the AP-1 protein is necessary for successful provirus transcription [192]. Heterodimeric protein AP-1 is formed upon phosphorylation of c-Jun N-terminal kinase (JNK) in JNK/MAPK pathway [193]. It is well established that activation of TLR signaling induces nuclear localization of NF- $\kappa$ B and AP-1 mediated via JNK pathway [194–196].

In addition to the already mentioned host factors, the potent viral trans-activating protein Tat and to a lesser extent the multifunctional viral protein, viral protein R (Vpr), positively affect viral transcription. Productive infection requires the presence of Tat. Exogenous expression of Tat rescues HIV from latency [197]. A defective Tat mutant (C22G) is incapable of full-length viral expression [198]. Additionally, the Tat mutant (H13L) is more prone to establish latency [197]. Tat recruits the positive transcription elongation factor b (P-TEFb), which shifts RNAPII promoter proximal pausing to transcriptional elongation leading to a productive infection [199,200]. P-TEFb consists of CDK9, a serine/threonine kinase, and CyclinT1. The N-terminal cystein-rich region of Tat (Cy22-Cy37) binds to CycT1 through Zn<sup>2+</sup>-mediated interactions [201–203].

Vpr is a multifunctional HIV-1 protein that plays a role in nuclear import of the PIC and cell cycle arrest in proliferating cells. Vpr also activates LTR activity through multiple mechanisms. Vpr recruits p300 to the 5' LTR increasing acetylation, resulting in HIV-1 transcription [204]. Moreover, Vpr interacts with Sp1 and TFIIB, part of the transcription initiation complex, stimulating proviral transcription [204–206].

#### 4.9. Repressive host factors at the 5' LTR

Not all host transcription factors have an activating effect on LTR activity (Figure 3). YY1 and LSF recognize binding sequences in the LTR and repress transcription through epigenetic

modification [207]. C-promoter binding factor-1 (CBF-1) also represses HIV through epigenetic silencing [208,209]. c-Myc recruits an epigenetic silencing factor to repress HIV-1 [210].

Transcription factors initiate LTR activity, but full-length transcripts are not produced because transcription elongation is inhibited. DRB sensitivity-inducing factor (DSIF), a heterodimer composed of hSpt4 and hSpt5 proteins, induces capping of RNA from newly initiated transcription complexes [211]. The subunit hSpt5 interacts directly with nascent RNA as it appears from the RNAPII exit site and recruits negative elongation factor (NELF) (Figure 3) [212–214]. Escape of transcripts from the promoter proximal pause site is prevented by NELF, which induces termination of transcription over several hundred bases [215]. Moreover, the binding sequence of NELF subunit E recognizes a homologous sequence on TAR, increasing association of NELF with the LTR, which results in transcription silencing. Indeed, experiments where NELF is knocked down show higher basal HIV transcription and reactivation from latency [216–218].

A novel, RNA interference independent, mechanism mediated by microprocessor and termination factors causes transcriptional silencing and chromatin remodeling at the HIV-1 promoter [219]. Microprocessor binds to TAR, which is then cleaved by Drosha into two RNAs, a 5'-end and 3'-end product. The 5' is further processed in an Rrp6-dependent manner into a transcription repressing RNA species. The 3' RNA recruits termination factor Xrn2 and Setx, which induces RNAPII pausing and premature termination of transcription [219].

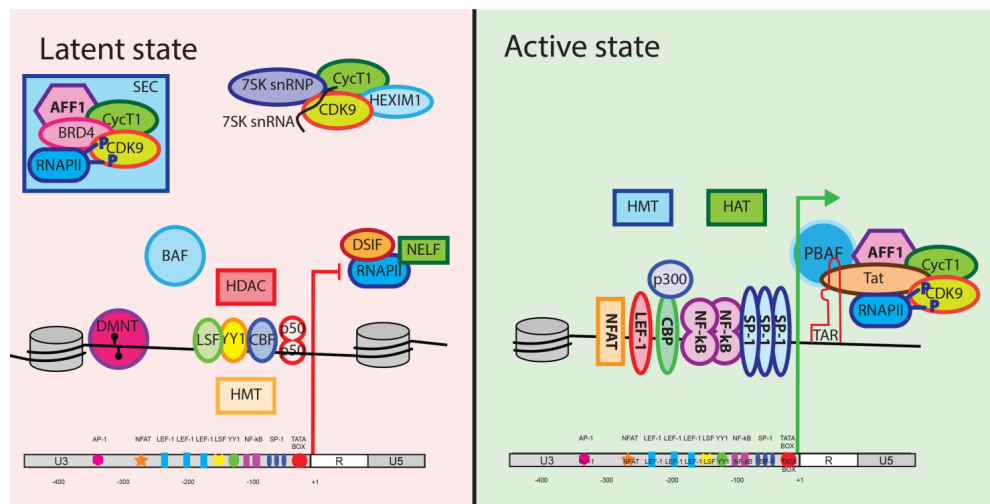


**Figure 3.** Molecular mechanisms in latent and productive HIV-1 infection

#### 4.10. Host factors induce transcriptional initiation, but not elongation

While some host transcription factors recruit RNAPII, in the absence of Tat, transcription elongation does not occur resulting in the generation of short abortive transcripts by promoter

proximal pausing [220,221]. These ~60nt transcripts include TAR, which has a stem-loop structure and binds near the HIV 5'LTR, inhibiting RNA-polymerase. TAR directly binds Tat, which recruits transcriptional elongation complex to the LTR [222].

#### **4.11. Tat-dependent transcription leads to productive infection**

If cells become activated or due to leaky transcription, Tat can be produced. Tat binding to P-TEFb induces significant conformational changes in P-TEFb, allowing Tat and CycT1 to cooperatively recognize and stably bind TAR [200,223].

Tat-P-TEFb phosphorylates NELF-E resulting in the dissociation of NELF from TAR and the paused RNAPII complex [214,216,218,224]. CDK9 phosphorylates RNAPII at the carboxyl terminal domain (CTD) at Ser2 and Ser5 residues of the 52 heptad repeats, which regulates progression to the elongation phase of transcription [225–227]. The phosphorylation status determines regular and alternative RNA splicing and the 3' end recruitment of polyadenylation factors [228,229]. Ser2 phosphorylation of the RNAPII CTD recruits splicing-associated c-Ski-interacting protein, SKIP, and stimulates elongation transcription and alternative splicing of the Tat-specific splice site through interactions with U5snRNP proteins and tri-snRNP110K [230].

Phosphorylation of hSpt5, a subunit of DSIF, by CDK9 converts it into a positive elongation factor that prevents nascent RNA from breaking off from the transcription complex prematurely and inhibits pausing of RNAPII at arrest sites [231,232]. By removing several blocks Tat-P-TEFb induces transcriptional elongation as well as co-transcriptional processing. During active transcription elongation, increased recruitment of RNAPII to TSS maintains a stable level of RNAPII at the promoter proximal region [218]. Throughout transcription, Tat-P-TEFb remains associated with the elongating transcription machinery [231,233,234].

#### **4.12. P-TEFb can be recruited in active and inactive form in the nucleus by Tat**

In activated T-cells, inactive P-TEFb predominantly resides in the 7SK small nuclear ribonucleoprotein (snRNP) complex (Figure 3) [235–237]. The 7SK snRNP complex consists of 7SK snRNA, HEXIM1 (or its homolog HEXIM2), the La-related protein 7 (LARP7), and the 7SK-specific 5' methylphosphate capping enzyme (MePCE). The snRNA functions as a scaffold: it binds two units of P-TEFb and one HEXIM1/2 homo-/heterodimers [238,239]. MePCE and LARP7 protect the 7SK RNA from nuclease degradation, MePCE binds the 5' end, LARP7 the polyuridine 3' end [240–242]. Tat disrupts the interaction between pTEFb and HEXIM1/7SK snRNA and recruits P-TEFb to 5' LTR, resulting in active transcription [226].

BRD4 can also recruit P-TEFb from 7SK snRNP [241,243], to promote transcription. Due to similarities in their C-terminal P-TEFb interacting domains [244], Tat and BRD4 compete for P-TEFb [245,246]. In a latent model, knockdown of BRD4 results in Tat-dependent reactivation of HIV-1 [247].

Bromodomain and extra-terminal domain family of proteins (BET) play an important role in repression of the HIV-1 transcription. BET proteins are responsible for the recruitment of P-

TEFb to transcribed genes [246,248]. BRD4 competes with viral protein Tat for binding site on pTEFb, and it represses HIV-1 transcription [245,246]. Knockdown of BRD2 indicates this protein contributes to the maintenance of latency. These results are consistent with the notion that BRD2 is binding to remodeling factors such as HDACs [249,250].

P-TEFb can be recruited to transcription complexes by other factors. CTIP2 recruits P-TEFb by binding HEXIM1 and negatively regulates the complex by repressing the CDK9 kinase activity of P-TEFb [251]. Phosphorylation of HEXIM1 at Tyr271 and Tyr 274 decreases retention of P-TEFb in the 7SK RNP [252]. Additionally, through the binding of nascent RNA, SRSF2 and P-TEFb are released from the 7SK complex and induce transcription elongation in a manner similar to TAR/Tat-mediated recruitment of P-TEFb [253].

#### **4.13. P-TEFb is a subunit of the super elongation complex**

P-TEFb is required for activation of HIV transcription but does not explain the maximum observed viral expression; therefore, additional factors are necessary [254,255]. P-TEFb is an integral part of the super elongation complex (SEC) (Figure 3), which is a potent activator of transcriptional elongation of host genes [234,256]. It is composed of one of two scaffold proteins, AF4/FMR2 proteins AFF1 or AFF4. Translocations of AFF1 and AFF4 resulting in fusion proteins are commonly found in mixed lineage leukemia (MLL) [257–259]. The resultant fusion proteins cause aberrant recruitment of SEC to MLL-specific genes [260]. AFF1 and AFF4 recruit many other proteins to the SEC [261], such as ELL family of elongation stimulatory factors ELL1 and ELL2, which inhibit RNAPII pausing and synergistically improve Tat-transactivation with P-TEFb [256]. Moreover, knockdown of ELL2 strongly suppresses viral expression. [203,210,230,252]. Tat and AFF4 inhibit the polyubiquitination-mediated degradation of ELL2, increasing available levels of SEC. [256,262].

#### **4.14. Tat can be extensively post-translationally modified – “Tat code”**

Modifications on numerous amino residues of Tat regulate the interaction with a wide variety of host proteins. In comparison to the histone code which is used to explain the multiple modification on histone tails and their function, a “Tat-code” has been proposed [34]. Tat is phosphorylated on Ser16 and Ser 46 by CDK2, modifications which result in transcription inhibition [263]. Acetylation of Lys28 increases affinity for P-TEFb binding and is removed by HDAC6 [264–266]. Tat dissociates from TAR and binds acetyltransferase PCAF which acetylates Tat at Lys50 and Lys51 [264,265,267–270]. Acetylated Lys50 allows recruitment of the PBAF (SWI/SNF B) chromatin remodeling complex to the LTR [267,271–273]. SIRT1 deacetylates Tat at Lys50 as part of a late phase of transcriptional regulation, stripping Tat of acetyl groups allowing its reuse in subsequent rounds of transcriptional cycles [274]. Mono-methyl-transferase Set7/9 and LSD1, respectively, methylate and demethylate Lys51. Demethylated Lys51 of Tat enhances HIV-1 transcription [275,276]. Hdm2 polyubiquitinates Lys71, activating Tat [277].



#### 4.15. Nucleosome positioning at the 5' LTR controls viral expression

Regardless of integration position, the latent 5' LTR typically contains two nucleosomes, Nuc-0 and Nuc-1, at fixed positions [278]. Nuc-1 blocks transcription elongation as it is positioned just downstream of the TSS. Nuc-1 is displaced upon virus reactivation [278–280]. Nucleosomes can be altered by chromatin remodeling complexes. A third unstable or loosely positioned nucleosome is located in between nuc-0 and nuc-1 [281] (Figures 2 and 3A).

BCL11B, together with the chromatin remodeling complex NuRD, strongly represses HIV-1 transcription [282]. BCL11B is specifically expressed in T-cells and neurons. Interestingly, the NuRD complex consists of several proteins with histone deacetylase activities – i.e., HDAC1 and HDAC2 [283,284].

The ATP-dependent chromatin remodeler BAF (SWI/SNF-A) was discovered by our group to be essential to both the establishment and maintenance of HIV latency (Figure 3). The BAF complex utilizes energy from ATP to push Nuc-1 from an energetically favorable position upstream of the TSS to a suboptimal region, downstream of TSS, resulting in a transcriptional block [281]. siRNA depletion of the BAF complex de-repressed proviral transcription. Furthermore, in siRNA-mediated BAF knockdown, latency establishment occurred less frequently than in the presence of the functional complex. The PIC through LEDGF interacts with INI-1 a subunit of BAF, allowing nucleosomes to be deposited at the provirus, contributing to latency establishment [118].

#### 4.16. Epigenetic modifications regulate latency

Epigenetic modifications of nucleosomes such as histone-acetylation and -methylation and of DNA such as DNA-methylation play an important role in regulating the proviral transcription. Nucleosomes are the basic units of organization of chromatin and consist of a combination of histone subunits. Histones have an amino acids tail that can be extensively modified. Two broadly studied modifications that regulate expression effects are histone-acetylation and histone-methylation

Histone-acetylation by histone acetyl transferases (HATs) induces chromatin loosening, while histone deacetylases (HDACs) reverse the effect by removing the acetyl group (Figure 3). HATs such as p300/CREB-binding protein (p300/CBP) and p300/CBP-associated factor (P/CAF) can be recruited to activate the HIV LTR [158,285]. HDAC1, HDAC2, HDAC3, and HDAC6 repress HIV [286–289]. Numerous host factors recruit HDACs to the LTR. A negative regulator of P-TEFb, CTIP2 in cooperation with COUP-TF and Sp1 also recruits HDAC1 and HDAC2 to the HIV LTR in microglial cells [290,291]. Host factors LSF and YY1 co-operatively bind to the LTR, where YY1 recruits HDAC1 to deacetylate Nuc-1 [207]. CBF-1 and c-Myc also repress HIV through the recruitment of HDAC1 [208–210].

Methylation of histones by histone methyltransferases (HMT) can act as an activating or repressing mark depending on the histone tail residue modified (e.g., methylation of lysine 4 on histone 3 (H3K4) is activating whereas H3K9, H3K27, and H4K20 methylation is repressive). HMTs modify specific histone residues, e.g., EZH2 (H3K27me3), SUV39H1 (H3K9me3), G9a (H3K9me2), and G9a like protein, GLP (H3K9me2). The repressive methyl groups deposited



by these HMTs contribute to the maintenance of latency [292–295]. Moreover, EZH2 is suspected to recruit additional repressive proteins such as HDACs and other HMTs [294].

DNA methylation at CpG dinucleotides represses transcription by disrupting the binding of transcription activators to their binding sites or indirectly through the binding methyl-CpG binding proteins (MeCPs). In cell line models of latency, the HIV-1 LTR contains two CpG islands that are hypermethylated (Figure 3) [296]. Methyl-CpG binding domain protein 2 (MDB2) and HDAC-2 bind to the second CpG island on the HIV LTR and are displaced from there when cells are treated with cytosine-methylation inhibitor 5-aza-2'-deoxycytidine [296]. In memory CD4+ T-cells from long-term aviremic and viremic patients, an increase in HIV LTR DNA methylation was observed in the aviremic patients [297]. The methylation of the HIV LTR in long-term non-progressors and elite controllers is increased compared to the LTR of aviremic patients on cART [298]. In contrast, this difference was not found in the first CpG island of resting memory CD4+ T-cells from aviremic patients, indicating that the mechanism by which DNA-methylation regulates latency deserves further exploration.

#### **4.17. Viral and host non-coding RNAs regulate viral expression**

Non-coding RNAs exert post transcriptional control on gene expression. Small non-coding RNAs (<200 nt) and in particular microRNAs (miRNAs) are well established to have regulatory function. The study of long non-coding RNAs (lncRNA, >200 nt) is an emerging field because of their epigenetic regulatory potential. Both viral and host miRNAs and lncRNAs affect replication of HIV-1 [146,299–301].

RNA interference (RNAi) is a post-transcriptional gene silencing mechanism. miRNAs post-transcriptionally suppress or silence gene expression as part of the RNA-induced silencing complex (RISC) forming a protein–RNA complex. Pri-miRNAs are generated by RNAPII and are subsequently processed by microprocessor into pre-miRNAs in the nucleus. Following export to the cytoplasm, they are cleaved by Dicer and incorporated into RISC. RISC generally binds in the 3'-untranslated region (3'UTR) of a target mRNA. The bound transcript is degraded or transcription is impeded depending on the level of homology, resulting in translational repression. The RNAi affects the infectivity of monocytes and macrophages [302]. Comparisons of productively infected, suppressed, and uninfected patients found difference in miRNA profiles, but it is very unlikely that the observed effects are due to viral activity because the number of infected cells is low in elite controllers or under cART [303–305]. Knockdown of Dicer or Drosha, a component of microprocessor, stimulates HIV-1 replication, indicating that miRNA generally are responsible for suppression of proviral transcription [299,300]. However, phenotypic effects are hard to interpret due to the pleiotropic side effects of microprocessor depletion. RNAi affects infectivity by targeting transcripts of key host factors and viral proteins involved in HIV-1 repression. In resting T-cells, the polycistronic miRNA cluster miR-17/92 is suppressed by HIV, resulting in PCAF upregulation [299]. Additionally, CycT1 is negatively regulated by miR27b [306]. Moreover, during differentiation from monocytes to macrophages, expression of miRNA198 and miR27b decreases relieving suppression of CycT1 [307,308]. In infected cells Tat, and possibly Vpr, inhibit RNAi [309–311]. In resting, but not activated, CD4+ T-cells a cluster of five miRNAs (miR-28, miR-125b,

miR-150, miR-223, and miR-382) were found to be upregulated. They all target viral mRNAs for degradation; therefore, these miRNAs are contributing to latency maintenance [312]. However, further studies are required as results thus far are inconsistent [313–319].

The viral protein Nef is targeted by miR29a which interferes with HIV replication [300,320]. TRIM32 activates HIV-1 expression through the NF- $\kappa$ B pathway and is downregulated by miRNA-155 [321]. Tat-induced upregulation of miR34a and miR217 inhibits SIRT1 expression, which in turn results in high abundance of NF- $\kappa$ B, enhancing proviral transcription [322,323]. miRNA-182 has a positive effect on LTR activation by Tat [324]. miR-1236 restricts viral replication by repressing Vpr (HIV-1)-binding protein expression, VprBP [325].

HIV-1-derived miRNAs (vmiRNAs) were predicted *in silico* [326]. Applying deep sequencing technologies vmiRNAs were observed in cell line model systems of latency [327,328]. The TAR-derived miRNA-TAR5p and miR-TAR3p are asymmetrically processed and both repress LTR activity [329]. The *Nef*-derived miR-N367 inhibits viral promoter activity [330]. Nevertheless, relevance of vmiRNAs is debatable as no vmiRNAs were detected in PBMCs or macrophages of infected patients [331].

lncRNAs can modulate gene expression through different proposed mechanisms: (1) affecting mRNAs through sequence recognition, (2) recruiting proteins to DNA, (3) blocking host factors by assuming a secondary structure, (4) functioning as a scaffold for protein complexes. An anti-sense lncRNA of HIV-1 inhibits viral replication[146]. The non-coding repressor of NFAT (NRON) inhibits LTR activity in a NFAT-dependent manner [301].

#### 4.18. Stochastic gene expression

The current model of HIV latency proposes that resting memory CD4<sup>+</sup> T-cells are deprived of host factors that are necessary for viral expression. An alternative model proposes that expression is highly stochastic. Due to fluctuations in chromatin state and availability of the transcription factors, the latent and productive state co-exist [332]. In support, clonal lines (containing the same integration) showed binominal distributions of viral expression [333]. Transcriptional bursts of 2–10 mRNA transcripts were estimated to be the source of HIV-1 gene expression [334]. Tat-controlled positive feedback extends the expression reactivation [335]. The sensitivity to reactivation is also stochastic, as cells derived from patients remained latent during a first round of activation and were reactivatable in the next round of activation [83]. Moreover, molecules that increase gene expression fluctuations synergistically enhance HIV-1 reactivation [336].

## 5. HIV cure

Mechanistic insight into the complex nature of latent HIV-1 infection provides a rationale for eradication strategies. Therefore, identification of molecules that inhibit activity of repressors or potentiate HIV-1 activators alongside with immune system boosting are important objectives in eradication strategies.

### 5.1. Shocking the virus: screening for Latency Reversal Agents (LRAs)

The initial step of LRA discovery is screening drug libraries with cell-line-based models. Positive hits are evaluated further using primary-cell-based models as they better recapitulate the nature of latent reservoirs. If effective and not toxic, putative LRAs should undergo reactivation studies using primary cells derived from HIV-1-positive individuals that are on cART as well as toxicology studies in animal models, in case of novel molecules. It is advantageous to include molecules that are already approved drugs in such putative LRAs libraries, employing them into clinical practice would be time and resources effective. Moreover, in order to easily diffuse through cell membranes, ideal LRAs are small molecules, with molecular weight below 900 daltons, although clinical practice shows that most effective compounds do not exceed 500 daltons [337,338].

The first attempts to reactivate proviral DNA failed, due to the use of agents (e.g., IL-2 or a monoclonal antibody against CD3 receptor) which resulted in global T-cell activation. Indeed, viral p24 and plasma HIV-1 RNA levels increased, but the toxicity of such treatment left this approach useless [339–341]. Therefore, there is a need for more specific agents, which are able to reactivate proviral transcription without T-cell activation.

### 5.2. HDAC inhibitors (HDACis)

Histone deacetylase inhibitors (HDACis) are a very promising class of LRAs which include valporic acid (VPA), Vorinostat (SAHA), Romidepsin, Panobinostat, Givinostat, Droxinostat, or Entinostat. Some (Vorinostat (SAHA), Romidepsin, Panobinostat) are undergoing clinical trials [94,342–344].

The focus on HDACis is due to their ability to loosen up the compact chromatin structure at the latent proviral promoter. Inhibition of HDACs results in an increase of histone acetylation level by HATs. HDACs 1, 2, and 3 are of particular interest as they considerably contribute to HIV-1 repression [287]. Fortunately, HDACis are already used in clinical therapies, e.g., VPA is used in epilepsy and bipolar disorders, Vorinostat and Romidepsin are used to treat cutaneous T-cell lymphoma (CTCL) while Panabinostat is used in patients with multiple myeloma. In a very promising study by Archin et al., a single treatment with Vorinostat resulted in an increase in proviral RNA [345]. Unfortunately, the follow-up study with additional, multiple-dose rounds of treatment showed that increase on HIV-1 transcription is neither sustained nor elevated [346]. It is possible that other mechanisms maintaining latency compensate histone acetylation, in order to restrain proviral transcription. Alternatively such low concentrations of Vorinostat result in activation of pTEF-b instead of HDAC inhibition [347]. Since HDACs are involved in general regulation of gene expression; they have pleiotropic effects causing toxicities. Therefore, their use must be strictly controlled and monitored in order to provide maximal safety [348]. Nevertheless, HDACis are still under much interest. Especially, finding more specific HDAC inhibitors is very appealing, as current drugs are inhibiting a wide range of different HDACs, contributing to high toxicity [349].

### 5.3. BET inhibitors (BETi's)

Since BET proteins repress the HIV-1 promoter, it is worth to use their inhibitors in latency reversal strategies. Treatment with BET protein inhibitor JQ1 reactivates HIV-1 transcription in Tat-independent fashion [247]. Furthermore, BET inhibitor activity was positively tested in more relevant primary model system of latency [249]. Unfortunately, JQ-1 is not clinically available, due to its short half-life.

### 5.4. HMT inhibitors (HMTis)

Several histone methyltransferases (HMTs) such as EZH2, SUV39H1, and G9a interact with 5' LTR contributing to maintenance of latency by deposition of repressive methyl groups on nucleosomal proteins [292–295]. Moreover, EZH2 recruits additional repressive proteins such as HDACs and other HMTs [294]. Several inhibitors of these proteins were tested in cell lines or primary cells from HIV-1 positive patients. Among which, Chaetocin (SUV39H1 inhibitor) and BIX-01294 (G9a inhibitor) were most potent [292,350]. However, high toxicity, due to pleiotropic effects, makes them unsuitable for clinical practice. Therefore, identification of novel compounds that are able to inhibit the activity of HMTs is needed.

### 5.5. DNMT inhibitors (DNMTis)

Inhibition of DNA methyltransferases (DNMTs) with 5-aza-2' deoxycytidine (aza-CdR or Decitabine) leads to modest reactivation of latent HIV-1. This activity can be further enhanced with PKC agonists [351]. However, 5' LTR methylation in patients material remains controversial [352]. Thus, further investigation of provirus methylation *in vivo* is needed.

### 5.6. Toll-like receptors (TLRs) stimulation

TLRs recently gained more attention, as their agonists are strong reactivators of HIV-1 [353–357]. The main role of these receptors is to activate an immune response against bacterial or viral infections [358]. Stimulating TLRs (as adjuvants in immunization) as well as opportunistic bacterial infections elevate plasma HIV-RNA and improve immune function [359–363].

Vaccine adjuvant – CPG 7909 (TLR 9 agonist) is able to decrease plasma HIV-1 RNA via activation of HIV-specific CD8<sup>+</sup> T-cells in peripheral blood [359]. More recently, in SIV-positive rhesus monkeys undergoing cART were treated with GS-9620, a TLR7 agonist, reversible CD8 cytotoxic T-cells activation alongside with modest CD4 T-cell activation were observed. Moreover, elevated plasma viremia was observed as well as decrease in HIV-1 DNA in blood, colon, and lymph nodes. Interestingly, viral load returned back to undetectable levels when GS-9620 was no longer administered. More strikingly, when cART was stopped, GS-9620-treated monkeys had 0.5 log lower viral set-point than untreated, infected animals. Additionally, in cells isolated from HIV-positive individuals transcription of HIV-1 was observed. However, some variability between samples was noticed. Clinical trials with the use of this compound are planned [364,365].

### 5.7. Super elongation complex stimulation

Treatment of cell lines and cells isolated from aviremic patients on cART with hexamethylene bisacetamide (HMBA), an anticancer drug that transiently activates PI3K/Akt pathway, results in phosphorylation of HEXIM1. P-TEFb is subsequently released and interacts with RNAP II, resulting in latency reversal [366–368]. Moreover, HMBA provides CDK9 recruitment to the viral promoter by interaction with SP1, which enhances transcription from proviral DNA. Furthermore, Klichko et al. showed that treatment with HMBA resulted in a decrease of CD4 receptor expression without affecting transcription of CCR5 and CXCR4 co-receptors [369]. Moreover, HMBA does not trigger activation of T-cells. Studies on P-TEFb's role in HIV-1 latency indicate that this heterocomplex might be an interesting target for inclusion in “shock and kill” therapies.

### 5.8. PKC pathway activation

Another interesting approach is the use of molecules that are able to selectively activate the protein kinase C (PKC) pathway. PKC pathway agonists trigger nuclear localization of NF- $\kappa$ B, NFAT, and AP-1 transcription factors. Therefore, PKC agonists are one of the most potent activators of HIV-1 transcription. Currently, two PKC agonists are being scrutinized clinically: prostratin and bryostatin, due to their safety and specificity toward HIV-1 reactivation. The latter is a clinically available drug [370]. Moreover, these two compounds prevent *de novo* infections, as they downregulate viral receptor and co-receptors CD4, CCR5 and CXCR4 in PBMCs [371]. A rather controversial molecule that reactivates HIV-1 transcription via NF- $\kappa$ B pathway is arsenic trioxide ( $As_2O_3$ ). In the Jurkat model system of latency,  $As_2O_3$  activates NF- $\kappa$ B leading to HIV-1 replication. Moreover, it synergizes with prostratin, tumor necrosis factor alpha (TNF $\alpha$ ), and VPA [372]. Interestingly, arsenic is already used in clinical practice to treat acute promyelocytic leukemia (APL). Therefore, it would be interesting to test this compound in more relevant models of HIV-1 latency such as primary cells infected *ex vivo* and in cells derived from aviremic patients.

The use of PKC agonists raises concerns about their safety in a clinical setting. The protein kinase enzyme family consists of several isoenzymes that play important roles in signal transduction cascades [373]. As activation of latent HIV-1 is mediated via PKC $\alpha$  and PKC $\theta$ , the identification of more specific agonists of PKC $\alpha$  and PKC $\theta$  is needed. Alternatively, lowering the concentration of a specific agonists might decrease toxicity and contribute to latency reversal [374].

### 5.9. JNK/MAPK pathway activation

Studies employing mutagenesis of binding sites for activator protein-1 (AP-1) within the proviral genome showed that the AP-1 transcription factor is a crucial activator of proviral transcription, as proviruses with altered AP-1 binding sites were less prone to reactivation even if treated with a strong activator such as phorbol 12-myristate 13-acetate – PMA [191]. Furthermore, the latent pool of cells infected by virus with deletion in AP-1 sites was bigger, implicating that AP-1 is necessary for provirus transcription [192]. Heterodimeric protein AP-1

is formed upon phosphorylation of c-Jun N-terminal kinase (JNK) in JNK/MAPK pathway [193]. It is well established that activation of TLR signaling induces nuclear localization of NF- $\kappa$ B and AP-1 mediated via JNK pathway [194,196,376,377].

Virtual screening followed by validation of positive hits in cell line model systems for HIV-1 latency discovered 8-methoxy-6-methylquinolin-4-ol (MMQO) as a specific activator of the JNK-AP-1 pathway, which is able to reactivate HIV-1 from its latent state. Interestingly, MMQO inhibits IL-2 and TNF $\alpha$  expression, contributing to maintenance of resting state of CD4 $^{+}$  T-cells [378]. The recently synthesized panel of inhibitors of farnesyl transferase (FTase) are able to moderately reactivate HIV-1 transcription via JNK pathway. Interestingly, strong synergy with other LRAs, such as Vorinostat or TNF- $\alpha$ , was observed for these molecules in latency reversal [379,380].

### 5.10. Canonical Wnt signaling pathway activation

Recently, our group showed that treatment with Wnt3A/Rsp (natural stimulators of Wnt pathway) and lithium (inhibitor of Wnt repressor protein GSK3) leads to latency reversal in latent cell lines and enhances the latency reversal potential of HDAC inhibitors in CD4 $^{+}$  T primary cells obtained from patient volunteers when co-treated [381]. This observation shows a functional role for three LEF1 binding sites in the 5' LTR contains, which are downstream targets of the classical Wnt pathway [381,382]. It would be very interesting to find more potent and selective inducers of Wnt pathway, as lithium exhibits many pleiotropic, toxic effects [383,384].

### 5.11. Chromatin loosening

It was discovered by our group that a main player in the establishment and maintenance of latency is the BAF complex (SWI/SNF-A), which belongs to ATP-dependent chromatin remodelers' family. Interestingly, Dykhuizen et al. [378] screened a library of compounds that would be able to mimic BRG-1 knock out. In their study, they found 20 compounds that were transcriptionally mimicking BAF complex disruption. We showed that several of those molecules were able to decrease the frequency of latency establishment and reactivate HIV-1 in cell line and primary cells models of latency [386, in press]. Moreover, they synergize with other LRAs – SAHA and prostratin. Two most potent inhibitors – caffeic acid phenethyl ester (CAPE) and pyrimethamine (PYR) did not activate T-cells derived from healthy donors and cells obtained from aviremic patients. Moreover, PYR is a registered drug used in malaria treatment. Therefore, these inhibitors are promising molecules to include in eradication strategies.

### 5.12. Multifunctional LRAs

*In vitro* treatment with cocaine leads to increase in HIV- replication in PBMCs as well as increased viral load in mouse models of HIV infection [387–389]. Interestingly, *in vivo* infected primary CD4 $^{+}$  cocaine treatment resulted in downregulation of miR125-b expression, which led to enhanced replication of HIV-1 [314]. In primary human macrophages and myeloid



cell systems of latency, cocaine increased replication of HIV-1. Cocaine treatment activates NF- $\kappa$ B and leads to phosphorylation of mitogen- and stress-activated kinase 1 (MSK1). Furthermore, pMSK1 phosphorylates RELA (p65), a subunit of NF- $\kappa$ B promoting the interaction of NF- $\kappa$ B with p300 and recruitment of P-TEFb to the proviral 5' LTR [390]. Moreover, treatment with cocaine results in histone H3 phosphorylation, thus increasing accessibility of HIV-1 promoter for transcription factors [390]. Therefore, cocaine not only reverses latency via NF- $\kappa$ B pathway but also causes epigenetic changes on 5' LTR as well as blocks repressive miRNA.

Oral bacteria secrete short-chain fatty acids (SCFAs) including butyric acid, propionic acid, isovaleric acid, and isobutyric acid that are capable of HIV-1 and herpesviruses latency reversal [384,385]. Some of these molecules are known HDACis (e.g. Butyric acid) [393]. Moreover, SCFAs not only promotes histone acetylation, but also inhibit repressive histone formation and DNA methylation. Furthermore, they activate P-TEFb resulting in increased elongation of transcription from 5' LTR. [345,385,386].

### **5.13. Immune clearance of reactivated cells – “Kill”**

The majority of chronic patients are facing immune exhaustion, characterized by low cytokine secretion, smaller proliferative capacity, and low cytopathic potential of CD8+ T-cells [394,395]. Therefore, the first line of action would be reviving normal immune activity. Indeed, inhibition of programmed cell death protein 1 (PD-1) leads to restoration of immune functions in mouse models of HIV-1 infection [396]. However, these results were obtained in viremic animals. Nevertheless, an IgG4 antibody targeting PD-1 receptor is undergoing clinical trials to assess safety, immunotherapeutic activity, and the ability of treatment to reduce pool of latently infected cells [397].

In so-called “elite controllers”, CD8+ T-cells effectively restrain infection without intervention of cART, by killing CD4+ T-cells that are actively producing HIV-1 particles [398,399]. The immune system can be boosted by specific amplification of HIV-1-specific CD8+ T-cells. These observations again aroused the idea of developing a vaccine. Indeed, rhesus monkeys vaccinated with CMV vectors resulted in broad cellular immune response to SIV [400–402]. However, safety issues related to the use of such vectors remain to be elucidated. Another platform being investigated to increase immune response against HIV-1 are Ad26 vectors, as it was shown that vaccinated rhesus monkeys were protected against infection with SIV as well as viral loads were lowered after vaccination [403,404].

A very interesting group of immunoglobulins to include in eradication strategies are broadly neutralizing monoclonal antibodies (mAbs or bNAbs) isolated from chronically infected patients. New generations of bNAbs exert higher potency and wider range of activity against many HIV-1 subtypes. It was shown that a combination of bNAbs is potent enough to transiently suppress viremia in rhesus monkeys as well as to reduce the amount of HIV-1 DNA in the blood, lymph nodes, and gastrointestinal mucosa [403,405,406].

## 6. Future perspectives and challenges

A reservoir of latent HIV is the main obstacle in finding a functional and sterilizing cure. Several challenges need to be addressed in order to overcome this obstacle. Defining the latent reservoir is impeded by the rare occurrence of a latent infection in a high background of defective proviral integration. Although HIV prefers integration in or near transcriptionally active genes which leaves ample room for variation in chromatin environment and available host transcription factors. This puts considerable demands on LRAs. LRAs should be effective, yet specific, without being toxic. As LRAs act via pathways involved in distinct cellular processes, pleiotropic effects are to be expected. Furthermore, recent studies on material obtained from HIV-1-positive suppressed patients revealed that currently available LRAs are not strong enough to reactivate the whole pool of latent proviruses, even after multiple rounds of stimulation. One of the concerns arising from “shock and kill” therapy is whether putative LRAs are strong enough to drive virus production to a level at which the immune system will be able to recognize and destroy HIV-1-producing cells. Indeed, trials aiming at testing HDAC inhibitors are inconsistent in showing depletion of latently infected cells while showing increased proviral transcription [407–412]. A complementary strategy would be to use multiple LRAs in combination to broadly and potentially synergistically reactivate the diversely integrated latent proviruses. Synergism between LRAs was already identified, e.g., Vorinostat and Prostratin [84]. Therefore, the quest for identification and characterization of novel compounds which are able to reactivate HIV-1 transcription as well as identifying combinations of drugs that can synergize to reverse latency is needed. Currently, no cell model is able to recapitulate the complexities of latency *in vivo*. A better system that more closely resembles the *in vivo* situation would greatly aid the understanding of molecular mechanisms underlying latency and the screening of new LRA. Moreover, as HIV-1 persists in a silent state, it contributes to a low level of inflammation, which over time leads to immune exhaustion. Furthermore, depletion of cells harboring latent provirus requires antigen-specific CTLs stimulation [399]. Most likely successful eradication therapies will be based on the combination of LRAs coupled with boosting HIV-1-specific immune response. A “shock and kill” approach in combination with immune therapies provides hope for reversing HIV-1 infection.

## Author details

Michael D. Röling<sup>‡</sup>, Mateusz Stoszek<sup>‡</sup>, Tokameh Mahmoudi<sup>\*</sup>

<sup>\*</sup>Address all correspondence to: t.mahmoudi@erasmusmc.nl

Department of Biochemistry, Erasmus Medical Centre, Rotterdam, The Netherlands

<sup>‡</sup>These authors contributed equally to this work.



## References

- [1] Carpenter CCJ, Fischl MA, Hammer SM, Hirsch MS, Jacobsen DM, Katzenstein DA, et al. Antiretroviral Therapy for HIV Infection in 1998. *JAMA*. American Medical Association; 1998;280:78.
- [2] Dinoso JB, Kim SY, Wiegand AM, Palmer SE, Gange SJ, Cranmer L, et al. Treatment intensification does not reduce residual HIV-1 viremia in patients on highly active antiretroviral therapy. *Proc. Natl. Acad. Sci. U. S. A.* 2009;106:9403–8.
- [3] Davey RT, Bhat N, Yoder C, Chun TW, Metcalf JA, Dewar R, et al. HIV-1 and T cell dynamics after interruption of highly active antiretroviral therapy (HAART) in patients with a history of sustained viral suppression. *Proc. Natl. Acad. Sci. U. S. A.* 1999;96(26):15109–14.
- [4] (WHO) WHO. WHO | Data and statistics [Internet]. World Health Organization; 2014 [cited 2015 Jul 29]. Available from: <http://www.who.int/hiv/data/en/>
- [5] Pau AK, George JM. Antiretroviral Therapy. *Infect. Dis. Clin. North Am.* Elsevier Inc; 2014;28:371–402.
- [6] Siliciano JD, Kajdas J, Finzi D, Quinn TC, Chadwick K, Margolick JB, et al. Long-term follow-up studies confirm the stability of the latent reservoir for HIV-1 in resting CD4+ T cells. *Nat. Med.* 2003;9:727–8.
- [7] Centers for Disease Control and Prevention - CDC. CDC - HIV Cost-effectiveness - Ongoing Research - Prevention Research - HIV/AIDS [Internet]. 2015 [cited 2015 Jul 29]. Available from: <http://www.cdc.gov/hiv/prevention/ongoing/costeffectiveness/>
- [8] Deeks SG. HIV infection, inflammation, immunosenescence, and aging. *Annu. Rev. Med.* 2011;62:141–55.
- [9] Meyerhans A, Vartanian JP, Hultgren C, Plikat U, Karlsson A, Wang L, et al. Restriction and enhancement of human immunodeficiency virus type 1 replication by modulation of intracellular deoxynucleoside triphosphate pools. *J. Virol.* 1994;68:535–40.
- [10] Zhou Y, Zhang H, Siliciano JD, Siliciano RF. Kinetics of human immunodeficiency virus type 1 decay following entry into resting CD4+ T cells. *J. Virol.* 2005;79:2199–210.
- [11] Bukrinsky MI, Stanwick TL, Dempsey MP, Stevenson M. Quiescent T lymphocytes as an inducible virus reservoir in HIV-1 infection. *Science*. 1991;254:423–7.
- [12] Zack JA, Arrigo SJ, Weitsman SR, Go AS, Haislip A, Chen IS. HIV-1 entry into quiescent primary lymphocytes: molecular analysis reveals a labile, latent viral structure. *Cell*. 1990;61:213–22.
- [13] Ganesh L, Burstein E, Guha-Niyogi A, Louder MK, Mascola JR, Klomp LWJ, et al. The gene product Murr1 restricts HIV-1 replication in resting CD4+ lymphocytes. *Nature*. 2003;426:853–7.

- [14] Pan X, Baldauf H-M, Keppler OT, Fackler OT. Restrictions to HIV-1 replication in resting CD4<sup>+</sup> T lymphocytes. *Cell Res. Shanghai Institutes for Biological Sciences, Chinese Academy of Sciences*; 2013;23:876–85.
- [15] Donahue D a, Wainberg M a. Cellular and molecular mechanisms involved in the establishment of HIV-1 latency. *Retrovirology. Retrovirology*; 2013;10:11.
- [16] Bleul CC, Wu L, Hoxie JA, Springer TA, Mackay CR. The HIV coreceptors CXCR4 and CCR5 are differentially expressed and regulated on human T lymphocytes. *Proc. Natl. Acad. Sci. U. S. A.* 1997;94:1925–30.
- [17] Stevenson M, Stanwick TL, Dempsey MP, Lamonica CA. HIV-1 replication is controlled at the level of T cell activation and proviral integration. *EMBO J.* 1990;9:1551–60.
- [18] Wang W, Guo J, Yu D, Vorster PJ, Chen W, Wu Y. A dichotomy in cortical actin and chemotactic actin activity between human memory and naive T cells contributes to their differential susceptibility to HIV-1 infection. *J. Biol. Chem.* 2012;287:35455–69.
- [19] Spear M, Guo J, Wu Y. The trinity of the cortical actin in the initiation of HIV-1 infection. *Retrovirology.* 2012;9:45.
- [20] Siliciano RF, Greene WC. HIV latency. *Cold Spring Harb. Perspect. Med.* 2011;1:a007096.
- [21] Ho DD, Neumann AU, Perelson AS, Chen W, Leonard JM, Markowitz M. Rapid turnover of plasma virions and CD4 lymphocytes in HIV-1 infection. *Nature.* 1995;373:123–6.
- [22] Wei X, Ghosh SK, Taylor ME, Johnson VA, Emini EA, Deutsch P, et al. Viral dynamics in human immunodeficiency virus type 1 infection. *Nature.* 1995;373:117–22.
- [23] Chavez L, Calvanese V, Verdin E. HIV Latency Is Established Directly and Early in Both Resting and Activated Primary CD4 T Cells. *PLoS Pathog.* 2015;11:e1004955.
- [24] Eriksson S, Graf EH, Dahl V, Strain MC, Yukl SA, Lysenko ES, et al. Comparative analysis of measures of viral reservoirs in HIV-1 eradication studies. *PLoS Pathog. Public Library of Science*; 2013;9:e1003174.
- [25] Chun T, Carruth L, Finzi D, Shen X, DiGiuseppe J, Taylor H, et al. Quantification of latent tissue reservoirs and total body viral load in HIV-1 infection. *Lett. to Nat.* 1997;246:170–170.
- [26] Finzi D, Blankson J, Siliciano JD, Margolick JB, Chadwick K, Pierson T, et al. Latent infection of CD4<sup>+</sup> T cells provides a mechanism for lifelong persistence of HIV-1, even in patients on effective combination therapy. *Nat. Med.* 1999;5:512–7.
- [27] Strain MC, Günthard HF, Havlir D V, Ignacio CC, Smith DM, Leigh-Brown AJ, et al. Heterogeneous clearance rates of long-lived lymphocytes infected with HIV: intrinsic stability predicts lifelong persistence. *Proc. Natl. Acad. Sci. U. S. A.* 2003;100:4819–24.

- [28] Chomont N, El-Far M, Ancuta P, Trautmann L, Procopio F a, Yassine-Diab B, et al. HIV reservoir size and persistence are driven by T cell survival and homeostatic proliferation. *Nat. Med.* 2009;15:893–900.
- [29] Wightman F, Solomon A, Khoury G, Green JA, Gray L, Gorry PR, et al. Both CD31(+) and CD31<sup>-</sup> naive CD4(+) T cells are persistent HIV type 1-infected reservoirs in individuals receiving antiretroviral therapy. *J. Infect. Dis.* 2010;202:1738–48.
- [30] Costiniuk CT, Jenabian M-A. The lungs as anatomical reservoirs of HIV infection. *Rev. Med. Virol.* 2014;24:35–54.
- [31] Salemi M, Lamers SL, Yu S, de Oliveira T, Fitch WM, McGrath MS. Phylodynamic analysis of human immunodeficiency virus type 1 in distinct brain compartments provides a model for the neuropathogenesis of AIDS. *J. Virol.* 2005;79:11343–52.
- [32] garashi T, Brown CR, Endo Y, Buckler-White A, Plishka R, Bischofberger N, et al. Macrophage are the principal reservoir and sustain high virus loads in rhesus macaques after the depletion of CD4<sup>+</sup> T cells by a highly pathogenic simian immunodeficiency virus/HIV type 1 chimera (SHIV): Implications for HIV-1 infections of humans. *Proc. Natl. Acad. Sci. U. S. A.* 2001;98:658–63.
- [33] Gartner S, Markovits P, Markovitz DM, Kaplan MH, Gallo RC, Popovic M. The role of mononuclear phagocytes in HTLV-III/LAV infection. *Science.* 1986;233:215–9.
- [34] Van Lint C, Bouchat S, Marcello A. HIV-1 transcription and latency: an update. *Retrovirology.* 2013;10:67.
- [35] Eisele E, Siliciano RF. Redefining the viral reservoirs that prevent HIV-1 eradication. *Immunity.* Elsevier Inc.; 2012;37:377–88.
- [36] Tyagi M, Bukrinsky M. Human immunodeficiency virus (HIV) latency: the major hurdle in HIV eradication. *Mol. Med.* 2012;18:1096–108.
- [37] Schnell G, Price RW, Swanstrom R, Spudich S. Compartmentalization and clonal amplification of HIV-1 variants in the cerebrospinal fluid during primary infection. *J. Virol.* 2010;84:2395–407.
- [38] Churchill MJ, Gorrry PR, Cowley D, Lal L, Sonza S, Purcell DFJ, et al. Use of laser capture microdissection to detect integrated HIV-1 DNA in macrophages and astrocytes from autopsy brain tissues. *J. Neurovirol.* 2006;12:146–52.
- [39] Wiley CA, Schrier RD, Nelson JA, Lampert PW, Oldstone MB. Cellular localization of human immunodeficiency virus infection within the brains of acquired immune deficiency syndrome patients. *Proc. Natl. Acad. Sci. U. S. A.* 1986;83:7089–93.
- [40] Yukl SA, Gianella S, Sinclair E, Epling L, Li Q, Duan L, et al. Differences in HIV burden and immune activation within the gut of HIV-positive patients receiving suppressive antiretroviral therapy. *J. Infect. Dis.* 2010;202:1553–61.

- [41] Chun T-W, Nickle DC, Justement JS, Meyers JH, Roby G, Hallahan CW, et al. Persistence of HIV in gut-associated lymphoid tissue despite long-term antiretroviral therapy. *J. Infect. Dis.* 2008;197:714–20.
- [42] Lerner P, Guadalupe M, Donovan R, Hung J, Flamm J, Prindiville T, et al. The gut mucosal viral reservoir in HIV-infected patients is not the major source of rebound plasma viremia following interruption of highly active antiretroviral therapy. *J. Virol.* 2011;85:4772–82.
- [43] Yilmaz A, Verhofstede C, D’Avolio A, Watson V, Hagberg L, Fuchs D, et al. Treatment intensification has no effect on the HIV-1 central nervous system infection in patients on suppressive antiretroviral therapy. *J. Acquir. Immune Defic. Syndr.* 2010;55:590–6.
- [44] Symons J, Vandekerckhove L, Hütter G, Wensing AMJ, Van Ham PM, Deeks SG, et al. Dependence on the CCR5 coreceptor for viral replication explains the lack of rebound of CXCR4-predicted HIV variants in the Berlin patient. *Clin. Infect. Dis.* 2014;59:596–600.
- [45] Hütter G, Nowak D, Mossner M, Ganepola S, Müssig A, Allers K, et al. Long-term control of HIV by CCR5 Delta32/Delta32 stem-cell transplantation. *N. Engl. J. Med.* 2009;360:692–8.
- [46] Deng H, Liu R, Ellmeier W, Choe S, Unutmaz D, Burkhart M, et al. Identification of a major co-receptor for primary isolates of HIV-1. *Nature.* 1996;381:661–6.
- [47] Dragic T, Litwin V, Allaway GP, Martin SR, Huang Y, Nagashima KA, et al. HIV-1 entry into CD4+ cells is mediated by the chemokine receptor CC-CKR-5. *Nature.* 1996;381:667–73.
- [48] Libert F, Cochaux P, Beckman G, Samson M, Aksenova M, Cao A, et al. The *deltaccr5* mutation conferring protection against HIV-1 in Caucasian populations has a single and recent origin in Northeastern Europe. *Hum. Mol. Genet.* 1998;7:399–406.
- [49] Yukl SA, Boritz E, Busch M, Bentsen C, Chun T-W, Douek D, et al. Challenges in detecting HIV persistence during potentially curative interventions: a study of the Berlin patient. *PLoS Pathog. Public Library of Science*; 2013;9:e1003347.
- [50] Martinson JJ, Chapman NH, Rees DC, Liu YT, Clegg JB. Global distribution of the CCR5 gene 32-basepair deletion. *Nat. Genet.* 1997;16:100–3.
- [51] Sabeti PC, Walsh E, Schaffner SF, Varilly P, Fry B, Hutcheson HB, et al. The case for selection at CCR5-Delta32. *PLoS Biol. Public Library of Science*; 2005;3:e378.
- [52] Yukl SA, Boritz E, Busch M, Bentsen C, Chun T-W, Douek D, et al. Challenges in detecting HIV persistence during potentially curative interventions: a study of the Berlin patient. *PLoS Pathog. Public Library of Science*; 2013;9:e1003347.

- [53] Henrich TJ, Hu Z, Li JZ, Sciaranghella G, Busch MP, Keating SM, et al. Long-term reduction in peripheral blood HIV type 1 reservoirs following reduced-intensity conditioning allogeneic stem cell transplantation. *J. Infect. Dis.* 2013;207:1694–702.
- [54] Passaes CP, Sáez-Cirión A. HIV cure research: advances and prospects. *Virology.* 2014;454-455:340–52.
- [55] Persaud D, Gay H, Ziemniak C, Chen YH, Piatak M, Chun T-W, et al. Absence of detectable HIV-1 viremia after treatment cessation in an infant. *N. Engl. J. Med.* 2013;369:1828–35.
- [56] Huang J, Burke PS, Cung TDH, Pereyra F, Toth I, Walker BD, et al. Leukocyte immunoglobulin-like receptors maintain unique antigen-presenting properties of circulating myeloid dendritic cells in HIV-1-infected elite controllers. *J. Virol.* 2010;84:9463–71.
- [57] Lewin SR, Rouzioux C. HIV cure and eradication: how will we get from the laboratory to effective clinical trials? *AIDS.* 2011;25:885–97.
- [58] Autran B, Descours B, Avettand-Fenoel V, Rouzioux C. Elite controllers as a model of functional cure. *Curr. Opin. HIV AIDS.* 2011;6:181–7.
- [59] Okulicz JF, Lambotte O. Epidemiology and clinical characteristics of elite controllers. *Curr. Opin. HIV AIDS.* 2011;6:163–8.
- [60] Blankson JN. Control of HIV-1 replication in elite suppressors. *Discov. Med.* 2010;9:261–6.
- [61] Shacklett BL. Understanding the ‘lucky few’: the conundrum of HIV-exposed, seronegative individuals. *Curr. HIV/AIDS Rep.* 2006;3:26–31.
- [62] Sáez-Cirión A, Bacchus C, Hocqueloux L, Avettand-Fenoel V, Girault I, Lecuroux C, et al. Post-treatment HIV-1 controllers with a long-term virological remission after the interruption of early initiated antiretroviral therapy ANRS VISCONTI Study. *PLoS Pathog. Public Library of Science;* 2013;9:e1003211.
- [63] Frange P, Faye A, Avettand-Fenoel V, Bellaton E, Deschamps D, Angin M, et al. HIV-1 virological remission for more than 11 years after interruption of early initiated antiretroviral therapy in a perinatally-infected child. 8th Int. AIDS Soc. Conf. HIV Pathog. Treat. Prev. (IAS 2015) Vancouver. 2015. p. MOAA0105LB.
- [64] Ru R, Yao Y, Yu S, Yin B, Xu W, Zhao S, et al. Targeted genome engineering in human induced pluripotent stem cells by penetrating TALENs. *Cell Regeneration;* 2013;2(1):5.
- [65] Mandal PK, Ferreira LMR, Collins R, Meissner TB, Boutwell CL, Friesen M, et al. Efficient Ablation of Genes in Human Hematopoietic Stem and Effector Cells using CRISPR/Cas9. *Cell Stem Cell. Elsevier Inc.;* 2014;15:643–52.

- [66] Tebas P, Stein D, Tang WW, Frank I, Wang SQ, Lee G, et al. Gene Editing of CCR5 in Autologous CD4 T Cells of Persons Infected with HIV. *N. Engl. J. Med.* 2014;370:901–10.
- [67] Allers K, Schneider T. CCR5 $\Delta$ 32 mutation and HIV infection: basis for curative HIV therapy. *Curr. Opin. Virol.* 2015;14:24–9.
- [68] Vrans CLJ, Out R, van Santbrink P, van der Zee A, Mahmoudi T, Groenendijk M, et al. Znf202 affects high density lipoprotein cholesterol levels and promotes hepatosteatosis in hyperlipidemic mice. *PLoS One.* 2013;8:e57492.
- [69] Huelsmann PM, Hofmann AD, Knoepfel SA, Popp J, Rauch P, Di Giallonardo F, et al. A suicide gene approach using the human pro-apoptotic protein tBid inhibits HIV-1 replication. *BMC Biotechnol.* 2011;11:4.
- [70] Hamer DH. Can HIV be Cured? Mechanisms of HIV persistence and strategies to combat it. *Curr. HIV Res.* 2004;2:99–111.
- [71] Deeks SG, Autran B, Berkhout B, Benkirane M, Cairns S, Chomont N, et al. Towards an HIV cure: a global scientific strategy. *Nat. Rev. Immunol.* Nature Publishing Group; 2012;12:607–14.
- [72] Barouch DH, Deeks SG. immunologic strategies for HIV-1 remission and eradication. *Science* (80-.). 2014;345:169–74.
- [73] Archin NM, Margolis DM. Emerging strategies to deplete the HIV reservoir. *Curr. Opin. Infect. Dis.* 2014;27:29–35.
- [74] Folks TM, Clouse KA, Justement J, Rabson A, Duh E, Kehrl JH, et al. Tumor necrosis factor alpha induces expression of human immunodeficiency virus in a chronically infected T-cell clone. *Proc. Natl. Acad. Sci. U. S. A.* 1989;86:2365–8.
- [75] Folks TM, Justement J, Kinter a, Dinarello C a, Fauci a S. Cytokine-induced expression of HIV-1 in a chronically infected promonocyte cell line. *Science.* 1987;238:800–2.
- [76] Emiliani S, Van Lint C, Fischle W, Paras P, Ott M, Brady J, et al. A point mutation in the HIV-1 Tat responsive element is associated with postintegration latency. *Proc. Natl. Acad. Sci. U. S. A.* 1996;93:6377–81.
- [77] Emiliani S, Fischle W, Ott M, Van Lint C, Amella CA, Verdin E. Mutations in the tat Gene Are Responsible for Human Immunodeficiency Virus Type 1 Postintegration Latency in the U1 Cell Line. *J. Virol.* 1998;72:1666–70.
- [78] Jordan A, Bisgrove D, Verdin E. HIV reproducibly establishes a latent infection after acute infection of T cells in vitro. *EMBO.* 2003;22:1868–77.
- [79] Folks TM, Justement J, Kinter A, Dinarello CA, Fauci AS. Cytokine-induced expression of HIV-1 in a chronically infected promonocyte cell line. *Science.* 1987;238:800–2.

- [80] Weiss A, Wiskocil RL, Stobo JD. The role of T3 surface molecules in the activation of human T cells: a two-stimulus requirement for IL 2 production reflects events occurring at a pre-translational level. *J. Immunol.* 1984;133:123–8.
- [81] Schneider U, Schwenk HU, Bornkamm G. Characterization of EBV-genome negative ‘null’ and ‘T’ cell lines derived from children with acute lymphoblastic leukemia and leukemic transformed non-Hodgkin lymphoma. *Int. J. Cancer.* 1977;19:621–6.
- [82] Schröder ARW, Shinn P, Chen H, Berry C, Ecker JR, Bushman F. HIV-1 integration in the human genome favors active genes and local hotspots. *Cell.* 2002;110:521–9.
- [83] Ho Y-C, Shan L, Hosmane NN, Wang J, Laskey SB, Rosenbloom DIS, et al. Replication-competent noninduced proviruses in the latent reservoir increase barrier to HIV-1 cure. *Cell*; 2013;155:540–51.
- [84] Spina C a, Anderson J, Archin NM, Bosque A, Chan J, Famiglietti M, et al. An in-depth comparison of latent HIV-1 reactivation in multiple cell model systems and resting CD4+ T cells from aviremic patients. *PLoS Pathog.* 2013;9:e1003834.
- [85] Sahu GK, Lee K, Ji J, Braciale V, Baron S, Cloyd MW. A novel in vitro system to generate and study latently HIV-infected long-lived normal CD4+ T-lymphocytes. *Virology.* 2006;355:127–37.
- [86] Bosque A, Planelles V. Induction of HIV-1 latency and reactivation in primary memory CD4+ T cells. *Blood.* 2009;113:58–65.
- [87] Yang H, Xing S, Shan L, Connell KO, Dinoso J, Shen A, et al. Small-molecule screening using a human primary cell model of HIV latency identifies compounds that reverse latency without cellular activation. 2009;119(11):3473-86..
- [88] Marini A, Harper JM, Romerio F. An in vitro system to model the establishment and reactivation of HIV-1 latency. *J. Immunol.* 2008;181:7713–20.
- [89] Chun TW, Finzi D, Margolick J, Chadwick K, Schwartz D, Siliciano RF. In vivo fate of HIV-1-infected T cells: quantitative analysis of the transition to stable latency. *Nat. Med.* 1995;1:1284–90.
- [90] Pierson T, McArthur J, Siliciano RF. Reservoirs for HIV-1: mechanisms for viral persistence in the presence of antiviral immune responses and antiretroviral therapy. *Annu. Rev. Immunol.* 2000;18:665–708.
- [91] Finzi D, Hermankova M, Pierson T, Carruth LM, Buck C, Chaisson RE, et al. Identification of a reservoir for HIV-1 in patients on highly active antiretroviral therapy. *Science.* 1997;278:1295–300.
- [92] Swiggard WJ, Baytop C, Yu JJ, Li C, Schretzenmair R, Doherty UO, et al. Human Immunodeficiency Virus Type 1 Can Establish Latent Infection in Resting CD4 + T Cells in the Absence of Activating Stimuli. *J.....* 2005;79:14179–88.



- [93] De Crignis E, Mahmoudi T. HIV eradication: combinatorial approaches to activate latent viruses. *Viruses*. 2014;6:4581–608.
- [94] Archin NM, Sung JM, Garrido C, Soriano-Sarabia N, Margolis DM. Eradicating HIV-1 infection: seeking to clear a persistent pathogen. *Nat. Rev. Microbiol.* Nature Publishing Group; 2014;12:750–64.
- [95] Denton PW, Olesen R, Choudhary SK, Archin NM, Wahl a., Swanson MD, et al. Generation of HIV Latency in Humanized BLT Mice. *J. Virol.* 2012;86:630–4.
- [96] Melkus MW, Estes JD, Padgett-Thomas A, Gatlin J, Denton PW, Othieno F a, et al. Humanized mice mount specific adaptive and innate immune responses to EBV and TSST-1. *Nat. Med.* 2006;12:1316–22.
- [97] Denton PW, Estes JD, Sun Z, Othieno F a., Wei BL, Wege AK, et al. Antiretroviral pre-exposure prophylaxis prevents vaginal transmission of HIV-1 in humanized BLT mice. *PLoS Med.* 2008;5:0079–89.
- [98] North TW, Higgins J, Deere JD, Hayes TL, Villalobos A, Adamson L, et al. Viral sanctuaries during highly active antiretroviral therapy in a nonhuman primate model for AIDS. *J. Virol.* 2010;84:2913–22.
- [99] Van Rompay KK a. Evaluation of antiretrovirals in animal models of HIV infection. *Antiviral Res.* 2010;85:159–75.
- [100] Hatziioannou T, Ambrose Z, Chung NPY, Piatak M, Yuan F, Trubey CM, et al. A macaque model of HIV-1 infection. *Proc. Natl. Acad. Sci. U. S. A.* 2009;106:4425–9.
- [101] Krebs FC, Hogan TH, Quiterio S, Gartner S, Wigdahl B. Lentiviral LTR-directed Expression, Sequence Variation, and Disease Pathogenesis Reviews. In: CL K, B F, B H, B K, F M, PA M, et al., editors. *HIV Seq. Compend.* 2001. Los Alamos: Theoretical Biology and Biophysics Group, Los Alamos National Laboratory: Los Alamos, NM; 2001. p. 1–42.
- [102] Bruner KM, Hosmane NN, Siliciano RF. Towards an HIV-1 cure: measuring the latent reservoir. *Trends Microbiol.* Elsevier Ltd; 2015;23:192–203.
- [103] Hindson BJ, Ness KD, Masquelier D a., Belgrader P, Heredia NJ, Makarewicz AJ, et al. High-throughput droplet digital PCR system for absolute quantitation of DNA copy number. *Anal. Chem.* 2011;83:8604–10.
- [104] Procopio FA, Fromentin R, Kulpa DA, Brehm JH, Bebin A-G, Strain MC, et al. A Novel Assay to Measure the Magnitude of the Inducible Viral Reservoir in HIV-infected Individuals. *EBioMedicine.* Elsevier; 2015;
- [105] Descours B, Cribier A, Chable-Bessia C, Ayinde D, Rice G, Crow Y, et al. SAMHD1 restricts HIV-1 reverse transcription in quiescent CD4+ T-cells. *Retrovirology.* Retrovirology; 2012;9:87.



- [106] Goldstone DC, Ennis-Adeniran V, Hedden JJ, Groom HCT, Rice GI, Christodoulou E, et al. HIV-1 restriction factor SAMHD1 is a deoxynucleoside triphosphate triphosphohydrolase. *Nature*. Nature Publishing Group; 2011;480:379–82.
- [107] Kim B, Nguyen L a., Daddacha W, Hollenbaugh J a. Tight interplay among SAMHD1 protein level, cellular dNTP levels, and HIV-1 proviral DNA synthesis kinetics in human primary monocyte-derived macrophages. *J. Biol. Chem.* 2012;287:21570–4.
- [108] Lahouassa H, Daddacha W, Hofmann H, Ayinde D, Logue EC, Dragin L, et al. SAMHD1 restricts the replication of human immunodeficiency virus type 1 by depleting the intracellular pool of deoxynucleoside triphosphates. *Nat. Immunol.* 2012;13:621–621.
- [109] Ryoo J, Choi J, Oh C, Kim S, Seo M, Diaz-griffero F, et al. The ribonuclease activity of SAMHD1 is required for HIV-1 restriction. *Nat. Med.* 2014;20:936–41.
- [110] Choi J, Ryoo J, Oh C, Hwang S, Ahn K. SAMHD1 specifically restricts retroviruses through its RNase activity. *Retrovirology*. BioMed Central; 2015;12:1–12.
- [111] Hofmann H, Logue EC, Bloch N, Daddacha W, Polsky SB, Schultz ML, et al. The Vpx lentiviral accessory protein targets SAMHD1 for degradation in the nucleus. *J. Virol.* 2012;86:12552–60.
- [112] Sheehy AM, Gaddis NC, Choi JD, Malim MH. Isolation of a human gene that inhibits HIV-1 infection and is suppressed by the viral Vif protein. *Nature*. 2002;418:646–50.
- [113] Schrijvers R, De Rijck J, Demeulemeester J, Adachi N, Vets S, Ronen K, et al. LEDGF/p75-independent HIV-1 replication demonstrates a role for HRP-2 and remains sensitive to inhibition by LEDGINs. *PLoS Pathog.* 2012;8.
- [114] Ciuffi A, Llano M, Poeschla E, Hoffmann C, Leipzig J, Shinn P, et al. A role for LEDGF/p75 in targeting HIV DNA integration. *Nat. Med.* 2005;11:1287–9.
- [115] Shun MC, Raghavendra NK, Vandegraaff N, Daigle JE, Hughes S, Kellam P, et al. LEDGF/p75 functions downstream from preintegration complex formation to effect gene-specific HIV-1 integration. *Genes Dev.* 2007;21:1767–78.
- [116] Engelman A, Cherepanov P. The lentiviral integrase binding protein LEDGF/p75 and HIV-1 replication. *PLoS Pathog.* 2008;4.
- [117] Wang H, Jurado KA, Wu X, Shun M-C, Li X, Ferris AL, et al. HRP2 determines the efficiency and specificity of HIV-1 integration in LEDGF/p75 knockout cells but does not contribute to the antiviral activity of a potent LEDGF/p75-binding site integrase inhibitor. *Nucleic Acids Res.* 2012;40:11518–30.
- [118] Lesbats P, Botbol Y, Chevereau G, Vaillant C, Calmels C, Arneodo A, et al. Functional coupling between HIV-1 integrase and the SWI/SNF chromatin remodeling complex for efficient in vitro integration into stable nucleosomes. *PLoS Pathog.* 2011;7:e1001280.

- [119] Maroun M, Delelis O, Coadou G, Bader T, Ségéral E, Mbemba G, et al. Inhibition of early steps of HIV-1 replication by SNF5/Ini1. *J. Biol. Chem.* 2006;281:22736–43.
- [120] Turelli P, Doucas V, Craig E, Mangeat B, Klages N, Evans R, et al. Cytoplasmic recruitment of INI1 and PML on incoming HIV preintegration complexes: Interference with early steps of viral replication. *Mol. Cell.* 2001;7:1245–54.
- [121] Ocwieja KE, Brady TL, Ronen K, Huegel A, Roth SL, Schaller T, et al. HIV integration targeting: A pathway involving transportin-3 and the nuclear pore protein RanBP2. *PLoS Pathog.* 2011;7:19–21.
- [122] Pierson TC, Kieffer TL, Ruff CT, Buck C, Gange SJ, Siliciano RF. Intrinsic Stability of Episomal Circles Formed during Human Immunodeficiency Virus Type 1 Replication. *J. Virol.* 2002;76:4138–44.
- [123] Pierson TC, Zhou Y, Kieffer TL, Christian T, Buck C, Siliciano RF, et al. Molecular Characterization of Preintegration Latency in Human Immunodeficiency Virus Type 1 Infection. *J. Virol.* 2002;76:8518–31.
- [124] Zamborlini A, Lehmann-Che J, Clave E, Giron M-L, Tobaly-Tapiero J, Roingeard P, et al. Centrosomal pre-integration latency of HIV-1 in quiescent cells. *Retrovirology.* 2007;4:63.
- [125] Trinité B, Ohlson EC, Voznesensky I, Rana SP, Chan CN, Mahajan S, et al. An HIV-1 replication pathway utilizing reverse transcription products that fail to integrate. *J. Virol.* 2013;87:12701–20.
- [126] Han Y, Lassen K, Monie D, Ahmad R, Shimoji S, Liu X, et al. Resting CD4 + T Cells from Human Immunodeficiency Virus Type 1 (HIV-1) -Infected Individuals Carry Integrated HIV-1 Genomes within Actively Transcribed Host Genes. *J. Virol.* 2004;78:6122.
- [127] Liu H, Dow EC, Arora R, Kimata JT, Bull LM, Arduino RC, et al. Integration of human immunodeficiency virus type 1 in untreated infection occurs preferentially within genes. *J. Virol.* 2006;80:7765–8.
- [128] Lewinski MK, Bisgrove D, Shinn P, Chen H, Hoffmann C, Hannenhalli S, et al. Genome-Wide Analysis of Chromosomal Features Repressing Human Immunodeficiency Virus Transcription. *J Virol.* 2005;79:6610–9.
- [129] Marini B, Kertesz-farkas A, Ali H, Lucic B, Lisek K, Manganaro L, et al. Nuclear architecture dictates HIV-1 integration site selection. *Nature.* 2015;521(7551):227-31
- [130] Wang GP, Ciuffi A, Leipzig J, Berry CC, Bushman FD. HIV integration site selection: analysis by massively parallel pyrosequencing reveals association with epigenetic modifications. *Genome Res.* 2007;17:1186–94.

- [131] Brady T, Agosto LM, Malani N, Berry CC, O'Doherty U, Bushman F. HIV integration site distributions in resting and activated CD4+ T cells infected in culture. *AIDS*. 2009;23:1461–71.
- [132] Albanese A, Arosio D, Terreni M, Cereseto A. HIV-1 pre-integration complexes selectively target decondensed chromatin in the nuclear periphery. *PLoS One*. 2008; 3(6): e2413.
- [133] Dieudonné M, Maiuri P, Biancotto C, Knezevich A, Kula A, Lusic M, et al. Transcriptional competence of the integrated HIV-1 provirus at the nuclear periphery. *EMBO J*. 2009;28:2231–43.
- [134] Cohn LB, Silva IT, Oliveira TY, Rosales RA, Parrish EH, Learn GH, et al. HIV-1 Integration Landscape during Latent and Active Infection. *Cell*. Elsevier Inc.; 2015;160:420–32.
- [135] Lusic M, Marini B, Ali H, Lucic B, Luzzati R, Giacca M. Proximity to PML nuclear bodies regulates HIV-1 latency in CD4+ T cells. *Cell Host Microbe*. Elsevier Inc.; 2013;13:665–77.
- [136] Gallastegui E, Millán-Zambrano G, Terme J-M, Chávez S, Jordan A. Chromatin reassembly factors are involved in transcriptional interference promoting HIV latency. *J. Virol*. 2011;85:3187–202.
- [137] Lenasi T, Contreras X, Peterlin BM. Transcriptional interference antagonizes proviral gene expression to promote HIV latency. *Cell Host Microbe*. 2008;4:123–33.
- [138] Han Y, Lin YB, An W, Xu J, Yang H-C, O'Connell K, et al. Orientation-dependent regulation of integrated HIV-1 expression by host gene transcriptional readthrough. *Cell Host Microbe*. 2008;4:134–46.
- [139] Shan L, Yang H-C, Rabi SA, Bravo HC, Shroff NS, Irizarry R a, et al. Influence of host gene transcription level and orientation on HIV-1 latency in a primary-cell model. *J. Virol*. 2011;85:5384–93.
- [140] De Marco A, Biancotto C, Knezevich A, Maiuri P, Vardabasso C, Marcello A. Intragenic transcriptional cis-activation of the human immunodeficiency virus 1 does not result in allele-specific inhibition of the endogenous gene. *Retrovirology*. 2008;5:98.
- [141] Klaver B, Berkhout B. Comparison of 5' and 3' long terminal repeat promoter function in human immunodeficiency virus. *J. Virol*. 1994;68:3830–40.
- [142] Cullen BR, Lomedico PT, Ju G. Transcriptional interference in avian retroviruses—implications for the promoter insertion model of leukaemogenesis. *Nature*. 1984;307:241–5.
- [143] Michael NL, Vahey MT, d'Arcy L, Ehrenberg PK, Mosca JD, Rappaport J, et al. Negative-strand RNA transcripts are produced in human immunodeficiency virus type 1-

- infected cells and patients by a novel promoter downregulated by Tat. *J. Virol.* 1994;68:979–87.
- [144] Landry S, Halin M, Lefort S, Audet B, Vaquero C, Mesnard J-M, et al. Detection, characterization and regulation of antisense transcripts in HIV-1. *Retrovirology.* 2007;4:71.
- [145] Ludwig LB, Ambrus JL, Krawczyk K a, Sharma S, Brooks S, Hsiao C-B, et al. Human Immunodeficiency Virus-Type 1 LTR DNA contains an intrinsic gene producing antisense RNA and protein products. *Retrovirology.* 2006;3:80.
- [146] Kobayashi-Ishihara M, Yamagishi M, Hara T, Matsuda Y, Takahashi R, Miyake A, et al. HIV-1-encoded antisense RNA suppresses viral replication for a prolonged period. *Retrovirology.* 2012;9:38.
- [147] Saayman S, Ackley A, Turner A-MW, Famiglietti M, Bosque A, Clemson M, et al. An HIV-encoded antisense long noncoding RNA epigenetically regulates viral transcription. *Mol. Ther.* 2014;22:1164–75.
- [148] Karn J, Stoltzfus CM. Regulation of HIV-1 Gene Expression. *Cold Spring Harb. Perspect. Med.* 2012;1–17.
- [149] Peeters a, Lambert PF, Deacon NJ. A fourth Sp1 site in the human immunodeficiency virus type 1 long terminal repeat is essential for negative-sense transcription. *J. Virol.* 1996;70:6665–72.
- [150] Bentley K, Deacon N, Sonza S, Zeichner S, Churchill M. Mutational analysis of the HIV-1 LTR as a promoter of negative sense transcription. *Arch. Virol.* 2004;149:2277–94.
- [151] Gaynor Richard. Cellular transcription factors involved in the regulation of HIV-1 gene expression. *Aids.* 1992. p. 347–63.
- [152] Rosen C a, Sodroski JG, Haseltine W a. Location of cis-acting regulatory sequences in the human T-cell leukemia virus type I long terminal repeat. *Proc. Natl. Acad. Sci. U. S. A.* 1985;82:6502–6.
- [153] Siekevitz M, Josephs SF, Dukovich M, Peffer N, Wong-Staal F, Greene WC. Activation of the HIV-1 LTR by T cell mitogens and the trans-activator protein of HTLV-I. *Science.* 1987;238:1575–8.
- [154] Pereira LA, Bentley K, Peeters A, Churchill MJ, Deacon NJ. SURVEY AND SUMMARY A compilation of cellular transcription factor interactions with the HIV-1 LTR promoter. 2000;28:663–8.
- [155] Kinoshita S, Su L, Amano M, Timmerman L a, Kaneshima H, Nolan GP. The T cell activation factor NF-ATc positively regulates HIV-1 replication and gene expression in T cells. *Immunity.* 1997;6:235–44.

- [156] Selliah N, Zhang M, DeSimone D, Kim H, Brunner M, Ittenbach RF, et al. The c-cytokine regulated transcription factor, STAT5, increases HIV-1 production in primary CD4 T cells. *Virology*. 2006;344:283–91.
- [157] Nabel G, Baltimore D. An inducible transcription factor activates expression of human immunodeficiency virus in T cells. *Nature*. 1987;326:711–3.
- [158] Gerritsen ME, Williams a J, Neish a S, Moore S, Shi Y, Collins T. CREB-binding protein/p300 are transcriptional coactivators of p65. *Proc. Natl. Acad. Sci. U. S. A.* 1997;94:2927–32.
- [159] Tesmer VM, Rajadhyaksha a, Babin J, Bina M. NF-IL6-mediated transcriptional activation of the long terminal repeat of the human immunodeficiency virus type 1. *Proc. Natl. Acad. Sci.* 1993;90:7298–302.
- [160] Henderson a J, Zou X, Calame KL. C/EBP proteins activate transcription from the human immunodeficiency virus type 1 long terminal repeat in macrophages/monocytes. *J. Virol.* 1995;69:5337–44.
- [161] Yang X, Chen Y, Gabuzda D. ERK MAP kinase links cytokine signals to activation of latent HIV-1 infection by stimulating a cooperative interaction of AP-1 and NF- $\kappa$ B. *J. Biol. Chem.* 1999;274:27981–8.
- [162] Krebs FC, Mehrens D, Pomeroy S, Goodenow MM, Wigdahl B. Human immunodeficiency virus type 1 long terminal repeat quasispecies differ in basal transcription and nuclear factor recruitment in human glial cells and lymphocytes. *J. Biomed. Sci.* 1998;5:31–44.
- [163] Coiras M, López-Huertas MR, Rullas J, Mittelbrunn M, Alcamí J. Basal shuttle of NF- $\kappa$ B/I  $\kappa$ B  $\alpha$  in resting T lymphocytes regulates HIV-1 LTR dependent expression. *Retrovirology*. 2007;4:56.
- [164] Colin L, Van Lint C. Molecular control of HIV-1 postintegration latency: implications for the development of new therapeutic strategies. *Retrovirology*. 2009;6:111.
- [165] Cron RQ, Bartz SR, Clausell A, Bort SJ, Klebanoff SJ, Lewis DB. NFAT1 enhances HIV-1 gene expression in primary human CD4 T cells. *Clin. Immunol.* 2000;94:179–91.
- [166] McKernan LN, Momjian D, Kulkosky J. Protein Kinase C: One Pathway towards the Eradication of Latent HIV-1 Reservoirs. *Adv. Virol.* 2012;2012:805347.
- [167] Mahmoudi T. The BAF complex and HIV latency. *Transcription*. 2012;3:171–6.
- [168] West MJ, Lowe AD, Karn J. Activation of Human Immunodeficiency Virus Transcription in T Cells Revisited: NF- $\kappa$ B p65 Stimulates Transcriptional Elongation Activation of Human Immunodeficiency Virus Transcription in T Cells Revisited: NF- $\kappa$ B p65 Stimulates Transcriptional Elonga. *J. Virol.* 2001;75:8524–37.

- [169] Li X, Josef J, Marasco W a. Hiv-1 Tat can substantially enhance the capacity of NIK to induce IkappaB degradation. *Biochem. Biophys. Res. Commun.* 2001;286:587–94.
- [170] Pazin MJ, Sheridan PL, Cannon K, Cao Z, Keck JG, Kadonaga JT, et al. NF- $\kappa$ B-mediated chromatin reconfiguration and transcriptional activation of the HIV-1 enhancer in vitro. *Genes Dev.* 1996;10:37–49.
- [171] Steger DJ, Workman JL. Stable co-occupancy of transcription factors and histones at the HIV-1 enhancer. *EMBO J.* 1997;16:2463–72.
- [172] Rothgiesser KM, Erener S, Waibel S, Lüscher B, Hottiger MO. SIRT2 regulates NF- $\kappa$ B dependent gene expression through deacetylation of p65 Lys310. *J. Cell Sci.* 2010;123:4251–8.
- [173] Kwon H-S, Ott M. The ups and downs of SIRT1. *Trends Biochem. Sci.* 2008;33:517–25.
- [174] Zhang JL, Sharma PL, Crumpacker CS. Enhancement of the basal-level activity of HIV-1 long terminal repeat by HIV-1 nucleocapsid protein. *Virology.* 2000;268:251–63.
- [175] Kim YK, Bourgeois CF, Pearson R, Tyagi M, West MJ, Wong J, et al. Recruitment of TFIIH to the HIV LTR is a rate-limiting step in the emergence of HIV from latency. *EMBO J.* 2006;25:3596–604.
- [176] Larochelle S, Amat R, Glover-Cutter K, Sansó M, Zhang C, Allen JJ, et al. Cyclin-dependent kinase control of the initiation-to-elongation switch of RNA polymerase II. *Nat. Struct. Mol. Biol.* 2012;19:1108–15.
- [177] Takahashi Y, Tanaka Y, Yamashita A. OX40 Stimulation by gp34/OX40 ligand enhances productive human immunodeficiency virus type1 infection. *J. Virol.* 2001;75:674806757.
- [178] Kundu M, Srinivasan a, Pomerantz RJ, Khalili K. Evidence that a cell cycle regulator, E2F1, down-regulates transcriptional activity of the human immunodeficiency virus type 1 promoter. *J. Virol.* 1995;69:6940–6.
- [179] Majello B, De Luca P, Hagen G, Suske G, Lania L. Different members of the Sp1 multigene family exert opposite transcriptional regulation of the long terminal repeat of HIV-1. *Nucleic Acids Res.* 1994;22:4914–21.
- [180] Millhouse S, Krebs FC, Yao J, McAllister JJ, Conner J, Ross H, et al. Sp1 and related factors fail to interact with the NF-kappaB-proximal G/C box in the LTR of a replication competent, brain-derived strain of HIV-1 (YU-2). *J. Neurovirol.* 1998;4:312–23.
- [181] Garcia-Rodriguez C, Rao A. Nuclear Factor of Activated T Cells (NFAT)-dependent Transactivation Regulated by the Coactivators p300/CREB-binding Protein (CBP). *J. Exp. Med.* 1998;187:2031–6.

- [182] Wang FX, Xu Y, Sullivan J, Souder E, Argyris EG, Acheampong E a., et al. IL-7 is a potent and proviral strain-specific inducer of latent HIV-1 cellular reservoirs of infected individuals on virally suppressive HAART. *J. Clin. Invest.* 2005;115:128–37.
- [183] Shuai K, Liu B. Regulation of JAK-STAT signalling in the immune system. *Nat. Rev. Immunol.* 2003;3:900–11.
- [184] Bovolenta C, Camorali L, Lorini a L, Ghezzi S, Vicenzi E, Lazzarin a, et al. Constitutive activation of STATs upon in vivo human immunodeficiency virus infection. *Blood.* 1999;94:4202–9.
- [185] Crotti A, Lusic M, Lupo R, Lievens PMJ, Liboi E, Della Chiara G, et al. Naturally occurring C-terminally truncated STAT5 is a negative regulator of HIV-1 expression. *Blood.* 2007;109:5380–9.
- [186] Della Chiara G, Crotti A, Liboi E, Giacca M, Poli G, Lusic M. Negative regulation of HIV-1 transcription by a heterodimeric NF- $\kappa$ B1/p50 and C-terminally truncated STAT5 complex. *J. Mol. Biol. Elsevier Ltd;* 2011;410:933–43.
- [187] Henderson AJ, Connor RI, Calame KL. C/EBP activators are required for HIV-1 replication and proviral induction in monocytic cell lines. *Immunity.* 1996;5:91–101.
- [188] Henderson a J, Calame KL. CCAAT/enhancer binding protein (C/EBP) sites are required for HIV-1 replication in primary macrophages but not CD4(+) T cells. *Proc. Natl. Acad. Sci. U. S. A.* 1997;94:8714–9.
- [189] Lee ES, Zhou H, Al LEEET, Irol J V. Endothelial Cells Enhance Human Immunodeficiency Virus Type 1 Replication in Macrophages through a C / EBP-Dependent Mechanism. *Society.* 2001;75:9703–12.
- [190] Combates J, Kwon P, Rzepka W, Cohen D. Involvement of the Transcription Factor NF-1L6 in Phorbol Ester Induction of P-glycoprotein in U937 Cells. *Cell.* 1997;8:213–9.
- [191] Colin L, Vandenhoudt N, de Walque S, Van Driessche B, Bergamaschi A, Martinelli V, et al. The AP-1 binding sites located in the pol gene intragenic regulatory region of HIV-1 are important for viral replication. *PLoS One. Public Library of Science;* 2011;6:e19084.
- [192] Duverger A, Wolschendorf F, Zhang M, Wagner F, Hatcher B, Jones J, et al. An AP-1 binding site in the enhancer/core element of the HIV-1 promoter controls the ability of HIV-1 to establish latent infection. *J. Virol.* 2013;87:2264–77.
- [193] Hess J, Angel P, Schorpp-Kistner M. AP-1 subunits: quarrel and harmony among siblings. *J. Cell Sci.* 2004;117:5965–73.
- [194] Challacombe SJ, Naglik JR. The effects of HIV infection on oral mucosal immunity. *Adv. Dent. Res.* 2006;19:29–35.

- [195] Long J, Wang Y, Wang W, Chang BHJ, Danesh FR. Identification of microRNA-93 as a novel regulator of vascular endothelial growth factor in hyperglycemic conditions. *J. Biol. Chem.* 2010;285:23457–65.
- [196] Novis CL, Archin NM, Buzon MJ, Verdin E, Round JL, Lichterfeld M, et al. Reactivation of latent HIV-1 in central memory CD4<sup>+</sup> T cells through TLR-1/2 stimulation. *Retrovirology.* 2013;10:119.
- [197] Pearson R, Kim YK, Hokello J, Lassen K, Friedman J, Tyagi M, et al. Epigenetic silencing of human immunodeficiency virus (HIV) transcription by formation of restrictive chromatin structures at the viral long terminal repeat drives the progressive entry of HIV into latency. *J. Virol.* 2008;82:12291–303.
- [198] Kim YK, Mbonye U, Hokello J, Karn J. T-cell receptor signaling enhances transcriptional elongation from latent HIV proviruses by activating P-TEFb through an ERK-dependent pathway. *J. Mol. Biol.* 2011;410:896–916.
- [199] Herrmann CH, Rice A P. Lentivirus Tat proteins specifically associate with a cellular protein kinase, TAK, that hyperphosphorylates the carboxyl-terminal domain of the large subunit of RNA polymerase II: candidate for a Tat cofactor. *J. Virol.* 1995;69:1612–20.
- [200] Wei P, Garber ME, Fang SM, Fischer WH, Jones K a. A novel CDK9-associated C-type cyclin interacts directly with HIV-1 Tat and mediates its high-affinity, loop-specific binding to TAR RNA. *Cell.* 1998;92:451–62.
- [201] Bieniasz PD, Grdina T a, Bogerd HP, Cullen BR. Recruitment of a protein complex containing Tat and cyclin T1 to TAR governs the species specificity of HIV-1 Tat. *EMBO J.* 1998;17:7056–65.
- [202] Fujinaga K, Cujec TP, Peng J, Garriga J, Price DH, Graña X, et al. The ability of positive transcription elongation factor B to transactivate human immunodeficiency virus transcription depends on a functional kinase domain, cyclin T1, and Tat. *J. Virol.* 1998;72:7154–9.
- [203] Garber ME, Wei P, KewalRamani VN, Mayall TP, Herrmann CH, Rice AP, et al. The interaction between HIV-1 Tat and human cyclin T1 requires zinc and a critical cysteine residue that is not conserved in the murine CycT1 protein. *Genes Dev.* 1998;12:3512–27.
- [204] Felzien LK, Woffendin C, Hottiger MO, Subbramanian R a, Cohen E a, Nabel GJ. HIV transcriptional activation by the accessory protein, VPR, is mediated by the p300 co-activator. *Proc. Natl. Acad. Sci. U. S. A.* 1998;95:5281–6.
- [205] Wang L, Mukherjee S, Jia F, Narayan O, Zhao LJ. Interaction of virion protein Vpr of human immunodeficiency virus type 1 with cellular transcription factor Sp1 and trans-activation of viral long terminal repeat. *J. Biol. Chem.* 1995;270:25564–9.



- [206] Agostini I, Navarro JM, Rey F, Bouhamdan M, Spire B, Vigne R, et al. The human immunodeficiency virus type 1 Vpr transactivator: cooperation with promoter-bound activator domains and binding to TFIIIB. *J. Mol. Biol.* 1996;261:599–606.
- [207] He G, Margolis DM. Counterregulation of chromatin deacetylation and histone deacetylase occupancy at the integrated promoter of human immunodeficiency virus type 1 (HIV-1) by the HIV-1 repressor YY1 and HIV-1 activator Tat. *Mol. Cell. Biol.* 2002;22:2965–73.
- [208] Tyagi M, Karn J. CBF-1 promotes transcriptional silencing during the establishment of HIV-1 latency. *EMBO J.* 2007;26:4985–95.
- [209] Tyagi M, Pearson RJ, Karn J. Establishment of HIV latency in primary CD4+ cells is due to epigenetic transcriptional silencing and P-TEFb restriction. *J. Virol.* 2010;84:6425–37.
- [210] Jiang G, Espeseth A, Hazuda DJ, Margolis DM. c-Myc and Sp1 contribute to proviral latency by recruiting histone deacetylase 1 to the human immunodeficiency virus type 1 promoter. *J. Virol.* 2007;81:10914–23.
- [211] Wen Y, Shatkin AJ. Transcription elongation factor hSPT5 stimulates mRNA capping. *Transcription elongation factor hSPT5 stimulates mRNA capping. Genes Dev.* 1999; 13(14): 1774–1779.
- [212] Cheng B, Price DH. Analysis of factor interactions with RNA polymerase II elongation complexes using a new electrophoretic mobility shift assay. *Nucleic Acids Res.* 2008;36:1–10.
- [213] Missra A, Gilmour DS. Interactions between DSIF (DRB sensitivity inducing factor), NELF (negative elongation factor), and the Drosophila RNA polymerase II transcription elongation complex. *Proc. Natl. Acad. Sci. U. S. A.* 2010;107:11301–6.
- [214] Yamaguchi Y, Inukai N, Narita T, Wada T, Handa H. Evidence that Negative Elongation Factor Represses Transcription Elongation through Binding to a DRB Sensitivity-Inducing Factor / RNA Polymerase II Complex and RNA. *Mol. Cell. Biol.* 2002;22:2918–27.
- [215] Renner DB, Yamaguchi Y, Wada T, Handa H, Price DH. A Highly Purified RNA Polymerase II Elongation Control System. *J. Biol. Chem.* 2001;276:42601–9.
- [216] Zhang Z, Klatt A, Gilmour DS, Henderson AJ. Negative elongation factor NELF represses human immunodeficiency virus transcription by pausing the RNA polymerase II complex. *J. Biol. Chem.* 2007;282:16981–8.
- [217] Natarajan M, Schiralli Lester GM, Lee C, Missra A, Wasserman G a., Steffen M, et al. Negative elongation factor (NELF) coordinates RNA polymerase II pausing, premature termination, and chromatin remodeling to regulate HIV transcription. *J. Biol. Chem.* 2013;288:25995–6003.

- [218] Jadowsky JK, Wong JY, Graham AC, Dobrowolski C, Devor RL, Adams MD, et al. Negative Elongation Factor Is Required for the Maintenance of Proviral Latency but Does Not Induce Promoter-Proximal Pausing of RNA Polymerase II on the HIV Long Terminal Repeat. *Mol. Cell. Biol.* 2014;34:1911–28.
- [219] Wagschal A, Rousset E, Basavarajaiah P, Contreras X, Harwig A, Laurent-Chabalier S, et al. Microprocessor, Setx, Xrn2, and Rrp6 co-operate to induce premature termination of transcription by RNAPII. *Cell.* 2012;150:1147–57.
- [220] Kao SY, Calman a F, Luciw P a, Peterlin BM. Anti-termination of transcription within the long terminal repeat of HIV-1 by tat gene product. *Nature.* 1987;330:489–93.
- [221] Laspia MF, Rice a P, Mathews MB. HIV-1 Tat protein increases transcriptional initiation and stabilizes elongation. *Cell.* 1989;59:283–92.
- [222] Dingwall C, Ernberg I, Gait MJ, Green SM, Heaphy S, Karn J, et al. HIV-1 tat protein stimulates transcription by binding to a U-rich bulge in the stem of the TAR RNA structure. *EMBO J.* 1990;9:4145–53.
- [223] Tahirov TH, Babayeva ND, Varzavand K, Cooper JJ, Sedore SC, Price DH. Crystal structure of HIV-1 Tat complexed with human P-TEFb. *Nature.* 2010;465:747–51.
- [224] Fujinaga K, Irwin D, Huang Y, Taube R, Kurosu T, Peterlin BM. Dynamics of human immunodeficiency virus transcription: P-TEFb phosphorylates RD and dissociates negative effectors from the transactivation response element. *Mol. Cell. Biol.* 2004;24:787–95.
- [225] Komarnitsky P, Cho EJ, Buratowski S. Different phosphorylated forms of RNA polymerase II and associated mRNA processing factors during transcription. *Genes Dev.* 2000;14:2452–60.
- [226] Kim YK, Bourgeois CF, Isel C, Churcher MJ, Karn J. Phosphorylation of the RNA polymerase II carboxyl-terminal domain by CDK9 is directly responsible for human immunodeficiency virus type 1 Tat-activated transcriptional elongation. *Mol. Cell. Biol.* 2002;22:4622–37.
- [227] Czudnochowski N, Böskén C a., Geyer M. Serine-7 but not serine-5 phosphorylation primes RNA polymerase II CTD for P-TEFb recognition. *Nat. Commun.* 2012;3:842.
- [228] Ahn SH, Kim M, Buratowski S. Phosphorylation of serine 2 within the RNA polymerase II C-terminal domain couples transcription and 3' end. *Process. Mol. Cell.* 2004;13:67–76.
- [229] Lenasi T, Peterlin BM, Barboric M. Cap-binding protein complex links pre-mRNA capping to transcription elongation and alternative splicing through positive transcription elongation factor b (P-TEFb). *J. Biol. Chem.* 2011;286:22758–68.

- [230] Briss V, Gomes N, Pickle L, Jones K a. A human splicing factor, SKIP, associates with P-TEFb and enhances transcription elongation by HIV-1 Tat. *Genes Dev.* 2005;19:1211–26.
- [231] Bourgeois CF, Kim YK, Churcher MJ, West MJ, Karn J. Spt5 cooperates with human immunodeficiency virus type 1 Tat by preventing premature RNA release at terminator sequences. *Mol. Cell. Biol.* 2002;22:1079–93.
- [232] Yamada T, Yamaguchi Y, Inukai N, Okamoto S, Mura T, Handa H. P-TEFb-mediated phosphorylation of hSpt5 C-terminal repeats is critical for processive transcription elongation. *Mol. Cell.* 2006;21:227–37.
- [233] Keen NJ, Churcher MJ, Karn J. Transfer of Tat and release of TAR RNA during the activation of the human immunodeficiency virus type-1 transcription elongation complex. *EMBO J.* 1997;16:5260–72.
- [234] Sobhian B, Laguette N, Yatim A, Nakamura M, Levy Y, Kiernan R, et al. HIV-1 Tat Assembles a Multifunctional Transcription Elongation Complex and Stably Associates with the 7SK snRNP. *Mol. Cell.* Elsevier Ltd; 2010;38:439–51.
- [235] Nguyen VT, Kiss T, Michels a, Bensaude O. 7SK small nuclear RNA binds to and inhibits the activity of CDK9/cyclin T complexes. *Nature.* 2001;414:322–5.
- [236] Yang Z, Zhu Q, Luo K, Zhou Q. The 7SK small nuclear RNA inhibits the CDK9/cyclin T1 kinase to control transcription. *Nature.* 2001;414:317–22.
- [237] Yik JHN, Chen R, Nishimura R, Jennings JL, Link AJ, Zhou Q. Inhibition of P-TEFb (CDK9/cyclin T) kinase and RNA polymerase II transcription by the coordinated actions of HEXIM1 and 7SK snRNA. *Mol. Cell.* 2003;12:971–82.
- [238] Li Q, Price JP, Byers SA, Cheng D, Peng J, Price DH. Analysis of the large inactive P-TEFb complex indicates that it contains one 7SK molecule, a dimer of HEXIM1 or HEXIM2, and two P-TEFb molecules containing Cdk9 phosphorylated at threonine 186. *J. Biol. Chem.* 2005;280:28819–26.
- [239] Peterlin BM, Brogie JE, Price DH. 7SK snRNA: A noncoding RNA that plays a major role in regulating eukaryotic transcription. *Wiley Interdiscip. Rev. RNA.* 2012;3:92–103.
- [240] Jeronimo C, Forget D, Bouchard A, Li Q, Chua G, Poitras C, et al. Systematic Analysis of the Protein Interaction Network for the Human Transcription Machinery Reveals the Identity of the 7SK Capping Enzyme. *Mol. Cell.* 2007;27:262–74.
- [241] Krueger BJ, Varzavand K, Cooper JJ, Price DH. The mechanism of release of P-TEFb and HEXIM1 from the 7SK snRNP by viral and cellular activators includes a conformational change in 7SK. *PLoS One.* 2010;5.

- [242] Markert A, Grimm M, Martinez J, Wiesner J, Meyerhans A, Meyuhas O, et al. The La-related protein LARP7 is a component of the 7SK ribonucleoprotein and affects transcription of cellular and viral polymerase II genes. *EMBO Rep.* 2008;9:569–75.
- [243] Schröder S, Cho S, Zeng L, Zhang Q, Kaehlcke K, Mak L, et al. Two-pronged binding with bromodomain-containing protein 4 liberates positive transcription elongation factor b from inactive ribonucleoprotein complexes. *J. Biol. Chem.* 2012;287:1090–9.
- [244] Bisgrove D a, Mahmoudi T, Henklein P, Verdin E. Conserved P-TEFb-interacting domain of BRD4 inhibits HIV transcription. *Proc. Natl. Acad. Sci. U. S. A.* 2007;104:13690–5.
- [245] Jang MK, Mochizuki K, Zhou M, Jeong H-S, Brady JN, Ozato K. The bromodomain protein Brd4 is a positive regulatory component of P-TEFb and stimulates RNA polymerase II-dependent transcription. *Mol. Cell.* 2005;19:523–34.
- [246] Yang Z, Yik JHN, Chen R, He N, Jang MK, Ozato K, et al. Recruitment of P-TEFb for stimulation of transcriptional elongation by the bromodomain protein Brd4. *Mol. Cell.* 2005;19:535–45.
- [247] Zhu J, Gaiha GD, John SP, Pertel T, Chin CR, Gao G, et al. Reactivation of latent HIV-1 by inhibition of BRD4. *Cell Rep.* 2012;2:807–16.
- [248] Wu S-Y, Chiang C-M. The double bromodomain-containing chromatin adaptor Brd4 and transcriptional regulation. *J. Biol. Chem.* 2007;282:13141–5.
- [249] Boehm D, Calvanese V, Dar RD, Xing S, Schroeder S, Martins L, et al. BET bromodomain-targeting compounds reactivate HIV from latency via a Tat-independent mechanism. *Cell Cycle.* 2013;12:452–62.
- [250] Denis G V, McComb ME, Faller D V, Sinha A, Romesser PB, Costello CE. Identification of transcription complexes that contain the double bromodomain protein Brd2 and chromatin remodeling machines. *J. Proteome Res.* 2006;5:502–11.
- [251] Cherrier T, Le Douce V, Eilebrecht S, Riclet R, Marban C, Dequiedt F, et al. CTIP2 is a negative regulator of P-TEFb. *Proc. Natl. Acad. Sci. U. S. A.* 2013;110:12655–60.
- [252] Mbonye UR, Wang B, Gokulrangan G, Chance MR, Karn J. Phosphorylation of HEX-IM1 at Tyr271 and Tyr274 Promotes Release of P-TEFb from the 7SK snRNP Complex and Enhances Proviral HIV Gene Expression. *Proteomics.* 2015;15:2078–86.
- [253] Ji X, Zhou Y, Pandit S, Huang J, Li H, Lin CY, et al. SR proteins collaborate with 7SK and promoter-associated nascent RNA to release paused polymerase. *Cell.* 2013;153:855–68.
- [254] Suñé C, Goldstrohm a C, Peng J, Price DH, Garcia-Blanco M a. An in vitro transcription system that recapitulates equine infectious anemia virus tat-mediated inhibition of human immunodeficiency virus type 1 Tat activity demonstrates a role for posi-

- tive transcription elongation factor b and associated proteins in th. *Virology*. 2000;274:356–66.
- [255] Lu H, Li Z, Xue Y, Schulze-Gahmen U, Johnson JR, Krogan NJ, et al. AFF1 is a ubiquitous P-TEFb partner to enable Tat extraction of P-TEFb from 7SK snRNP and formation of SECs for HIV transactivation. *Proc. Natl. Acad. Sci.* 2014;111 :E15–24.
  - [256] He N, Liu M, Hsu J, Xue Y, Chou S, Burlingame A, et al. HIV-1 Tat and host AFF4 recruit two transcription elongation factors into a bifunctional complex for coordinated activation of HIV-1 transcription. *Mol. Cell*. 2010;38:428–38.
  - [257] Mueller D, García-Cuellar MP, Bach C, Buhl S, Maethner E, Slany RK. Misguided transcriptional elongation causes mixed lineage leukemia. *PLoS Biol*. 2009;7.
  - [258] Lin C, Smith ER, Takahashi H, Lai K, Martin- S, Florens L, et al. AFF4, a component of the ELL/p-TEFb elongation complex and a shared subunit of MLL chimeras can link transcription elongation to leukemia. *Mol. Cell*. 2010;37:429–37.
  - [259] Yokoyama A, Lin M, Naresh A, Kitabayashi I, Cleary ML. A Higher-Order Complex Containing AF4 and ENL Family Proteins with P-TEFb Facilitates Oncogenic and Physiologic MLL-Dependent Transcription. *Cancer Cell*. 2010;17:198–212.
  - [260] Smith E, Lin C, Shilatifard A. The super elongation complex (SEC) and MLL in development and disease. *Genes Dev*. 2011;25:661–72.
  - [261] Chou S, Upton H, Bao K, Schulze-Gahmen U, Samelson AJ, He N, et al. HIV-1 Tat recruits transcription elongation factors dispersed along a flexible AFF4 scaffold. *Proc. Natl. Acad. Sci. U. S. A.* 2013;110:E123–31.
  - [262] Liu M, Hsu J, Chan C, Li Z, Zhou Q. The Ubiquitin Ligase Siah1 Controls ELL2 Stability and Formation of Super Elongation Complexes to Modulate Gene Transcription. *Mol. Cell*. Elsevier Inc.; 2012;46:325–34.
  - [263] Ammosova T, Berro R, Jerebtsova M, Jackson A, Charles S, Klase Z, et al. Phosphorylation of HIV-1 Tat by CDK2 in HIV-1 transcription. *Retrovirology*. 2006;3:78.
  - [264] Kiernan RE, Vanhulle C, Schiltz L, Adam E, Xiao H, Maudoux F, et al. HIV-1 tat transcriptional activity is regulated by acetylation. *EMBO J*. 1999;18:6106–18.
  - [265] Brès V, Tagami H, Péloponèse JM, Loret E, Jeang KT, Nakatani Y, et al. Differential acetylation of Tat coordinates its interaction with the co-activators cyclin T1 and PCAF. *EMBO J*. 2002;21:6811–9.
  - [266] Huo L, Li D, Sun X, Shi X, Karna P, Yang W, et al. Regulation of Tat acetylation and transactivation activity by the microtubule-associated deacetylase HDAC6. *J. Biol. Chem*. 2011;286:9280–6.
  - [267] Ott M, Schnölzer M, Garnica J, Fischle W, Emiliani S, Rackwitz HR, et al. Acetylation of the HIV-1 tat protein by p300 is important for its transcriptional activity. *Curr. Biol*. 1999;9:1489–92.

- [268] Col E, Caron C, Seigneurin-Berny D, Gracia J, Favier A, Khochbin S. The Histone Acetyltransferase, hGCN5, Interacts with and Acetylates the HIV Transactivator, Tat. *J. Biol. Chem.* 2001;276:28179–84.
- [269] Dorr A, Kiermer V, Pedal A, Rackwitz HR, Henklein P, Schubert U, et al. Transcriptional synergy between Tat and PCAF is dependent on the binding of acetylated Tat to the PCAF bromodomain. *EMBO J.* 2002;21:2715–23.
- [270] Kaehlcke K, Dorr A, Hetzer-Egger C, Kiermer V, Henklein P, Schnoelzer M, et al. Acetylation of Tat defines a CyclinT1-independent step in HIV transactivation. *Mol. Cell.* 2003;12:167–76.
- [271] Mahmoudi T, Parra M, Vries RGJ, Kauder SE, Verrijzer CP, Ott M, et al. The SWI/SNF chromatin-remodeling complex is a cofactor for Tat transactivation of the HIV promoter. *J. Biol. Chem.* 2006;281:19960–8.
- [272] Tréand C, du Chéné I, Brès V, Kiernan R, Benarous R, Benkirane M, et al. Requirement for SWI/SNF chromatin-remodeling complex in Tat-mediated activation of the HIV-1 promoter. *EMBO J.* 2006;25:1690–9.
- [273] Agbottah E, Deng L, Dannenberg LO, Pumfery A, Kashanchi F. Effect of SWI/SNF chromatin remodeling complex on HIV-1 Tat activated transcription. *Retrovirology.* 2006;3:48.
- [274] Pagans S, Pedal A, North BJ, Kaehlcke K, Marshall BL, Dorr A, et al. SIRT1 regulates HIV transcription via Tat deacetylation. *PLoS Biol.* 2005;3:0210–20.
- [275] Pagans S, Kauder SE, Kaehlcke K, Sakane N, Schroeder S, Dormeyer W, et al. The Cellular lysine methyltransferase Set7/9-KMT7 binds HIV-1 TAR RNA, monomethylates the viral transactivator Tat, and enhances HIV transcription. *Cell Host Microbe.* 2010;7:234–44.
- [276] Sakane N, Kwon HS, Pagans S, Kaehlcke K, Mizusawa Y, Kamada M, et al. Activation of hiv transcription by the viral tat protein requires a demethylation step mediated by lysine-specific demethylase 1 (LSD1/KDM1). *PLoS Pathog.* 2011;7:1–12.
- [277] Brès V, Kiernan RE, Linares LK, Chable-Bessia C, Plechakova O, Tréand C, et al. A non-proteolytic role for ubiquitin in Tat-mediated transactivation of the HIV-1 promoter. *Nat. Cell Biol.* 2003;5:754–61.
- [278] Verdin E. DNase I-hypersensitive sites are associated with both long terminal repeats and with the intragenic enhancer of integrated human immunodeficiency virus type 1. *J. Virol.* 1991;65:6790–9.
- [279] Verdin E, Paras P, Van Lint C. Chromatin disruption in the promoter of human immunodeficiency virus type 1 during transcriptional activation. *EMBO J.* 1993;12:3249–59.

- [280] Van Lint C, Emiliani S, Ott M, Verdin E. Transcriptional activation and chromatin remodeling of the HIV-1 promoter in response to histone acetylation. *EMBO J.* 1996;15:1112–20.
- [281] Rafati H, Parra M, Hakre S, Moshkin Y, Verdin E, Mahmoudi T. Repressive LTR nucleosome positioning by the BAF complex is required for HIV latency. *PLoS Biol.* 2011;9:e1001206.
- [282] Cismasiu VB, Paskaleva E, Suman Daya S, Canki M, Duus K, Avram D. BCL11B is a general transcriptional repressor of the HIV-1 long terminal repeat in T lymphocytes through recruitment of the NuRD complex. *Virology.* 2008;380:173–81.
- [283] Xue Y, Wong J, Moreno GT, Young MK, Côté J, Wang W. NURD, a novel complex with both ATP-dependent chromatin-remodeling and histone deacetylase activities. *Mol. Cell.* 1998;2:851–61.
- [284] Zhang Y, Li Y. The Expanding Mi-2/NuRD Complexes: A Schematic Glance. *Proteomics Insights. Libertas Academica;* 2011;2010:79.
- [285] Perkins ND, Felzien LK, Betts JC, Leung K, Beach DH, Nabel GJ. Regulation of NF-kappaB by cyclin-dependent kinases associated with the p300 coactivator. *Science.* 1997;275:523–7.
- [286] Williams SA, Chen L-F, Kwon H, Ruiz-Jarabo CM, Verdin E, Greene WC. NF-kappaB p50 promotes HIV latency through HDAC recruitment and repression of transcriptional initiation. *EMBO J.* 2006;25:139–49.
- [287] Keedy KS, Archin NM, Gates AT, Espeseth A, Hazuda DJ, Margolis DM. A limited group of class I histone deacetylases acts to repress human immunodeficiency virus type 1 expression. *J. Virol.* 2009;83:4749–56.
- [288] Huber K, Doyon G, Plaks J, Fyne E, Mellors JW, Sluis-Cremer N. Inhibitors of histone deacetylases: Correlation between isoform specificity and reactivation of HIV type 1 (HIV-1) from latently infected cells. *J. Biol. Chem.* 2011;286:22211–8.
- [289] Ying H, Zhang Y, Zhou X, Qu X, Wang P, Liu S, et al. Selective Histone deacetylase Inhibitor M344 Intervenes in HIV-1 Latency through Increasing Histone Acetylation and Activation of NF-kappaB. *PLoS One.* 2012;7.
- [290] Marban C, Suzanne S, Dequiedt F, de Walque S, Redel L, Van Lint C, et al. Recruitment of chromatin-modifying enzymes by CTIP2 promotes HIV-1 transcriptional silencing. *EMBO J.* 2007;26:412–23.
- [291] Marban C, Redel L, Suzanne S, Van Lint C, Lecestre D, Chasserot-Golaz S, et al. COUP-TF interacting protein 2 represses the initial phase of HIV-1 gene transcription in human microglial cells. *Nucleic Acids Res.* 2005;33:2318–31.



- [292] Bouchat S, Gatot J-S, Kabeya K, Cardona C, Colin L, Herbein G, et al. Histone methyltransferase inhibitors induce HIV-1 recovery in resting CD4(+) T cells from HIV-1-infected HAART-treated patients. *AIDS*. 2012;26:1473–82.
- [293] Du Chéné I, Basyuk E, Lin Y-L, Triboulet R, Knezevich A, Chable-Bessia C, et al. Suv39H1 and HP1gamma are responsible for chromatin-mediated HIV-1 transcriptional silencing and post-integration latency. *EMBO J*. 2007;26:424–35.
- [294] Friedman J, Cho W-K, Chu CK, Keedy KS, Archin NM, Margolis DM, et al. Epigenetic silencing of HIV-1 by the histone H3 lysine 27 methyltransferase enhancer of Zeste 2. *J. Virol*. 2011;85:9078–89.
- [295] Imai K, Togami H, Okamoto T. Involvement of histone H3 lysine 9 (H3K9) methyltransferase G9a in the maintenance of HIV-1 latency and its reactivation by BIX01294. *J. Biol. Chem*. 2010;285:16538–45.
- [296] Kauder SE, Bosque A, Lindqvist A, Planelles V, Verdin E. Epigenetic regulation of HIV-1 latency by cytosine methylation. *PLoS Pathog*. 2009;5:e1000495.
- [297] Blazkova J, Trejbalova K, Gondois-Rey F, Halfon P, Philibert P, Guiguen A, et al. CpG methylation controls reactivation of HIV from latency. *PLoS Pathog*. 2009;5.
- [298] Palacios JA, Pérez-Piñar T, Toro C, Sanz-Minguella B, Moreno V, Valencia E, et al. Long-term nonprogressor and elite controller patients who control viremia have a higher percentage of methylation in their HIV-1 proviral promoters than aviremic patients receiving highly active antiretroviral therapy. *J. Virol*. 2012;86:13081–4.
- [299] Triboulet R, Mari B, Lin Y, Chable-bessia C, Bennasser Y, Lebrigand K, et al. Suppression of MicroRNA-Silencing Pathway by HIV-1 During Virus Replication. *Science* (80-). 2007;1579–82.
- [300] Nathans R, Chu C-Y, Serquina AK, Lu C-C, Cao H, Rana TM. Cellular microRNA and P bodies modulate host-HIV-1 interactions. *Mol. Cell*. Elsevier Ltd; 2009;34:696–709.
- [301] Imam H, Shahr Bano A, Patel P, Holla P, Jameel S. The lncRNA NRON modulates HIV-1 replication in a NFAT-dependent manner and is differentially regulated by early and late viral proteins. *Sci. Rep*. 2015;5:8639.
- [302] Wang X, Ye L, Hou W, Zhou Y, Wang Y-J, Metzger DS, et al. Cellular microRNA expression correlates with susceptibility of monocytes/macrophages to HIV-1 infection. *Blood*. 2009;113:671–4.
- [303] Houzet L, Yeung ML, de Lame V, Desai D, Smith SM, Jeang K-T. MicroRNA profile changes in human immunodeficiency virus type 1 (HIV-1) seropositive individuals. *Retrovirology*. 2008;5:118.



- [304] Witwer KW, Watson AK, Blankson JN, Clements JE. Relationships of PBMC micro-RNA expression, plasma viral load, and CD4+ T-cell count in HIV-1-infected elite suppressors and viremic patients. *Retrovirology*. 2012;9:5.
- [305] Bignami F, Pilotti E, Bertoncelli L, Ronzi P, Gulli M, Marmioli N, et al. Stable changes in CD4 + T lymphocyte miRNA expression after exposure to HIV-1. *Blood*. 2013;119:6259–67.
- [306] Chiang K, Sung T-L, Rice a. P. Regulation of Cyclin T1 and HIV-1 Replication by MicroRNAs in Resting CD4+ T Lymphocytes. *J. Virol*. 2012;86:3244–52.
- [307] Sung TL, Rice AP. miR-198 inhibits HIV-1 gene expression and replication in monocytes and its mechanism of action appears to involve repression of cyclin T1. *PLoS Pathog*. 2009;5.
- [308] Chiang K, Rice AP. MicroRNA-mediated restriction of HIV-1 in resting CD4+ T cells and monocytes. *Viruses*. 2012;4:1390–409.
- [309] Qian S, Zhong X, Yu L, Ding B, de Haan P, Boris-Lawrie K. HIV-1 Tat RNA silencing suppressor activity is conserved across kingdoms and counteracts translational repression of HIV-1. *Proc. Natl. Acad. Sci. U. S. A*. 2009;106:605–10.
- [310] Hayes AM, Qian S, Yu L, Boris-Lawrie K. Tat RNA silencing suppressor activity contributes to perturbation of lymphocyte miRNA by HIV-1. *Retrovirology*. BioMed Central Ltd; 2011;8:36.
- [311] Coley W, Van Duyne R, Carpio L, Guendel I, Kehn-Hall K, Chevalier S, et al. Absence of DICER in monocytes and its regulation by HIV-1. *J. Biol. Chem*. 2010;285:31930–43.
- [312] Huang J, Wang F, Argyris E, Chen K, Liang Z, Tian H, et al. Cellular microRNAs contribute to HIV-1 latency in resting primary CD4+ T lymphocytes. *Nat. Med*. 2007;13:1241–7.
- [313] Jiménez VC, Booiman T, de Taeye SW, van Dort K a., Rits M a. N, Hamann J, et al. Differential expression of HIV-1 interfering factors in monocyte-derived macrophages stimulated with polarizing cytokines or interferons. *Sci. Rep*. 2012;2:1–7.
- [314] Mantri CK, Pandhare Dash J, Mantri JV, Dash CC V. Cocaine enhances HIV-1 replication in CD4+ T cells by down-regulating MiR-125b. *PLoS One*. Public Library of Science; 2012;7:e51387.
- [315] Wang X, Ye L, Zhou Y, Liu MQ, Zhou DJ, Ho WZ. Inhibition of anti-HIV microRNA expression: A mechanism for opioid-mediated enhancement of HIV infection of monocytes. *Am. J. Pathol*. 2011;178:41–7.
- [316] Swaminathan S, Murray DD, Kelleher AD. Mirnas and HIV: Unforeseen Determinants Of Host-Pathogen Interaction. *Immunol. Rev*. 2013;254:265–80.

- [317] Sun G, Li H, Wu X, Covarrubias M, Scherer L, Meinking K, et al. Interplay between HIV-1 infection and host microRNAs. *Nucleic Acids Res.* 2012;40:2181–96.
- [318] Betel D, Wilson M, Gabow A, Marks DS, Sander C. The microRNA.org resource: Targets and expression. *Nucleic Acids Res.* 2008;36:149–53.
- [319] Landgraf P, Rusu M, Sheridan R, Sewer A, Iovino N, Aravin A, et al. A Mammalian microRNA Expression Atlas Based on Small RNA Library Sequencing. *Cell.* 2009;129:1401–14.
- [320] Ahluwalia JK, Khan SZ, Soni K, Rawat P, Gupta A, Hariharan M, et al. Human cellular microRNA hsa-miR-29a interferes with viral nef protein expression and HIV-1 replication. *Retrovirology.* 2008;5:117.
- [321] Ruelas DS, Chan JK, Oh E, Heidersbach AJ, Hebbeler AM, Chavez L, et al. MicroRNA-155 Reinforces HIV Latency. *J. Biol. Chem.* 2015;290:jbc.M115.641837.
- [322] Zhang HS, Chen XY, Wu TC, Sang WW, Ruan Z. MiR-34a is involved in Tat-induced HIV-1 long terminal repeat (LTR) transactivation through the SIRT1/NF- $\kappa$ B pathway. *FEBS Lett. Federation of European Biochemical Societies;* 2012;586:4203–7.
- [323] Zhang H-S, Wu T-C, Sang W-W, Ruan Z. MiR-217 is involved in Tat-induced HIV-1 long terminal repeat (LTR) transactivation by down-regulation of SIRT1. *Biochim. Biophys. Acta.* 2012;1823:1017–23.
- [324] Chen XY, Zhang HS, Wu TC, Sang WW, Ruan Z. Down-regulation of NAMPT expression by miR-182 is involved in Tat-induced HIV-1 long terminal repeat (LTR) transactivation. *Int. J. Biochem. Cell Biol. Elsevier B.V.;* 2013;45:292–8.
- [325] Ma L, Shen CJ, Cohen É a., Xiong SD, Wang JH. MiRNA-1236 inhibits HIV-1 infection of monocytes by repressing translation of cellular factor VprBP. *PLoS One.* 2014;9:1–7.
- [326] Bennasser Y, Le S-Y, Yeung ML, Jeang K-T. HIV-1 encoded candidate micro-RNAs and their cellular targets. *Retrovirology.* 2004;1:43.
- [327] Yeung ML, Houzet L, Yedavalli VSRK, Jeang K-T. A genome-wide short hairpin RNA screening of jurkat T-cells for human proteins contributing to productive HIV-1 replication. *J. Biol. Chem.* 2009;284:19463–73.
- [328] Schopman NCT, Willemsen M, Liu YP, Bradley T, Van Kampen A, Baas F, et al. Deep sequencing of virus-infected cells reveals HIV-encoded small RNAs. *Nucleic Acids Res.* 2012;40:414–27.
- [329] Ouellet DL, Plante I, Landry P, Barat C, Janelle M-E, Flamand L, et al. Identification of functional microRNAs released through asymmetrical processing of HIV-1 TAR element. *Nucleic Acids Res.* 2008;36:2353–65.
- [330] Omoto S, Fujii YR. Regulation of human immunodeficiency virus 1 transcription by nef microRNA. *J. Gen. Virol.* 2005;86:751–5.

- [331] Whisnant AW, Bogerd HP, Flores O, Ho P, Powers JG, Sharova N, et al. In-depth analysis of the interaction of HIV-1 with cellular microRNA biogenesis and effector mechanisms. *MBio*. 2013;4:e000193.
- [332] Raj A, van Oudenaarden A. Nature, Nurture, or Chance: Stochastic Gene Expression and Its Consequences. *Cell*. 2008;135:216–26.
- [333] Weinberger LS, Burnett JC, Toettcher JE, Arkin AP, Schaffer D V. Stochastic gene expression in a lentiviral positive-feedback loop: HIV-1 Tat fluctuations drive phenotypic diversity. *Cell*. 2005;122:169–82.
- [334] Singh A, Razooky B, Cox CD, Simpson ML, Weinberger LS. Transcriptional bursting from the HIV-1 promoter is a significant source of stochastic noise in HIV-1 gene expression. *Biophys. J. Biophysical Society*; 2010;98:L32–4.
- [335] Weinberger AD, Weinberger LS. Stochastic fate selection in HIV-infected patients. *Cell. Elsevier*; 2013;155:497–9.
- [336] Dar RD, Hosmane NN, Michelle RA, Siliciano RF, Weinberger LS. Screening for noise in gene expression identifies drug synergies. *Science (80-.)*. 2014;344:1392–6.
- [337] Lipinski CA. Lead- and drug-like compounds: the rule-of-five revolution. *Drug Discov. Today. Technol.* 2004;1:337–41.
- [338] Leeson PD, Springthorpe B. The influence of drug-like concepts on decision-making in medicinal chemistry. *Nat. Rev. Drug Discov.* 2007;6:881–90.
- [339] Chun TW, Engel D, Mizell SB, Ehler LA, Fauci AS. Induction of HIV-1 replication in latently infected CD4+ T cells using a combination of cytokines. *J. Exp. Med.* 1998;188:83–91.
- [340] Prins JM, Jurriaans S, van Praag RM, Blaak H, van Rij R, Schellekens PT, et al. Immuno-activation with anti-CD3 and recombinant human IL-2 in HIV-1-infected patients on potent antiretroviral therapy. *AIDS*. 1999;13:2405–10.
- [341] Brooks DG, Hamer DH, Arlen PA, Gao L, Bristol G, Kitchen CMR, et al. Molecular characterization, reactivation, and depletion of latent HIV. *Immunity*. 2003;19:413–23.
- [342] Rasmussen TA, Schmeltz Søgaard O, Brinkmann C, Wightman F, Lewin SR, Melchjorsen J, et al. Comparison of HDAC inhibitors in clinical development: effect on HIV production in latently infected cells and T-cell activation. *Hum. Vaccin. Immunother.* 2013;9:993–1001.
- [343] Wightman F, Lu HK, Solomon AE, Saleh S, Harman AN, Cunningham AL, et al. Entinostat is a histone deacetylase inhibitor selective for class 1 histone deacetylases and activates HIV production from latently infected primary T cells. *AIDS*. 2013;27:2853–62.
- [344] Wei DG, Chiang V, Fyne E, Balakrishnan M, Barnes T, Graupe M, et al. Histone deacetylase inhibitor romidepsin induces HIV expression in CD4 T cells from patients

- on suppressive antiretroviral therapy at concentrations achieved by clinical dosing. *PLoS Pathog.* Public Library of Science; 2014;10:e1004071.
- [345] Archin NM, Liberty AL, Kashuba AD, Choudhary SK, Kuruc JD, Crooks AM, et al. Administration of vorinostat disrupts HIV-1 latency in patients on antiretroviral therapy. *Nature.* 2012;487:482–5.
- [346] Archin NM, Bateson R, Tripathy MK, Crooks AM, Yang K-H, Dahl NP, et al. HIV-1 expression within resting CD4+ T cells after multiple doses of vorinostat. *J. Infect. Dis.* 2014;210:728–35.
- [347] Bartholomeeusen K, Xiang Y, Fujinaga K, Peterlin BM. Bromodomain and extra-terminal (BET) bromodomain inhibition activate transcription via transient release of positive transcription elongation factor b (P-TEFb) from 7SK small nuclear ribonucleoprotein. *J. Biol. Chem.* 2012;287:36609–16.
- [348] Falkenberg KJ, Johnstone RW. Histone deacetylases and their inhibitors in cancer, neurological diseases and immune disorders. *Nat. Rev. Drug Discov.* Nature Publishing Group, a division of Macmillan Publishers Limited. All Rights Reserved.; 2014;13:673–91.
- [349] Xing S, Siliciano RF. Targeting HIV latency: pharmacologic strategies toward eradication. *Drug Discov. Today.* Elsevier Ltd; 2013;18:541–51.
- [350] Bernhard W, Barreto K, Saunders A, Dahabieh MS, Johnson P, Sadowski I. The Suv39H1 methyltransferase inhibitor chaetocin causes induction of integrated HIV-1 without producing a T cell response. *FEBS Lett.* 2011;585:3549–54.
- [351] Fernandez G, Zeichner SL. Cell line-dependent variability in HIV activation employing DNMT inhibitors. *Virol. J.* 2010;7:266.
- [352] Blazkova J, Murray D, Justement JS, Funk EK, Nelson AK, Moir S, et al. Paucity of HIV DNA methylation in latently infected, resting CD4+ T cells from infected individuals receiving antiretroviral therapy. *J. Virol.* 2012;86:5390–2.
- [353] Thibault S, Imbeault M, Tardif MR, Tremblay MJ. TLR5 stimulation is sufficient to trigger reactivation of latent HIV-1 provirus in T lymphoid cells and activate virus gene expression in central memory CD4+ T cells. *Virology.* 2009;389:20–5.
- [354] Chang JJ, Altfeld M. Immune activation and the role of TLRs and TLR agonists in the pathogenesis of HIV-1 infection in the humanized mouse model. *J. Infect. Dis.* 2013;208 Suppl :S145–9.
- [355] De Jong MAWP, de Witte L, Oudhoff MJ, Gringhuis SI, Gallay P, Geijtenbeek TBH. TNF-alpha and TLR agonists increase susceptibility to HIV-1 transmission by human Langerhans cells ex vivo. *J. Clin. Invest.* American Society for Clinical Investigation; 2008;118:3440–52.

- [356] Moody MA, Santra S, Vandergrift NA, Sutherland LL, Gurley TC, Drinker MS, et al. Toll-like receptor 7/8 (TLR7/8) and TLR9 agonists cooperate to enhance HIV-1 envelope antibody responses in rhesus macaques. *J. Virol.* 2014;88:3329–39.
- [357] Sanders CM, Cruse JM, Lewis RE. Toll-like receptors, cytokines and HIV-1. *Exp. Mol. Pathol.* 2008;84:31–6.
- [358] De Nardo D. Toll-like receptors: Activation, signalling and transcriptional modulation. *Cytokine.* 2015;74:181–9.
- [359] Winckelmann AA, Munk-Petersen L V, Rasmussen TA, Melchjorsen J, Hjelholt TJ, Montefiori D, et al. Administration of a Toll-like receptor 9 agonist decreases the proviral reservoir in virologically suppressed HIV-infected patients. *PLoS One. Public Library of Science*; 2013;8:e62074.
- [360] Offersen R, Melchjorsen J, Paludan SR, Østergaard L, Tolstrup M, Søgaard OS. TLR9-adjuvanted pneumococcal conjugate vaccine induces antibody-independent memory responses in HIV-infected adults. *Hum. Vaccin. Immunother.* 2012;8:1042–7.
- [361] Scheller C, Ullrich A, Lamla S, Dittmer U, Rethwilm A, Koutsilieri E. Dual activity of phosphorothioate CpG oligodeoxynucleotides on HIV: reactivation of latent provirus and inhibition of productive infection in human T cells. *Ann. N. Y. Acad. Sci.* 2006;1091:540–7.
- [362] Scheller C, Ullrich A, McPherson K, Hefele B, Knöferle J, Lamla S, et al. CpG oligodeoxynucleotides activate HIV replication in latently infected human T cells. *J. Biol. Chem.* 2004;279:21897–902.
- [363] Søgaard OS, Lohse N, Harboe ZB, Offersen R, Bukh AR, Davis HL, et al. Improving the immunogenicity of pneumococcal conjugate vaccine in HIV-infected adults with a toll-like receptor 9 agonist adjuvant: a randomized, controlled trial. *Clin. Infect. Dis.* 2010;51:42–50.
- [364] Sloan DD, Irrinki A, Tsai A, Kaur J, Lalezari J, Murry J, et al. TLR7 Agonist GS-9620 Activates HIV-1 in PBMCs From HIV-Infected Patients on cART. *Conf. Retroviruses Opportunistic Infect.* 2015, Bost. Massachusetts. 2015. p. P – F7, 417.
- [365] Whitney JB, Lim S-Y, Osuna CE, Sanisetty S, Barnes TL, Hraber PT, et al. Treatment With a TLR7 Agonist Induces Transient Viremia in SIV-Infected ART-Suppressed Monkeys. *Conf. Retroviruses Opportunistic Infect.* 2015, Bost. Massachusetts. 2015. p. O – 9, 108.
- [366] Antoni BA, Rabson AB, Kinter A, Bodkin M, Poli G. NF-kappa B-dependent and -independent pathways of HIV activation in a chronically infected T cell line. *Virology.* 1994;202:684–94.
- [367] Contreras X, Barboric M, Lenasi T, Peterlin BM. HMBA releases P-TEFb from HEX-IM1 and 7SK snRNA via PI3K/Akt and activates HIV transcription. *PLoS Pathog.* 2007;3:1459–69.

- [368] Choudhary SK, Archin NM, Margolis DM. Hexamethylbisacetamide and disruption of human immunodeficiency virus type 1 latency in CD4(+) T cells. *J. Infect. Dis.* 2008;197:1162–70.
- [369] Klichko V, Archin N, Kaur R, Lehrman G, Margolis D. Hexamethylbisacetamide remodels the human immunodeficiency virus type 1 (HIV-1) promoter and induces Tat-independent HIV-1 expression but blunts cell activation. *J. Virol.* 2006;80:4570–9.
- [370] Pérez M, de Vinuesa AG, Sanchez-Duffhues G, Marquez N, Bellido ML, Muñoz-Fernandez MA, et al. Bryostatin-1 synergizes with histone deacetylase inhibitors to reactivate HIV-1 from latency. *Curr. HIV Res.* 2010;8:418–29.
- [371] Biancotto A, Grivel J-C, Gondois-Rey F, Bettendroffer L, Vigne R, Brown S, et al. Dual role of prostratin in inhibition of infection and reactivation of human immunodeficiency virus from latency in primary blood lymphocytes and lymphoid tissue. *J. Virol.* 2004;78:10507–15.
- [372] Wang P, Qu X, Wang X, Liu L, Zhu X, Zeng H, et al. As2O3 synergistically reactivate latent HIV-1 by induction of NF- $\kappa$ B. *Antiviral Res.* 2013. p. 688–97.
- [373] Mochly-Rosen D, Khaner H, Lopez J. Identification of intracellular receptor proteins for activated protein kinase C. *Proc. Natl. Acad. Sci.* 1991;88:3997–4000.
- [374] Trushin SA, Bren GD, Asin S, Pennington KN, Paya C V, Badley AD. Human immunodeficiency virus reactivation by phorbol esters or T-cell receptor ligation requires both PKC $\alpha$  and PKC $\theta$ . *J. Virol.* 2005;79:9821–30.
- [375] Colin L, Vandenhoult N, de Walque S, Van Driessche B, Bergamaschi A, Martinelli V, et al. The AP-1 binding sites located in the pol gene intragenic regulatory region of HIV-1 are important for viral replication. *PLoS One. Public Library of Science;* 2011;6:e19084.
- [376] Hirsch I, Caux C, Hasan U, Bendriss-Vermare N, Olive D. Impaired Toll-like receptor 7 and 9 signaling: from chronic viral infections to cancer. *Trends Immunol.* 2010;31:391–7.
- [377] Chang JJ, Altfeld M. Immune activation and the role of TLRs and TLR agonists in the pathogenesis of HIV-1 infection in the humanized mouse model. *J. Infect. Dis.* 2013;208 Suppl :S145–9.
- [378] Gallastegui E, Marshall B, Vidal D, Sanchez-Duffhues G, Collado JA, Alvarez-Fernández C, et al. Combination of biological screening in a cellular model of viral latency and virtual screening identifies novel compounds that reactivate HIV-1. *J. Virol.* 2012;86:3795–808.
- [379] Das B, Dobrowolski C, Mao H, Powell D, Miller M, Hazuda D, et al. Farnesyl transferase: A new target for eradication of latent HIV-1 provirus in jurkat T-cells. *Proc. 6th Int. Work. HIV Persistence Dur. Ther. Miami, FL, USA, 3–6 December 2013.* 2013.

- [380] Hazuda D, Barnard R, Wolkenberg S, Powell D, Karn J, Das B, et al. HIV latency drug discovery: Optimizing drugs to induce latent HIV expression. Proc. 6th Int. Work. HIV Persistence Dur. Ther. Miami, FL, USA, 3–6 December 2013. 2013;
- [381] Rafati H, LeMasters E, Lennert VDD, El-Sayyed M, Boucher C, Vries R, et al. Activation of the Wnt pathway by natural ligands or small molecule inhibitors activates latent HIV. Proc. 7th IAS Conf. HIV Pathog. Treat. Prev. (IAS), Kuala Lumpur, Malaysia, 30 June–3 July 2013.
- [382] Sheridan PL, Sheline CT, Cannon K, Voz ML, Pazin MJ, Kadonaga JT, et al. Activation of the HIV-1 enhancer by the LEF-1 HMG protein on nucleosome-assembled DNA in vitro. *Genes Dev.* 1995;9:2090–104.
- [383] McKnight RF, Adida M, Budge K, Stockton S, Goodwin GM, Geddes JR. Lithium toxicity profile: a systematic review and meta-analysis. *Lancet.* 2012;379:721–8.
- [384] Oruch R, Elderbi MA, Khattab HA, Pryme IF, Lund A. Lithium: a review of pharmacology, clinical uses, and toxicity. *Eur. J. Pharmacol.* 2014;740:464–73.
- [385] Dykhuizen EC, Carmody LC, Tolliday N, Crabtree GR, Palmer M a J. Screening for inhibitors of an essential chromatin remodeler in mouse embryonic stem cells by monitoring transcriptional regulation. *J. Biomol. Screen.* 2012;17:1221–30.
- [386] Stoszko; M, Crignis; E De, Khalid; MM, Lungu; C, Palstra; R-J, Dykhuizen; EC, et al. Small molecule inhibitors of BAF; a new family of compounds in HIV latency reversal Article. *EBioMedicine.* 2015, submitted.
- [387] Roth MD, Tashkin DP, Choi R, Jamieson BD, Zack JA, Baldwin GC. Cocaine Enhances Human Immunodeficiency Virus Replication in a Model of Severe Combined Immunodeficient Mice Implanted with Human Peripheral Blood Leukocytes. *J. Infect. Dis.* 2002;185:701–5.
- [388] Bagasra O, Pomerantz RJ. Human immunodeficiency virus type 1 replication in peripheral blood mononuclear cells in the presence of cocaine. *J. Infect. Dis.* 1993;168:1157–64.
- [389] Peterson PK, Gekker G, Chao CC, Schut R, Molitor TW, Balfour HH. Cocaine potentiates HIV-1 replication in human peripheral blood mononuclear cell cocultures. Involvement of transforming growth factor-beta. *J. Immunol.* 1991;146:81–4.
- [390] Sahu G, Farley K, El-Hage N, Aiamkitsumrit B, Fassnacht R, Kashanchi F, et al. Cocaine promotes both initiation and elongation phase of HIV-1 transcription by activating NF- $\kappa$ B and MSK1 and inducing selective epigenetic modifications at HIV-1 LTR. *Virology.* 2015;483:185–202.
- [391] Imai K, Yamada K, Tamura M, Ochiai K, Okamoto T. Reactivation of latent HIV-1 by a wide variety of butyric acid-producing bacteria. *Cell. Mol. Life Sci.* 2012;69:2583–92.



- [392] Ye F, Karn J. Bacterial Short Chain Fatty Acids Push All The Buttons Needed To Re-activate Latent Viruses. *Stem cell epigenetics*. 2015;2.
- [393] Shirakawa K, Chavez L, Hakre S, Calvanese V, Verdin E. Reactivation of latent HIV by histone deacetylase inhibitors. *Trends Microbiol. Elsevier Ltd*; 2013;21:277–85.
- [394] Wherry EJ, Blattman JN, Murali-Krishna K, van der Most R, Ahmed R. Viral persistence alters CD8 T-cell immunodominance and tissue distribution and results in distinct stages of functional impairment. *J. Virol.* 2003;77:4911–27.
- [395] Khaitan A, Unutmaz D. Revisiting immune exhaustion during HIV infection. *Curr. HIV/AIDS Rep.* 2011;8:4–11.
- [396] Palmer BE, Neff CP, Lecureux J, Ehler A, Dsouza M, Remling-Mulder L, et al. In vivo blockade of the PD-1 receptor suppresses HIV-1 viral loads and improves CD4+ T cell levels in humanized mice. *J. Immunol.* 2013;190:211–9.
- [397] (NIAID) NI of A and ID. Safety and Immune Response of BMS-936559 in HIV-Infected People Taking Combination Antiretroviral Therapy. 2015.
- [398] Migueles SA, Osborne CM, Royce C, Compton AA, Joshi RP, Weeks KA, et al. Lytic granule loading of CD8+ T cells is required for HIV-infected cell elimination associated with immune control. *Immunity*. 2008;29:1009–21.
- [399] Shan L, Deng K, Shroff NS, Durand CM, Rabi SA, Yang H-C, et al. Stimulation of HIV-1-specific cytolytic T lymphocytes facilitates elimination of latent viral reservoir after virus reactivation. *Immunity*. 2012;36:491–501.
- [400] Hansen SG, Ford JC, Lewis MS, Ventura AB, Hughes CM, Coyne-Johnson L, et al. Profound early control of highly pathogenic SIV by an effector memory T-cell vaccine. *Nature*. 2011;473:523–7.
- [401] Hansen SG, Piatak M, Ventura AB, Hughes CM, Gilbride RM, Ford JC, et al. Immune clearance of highly pathogenic SIV infection. *Nature*. 2013;502:100–4.
- [402] Hansen SG, Sacha JB, Hughes CM, Ford JC, Burwitz BJ, Scholz I, et al. Cytomegalovirus vectors violate CD8+ T cell epitope recognition paradigms. *Science*. 2013;340:1237874.
- [403] Barouch DH, Whitney JB, Moldt B, Klein F, Oliveira TY, Liu J, et al. Therapeutic efficacy of potent neutralizing HIV-1-specific monoclonal antibodies in SHIV-infected rhesus monkeys. *Nature*.; 2013;503:224–8.
- [404] Barouch DH, Stephenson KE, Borducchi EN, Smith K, Stanley K, McNally AG, et al. Protective efficacy of a global HIV-1 mosaic vaccine against heterologous SHIV challenges in rhesus monkeys. *Cell*. 2013;155:531–9.
- [405] Klein F, Halper-Stromberg A, Horwitz JA, Gruell H, Scheid JF, Bournazos S, et al. HIV therapy by a combination of broadly neutralizing antibodies in humanized mice. *Nature*. 2012;492:118–22.



- [406] Shingai M, Nishimura Y, Klein F, Mouquet H, Donau OK, Plishka R, et al. Antibody-mediated immunotherapy of macaques chronically infected with SHIV suppresses viraemia. *Nature*. 2013;503:277–80.
- [407] Lehrman G, Hogue IB, Palmer S, Jennings C, Spina C a, Wiegand A, et al. Depletion of latent HIV-1 infection in vivo: a proof-of-concept study. *Lancet*. 2005;366:549–55.
- [408] Steel A, Clark S, Teo I, Shaunak S, Nelson M, Gazzard B, et al. No change to HIV-1 latency with valproate therapy. *AIDS*. 2006;20:1681–2.
- [409] Siliciano JD, Lai J, Callender M, Pitt E, Zhang H, Margolick JB, et al. Stability of the latent reservoir for HIV-1 in patients receiving valproic acid. *J. Infect. Dis*. 2007;195:833–6.
- [410] Archin NM, Eron JJ, Palmer S, Hartmann-Duff A, Martinson JA, Wiegand A, et al. Valproic acid without intensified antiviral therapy has limited impact on persistent HIV infection of resting CD4+ T cells. *AIDS*. 2008;22:1131–5.
- [411] Archin NM, Cheema M, Parker D, Wiegand A, Bosch RJ, Coffin JM, et al. Antiretroviral intensification and valproic acid lack sustained effect on residual HIV-1 viremia or resting CD4+ cell infection. *PLoS One*. 2010;5:e9390.
- [412] Sagot-Lerolle N, Lamine A, Chaix M-L, Boufassa F, Aboulker J-P, Costagliola D, et al. Prolonged valproic acid treatment does not reduce the size of latent HIV reservoir. *AIDS*. 2008;22:1125–9.



# Chapter 1

## General introduction

II.

**A broad drug arsenal to attack a strenuous latent HIV reservoir.**

**Mateusz Stoszko**, Enrico Ne and Tokameh Mahmoudi

Published: Current opinions in Virology 2019. 38, 37–53. [doi.org/10.1016/J.COVIRO.2019.06.001](https://doi.org/10.1016/J.COVIRO.2019.06.001)





# A broad drug arsenal to attack a strenuous latent HIV reservoir

Mateusz Stoszko<sup>1,3</sup>, Enrico Ne<sup>1,3</sup>, Erik Abner<sup>2</sup> and Tokameh Mahmoudi<sup>1</sup>

HIV cure is impeded by the persistence of a strenuous reservoir of latent but replication competent infected cells, which remain unsusceptible to c-ART and unrecognized by the immune system for elimination. Ongoing progress in understanding the molecular mechanisms that control HIV transcription and latency has led to the development of strategies to either permanently inactivate the latent HIV infected reservoir of cells or to stimulate the virus to emerge out of latency, coupled to either induction of death in the infected reactivated cell or its clearance by the immune system. This review focuses on the currently explored and non-exclusive pharmacological strategies and their molecular targets that 1. stimulate reversal of HIV latency in infected cells by targeting distinct steps in the HIV-1 gene expression cycle, 2. exploit mechanisms that promote cell death and apoptosis to render the infected cell harboring reactivated virus more susceptible to death and/or elimination by the immune system, and 3. permanently inactivate any remaining latently infected cells such that c-ART can be safely discontinued.

## Addresses

<sup>1</sup> Department of Biochemistry, Erasmus University Medical Center, Ee634 PO Box 2040, 3000CA, Rotterdam, The Netherlands

<sup>2</sup> Institute of Genomics, University of Tartu, Tartu, Estonia

Corresponding author:

Mahmoudi, Tokameh ([t.mahmoudi@erasmusmc.nl](mailto:t.mahmoudi@erasmusmc.nl))

<sup>3</sup> These authors contributed equally.

**Current Opinion in Virology** 2019, **38**:37–53

This review comes from a themed issue on **Engineering for viral resistance**

Edited by **Ben Berkhout** and **Liang Chen**

<https://doi.org/10.1016/j.coviro.2019.06.001>

1879-6257/© 2019 The Authors. Published by Elsevier B.V. This is an open access article under the CC BY license (<http://creativecommons.org/licenses/by/4.0/>).

## Introduction

Millions worldwide are infected with HIV and depend on daily antiretrovirals for survival. Combination antiretroviral therapy (cART) suppresses HIV replication and halts disease progression. However, a small reservoir of replication-competent virus lingers in long-lived resting memory CD4<sup>+</sup>T cells, which, because the virus is in a latent state, are not targeted by cART [1]. Persistence of these cells leads to

inevitable rebound of viral replication once cART is interrupted and constitutes a roadblock to cure. Viable HIV cure dictates either elimination of the latent reservoir or its permanent containment such that cART can be safely discontinued. Ongoing progress in molecular understanding of HIV latency has led to development of pharmacological strategies that target the latent HIV infected cell reservoir (Figure 1). While ‘block and lock’ [2<sup>\*</sup>] relies on permanent suppression of latent virus, other approaches aim to reverse HIV-1 latency in infected cells via latency reversal agents (LRAs) [3] such that either cell death is induced, or HIV infected cells are ‘seen’ and eliminated by an immune response. This review focuses on the arsenal of pharmacological agents and mechanisms they exploit to target the reservoir for latency reversal, permanent inactivation, and/or cell death. Other important strategies not discussed include the breadth of interventions to boost HIV-specific immunity for viral elimination [4–7].

## Pipeline of latency reversal agents (LRAs)

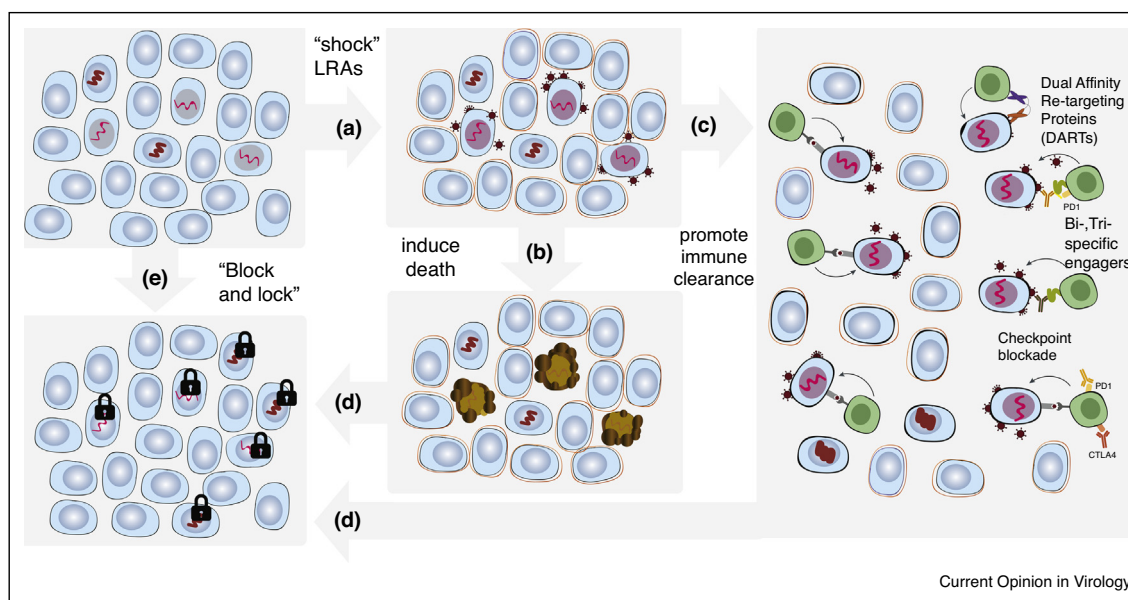
Following integration, transcription at the proviral promoter or 5′ long terminal repeat (5′LTR) is controlled by the host transcription machinery and influenced by surrounding chromatin landscape [8]. Regardless of genomic position, 5′LTR latent structure is defined by Nucleosome-0 (Nuc0) connected by a stretch of accessible DNA (HSS1) to the strictly positioned repressive Nuc1 downstream of the transcription start site (TSS), which is remodeled upon activation (Figure 2a) [8,12,15]. HIV-1 transcription is initiated by engagement of inducible sequence-specific transcription factors (TFs) and associated cofactors at the 5′LTR, controlling accessibility to RNA Polymerase II (Pol II) and permissiveness to transcription (Figure 2). Under basal conditions transcription is initiated but Pol II pauses, producing short transcripts [9,12,15]. The HIV transactivator Tat, a major determinant of reactivation from latency, when expressed, recruits the positive transcription elongation factor (PTEFb) to the nascent TAR RNA, releases Pol II pausing, activating transcription elongation [8,12,15]. HIV-1 expression is also restricted post-transcriptionally via previously underappreciated mechanisms that can also be explored pharmacologically to modulate latency [10,11].

## De-repressors: pharmacological interventions that counter repressive chromatin

### Targeting PTMs

A broad category of LRAs affect post-translational modifications (PTMs) of N-terminal histone tails, modulating

Figure 1



Pharmacological strategies to target the latent HIV-1 reservoir. **(a)** The inducible fraction of the HIV-1 latent reservoir is 'shocked' with LRAs to induce expression of the provirus. **(b)** Cells expressing viral particles die due to the associated cytotoxicity and via pharmacological interventions that sensitize HIV reactivated cells toward cell death. **(c)** Reactivated cells are also recognized and killed by the immune system which can be strengthened and boosted via a number of strategies including small molecule checkpoint inhibitors that enhance T cell function, bi/tri-specific T cell engagers (BI/TRIES) and dual-affinity re-targeting proteins (DARTs). **(d)** In case of inefficient activation and insufficient clearance of latently infected cells, a deeper state of latency is pharmacologically promoted in the remaining fraction of the reservoir ('block and lock'). **(e)** Efficient 'block and lock' strategies, capable of driving the whole reservoir into a deep latency state, could also, in principle, be used alone without the need of additional interventions.

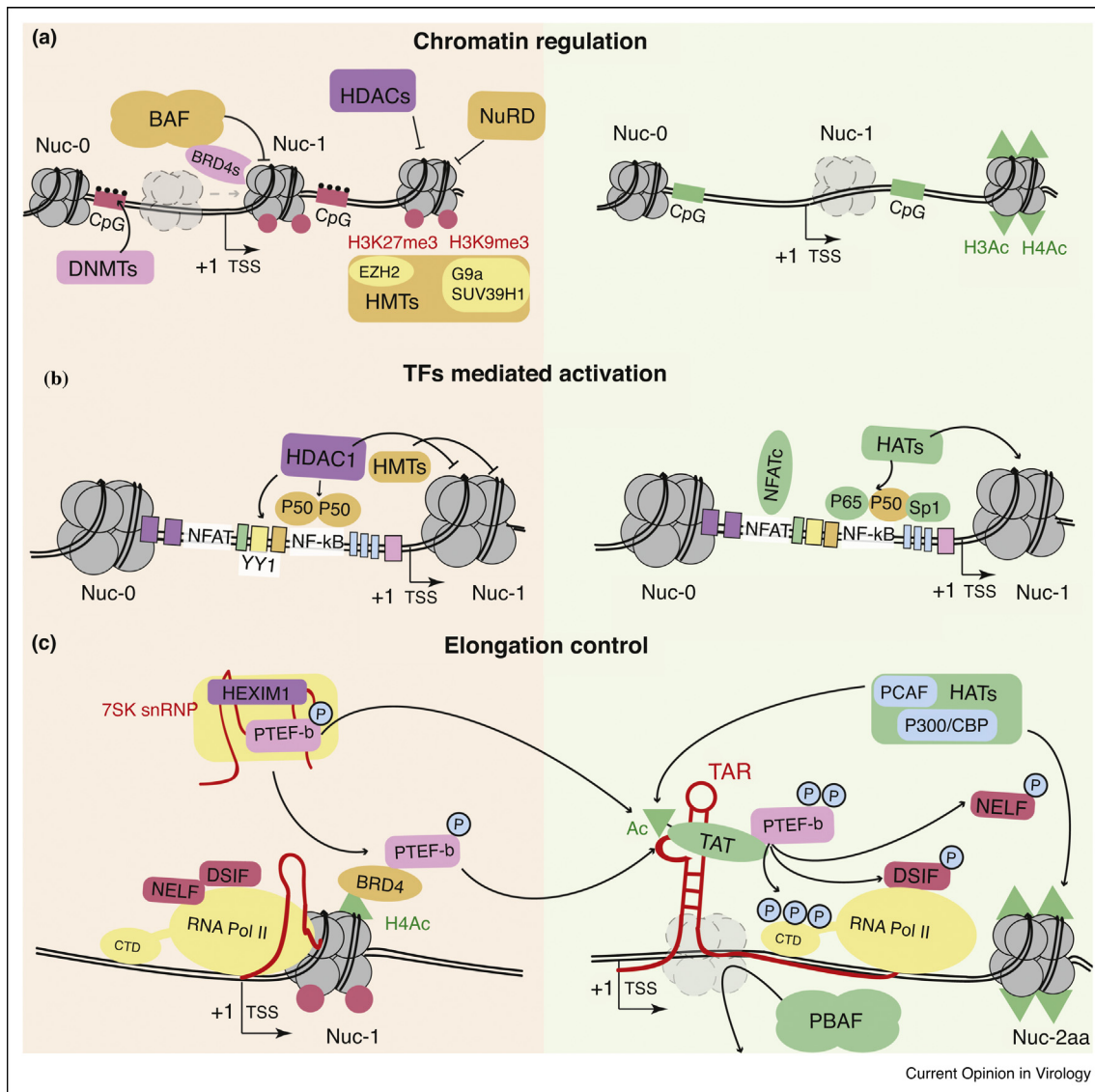
the strength of DNA-nucleosomal core interaction and can serve as marks for recruitment of protein complexes that regulate chromatin structure [12,13]. The best-characterized modification, histone acetylation is deposited by histone acetyltransferases (HATs) and removed by histone deacetylases (HDACs), which are associated with the latent HIV-1 promoter and can be targeted with HDAC inhibitors (HDACis) for derepression [13]. The repressed HIV-1 promoter is also characterized by latency-associated H3K27me3, deposited by polycomb group repressive complex 2 (PRC2) histone methyltransferase (HMT) EZH2, and serves as a mark to recruit other repressors including HDACs, PRC1 and DNA methyltransferases (DNMTs) [14–16]. As well, heterochromatin associated HMTs G9a and Suv39H1-deposited H3K9di/tri-methyl marks [14–16] occupy the latent LTR. A previously underappreciated modification, H4K3 Crotonylation, found to be associated with latency reversal, can be enhanced by sodium crotonate as substrate [17].

**HDACis** Romidepsin, Panobinostat, Vorinostat, and Valproic acid have been extensively studied for their latency reversal potential [18–21]. The metabolite acetate, highly concentrated in the gut and blood, inhibits HDAC activity and boosted HIV replication [22]. Clinical trials

and *in vitro* data have confirmed their sufficient clinical tolerance and effectiveness as LRAs that mechanistically enhance transcriptional noise and synergize with signal-dependent HIV-1 activation [23,8], inducing viral RNA and protein [24]. But clinically, no significant reservoir depletion with HDACis has been observed [18–22]. A multitude of HDACis, targeting all or specific HDAC classes have been developed (Table 1). Class I appear to play a prominent role in latency with Class I HDACis inducing stronger HIV-1 derepression [25,26]. A recent comparison of HDACis pointed to benzamide moiety and pyridyl cap group molecules, such as Chidamide to be most active with least associated cytotoxicity [27].

**HMTis.** The potential of HMTis as LRAs has more recently emerged. Inhibition of SUV39H1 with Chacotocin, or targeting G9a with the quinazoline BIX-01294 and more recently UNC-0638, a BIX-01294 derivative with better toxicity profile, reversed latency in CD4+T cells of suppressed patients [14–16,28]. H4K20 monomethylation, deposited by SMYD2, was linked to HIV-1 latency and its inhibition by AZ391 led to increased cell associated HIV-1 RNA in c-ART treated patient CD4+T cells [29]. Wide spectrum EZH2 HMTis including

Figure 2



Distinct steps in control of the HIV-1 LTR transcription cycle represented in the latent and active states, simplified overview. **(a)** The chromatin architecture of the HIV-1 promoter consists of three strictly positioned nucleosomes (Nuc-0, Nuc-1 and Nuc-2) separated by nucleosome free regions. In the repressed state (left panel), the BAF complex is recruited to the LTR tethered by BRD4S and mediates the positioning of the repressive Nuc-1, downstream of the transcriptional start site (TSS). The latent HIV-1 promoter is also characterized by the presence of repressive cofactors, including HDACs, HMTs and the NuRD complex. **(b)** Upon signal-dependent activation, sequence-specific TFs bind their consensus sites at the HIV-1 5' LTR and mediate the recruitment of RNA Pol II, required for transcription initiation, and HATs, rendering the chromatin more permissive to transcription. **(c)** In basal conditions RNA Pol II processivity is restricted by the activity of negative elongation factors NELF and DSIF which promote the early dissociation of RNA Pol II from the DNA template, and inhibit the production of full length viral RNAs. Additionally, the availability of P-TEFb is restricted by sequestration within the 7SK snRNP complex and by BRD4-dependent chromatin recruitment. Productive infection requires sufficient expression of the viral transactivator Tat that dramatically potentiates transcription elongation. Tat binds TAR, a hairpin loop RNA structure of the nascent transcript, and recruits P-TEFb to the 5' LTR. Within P-TEFb, the kinase activity of CDK9 promotes phosphorylation of NELF, DSIF and the RNA Pol II CTD, hence increasing RNA Pol II processivity. Tat PTMs modulates its association with cellular cofactors including HATs and PBAF, remodeling chromatin and enhancing transcription.

DZNep reactivated latent HIV in cell lines, although with substantial toxicity, while recently, specific EZH2 inhibitors EPZ-6438, GSK-343 more effectively reversed latency in resting CD4<sup>+</sup>T cells from infected individuals [14–16,28\*].

**DNMTis.** HIV 5'LTR CpG methylation promotes binding of methyl-CpG-binding protein (MBD2) and recruitment of the repressive NuRD complex [8]. While the importance of this mechanism *in vivo* has been questioned [8,12,15], sequential treatment with DNMTis and

Table 1

## Pharmacologic interventions to target the latent HIV-1 reservoir

Class	Subclass	Function/Target	Compounds	Experimental system	References (Fully listed in reference list)
Chromatin modulators		ACSS2 agonist	Sodium crotonate (Na-Cro)	A, F	Jiang <i>et al.</i> , 2018
		HMT (SMYD2 inhibitor)	AZ391	A, F	Boehm <i>et al.</i> , 2017
		HMT (G9a inhibitor)	BIX-01294	A	Imai <i>et al.</i> , 2010
		Polycomb (L3MBTL1 inhibitor)	UNC-0638	D, F	Nguyen <i>et al.</i> , 2017
		Polycomb (SUV39H1 inhibitor)	UNC-926	A, F	Boehm <i>et al.</i> , 2017
	Histone methyl transferases inhibitors (HMTis)	Polycomb (EZH1/EZH2 inhibitor)	Chaetocin	A	Bernhard <i>et al.</i> , 2011
		Polycomb (EZH2 inhibitor)	UNC-1999	D	Kobayashi <i>et al.</i> , 2017
			3-deazaneplanocin A (DZNep)	A	Friedman <i>et al.</i> , 2011
			EPZ-6438; GSK-343	A, F	Nguyen <i>et al.</i> , 2017
			CG05; CG06	A	Choi <i>et al.</i> , 2010
			Thiophenyl benzamide (TPB)	A, F	Huang <i>et al.</i> , 2018
			Chidamide	A, F, G (NCT02902185, NCT02513901)	Yang <i>et al.</i> , 2018
			Entinostat	A, F	Wightman <i>et al.</i> , 2013
			Largazoles (SDL148; JMF1080; SDL256)	A, D	Albert <i>et al.</i> , 2017
			Mocetinostat	C	Zaikos <i>et al.</i> , 2018
	HDAC Class I		Romidepsin	D; G (NCT02092116, NCT01933594, NCT02850016, NCT03041012, NCT03619278, NCT02616874, NCT01933594)	Wei <i>et al.</i> , 2014
			Pimelic diphenylamide 106, Pyroxamide	D	Kobayashi <i>et al.</i> , 2017
			Apicidin	A	Lin <i>et al.</i> , 2011
			BRD3308	A, F	Barton <i>et al.</i> , 2014
			Droxinostat	A	Matalon <i>et al.</i> , 2011
			Belinostat	A	Matalon <i>et al.</i> , 2010
			Givinostat	D	Kobayashi <i>et al.</i> , 2017
			KD5170, Pracinostat (SB939)	A	Ying <i>et al.</i> , 2012
			M344	A	Shehu-Xhila <i>et al.</i> , 2009
		(pan)HDAC	Metacept-1; Metacept-2; Oxamflatin	F, G (NCT02471430, NCT01680094)	Bullen <i>et al.</i> , 2014
	Histone deacetylases inhibitors (HDACis)		Panobinostat		



Table 1 (Continued)

Class	Subclass	Function/Target	Compounds	Experimental system	References (Fully listed in reference list)
<b>Chromatin modulators</b>		(pan)HDAC	Psammaplin A	A, E	Richard K <i>et al.</i> , 2018
			Scrpitaid	A	Ying <i>et al.</i> , 2010
			Sodium butyrate (Na-But)	A	Reuse <i>et al.</i> , 2009
			ST7612AA1	E	Badia <i>et al.</i> , 2015
			Trichostatin A (TSA); Trapoxin A (TPX)	A	Van Lint <i>et al.</i> , 1996
	<b>Histone deacetylases inhibitors (HDACis)</b>		Valproic Acid (VPA)	G (NCT03525730, NCT00614458)	Lehman <i>et al.</i> , 2005
			Vorinostat (SAHA)	D, F, G (NCT02336074, NCT03198559, NCT03803605, NCT03212989, NCT03382834, NCT02475915, NCT02707900, NCT01319383)	Contreras <i>et al.</i> , 2009
				D	Kobayashi <i>et al.</i> , 2017
				E	Bolduc <i>et al.</i> , 2017
				D, F, G (NCT03525730)	Stoszko <i>et al.</i> , 2016
<b>Activators of Transcription</b>	<b>BRG-1-associated factors complex inhibitors (BAFis)</b>	SIRT2 inhibitor HDAC/II BAF complex  ARID1A subunit of BAF	AGK2	D	Marian <i>et al.</i> , 2018
			acetate	A, D	Kauder <i>et al.</i> , 2009
			CAPE; MGD-486; Pyrimethamine	A, F	Blazkova <i>et al.</i> , 2009
			Macrolactams	D, E (NCT02191098)	Jones <i>et al.</i> , 2016
			Decitabine (5-aza-2'-deoxycytidine)	F, G (NCT03382834)	Tae-Wook Chun <i>et al.</i> , 1998
	<b>DNA methyltransferases inhibitors (DNMTis)</b>	CD122/CD132  CD122/CD132 CD127/CD132	Zebularine	F, G (NCT01019551)	Wang <i>et al.</i> , J 2005; Katlama <i>et al.</i> , 2016
			ALT-803 (IL-15 superagonist complex)	A, D	Tong-Starkesen <i>et al.</i> , 1989; Spina <i>et al.</i> , 2013
			IL-2, IL-6, TNF $\alpha$	A, F	Abdel-Mohsen <i>et al.</i> , 2016
			CYT107 (recombinant IL-7)	A, D	Spina <i>et al.</i> , 2013
			$\alpha$ CD28	A, D	Calvanese <i>et al.</i> , 2013
<b>Extracellular stimulators</b>		Surface glycans  EGFR inhibitor TCR agonist S1P1 $\alpha$ PD1 antibodies	rGal9 (recombinant Gal9)	C, E, G (NCT02595866, NCT03239899)	Duquenne <i>et al.</i> , 2017
			Phytohemagglutinin (PHA)		Fromentin <i>et al.</i> , 2019
			AG555		
			$\alpha$ CD3		
			S1P1 agonists		

Table 1 (Continued)

Class	Subclass	Function/Target	Compounds	Experimental system	References (Fully listed in reference list)
Activators of transcription			12-deoxyphorbol 13-phenylacetate (DPP)	A	Bocklandt <i>et al.</i> , 2003
			3-(2-Naphthoyl)ingenol	A	Liu <i>et al.</i> , 2018
Protein kinase C agonists (PKC agonists)			Aplysiatoxin;	A, E	Richard <i>et al.</i> , 2018
			Debromoaplysiatoxin	A, D	Marsden <i>et al.</i> , 2018
			Bryostatin-1	G (NCT02269605)	Gutiérrez <i>et al.</i> , 2016
			C3-esterified ingenol derivatives	A, F	Spivak <i>et al.</i> , 2018
			EK-16A	A, F	Wang <i>et al.</i> , 2017
			Euphoria Kansui extract	D, E, G (NCT02531295)	Cary <i>et al.</i> , 2016
			Gnidimacrin	A, E	Huang <i>et al.</i> , 2011; Lai <i>et al.</i> , 2015
			IDB (ingenol 3, 20-dibenzoate)	F	Spivak <i>et al.</i> , 2015
			Ingenol-B (ingenol-3-hexanoate)	D, F	Jiang <i>et al.</i> , 2014; Pandeló José <i>et al.</i> , 2014
			LMC03; LMC07	F	Hamer <i>et al.</i> , 2003
			Namushen-1; Namushen-2	A	Tietjen <i>et al.</i> , 2018
			PEP005 (ingenol-3-angelate)	A, F,	Jiang <i>et al.</i> , 2015
			Phorbol 12-myristate 13-acetate (PMA)	A, D	Folks <i>et al.</i> , 1988; Spina <i>et al.</i> , 2013
			Prostratin	A, E	Gulatosky <i>et al.</i> , 1997; Kulkosky <i>et al.</i> , 2001
			Sesterterpenoids	A	Wang <i>et al.</i> , 2016
			SJ23B	A	Bedoya <i>et al.</i> , 2009
			Pam2CSK4, Pam3CSK4; Imiquimod	D, E	Novis <i>et al.</i> , 2013; Macedo <i>et al.</i> , 2018
			HKLM	A	Alvarez-Carbonell <i>et al.</i> , 2017
Toll-like receptor agonists		TLR1/2	PIM6	D	Rodriguez <i>et al.</i> , 2013
			Poly-ICLC	A, G (NCT02071095)	Alvarez-Carbonell <i>et al.</i> , 2017
		TLR2	CL413	D, E	Macedo <i>et al.</i> , 2018
			Flagellin	A	Thibault <i>et al.</i> , 2009
		TLR7/8	R-848	A, C (productive infection)	Schlaepfer <i>et al.</i> , 2006
			vesatolimod (GS- 9620)	E, G (NCT03060447, NCT02858401)	Tsai <i>et al.</i> , 2017
		TLR7	GS-986	H	Lim <i>et al.</i> , 2018
		TLR8	3M-002	A, F	Schlaepfer and Speck, J, 2011; Rochat <i>et al.</i> , 2017

**Table 1 (Continued)**

Class	Subclass	Function/Target	Compounds	Experimental system	References (Fully listed in reference list)
Activators of transcription	Toll-like receptor agonists	TLR9	CPG-7909 MGN1703 CpG oligonucleotides: ODN-2006; ODN-2040 Maraviroc	G (NCT00562939) A, E, G (NCT02443935) A	Winckelmann <i>et al.</i> , 2013 Offersen <i>et al.</i> , 2016 Scheller <i>et al.</i> , 2004
		NF-κB - CCR5		D, G (NCT02486510, NCT02475915, NCT00935480, NCT00808002) A, D A A	López-Huertas <i>et al.</i> , 2017; Madrid-Elena <i>et al.</i> , 2018
		NF-κB NF-κB and MSK1 activation NF-κB activation	Juglone (5HN) Cocaine As2O3 (Arsenic trioxide; FDA-approved drug) Benzotriazoles (HODHBt, HBt, HOBt, HOAt) AV6 Ro5-3335 MCB-613	F F D E A, B	Yang <i>et al.</i> , 2009 Sahu <i>et al.</i> , 2015 Wang <i>et al.</i> , 2013 Bosque <i>et al.</i> , 2017
		STAT5 sumoylation inhibitors NFAT activator RUNX1 inhibitor SRC agonist			Micheva-Viteva <i>et al.</i> , 2011 Klase <i>et al.</i> , 2014 Nikolai <i>et al.</i> , 2017 (8th HIV Persistence during Therapy Workshop) Pan <i>et al.</i> , 2016; Zeng <i>et al.</i> , 2017
		HSF-1 stimulators	Resveratrol; Triacetyl resveratrol	A	Elliott <i>et al.</i> , HIV 2015; Spivak <i>et al.</i> , 2014
		PTEN dysregulation	Disulfiram	D, G (NCT03198559; NCT01286259; NCT01944371, NCT01571466) A A, E A F	Lin <i>et al.</i> , 2018 Doyon <i>et al.</i> , 2014 Shankaran <i>et al.</i> , 2011 Gramatica <i>et al.</i> , 2017 (8th HIV Persistence during Therapy Workshop) Pan <i>et al.</i> , 2016 Siekvitz <i>et al.</i> , 1988; Spina <i>et al.</i> , 2013
		PKA agonist PI3K agonist Heme oxygenase-1 agonist GSK3 inhibitors	Bucladesine (dibutyl-γ-cAMP) Oxoglucine (57704) Heme arginate SB-216763; Tideglusib	A A, E A F	Calvanese <i>et al.</i> , 2013 Oguariri <i>et al.</i> , 2007 Bobardt, Kuo, Galloway, 2019 Pache <i>et al.</i> , 2015
		GADD34 / PP1 inhibitor Calcineurin agonist	Salubrinal Ionomycin	A, F A, D	
		BTk inhibitor Sp1	Terreic acid Hydroxyurea Debio 1143	A A B, F F	
		BIRC2	Birinapant; SBI-0637142; LCL-161		
Inhibitors of apoptosis (IAPs)					

Table 1 (Continued)

Class	Subclass	Function/Target	Compounds	Experimental system	References (Fully listed in reference list)
Transcription elongation control	Inhibition of BET	KAT5 inhibitor	MG-149	D, F	Li <i>et al.</i> , 2018
			8-methoxy-6-methylquinolin-4-ol (MMQO)	D, E	Abner <i>et al.</i> , 2018;
			Apabetalone (RVX-208), PFI-1	A, F	Gallastegui <i>et al.</i> , 2012
			I-BET; I-BET-151; MS-417	A, D	Lu <i>et al.</i> , 2017
			JQ1	D, F	Nilsson <i>et al.</i> , 2016
		BET inhibitors	OTX-015	A, F	Banerjee <i>et al.</i> , 2012
			UMB-136	D, F	Lu <i>et al.</i> , 2016
			Hexamethylene bisacetamide (HMBA)	C, F	Huang <i>et al.</i> , 2017
			HMBA	A, C, D	Vlach and Pitha, 1993;
			Glutoxin	D, F	Klichko <i>et al.</i> , 2005
7SK snRNP	7SK RNA	TAR-LTR	HEXIM	A, C, D	Contreras <i>et al.</i> , 2009; Spina <i>et al.</i> , Pathogens 2013
			7SK RNA	D, F	Stoszko <i>et al.</i> , 8th HIV Persistence during therapy workshop, Miami 2017
			TatR5M4	A, D, F	Geng <i>et al.</i> , 2016
			EXO-Tat	A, D, F	Tang <i>et al.</i> , 2018
			Durvalumab (anti-PD1)	G	NCT03094286
			Cemiplimab (anti-PD1)	G	NCT03787095
			Nivolumab (anti-PD1)	G	NCT02408861
			BMS-936559 (anti-PD1)	G	NCT02028403
			Pembrolizumab	F, G case study, N = 1	Fromentin <i>et al.</i> , 2019, NCT02595866
			Ipilimumab (anti-CTLA-4)	E (case study, N = 1); G (NCT02408861, NCT03407105)	Wightman <i>et al.</i> , 2015
Post transcriptional control	SF3B1 inhibitor	SR protein family; SRp20/SRSF3	siRNA	A, D	Kyei <i>et al.</i> , 2018
			Digoxin	C, E	Wong <i>et al.</i> , 2013
			Cardiac glycoside/aglycones	A, C, E	Wong <i>et al.</i> , 2018
			DHA-type compound 9 (1C8)	A	Cheung <i>et al.</i> , 2016
			Clomifene	A	Prado <i>et al.</i> , 2016
			8-Azaguanine, 2-(2-[5-Nitro-2-thienyl]vinyl)quinolone	C, E	Wong <i>et al.</i> , 2013
			LMB, ratiadone A	A	Fieta-Soriano <i>et al.</i> , 2014
			PKF050-638	A	Daelemans <i>et al.</i> , 2002
			ABX464	D, G (NCT02735863, NCT02990325)	Vautrin <i>et al.</i> , 2019; Steens <i>et al.</i> , 2017
			Deferiprone	C, G (NCT02191657)	Saxena <i>et al.</i> , 2016
Miscellaneous	Deoxyhypusyl hydroxylase	CRM1 inhibitors	ABX464	D, G (NCT02735863, NCT02990325)	Vautrin <i>et al.</i> , 2019; Steens <i>et al.</i> , 2017
			Deferiprone	C, G (NCT02191657)	Saxena <i>et al.</i> , 2016
			Deferiprone	C, G (NCT02191657)	Saxena <i>et al.</i> , 2016
			Deferiprone	C, G (NCT02191657)	Saxena <i>et al.</i> , 2016
			Deferiprone	C, G (NCT02191657)	Saxena <i>et al.</i> , 2016
			Deferiprone	C, G (NCT02191657)	Saxena <i>et al.</i> , 2016
			Deferiprone	C, G (NCT02191657)	Saxena <i>et al.</i> , 2016
			Deferiprone	C, G (NCT02191657)	Saxena <i>et al.</i> , 2016
			Deferiprone	C, G (NCT02191657)	Saxena <i>et al.</i> , 2016
			Deferiprone	C, G (NCT02191657)	Saxena <i>et al.</i> , 2016
			Deferiprone	C, G (NCT02191657)	Saxena <i>et al.</i> , 2016

Table 1 (Continued)

Class	Subclass	Function/Target	Compounds	Experimental system	References (Fully listed in reference list)
Miscellaneous	Adenosine reuptake inhibitor	Proteasome inhibitors	Dilazep	A	Calvanese <i>et al.</i> , 2013
			Carfilzomib (CFZ)	A, F	Pan <i>et al.</i> , JBC 2016
	Unknown		MG-132 (ONX-0914/PR-957); Velcade; CLBL	A, D	Miller <i>et al.</i> , 2013
			PR-957 (ONX-0914/MG-132)	A, F	Li <i>et al.</i> , 2018
			Abyssomicin-2	D, F	Leon <i>et al.</i> , 2015
			HHODC	A, E	Kapewangolo <i>et al.</i> , 2017
	Kinase inhibitors	mTOR inhibitors	Piceatannol	A	Elbezanti <i>et al.</i> , 2017 (oral presentation); Zeng <i>et al.</i> , JAF 2017
			PH01; PH02; PH03; PH04; PH05	A, F	Hashemi <i>et al.</i> , 2018
			Quinolin-8-ol derivatives	A, D	Xing <i>et al.</i> , J 2011
			Radical; Pochonin B; Pochonin C	D	Mejia <i>et al.</i> , J 2014
Block and Lock approaches	Tat inhibitor	JAK-STAT inhibitors	Danuserib, PF-3758309	D	Vargas <i>et al.</i> , 2018
			Torin1, pp242 and rapamycin (Sirolimus)	F, G (NCT02440789)	Besnard <i>et al.</i> , 2017
			Didehydro-cortistatin A (dCA)	A, B, F	Mosseu <i>et al.</i> , 2015;
			Triptolide wilfordii	A, G (NCT02219672)	Kessing <i>et al.</i> , 2017
	CDK9 inhibitors	LEDGF/p75 inhibitors	Tofacitinib and ruxolitinib	D, F	Wan and Chen, 2014
			LEDGINS	D	Gavagnano <i>et al.</i> , 2017
			curaxin 100 (CBL0100)	D, E	Vranckx <i>et al.</i> , 2016
			GV1001	A	Jean <i>et al.</i> , 2017
	PKC	Bcl-2 agonists	cyclosporin A	A, D	Kim <i>et al.</i> , 2016
			F07#13	B	Chan <i>et al.</i> , 2013
Induction of cell death	PI3K/Akt inhibitors	SMAC mimetics	FIT-039	A	Van Duyne <i>et al.</i> , 2013
			Panel of inhibitors	A	Okamoto <i>et al.</i> , 2015
			2-fluorophenyl (12 d), flavopiridol analogue	A	Nemeth <i>et al.</i> , 2011
			Benzolactam derivative, BL-V8-310	A, E	Ali <i>et al.</i> , 2009
	BET inhibitor	RIG-I	Apabetalone	A, F	Matsuda <i>et al.</i> , 2019
			Venetoclax, Navitoclax	F	Xuan-xuan Zhang <i>et al.</i> , 2019
			Edelfosine, Perifosine, Miltefosine	A	Campbell <i>et al.</i> , 2015, CROI, conference
			Lancemaside A, Compound K, Arctigenin	A	Lucas <i>et al.</i> , 2010
Induction of cell death	BET inhibitor	RIG-I	Birinapant, GDC-0152, Embelin	F	Kim <i>et al.</i> , 2016
			AZD5582; AT406; BV6; SM164; GDC0152	A, F	Campbell <i>et al.</i> , 2018, Hattori, 2018
			SM-AEG40730, SM-LCL161	A, C	Sampey <i>et al.</i> , 2018
			Acitretin	F	Ashok Kumar <i>et al.</i> , 2019
	BET inhibitor	RIG-I	Panel of inhibitors	A	Li <i>et al.</i> , 2016; Garcia-Vidal <i>et al.</i> [90]
			2-fluorophenyl (12 d), flavopiridol analogue	A	
			Benzolactam derivative, BL-V8-310	A, E	
			Apabetalone	A, F	
	BET inhibitor	RIG-I	Venetoclax, Navitoclax	F	
			Edelfosine, Perifosine, Miltefosine	A	

Table 1 (Continued)

Class	Subclass	Function/Target	Compounds	Experimental system	References (Fully listed in reference list)
Promote cell killing		Bispecific T-cell engaging (BiTE) antibodies	B12; VRC01; CD4(1+2)L17b	C	Brozy <i>et al.</i> , 2018
		Dual-affinity re- targeting (DART)	MGD014 HIVxCD3 HIVxCD3	G A, D, F D, E	NCT03570918 Sung <i>et al.</i> , 2015 Sloan <i>et al.</i> , 2015
Model systems: A – cell lines. B – mouse models. C – <i>ex vivo</i> infected PBMCs. D – <i>ex vivo</i> infected primary CD4+ T cells. E – PBMCs from aviremic participants. F – CD4+ T cells from aviremic participants. G – aviremic participants ( <i>in vivo</i> ).					

HDACis synergized to reactivate HIV-1 in cART treated patient cells [30].

#### Targeting chromatin structure

A major determinant of HIV latency, chromatin, is restructured by the activity of ATP-dependent remodelers. The CHD3 containing NuRD remodeller and related CHD1 repress HIV-1 [8,9]. The INI-1 containing ATP-dependent BAF remodeller is associated with the 5'/LTR and represses HIV-1 by actively positioning Nuc-1 [8]. Interestingly, BRD4S, a short isoform of the bromodomain protein BRD4, tethers BAF to the 5'/LTR, silencing HIV-1 [31]. Such enforced chromatin structure represents a mechanical block for HIV-1 transcription, subject to pharmacological intervention for reversal [8,31,32,33,34].

**BAF inhibitors (BAFis).** Small molecule BAFis re-activated latent HIV-1 in a spectrum of *in vitro* latency models and in c-ART suppressed HIV-1 infected patient CD4+T cells [32]. BAFis CAPE and Pyrimethamine enhance transcriptional noise [34]. When combined with PKC agonists showed significantly increased potency than single treatments, pointing, similar to HDACis, to their potential in combinatorial LRA approaches. Recently, a screen of almost 350 000 compounds led to identification of ARID1A targeting macrolactam scaffold BAFis, which reversed HIV-1 latency in primary CD4+T cells with limited cytotoxicity, representing promising LRAs for clinical investigation [33].

**BET inhibitors (BETis),** in addition to enhancing HIV-1 transcription elongation (Section 'Enhancing HIV-1 transcriptional elongation'), act as derepressors of HIV-1 transcription in a Tat independent manner [8]. BETis inhibited 5'/LTR-bound BRD2, and BRD4S, inducing LTR chromatin derepression in a BAF-dependent manner [8,31]. Small molecule BETis are under development with differing potency and specificity to circumvent clinical limitations of JQ1 (Table 1).

#### Inducing HIV-1 transcription activation

The 5'/LTR contains a plethora of consensus sequences for TFs whose binding leads to HIV-1 5'/LTR recruitment of Pol II and basal TFs [8,12,15] (Figure 2b). NF-κB/p65, arguably the strongest activator of HIV-1 transcription initiation, and molecular effectors that facilitate its binding such as those in the protein kinase C (PKC), TLR, and TNFα signaling pathways, are high potential pharmacological targets for latency reversal [9,35]. AP-1, STAT5 and NFAT are also among important HIV-1 transcription activators [8,9,36].

#### Targeting NFκB

In latent HIV-1 infected resting CD4+T cells, p65 is sequestered in the cytoplasm while the 5'/LTR is repressed by p50 homodimers. Upon canonical NFκB

activation, p65 translocates to the nucleus, binds 5′LTR as a p65/p50 heterodimer and recruits Pol II, HATs, as well as PTEFb, leading to initiation and elongation of HIV transcription [8,9,35]. While an attractive pathway for LRA-based interventions, NFκB signaling is a master regulator of immune and other functions and its pharmacological modulation exposes risks of serious side effects [35]. Interestingly, small molecule mimetics of mitochondria-derived activator of caspases (SMAC mimetics) (Section ‘Inhibitors of IAPs’), activated non-canonical NFκB and binding of RELB/p52 heterodimers to the 5′LTR resulting in latency reversal (Table 1) without causing T cell activation, pointing to non-canonical NFκB as an interesting avenue for further exploration [27,37,38].

**PKC agonists.** A spectrum of drugs targeting the PKC pathway, including Prostratin, Bryostatin-1 and Ingenol activate NFAT, NFκB and AP-1 binding to the 5′LTR (Table 1), leading to strong proviral transcription initiation [18,39–45]. While PKCα and PKCθ stimulation targets HIV-1 [46], most currently available PKC agonists target many PKC isoforms resulting in pleiotropic and consequent toxic effects, highlighting need for novel more specific PKC agonists [18,45,46].

**Maraviroc,** a CCR5 antagonist HIV entry blocker was shown to also reverse latency via NFκB activation [47,48]. Maraviroc induced NFκB phosphorylation and HIV transcription as shown by increased cell associated HIV-1 RNA in patient CD4+ T cells [48]. Maraviroc is attractive for inclusion in pharmacological LRA strategies because of its mechanistic versatility as an LRA and antiviral.

**TLR agonists** have gained much attention due to their multifactorial effects on the HIV-1 reservoir [49–54]. At least ten TLRs are described that function as first line of pathogen recognition and induce innate and adaptive immune defenses. Dual TLR agonists such as CL413 showed potent HIV-1 reactivation via complementary targeting of TLR2 and TLR7, leading to NFκB activation concomitant with TNFα production [49]. MGN1703, a TLR9 agonist induced HIV plasma RNA in 6 of 15 study participants concomitant with increased activation of NK and CD8+T cells, although no reduction in latent reservoir was observed [50]. The TLR7 agonists GS-986 and GS-9620, suggested to also enhance anti-HIV immune effector function, reversed latency in patient cells [51]. These TLR7 agonists also increased plasma HIV-1 RNA concomitant with decreased HIV-1 DNA in the infected rhesus model, where two of nine animals have remained aviremic [52]. Because of this functional versatility, TLR agonists show much promise in reservoir elimination strategies.

#### Other TFs

LRAs can reduce or enhance HIV-1 5′LTR binding of repressive/activating TFs [8,12,15]. Resveratrol

promotes histone acetylation and activation of HSF1, an HIV-1 transcription activator [55]. Benzotriazoles were recently shown to stabilize the active form of STAT5 and reactivate HIV-1 [36].

#### Enhancing HIV-1 transcriptional elongation

Inefficient transcription elongation via promoter-proximal Pol II 5′LTR pausing is a major rate-limiting step in latency reversal [56] (Figure 2c), which is released by Tat; when expressed at sufficient levels, Tat orchestrates a strong positive transcriptional feedback loop [8]. Tat binds TAR and recruits PTEFb, whose CDK9 component phosphorylates the Pol II C-terminal domain (CTD) as well as NELF and DSIF (which promote Pol II dissociation when unphosphorylated), enhancing Pol II processivity. In latent cells, PTEFb is predominantly sequestered within the 7SKsnRNP complex, a ribonucleoprotein scaffold in which PTEFb activity is inhibited [8]. Tat also competes for PTEFb with BRD4, which binds and sequesters PTEFb [9]. To enhance transcription elongation, in addition to PTEFb, Tat recruits a number of other interactors, including chromatin modifiers, whose binding is regulated by deposition and removal of PTMs and these can also be exploited pharmacologically [8,57–59].

**BETis.** Inhibition of BRD4 releases PTEFb, increasing its availability for binding Tat. BETis activate latent HIV in a spectrum of latency models and after treatment of cells from HIV infected patients [60–63] (Table 1). Interestingly, inhibition of the lysine acetyltransferase KAT5 reduced 5′LTR histone H4 acetylation and impaired BRD4 recruitment, similar to BETis, resulting in increased PTEFb pool for Tat reactivation of latent HIV-1 [64]. Thus BETis are promising LRAs that act via a dual mechanism, relieving BRD4S-BAF-mediated LTR repression as well as increasing availability of PTEFb for Tat.

**Compounds disrupting 7SK snRNP.** In resting CD4+T cells the majority of PTEFb is sequestered in an inactive form within the 7SK snRNP complex [8]. Inhibition of the HEXIM subunit of 7SK snRNP by HMBA enhanced PTEFb activity and latency reversal [9,63,65]. We recently found Gliotoxin, a small molecule secreted by *Aspergillus fumigatus* reversed latency in HIV infected patient CD4+T cells by disrupting 7SK snRNP causing PTEFb release and transcription elongation at the HIV LTR (submitted).

**Tat** has remarkable specificity for the HIV 5′LTR and can penetrate cell membranes. In an attenuated form [66], or exosomally delivered [67], Tat activated HIV-1 in CD4+T cells obtained from c-ART suppressed infected individuals and significantly increased the potency of other LRAs. The potential of Tat as a therapeutic vaccine

candidate has also been explored [68] and may play a role in efforts toward reservoir depletion.

**Immune checkpoint (IC) blockers.** PD-1 has been suggested to confer persistence of HIV-1 latency during c-ART, likely via inhibition of signaling pathways that lead to PTEFb activity [69,70]. IC blockers reversed latency in cells obtained from suppressed patients [71], although another study found less robust effects [72]. Further investigation will determine effectiveness of IC blockers as LRAs and/or in alleviating CD8+T cell exhaustion.

### Targeting post transcriptional regulation

Viral proteins were shown to be produced in a small fraction of LRA-reactivated cells which transcribed viral RNA [73<sup>••</sup>]. This points to the presence of post-transcriptional blocks in viral reactivation [56<sup>••</sup>], where HIV-1 RNA is subjected to splicing and polyadenylation and RNA surveillance proteins influence viral RNA metabolism. Lack of polyadenylated mRNA compromises transcript stability, export and HIV-1 protein production while block in splicing decreases HIV-1 expression [10,11,56<sup>••</sup>,74–77]. The significant contribution of post-transcriptional and transcription elongation blocks to efficient HIV latency reversal have only recently come to light. Although these regulatory mechanisms have not been extensively explored in the context of HIV reactivation, effective latency reversal may require interventions that improve viral RNA stability, splicing, export and translation in order to boost viral protein production.

### Pipeline of block and lock agents

On the flip side of reversing latency as a stepping stone to viral elimination, ‘block and lock’ [2<sup>•</sup>] is a functional cure strategy to permanently shut down viral expression, eliminating the need for continued antiviral therapy.

### Tat inhibition

The HIV-1 Tat inhibitor Didehydro-Cortistatin A (dCA) binds Tat and effectively disrupts Tat/TAR axis [78], restricting HIV-1 transcription and replication. dCA treatment was shown to restrict PBAF recruitment while enhancing BAF 5’LTR occupancy and Nuc-1 mediated repression [79]. Consistently, *ex vivo* dCA treatment of CD4+T cells from HIV-1 infected individuals both improved c-ART suppression of infection and led to strengthened 5’LTR chromatin and epigenetic repression, restricting viral reactivation in latently infected cells and leading to a delayed viral rebound after c-ART interruption [2<sup>•</sup>].

### Targeting host factors to reinforce latency

In line with block and lock, compounds targeting host factors DDX3, DDX5, Matrin3, Mov10, splicing factors, UPF proteins, involved in HIV-1 post-transcriptional processing, including inhibitors of mTOR, cardiotonic steroids, SR proteins, inhibit HIV-1 latency reversal

and lead to a block in translation [74–81]. Inhibition of HIV-1 Rev and Rev response element (RRE) association on the viral RNA or the cellular factor CRM1 can block nuclear export of unspliced viral mRNA [82]. ABX464-mediated inhibition of the cap binding complex increased viral splicing, halting production of unspliced RNA required for viral assembly [83]. LEDGINS, molecules that inhibit HIV-1 integrase-LEDGF interaction were described to shift preferential sites of HIV-1 integration out of active transcription units, and retarget HIV into regions refractory to reactivation [84]. Block and lock strategies, similarly to LRAs, can in principle work most effectively in combination; dCA, LEDGINS, compounds that strengthen proviral epigenetic repression, and ultimately modulators of splicing and viral export, may act synergistically to induce a deeper state of latency to delay or permanently suppress viral rebound.

### Inducing cell death

An attractive approach to eliminate HIV-1 emerging out of latency is to pharmacologically target danger sensing, stress and apoptotic pathways in order to induce cell death in LRA-reactivated HIV expressing cells [85]. This would bypass necessity for an anti-HIV immune response to eliminate reactivated cells. To this end, coupling LRA-induced HIV activation with inhibitors of inhibitors of apoptosis (IAPs), stimulation of danger sensing pathways, and indirect triggering of stress by blocking the cell’s physiological processes have drawn much attention as a way to eliminate latently infected cells.

### Inhibitors of IAPs

SMAC mimetics (SMs), molecules which target cell survival factors XIAP and cIAP1/BIRC2 have shown much promise as both LRAs that act through noncanonical NFκB activation as well as compounds that induce apoptosis in HIV-1 infected cells through proteasomal degradation of IAPs. SMs SBI-0637142 and LCL161 down-regulated BIRC2/IAP, leading to proviral transcription [37]. Debio 1143 targets BIRC2 for degradation inducing non-canonical NFκB with subsequent HIV-1 latency reversal in resting CD4+T cell from aviremic participants [86]. SMs birinapant [38], GDC-0152, and embelin induced apoptosis selectively in HIV-1 infected (but not uninfected) central memory CD4+Tcells, leading to their elimination [87<sup>••</sup>]. Benzolactam related compound BL-V8-310 induced apoptosis in HIV infected cells reactivated in a PKC induced manner [44]. Interestingly, *in vitro* treatment with the pro-apoptotic drug Venetoclax, which blocks Bcl-2, followed by anti-CD3/CD28 stimulation resulted in fast decay of productively infected primary T cells *in vitro* and reduction of the latent reservoir *in vitro* [88].

### Stimulation of TLRs and RIG-I-like receptors (RLRs)

When latent HIV is reactivated, TLRs, RLRs and their molecular effectors, act as sensors that trigger NFκB,



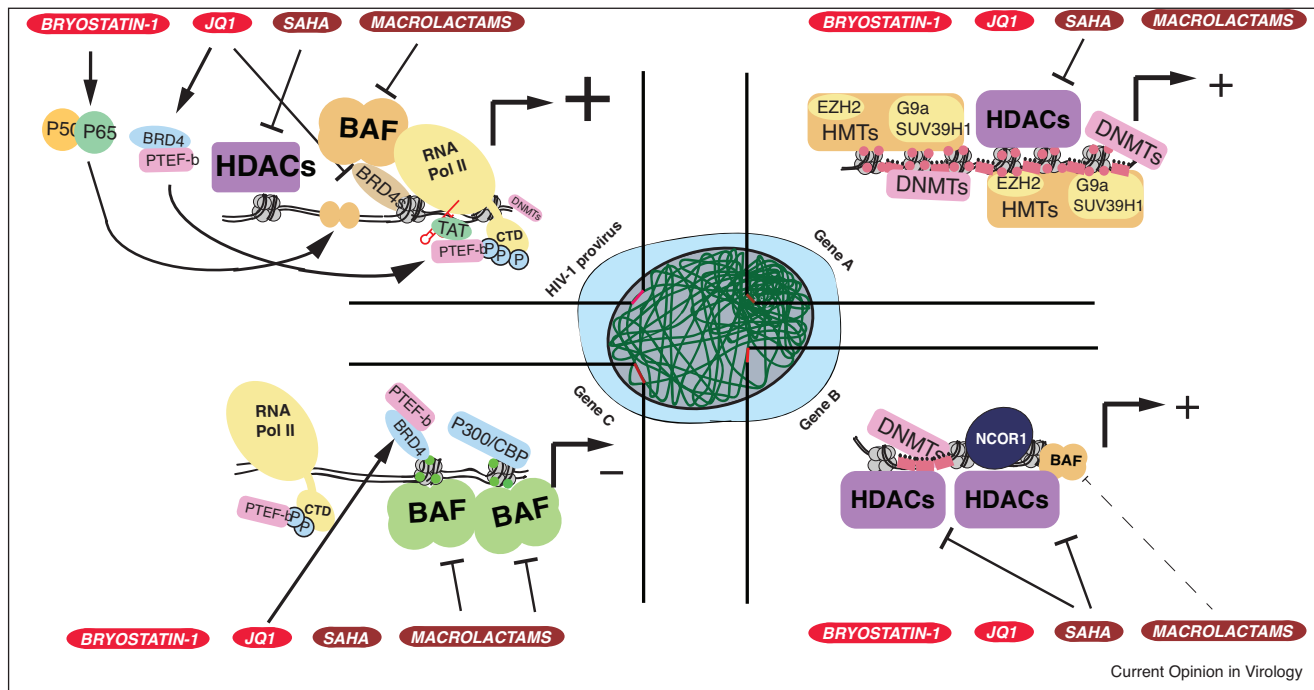
MAP kinase and interferon signaling and initiate an innate immune response. Subsequent to detection of viral RNA, RIG-1 induces apoptosis. Interestingly, retinoic acid (RA) induces expression of RIG-I and p300, which in turn stimulates HIV-1. Acitretin a derivative of RA reversed HIV-1 latency and induced apoptosis in infected cells [89,90]. When combined with Vorinostat even higher depletion of proviral DNA was observed. A later study however challenged these findings showing only weak latency reversal and cell death, pointing to need for further evaluation. TLRs may also play multiple roles, as LRAs, and mediators of HIV-infected cell death [51,54]. A remaining question is whether and which TLRs become activated by HIV-1 transcripts and proteins upon latency reversal.

## Combination, synergism and scalable therapy

Current LRAs reactivate only 5% of latently infected cells [91\*\*], of which only an approximated 2–10% produce viral protein in addition to expressing viral RNA [73\*\*]. Administration of certain LRA combinations in intervals, rather than at once [19,30], stimulated higher proviral expression, while sequential treatment rounds yielded

new infectious particles. These observations point to a limitation in potency of current LRAs as well as transcriptional stochasticity of a diverse and strenuous latent reservoir. The heterogeneous nature of molecular mechanisms controlling HIV latency predicts that a combination of compounds targeting distinct regulatory pathways will be most effective to activate the reservoir. Synergistic effects of LRAs have been shown *ex vivo* [8,9,30,32,33\*,40,43,63]. While ongoing and future clinical trials will shed more light on which mechanisms of latency should be targeted in concert for most robust reversal, mechanistic and preclinical observations point to combinations that include derepressors (eg. Vorinostat, BAFis), activators of NFkB (eg. dual TLR agonists or SMAC mimetics) and activators of transcription elongation (eg. BETis, Gliotoxin) to have high potential. The use of LRAs in combination allows for lower concentrations of each molecule to induce HIV activation. Hence, combinatorial approaches emerge not only as a way to improve the activation efficacy of individual LRAs, but also as a way to govern a level of specificity towards HIV-1 latency reversal, limiting the pleiotropic and toxic effects of each intervention (Figure 3).

### Figure 3



Combinatorial targeting to obtain synergism and selectivity for the HIV promoter to achieve HIV latency reversal with minimal associated pleiotropic effects and cytotoxicity. Combinatorial use of different classes of LRAs (e.g. bryostatins-1, JQ1, Vorinostat and macrolactam scaffold BAFs shown here) may confer specificity for transcriptional reactivation at the latent HIV-1 promoter relative to endogenous genes. The HIV-1 promoter is targeted by the activity of each LRA, which together strongly synergize to re-activate HIV-1 transcription. Gene A, is highly repressed and targeted only by Vorinostat for re-activation, with limited effect. Gene B, predominantly repressed by NCOR1, histone hypoacetylation and DNA methylation, and partially by the repressive BAF is moderately re-activated by the combination of LRAs. Gene C is an actively transcribed gene, dependent on p300, BAF and BRD4 and undergoes partial repression as result of the combination LRAs.

In contrast to antivirals, which target HIV, pharmacological interventions to eliminate the HIV reservoir (Table 1), with the exception of Tat and Tat and Rev-RRE inhibitors, all target host molecular effectors, harbor inherent pleiotropic effects and are subject to variability in response. In this context, pharmacogenetics to investigate the patient-specific response to distinct molecules may identify robust treatments, which synergize at sufficient magnitudes to overrule individual variability, paving the way for scalable therapy options. Importantly, the complex nature of the latent reservoir points to the likelihood of future combinations of nonexclusive pipelines of interventions. For example, potent latency reversal and cell death promoting combination regimens could be used, in presence of c-ART, to activate and eliminate a more reactivatable fraction of the reservoir. Here promoting clearance of latent cells via apoptosis and immune boosting strategies could be used concomitantly to improve reservoir elimination. Upon clearance of this more labile latent reservoir, 'block and lock' regimens may be employed to lock the remaining reservoir in a permanently repressed state. A strengthened immune system would then control the latent virus in case of escape from the blocked state, in combination allowing cessation of c-ART.

## Conflict of interest statement

Nothing declared.

## Acknowledgements

TM received funding from the European Research Council (ERC) under the European Union's Seventh Framework Programme(FP/2007-2013)/ERC STG 337116 Trxn-PURGE, the Dutch AIDS Fonds grant 2014021 and Erasmus MC mRACE research grant.

## References and recommended reading

Papers of particular interest, published within the period of review, have been highlighted as:

- of special interest
- of outstanding interest

1. Siliciano JM, Siliciano RF: **The remarkable stability of the latent reservoir for HIV-1 in resting memory CD4+ T cells.** *J Infect Dis* 2015, **212**:1345-1347.
2. Kessing CF, Nixon CC, Li C, Tsai P, Takata H, Mousseau G, Ho PT, Honeycutt JB, Fallahi M, Trautmann L *et al.*: **In vivo suppression of HIV rebound by Didehydro-Cortistatin A, a "Block-and-Lock" strategy for HIV-1 treatment.** *Cell Rep* 2017, **17**:600-611.
- The authors describe the use of dCA, an inhibitor of Tat-TAR in the 'Block and lock' approach which aims to induce a deep and stable state of HIV-1 latency whereby c-ART could be discontinued.
3. Deeks SG: **HIV: shock and kill.** *Nature* 2012, **25**:439-40.6.
4. Kuhlmann A-S, Peterson CW, Kiem H-P: **Chimeric antigen receptor T-cell approaches to HIV cure.** *Curr Opin HIV AIDS* 2018:446-453.
5. Gao Y, McKay PF, Mann JFS: **Advances in HIV-1 vaccine development.** *Viruses* 2018, **10**.
6. Jones RB, Walker BD: **HIV-specific CD8+T cells and HIV eradication.** *J Clin Invest* 2016, **126**:455-463.
7. Kumar R, Qureshi H, Deshpande S, Bhattacharya J: **Broadly neutralizing antibodies in HIV-1 treatment and prevention.** *Ther Adv Vaccines Immunother* 2018, **6**:61-68.
8. Ne E, Palstra RJ, Mahmoudi T: **Transcription: insights from the HIV-1 promoter.** *Int Rev Cell Mol Biol* 2018, **335**:191-243.
9. De Crignis E, Mahmoudi T: **The multifaceted contributions of chromatin to HIV-1 integration, transcription, and latency.** *Int Rev Cell Mol Biol* 2017, **328**:197-252.11.
10. Sarracino A, Marcello A: **The relevance of post-transcriptional mechanisms in HIV latency reversal.** *Curr Pharm Des* 2017, **23**.
11. Baxter AE, O'Doherty U, Kaufmann DE: **Beyond the replication-competent HIV reservoir: transcription and translation-competent reservoirs.** *Retrovirology* 2018, **15**:18.
12. Cary DC, Fujinaga K, Peterlin BM, Barre-Sinoussi F, Alison M, Sanchez-Pescador R *et al.*: **Molecular mechanisms of HIV latency.** *J Clin Invest* 2016, **126**:448-454.
13. Margolis DM, Archin NM: **Proviral latency, persistent human immunodeficiency virus infection, and the development of latency reversing agents.** *J Infect Dis* 2017, **215**:S111-S118.
14. Khan S, Iqbal M, Tariq M, Baig SM, Abbas W: **Epigenetic regulation of HIV-1 latency: focus on polycomb group (PcG) proteins.** *Clin Epigenet* 2018, **5**:14.
15. Mbonye U, Karn J: **The molecular basis for human immunodeficiency virus latency.** *Annu Rev Virol* 2017, **29**:261-285.
16. Boehm D, Ott M: **Host methyltransferases and demethylases: potential new epigenetic targets for HIV cure strategies and beyond.** *AIDS Res Hum Retrovirus* 2017, **33**:S8-S22.
17. Jiang G, Nguyen D, Archin NM, Yuki SA, Méndez-Lagares G, Tang Y, Elsheikh MM, Thompson GR 3rd, Hartigan-O'Connor DJ, Margolis DM *et al.*: **HIV latency is reversed by ACSS2-driven histone crotonylation.** *J Clin Invest* 2018, **128**:1190-1198.
18. Rasmussen TA, Søgaard OS: **Clinical interventions in HIV cure research.** *Adv Exp Med Biol* 2018, **1075**:285-318.
19. Archin NM, Kirchherr JL, Sung JA, Clutton G, Sholtis K, Xu Y, Allard B, Stuelke E, Kashuba AD, Kuruc JD *et al.*: **Interval dosing with the HDAC inhibitor vorinostat effectively reverses HIV latency.** *J Clin Invest* 2017, **1**:3126-3135.
20. Brinkmann CR, Højen JF, Rasmussen TA, Kjær AS, Olesen R, Denton PW, Østergaard L, Ouyang Z, Lichterfeld M, Yu X *et al.*: **Treatment of HIV-infected individuals with the histone deacetylase inhibitor panobinostat results in increased numbers of regulatory T cells and limits ex vivo lipopolysaccharide-induced inflammatory responses.** *mSphere* 2018, **14** pii: e00616-17.
21. Spivak AM, Planelles V: **Novel latency reversal agents for HIV-1 cure.** *Annu Rev Med* 2017, **69** annurev-med-052716-031710.
22. Bolduc JF, Hany L, Barat C, Ouellet M, Tremblay MJ: **Epigenetic metabolite acetate inhibits class I/II histone deacetylases, promotes histone acetylation, and increases HIV-1 integration in CD4+ T cells.** *J Virol* 2017, **91** e01943-16.
23. Dar RD, Hosmane NN, Arkin MR, Siliciano RF, Weinberger LS: **Screening for noise in gene expression identifies drug synergies.** *Science* 2014, **344**:1392-1396.
24. Wu G, Swanson M, Talla A, Graham D, Strizki J, Gorman D, Barnard RJO, Blair W, Søgaard OS, Tolstrup M *et al.*: **HDAC inhibition induces HIV-1 protein and enables immune-based clearance following latency reversal.** *JCI Insight* 2017, **2**: e92901.
25. Albert BJ, Niu A, Ramani R, Marshall GR, Wender PA, Williams RM, Ratner L, Barnes AB, Kyei GB: **Combinations of isoform-targeted histone deacetylase inhibitors and bryostatin analogues display remarkable potency to activate latent HIV without global T-cell activation.** *Sci Rep* 2017, **7** 7456.38.
26. Zaikos TD, Painter MM, Sebastian Kettinger NT, Terry VH, Collins KL: **Class 1-Selective Histone Deacetylase (HDAC) inhibitors enhance HIV latency reversal while preserving the**

**activity of HDAC isoforms necessary for maximal HIV gene expression.** *J Virol* 2018, **92** e02110-17.

The authors demonstrate that specific class I HDACs more potently reverse latency, alone or in synergy with other LRAs, than pan-HDACs. They provide evidence that certain non-class I HDACs support the activity of factors required for proviral activation thus explaining the limited potency of pan-HDACs.

27. Kobayashi Y, Gélinas C, Dougherty JP: **HDAC inhibitors containing a benzamide functional group and a Pyridyl cap are preferentially effective HIV-1 latency reversing agents in primary resting CD4+ T cells.** *J Gen Virol* 2017:799-809.
28. Nguyen K, Das B, Dobrowolski C, Karn J: **Multiple histone lysine methyltransferases are required for the establishment and maintenance of HIV-1 latency.** *mBio* 2017, **28** e00133-17.  
The authors provide a thorough characterization of the histone lysine methyltransferases implicated in HIV-1 latency establishment and maintenance and propose novel epigenetic drugs for use in latency reversal strategies.
29. Boehm D, Jeng M, Camus G, Gramatica A, Schwarzer R, Johnson JR, Hull PA, Montano M, Sakane N, Pagans S et al.: **SMYD2-mediated histone methylation contributes to HIV-1 latency.** *Cell Host Microbe* 2017, **21**:569-579.e6.
30. Bouchat S, Delacourt N, Kula A, Darcis G, Van Driessche B, Corazza F, Gatot JS, Melard A, Vanhulle C, Kabeya K et al.: **Sequential treatment with 5-aza-2'-deoxycytidine and deacetylase inhibitors reactivates HIV-1.** *EMBO Mol Med* 2016, **8**:117-138.
31. Conrad RJ, Fozouni P, Thomas S, Sy H, Zhang Q, Zhou MM, Ott M: **The short isoform of BRD4 promotes HIV-1 latency by engaging repressive SWI/SNF chromatin-remodeling complexes.** *Mol Cell* 2017, **67**:1001-1012.e6.  
The authors show that a short BRD4 isoform tethers the repressive BAF complex to the LTR, and that JQ1 leads to a BAF-dependent remodeling of the latent HIV LTR.
32. Stoszko M, De Crignis E, Rokx C, Khalid MM, Lungu C, Palstra RJ, Kan TW, Boucher C, Verbon A, Dykhuizen EC, Mahmoudi T: **Small molecule inhibitors of BAF; a promising family of compounds in HIV-1 latency reversal.** *BioMedicine* 2015, **27**:108-121.
33. Marian CA, Stoszko M, Wang L, Leighty MW, de Crignis E, Maschinot CA, Gatchalian J, Carter BC, Chowdhury B, Hargreaves DC et al.: **Small molecule targeting of specific BAF (mSWI/SNF) complexes for HIV latency reversal.** *Cell Chem Biol* 2018, **25**:1443-1455.e14.  
The authors describe identification, from a screen of 350 000 molecules, a macrolactam scaffold class of small molecules that target and inhibit the ARID1a subunit of the BAF complex and reverse HIV latency with less associated cytotoxicity.
34. Megaridis MR, Lu Y, Tevonian EN, Junger KM, Moy JM, Bohn-Wippert K, Dar RD: **Fine-tuning of noise in gene expression with nucleosome remodeling.** *APL Bioeng* 2018, **2**:026106.
35. Jiang G, Dandekar S: **Targeting NF-κB signaling with protein kinase C agonists as an emerging strategy for combating HIV latency.** *AIDS Res Hum Retroviruses* 2015, **31**:4-12.
36. Bosque A, Nilson KA, Macedo AB, Spivak AM, Archin NM, Van Wagoner RM, Martins LJ, Novis CL, Szaniawski MA, Ireland CM et al.: **Benzotriazoles reactivate latent HIV-1 through inactivation of STAT5 SUMOylation.** *Cell Rep* 2017, **18**:1324-1334.
37. Pache L, Dutra MS, Spivak AM, Marlett JM, Murry JP, Hwang Y, Maestre AM, Manganaro L, Vámos M, Teriete P et al.: **BIRC2/cIAP1 is a negative regulator of HIV-1 transcription and can be targeted by Smac mimetics to promote reversal of viral latency.** *Cell Host Microbe* 2015, **18**:345-353.
38. Hattori SI, Matsuda K, Tsuchiya K, Gatanaga H, Oka S, Yoshimura K, Mitsuya H, Maeda K: **Combination of a latency-reversing agent with a Smac mimetic minimizes secondary HIV-1 infection in vitro.** *Front Microbiol* 2018, **9**:2022.
39. Brogdon J, Ziani W, Wang X, Veazey RS, Xu H: **In vitro effects of the small-molecule protein kinase C agonists on HIV latency reactivation.** *Sci Rep* 2016, **6**:39032.
40. Spivak AM, Nell RA, Petersen M, Martins L, Sebahar P, Looper RE, Planelles V: **Synthetic ingenols maximize protein kinase C-**

**induced HIV-1 latency reversal.** *Antimicrob Agents Chemother* 2018, **62** e01361-18.

41. Marsden MD, Loy BA, Wu X, Ramirez CM, Schrier AJ, Murray D, Shimizu A, Ryckbosch SM, Near KE, Chun TW et al.: **In vivo activation of latent HIV with a synthetic bryostatin analog effects both latent cell "kick" and "kill" in strategy for virus eradication.** *PLoS Pathog* 2017, **13**:e1006575.
42. Marsden MD, Wu X, Navab SM, Loy BA, Schrier AJ, De Christopher BA, Shimizu AJ, Hardman CT, Ho S, Ramirez CM et al.: **Characterization of designed, synthetically accessible bryostatin analog HIV latency reversing agents.** *Virology* 2018, **520**:83-93.
43. Hashemi P, Barreto K, Bernhard W, Lomness A, Honson N, Pfeifer TA, Harrigan PR, Sadowski I: **Compounds producing an effective combinatorial regimen for disruption of HIV-1 latency.** *EMBO Mol Med* 2018, **10**:160-174.
44. Matsuda K, Kobayakawa T, Tsuchiya K, Hattori SI, Nomura W, Gatanaga H, Yoshimura K, Oka S, Endo Y, Tamamura H et al.: **Benzolactam-related compounds promote apoptosis of HIV-infected human cells via protein kinase C-induced HIV latency reversal.** *J Biol Chem* 2019, **294**:116-129.
45. Gutiérrez C, Serrano-Villar S, Madrid-Elena N, Pérez-Eliás MJ, Martín ME, Barbas C, Ruipérez J, Muñoz E, Muñoz-Fernández MA, Castor T, Moreno S: **Bryostatin-1 for latent virus reactivation in HIV-infected patients on antiretroviral therapy.** *AIDS* 2016, **30**:1385-1392.
46. Phetsouphanh C, Kelleher AD: **The role of PKC-θ in CD4+ T cells and HIV infection: to the nucleus and back again.** *Front Immunol* 2015, **30**:391.
47. López-Huertas MR, Jiménez-Tormo L, Madrid-Elena N, Gutiérrez C, Rodríguez-Mora S, Coiras M, Alcamí J, Moreno S: **The CCR5-antagonist maraviroc reverses HIV-1 latency in vitro alone or in combination with the PKC-agonist Bryostatin-1.** *Sci Rep* 2017, **7**:2385.
48. Madrid-Elena N, García-Bermejo ML, Serrano-Villar S, Díaz-de Santiago A, Sastre B, Gutiérrez C, Dronda F, Coronel Díaz M, Domínguez E, López-Huertas MR et al.: **Maraviroc is associated with latent HIV-1 reactivation through NF-κB activation in resting CD4+ T cells from HIV-infected individuals on suppressive antiretroviral therapy.** *J Virol* 2018, **92**.
49. Macedo AB, Novis CL, De Assis CM, Sorensen ES, Moszczynski P, Huang SH, Ren Y, Spivak AM, Jones RB, Planelles V, Bosque A: **Dual TLR2 and TLR7 agonists as HIV latency-reversing agents.** *JCI Insight* 2018, **3** pii: 122673.  
The authors describe dual TLR2/7 agonists that reverse latency in a complementary manner via both inducing NFκB in CD4+ T cells via the TLR2 component and TLR7 mediated production of TNFα by monocytes and dendritic cells.
50. Vibholm L, Schleimann MH, Hojen JF, Benfield T, Offersen R, Rasmussen K, Olesen R, Dige A, Agnholt J, Grau J et al.: **Short-course toll-like receptor 9 agonist treatment impacts innate immunity and plasma viremia in individuals with human immunodeficiency virus infection.** *Clin Infect Dis* 2017, **64**:1686-1695.
51. Tsai A, Irrinki A, Kaur J, Cihlar T, Kukolj G, Sloan DD, Murry JP: **Toll-like receptor 7 agonist GS-9620 induces HIV expression and HIV-specific immunity in cells from HIV-infected individuals on suppressive antiretroviral therapy.** *J Virol* 2017, **91** e02166-16.
52. Lim SY, Osuna CE, Hraber PT, Hesselgesser J, Gerold JM, Barnes TL, Sanisetty S, Seaman MS, Lewis MG, Gelezianus R et al.: **TLR7 agonists induce transient viremia and reduce the viral reservoir in SIV-infected rhesus macaques on antiretroviral therapy.** *Sci Transl Med* 2018, **10** pii: eaao4521.119.
53. Rochat MA, Schlaepfer E, Speck RF: **Promising role of toll-like receptor 8 agonist in concert with prostratin for activation of silent HIV.** *J Virol* 2017, **91** e02084-16.
54. Cheng L, Wang Q, Li G, Banga R, Ma J, Yu H, Yasui F, Zhang Z, Pantaleo G, Perreau M et al.: **TLR3 agonist and CD40-targeting vaccination induces immune responses and reduces HIV-1 reservoirs.** *J Clin Invest* 2018, **128**:4387-4396.



55. Zeng X, Pan X, Xu X, Lin J, Que F, Tian Y, Li L, Liu S: **Resveratrol reactivates latent HIV through increasing histone acetylation and activating heat shock factor 1**. *J Agric Food Chem* 2017, **65**:4384-4394.
56. Yuki SA, Kaiser P, Kim P, Telwate S, Joshi SK, Vu M, Lampiris H, ●● Wong JK: **HIV latency in isolated patient CD4+ T cells may be due to blocks in HIV transcriptional elongation, completion, and splicing**. *Sci Transl Med* 2018, **10** pii: eaap9927.  
The authors use RT-ddPCR to demonstrate that major blocks to transcription of the HIV virus occur beyond the level of transcription initiation, at the transcription elongation, polyadenylation and splicing stages, and that LRAs showed differing effects on these distinct blocks.
57. Jean M, Power D, Kong W, Huang H, Santoso N, Zhu J: **Identification of HIV-1 Tat-associated proteins contributing to HIV-1 transcription and latency**. *Viruses* 2017, **9**:67.
58. Khoury G, Mota TM, Li S, Tumpach C, Lee MY, Jacobson J, Harty L, Anderson JL, Lewin SR, Purcell DFJ: **HIV latency reversing agents act through Tat post translational modifications**. *Retrovirology* 2018, **15** 36:146.
59. Mousseau G, Valente ST: **Role of host factors on the regulation of Tat-mediated HIV-1 transcription**. *Curr Pharm Des* 2017, **23**:4079-4090.
60. Abner E, Stoszko M, Zeng L, Chen HC, Izquierdo-Bouldstridge A, Konuma T, Zorita E, Fanunza E, Zhang Q, Mahmoudi T *et al.*: **A new quinoline BRD4 inhibitor targets a distinct latent HIV-1 reservoir for reactivation from other "Shock" drugs**. *J Virol* 2018, **92** e02056-17.
61. Lu P, Qu X, Shen Y, Jiang Z, Wang P, Zeng H, Ji H, Deng J, Yang X, Li X *et al.*: **The BET inhibitor OTX015 reactivates latent HIV-1 through P-TEFb**. *Sci Rep* 2016, **12**:24100.
62. Huang H, Liu S, Jean M, Simpson S, Huang H, Merkley M, Hayashi T, Kong W, Rodríguez-Sánchez I, Zhang X *et al.*: **A novel bromodomain inhibitor reverses HIV-1 latency through specific binding with BRD4 to promote Tat and P-TEFb association**. *Front Microbiol* 2017, **7**:1035.
63. Darcis G, Kula A, Bouchat S, Fujinaga K, Corazza F, Ait-Ammar A, Delacourt N, Melard A, Kabeya K, Vanhulle C *et al.*: **An in-depth comparison of latency-reversing agent combinations in various in vitro and ex vivo HIV-1 latency models identified bryostatin-1+JQ1 and ingenol-B+JQ1 to potentially reactivate viral gene expression**. *PLoS Pathog* 2015, **11**:e1005063.
64. Li Z, Mbonye U, Feng Z, Wang X, Gao X, Karn J, Zhou Q: **The KAT5-Acetyl-Histone4-Brd4 axis silences HIV-1 transcription and promotes viral latency**. *PLoS Pathog* 2018, **14**:e1007012.
65. Chen D, Wang H, Aweya JJ, Chen Y, Chen M, Wu X, Chen X, Lu J, Chen R, Liu M: **HMBA enhances prostratin-induced activation of latent HIV-1 via suppressing the expression of negative feedback regulator A20/TNFAIP3 in NF-κB signaling**. *Biomed Res Int* 2016, **2016**:5173205.
66. Geng G, Liu B, Chen C, Wu K, Liu J, Zhang Y, Pan T, Li J, Yin Y, Zhang J *et al.*: **Development of an attenuated Tat protein as a highly-effective agent to specifically activate HIV-1 latency**. *Mol Ther* 2016, **24**:1528-1537.
67. Tang X, Lu H, Dooner M, Chapman S, Quesenberry PJ, Ramratnam B: **Exosomal Tat protein activates latent HIV-1 in primary, resting CD4+ T lymphocytes**. *JCI Insight* 2018, **3** pii: 95676.
68. Sgadari C, Monini P, Tripiciano A, Picconi O, Casabianca A, Orlandi C, Moretti S, Francavilla V, Arancio A, Panicia G *et al.*: **Continued decay of HIV proviral DNA upon vaccination with HIV-1 Tat of subjects on long-term ART: an 8-year follow-up study**. *Front Immunol* 2019, **10** 233:156.
69. Boyer Z, Palmer S: **Targeting immune checkpoint molecules to eliminate latent HIV**. *Front Immunol* 2018, **9**:2339.
70. Evans VA, van der Sluis RM, Solomon A, Dantanarayana A, McNeil C, Garsia R, Palmer S, Fromentin R, Chomont N, Sékaly RP *et al.*: **Programmed cell death-1 contributes to the establishment and maintenance of HIV-1 latency**. *AIDS* 2018, **32**:1491-1497.
71. Fromentin R, DaFonseca S, Costiniuk CT, El-Far M, Procopio FA, Hecht FM, Hoh R, Deeks SG, Hazuda DJ, Lewin SR *et al.*: **PD-1 blockade potentiates HIV latency reversal ex vivo in CD4+ T cells from ART-suppressed individuals**. *Nat Commun* 2019, **10**:814.
72. Bui JK, Cyktor JC, Fyne E, Campellone S, Mason SW, Mellors JW: **Blockade of the PD-1 axis alone is not sufficient to activate HIV-1 virion production from CD4+ T cells of individuals on suppressive ART**. *PLoS One* 2019, **25**:e0211112.
73. Grau-Expósito J, Serra-Peinado C, Miguel L, Navarro J, Curran A, Burgos J, Ocaña I, Ribera E, Torrella A, Planas B *et al.*: **A novel single-cell FISH-Flow assay identifies effector memory CD4+ T cells as a major niche for HIV-1 transcription in HIV-infected patients**. *mBio* 2017, **8** e00876-17.  
The authors show, using FISH-Flow technology, that effector memory CD4 T cells are the main population that harbor HIV transcription in infected patients, and that after reactivation, only up to 10% of cells that express viral RNA also express gag (protein).
74. Rao S, Amorim R, Niu M, Temzi A, Moulard AJ: **The RNA surveillance proteins UPF1, UPF2 and SMG6 affect HIV-1 reactivation at a post-transcriptional level**. *Retrovirology* 2018, **28**:42.
75. Sarracino A, Gharu L, Kula A, Pasternak AO, Avettand-Fenoel V, Rouzioux C, Bardina M, De Wit S, Benkirane M, Berkhout B *et al.*: **Posttranscriptional regulation of HIV-1 gene expression during replication and reactivation from latency by nuclear matrix protein MATR3**. *mBio* 2018, **9** e02158-18.
76. Cheung PK, Horhant D, Bandy LE, Zamiri M, Rabea SM, Karagiosov SK, Matloobi M, McArthur S, Harrigan PR, Chabot B, Grierson DS: **Parallel synthesis approach to the identification of novel diheteroarylamine-based compounds blocking HIV replication: potential inhibitors of HIV-1 Pre-mRNA alternative splicing**. *J Med Chem* 2016, **59**:1869-1879.
77. Kyei GB, Meng S, Ramani R, Niu A, Lagisetty C, Webb TR, Ratner L: **Splicing factor 3B subunit 1 interacts with HIV Tat and plays a role in viral transcription and reactivation from latency**. *mBio* 2018, **9** e01423-18.
78. Mediouni S, Chinthalapudi K, Ekka MK, Usui I, Jablonski JA, Clementz MA, Mousseau G, Nowak J, Macherla VR, Beverage JN *et al.*: **Didehydro-Cortistatin A inhibits HIV-1 by specifically binding to the unstructured basic region of Tat**. *mBio* 2019, **10**:e02662-1.
79. Li C, Mousseau G, Valente ST: **Tat inhibition by didehydro-Cortistatin A promotes heterochromatin formation at the HIV-1 long terminal repeat**. *Epigenetics Chromatin* 2019, **12**:23.
80. Besnard E, Hakre S, Kampmann M, Lim HW, Hosmane NN, Martin A, Bassik MC, Verschueren E, Battivelli E, Chan J: **The mTOR complex controls HIV latency**. *Cell Host Microbe* 2016, **20**:785-797.
81. Wong RW, Lingwood CA, Ostrowski MA, Cabral T, Cochrane A: **Cardiac glycoside/aglycones inhibit HIV-1 gene expression by a mechanism requiring MEK1/2-ERK1/2 signaling**. *Sci Rep* 2018, **8**:850.
82. Balachandran A, Wong R, Stoilov P, Pan S, Blencowe B, Cheung P, Harrigan PR, Cochrane A: **Identification of small molecule modulators of HIV-1 Tat and Rev protein accumulation**. *Retrovirology* 2017, **14**:7.
83. Vautrin A, Manchon L, Garcel A, Campos N, Lapasset L, Laeref AM, Bruno R, Gislard M, Dubois E, Scherrer D *et al.*: **Both anti-inflammatory and antiviral properties of novel drug candidate ABX464 are mediated by modulation of RNA splicing**. *Sci Rep* 2019, **9**.
84. Debyser Z, Vansant G, Bruggemans A, Janssens J, Christ F: **Insight in HIV integration site selection provides a block-and-lock strategy for a functional cure of HIV infection**. *Viruses* 2018, **11** pii: E12.
85. Kim Y, Anderson JL, Lewin SR: **Getting the "kill" into "shock and kill": strategies to eliminate latent HIV**. *Cell Host Microbe* 2018, **23**:14-26.
86. Bobardt M, Kuo J, Chatterji U, Chanda S, Little SJ, Wiedemann N, Vagniaux G, Gallay PA: **The inhibitor apoptosis protein**

antagonist **Debio 1143** is an attractive **HIV-1** latency reversal candidate. *PLoS One* 2019, **14**:e0211746.

87. Campbell GR, Bruckman RS, Chu YL, Trout RN, Spector SA:  
●● **SMAC mimetics induce autophagy-dependent apoptosis of HIV-1-infected resting memory CD4+ T cells.** *Cell Host Microbe* 2018, **24**:689-702.e7.

The authors show selective elimination of HIV infected and not uninfected TCM by SMAC mimetic molecules, which degrade inhibitors of apoptosis (IAPs), inducing autophagy and apoptosis in infected cells.

88. Cummins NW, Sainski-Nguyen AM, Natesampillai S, Aboulnasr F, Kaufmann S, Badley AD: **Maintenance of the HIV reservoir is antagonized by selective BCL2 inhibition.** *J Virol* 2017, **91** e00012-17.
89. Li P, Kaiser P, Lampiris HW, Kim P, Yukl SA, Havlir DV, Greene WC, Wong JK: **Stimulating the RIG-I pathway to kill cells in the**

**latent HIV reservoir following viral reactivation.** *Nat Med* 2016, **22**:807-811.

90. Garcia-Vidal E, Castellvi M, Pujantell M, Badia R, Jou A, Gomez L, Puig T, Clotet B, Ballana E, Riveira-Muñoz E, Esté JA: **Evaluation of the innate immune modulator acitretin as a strategy to clear the HIV reservoir.** *Antimicrob Agents Chemother* 2017, **61** e01368-17.

91. Battivelli E, Dahabieh MS, Abdel-Mohsen M, Svensson JP, Tojal Da Silva I, Cohn LB, Gramatica A, Deeks S, Greene WC, Pillai SK, Verdin E: **Distinct chromatin functional states correlate with HIV latency reactivation in infected primary CD4+ T cells.** *eLife* 2018, **7** pii: e34655.

The authors show that transcription competent latent viruses exist in distinct chromatin domains with differing reactivation potential in primary latently infected CD4+ T cells, and that LRAs reactivate a small fraction, which are integrated in more accessible, reactivatable chromatin domains.



# General introduction

## III.

### Scope of the thesis

Pharmacological reversal of HIV-1 latency with subsequent immunological clearance of the virus has been proposed as a means to eradicate HIV, in a so called “shock and kill” approach. Up to now several latency reversing agents (LRAs) have been described. Unfortunately, so far none of them were potent enough to strongly “shock” the virus from hiding in clinical trials. It becomes clear that we need to identify stronger drugs to carry the task. Most likely we will also have to combine different classes of LRAs in order to achieve clinically relevant latency reversal.

The main aim of the work presented in this thesis is to identify and characterize novel, therapeutically relevant latency reversal agents – LRAs, which induce expression of the HIV-1 genome at the RNA and protein levels. Secondly, we intensively investigate dual treatments with different classes of these drugs to identify combinations exerting synergistic latency reversal.

We have previously shown in cell line models of latency that the BAF complex is responsible for re-positioning of nucleosome 1 in a thermodynamically disfavored position just after the transcription start site (TSS) on the pro-viral promoter or 5’LTR. Such enforced chromatin structure represents a mechanical block for RNA Polymerase II processing and causes inhibition of transcription of the HIV-1 provirus. BAF, as a repressor of HIV-1 transcription represented an ideal molecular target for pharmacological targeting to reverse latency.

In chapter two we tested whether a set of molecules recently identified to mimic a BAF knock-out in ES cells (Dykhuizen, Carmody, Tolliday, Crabtree, & Palmer, 2012) was capable of reversing HIV-1 latency. First, we focused on cell line models of latency, where we could assess efficacy and toxicity of these small molecules. Additionally, we employed ChIP assays to examine how BAF inhibitors (BAFis) reverse latency. We showed that while in untreated cells BAF complex occupies nucleosome 1 of the proviral promoter, treatment with BAFis lead to displacement of the complex resulting in more open chromatin. Cell lines do not adequately represent the physiological reservoir of latent HIV-1, the most functionally relevant of which are primary resting memory CD4+ T cells. We therefore next

examined the potential of putative BAF inhibitor compounds to reverse latency in primary ex vivo infected HIV-1 latency models, and more importantly in cells obtained from aviremic persons living with HIV-1. Furthermore, we examined whether the putative BAF inhibitors would synergize with compounds belonging to other LRA families of molecules. Given the importance of the BAF complex in gene regulation we were also interested in determining toxicity profile and potential pleiotropic effects of these drugs on immune cells.

In chapter three, in collaboration with the Dykhuizen lab, we examined HIV latency reversal potential of more specific BAFs identified in high throughput unbiased screen of almost 350 000 molecules of various sources (ie. Natural products, known bioactives, commercially available compound libraries, and compound libraries designed by scientists at the Broad Institute, MIT). Identified candidate BAFs tested were based on a macrolactam structure. Target identification and mechanistic experiments showed that macrolactams target ARID1A subunit of the BAF complex. In order to examine their effectiveness, we employed multiple models of latency, including cells obtained from people living with HIV. We also assessed toxicity of these drugs on cells to investigate how safe their use would be. We showed that, similarly to CAPE and PYR, treatment with macrolactams results in more open LTR chromatin as assessed by FAIRE assay. However, likely because of their specific targeting of the ARID1A subunit, the macrolactam structure BAFi's exhibited less toxicity concomitant with more potency.

A growing body of evidence suggests that activating transcription elongation is of utmost importance in "shock and kill" approaches (Yukl et al., 2018). In fact, it has been demonstrated that in replication competent latent HIV infected cells from aviremic patients, the main barrier to expression of the virus stems from series of blocks to proximal elongation, distal transcription/polyadenylation (completion), and multiple splicing rather than from blocks to transcriptional initiation (as previously assumed (Röling et al., 2016)). Up until now, there were only two small molecules able to trigger transcriptional elongation, namely JQ1 and HMBA (Banerjee et al., 2012; Contreras et al., 2007; Filippakopoulos et al., 2010). Unfortunately, short half-life of JQ1 limits its potential therapeutic usefulness (Trabucco et al., 2015; Wroblewski et al., 2018). The Jordan group has recently identified MMQO small molecule to be a promising BET targeting LRA.

In chapter four, together with Jordan lab we investigated in more detail the mechanisms governing the activity of MMQO. Analysis of transcriptomes of cells treated with MMQO and other LRAs were used to compare how these drugs influence transcription and to find common gene targets. Importantly, nuclear magnetic resonance (NMR) binding studies were done to determine if MMQO binds to BRD4. Interestingly, we also investigated if and how different classes of LRAs target latency reversal in distinct subsets of latently infected cells.



In the final chapter, we screened for novel putative LRA(s) using a largely untapped source for potentially bioactive molecules. We focused on fungal secondary metabolites, as fungi are well known for producing a plethora of diverse array of molecules. Combination of academic knowledge of mycology, low and medium throughput biological screening systems and state-of-art fractionation and purification techniques resulted in identification of three fungi producing putative LRAs. We focused on the strongest hit, supernatants of *Aspergillus fumigatus*, which we showed contain gliotoxin (GTX) as a novel LRA. Activity and toxicity of the identified hit was further determined in variety of model systems of HIV-1 latency, including cells obtained from aviremic people living with HIV-1. We focused on understanding, at the mechanistic, molecular level, how latency is reversed by gliotoxin. Therefore, we employed transcriptome analysis coupled with biochemical assays to unravel the steps targeted by GTX to reverse latency. Additionally, we assed efficacy of synergistic combinations of gliotoxin with other known LRAs.

In this thesis we have identified and described the mechanism of function of a wide array of small molecules with potential to reverse HIV-1 latency, a first step towards eradication of the virus. These drugs, namely caffeic phenethyl ester (CAPE), pyrimethamine (PYR) and macrolactams, MMQO, and gliotoxin belong to BAF targeting, BET targeting, and 7SKsnRNP complex targeting classes of molecules, respectively, and we investigated and described how mechanistically they induce proviral transcription. We also assessed effective combination of these molecules with other known LRAs with the aim to find co-treatments exerting synergistic effect. Additionally, we evaluated the toxicity profile and potential pleiotropic effects of these molecules on other immune cells, namely CD8<sup>+</sup> T cells responsible for eliminating the infected CD4<sup>+</sup> T cells. Importantly, we studied the effectiveness of these molecules to reverse HIV latency ex vivo in cells obtained from aviremic participants living with HIV, the gold standard for in vitro effectiveness of LRAs.



# Chapter 2

## **Small Molecule Inhibitors of BAF; A Promising Family of Compounds in HIV-1 Latency Reversal.**

Mateusz Stoszko<sup>a,1</sup>, Elisa De Crignis<sup>a,1</sup>, Casper Rokx<sup>c</sup>, Mir Mubashir Khalid<sup>a</sup>, Cynthia Lungu<sup>a</sup>, Robert-Jan Palstra<sup>a</sup>, Tsung Wai Kan<sup>a</sup>, Charles Boucher<sup>d</sup>, Annelies Verbon<sup>c</sup>, Emily C. Dykhuizen<sup>b</sup>, Tokameh Mahmoudi<sup>a</sup>,

a Department of Biochemistry, Erasmus University Medical Center, Ee634, PO Box 2040 3000CA, Rotterdam, The Netherlands

b Department of Medicinal Chemistry and Molecular Pharmacology, Purdue University, West Lafayette, IN, USA

c Department of Internal Medicine, Section of Infectious Diseases, Erasmus University Medical Center, PO Box 2040 3000CA, Rotterdam, The Netherlands

d Department of Viroscience, Erasmus University Medical Center, PO Box 2040 3000CA, Rotterdam, the Netherlands

Published:

EBioMedicine 2015, 3, p. 108-121





## Research Paper

# Small Molecule Inhibitors of BAF; A Promising Family of Compounds in HIV-1 Latency Reversal



Mateusz Stoszko<sup>a,1</sup>, Elisa De Crignis<sup>a,1</sup>, Casper Rokx<sup>c</sup>, Mir Mubashir Khalid<sup>a</sup>, Cynthia Lungu<sup>a</sup>, Robert-Jan Palstra<sup>a</sup>, Tsung Wai Kan<sup>a</sup>, Charles Boucher<sup>d</sup>, Annelies Verbon<sup>c</sup>, Emily C. Dykhuizen<sup>b</sup>, Tokameh Mahmoudi<sup>a,\*</sup>

<sup>a</sup> Department of Biochemistry, Erasmus University Medical Center, Ee634, PO Box 2040 3000CA, Rotterdam, The Netherlands

<sup>b</sup> Department of Medicinal Chemistry and Molecular Pharmacology, Purdue University, West Lafayette, IN, USA

<sup>c</sup> Department of Internal Medicine, Section of Infectious Diseases, Erasmus University Medical Center, PO Box 2040 3000CA, Rotterdam, The Netherlands

<sup>d</sup> Department of Viroscience, Erasmus University Medical Center, PO Box 2040 3000CA, Rotterdam, the Netherlands

## ARTICLE INFO

## Article history:

Received 29 June 2015

Received in revised form 19 November 2015

Accepted 25 November 2015

Available online 27 November 2015

## Keywords:

HIV

Latency

BAF complex

Chromatin remodeling

latency reversal agents

## ABSTRACT

Persistence of latently infected cells in presence of Anti-Retroviral Therapy presents the main obstacle to HIV-1 eradication. Much effort is thus placed on identification of compounds capable of HIV-1 latency reversal in order to render infected cells susceptible to viral cytopathic effects and immune clearance. We identified the BAF chromatin remodeling complex as a key player required for maintenance of HIV-1 latency, highlighting its potential as a molecular target for inhibition in latency reversal. Here, we screened a recently identified panel of small molecule inhibitors of BAF (BAFi's) for potential to activate latent HIV-1. Latency reversal was strongly induced by BAFi's Caffeic Acid Phenethyl Ester and Pyrimethamine, two molecules previously characterized for clinical application. BAFi's reversed HIV-1 latency in cell line based latency models, in two ex vivo infected primary cell models of latency, as well as in HIV-1 infected patient's CD4+ T cells, without inducing T cell proliferation or activation. BAFi-induced HIV-1 latency reversal was synergistically enhanced upon PKC pathway activation and HDAC-inhibition. Therefore BAFi's constitute a promising family of molecules for inclusion in therapeutic combinatorial HIV-1 latency reversal.

© 2015 The Authors. Published by Elsevier B.V. This is an open access article under the CC BY-NC-ND license (<http://creativecommons.org/licenses/by-nc-nd/4.0/>).

## 1. Introduction

The use of fully suppressive combination Anti-Retroviral Therapy (c-ART), aside from efficiently inhibiting viral replication, has provided

important insights into the characteristics and dynamics of the persistent latent pool of the HIV-1 virus in infected patients (Pierson et al., 2000; Dahabieh et al., 2015; Geeraert et al., 2008; Chun et al., 1995, 2007). Studies have led to the identification of quiescent latently infected CD4+ memory T cells, which harbor latent HIV-1, as the major barrier to a cure (Finzi et al., 1999; Siliciano et al., 2003). The majority of HIV-1 infected patients are diagnosed during the chronic phase of the infection, when a large reservoir of latently infected cells is already established (Strain et al., 2005; Watanabe et al., 2011; Whitney et al., 2014). Therefore, to achieve a functional cure, recent pharmacological efforts have centered on targeting the reservoir harboring latent HIV-1 for activation in order to induce viral replication. As a second step, following latency reversal, the infected cells would be exposed to viral cytopathic effects and the immune system, thereby eliminating or depleting the infected cells that constitute the latent reservoir (Deeks, 2012).

Latently HIV-1 infected cells harbor replication competent HIV-1 virus, whose gene expression is transcriptionally blocked. Once integrated, the double stranded HIV-1 provirus behaves as a cellular gene and becomes subject to a complex network of molecular mechanisms that determine its transcriptional state (Mbonye and Karn, 2014; Mahmoudi, 2012; Dahabieh et al., 2015). As part of the genome, the

**Abbreviations:** BAF250a, BAF Associated Factor 250 a; BAF, BRG-Brahma Associated Factors; BAFi, BAF inhibitor; bp, base pairs; BRG-1, Brahma Related Gene 1; CAPE, caffeic acid phenethyl ester; cART, combination Antiretroviral Therapy; ChIP, Chromatin Immunoprecipitation; CycA, Cyclophilin A; DHS-1, DNase Hypersensitive Site 1; ES cells, embryonic stem cells; FAIRE, Formaldehyde Assisted Isolation of Regulatory Elements; FBS, Fetal Bovine Serum; GFP, Green Fluorescent Protein; HDAC, histone deacetylase; HIV-1, human immunodeficiency virus type 1; IFN $\beta$ , Interferon beta; IL10, Interleukin 10; IL12, Interleukin 12; IL4, Interleukin 4; IL6, Interleukin 6; INI-1, Integrase Interactor 1; IRES, Internal Ribosome Entry Site; I $\kappa$ B- $\alpha$ , Inhibitor of NF- $\kappa$ B – alpha; LRA, latency reversal agent; LTR, Long Terminal Repeat; MIP26, Major Intrinsic Protein; MMP9, Matrix Metalloproteinase 9; NF- $\kappa$ B, Nuclear Factor Kappa-light-chain-enhancer of activated B cells; nuc, nucleosome; PBMC, peripheral blood mononuclear cell; PBS, Phosphate Buffered Saline; PKC, Protein Kinase C; PYR, Pyrimethamine; RT-qPCR, Reverse Transcriptase, quantitative Polymerase Chain Reaction; SAHA, Suberoylanilide Hydroxamic Acid; SD, Standard Deviation; siRNA, small interfering RNA; SOCS3, Suppressor Of Cytokine Signaling 3; TGF- $\beta$ , Transforming Growth Factor beta; TLR2, Toll-like Receptor 2.

\* Corresponding author.

E-mail address: [t.mahmoudi@erasmusmc.nl](mailto:t.mahmoudi@erasmusmc.nl) (T. Mahmoudi).

<sup>1</sup> Authors contributed equally.

HIV-1 chromatin structure at the 5' LTR, the HIV-1 promoter, is highly organized into specifically deposited nucleosomes: in its latent state, the 5'LTR is organized into nuc-0 and nuc-1, two strictly positioned nucleosomes that are separated by DHS1, a region sensitive to nuclease digestion, which encompasses a loosely positioned nucleosome (Verdin, 1991; Verdin and Van Lint, 1995; Rafati et al., 2011). The positioning of nuc-1, downstream of the core promoter transcription start site, is the hallmark of the repressed 5' LTR. Upon activation, nuc-1 becomes rapidly and specifically disrupted, allowing for HIV-1 gene expression to occur (Verdin and Van Lint, 1995; Verdin et al., 1993; Van Lint et al., 1996; Rafati et al., 2011).

The chromatin structure of the HIV-1 promoter, as with cellular promoters, is generated through the concerted activity of protein complexes, which remodel chromatin (Mbonye and Karn, 2014; Lusica and Giacca, 2015). This is in part accomplished by loosening or tightening histone-DNA interaction via posttranslational modifications on histone tails, which include acetylation and methylation (Zentner and Henikoff, 2013). Of particular interest for regulation of HIV-1 transcription, histone deacetylases have been shown to play a critical role in repressing gene expression at the HIV-1 LTR (Van Lint et al., 1996; Keedy et al., 2009; Marban et al., 2007; Williams et al., 2006; Barton and Margolis, 2013; Barton et al., 2014; Lu et al., 2014) and represent an important target for therapies aimed at activation of latent virus or latency reversal. Accordingly, a number of small molecule HDAC inhibitors including valproic acid (Edelstein et al., 2009), suberoylanilide hydroxamic acid (SAHA) (Contreras et al., 2009), Panobinostat (Rasmussen et al., 2013), and Romidepsin (Wei et al., 2014) have been or are currently under clinical investigation for their potential in therapeutic HIV-1 latency reversal (Archin et al., 2012, 2014; Elliott et al., 2014; Barton et al., 2015; Rasmussen et al., 2014).

Initial data from preclinical and clinical studies using HDAC inhibitors in therapeutic latency reversal suggest that while promising, HDAC inhibitors alone may not be sufficient in activation of the latent HIV-1 to the extent required to accomplish clinically significant depletion of the latent reservoir in patients. HIV-1 transcriptional latency is a complex molecular phenomenon, driven and controlled by multiple mechanisms, including the position of virus integration in the genome, its orientation and proximity to endogenous genes, and the presence and activity of host transcription factors and cofactors on the HIV-1 promoter (Van Lint et al., 2013; Dahabieh et al., 2015; Mbonye and Karn, 2014; Ruelas and Greene, 2013; Matsuda et al., 2015). Therefore, the specific transcriptional environment of each latently infected cell is likely to impact its responsiveness to activating molecules. Accordingly, the molecular mechanisms at play in transcriptionally silencing the latent reservoir are likely to be diverse and heterogeneous. Indeed, data obtained from in vitro models using latently infected cell lines support the notion that targeting two or more pathways in combination is more effective in activating latent HIV-1 by inducing synergistic activation of the latent promoter (De Crignis and Mahmoudi, 2014; Laird et al., 2015). It is therefore critical to identify and target multiple molecular effectors with distinct mechanisms that drive HIV-1 latency in order to obtain more effective and synergistic activation of the latent reservoir.

ATP dependent chromatin remodeling complexes are another group of factors, which the cell has co-evolved in addition to post-translational histone modifications, in order to alter histone-DNA contacts and change chromatin structure. These multi-subunit protein complexes use energy from ATP hydrolysis to disrupt or move nucleosomes, thereby remodeling chromatin and modulating access to DNA (Narlikar et al., 2013; Petty and Pillus, 2013; Hargreaves and Crabtree, 2011; Mahmoudi and Verrijzer, 2001). We have recently found that the BAF chromatin remodeling complex uses energy from ATP hydrolysis to position the transcriptionally repressive nuc-1 over thermodynamically sub-optimal DNA sequences leading to the establishment and maintenance of HIV-1 latency. Consistent with the pivotal role of BAF complex in HIV-1 latency, we have shown that siRNA mediated

depletion of BAF specific subunits significantly decreases the percentage of latent events at the time of infection. Similarly, in cells in which latency is already established, such as in vitro T cell line models of latency, depletion of BAF subunits results in reactivation of latent virus. Our data identified the BAF chromatin remodeling complex as a putative molecular target in therapeutic efforts aimed at HIV-1 latency reversal (Rafati et al., 2011; Mahmoudi, 2012). Recently, a spectrum of potential small molecule inhibitors of the BAF complex were identified in a screen of more than 30,000 compounds, which included synthetic molecules, natural products, drug-like compounds and molecules with known bioactivity (Dykhuizen et al., 2012). 34 BAF inhibitors were initially identified by monitoring mRNA expression of well characterized BAF target genes in mouse embryonic stem cells. A second screen then eliminated molecules with non-specific targets and general repressive activities, leading to the identification of 20 compounds that transcriptionally mimic genetic deletion of *BRG1* (the ATPase subunit of the complex), indicating specific activity against the BAF complex.

Here we have tested a panel of BAF inhibitors for their potential to activate latent HIV-1. Following the initial screening, we focused on functional characterization of A01, A11, and C09, the three compounds that displayed most significant activity on the latent LTR with the lowest toxicity. We found that BAF inhibitors (BAFi's) activate latent HIV-1 in both Jurkat cell lines harboring latent full length HIV-1 and HIV-1 derived viruses, in two distinct ex vivo infected primary CD4+ T cell models of HIV-1 latency, as well as in cells obtained from virologically suppressed HIV-1 infected patients. BAFi-mediated activation of latent HIV-1 was accompanied by the displacement of the BAF complex from the HIV-1 LTR, as demonstrated by ChIP assay, and was synergistically enhanced in presence of the HDAC inhibitor SAHA and the PKC agonist Prostratin. Consistently, FAIRE assays demonstrated removal of the repressive positioned nuc-1 in response to treatment with BAFi's, and synergism at the molecular level when cells were co-treated with BAFi's together with Prostratin. While efficiently activating latent HIV-1, treatment with BAFi's did not induce T cell proliferation or general T cell activation of primary CD4+ T cells. Our data identifies BAFi's as a promising family of small molecules for inclusion in therapeutic combinations aiming to reverse HIV-1 latency.

## 2. Materials and Methods

### 2.1. Cell Culture and Reagents

Jurkat, J-Lat A2 (LTR-Tat-IRES-GFP), J-Lat 11.1 (integrated full-length HIV-1 genome mutated in *env* gene and GFP replacing *Nef*) (Jordan et al., 2001, 2003) cells were cultured in RPMI-1640 medium (Sigma Aldrich, Zwijndrecht, The Netherlands) supplemented with 10% FBS and 100 µg/ml penicillin-streptomycin at 37 °C in a humidified 95% air-5% CO<sub>2</sub> atmosphere. Cells were treated with the following compounds: Phorbol 12-myristate 13-acetate (PMA, Sigma Aldrich); Ionomycin (Sigma Aldrich); SAHA-Vorinostat (Selleck Chemicals); Prostratin (Sigma Aldrich); A01 (N-hydroxy-N'-phenyl-octanediamide 2-hydroxy-N'-[(E)-(5-hydroxy-6-oxocyclohexa-2,4-dien-1-ylidene)methyl]benzohydrazide (BRD-K70161581-001-01-5), Vitas-M Laboratory, Ltd., Apeldoorn, Netherlands.); A11 (5-(4-chlorophenyl)-6-ethyl-2,4-pyrimidinediamine (BRD-K88429204-001-18-7), Sigma Aldrich); C09 (2-phenylethyl (E)-3-(3,4-dihydroxyphenyl)prop-2-enoate (BRD-K91370081-001-04-6), MP Biomedicals, Eindhoven, The Netherlands).

### 2.2. Flow Cytometry

GFP expression in the J-Lat cell lines was analyzed by Flow Cytometry. The live population was defined by forward versus side scatter profiles. Cells were further gated by using forward scatter versus GFP intensity to differentiate between GFP-positive and -negative cells.

In primary models of latency, the phenotypic characteristics of the cell population at the moment of reactivation were determined using

flow cytometry: cells were stained with anti-CD4-PB (Becton Dickinson, Breda, The Netherlands), anti-CCR7-PE (eBioscience, Uithoorn, The Netherlands), anti-CD27-APC (Becton Dickinson), and anti CD45RO-FITC (Dako, Heverlee, Belgium). Cells were stained for 30 min at 4 °C, washed with PBS, and re-suspended for flow cytometric analysis.

To determine cell activation following BAF complex inhibition, cells were treated with BAFi's for 72 h. Untreated cells and PMA/Ionomycin treated cells were used as negative and positive control, respectively. At 24 and 72 h post treatment cells were collected and stained with Fixable Viability Dye eFluor® 450 and anti-CD25-PE (Becton Dickinson). Cells were stained for 30 min at 4 °C, washed with PBS, and resuspended for flow cytometric analysis. To determine the expression of Ki67, cells were collected and stained with Fixable Viability Dye eFluor® 450 for 15 min. Following 2% PFA fixation, cells were permeabilized with 0.3% saponin for 30 min, incubated with anti-Ki67-PE (eBioscience) antibody for 60 min at 4 °C, washed in PBS and resuspended for flow cytometry. All samples were analyzed with a Becton Dickinson Fortessa instrument.

### 2.3. Primary CD4 + T Cell Isolation and Infection

Primary CD4 + T cells were isolated from buffy coats from healthy donors by Ficoll gradient followed by magnetic separation with EasyStep Human CD4 + T cell Enrichment kit (StemCells Technologies, Grenoble, France).

Two in vitro models of HIV-1 latency were set up following the method developed by Bosque and Planelles (Bosque and Planelles, 2009) and Lassen and Greene (Lassen et al., 2012). Infections were performed using a pseudotyped virus expressing luciferase. Viral pseudotyped particles were obtained by co-transfecting HXB2 Env together with the HIV-1 backbone plasmid (pNL4.3.Luc.R-E-) into HEK 293 T cells using PEI (Polyethylenimine) transfection reagent. Twenty four, 48 and 72 h post-transfection, the pseudovirus-containing supernatant was collected, filtered through a 0.45 µm filter, aliquoted, and stored at –80 °C.

For generation of latently infected primary cells according to the Bosque and Planelles method, purified CD4 + T cells were cultured in RPMI 1640 containing 10% FBS in presence of 10 ng/ml of TGF-β (Sigma-Aldrich), 1 µg/ml α-IL4 (PeproTech, London, UK), 2 µg/ml α-IL12 (PeproTech), and α-CD3-CD28 (Life Technologies, Breda, The Netherlands) coated beads in 1:1 ratio for 3 days. After 3 days α-CD3-CD28 coated beads were removed and cells were cultured in RPMI 1640 containing 10% FBS, 100 µg/ml penicillin-streptomycin and 5 ng/ml of IL2 (Sigma-Aldrich) for 4 days. On day 7 post stimulation cells were infected with HIV-derived virus particles. Primary CD4 + T cells, were infected with the PNL4.3.LUC.R-E- virus by spinoculation (90 min at 1200 g), washed in PBS and cultured in RPMI 1640 containing 10% FBS, 100 µg/ml penicillin-streptomycin, IL2 (5 ng/ml) and Saquinavir Mesylate (5 µM). Six days after infection cells were treated with BAFi's in presence of Raltegravir (30 µM).

Generation of latently infected cells according to Lassen and Greene method was performed as follows: CD4 + T cells were infected with the PNL4.3.LUC.R-E- virus by spinoculation (120 min at 1200 g) right after isolation and cultured for three days in RPMI 10% FBS and 100 µg/ml penicillin-streptomycin in presence of Saquinavir Mesylate (5 µM). Three days after infection cells were treated with BAFi's in presence of Raltegravir (30 µM).

Cells were harvested 24 h after stimulation with BAF inhibitors, washed once in PBS and luciferase activity was measured using Luciferase Assay System (Promega, Leiden, The Netherlands). Relative light units were normalized to protein content determined by Bradford assay (Bio Rad, Veenendaal, The Netherlands).

HIV-1 molecular clone pNL4.3.Luc.R-E-, HIV-1 HXB2-Env expression vector, Saquinavir Mesylate and Raltegravir were kindly provided by the Centre for AIDS Reagents, NIBSC. HIV-1 molecular clone pNL4.3.Luc.R-E- and HIV-1 HXB2-Env expression vector were donated

by Dr. Nathaniel Landau and Drs Kathleen Page and Dan Littman, respectively.

### 2.4. Activation of HIV-1 Transcription in Patient CD4 + T Cells

Total PBMCs were obtained from HIV-infected patients without (overt) clinical symptoms by leukapheresis, and isolated by Ficol gradient density sedimentation. CD4 + T cells were isolated using the CD4 + T-Cell enrichment kit (Stem Cell Technologies) and frozen. Inclusion criteria were as follows: age > 18 years; confirmed HIV-1 infection; plasma HIV-1 RNA viral load below 50 copies/ml for more than 12 months; cART for at least 3 years. 2.5 million CD4 + T cells were plated in 6 wells plates in 2.5 ml of RPMI supplemented with 10% FBS and left untreated or treated with 1 µM C09, 20 µM A11 or 300 nM Prostratin alone or in combination as indicated. As a positive control, cells were treated with CD3-CD28 beads or PMA-Ionomycin. Twelve hours after stimulation cells were collected and lysed in RNA lysis buffer (Promega). RNA was extracted and reverse transcribed using Random primers (Life Technologies) and Superscript II (Life Technologies) following manufacturer's instructions. Levels of cellular associated RNA were quantified using a PCR targeting the HIV-1 *POL* gene. qPCR was performed in a final volume of 25 µl using 4 µl of cDNA, 2.5 µl of 10× PCR buffer (Life Technologies), 1.75 µl of 50 mM MgCl<sub>2</sub> (Life Technologies), 1 µl of 10 mM dNTPs (Life Technologies), 0.125 µl of 100 µM Pol For (HXB2 genome 4901 → 4924), 0.125 µl of 100 µM Pol Rev. (HXB2 genome 5060 → 5040), 0.075 µl of 50 µM of Pol Probe, and 0.2 µl Platinum Taq (Life Technologies). The lower limit of detection of this method was of 20 copies of HIV-1 RNA in 1 µg of total RNA. The absolute number of *POL* copies in PCR was calculated using a standard curves ranging from 4 to 4 × 10<sup>5</sup> copies of a plasmid containing the full-length HIV-1 genome. The amount of HIV-1 cellular associated RNA was expressed as number of copies/µg of input RNA in reverse transcription. Preparations of cell-associated RNA were tested for potential contamination with HIV-1 DNA and/or host DNA by performing the PCR amplification in the presence and absence of reverse transcriptase.

This study was conducted in accordance with the ethical principles of the Declaration of Helsinki. The patients involved in the study provided signed informed consent and the study protocol was approved by The Netherlands Medical Ethics Committee (MEC-2012-583).

### 2.5. Total RNA Isolation and Quantitative RT-PCR (RT-qPCR)

Total RNA was isolated from the cells using RealiaPrep RNA Cell Miniprep System (Promega), cDNA synthesis was performed using Superscript II Reverse Transcriptase (Life Technologies) kit following manufactures protocol. RT-qPCR was performed using GoTaq qPCR Master Mix (Promega) following manufacturer protocol. Amplification was performed on the CFX Connect Real-Time PCR Detection System thermocycler (BioRad) using following thermal program starting with 3 min at 95 °C, followed by 40 cycles of 95 °C for 10 s and 60 °C for 30 s. Specificity of the RT-qPCR products was assessed by melting curve analysis. Primers used for real-time PCR are listed in Table 1. Expression data was calculated using 2<sup>–ΔΔCt</sup> method by Livak Schmittgen (Schmittgen and Livak, 2008). Cyclophilin A (CycA) and β-2-microglobulin were used as housekeeping genes for J-Lat cell lines and primary cells, respectively.

### 2.6. Knock-down Experiments

Pre-designed siRNA pools targeting transcripts of the human ARID1a-BAF250a (L-017,263-00-0005) and non-target control siRNA pool (D-001,810-10-20) were purchased from Dharmacon (Dharmacon, Etten-Leur, The Netherlands). Small-interfering RNAs were delivered by nucleofection using Amaxa Nucleofector (Amaxa AG-Lonza, Cologne, Germany) as previously described (Rafati et al., 2011). Briefly, cells were split to 3 × 10<sup>5</sup> cells/ml one day before nucleofection. Five million



**Table 1**  
List of RT-qPCR primers.

Primer	Sequence (5'–3')
β – Actin For	CGAAAGACCTGTACGCCAAC
β – Actin Rev	GAGCCGCCGATCCACAG
β2Microglobulin For	AGCGTACTCCAAAGATTACGGTT
β2Microglobulin Rev	ATGATGCTGCTTACATGTCCTCGAT
BAF250a For	CTTCAACCTCAGTCAGCTCCCA (Wang et al., 2012)
BAF250a Rev	GGTCAACCCACCTCATCTCTTT (Wang et al., 2012)
BRG-1 For	GCAGGCTCGCATCGCACAC
BRG-1 Rev	GCTCAATGGTCGCTTTGGTTCCG
CycA (PPIA) For	TCATCTGCACTGCCAAGACTG
CycA (PPIA) Rev	CATGCCTTCTTTCATTTGCG
Gag For	AGTAGTGTGTGCCCCGTCTGT
Gag Rev	TGCCTTTTCAGGTCCTGTTCG
Gfp For	GAAGCAGCAGCACTTCTTCAA
Gfp Rev	GCTTGTGCGCCATGATATAGA
IFNβ For	GGAGGACGCCGATTGAC
IFNβ Rev	TGATAGACATTAGCAGGAGGTTCT
IL6 For	CCCTGACCAACCAAAATGC
IL6 Rev	CAACAACAATCTGAGGTGCCAT
IL10 For	ACATCAAGGCCGATGTGAAC
IL10 Rev	GCCACCTGATGTCTCAGTT
Luc For	TCTAAGGAAGTCGGGGAAGC (Barakat et al., 2011)
Luc Rev	CCCTCGGGTGAATCAGAAT (Barakat et al., 2011)
MIP26 For	AGTGTGTGGCTCTTGTATTCTGAGG
MIP26 Rev	CCACCTCCCTGAGTCCCTTCTC
MMP9 For	TGGTCTGGTGTCTCTGGTG
MMP9 Rev	GCTGCTGTGCTGAGATTGG
SOC3 For	CCAAGGACGAGACTTCGAT
SOC3 Rev	GGTACTCGCTCTTGAGGCTG
TLR2 For	TGGATGGTGTGGGTCTTGG
TLR2 Rev	AGGTCACTGTGCTAATGTAGG
Nuc-0 For	ATCTACCACACAAAGCTAC
Nuc-0 Rev	GTACTAATCTGAAGCACCATCC
DHS-1 For	AAGTTTGACAGCTCTAGC
DHS-1 Rev	CACACCTCCCTGGAAGTC
Nuc-1 For	TCTCTGGCTAACTAGGGAACC
Nuc-1 Rev	AAAGGCTCTGAGGGATCTCTAG
ChIP CTRL Reg For	GCCAGAGTCAAGCCAGTAGTC
ChIP CTRL Reg Rev	TAGCTAATGTGGAGTGGATGTG
Alu For	GCCTCCCAAGTGTGGGATTACAG
AluGag For	GGTGGGAGAGCGTCAGTAT
AluGag Rev	AGCTCCCTGCTTCCCATA
AluGag probe	[6FAM]AAAAATTCGGTTAAGGCCAGGGGAAAGAA[BHQ1]
ALB For	TGCATGAGAAAACGCCAGTAA
ALB Rev	ATGGTCGCTGTTCACCA
ALB probe	[FAM]TCACAGAGTCACCAATGATGCACAGAA[BHQ1]
Pol For	GGTTTATTACAGGGACAGCAGAGA
Pol Rev	ACCTGCCATCTGTTTCCATA
Pol Probe	[6FAM]ACTACTGCCCTTCACTTTCCAGAG[BHQ1]

cells were centrifuged at 200 g for 10 min at room temperature, re-suspended in 100 µl of solution R, and nucleofected with 2 µM siRNA using program O28. Nucleofected cells were re-suspended in 500 µl of pre-warmed, serum-free antibiotic-free RPMI at 37 °C for 15 min and then plated in 4 ml of pre-warmed complete media. Seventy-two hours post-nucleofection cells were treated with SAHA [350 nM] or Prostratin [100 nM]. LTR-driven GFP expression was assessed after 24 and 48 h after treatment by FACS. RNA and protein for RT-qPCR and Western blot analysis were isolated 96 h after nucleofection.

## 2.7. Western blot Analysis

Cells were treated with BAF inhibitors for 36 h and then lysed with IP buffer (25 mM HEPES, pH 7.9, 150 mM KCl, 1 mM EDTA, 5 mM MgCl<sub>2</sub>, 5% glycerol, 1% NP40, 0.5 mM dithiothreitol and a protease inhibitor cocktail (Sigma Aldrich)) for 30 min on ice. Whole-cell protein lysate was used for SDS-PAGE in order to detect BAF250a, BRG-1, INI-1, IκB, and GAPDH. The following antibodies were used in Western blot analysis: anti-SMARCA4-BRG1 (sc-17,796, Santa Cruz Biotechnology; ab4081-100, Abcam), anti-ARID1a-BAF250a (kind gift from C.P.

Verrijzer), anti-SMARCA1-hSNF5 (ab4552, Abcam), anti- IκB (sc-371, Santa Cruz Biotechnology) and anti-GAPDH (ab8245, Abcam). Signal intensity for representative blots was quantified using ImageJ software according to NIH guidelines. Briefly, specific bands, related to protein of interest were marked in order to generate plots of relative density. Area under the plots, representing each band intensity, was normalized to its loading control and then to its untreated sample for BAF250a and INI-1, each band intensity for BRG-1 was normalized to its corresponding loading control and to untreated control, band intensity of treated samples for GAPDH was normalized with untreated controls.

## 2.8. Latency Establishment Experiment

HIV-derived virus particles were generated as described (Jordan et al., 2001). Briefly, HEK 293 T cells were transfected with VSVG, the R8.9 packaging vector, and the retroviral vector LTR-Tat-IRES-EGFP (pEV731). Virus was harvested every 12 h starting at 24 h after transfection. Jurkat cells were treated with 1 µM BAFi's as indicated 1 h prior to infection. Cells were then infected in presence or absence of BAFi's with the LTR-Tat-IRES-EGFP virus at low multiplicity of infection (MOI), such that approximately 10% of cells were infected. Ninety six hours after infection, the GFP negative cell population was sorted using a FACS Aria II cell sorter (Becton Dickinson) and treated with PMA. Percentage of GFP positive (latent) infections was determined by FACS analysis 48 h after PMA stimulation.

For Alu-PCR, 2–5 · 10<sup>6</sup> cells were subjected to genomic DNA isolation using DNeasy Blood & Tissue Kit (Qiagen, Hilden, The Netherlands). The following reaction mix was used for the first round PCR: 1X PCR buffer (Life Technologies), 1.5 mM MgCl<sub>2</sub> (Life Technologies), 0.5 mM dNTPs (Thermo Scientific, Waltham, MA USA) 1 µM Alu forward primer, 6 µM Gag reverse primer, 2.5 U of Platinum Taq polymerase (Life Technologies) and 150 ng of genomic DNA. Amplification was performed in a T100 Thermal Cycler (BioRad) with following thermal program: 2 min at 95 °C, followed by 14 cycles of 95 °C for 30 s, 50 °C for 30 s and 72 °C for 210 s. A nested PCR targeting the Gag gene was performed using the following reaction mix: 1 X PCR buffer, 1.5 mM MgCl<sub>2</sub>, 0.5 mM dNTPs, 0.5 µM AluGag For and AluGag Rev. primers, 0.15 µM AluGag probe (FAM-AAAATTCGGTTAAGGCCAGGGGAAAGAA-BHQ1), 1 U Platinum Taq polymerase and 3 ng of genomic DNA or 2 µl of AluGag PCR product. Amplification was performed on the CFX Connect Real-Time PCR Detection System thermocycler (BioRad) using following thermal program starting with 5 min 95 °C, followed by 30 cycles 95 °C for 30 s, 60 °C for 30 s. Albumin gene was used for normalization. Primer sequences used are listed in Table 1.

## 2.9. Chromatin Immunoprecipitation (ChIP)

Eighteen hours prior to analysis J-Lat 11.1 cells were untreated or treated with BAFi's as indicated. Twenty million cells were used per sample. Cells were washed with PBS<sup>++</sup> (PBS, 1 mM CaCl<sub>2</sub>, 1 mM MgCl<sub>2</sub>) and cross-linked for 30 min at room temperature by adding buffer A (1% HCHO, 10 mM NaCl, 100 µM EDTA, 50 µM EGTA, 2 mM HEPES pH 7.6). The reaction was quenched with 125 mM glycine. Cross-linked cells were washed in ice-cold PBS<sup>++</sup> followed by washes with buffer B (0.25% Triton-X 100, 1 mM EDTA, 0.5 mM EGTA, 20 mM HEPES, pH 7.6) and buffer C (150 mM NaCl, 1 mM EDTA, 0.5 mM EGTA, 20 mM HEPES, pH 7.6) for 10 min at 4 °C. For sonication, cells were re-suspended in ChIP incubation buffer (1% SDS, 1% Triton-X 100, 0.15 M NaCl, 1 mM EDTA, 0.5 mM EGTA, 20 mM HEPES, pH 7.6, Protease inhibitors cocktail) and chromatin was sheared by sonication to an apparent length of ~500 bp using a Bio Ruptor sonicator (Cosmo Bio Co., Ltd., Tokyo, Japan) with 20 times 60-s pulses at maximum setting at 4 °C. At least 150 µl of each sample were collected for input. Chromatin from approximately 20 million cells was diluted 7 times with ChIP incubation buffer lacking SDS, in order to decrease SDS concentration in sonicated samples. Chromatin was immunoprecipitated



with 2–5 µg of antibody specific to BAF250a (kind gift of gift from C.P. Verrijzer or sc-32761, SantaCruz Biotechnology) and BSA-blocked protein-A agarose beads (GE Healthcare) at 4 °C overnight. Beads were washed twice with the following buffers buffer 1 (0.1% SDS, 0.1% deoxycholate, 1% Triton-X 100, 150 mM NaCl, 1 mM EDTA, 0.5 mM EGTA, 20 mM HEPES pH 7.6), buffer 2 (0.1% SDS, 0.1% deoxycholate, 1% Triton-X 100, 500 mM NaCl, 1 mM EDTA, 0.5 mM EGTA, 20 mM HEPES pH 7.6), buffer 3 (250 mM LiCl, 0.5% deoxycholate, 0.5% NP-40, 1 mM EDTA, 0.5 mM EGTA, 20 mM HEPES, pH 7.6), and buffer 4 (1 mM EDTA, 0.5 mM EGTA, 20 mM HEPES, pH 7.6). Immunoprecipitated complexes and inputs were eluted in elution buffer (1% SDS, 0.1 M NaHCO<sub>3</sub>) for 30 min at room temperature, and decrosslinked overnight at 65 °C in presence of 200 mM NaCl<sub>2</sub>. DNA was extracted with phenol:chloroform:isoamylalcohol 24:24:1 (Sigma) followed by chloroform:isoamylalcohol 24:1 extraction, ethanol precipitated, and resuspended in 100 µl H<sub>2</sub>O by shaking at 37 °C. Input and immunoprecipitated DNA were subjected to Sybergreen qPCR cycles with specific primers (sequences provided in Table. 1) with an CFX Connect Real-Time PCR Detection System thermocycler (BioRad) and GoTaq qPCR Mastermix (Promega).

## 2.10. Formaldehyde-Assisted Isolation of Regulatory Elements (FAIRE)

Eighteen hours prior to analysis, J-Lat A2 and 11.1 cells were treated with BAFi's where indicated. J-Lat cells were fixed for 30 min by adding formaldehyde to a final concentration of 1% at room temperature. Twenty million cells were used per FAIRE experiment. The reaction was quenched with 125 mM glycine. Cross-linked cells were washed with PBS followed by washes with buffer B (0.25% Triton-X 100, 1 mM EDTA, 0.5 mM EGTA, 20 mM HEPES, pH 7.6) and buffer C (150 mM NaCl, 1 mM EDTA, 0.5 mM EGTA, 20 mM HEPES, pH 7.6). For sonication, cells were re-suspended in ChIP incubation buffer (1% SDS, 1% Triton-X 100, 0.15 M NaCl, 1 mM EDTA, 0.5 mM EGTA, 20 mM HEPES, pH 7.6) and chromatin was sheared by sonication to an apparent length of ~200–400 bp (corresponding to ~100–200 bp of free DNA) using a BioRuptor sonicator (Cosmo Bio Co., Ltd) with 20 times 30-s pulses at maximum setting at 4 °C. Sonicated chromatin was twice phenol:chloroform:isoamyl alcohol (24:24:1) extracted, washed with chloroform:isoamylalcohol (24:1) and ethanol precipitated. Isolated DNA was subjected to Sybergreen qPCR cycles with specific primers (sequences provided in Table. 1) with a CFX Connect Real-Time PCR Detection System (BioRad) and GoTaq qPCR Mastermix (Promega), using following thermal program starting with 3 min at 95 °C, followed by 40 cycles of 95 °C for 10 s and 60 °C for 30 s.

## 2.11. Statistical Analysis

Data are shown as the average + S.D. of three or more independent experiments. Statistical significance for multiple comparisons was calculated using Student's t test or, when appropriate, Mann–Whitney non parametric test.

According to the Bliss independence method (Bliss, 1939), threshold for synergism was calculated using the following equation  $\mu_{(1+2)exp.} = [1 - (1 - \mu_1) \times (1 - \mu_2)]$ , where  $\mu_{(1+2)exp.}$  is the expected percentage of cells reactivated after combinatorial treatment in absence of synergism and  $\mu_1$  and  $\mu_2$  correspond to the percentage of cells reactivated by the single treatments. The difference between the observed percentage of cells activated by combination treatment and the expected percentage ( $\mu_{(1+2)exp.}$ ) describes the interaction between two treatments. Combination was considered synergistic if the difference and its 95% normal confidence interval (CI) were >0. Synergistic effect of BAFi's over SAHA + Prostratin combination was calculated considering Prostratin + SAHA as a single treatment.

## 3. Results

### 3.1. Small Molecule Inhibitors of BAF Activate Latent HIV

We tested a panel of compounds (Figure S1 and Table S1), identified in a screen for inhibitors of the BAF chromatin remodeling complex (Dykhuizen et al., 2012) for their potential to activate latent HIV-1 in J-Lat A2 (Fig. 1a) and J-Lat 11.1 (Fig. 1b) cells. These Jurkat clonal cell lines contain, respectively, an integrated latent LTR-Tat-IRES-GFP virus or a defective full-length HIV-1 genome expressing GFP in place of Nef (Jordan et al., 2003). Six compounds significantly activated the latent HIV-1 in both cell lines, however 3 of these displayed significant toxicity at the concentrations tested in the screening. Therefore we focused on A01, A11, and C09, the three BAF inhibitors displaying the strongest capacity to activate latent HIV-1 while not significantly affecting cell viability. Titration experiments indicated optimal concentrations for these compounds in HIV-1 activation to be in the 0.5–2 µM range in J-Lat cell lines (Fig. 1c).

As the BAF inhibitors were identified in a screen in mouse ES cells, we set out to confirm their specificity in inhibition of the BAF complex in human CD4+ T cells. Thus, we analyzed the gene expression profile of human CD4+ T cells after siRNA depletion of the BAF-specific subunit BAF250a and compared it with the gene expression profile obtained after treatment with BAFi's. J-Lat 11.1 cells were transfected with a siRNA targeting the BAF250a subunit and the expression levels of the LTR driven transcripts as well as those of endogenous BAF target genes were analyzed by RT-qPCR 48 h after transfection. Depletion of BAF250a was confirmed by RT-qPCR and Western blot analysis (Fig. 2a). As observed previously (Rafati et al., 2011), depletion of BAF250a resulted in activation of latent HIV-1 as determined by an increase in expression of the HIV-1 LTR-driven *P24* and *GFP* reporter (Fig. 2b). Moreover, qRT-PCR analysis identified a set of endogenous previously described BAF target genes which were positively or negatively modulated after BAF250a knock down. In particular, BAF250a depletion induced the expression of *IL10* (Wurster et al., 2012), and *SOC3* (Dykhuizen et al., 2012), and decreased the expression of *TLR2*, *MMP9*, *INFβ*, and *IL6* (Barker et al., 2001; Ni and Bremner, 2007) (Fig. 2b). To determine the level of activity and specificity of the BAFi's, we examined the gene expression profile of J-Lat11.1 cells 18 h after treatment with A01, A11, and C09 (1 µM). Mirroring BAF250a depletion, treatment with A11 and C09 upregulated *IL-10* and *SOC3* while downregulating the expression of endogenous BAF target genes *TLR2*, *MMP9*, *INFβ*, *IL-6*, whereas treatment with A01 resulted in significant down-regulation of *MMP9* only, together with a significant upregulation of both *IL-10* and *SOC3* (Fig. 2c). All BAFi's activated latent HIV-1 as demonstrated by the increase in *P24* and *GFP* expression (Fig. 2c). Thus, inhibition of BAF with BAFi's functionally mimicked the effect of siRNA depletion of BAF250a in modulating the expression of endogenous BAF target genes and resulted in activation of the latent HIV-1 as demonstrated by an increase in *GFP* and *P24* expression.

To determine the direct effects of BAFi treatment on the latent HIV-1 promoter, we examined the BAF complex occupancy of the promoter by ChIP assay. We have shown previously that, while bound to the latent HIV-1 LTR, the BAF complex is displaced upon LTR activation (Rafati et al., 2011). Similarly, as shown in Fig. 2d, the stimulation with the BAFi's A11 and C09 results in the displacement of the BAF specific subunit BAF250a, which is specifically enriched in the DHS1 and nuc-1 regions on the latent HIV-1 promoter. These results provide a direct mechanistic evidence for the function of BAFi's in HIV-1 latency.

To investigate the mechanism mediating the activity of the BAFi's, we analyzed the expression of the BAF subunits at the RNA and at the protein level. To determine whether BAFi's directly affect the BAF complex at the protein level, we quantitated the relative expression of the BAF subunits BAF250a, BRG1, and INI-1 by Western blotting after treatment with increasing concentrations of BAFi's (Figure S2a). Treatment of cells for 36 h with increasing concentrations of A11 and C09

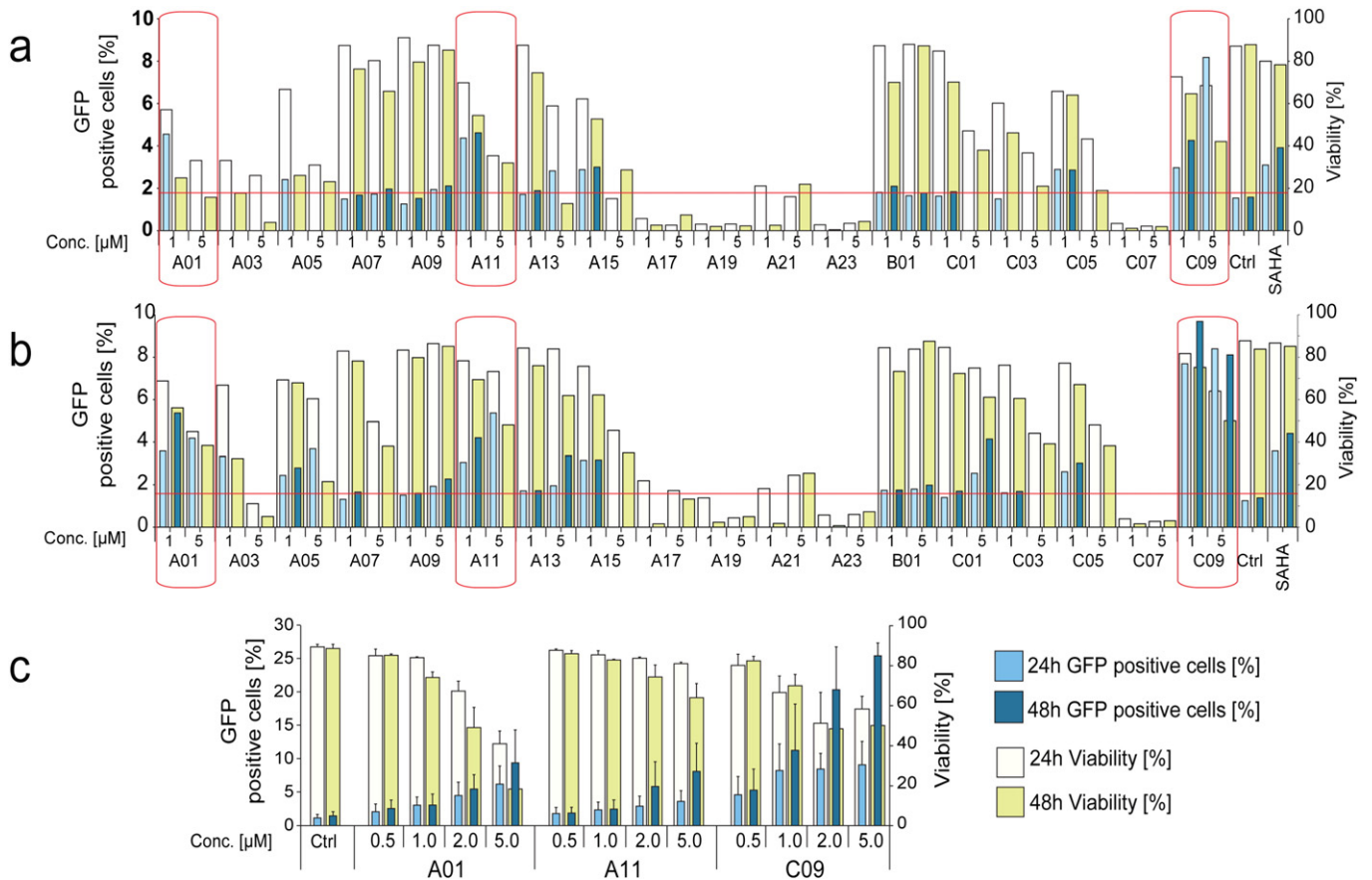


**Fig. 1.** Small molecule inhibitors of the BAF complex (BAFi's) re-activate latent HIV. J-Lat A2 (Panel a) and 11.1 (Panel b) cells were treated with BAFi's at 1 μM and 5 μM concentrations and re-activation quantitated at 24 and 48 h post treatment. Percent of GFP positive cells (left axes, dark colored bars), corresponding to the level of HIV-1 activation, and cell viability (right axes light colored bars) were evaluated by FACS analysis. GFP levels of samples in which cell viability was below 50% are not shown. HIV-1 activation was considered significant when GFP levels exceeded the average + 2SD of untreated controls (red horizontal line). Red squares identify BAFi's which induced activation of HIV-1 without significantly affecting cell viability. These compounds were further investigated for their ability to activate HIV-1 transcription in 11.1 cells (Panel c). Data are presented as mean ± SD.

resulted in a decrease in the BAF-specific subunit BAF250a protein levels, while not affecting the BRG1 and INI-1 subunits. We observed a decrease of BAF250a levels of up to 50% after treatment with the highest concentrations of A11, while C09 treatment resulted in a substantial (up to 70%) decrease in BAF250a (Figure S2a). At the RNA level, the expression of BAF250a did not change in response to BAFi's (Figure S2b), excluding an indirect mechanism whereby BAFi's treatment would cause a decrease in transcription of the BAF subunits. Conversely, the negative effect of A11 and C09 on stability of BAF250a is consistent with a mechanism of direct inhibition, in which destabilization and degradation of BAF250a at the protein level results in the specific inhibition of the BAF complex.

### 3.2. HIV-1 Latency Reversal by BAFi's is Synergistically Enhanced by Co-treatment With Prostratin and SAHA

Combination therapy using latency reversal agents (LRAs) targeting different pathways is considered the most effective strategy for reactivation of latent HIV-1 (De Crignis and Mahmoudi, 2014; Laird et al., 2015). HDAC inhibitors (HDACi's) and PKC agonists are two promising classes of compounds currently under clinical investigation for their potential to reverse HIV-1 latency. HDACi's counteract the activity of histone deacetylases which repress HIV-1 transcription by compacting chromatin structure, whereas Prostratin induces translocation of NF-κB to the nucleus where it binds to the HIV-1 LTR and activates its transcription. To examine whether the combination of these mechanisms with BAF inhibition would enhance the activation of latent HIV-1 we evaluated the effect of SAHA and Prostratin after siRNA mediated

knock down of BAF complex or treatment with BAFi's. The Bliss independence model for combined drug effects was used to calculate the threshold for synergism (Bliss, 1939; Zhao et al., 2014a).

J-Lat 11.1 cells were treated with SAHA or Prostratin after nucleofection with BAF250a-specific siRNA. siRNA treatment alone induced a limited activation of HIV-1 LTR as shown by the slight increase in the percentage of GFP positive cells at 48 h; when BAF250a-depleted cells were co-treated with Prostratin or SAHA, however, we observed a synergistic or additive, respectively, increase in reactivation of latent HIV-1 (Fig. 3a). Neither treatment significantly affected cell viability. Notably, we observed a similar effect when BAF complex activity was inhibited using BAFi's. J-Lat 11.1 cells were treated with Prostratin or SAHA alone or together with increasing concentrations of A01, A11, and C09 ranging from 0.5 μM to 4 μM (Fig. 3b). C09 demonstrated the most potent activity, synergistically enhancing HIV-1 transcription with both Prostratin and SAHA at all tested concentrations, whereas combination of LRAs with either A01 or A11 induced a synergistic or additive increase in activity depending on the concentration tested as shown (Fig. 3b). Interestingly, all BAFi's showed synergism used in triple treatment, i. e. when cells were treated with a combination of SAHA and Prostratin together with sub-optimal concentrations of BAFi's (Fig. 3c). We performed Formaldehyde Assisted Isolation of regulatory Elements (FAIRE) in order to examine the effect of BAFi's on the positioning of the latent HIV-1 LTR nuc-1 (Fig. 3d). Consistent with the previously observed HIV-1 activation and the displacement of BAF250a from DHS-1 and Nuc-1 demonstrated by ChIP assay, treatment with BAFi's resulted in a dose dependent remodeling of nuc-1 as demonstrated by

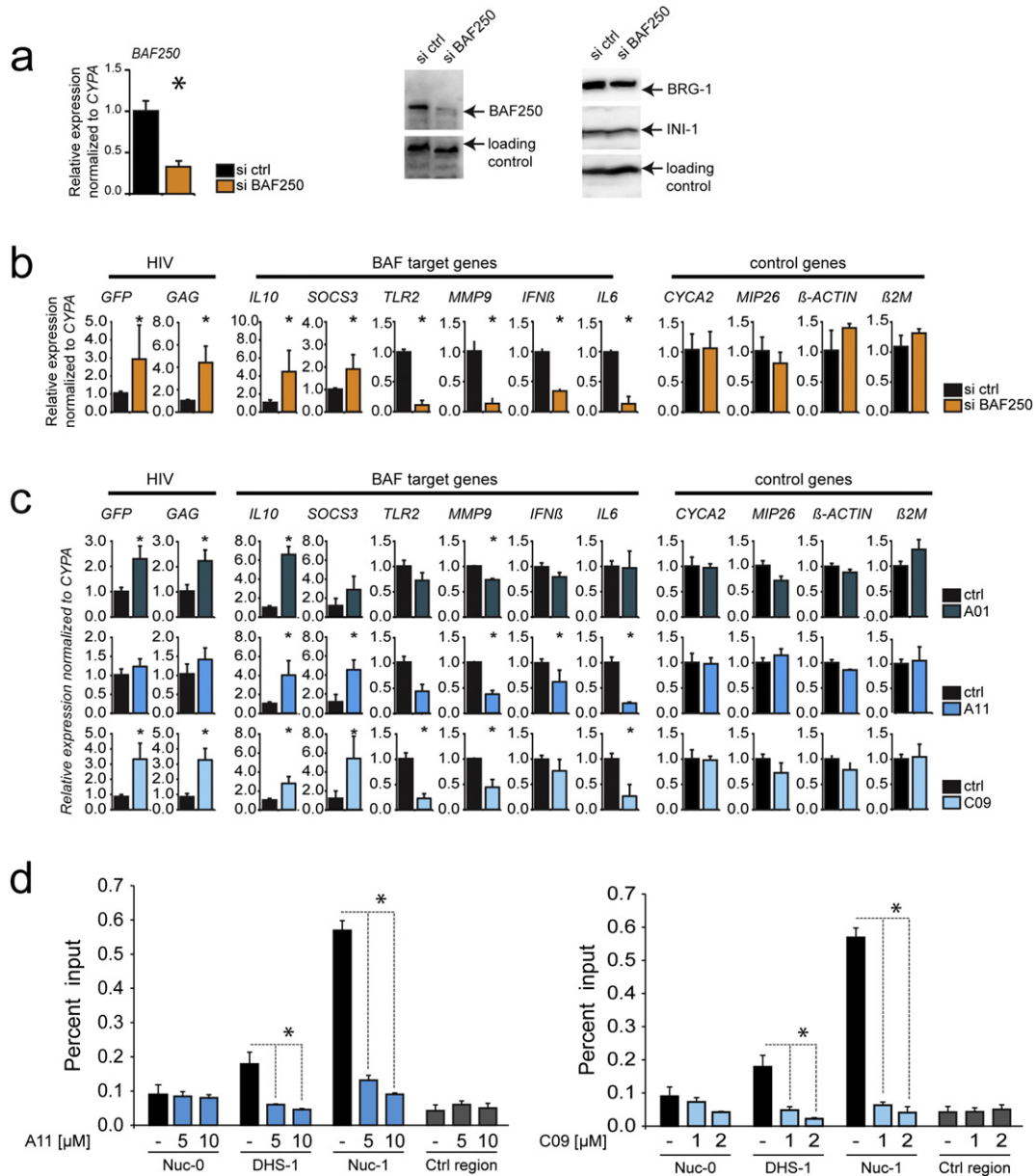


**Fig. 2.** Treatment with BAFi's specifically modulates BAF target genes, and displaces the BAF complex from the latent HIV-1 LTR. (Panel a) Knockdown of BAF complex was obtained by nucleofecting J-Lat 11.1 cells with siRNA targeting the BAF complex specific subunit BAF250a. RNA levels of BAF250a were quantitated by RT-PCR analysis, whereas protein levels of BAF250a as well as of the other subunits of the complex were determined by Western blot. RT-PCR analysis of J-Lat 11.1 cells after BAF250a knockdown (Panel b) or treatment with BAFi's A01 (1  $\mu$ M), A11 (1  $\mu$ M) and C09 (1  $\mu$ M) for 18 h (Panel c). The effect of BAFi's treatment was monitored analyzing the changes in gene expression of HIV-1 LTR driven genes (*GFP*, *GAG*) and BAF target genes (*TLR2*, *MMP9*, *IFN $\beta$* , *IL6*, *IL10*, *SOC3*). A set of BAF independent genes (*CYCA2*, *MIP26*,  $\beta$ -*ACTIN*,  $\beta$ -*MICROGLOBULIN*) was used as control. RT-qPCR data are presented as mean  $\pm$  SD. (Panel d) BAFi treatment results in displacement of the BAF complex-specific subunit BAF250a from DHS1 and nuc-1 regions of the HIV-1 LTR. J-Lat 11.1 cells untreated or treated with BAFi's at indicated concentrations were subjected to ChIP using antibodies specific for the BAF250a subunit. Input and immunoprecipitated DNA were analyzed by PCR using primer pairs specific for the HIV-1 LTR nuc-0, DHS1, and nuc-1 regions and for a control region located upstream of the Axin gene promoter. ChIP results are presented as percent of immunoprecipitated material over input, error bars represent the standard deviation of three independent experiments. \* indicates the level of significance at  $p < 0.05$ .

increased accessibility of the DNA encompassing the positioned nuc-1 (Fig. 3d and Figure S3). Moreover, BAFi-induced remodeling of nuc-1 was also synergistically enhanced at the molecular level after co-treatment with Prostratin (Fig. 3d and Figure S3b).

The striking synergism observed when cells were co-treated with the BAFi C09 and the PKC agonist Prostratin was unexpected, as C09 or Caffeic Acid Phenethyl Ester (CAPE) has been previously described to be an inhibitor of NF- $\kappa$ B, albeit at significantly higher concentrations (Marquez et al., 2004; Natarajan et al., 1996; Wang et al., 2010). We therefore examined the activity of C09 in a range of concentrations on Prostratin-induced I $\kappa$ B $\alpha$  degradation and HIV-1 activation. At concentrations effective in latency reversal (0.5–2  $\mu$ M), C09 did not inhibit

I $\kappa$ B $\alpha$  degradation induced by Prostratin (Figure S4a). Moreover, while synergistic with Prostratin in activation of the latent HIV-1 promoter at low concentrations, C09 interfered with the ability of Prostratin to re-activate latent HIV-1 when used at higher concentrations (30–100  $\mu$ M) (Figure S4b), consistent with its previously described activity as an NF- $\kappa$ B inhibitor.

### 3.3. BAFi's Reverse HIV-1 Latency in Primary Infected CD4 + T Cells Without Inducing Cell Activation

The main reservoir of latent HIV-1 in infected patients resides in resting CD4 + T cells. Due to their extended life span and the capacity



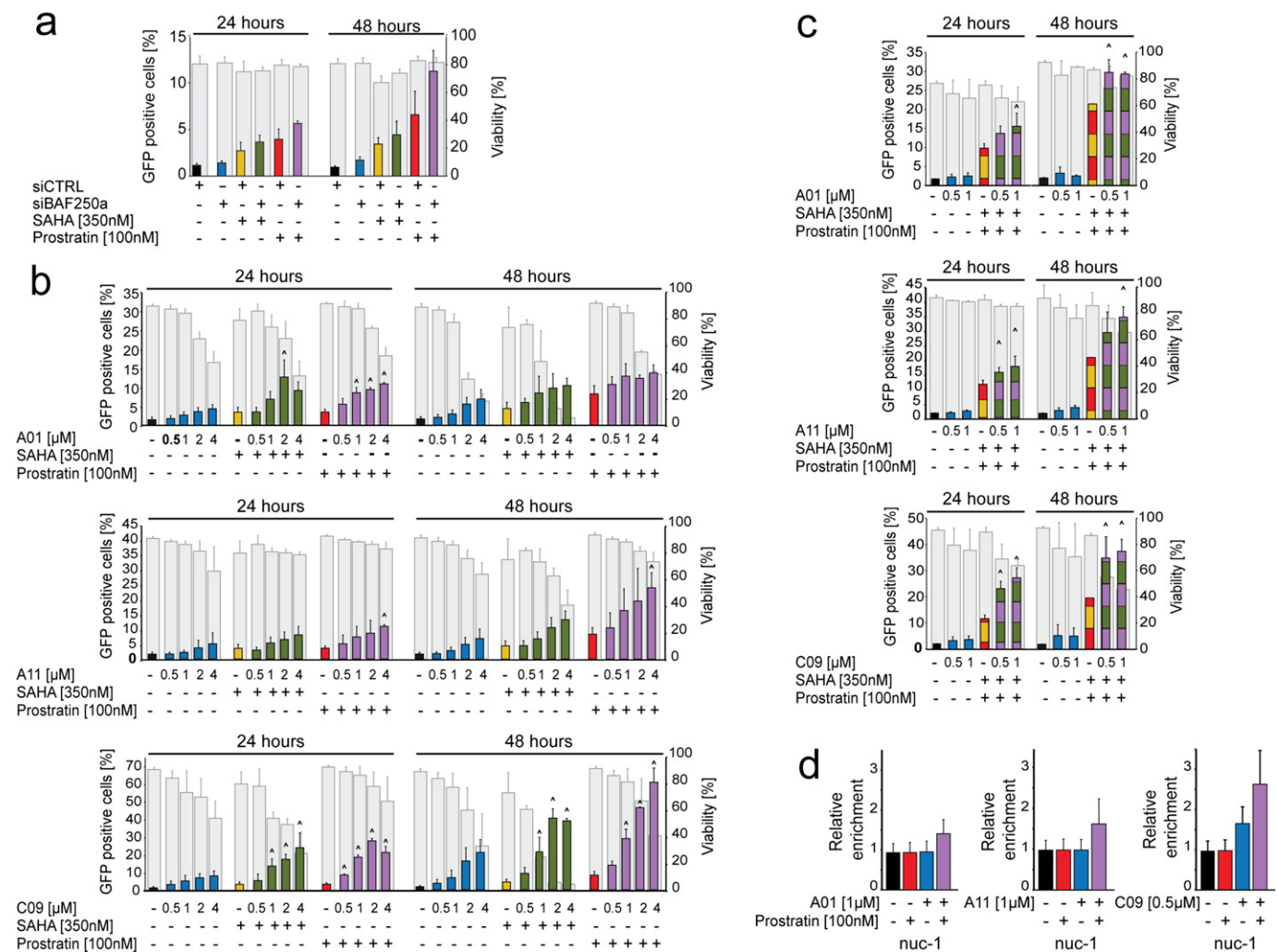


**Fig. 3.** Re-activation of latent HIV-1 by BAF inhibition is synergistically enhanced with co-treatment with HDACi's and PKC agonists. (Panel a) Percent of GFP positive cells was evaluated in BAF complex depleted J-Lat 11.1 cells 24 and 48 h after treatment with suboptimal concentrations of Prostratin and SAHA. (Panel b and c) J-Lat 11.1 cells were treated with BAFi's A01, A11 and C09 alone or together with SAHA and/or Prostratin. HIV-1 re-activation was monitored by measuring the percentage of cells expressing GFP: colored bars show the percent of GFP positive cells after treatment, whereas gray bars show cell viability. (Panel d) Levels of nucleosome occupancy of the HIV-1 5'LTR Nuc-1 region following treatment with BAFi's alone and in combination with Prostratin were analyzed using FAIRE assay. Data are presented as mean  $\pm$  SD. The (\*) symbol indicates a synergistic interaction between treatments.

of self-renewal these latently infected cells constitute the major barrier to HIV-1 eradication and are the most relevant target to determine the activity and efficiency of potential LRAs. Therefore, while T cell line models of HIV-1 latency represent useful models for compound screens and the initial molecular characterization of putative LRAs that requires large scale techniques, it is critical that potential LRAs are characterized also in primary T cell models of HIV-1 latency.

Several primary cell models of HIV-1 latency have been developed and validated in past years. In this study we first tested the activity of BAFi's using two in vitro primary models that recapitulate two different mechanisms that are thought to mediate the establishment of HIV-1 latency in vivo (Fig. 4a and b). In the first model, initially developed by O' Doherty (Swiggard et al., 2005) and further modified by Lassen and Greene (Lassen et al., 2012), primary cells are infected without activation; the lack of specific transcription factors and the reduced metabolic rate in resting cells prevents the establishment of a productive infection and drives the virus into the latent state (Fig. 4a). In this model, infected cells mainly belong to the Transitional (CD4 + CD45RO + CCR7- CD27 +) and Central Memory (CD4 + CD45RO + CCR7 + CD27 +) populations. In the second method, developed by Bosque and Planelles, primary CD4 + T cells are stimulated for three days and infection is performed after removing the activating stimuli,

i.e. during reversion to the resting state (Bosque and Planelles, 2009) (Fig. 4b). Cells generated via this model acquire a phenotype that closely resembles the CD4 + Central Memory population (CD4 + CD45RO + CCR7 + CD27 +), which is thought to harbor the majority of latent proviruses in HIV-1 infected individuals under suppressive cART (Chomont et al., 2009). In both protocols, cells were infected with a defective virus harboring luciferase in place of the envelope gene and latency reversal activity was monitored determining the levels of luciferase activity 24 h after treatment with BAFi's.

To verify the activity of BAFi's on latent HIV-1, primary cells were treated with increasing concentrations of A11 and C09, the two compounds showing the maximum activity in cell line models of latency. The range of concentrations was selected based on their toxicity profile on primary cells. We observed a dose dependent increase in luciferase activity after treatment with C09 (Fig. 4c and d) with significantly higher levels of luciferase activity compared to untreated control at 1  $\mu$ M and 2  $\mu$ M concentrations ( $p < 0.05$ ). Treatment with A11 did not induce significant activation of latent HIV-1, however we observed a tendency towards activation at the highest concentration (10  $\mu$ M).

CD4+ T cells obtained from virologically suppressed HIV-1 infected patients are considered the most relevant model system for assessing the efficacy of potential latency reversal compounds. In light of our

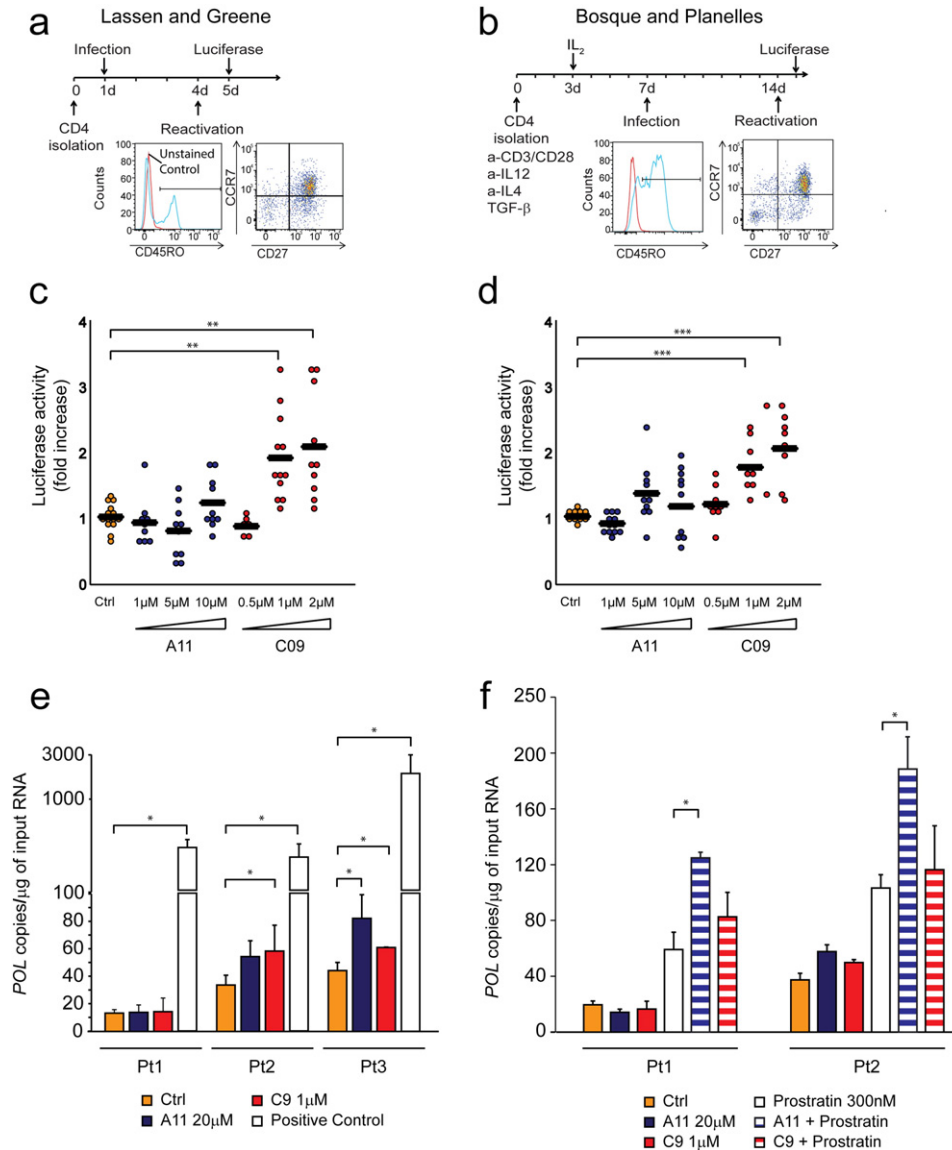


**Fig. 4.** BAFi treatment re-activates latent HIV-1 in two distinct primary model systems of HIV-1 latency. Latency reversal activity of the BAFi's A11 and C09 was tested on two models of HIV-1 latency. Panel a (Lassen and Greene) and b (Bosque and Planelles) depict the protocols for latency establishment in primary human CD4 + T cells. FACS plots show the characteristic of the cells population at the moment of reactivation for each method. Dotplots (Panels c and d) show the fold increase in luciferase activity after treatment with different concentrations of A11 and C09. Each dot represents a single measurement, black horizontal lines show the average fold increase for each treatment. Experiments were performed in duplicate using cells obtained from 6 healthy blood donors. Panel e shows the levels of cell associated HIV-1 RNA in CD4 + T cells isolated from three virologically suppressed HIV-infected patients after treatment with the BAFi's C09 and A11. Cells obtained from Patient 1 and Patient 2 were further analyzed and treated with BAFi's in combination with Prostratin (Panel f). Cell associated HIV-1 RNA was measured as the number of copies of HIV-1 POL per  $\mu\text{g}$  of input RNA; for each condition, bars represent the average of experiments performed at least in triplicate. Statistical significance was calculated within patient, based on at least three independent replicates performed for each condition. Asterisks indicate the level of significance (\*  $p < 0.05$ , \*\*  $p < 0.01$ , \*\*\*  $p < 0.001$ ).

results showing the activity of A11 and C09 in latency reversal in primary ex-vivo infected cells, we sought to confirm these observations in CD4 + T cells obtained from HIV-1 infected patients. Three patients who maintained HIV-1 viremia below 50 copies/ml for at least two years (Pt1 3 years; Pt2 2 years; Pt 3 3 years) were enrolled in the study. Untouched total CD4 + T cells were purified from PBMCs and used to assess the effect of BAFi's on the latent HIV-1 reservoir. Treatment with BAFi's alone increased the levels of cellular associated HIV-1 RNA in CD4 + T cells obtained from two out of three patients. In this model, increase in HIV-1 transcription after BAFi treatment mirrored the results obtained in the ex vivo infected primary cells: C09 elicited HIV-1 transcription at 1  $\mu\text{M}$  concentration, and A11 showed reversal activity at 20  $\mu\text{M}$ , confirming the trend observed in the ex vivo infected model (Fig. 4e). A variable response to treatment with de-repressors in primary cells obtained from HIV-1 infected patients has

been observed previously (Archin et al., 2012; Wei et al., 2014; Laird et al., 2015); however, even in absence of a detectable effect, the removal of a repressive mechanism has been suggested to facilitate triggering of transcription by enhancing noise and increasing the likelihood of stochastic promoter activation (Dar et al., 2014). We therefore examined the effect of the co-treatment of BAFi's together with the PKC agonist Prostratin on cells obtained from Patients 1 and 2. CD4 + T cells obtained from Patient 1, which did not respond to BAFi's alone, and CD4 + T cells obtained from Patient 2, which showed a BAFi-induced increase in HIV-1 cellular associated RNA, were treated with BAFi's alone or in combination with a sub-optimal concentration of Prostratin. As shown in Fig. 4f, treatment with BAFi's enhanced Prostratin-mediated HIV-1 transcription, independently of the response of cells to BAFi treatment alone. In particular, combination treatment with A11 together with Prostratin resulted in a significant enhancement

of Prostratin-induced increase in cellular associated HIV-1 RNA in both patients. Interestingly, C09, although capable of significantly inducing latency reversal in patient cells when used alone, did not significantly enhance Prostratin-mediated latency reversal, consistent with its role in NF- $\kappa$ B pathway inhibition. Given this limitation, C09 will likely be more effective in latency reversal combinations lacking PKC activators. Taken together, these results showed that treatment with BAFi's either alone or in combination with Prostratin resulted in latency reversal in all three patients included in the study.

Activation of bystander uninfected cells is a side effect which can be observed after treatment with LRAs (DeChristopher et al., 2012; Korin et al., 2002). Massive stimulation of T cells can result in general immune activation and thus will decrease the potential usefulness of latency reversal molecules in clinical settings. To investigate the effect of BAFi's on primary cells we treated human CD4+ T cells isolated from healthy donors with A11 and C09 for 72 h, and determined the levels of T cell activation and proliferation by flow cytometric analysis of CD25 and Ki67, respectively. Treatment with PMA-Ionomycin was used as a positive control. As shown in Fig. 5, in contrast to

PMA, treatment with BAFi's did not induce CD25 (Fig. 5a) and Ki67 (Fig. 5b) expression compared to untreated control during 3 days of treatment.

#### 3.4. Treatment with BAF Inhibitors Prevents Latency Establishment in Jurkat Cells

We have previously demonstrated that, in addition to its role in maintenance of HIV-1 latency, the BAF complex also contributes to the establishment of latency, as siRNA depletion of BAF subunits significantly decreased the incidence of latent infections in T cell lines (Rafati et al., 2011). We therefore examined whether inhibition of the BAF complex with A01, A11, and C09 interfered with the establishment of HIV-1 latency.

Jurkat cells were pre-treated with 1  $\mu$ M A01, A11, or C09 for 30 min prior to infection with an HIV-1 derived virus containing a GFP reporter, LTR-Tat-IRES-GFP in presence of BAFi's. Percentage of GFP positive cells and relative amount of integrated DNA were measured five days after infection to evaluate infection efficiency. GFP-negative cell population

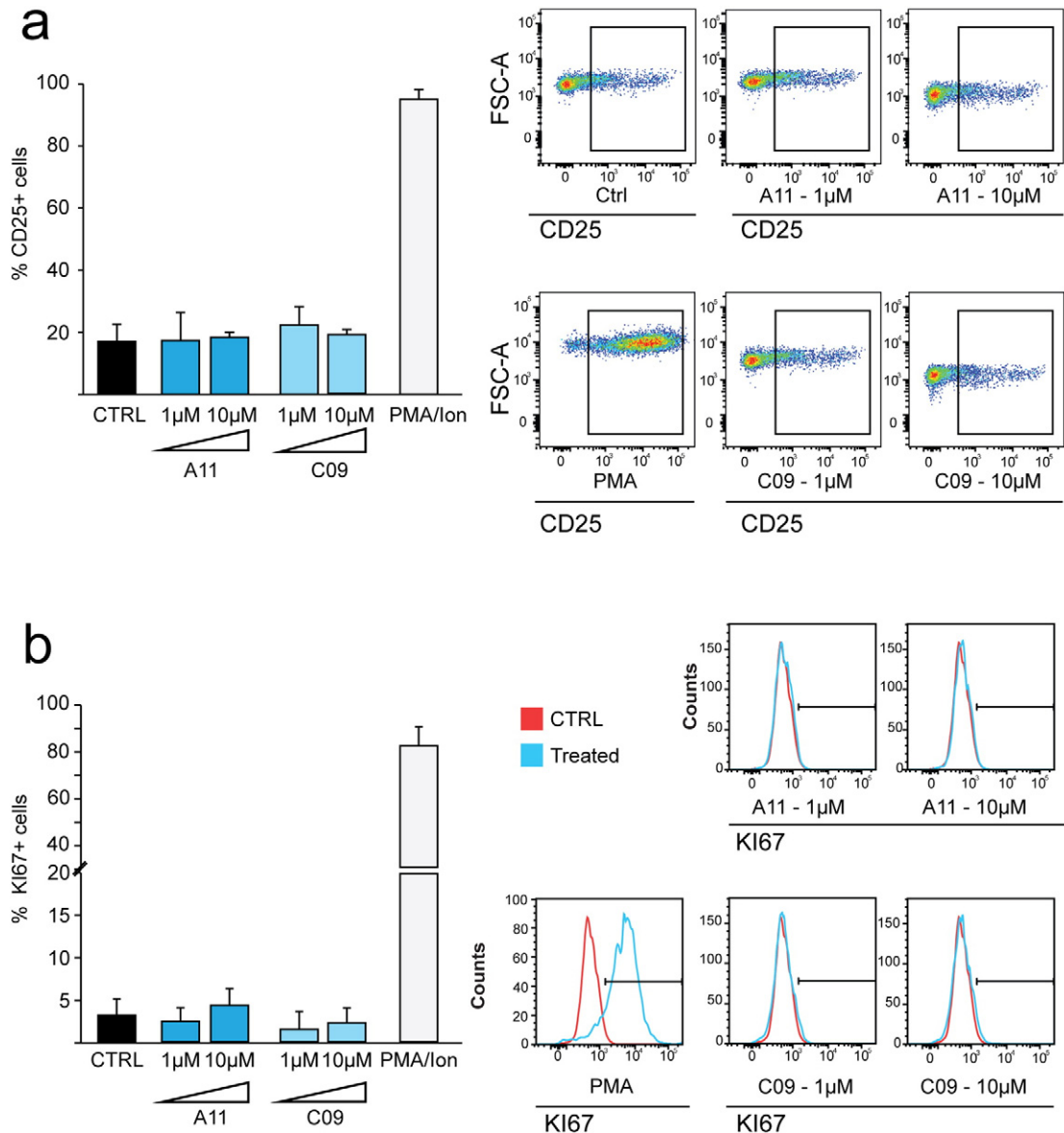


**Fig. 5.** BAF inhibitors do not induce T cell activation or proliferation. Percentage of cells expressing the markers of cell activation (CD25, panel a) and proliferation (Ki67, panel b) in primary CD4+ T cells treated with A11 and C09. Treatment with PMA/Ionomycin was used as a positive control. Bars represent the average  $\pm$  SD of experiments performed on samples deriving from three healthy blood donors. Images on the figure shows representative FACS plots for each marker.

consisting of uninfected and potentially latently infected cells were sorted by flow cytometry and stimulated with PMA. The percentage of GFP positive, latently infected cells was then determined and quantitate by FACS analysis (Fig. 6a). While treatment with A01 caused a slight increase in productive integrations, treatment of cells with A11 and C09 did not significantly affect the percentage of cells productively infected with the HIV-1 derived virus (Fig. 6b and c). However, when cells were treated with either A11 or C09, we observed a significant decrease in the percentage of GFP positive cells after PMA treatment, corresponding to a lower incidence of latent infections (Fig. 6d). Taken together these data show that inhibition of BAF activity using A11 and C09 interferes with the establishment of latency.

#### 4. Discussion

Recent pharmacological efforts aimed at HIV-1 eradication have focused on the development of “shock and kill” strategies, where HIV-1 is induced from latency in order to render infected cell recognizable to the immune system for clearance. We showed previously that the BAF chromatin remodeling complex plays an important role in the establishment and maintenance of HIV-1 latency, highlighting BAF as an attractive molecular target in HIV-1 eradication efforts. We have now tested a panel of small molecules, recently discovered in a screen for inhibition of BAF activity, for their potential to reverse HIV-1 latency. Treatment with BAFi's results in activation of latent virus in cell line as well as primary cell models harboring latent HIV-1. BAFi's constitute a group of molecules including compounds with different chemical structures targeting BAF activity with different degrees of specificity and potency. In the present screening we found the highest levels of HIV-1 activation for two compounds, A11 and C09.

A11, or Pyrimethamine (PYR), is an FDA approved licensed anti-protozoan drug which has been used to control opportunistic infections in HIV-1 infected patients (Rosenblatt, 1999; Klinker et al., 1996; Mathanga et al., 2011). Consistent with our results describing PYR as an activator of HIV-1 transcription, a previous report has shown that PYR, in the 10–100  $\mu$ M range, can enhance HIV-1 replication in vitro in

human PBMCs (Oguariri et al., 2010). C09, caffeic acid phenethyl ester (CAPE), is a bioactive compound found in many plants and isolated from honey bee propolis (Wu et al., 2011) shown to possess anti-inflammatory and immunomodulatory capacities (Tolba et al., 2013). CAPE, currently under clinical investigation (Clinical trial.gov identifier: NCT02050334 and NCT02351622), has been proposed in the treatment of several diseases including thrombocytopenia and cancer. CAPE has also been shown to function as a non-competitive inhibitor of the enzyme HIV-1 integrase and thus inhibits HIV-1 replication (Fesen et al., 1994). In the 0.5–2  $\mu$ M concentration range in which CAPE efficiently reactivates latent HIV-1, we did not observe an inhibitory effect on HIV-1 integration. We did however observe a decreased propensity for latency establishment in Jurkat cells in presence of low concentrations of both PYR and CAPE, mimicking decreased latency establishment upon siRNA mediated depletion of BAF shown previously (Rafati et al., 2011). The ability of BAFi's to prevent establishment of latency is of great interest in light of their potential use as LRAs. Indeed, despite the high efficiency of cART, the concentrations of antiretroviral drugs might not reach the optimal levels in some anatomical compartments. If reactivation of latent HIV-1 takes place in these compartments, de novo infections may occur and possibly lead to the establishment of a new reservoir. The use of LRAs that also inhibit infection and latency establishment, such as BAFi's and Romidepsin (Jonsson et al., 2015), could therefore increase the overall safety of latency reactivation strategies.

One important clinical consideration to be made in evaluating the potential of candidate molecules for latency reversal is whether they are able to generate sufficient levels of HIV-1 activation without inducing immune activation. Using two primary cell models of latency, we found that BAFi's induce reversal of HIV-1 latency in primary CD4+ T cells, which represent the main target of HIV-1 infection and harbor the majority of latent virus. Importantly, treatment of primary cells with BAFi's, at concentrations which efficiently induce latency reversal, did not result in cell proliferation nor caused general activation of primary CD4+ T cells. We also examined the activity of BAFi's in CD4+ T cells obtained from three long-term virologically suppressed

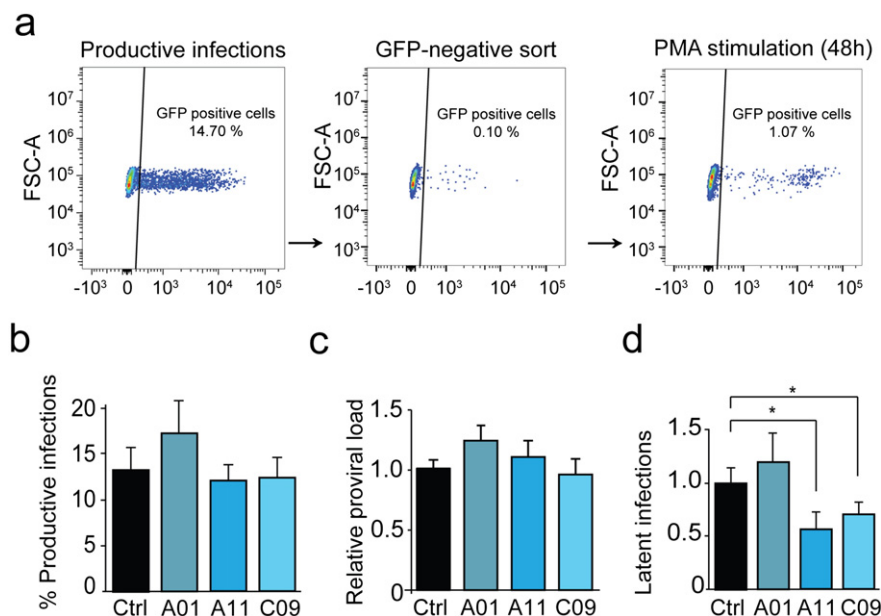


**Fig. 6.** Inhibition of BAF prevents the establishment of latent HIV-1 infections. (Panel a) FACS plots show the protocol for quantification of latently infected cells. GFP-negative cells were sorted (left panel) five days after infections. Following sorting, the GFP-negative population (middle panel) was stimulated with PMA and the percentage of reactivated cells was measured 48 h after reactivation (right panel). (Panel b) Infection efficiency in untreated vs BAFi's treated samples was determined by FACS. Bars represent the percent of GFP positive cells (i.e. productive infections) 5 days after infection. (Panel c) Proviral load from the infected population was measured by Alu-PCR. Bars represent the relative amount of HIV-1 DNA compared to untreated control. (Panel d) GFP-negative population (containing uninfected as well as latently infected cells) was treated with PMA for 48 h. Bars represent the percentage of GFP positive cells (i.e. latently infected cells) for each treatment. Data are presented as mean  $\pm$  SD, \* indicates the level of significance at  $p < 0.05$ .



HIV-1 infected patients, as this model is currently considered the most relevant model of latency. The patients included in our study were treated for at least 3 years and showed no sign of viral replication for at least 2 years. In fully suppressed c-ART treated patients, the presence of HIV-1 in activated T cells has been shown to be negligible (Finzi et al., 1997). To assess BAFi-mediated latency reversal, we therefore used total CD4 + patient T cells that include both activated and resting T cells as a surrogate for resting CD4 + T cell response, an approach also used in other recent studies to examine latency reversal ex vivo (Wei et al., 2014; Jiang et al., 2014, 2015).

In Patient 2 and 3, treatment with BAFi's alone increased the levels of cellular associated HIV-1 RNA. Although limited, the two fold increase in HIV-1 cellular associated RNA levels observed is similar to the modest effects of BAFi treatment alone observed in both cell line models and in vitro infected primary cells, and is consistent with de-repression, which results from removal of an LTR-bound repressive complex. Similar levels of activity have been observed for other candidate LRAs such as Vorinostat, Disulfiram, JQ1, and Romidepsin (Jiang et al., 2014; Laird et al., 2015; Wei et al., 2014). Importantly, many of the putative LRAs which showed limited latency reversal activity when used alone, have been shown to effectively induce HIV-1 transcription when used in combination (Laird et al., 2015; Spivak et al., 2015; Barton et al., 2014). Similarly, in cells obtained from both Patient 1, in which treatment with BAFi's alone did not upregulate the levels of HIV-1 RNA, and Patient 2, which responded to BAFi treatment, co-treatment using PYR together with the bona fide activator Prostratin resulted in significant enhancement of Prostratin mediated HIV-1 activation.

Interestingly, although CAPE when used alone induced significant latency reversal in cells from two of the three patients examined, it did not result in significant enhancement of Prostratin-mediated latency reversal. This lack of synergy is likely due to the described effect of CAPE in inhibition of NF- $\kappa$ B. At high concentrations (10–85  $\mu$ M) CAPE has been shown to block phosphorylation and degradation of I $\kappa$ B (Zhao et al., 2014b; Wang et al., 2010; Shvarzbeyn and Huleihel, 2011), and to inhibit translocation and DNA binding of p65 (Natarajan et al., 1996; Marquez et al., 2004). It is noteworthy that, in our experimental setting, CAPE was effective in activating latent HIV-1 at concentrations ranging from 0.5 to 2  $\mu$ M. At these relatively low concentrations, CAPE showed significant synergy in latency reversal and did not show an inhibitory effect towards either Prostratin-induced activation of latent HIV-1 or Prostratin-mediated degradation of I $\kappa$ B in cell lines. The difference between cell line and patient cell response to CAPE in latency reversal highlights the importance of validation of potential LRA activity in primary cells.

Another clinical consideration in appraising the potential for candidate LRAs, is the question of target specificity; most LRAs currently under investigation target chromatin modifying factors or transcriptional pathways, which are essential for normal regulation of host gene expression. Targeting these complexes will therefore have pleiotropic consequences and result in mis-regulation of host gene expression as it was recently shown for SAHA (Elliott et al., 2014). Similarly to SAHA, treatment with BAFi's, particularly at high concentrations, may result in adverse pleiotropic effects, including induction of genes counteracting HIV-1 activation (White et al., 2015). Further studies, such as transcriptome and proteome analysis, are needed to determine the array of cellular modifications induced by these compounds. In this context, inclusion of distinct LRAs, which function via different molecular targets in a combination therapy, would decrease the adverse pleiotropic effects of each compound, decrease toxicity issues, and provide a higher degree of specificity for the HIV-1 LTR.

Transcription of integrated HIV-1 is stochastic, and reversal of the latent state using a single agent can be limited by specific factors, including restrictions posed by the site of integration of the virus and its molecular environment, subtypes of the latent virus and their susceptibility to a single agent, and the cell type in which latency is established. Data obtained from in vitro cell line HIV-1 latency models support the

effectiveness of combinatorial approaches for the synergistic activation of HIV-1 transcription. These synergistic effects are likely the result of the combination of two mechanisms: the removal or decrease in a repressive chromatin environment together with the triggering and recruitment of bona fide activators. Combination of Prostratin with HDACi's results in synergistic activation of HIV-1 in vitro (Reuse et al., 2009; Ying et al., 2012; Qu et al., 2013; Burnett et al., 2010; Pandeló et al., 2014; Micheva-Viteva et al., 2011) as well as ex vivo (Laird et al., 2015). Similarly, BAFi-mediated reversal of transcriptional latency was synergistically enhanced when latent cells were co-treated with the HDAC inhibitor SAHA or the PKC agonist Prostratin. FAIRE assays indicate remodeling of the repressive LTR nuc-1 in response to BAFi treatment at the molecular level, and demonstrate the molecular synergism between Prostratin and BAFi's leading to eviction of nuc-1. These findings point to the importance of combining molecules that target multiple pathways to disrupt and reverse the latent transcriptional state of the virus in shock and kill strategies.

Our data highlights the potential of BAFi's as a source of molecules for inclusion in latency reversal therapies. BAFi's effectively reverse latency either alone or in combination with Prostratin in all three patients enrolled in this study. A caveat of the current study is the limited number of patients enrolled, which does not allow for a strong statistical validation of the effect of BAFi's across patients. Nevertheless, although not sufficient to fully recapitulate the variability in response to LRAs across patients, the data from the three included patients support our observations in cell lines and other primary models of latency. As with other molecules currently under clinical characterization in latency reversal, it is conceivable that with BAF inhibitors too, there will be some variability in patient response. Thus ex vivo studies performed on a larger number of HIV-1 infected patients are required in order to statistically validate the present observations. These studies, together with proof-of-concept clinical studies are the necessary next steps in order to further characterize the potency and applicability of BAFi's to reverse the latent HIV-1 reservoir in vivo. Given their demonstrated promising activity and the available information concerning their toxicity and pharmacokinetics profiles, CAPE and PYR, represent attractive candidates for future clinical development. Further screenings will likely identify additional molecules targeting HIV-1 latency via counteracting the activity of the repressive BAF complex. Importantly, since targeting a previously unexplored pathway, this promising class of drugs has high potential for inclusion in combination therapy.

## Funding Source

This work was supported by a Dutch 'Aids Fonds' grant (2014021), an Erasmus MC mRACE Research Grant and an ERC Starting Grant (337116 - Trxn-PURGE).

## Conflicts of Interest

The authors declare no conflict of interest.

## Author Contributions

MS, EDC and RJP carried out the experiments and performed data analysis. MMK participated in gene expression analysis experiments. TWK and CL participated in FACS experiments. RJP performed FAIRE experiments. CR and AV recruited patients. CB provided expertise and contributed to the writing of the manuscript. ECD provided compounds, expertise and contributed to the writing of the manuscript. MS, EDC and TM conceived the study and wrote the manuscript. All authors read and approved the final manuscript. MS and EDC contributed equally to this work.



## Acknowledgements

We would like to thank Dr. Michelle Palmer and Dr. Christina Scherer (Broad Institute of MIT and Harvard) for kindly providing the compounds used in the screening, and Professor C.P. Verrijzer for providing BAF250a antibodies. We would like to thank the Centre for AIDS Reagents (NIBSC, UK) for providing the PL4.3.Luc.R-E- and the HIV-1 HXB2-Env expression vectors, Saquinavir Mesylate, and Raltegravir.

## Appendix A. Supplementary Material

Supplementary data to this article can be found online at <http://dx.doi.org/10.1016/j.ebiom.2015.11.047>.

## References

- Archin, N.M., Liberty, A.L., Kashuba, A.D., Choudhary, S.K., Kuruc, J.D., Crooks, A.M., Parker, D.C., Anderson, E.M., Kearney, M.F., Strain, M.C., Richman, D.D., Hudgens, M.G., Bosch, R.J., Coffin, J.M., Eron, J.J., Hazuda, D.J., Margolis, D.M., 2012. Administration of vorinostat disrupts HIV-1 latency in patients on antiretroviral therapy. *Nature* 487, 482–485.
- Archin, N.M., Bateson, R., Tripathy, M.K., Crooks, A.M., Yang, K.H., Dahl, N.P., Kearney, M.F., Anderson, E.M., Coffin, J.M., Strain, M.C., Richman, D.D., Robertson, K.R., Kashuba, A.D., Bosch, R.J., Hazuda, D.J., Kuruc, J.D., Eron, J.J., Margolis, D.M., 2014. HIV-1 expression within resting CD4+ T cells after multiple doses of vorinostat. *J. Infect. Dis.* 210, 728–735.
- Barakat, T.S., Gunhanlar, N., Pardo, C.G., Achame, E.M., Ghazvini, M., Boers, R., Kenter, A., Rentmeester, E., Grootegoed, J.A., Gribnau, J., 2011. RNF12 activates Xist and is essential for X chromosome. *PLoS Genet.* 7 (1), 2011, e1002001. <http://dx.doi.org/10.1371/journal.pgen.1002001>.
- Barker, N., Hurlstone, A., Musisi, H., Miles, A., Bienz, M., Clevers, H., 2001. The chromatin remodelling factor Brg-1 interacts with beta-catenin to promote target gene activation. *EMBO J.* 20, 4935–4943.
- Barton, K., Margolis, D., 2013. Selective targeting of the repressive transcription factors YY1 and cMyc to disrupt quiescent human immunodeficiency viruses. *AIDS Res. Hum. Retrovir.* 29, 289–298.
- Barton, K.M., Archin, N.M., Keedy, K.S., Espeseth, A.S., Zhang, Y.L., Gale, J., Wagner, F.F., Holson, E.B., Margolis, D.M., 2014. Selective HDAC inhibition for the disruption of latent HIV-1 infection. *PLoS One* 9, e102684.
- Barton, K., Hiener, B., Palmern, S., Rasmussen, T.A., Tolstrup, M., Østergaard, L., Søgaard, O., Solomon, A., Lewin, S., Shao, W., 2015. CROI, February 23–26, 2015. Year. Panobinostat Broadly Activates Latent HIV-1 Proviruses in Patients (Seattle, Washington).
- Bliss, C.I., 1939. The toxicity of poisons applied jointly. *Ann. Appl. Biol.* 26, 585–615.
- Bosque, A., Planelles, V., 2009. Induction of HIV-1 latency and reactivation in primary memory CD4+ T cells. *Blood* 113, 58–65.
- Burnett, J.C., Lim, K.I., Calafi, A., Rossi, J.J., Schaffer, D.V., Arkin, A.P., 2010. Combinatorial latency reactivation for HIV-1 subtypes and variants. *J. Virol.* 84, 5958–5974.
- Chomont, N., El-Far, M., Ancuta, P., Trautmann, L., Procopio, F.A., Yassine-Diab, B., Boucher, G., Boulassel, M.R., Ghattas, G., Brechley, J.M., Schacker, T.W., Hill, B.J., Douek, D.C., Routy, J.P., Haddad, E.K., Sekaly, R.P., 2009. HIV reservoir size and persistence are driven by T cell survival and homeostatic proliferation. *Nat. Med.* 15, 893–900.
- Chun, T.W., Finzi, D., Margolick, J., Chadwick, K., Schwartz, D., Siliciano, R.F., 1995. In vivo fate of HIV-1-infected T cells: quantitative analysis of the transition to stable latency. *Nat. Med.* 1, 1284–1290.
- Chun, T.W., Justement, J.S., Moir, S., Hallahan, C.W., Maenza, J., Mullins, J.I., Collier, A.C., Corey, L., Fauci, A.S., 2007. Decay of the HIV reservoir in patients receiving antiretroviral therapy for extended periods: implications for eradication of virus. *J. Infect. Dis.* 195, 1762–1764.
- Contreras, X., Schwenecker, M., Chen, C.S., McCune, J.M., Deeks, S.G., Martin, J., Peterlin, B.M., 2009. Suberoylanilide hydroxamic acid reactivates HIV from latently infected cells. *J. Biol. Chem.* 284, 6782–6789.
- Dahabieh, M.S., Battivelli, E., Verdin, E., 2015. Understanding HIV latency: the road to an HIV cure. *Annu. Rev. Med.* 66, 407–421.
- Dar, R.D., Hosmane, N.N., Arkin, M.R., Siliciano, R.F., Weinberger, L.S., 2014. Screening for noise in gene expression identifies drug synergies. *Science* 344, 1392–1396.
- De Grignis, E., Mahmoudi, T., 2014. HIV eradication: combinatorial approaches to activate latent viruses. *Virus* 6, 4581–4608.
- Dechristopher, B.A., Loy, B.A., Marsden, M.D., Schrier, A.J., Zack, J.A., Wender, P.A., 2012. Designed, synthetically accessible bryostatin analogues potently induce activation of latent HIV reservoirs in vitro. *Nat. Chem.* 4, 705–710.
- Deeks, S.G., 2012. HIV: shock and kill. *Nature* 487, 439–440.
- Dykhuizen, E.C., Carmody, L.C., Tolliday, N., Crabtree, G.R., Palmer, M.A., 2012. Screening for inhibitors of an essential chromatin remodeler in mouse embryonic stem cells by monitoring transcriptional regulation. *J. Biomol. Screen.* 17, 1221–1230.
- Edelstein, L.C., Micheva-Viteva, S., Phelan, B.D., Dougherty, J.P., 2009. Short communication: activation of latent HIV type 1 gene expression by suberoylanilide hydroxamic acid (SAHA), an HDAC inhibitor approved for use to treat cutaneous T cell lymphoma. *AIDS Res. Hum. Retrovir.* 25, 883–887.
- Elliott, J.H., Wightman, F., Solomon, A., Ghneim, K., Ahlers, J., Cameron, M.J., Smith, M.Z., Spelman, T., McMahon, J., Velayudham, P., Brown, G., Roney, J., Watson, J., Prince, M.H., Hoy, J.F., Chomont, N., Fromentin, R., Procopio, F.A., Zeidan, J., Palmer, S., Odevall, L., Johnstone, R.W., Martin, B.P., Sinclair, E., Deeks, S.G., Hazuda, D.J., Cameron, P.U., Sekaly, R.P., Lewin, S.R., 2014. Activation of HIV transcription with short-course vorinostat in HIV-infected patients on suppressive antiretroviral therapy. *PLoS Pathog.* 10, e1004473.
- Fesen, M.R., Pommier, Y., Letaut, F., Hiroguchi, S., Yung, J., Kohn, K.W., 1994. Inhibition of HIV-1 integrase by flavones, caffeic acid phenethyl ester (CAPE) and related compounds. *Biochem. Pharmacol.* 48, 595–608.
- Finzi, D., Hermankova, M., Pierson, T., Carruth, L.M., Buck, C., Chaisson, R.E., Quinn, T.C., Chadwick, K., Margolick, J., Brookmeyer, R., Gallant, J., Markowitz, M., Ho, D.D., Richman, D.D., Siliciano, R.F., 1997. Identification of a reservoir for HIV-1 in patients on highly active antiretroviral therapy. *Science* 278, 1295–1300.
- Finzi, D., Blankson, J., Siliciano, J.D., Margolick, J.B., Chadwick, K., Pierson, T., Smith, K., Lisiewicz, J., Lori, F., Flexner, C., Quinn, T.C., Chaisson, R.E., Rosenberg, E., Walker, B., Gange, S., Gallant, J., Siliciano, R.F., 1999. Latent infection of CD4+ T cells provides a mechanism for lifelong persistence of HIV-1, even in patients on effective combination therapy. *Nat. Med.* 5, 512–517.
- Geeraert, L., Kraus, G., Pomerantz, R.J., 2008. Hide-and-seek: the challenge of viral persistence in HIV-1 infection. *Annu. Rev. Med.* 59, 487–501.
- Hargreaves, D.C., Crabtree, G.R., 2011. ATP-dependent chromatin remodeling: genetics, genomics and mechanisms. *Cell Res.* 21, 396–420.
- Jiang, G., Mendes, E.A., Kaiser, P., Sankaran-Walters, S., Tang, Y., Weber, M.G., Melcher, G.P., Thompson, G.R., Tanuri, I.I., A., Pianowski, L.F., Wong, J.K., Dandekar, S., 2014. Reactivation of HIV latency by a newly modified Ingenol derivative via protein kinase Cdelta-NF-kappaB signaling. *AIDS* 28, 1555–1566.
- Jiang, G., Mendes, E.A., Kaiser, P., Wong, D.P., Tang, Y., Cai, L., Fenton, A., Melcher, G.P., Hildreth, J.E., Thompson, G.R., Wong, J.K., Dandekar, S., 2015. Synergistic reactivation of latent HIV Expression by ingenol-3-angelate, PEPO05, targeted NF-kB signaling in combination with JQ1 induced p-TEFb activation. *PLoS Pathog.* 11, e1005066.
- Jonsson, K.L., Tolstrup, M., Vad-Nielsen, J., Kjaer, K., Laustsen, A., Andersen, M.N., Rasmussen, T.A., Søgaard, O.S., Østergaard, L., Denton, P.W., Jakobsen, M.R., 2015. Histone deacetylase inhibitor romidepsin inhibits de novo HIV-1 Infections. *Antimicrob. Agents Chemother.*
- Jordan, A., Defechereux, P., Verdin, E., 2001. The site of HIV-1 integration in the human genome determines basal transcriptional activity and response to Tat transactivation. *EMBO J.* 20, 1726–1738.
- Jordan, A., Bisgrove, D., Verdin, E., 2003. HIV reproducibly establishes a latent infection after acute infection of T cells in vitro. *EMBO J.* 22, 1868–1877.
- Keedy, K.S., Archin, N.M., Gates, A.T., Espeseth, A., Hazuda, D.J., Margolis, D.M., 2009. A limited group of class I histone deacetylases acts to repress human immunodeficiency virus type 1 expression. *J. Virol.* 83, 4749–4756.
- Klinker, H., Langmann, P., Richter, E., 1996. Plasma pyrimethamine concentrations during long-term treatment for cerebral toxoplasmosis in patients with AIDS. *Antimicrob. Agents Chemother.* 40, 1623–1627.
- Korin, Y.D., Brooks, D.G., Brown, S., Korotzer, A., Zack, J.A., 2002. Effects of prostratin on T-cell activation and human immunodeficiency virus latency. *J. Virol.* 76, 8118–8123.
- Laird, G.M., Bullen, C.K., Rosenbloom, D.I., Martin, A.R., Hill, A.L., Durand, C.M., Siliciano, J.D., Siliciano, R.F., 2015. Ex vivo analysis identifies effective HIV-1 latency-reversing drug combinations. *J. Clin. Invest.*
- Lassen, K.G., Hebbeler, A.M., Bhattacharyya, D., Lobritz, M.A., Greene, W.C., 2012. A flexible model of HIV-1 latency permitting evaluation of many primary CD4 T-cell reservoirs. *PLoS One* 7, e30176.
- Lu, H.K., Gray, L.R., Wightman, F., Ellenberg, P., Khoury, G., Cheng, W.J., Mota, T.M., Wesselingh, S., Gorro, P.R., Cameron, P.U., Churchill, M.J., Lewin, S.R., 2014. Ex vivo response to histone deacetylase (HDAC) inhibitors of the HIV long terminal repeat (LTR) derived from HIV-infected patients on antiretroviral therapy. *PLoS One* 9, e113341.
- Lusis, M., Giacca, M., 2015. Regulation of HIV-1 latency by chromatin structure and nuclear architecture. *J. Mol. Biol.* 427, 688–694.
- Mahmoudi, T., 2012. The BAF complex and HIV latency. *Transcription* 3, 171–176.
- Mahmoudi, T., Verrijzer, C.P., 2001. Chromatin silencing and activation by polycomb and trithorax group proteins. *Oncogene* 20, 3055–3066.
- Marban, C., Suzanne, S., Dequiedt, F., De Walque, S., Redel, L., Van Lint, C., Aunis, D., Rohr, O., 2007. Recruitment of chromatin-modifying enzymes by CTIP2 promotes HIV-1 transcriptional silencing. *EMBO J.* 26, 412–423.
- Marquez, N., Sancho, R., Macho, A., Calzado, M.A., Fiebig, B.L., Munoz, E., 2004. Caffeic acid phenethyl ester inhibits T-cell activation by targeting both nuclear factor of activated T-cells and NF-kappaB transcription factors. *J. Pharmacol. Exp. Ther.* 308, 993–1001.
- Mathanga, D.P., Uthman, O.A., Chinkhumba, J., 2011. Intermittent preventive treatment regimens for malaria in HIV-positive pregnant women. *Cochrane Database Syst. Rev.*, CD006689.
- Matsuda, Y., Kobayashi-Ishihara, M., Fujikawa, D., Ishida, T., Watanabe, T., Yamagishi, M., 2015. Epigenetic heterogeneity in HIV-1 latency establishment. *Sci. Rep.* 5, 7701.
- Mbonye, U., Karn, J., 2014. Transcriptional control of HIV latency: cellular signaling pathways, epigenetics, happenstance and the hope for a cure. *Virology* 454–455, 328–339.
- Micheva-Viteva, S., Kobayashi, Y., Edelstein, L.C., Pacchia, A.L., Lee, H.L., Graci, J.D., Breslin, J., Phelan, B.D., Miller, L.K., Colacino, J.M., Gu, Z., Ron, Y., Peltz, S.W., Dougherty, J.P., 2011. High-throughput screening uncovers a compound that activates latent HIV-1 and acts cooperatively with a histone deacetylase (HDAC) inhibitor. *J. Biol. Chem.* 286, 21083–21091.
- Narlikar, G.J., Sundaramoorthy, R., Owen-Hughes, T., 2013. Mechanisms and functions of ATP-dependent chromatin-remodeling enzymes. *Cell* 154, 490–503.

- Natarajan, K., Singh, S., Burke Jr., T.R., Grunberger, D., Aggarwal, B.B., 1996. Caffeic acid phenethyl ester is a potent and specific inhibitor of Activation of nuclear transcription factor NF-kappa B. *Proc. Natl. Acad. Sci. U. S. A.* 93, 9090–9095.
- Ni, Z., Bremner, R., 2007. Brahma-related gene 1-dependent STAT3 recruitment at IL-6-inducible genes. *J. Immunol.* 178, 345–351.
- Oguariri, R.M., Adelsberger, J.W., Baseler, M.W., Imachi, T., 2010. Evaluation of the effect of pyrimethamine, an anti-malarial drug, on HIV-1 replication. *Virus Res.* 153, 269–276.
- Pandeló, J.D., Bartholomeeusen, K., Da Cunha, R.D., Abreu, C.M., Glinski, J., Da Costa, T.B., Bacchi Rabay, A.F., Pianowski Filho, L.F., Dudycz, L.W., Ranga, U., Peterlin, B.M., Pianowski, L.F., Tanuri, A., Aguiar, R.S., 2014. Reactivation of latent HIV-1 by new semi-synthetic ingenol esters. *Virology* 462–463, 328–339.
- Petty, E., Pillus, L., 2013. Balancing chromatin remodeling and histone modifications in transcription. *Trends Genet.* 29, 621–629.
- Pierson, T., McArthur, J., Siliciano, R.F., 2000. Reservoirs for HIV-1: mechanisms for viral persistence in the presence of antiviral immune responses and antiretroviral therapy. *Annu. Rev. Immunol.* 18, 665–708.
- Qu, X., Ying, H., Wang, X., Kong, C., Zhou, X., Wang, P., Zhu, H., 2013. Histone deacetylase inhibitor MC1293 induces latent HIV-1 reactivation by histone modification in vitro latency cell lines. *Curr. HIV Res.* 11, 24–29.
- Rafati, H., Parra, M., Hakre, S., Moshkin, Y., Verdin, E., Mahmoudi, T., 2011. Repressive LTR nucleosome positioning by the BAF complex is required for HIV latency. *PLoS Biol.* 9, e1001206.
- Rasmussen, T.A., Schmeltz Sogaard, O., Brinkmann, C., Wightman, F., Lewin, S.R., Melchjorsen, J., Dinarello, C., Ostergaard, L., Tolstrup, M., 2013. Comparison of HDAC inhibitors in clinical development: effect on HIV production in latently infected cells and T-cell activation. *Hum. Vaccin Immunother.* 9, 993–1001.
- Rasmussen, T.A., Tolstrup, M., Brinkmann, C., Olesen, R., Erikstrup, C., Solomon, A., Winckelmann, A., Palmer, S., Dinarello, C., Buzon, M., Lichterfeld, M., Lewin, S., Østergaard, L., Sogaard, O., 2014. Year. Panobinostat Induces HIV Transcription and Plasma Viremia in HIV Patients on Suppressive cART. *CROI*, Boston.
- Reuse, S., Calao, M., Kabeya, K., Guiguen, A., Gatot, J.S., Quivy, V., Vanhulle, C., Lamine, A., Vaira, D., Demonte, D., Martinelli, V., Veithen, E., Cherrier, T., Avettand, V., Poutrel, S., Piette, J., DE Launoit, Y., Moutschen, M., Burny, A., Rouzioux, C., De Wit, S., Herbein, G., Rohr, O., Collette, Y., Lambotte, O., Clumeck, N., Van Lint, C., 2009. Synergistic activation of HIV-1 expression by deacetylase inhibitors and prostratin: implications for treatment of latent infection. *PLoS One* 4, e6093.
- Rosenblatt, J.E., 1999. Antiparasitic agents. *Mayo Clin. Proc.* 74, 1161–1175.
- Ruelas, D.S., Greene, W.C., 2013. An integrated overview of HIV-1 latency. *Cell* 155, 519–529.
- Schmittgen, T.D., Livak, K.J., 2008. Analyzing real-time PCR data by the comparative (C/T) method. *Nat. Protoc.* 3, 1101–1108.
- Shvarzbeyn, J., Huleihel, M., 2011. Effect of propolis and caffeic acid phenethyl ester (CAPE) on NF-kappaB activation by HTLV-1 Tax. *Antivir. Res.* 90, 108–115.
- Siliciano, J.D., Kajdas, J., Finzi, D., Quinn, T.C., Chadwick, K., Margolick, J.B., Kovacs, C., Gange, S.J., Siliciano, R.F., 2003. Long-term follow-up studies confirm the stability of the latent reservoir for HIV-1 in resting CD4+ T cells. *Nat. Med.* 9, 727–728.
- Spivak, A.M., Bosque, A., Balch, A.H., Smyth, D., Martins, L., Planelles, V., 2015. Ex vivo bio-activity and HIV-1 latency reversal by ingenol Dibenzoate and panobinostat in resting CD4+ T cells from aviremic patients. *Antimicrob. Agents Chemother.* 59, 5984–5991.
- Strain, M.C., Little, S.J., Daar, E.S., Havlir, D.V., Gunthard, H.F., Lam, R.Y., Daly, O.A., Nguyen, J., Ignacio, C.C., Spina, C.A., Richman, D.D., Wong, J.K., 2005. Effect of treatment, during primary infection, on establishment and clearance of cellular reservoirs of HIV-1. *J. Infect. Dis.* 191, 1410–1418.
- Swiggard, W.J., Baytop, C., Yu, J.J., Dai, J., Li, C., Schretzenmair, R., Theodosopoulos, T., O'Doherty, U., 2005. Human immunodeficiency virus type 1 can establish latent infection in resting CD4+ T cells in the absence of activating stimuli. *J. Virol.* 79, 14179–14188.
- Tolba, M.F., Azab, S.S., Khalifa, A.E., Abdel-Rahman, S.Z., Abdel-Naim, A.B., 2013. Caffeic acid phenethyl ester, a promising component of propolis with a plethora of biological activities: a review on its anti-inflammatory, neuroprotective, hepatoprotective, and cardioprotective effects. *IUBMB Life* 65, 699–709.
- Van Lint, C., Emiliani, S., Ott, M., Verdin, E., 1996. Transcriptional activation and chromatin remodeling of the HIV-1 promoter in response to histone acetylation. *EMBO J.* 15, 1112–1120.
- Van Lint, C., Bouchat, S., Marcello, A., 2013. HIV-1 transcription and latency: an update. *Retrovirology* 10, 67.
- Verdin, E., 1991. DNase I-hypersensitive sites are associated with both long terminal repeats and with the intragenic enhancer of integrated human immunodeficiency virus type 1. *J. Virol.* 65, 6790–6799.
- Verdin, E., Van Lint, C., 1995. Internal transcriptional regulatory elements in HIV-1 and other retroviruses. *Cell. Mol. Biol.* 41, 365–369.
- Verdin, E., Paras Jr., P., Van Lint, C., 1993. Chromatin disruption in the promoter of human immunodeficiency virus type 1 during transcriptional activation. *EMBO J.* 12, 3249–3259.
- Wang, D.D., Chen, Y.B., Pan, K., Wang, W., Chen, S.P., Chen, J.G., Zhao, J.J., Lv, L., Pan, Q.Z., Li, Y.Q., et al., 2012. Decreased expression of the ARID1A gene is associated with poor prognosis in primary gastric cancer. *PLoS One* 7, e40364.
- Wang, L.C., Chu, K.H., Liang, Y.C., Lin, Y.L., Chiang, B.L., 2010. Caffeic acid phenethyl ester inhibits nuclear factor-kappaB and protein kinase B signalling pathways and induces caspase-3 expression in primary human CD4+ T cells. *Clin. Exp. Immunol.* 160, 223–232.
- Watanabe, D., Ibe, S., Uehira, T., Minami, R., Sasakawa, A., Yajima, K., Yonemoto, H., Bando, H., Ogawa, Y., Taniguchi, T., Kasai, D., Nishida, Y., Yamamoto, M., Kaneda, T., Shirasaka, T., 2011. Cellular HIV-1 DNA levels in patients receiving antiretroviral therapy strongly correlate with therapy initiation timing but not with therapy duration. *BMC Infect. Dis.* 11, 146.
- Wei, D.G., Chiang, V., Fyne, E., Balakrishnan, M., Barnes, T., Graupe, M., Hesselgesser, J., Irrinki, A., Murry, J.P., Stepan, G., Stray, K.M., Tsai, A., Yu, H., Spindler, J., Kearney, M., Spina, C.A., McMahon, D., Lalezari, J., Sloan, D., Mellors, J., Geleziunas, R., Cihlar, T., 2014. Histone deacetylase inhibitor romidepsin induces HIV expression in CD4 T cells from patients on suppressive antiretroviral therapy at concentrations achieved by clinical dosing. *PLoS Pathog.* 10, e1004071.
- White, C.H., Johnston, H.E., Moesker, B., Manousopoulou, A., Margolis, D.M., Richman, D.D., Spina, C.A., Garbis, S.D., Woelk, C.H., Beliakova-Bethell, N., 2015. Mixed effects of suberoylanilide hydroxamic acid (SAHA) on the host transcriptome and proteome and their implications for HIV reactivation from latency. *Antivir. Res.* 123, 78–85.
- Whitney, J.B., Hill, A.L., Sanisetty, S., Penaloza-Macmaster, P., Liu, J., Shetty, M., Parenteau, L., Cabral, C., Shields, J., Blackmore, S., Smith, J.Y., Brinkman, A.L., Peter, L.E., Mathew, S.I., Smith, K.M., Borducchi, E.N., Rosenbloom, D.I., Lewis, M.G., Hattersley, J., Li, B., Hesselgesser, J., Geleziunas, R., Robb, M.L., Kim, J.H., Michael, N.L., Barouch, D.H., 2014. Rapid seeding of the viral reservoir prior to SIV viraemia in rhesus monkeys. *Nature* 512, 74–77.
- Williams, S.A., Chen, L.F., Kwon, H., Ruiz-Jarabo, C.M., Verdin, E., Greene, W.C., 2006. NF-kappaB p50 promotes HIV latency through HDAC recruitment and repression of transcriptional initiation. *EMBO J.* 25, 139–149.
- Wu, J., Omene, C., Karkoszka, J., Bosland, M., Eckard, J., Klein, C.B., Frenkel, K., 2011. Caffeic acid phenethyl ester (CAPE), derived from a honeybee product propolis, exhibits a diversity of anti-tumor effects in pre-clinical models of human breast cancer. *Cancer Lett.* 308, 43–53.
- Wurster, A.L., Precht, P., Becker, K.G., Wood, W.H., Zhang III, Y., Wang, Z., Pazin, M.J., 2012. IL-10 transcription is negatively regulated by BAF180, a component of the SWI/SNF chromatin remodeling enzyme. *BMC Immunol.* 13, 9.
- Ying, H., Zhang, Y., Zhou, X., Qu, X., Wang, P., Liu, S., Lu, D., Zhu, H., 2012. Selective histone deacetylase inhibitor M344 intervenes in HIV-1 latency through increasing histone acetylation and activation of NF-kappaB. *PLoS One* 7, e48832.
- Zentner, G.E., Henikoff, S., 2013. Regulation of nucleosome dynamics by histone modifications. *Nat. Struct. Mol. Biol.* 20, 259–266.
- Zhao, W., Sachsenmeier, K., Zhang, L., Sult, E., Hollingsworth, R.E., Yang, H., 2014a. A new bliss independence model to analyze drug combination data. *J. Biomol. Screen.* 19, 817–821.
- Zhao, W.X., Wang, L., Yang, J.L., Li, L.Z., Xu, W.M., Li, T., 2014b. Caffeic acid phenethyl ester attenuates pro-inflammatory and fibrogenic phenotypes of LPS-stimulated hepatic stellate cells through the inhibition of NF-kappaB signaling. *Int. J. Mol. Med.* 33, 687–694.

**Supplementary materials to**

**Chapter 2.**

**Small Molecule Inhibitors of BAF; A Promising Family of Compounds in HIV-1 Latency Reversal.**

Figure S1. Chemical structures of compounds tested for HIV-1 latency reversal potential.

## Figure S1

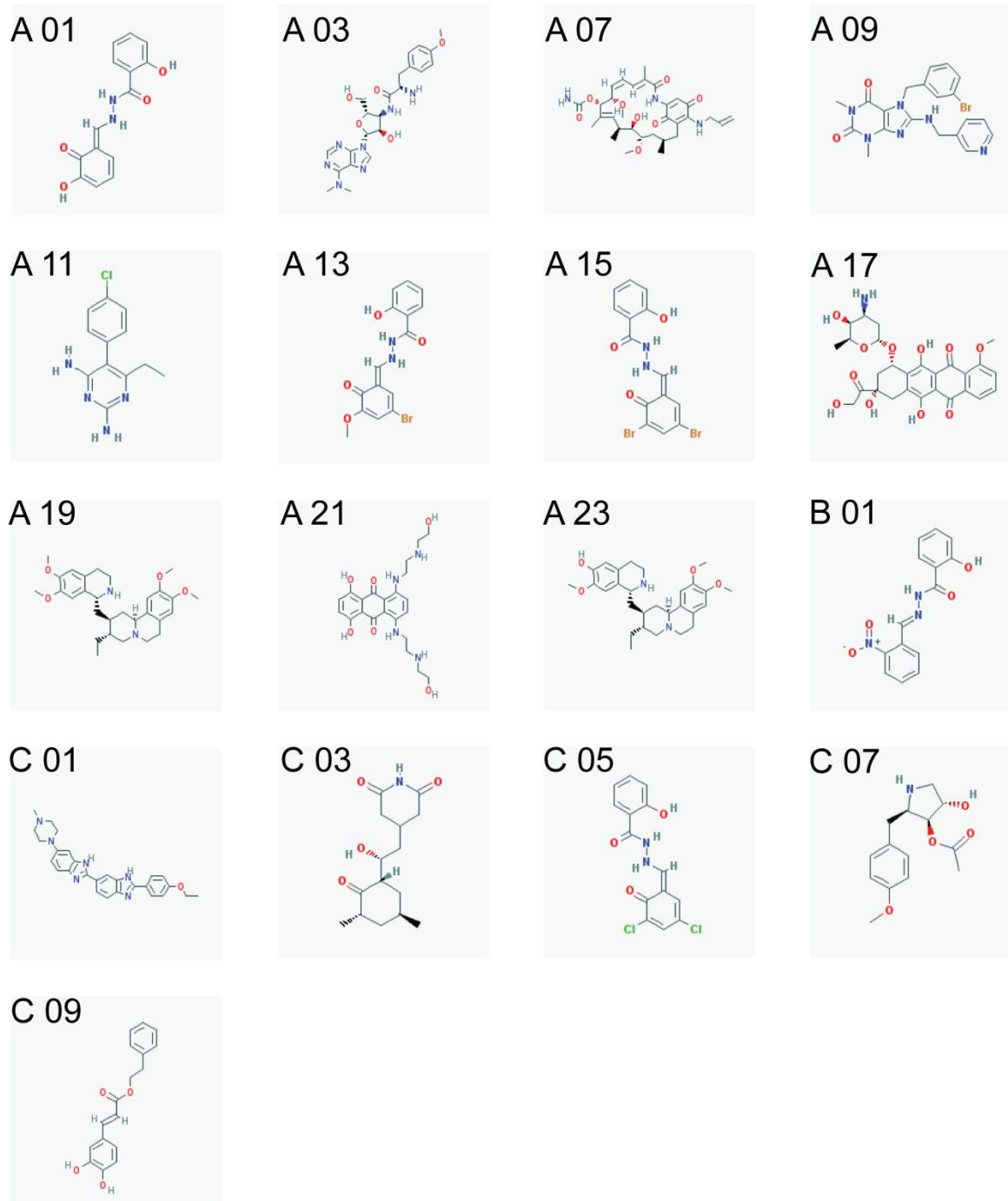


## Figure S2. Treatment with BAFi's induces degradation of BAF250a

(a) Western blot analysis showing the levels of different BAF complex subunits after treatment with BAFi's. The numbers on top of the gel images represent the relative intensity of each band according to ImageJ software analysis.

(b) RT-qPCR analysis of BAF250a expression after treatment with BAFi's. RT-qPCR data are presented as mean  $\pm$ SD.

## Figure S2

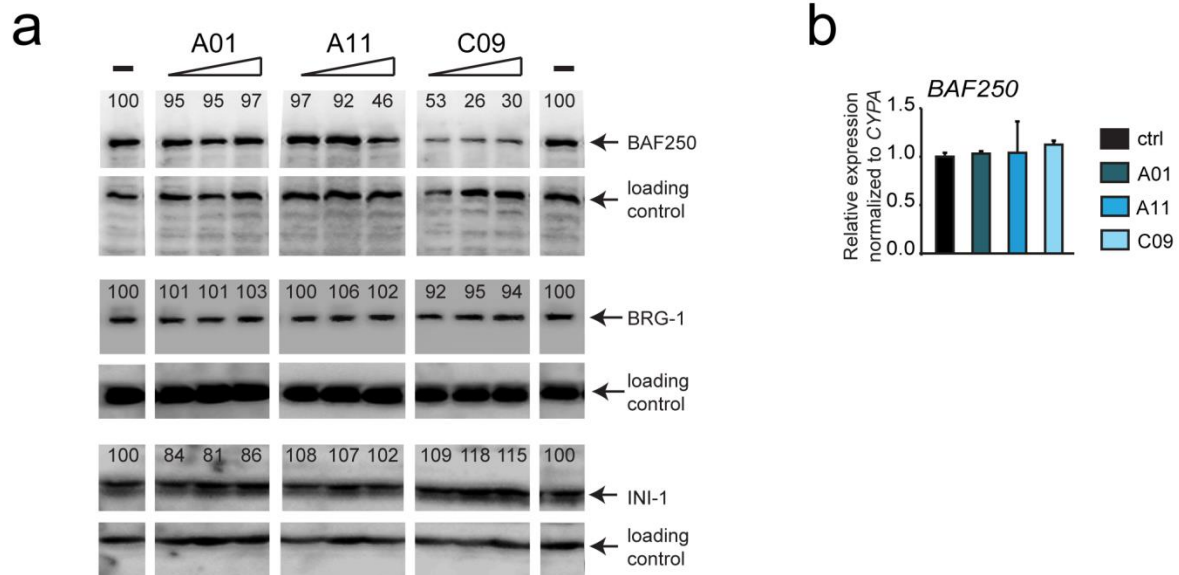


**Figure S3. BAFi-induced remodeling of HIV LTR.**

**(a)** FAIRE across nuc-0 and nuc-1 regions in J-Lat 11.1 cells treated with increasing concentrations of BAFi's.

**(b)** Effects of BAFi's and Prostratin co-treatment on chromatin remodeling of nuc-1 region in J-Lat A2 cell line. Bars represent the enrichment of nuc-0 and nuc-1 over an control region. Data are presented as mean  $\pm$ SD.

**Figure S3.**

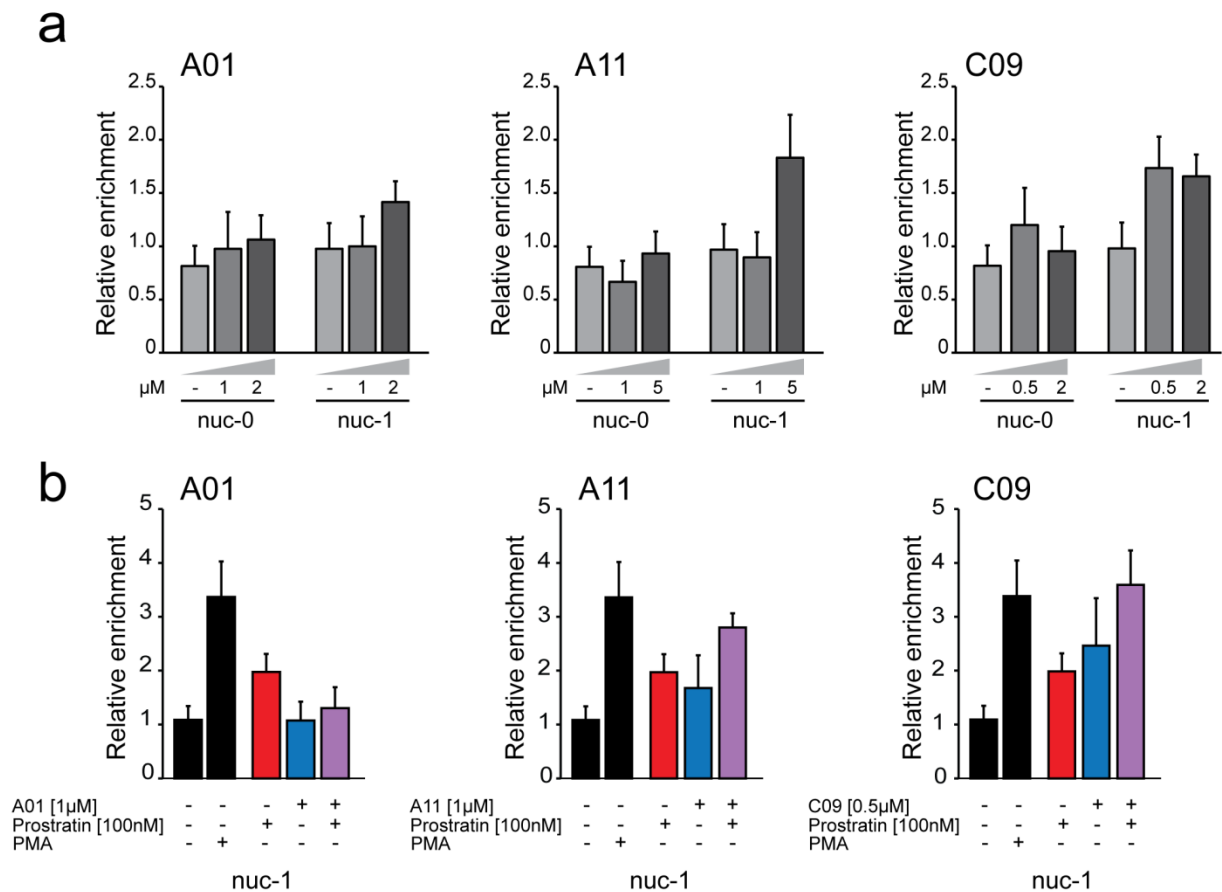


**Figure S4. BAFi C09 in 0.5-2μM concentration range does not inhibit NFκB-mediated activation of latent HIV-1.**

**(a)** J-Lat 11.1 cells were pretreated for 30 minutes with indicated concentrations of C09. Cells were stimulated with 2 μM Prostratin for 45 minutes and incubated at 37°C in a humidified 95% air/ 5% CO<sub>2</sub> atmosphere. Cells were then lysed and lysates subjected to western blot analysis using antibodies specific for IκBα and Tubulin. The numbers below each band represent the relative intensity of each band compared to the untreated control according to ImageJ software analysis.

**(b)** J-Lat 11.1 cells were pretreated for 30 minutes with indicated concentrations of C09. Cells were stimulated with 2 μM Prostratin or left unstimulated for 12 hours and incubated at 37°C in a humidified 95% air/ 5% CO<sub>2</sub> atmosphere. Percent of GFP positive cells (left axes, black bars), corresponding to the level of HIV-1 activation, and cell viability (right axes grey bars) were evaluated by FACS analysis.

**Figure S4**

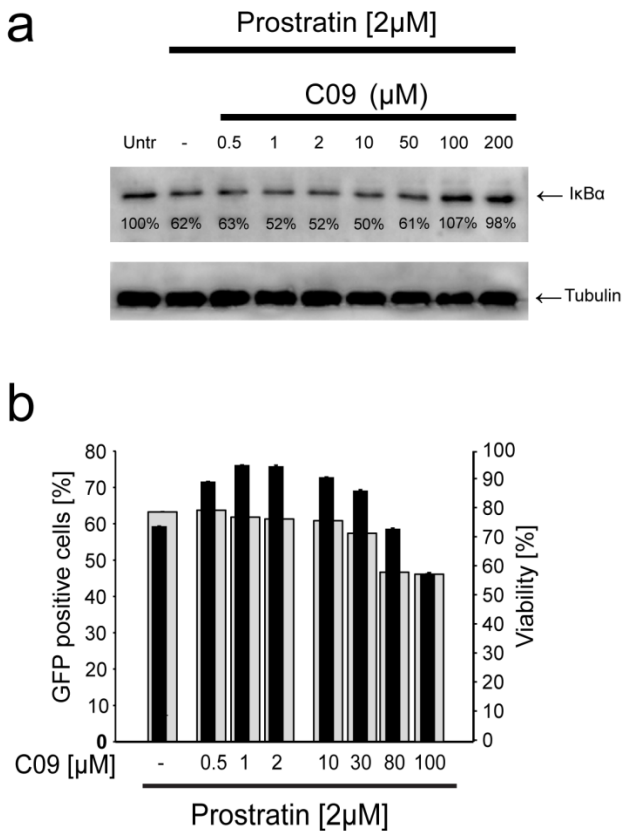




**Table S1. List of BAF inhibitors included in the screening**

A01	BRD-K70161581-001-01-5	<a href="https://pubchem.ncbi.nlm.nih.gov/substance/85815116#section=Identity">https://pubchem.ncbi.nlm.nih.gov/substance/85815116#section=Identity</a> , 29 september 2015
A03	BRD-K36007650-001-01-9	Berman HM, Westbrook J, Feng Z, Gilliland G, Bhat TN, Weissig H, Shindyalov IN, Bourne PE: The Protein Data Bank. <i>Nucleic Acids Res.</i> 2000 Jan 1;28(1):235-42
A05	BRD-K63750851-001-06-6	Bernard J. Abbott, John G. Whitney, "Method of preparing mycophenolic acid glucoside." U.S. Patent US4234684, issued January, 1976.
A07	BRD-K81473043-001-08-8	<a href="https://ncit.nci.nih.gov/ncitbrowser/pages/concept_details.jsf?dictionary=NCIThesaurus&amp;version=15.08e&amp;code=C37899&amp;ns=NCI_Thesaurus&amp;type=properties&amp;key=null&amp;b=1&amp;n=0&amp;vse=null">https://ncit.nci.nih.gov/ncitbrowser/pages/concept_details.jsf?dictionary=NCIThesaurus&amp;version=15.08e&amp;code=C37899&amp;ns=NCI_Thesaurus&amp;type=properties&amp;key=null&amp;b=1&amp;n=0&amp;vse=null</a>
A09	BRD-K81609421-001-01-4	<a href="https://pubchem.ncbi.nlm.nih.gov/substance/85834545#section=Top">https://pubchem.ncbi.nlm.nih.gov/substance/85834545#section=Top</a> , 29 september 2015
A11	BRD-K88429204-001-18-7	Ansdell VE, Wright SG, Hutchinson DB. Megaloblastic anaemia associated with combined pyrimethamine and co-trimoxazole administration. <i>Lancet.</i> 1976 Dec 4;2(7997):1257.
A13	BRD-K53795576-001-01-8	<a href="https://pubchem.ncbi.nlm.nih.gov/substance/85814970#section=Top">https://pubchem.ncbi.nlm.nih.gov/substance/85814970#section=Top</a> , 29 september 2015
A15	BRD-K72615639-001-01-0	<a href="https://pubchem.ncbi.nlm.nih.gov/substance/85814973#section=Top">https://pubchem.ncbi.nlm.nih.gov/substance/85814973#section=Top</a> , 29 september 2015
A17	BRD-K92093830-003-25-8	Tan C, Tasaka H, Yu KP, Murphy ML, Karnofsky DA. Daunomycin, an antitumor antibiotic, in the treatment of neoplastic disease. Clinical evaluation with special reference to childhood leukemia. <i>Cancer.</i> 1967 Mar;20(3):333-53.
A19	BRD-K03067624-001-01-5	Tan GT, Pezzuto JM, Kinghorn AD, Hughes SH. Evaluation of natural products as inhibitors of human immunodeficiency virus type 1 (HIV-1) reverse transcriptase. <i>J Nat Prod.</i> 1991 Jan-Feb;54(1):143-54.
A21	BRD-K21680192-001-11-4	Fesen MR, Kohn KW, Leteurtre F, Pommier Y. Inhibitors of human immunodeficiency virus integrase. <i>Proc Natl Acad Sci U S A.</i> 1993 Mar 15;90(6):2399-403.
A23	BRD-K80348542-001-01-4	Tan GT, Pezzuto JM, Kinghorn AD, Hughes SH. Evaluation of natural products as inhibitors of human immunodeficiency virus type 1 (HIV-1) reverse transcriptase. <i>J Nat Prod.</i> 1991 Jan-Feb;54(1):143-54.
B01	BRD-K50778578-001-02-3	<a href="https://pubchem.ncbi.nlm.nih.gov/substance/131404656#section=Top">https://pubchem.ncbi.nlm.nih.gov/substance/131404656#section=Top</a> , 29 september 2015
C01	BRD-K08554278-001-02-4	<a href="https://pubchem.ncbi.nlm.nih.gov/compound/1464#section=Information-Sources">https://pubchem.ncbi.nlm.nih.gov/compound/1464#section=Information-Sources</a> , 29 september 2015
C03	BRD-K36055864-001-16-8	Dinsdale D., Colchicine-induced lesions in the rat duodenum. <i>Pathol Eur.</i> 1975;10(2):95-104.
C05	BRD-K82837433-001-01-6	<a href="https://pubchem.ncbi.nlm.nih.gov/substance/85814974">https://pubchem.ncbi.nlm.nih.gov/substance/85814974</a> , 29 september 2015
C07	BRD-K91370081-001-04-6	Alarcón B, Lacal JC, Fernández-Sousa JM, Carrasco L., Screening for new compounds with antiherpes activity. <i>Antiviral Res.</i> 1984 Oct;4(5):231-44.
C09	BRD-K96188950-001-04-5	Fesen MR, Kohn KW, Leteurtre F, Pommier Y. Inhibitors of human immunodeficiency virus integrase. <i>Proc Natl Acad Sci U S A.</i> 1993 Mar 15;90(6):2399-403.



# Chapter 3

## Small Molecule Targeting of Specific BAF (mSWI/SNF) Complexes for HIV Latency Reversal

Christine A. Marian<sup>1,6</sup>, Mateusz Stoszek<sup>2,6</sup>, Lili Wang<sup>3</sup>, Matthew W. Leighty<sup>3</sup>, Elisa de Crignis<sup>2</sup>, Chad A. Maschinot<sup>1</sup>, Jovylyn Gatchalian<sup>4</sup>, Benjamin C. Carter<sup>1</sup>, Basudev Chowdhury<sup>1</sup>, Diana C. Hargreaves<sup>4</sup>, Jeremy R. Duvall<sup>3</sup>, Gerald R. Crabtree<sup>5</sup>, Tokameh Mahmoudi<sup>2</sup> and Emily C. Dykhuizen<sup>1</sup>.

<sup>1</sup>Department of Medicinal Chemistry and Molecular Pharmacology, Purdue University, 201 S. University St., West Lafayette, IN 47907, USA

<sup>2</sup>Department of Biochemistry, Erasmus University Medical Center, Ee634, P.O. Box 2040, 3000CA Rotterdam, the Netherlands

<sup>3</sup>The Broad Institute of Harvard and MIT, 415 Main Street, Cambridge, MA 02142, USA

<sup>4</sup>Department of Molecular and Cell Biology, Salk Institute for Biological Studies, 10010 N Torrey Pines Road, La Jolla, CA 92037, USA

<sup>5</sup>HHMI and the Departments of Developmental Biology and Pathology, Stanford University School of Medicine, 279 Campus Drive, Stanford, CA 94305, USA

<sup>6</sup>These authors contributed equally

Published:

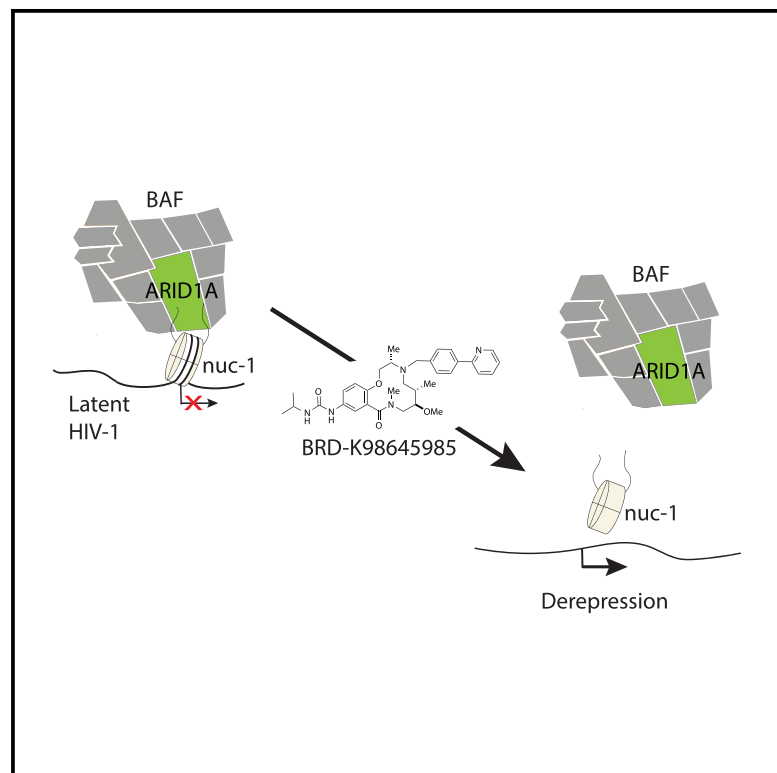
Cell Chemical Biology 2018, 25, 1–13



# Cell Chemical Biology

## Small Molecule Targeting of Specific BAF (mSWI/SNF) Complexes for HIV Latency Reversal

### Graphical Abstract



### Authors

Christine A. Marian, Mateusz Stoszko, Lili Wang, ..., Gerald R. Crabtree, Tokameh Mahmoudi, Emily C. Dykhuizen

### Correspondence

crabtree@stanford.edu (G.R.C.),  
t.mahmoudi@erasmusmc.nl (T.M.),  
edykhui@purdue.edu (E.C.D.)

### In Brief

The BAF (SWI/SNF) chromatin remodeling complex is involved in repressing HIV-1 transcription in latently infected T cells. Using high-throughput screening, we identified a macrolactam that inhibits ARID1A-containing BAF complexes to reverse HIV-1 latency without T cell activation or toxicity.

### Highlights

- HTS identifies a macrolactam that inhibits BAF transcriptional repression
- The macrolactams are likely targeting specific ARID1A-containing BAF complexes
- The macrolactams reverse HIV-1 latency and are non-toxic to T cells
- The macrolactams can be combined with other latency reversal agents

# Small Molecule Targeting of Specific BAF (mSWI/SNF) Complexes for HIV Latency Reversal

Christine A. Marian,<sup>1,6</sup> Mateusz Stoszek,<sup>2,6</sup> Lili Wang,<sup>3</sup> Matthew W. Leighty,<sup>3</sup> Elisa de Crignis,<sup>2</sup> Chad A. Maschiot,<sup>1</sup> Jovelyn Gatchalian,<sup>4</sup> Benjamin C. Carter,<sup>1</sup> Basudev Chowdhury,<sup>1</sup> Diana C. Hargreaves,<sup>4</sup> Jeremy R. Duvall,<sup>3</sup> Gerald R. Crabtree,<sup>5,\*</sup> Tokameh Mahmoudi,<sup>2,\*</sup> and Emily C. Dykhuizen<sup>1,7,\*</sup>

<sup>1</sup>Department of Medicinal Chemistry and Molecular Pharmacology, Purdue University, 201 S. University St., West Lafayette, IN 47907, USA

<sup>2</sup>Department of Biochemistry, Erasmus University Medical Center, Ee634, P.O. Box 2040, 3000CA Rotterdam, the Netherlands

<sup>3</sup>The Broad Institute of Harvard and MIT, 415 Main Street, Cambridge, MA 02142, USA

<sup>4</sup>Department of Molecular and Cell Biology, Salk Institute for Biological Studies, 10010 N Torrey Pines Road, La Jolla, CA 92037, USA

<sup>5</sup>HHMI and the Departments of Developmental Biology and Pathology, Stanford University School of Medicine, 279 Campus Drive, Stanford, CA 94305, USA

<sup>6</sup>These authors contributed equally

<sup>7</sup>Lead Contact

\*Correspondence: [crabtree@stanford.edu](mailto:crabtree@stanford.edu) (G.R.C.), [t.mahmoudi@erasmusmc.nl](mailto:t.mahmoudi@erasmusmc.nl) (T.M.), [edykhui@purdue.edu](mailto:edykhui@purdue.edu) (E.C.D.)

<https://doi.org/10.1016/j.chembiol.2018.08.004>

## SUMMARY

The persistence of a pool of latently HIV-1-infected cells despite combination anti-retroviral therapy treatment is the major roadblock for a cure. The BAF (mammalian SWI/SNF) chromatin remodeling complex is involved in establishing and maintaining viral latency, making it an attractive drug target for HIV-1 latency reversal. Here we report a high-throughput screen for inhibitors of BAF-mediated transcription in cells and the subsequent identification of a 12-membered macrolactam. This compound binds ARID1A-specific BAF complexes, prevents nucleosomal positioning, and relieves transcriptional repression of HIV-1. Through this mechanism, these compounds are able to reverse HIV-1 latency in an *in vitro* T cell line, an *ex vivo* primary cell model of HIV-1 latency, and in patient CD4<sup>+</sup> T cells without toxicity or T cell activation. These macrolactams represent a class of latency reversal agents with unique mechanism of action, and can be combined with other latency reversal agents to improve reservoir targeting.

## INTRODUCTION

Since the discovery of HIV-1 as the causative agent of AIDS in 1983 (Barré-Sinoussi et al., 1983), enormous progress has been made in treating HIV-1 infections and prolonging the lifespan of HIV-1-infected individuals. State-of-the-art treatment is a cocktail of drugs acting on different viral targets, known as combination anti-retroviral therapy (c-ART). c-ART is extremely effective at suppressing HIV-1 to undetectable levels, preventing progression to AIDS; however, treatment must be maintained for life and, as of yet, HIV-1 eradication is not achievable (Deeks

et al., 2013; Maartens et al., 2014). Despite being highly efficient in stopping active viral replication, anti-retroviral drugs do not target latently infected cells that harbor replication competent but transcriptionally silent proviruses. Latently infected cells persist in the body for life and, not being targeted by either c-ART or immune cells, they constitute the viral reservoir (Chun et al., 1997; Finzi et al., 1997, 1999). When these cells are activated, transcription from latent HIV-1 provirus is induced and, in the absence of c-ART, viral replication rebounds (Chun et al., 2010; Dahabieh et al., 2015; De Crignis and Mahmoudi, 2017; Ruelas and Greene, 2013; Siliciano et al., 2003).

Currently, there are two major non-redundant strategies to eliminate this population of latently infected cells in HIV-1-infected individuals (Churchill et al., 2016; Cillo and Mellors, 2016; Margolis, 2017; Siliciano and Siliciano, 2016). The first approach is harnessing the immune system to eliminate latently infected cells (Barouch and Deeks, 2014; Brockman et al., 2015; Martus and Altfeld, 2016; Perreau et al., 2017; Trautmann, 2016); the second, also known as the “shock-and-kill” strategy, is aimed at inducing HIV-1 transcription in latently infected cells such that all cells harboring replication competent virus can be targeted by the immune system (Deeks, 2012; Margolis and Archin, 2017; Margolis et al., 2016; Rasmussen et al., 2016).

HIV-1 latency is established and maintained through complex genetic and epigenetic mechanisms that create a specific repressive chromatin configuration at the viral promoter or 5'-long terminal repeat (LTR) (Verdin, 1991; Verdin et al., 1993). Active HIV-1 transcription is driven by Tat and its multiple activating co-factor complexes, while HIV-1 latency is driven through epigenetic regulators that maintain increased nucleosome occupancy at the 5'-LTR (Kumar et al., 2015; Mbonye and Karn, 2014; Turner and Margolis, 2017; Van Lint et al., 2013). Histone deacetylases (HDACs) play a prominent role in the repressive chromatin environment that drives HIV-1 latency and, as such, HDAC inhibitors are able to reverse HIV-1 latency in *in vitro* and *ex vivo* models (Archin et al., 2014, 2012; Conrad and Ott, 2016; De Crignis and Mahmoudi, 2017; Rasmussen et al., 2013; Sheridan et al., 1997; Van Lint et al., 1996; Wei

et al., 2014; Wightman et al., 2013). Results from clinical trials, however, indicate that the HDAC inhibitors tested are unable to significantly reduce the frequency of latently infected cells (Elliott et al., 2014; Rasmussen et al., 2013; Spivak and Planelles, 2016; Søgaard et al., 2015; Delagrèverie et al., 2016). Among the alternative epigenetic targets being investigated for reversing HIV-1 latency, one potential candidate is the mammalian SWI/SNF chromatin remodeling complex, BAF, which has been shown to contribute to HIV-1 transcriptional repression (Boese et al., 2009; Rafati et al., 2011; Van Duyne et al., 2011). BAF complexes are multisubunit ATP-dependent chromatin remodelers known for their roles in development and cancer (Ho and Crabtree, 2010; Hodges et al., 2016; Pulice and Kadoch, 2017). In latent cells harboring HIV-1 proviruses, BAF complexes are required for maintaining increased nucleosome density immediately downstream of the HIV-1 transcription start site (Rafati et al., 2011). During latency reversal, the closely related PBAF complex, which shares many of the same subunits, replaces BAF and directly or indirectly promotes removal of the repressive Nuc-1, activating HIV-1 transcription (Agbottah et al., 2006; Easley et al., 2010; Mahmoudi et al., 2006; Rafati et al., 2011; Tréand et al., 2006; Van Duyne et al., 2011). Consistent with the pivotal role of the BAF complex in HIV-1 latency, a recent report demonstrated that the latency reversal activity of BRD4 bromodomain inhibitors is due to the requirement for a short BRD4 isoform that recruits BAF to the HIV-1 5' LTR (Conrad et al., 2017).

Inhibitors specifically targeting the ARID1A subunit-containing BAF complex (but not PBAF) would be invaluable as HIV-1 latency reversal agents (LRAs). We recently reported a medium-throughput screen using qRT-PCR to identify compounds that alter the transcription of BAF target genes in mouse embryonic stem cells (mESCs) (Dykhuizen et al., 2012), and several compounds identified from this screen displayed an ability to reverse HIV-1 latency; however, many of these compounds have known targets besides BAF, raising the possibility for toxic off-target effects (Stoszko et al., 2016). To identify specific and non-toxic small molecule inhibitors of the BAF complex, we developed a high-throughput assay for screening large libraries of diverse small molecules in embryonic stem cells (ESCs). From a screen of almost 350,000 compounds, we identified a 12-membered macrolactam scaffold with low toxicity in cells and the ability to regulate a panel of BAF target genes. These macrolactams reverse HIV-1 latency in several relevant *in vitro* cell line and primary cell models of HIV-1 latency. In addition, they enhance the activity of other clinically used LRAs targeting HDACs and protein kinase C (PKC). Target identification experiments implicate ARID1A-containing BAF complexes as the primary target, and the compounds act to reverse HIV-1 latency by reducing repressive nucleosome occupancy at the 5' LTR.

## RESULTS

### Development and Confirmation of a Luciferase Reporter Cell Line

In murine ESCs the BAF complex is essential for maintaining repression of certain polycomb repressive complex 1 subunit genes, including *Bmi1* and *Ring1a*, while activating genes involved in maintaining the pluripotent state, such as *Fgf4* (Dykhuizen et al., 2012; Ho et al., 2009). For high-throughput

screening of BAF inhibitors, we developed a knockin luciferase reporter of BAF transcriptional repression. We used homologous recombination to construct a mESC line with firefly luciferase inserted at exon 1 of *Bmi1*. Southern blotting confirmed successful recombination of the original targeting vector, as well as subsequent Cre-mediated excision of the *Neo* selection marker (Figure 1A). To confirm that the reporter line was a reliable indicator of esBAF-mediated repression of *Bmi1*, we knocked down the gene encoding the BAF ATPase BRG1 using lentiviral shRNA. Three days after infection, a stable 4-fold increase in luciferase levels was observed when corrected for cell number, indicating successful de-repression of *Bmi1* (Figure 1B). In an effort to simplify the requirements for high-throughput screening, we performed the *Brg1* knockdown without correcting for cell number and found that the reporter line still displays robust 3-fold induction of luciferase 72 hr after infection with sh*Brg1*-expressing lentivirus (Figure 1B).

### High-Throughput Assay Development

The knockin ESC line was generated on mouse embryonic fibroblasts (MEFs) as a feeder layer, which is not compatible with high-throughput screening. Therefore, we first made the cell line feeder free by passaging at high density five times on gelatin. While we previously developed methods to gelatin coat 384-well plates (Dykhuizen et al., 2012), this was not feasible for this scale of screening effort. Instead we identified the Corning High Bind surface to support normal ESC morphology and normal alkaline phosphatase levels (indicative of maintained pluripotency) compared with gelatin-coated plates (Figure S1A). The assay was optimized in 384-well format at the Broad Institute Probe Development Center. The coefficient of variance for firefly luciferase reading across a 384-well plate was 4.5% and, using a non-specific hit identified in the pilot qRT-PCR screen (compound 63) as our positive control (Dykhuizen et al., 2012), we calculated a Z factor of 0.6, indicating a robust screen (Figure 1C).

### High-Throughput Screen

We screened 347,670 compounds in duplicate (Figure S1B for illustration of reproducibility). The compounds included the MLPCN validation set of natural products, known bioactives, commercially available compound libraries, and compound libraries designed by scientists at the Broad Institute (PubChem assay entry AID 602393 for full description of library). We defined hits as compounds with luciferase inductions that were at least 3 SDs above the mean, which corresponded to approximately 40% of the maximal activity observed with *Brg1* knockdown. We identified 7,048 hits (hit rate of 2%), which is high but not unexpected from cell-based luciferase assays, which tend to identify non-specific luciferase stabilizers (Auld et al., 2008). Hits identified in more than five luciferase screens or more than 10% of luciferase screens on PubMed were eliminated, as were compounds containing functional groups with known reactivity, including  $\alpha$ -chloroketones, imines, and nitro groups. This resulted in a refined hit list of 1,157 compounds for a hit rate of 0.33%, more in line with the expected hit rate for a robust screen (see Figure S1C for summary of the screening tree). We rescreened the 1,157 compounds at eight doses in the cell-based luciferase assay as a confirmatory assay along with a counter-screen for viability. We confirmed 548 hits with the concentration giving half-maximal response (EC<sub>50</sub>) less than 10  $\mu$ M

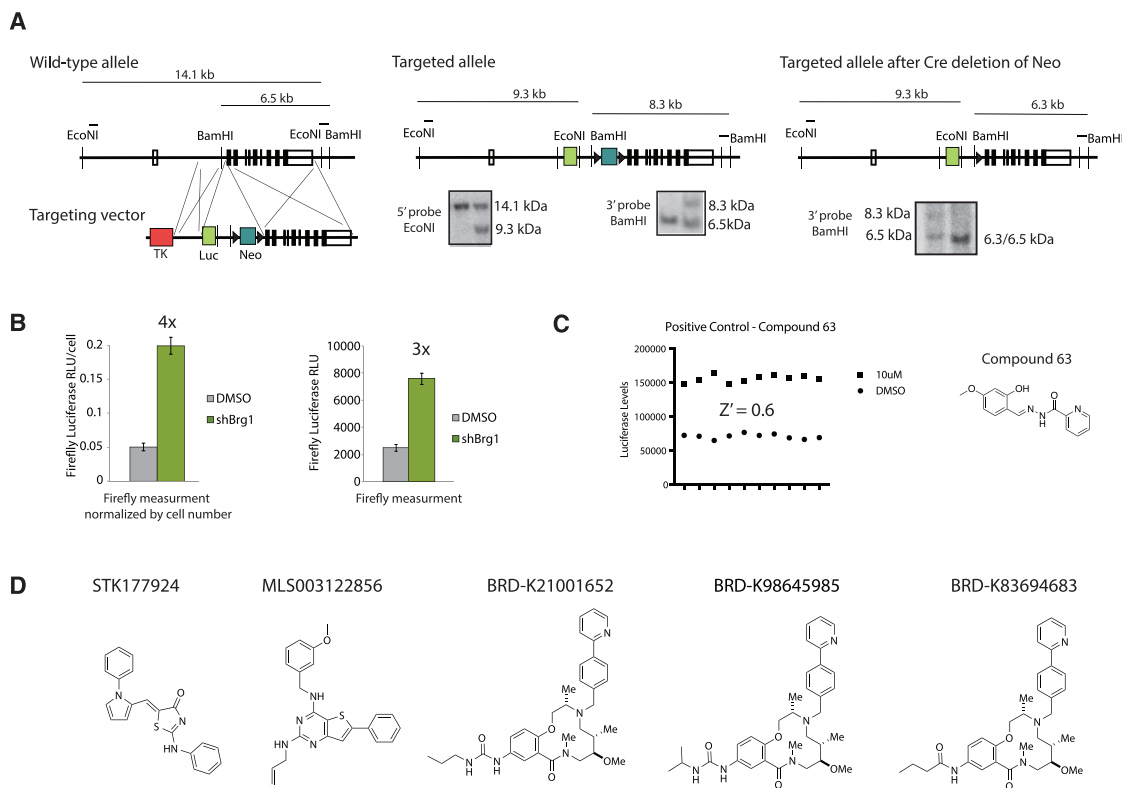


**Figure 1. High-Throughput screen for Inhibitors of BAF-Mediated Transcriptional Repression**

(A) The generation of a luciferase knockin at the *Bmi1* locus using homologous recombination in mouse ESCs and validation using Southern blot analysis. (B) Validation of the *Bmi1*-luciferase reporter cell line using lentiviral-mediated knockdown of *Brg1* either with (above) or without (below) normalizing by cell number. RLU, relative light units. Error bars represent mean  $\pm$  standard deviation.  $n = 3$ . (C) The robustness of the screen was determined using positive control compound 63. (D) The five hits identified from high-throughput screening efforts. See also Figure S1.

and toxicity  $EC_{50}$  greater than 30  $\mu$ M. We then treated cells with these hits at a single dose (30  $\mu$ M) in the qRT-PCR screen previously reported (Dykhuizen et al., 2012). From this secondary assay, we found five compounds that increase *Bmi1* at least 6-fold, and *Ring1* at least 2-fold, and decreased *Fgf4* at least 5-fold (Figure 1D). STK177924, a known non-specific pan-assay interference (PAIS) scaffold, was eliminated (Figure 1D) (Baell and Holloway, 2010). We next used chemoinformatics to investigate the structure activity relationship (SAR) of the thiophene (MLS003122856) from the primary screen and developed a small library of analogs to explore additional SAR for linker attachment (Figure S1D). The biotin-linked compound on solid support failed to enrich subunits of the BAF complex from lysates (Figure S1E), and, in addition, this compound had only moderate HIV latency reversal activity (Figure S1F). Therefore, while the thiophene may have interesting biological activity worth investigating, there is substantial evidence that it does not directly target the BAF complex or phenocopy the effects of BAF deletion in latent HIV-1-infected T cells.

### Broad Diversity-Oriented Synthesis Library Macrocyclic SAR

The three remaining hits shared a similar macrocyclic scaffold with only slight variations of substituents off macrocycle aniline:

n-propyl amide (BRD-K83694683), n-propyl urea (BRD-K21001652), and isopropyl urea (BRD-K98645985). Re-evaluation of hit BRD-K98645985 in the luciferase assay provided an  $EC_{50}$  of approximately  $2.37 \pm 0.98$   $\mu$ M (Figure 2A). In addition, we observed a 5-fold increase in *Bmi1*, 2.6-fold increase in *Ring1*, and 3.3-fold decrease in *Fgf4* upon treatment with 30  $\mu$ M compound, a profile that closely mimics Brg1 knockout (KO) (Figure 2B). We observed no toxicity to ESCs up to 30  $\mu$ M (Figure 2C), or to HepG2, HEK293T, and A549 cells (Figure S2A), increasing enthusiasm for this scaffold. The three hits containing this scaffold are members of the diversity-oriented synthesis (DOS) library synthesized using head-to-tail scaffold design (Fitzgerald et al., 2012). The primary screen contained 3,618 compounds containing the same 12-membered macrolactam scaffold. Substituents off the scaffold vary at two positions ( $R_1$  off the core aniline and  $R_2$  off the core secondary amine) and the stereochemistry varies at three positions along the ring (C2, C5, and C6). While all stereoisomers with varying stereochemistry at C2, C5, and C6 were included for BRD-K98645985, BRD-K83694683, and BRD-K21001652, all of the top hits have the same stereochemical configuration. Taking a closer look at the primary screen scores for the eight stereoisomers of BRD-K98645985, the stereoisomer S,S,R showed significantly increased activity over the other stereoisomers,

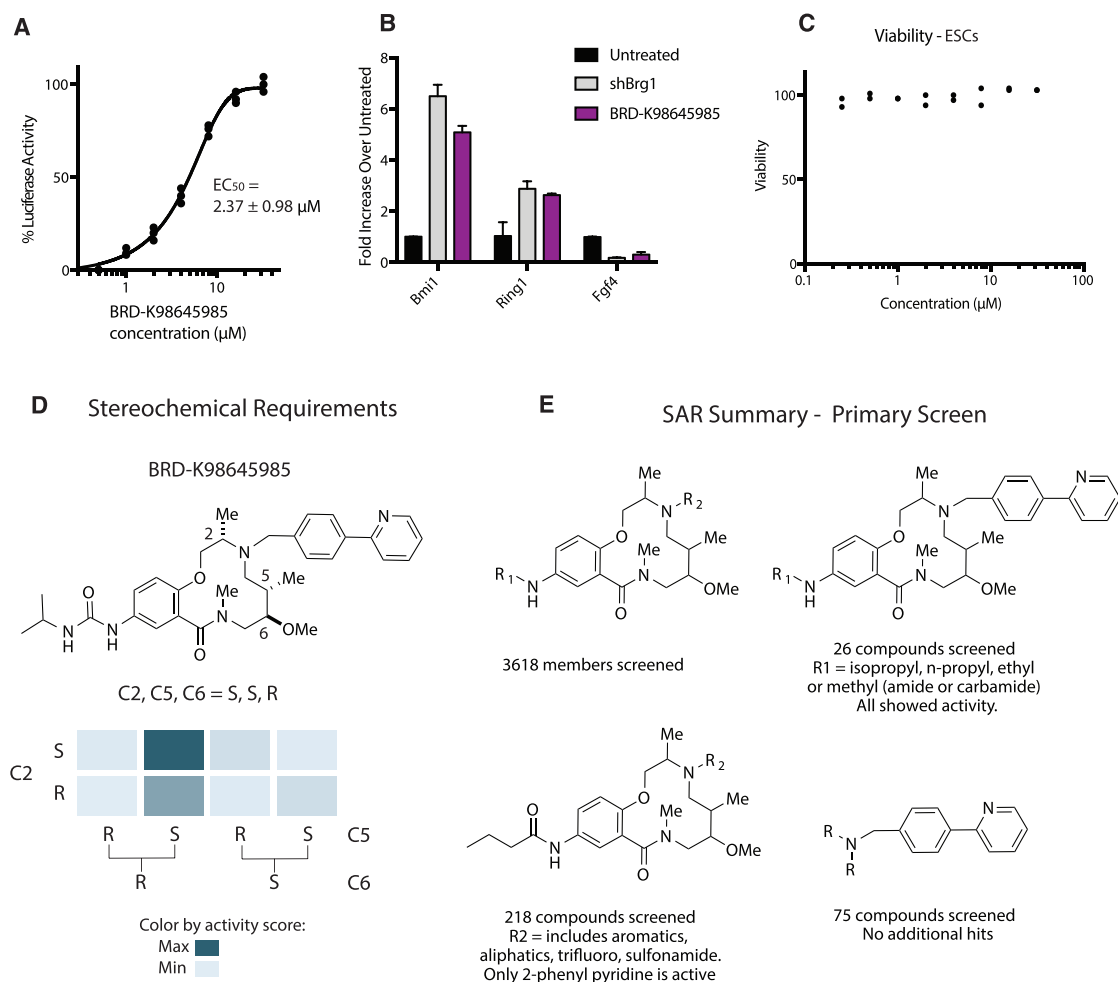


**Figure 2. Twelve-Membered Macrolactams Are Inhibitors of BAF-Mediated Transcription**

(A) The EC<sub>50</sub> was measured for the best screen hit BRD-K98645985 after 24 hr compound treatment with the Bmi1-luciferase reporter cell line. Each concentration was dosed in triplicate.

(B) The fold change of the transcription of three BAF target genes was calculated using qRT-PCR after 18 hr BRD-K98645985 treatment (30 μM) or *Brg1* knockdown compared with untreated cells. Gene expression was normalized to GAPDH levels. Error bars represent mean ± standard deviation. n = 3.

(C) Viability measurements in wild-type ESCs were performed after 72 hr of compound or DMSO treatment using CellTiter-Glo.

(D) The SAR of the eight stereoisomers of BRD-K98645985 based on initial luciferase induction from the primary screen.

(E) The SAR of the 3,618 macrolactam library members based on initial luciferase induction from the primary screen.

See also Figure S2.

supporting a specific target (Figure 2D). A similar profile was observed for BRD-K83694683 and BRD-K21001652 (Figure S2B).

To further define the SAR from initial screen data, we also looked at varied substituents at two positions, R<sub>1</sub> and R<sub>2</sub> (Figure 2E). The most common building block used at R<sub>1</sub> was n-propyl amide, which was included in 218 macrolactam library members. For these 218 library members, R<sub>2</sub> groups included aliphatic groups, aromatic groups, and sulfonamides, but only compounds with 2-phenyl pyridine moiety at R<sub>2</sub> were hits in the primary screen. To ensure that the preference for 2-phenyl pyridine is not due to non-specific interactions, we also looked at the 75 compounds in the initial compound library that contained the 2-phenyl pyridine moiety and confirmed that only the DOS macrolactams were hits. Substituting phenyl for

2-phenyl pyridine at R<sub>2</sub> increased the cLogP from 3.5 to 4.2, which, in conjunction with a lowered efflux ratio, could indicate that the increased activity is due to improved cell permeability (Over et al., 2016). There were 26 compounds that contained the 2-phenyl pyridine at position R<sub>2</sub> and varying substituents at R<sub>1</sub> and all were hits to some degree in the primary screen. This likely indicates that the R<sub>1</sub> position is more permissible to variation than the R<sub>2</sub> position; however, the variations at R<sub>1</sub> in the screen were minimal, including only simple aliphatic groups connected via amides, ureas, and carbamates.

### Solution Phase Macrolactam Library

Based on these initial SAR data, we synthesized a 30-membered library to further investigate substitutions at the R<sub>1</sub> and R<sub>2</sub> positions (Figure 3). For this library, we developed a



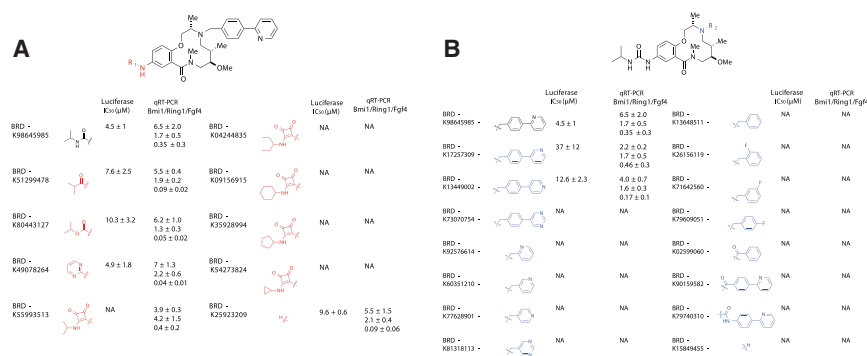


**Figure 3. The SAR between Members of a Solution Phase 12-Membered Macrolactam Analog Library**

(A and B) A solution phase library of 30 analogs was synthesized and tested to further explore SAR for compounds with variations at (A) the aniline ( $R_1$ ) and (B) the secondary amine ( $R_2$ ). Activity was defined as the  $EC_{50}$  in the luciferase reporter screen and as the fold transcriptional change of three BAF targets (*Bmi1*, *Ring1*, *Fgf4*) at a single compound concentration (30  $\mu$ M) determined using qRT-PCR.  $n = 3$ . Data presented as mean  $\pm$  SD. NA, no activity. See also Figure S3 and Table S1.

solution phase synthesis based on the previously published solid phase synthesis of the scaffold with minor alterations (Figure S3) (Fitzgerald et al., 2012). For the 30 library members, we performed the luciferase screen in dose and also calculated the fold change in *Bmi1*, *Fgf4*, and *Ring1* at a single dose (30  $\mu$ M) using qRT-PCR (Figures 3 and S3). We found high correlation between activity in the two assay formats. We varied substituents at the  $R_1$  position and confirmed that small aliphatic substituents linked via amide, urea, and carbamates are tolerated (Figure 3A). Interestingly, a small aromatic ring is tolerated at  $R_1$ , while a squarate linkage is not. Importantly, it is revealed that the free aniline is almost as potent as the parent compound and that no substituent is actually required at the  $R_1$  position. At the  $R_2$  position, 2-benzyl pyridine is still the best substituent, although 3-benzyl pyridine and 4-benzyl pyridine are tolerated (Figure 3B). Not surprisingly, smaller substituents containing a single aromatic ring are not active, but, interestingly, the closely related 2-benzoyl pyridine and amide phenyl pyridine are also not active, indicating that the benzyl pyridine may be involved in a specific binding mechanism and not simply functioning to increase cell permeability.

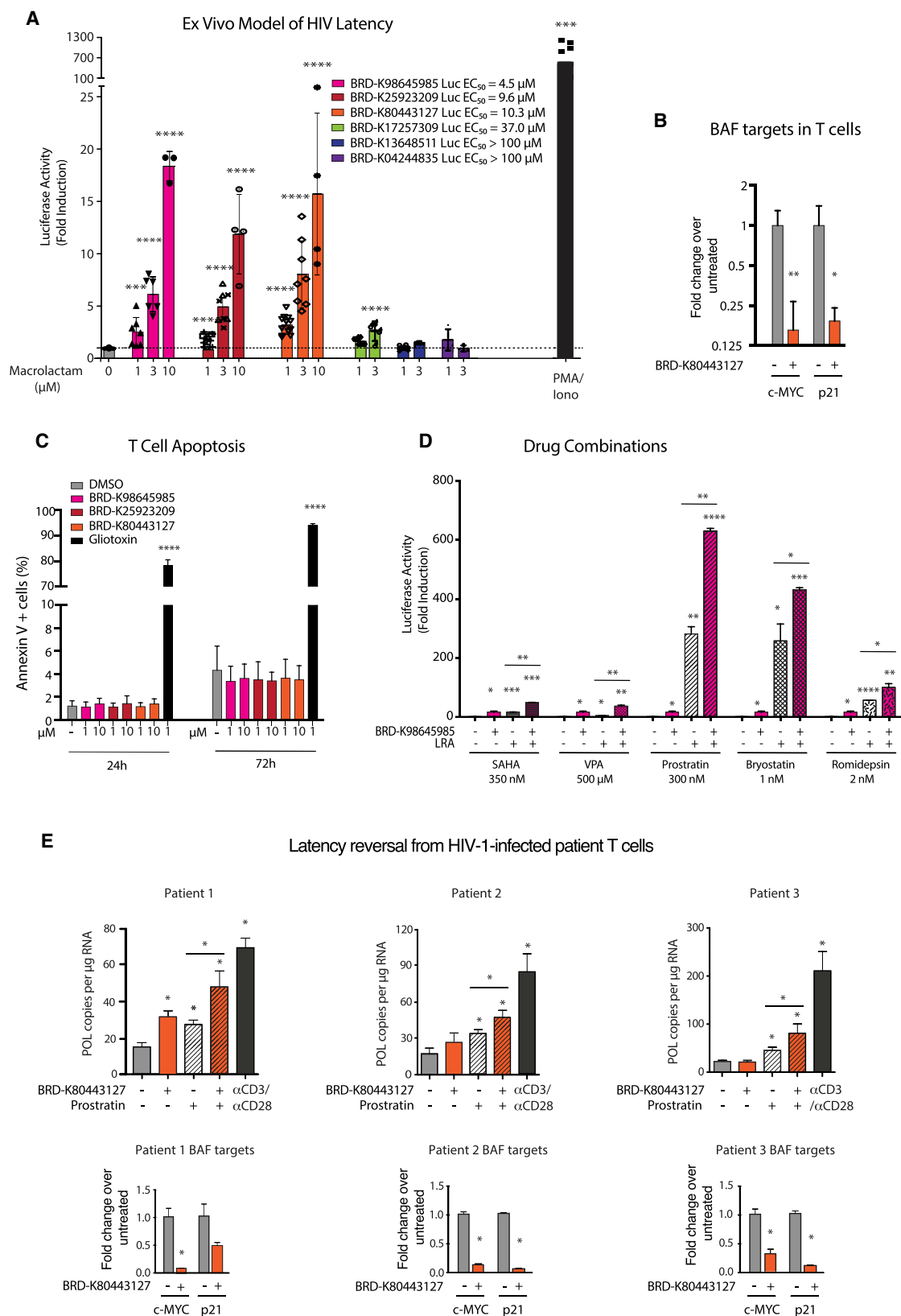
The last thing we looked at is the position of the  $R_2$  substituent off the macrocycle aromatic. We found no tolerance for moving the phenyl pyridine from the para to the meta position (Figure S3D). We measured solubility and neither this value nor the cLogP values for library members strongly correlated with activity (Table S1). Additionally, the compounds all displayed low toxicity toward cell lines with the exception of a few, which showed slight toxicity, possibly correlated to low solubility (Table S1).

### Latency Reversal

Using a primary cell model of HIV-1 latency established in ex vivo infected human CD4+ T cells (Lassen et al., 2012), we measured HIV-1 reversal activity of six compounds from the follow-up library: three with high activity in the *Bmi1* luciferase reporter assays (BRD-K98645985, BRD-K25923209, BRD-K80443127), one with moderate activity (BRD-K17257309), and two with low or no activity (BRD-K13648511, BRD-K04244835). We found remarkable correlation between the ability to induce *Bmi1* transcription in ESCs and the ability to increase transcription of latent HIV-1 in a concentration-dependent manner (Figure 4A). The activity of three potent compounds (BRD-K98645985, BRD-K25923209, BRD-K80443127)

was similar in this assay (Figure 4A); however, since BRD-K80443127 displayed slightly higher activity at low concentrations, we continued with this carbamate analog for further characterization. The activation was confirmed in a second ex vivo model of HIV-1 latency (Figure S4A) (Bosque and Planelles, 2009) and the differential expression of two BAF target genes, namely *c-MYC* and *p21*, upon treatment with BRD-K80443127 was consistent with BAF inhibition (Figure 4B) (Guan et al., 2011; Cheng et al., 1999; Pham et al., 2010; Shi et al., 2013). The compounds show excellent activity even in the low concentration range of 1–10  $\mu$ M, and, importantly, the compounds show no toxicity to T cells at these concentrations (Figures 4C and S4B). Unwanted general immune activation reduces the clinical applicability of LRAs (DeChristopher et al., 2012; Korin et al., 2002); therefore, to investigate whether inhibitor treatment results in stimulation of T cells, we treated human primary CD4+ T cells isolated from two healthy donors with BRD-K80443127 for 24 and 72 hr, followed by detection of activation markers CD25 and CD69. As expected, propidium monoazide (PMA)/ionomycin treatment resulted in activation of T cells, while BRD-K80443127 treatment had no effect on CD25 and CD69 expression (Figure S4C). We also found that the compounds can be used in conjunction with other HIV LRAs, such as HDAC inhibitors (SAHA [suberoylanilide hydroxamic acid], valproic acid, and romidepsin) or PKC modulators (prostratin and bryostatin), to boost activity compared with single-agent treatments (Figure 4D). The activities were primarily additive, with slight synergy when compared across multiple drug concentrations (Figure S4D) (Laird et al., 2015). To confirm whether inhibitors could reverse HIV-1 latency in T cells obtained from HIV-1-infected patients, we treated CD4+ T cells from three aviremic patients with BRD-K80443127, prostratin, BRD-K80443127, and prostratin, and  $\alpha$ CD3/ $\alpha$ CD28 magnetic beads as a positive control (Figure 4E). Patient 1 CD4 T cells responded to all treatments, while, interestingly, double treatment with BRD-K80443127 and prostratin resulted in 63% latency reversal compared with positive control  $\alpha$ CD3/ $\alpha$ CD28 (Figure 4E). Cells from patients 2 and 3 did not result in a significant increase in cell-associated HIV-1 *POL* after treatment with BRD-K80443127 alone; however, when co-treated with the PKC agonist prostratin, BRD-K80443127 showed significant increase in *POL* copies (Figure 4E). As biomarkers can be clinically useful as surrogate measures of compound activity, we examined expression levels of BAF target genes *p21* and





(legend on next page)

C-MYC in the three patients and we observed significant decrease of *p21* and C-MYC transcripts levels, confirming BRDK80443127 activity in these cells.

### Validation of BAF-Mediated Transcriptional Effects

To define how well the BAF inhibitors mimic the transcriptional profile of BAF deletion, we performed RNA sequencing (RNA-seq) analysis on mESCs treated with 30  $\mu$ M BRD-K98645985 or DMSO for 18 hr. We found 3,534 differentially regulated genes upon compound treatment (1.5-fold change,  $p < 0.05$ ), with 1,518 upregulated and 1,916 downregulated upon compound treatment. Comparing the gene overlap with published RNA-seq data from *Brg1* KO in mESCs (King and Klose, 2017) reveals a significant (2.3-fold enrichment over predicted,  $p = 1.47 \times 10^{-33}$ ) overlap of gene expression (Figure 5A). This high degree in overlap indicates that BRD-K98645985 targets similar pathways regulated by BRG1 in ESCs. The incomplete overlap could be due to off-target effects, phenotypic difference between acute inhibition and genetic deletion, compound targeting a subset of BRG1 function, heterogeneity of different ESC lines, different experimental conditions, and/or different analysis conditions. Pathway analysis of the overlapping genes shows significant enrichment of genes related to neuronal development and morphogenesis, consistent with the loss of pluripotency and a propensity for neuronal differentiation reported for *Arid1a* KO ESCs (Gao et al., 2008). We then performed RNA-seq analysis with *Arid1a* KO ESCs and identified 1,141 differentially regulated genes (1.5-fold change,  $p < 0.05$ ). A higher percentage of the ARID1A-regulated genes overlapped with compound-treated cells (2.7-fold enrichment over predicted,  $p = 6.55 \times 10^{-58}$ ) than BRG1-regulated genes. In addition, the canonical pathways identified for the differential genes from each dataset were most similar between the *Arid1a* KO cells and BRD-K98645985-treated cells. This, in conjunction with parallel studies with screen hits in the context of *ARID1A* mutant cancer cell lines and ATR synergy (unpublished data), led us to hypothesize ARID1A as the primary target of the macrolactams. Still, the incomplete overlap of gene expression between *Arid1a* KO cells and BRD-K98645985 treatment raises the possibility that BRD-K98645985 modulates *Arid1a* function

in a manner different from genetic deletion, and/or that it has additional biological targets.

### Validation of ARID1A as a Target

Based on the SAR we hypothesized that the  $R_1$  position would be amenable to linker attachment for protein target identification; however, the synthesis of analog CAM 2-64 with a single methylene addition compared with BRD-K83694683 resulted in a significant decrease in activity (Figure 5B). Further modification with a longer linker attached to biotin in CAM 2-56 further reduced activity in a cell-based system (Figure 5B). While CAM 2-56 may suffer from poor cell permeability due to the addition of biotin, it is unlikely that the pharmacokinetics of CAM 2-64 are significantly altered due to the addition of a single methylene onto BRD-K83694683, implying that the binding site does not tolerate additional bulk at  $R_1$ . Nevertheless, since we observed some activity of the biotin-linked compound CAM 2-56, we used it in combination with streptavidin support for affinity purification. In accordance with reduced binding affinity of these linked macrolactams, we saw only moderate enrichment of ARID1A from ESC lysates (Figures 5C and S5A); however, we did observe a complete reduction of ARID1A enrichment upon preincubation of lysates with 200  $\mu$ M soluble BRD-K25923209, indicating selective binding (Figures 5C and S5A). In addition, we observed only non-specific enrichment of PBAF subunit PBRM1 and loading control LaminB1. In agreement with the compounds targeting the ARID1A-containing BAF complexes, we observed a decrease in enrichment for BAF155 and BAF47, which are subunits of both BAF and PBAF. While these experiments indicate direct binding to ARID1A-containing BAF complexes, they are complicated by the decrease in affinity upon linking the compound to solid support. To circumvent the need for a derivatized scaffold for target ID, we turned to cellular thermal shift assay (CETSA), a cell-based technique (Savitski et al., 2014). CETSA is based on the principle that the stability of a protein will be increased upon binding to a small molecule ligand, which can be visualized using immunoblot analysis after incubation of cells across a temperature gradient followed by removal of the insoluble, denatured proteins. Since ARID1A is a dedicated member of the large, 1–2 MDa SWI/SNF complex,

### Figure 4. Twelve-Membered Macrolactams Reactivate Latent HIV-1 in Primary Model Systems of HIV-1 Latency and Patient Samples with Limited Toxicity or T Cell Activation

(A) A panel of six macrolactams with varying  $EC_{50}$  values from the Bmi1-luciferase assay were tested in an ex vivo model of HIV-1 latency using primary CD4+ T cells from healthy donors (Lassen et al., 2012). Each point represents a single experiment using T cells from at least two different healthy donors. Luciferase levels are normalized with total protein levels. Error bars represent mean  $\pm$  SD. Asterisks indicate the level of significance compared with untreated cells using Student's t test (\*\*\* $p < 0.001$ , \*\*\*\* $p < 0.0001$ ).

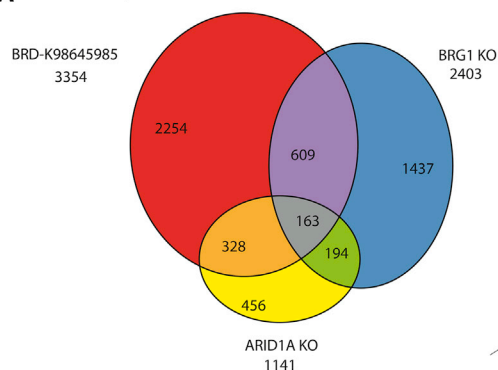
(B) mRNA expression levels of two BAF target genes were determined after treatment of CD4+ T cells isolated from three healthy donors with BRD-K80443127. Bars represent the average  $\pm$ SD. Asterisks indicate the level of significance compared with untreated cells using Student's t test (\* $p < 0.05$ , \*\* $p < 0.01$ ).

(C) The number of apoptotic human primary CD4+ T cells in the presence of macrolactams was measured using annexin V staining and flow cytometry analysis. Data presented as mean  $\pm$  SD of experiments performed on cells isolated from six healthy donors (\*\*\*\* $p < 0.0001$ ).

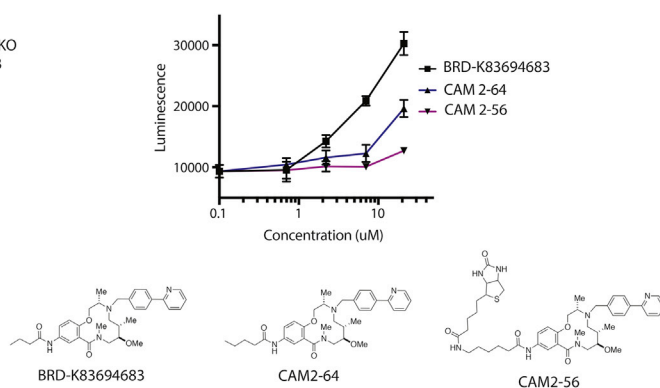
(D) Latency reversal activity of BRD-K80443127 in combination with known LRAs was assessed in the ex vivo model of HIV-1 latency. BRD-K80443127 was used at a concentration of 5  $\mu$ M alone or in combination with known LRAs at a single dose. Luciferase levels are normalized with total protein levels. Data presented as mean  $\pm$  SD of experiments performed in duplicate using cells from two healthy donors. Asterisks indicate the level significance compared with untreated cells using Student's t test (\* $p < 0.05$ , \*\* $p < 0.01$ , \*\*\* $p < 0.001$ , \*\*\*\* $p < 0.0001$ ).

(E) Cell-associated HIV Pol mRNA levels were quantitated in CD4+ T cells obtained from three c-ART-treated virologically suppressed HIV-1-infected patients after ex vivo treatment with BRD-K80443127 (10  $\mu$ M), Prostratin (200 nM), or  $\alpha$ CD3/ $\alpha$ CD28 Dynabeads as indicated in triplicate. Bars represent average of treatments in triplicate  $\pm$ SD; asterisks indicate the level of significance using one-way ANOVA followed by Tukey test (\* $p < 0.05$ ). mRNA expression levels of biomarker genes of BAF activity, c-MYC, and p-21 were also quantitated in the patient CD4+ T cells after treatment with DMSO or BRD-K80443127 (10  $\mu$ M). See also Figure S4.

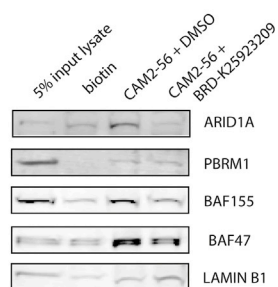
## A RNA-Seq Profiles



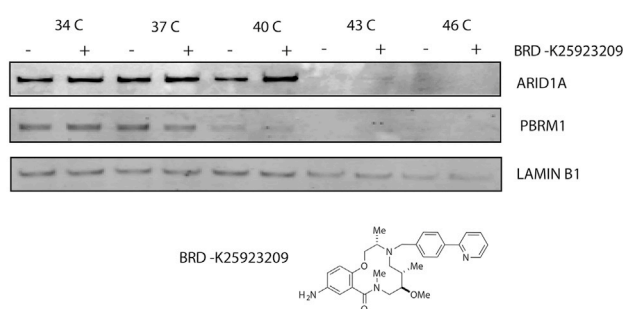
## B Activity of Linked Analogs



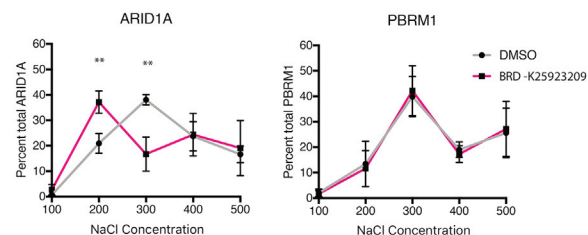
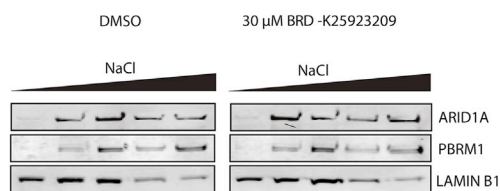
## C Enrichment of BAF from lysates



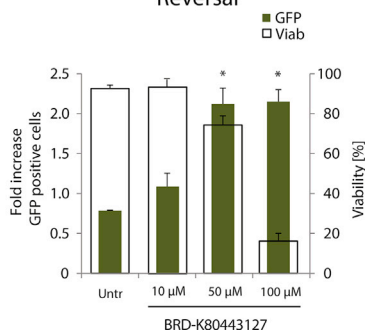
## D CETSA



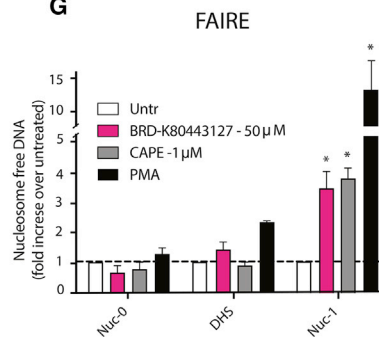
## E Sequential Salt Extraction



## F J-Lat 11.1 Latency Reversal



## G FAIRE



(legend on next page)

changes in protein stability from binding a small molecule would be difficult to discern; however, we did observe a small but reproducible increase in ARID1A stability, but not PBRM1 or LaminB1 stability, upon compound treatment, providing further preliminary evidence that the compound binds ARID1A-containing complexes (Figure 5D). The known enzymatic activity of the BAF chromatin remodeling complex is DNA-stimulated ATP hydrolysis via the BRG1 subunit; however, we observed only slight inhibition of the ATPase activity at high concentrations of compound (Figure S5B), indicating that this is not its primary mode of action. Similarly, we performed glycerol gradients to assess whether compounds affect BAF complex formation and did not observe any significant disruption to BAF complex integrity upon compound treatment (Figure S5C). When we used a sequential salt extraction to investigate the possibility of the compounds inhibiting ARID1A association with chromatin, we saw a significant and reproducible shift in ARID1A elution but not PBRM1 elution upon treatment with compound (Figure 5E). Although these shifts are small in nature, they are very reproducible between experiments and consistent with affinity shifts previously observed upon deletion of a single BAF complex subunit or mutation of a single chromatin binding domain within large BAF complexes (Porter and Dykhuizen, 2017).

### Mechanism of Action in HIV Latency Reversal

To examine the mechanism for how these BAF inhibitors might be inhibiting ARID1A-mediated repression, we used the J-Lat T cell line models of HIV-1 latency, in which activation of transcription from the latent provirus results in GFP synthesis. We confirmed concentration-dependent latency reversal upon treatment with BRD-K98645985, although at higher concentrations than in primary cells (Figures 5F and S5D). We investigated how nucleosome occupancy at the 5'-LTR changes upon treatment with BRD-K80443127 in J-Lat 11.1 using the formaldehyde-assisted isolation of regulatory elements (FAIRE) assay, which is a measure of chromatin accessibility (Giresi et al., 2007). Overnight compound treatment resulted in increased chromatin accessibility at the Nuc-1 position of the 5' LTR (Figure 5G), mimicking the effect elicited by the small interfering RNA knockdown of *ARID1A* and treatment with BAF inhibitors identified in our previous studies (Rafati et al., 2011; Stoszko et al., 2016).

## DISCUSSION

While the mammalian SWI/SNF chromatin remodeling complex is often referred to as a single protein complex, it is actually a heterogeneous assembly of closely related protein complexes with different biochemical and biological functions (Hargreaves and Crabtree, 2011; Wu et al., 2009). Several of these subcomplexes have been determined to be misregulated in disease, implicating subunits of SWI/SNF complexes as potential drug targets (Hohmann and Vakoc, 2014; Schiaffino-Ortega et al., 2014). A significant challenge for drug development is that general inhibition of SWI/SNF chromatin remodeling function may have undesirable toxicity, as many, if not most, cell types require some form of SWI/SNF chromatin remodeling for basic viability (Dykhuizen et al., 2013; Hohmann and Vakoc, 2014). Further complicating matters, it is still unclear how the biochemical functions of individual subunits of chromatin remodeling complexes are related to desired phenotypes, making it difficult to design and implement biochemical screening programs. To circumvent these issues, we developed a robust high-throughput phenotypic screen designed to identify small molecules that inhibit BAF-mediated transcription without affecting cellular viability. From this screen, we have identified a 12-membered macrolactam with low toxicity and the ability to inhibit the transcriptional activities of the BAF complex. These compounds have significant promise as HIV-1 LRAs, particularly because of their potential for clinical use in combination therapy with other currently available LRAs. Indeed, we show that treatment with the structurally similar macrolactams, BRD-K98645985, BRD-K25923209, and BRD-K80443127, triggered HIV transcription in *ex vivo* infected primary CD4+ T cells harboring latent HIV and potentiated the effect of other LRAs when used in combination. In CD4+ T cells isolated from c-ART-treated virologically suppressed HIV-1-infected patients, a significant increase in cell-associated HIV mRNA was observed after *ex vivo* treatment with BRD-K80443127 alone in one patient, while, in all three patients, BRD-K80443127 treatment led to significant potentiation of prostratin activity. The mechanism of action appears to be that of de-repression, or inhibition of the HIV-1 LTR-bound repressive BAF complex. Our observed modest and variable effects in latency reversal by BRD-K80443127 alone are consistent with

### Figure 5. Twelve-Membered Macrolactams Are Inhibitors of ARID1A-Containing BAF Complexes

(A) Differential gene expression of mESCs treated with 30  $\mu$ M BRD-K98645985 for 18 hr was compared with published differential gene expression in *Brg1* KO mESCs (King and Klose, 2017) to determine overlapping gene sets. Data were acquired from RNA-seq analyses.

(B) The luciferase induction upon treatment with macrolactams with propyl amide (BRD-K83694683), butyl amide (CAM2-64), and biotin-hexylamide (CAM2-56) appended off the aniline was determined using the BMI1-luciferase reporter cell line. Points represent mean  $\pm$  standard deviation.  $n = 3$ .

(C) Pulldowns were performed from ESC lysates pretreated with DMSO or 200  $\mu$ M BRD-K25923209 using biotin or CAM2-56 prebound to streptavidin resin. Protein enrichment was determined using immunoblot analysis.

(D) Protein stabilization by BRD-K25923209 was determined using CETSA in mESCs. The stabilization of ARID1A, PBRM1, and LAMINB1 was detected using immunoblot analysis of soluble proteins after incubation in a temperature gradient.

(E) Sequential salt extractions were performed on ESC nuclei. The chromatin was washed with increasing concentrations of salt containing DMSO or BRD-K98645985 (30  $\mu$ M) and the elutions of ARID1A and PBRM1 were analyzed using immunoblot analysis. The percentage of protein elution was calculated across all five washes using ImageJ for ARID1A and PBRM1.  $n = 3$ .

(F) J-Lat 11.1 cells were treated with increasing concentrations of BRD-K80443127 and reactivation was quantitated at 48 hr post treatment. Percentage GFP-positive cells (left axis, green bars), which corresponds to the level of HIV-1 activation, and cell viability (right axis, transparent bars) were both evaluated by flow cytometry.  $n = 3$ . Viab, viability.

(G) Levels of nucleosome occupancy at the HIV-1 5'-LTR region following treatment with BRD-K80443127, CAPE (caffeic acid phenethyl ester), and PMA were analyzed using FAIRE assay.  $n = 3$ .

Data are presented as mean  $\pm$  SD. Asterisks indicate the level significance compared with untreated cells using Student's *t* test (\* $p < 0.05$ , \*\* $p < 0.01$ , \*\*\* $p < 0.001$ , \*\*\*\* $p < 0.0001$ ). See also Figure S5.

this notion and point to the need for larger patient cohorts in order to test the activity of this compound with robust across-patient statistics. Importantly, in line with the mechanism of action of BRD-K80443127 as an LTR de-repressor, co-treatment with the PKC agonist prostratin, which is a *bona fide* activator of HIV transcription resulted in significant increase in cell-associated HIV RNA in all patients. This is in line with recent findings that ARID1A degraders from our previous studies (Stoszko et al., 2016) act to increase transcriptional noise (frequency or burst) at the HIV-1 LTR promoter (Megaridis et al., 2018). This points to the potential for this class of compounds for inclusion in combinatorial therapy with other drugs targeting different steps in HIV-1 transcription.

Target identification and mechanistic work indicate that this inhibitor binds the ARID1A-containing BAF complexes and prevent ARID1A function at the 5' LTR of HIV-1, although the exact mechanism of compound action is still to be resolved. The SAR from this study indicates that further variation of substituents at the R<sub>1</sub> and R<sub>2</sub> positions on the macrolactam scaffold will likely not improve potency much, but optimization at other unexplored positions around the macrolactam ring could increase potency and also facilitate derivatization for more in-depth target identification. Deciphering how this class of compounds inhibits ARID1A activity will be critical for further optimization of these inhibitors as HIV-1 LRAs targeting the BAF complex. In addition, we have found that BAF inhibitor synergizes with ATR inhibitors for the killing of specific types of cancer, particularly those with high mutational backgrounds (unpublished data). Here again, a detailed understanding of the exact mechanism of actions for these inhibitors will be necessary for pharmacologic and therapeutic optimization as well as to provide a tool to understand the mechanism of action of ARID1A-containing BAF complexes in polycomb eviction and resolution of facultative heterochromatin (Kadoch et al., 2017; Miller et al., 2017; Stanton et al., 2017).

## SIGNIFICANCE

**The BAF (SWI/SNF) chromatin remodeling complex has long been an attractive target for drug development; however, the heterogeneous nature of BAF complexes, along with undefined biochemical functions for disease-related subunits, has made the development of small molecule screening platforms particularly challenging. Here, we have developed a reporter cell line of BAF-mediated transcriptional repression and identified a macrolactam inhibitor of the BAF chromatin remodeling complex using high-throughput screening. This optimized class of compounds activates the expression of BAF-repressed genes in ESCs and are similarly able to activate transcription in *in vitro* cell line models of HIV-1 latency and in primary human CD4+ T cells harboring latent HIV-1. Importantly, these compounds do not display T cell toxicity or T cell activation, which are associated with many LRAs. Target identification and phenotypic analysis point to the inhibition of ARID1A-containing BAF complexes, which are selectively involved in maintaining HIV-1 latency. This study validates the strategy of targeting individual BAF subcomplexes involved in disease and identifies a macrolactam scaffold developed using DOS. This class of compounds is a useful starting**

**point for more potent and selective BAF inhibitors, which can be used in combination with other LRAs to activate HIV-1 transcription and eliminate the latently infected cell population.**

## STAR★METHODS

Detailed methods are provided in the online version of this paper and include the following:

- KEY RESOURCES TABLE
- CONTACT FOR REAGENT AND RESOURCE SHARING
- EXPERIMENTAL MODEL AND SUBJECT DETAILS
  - Cell Line Authentication
  - Cell Culture Conditions
  - Subject Details
- METHOD DETAILS
  - Bmi1-Luciferase Reporter Cell Line
  - Lentiviral Infection
  - Compound Treatment
  - Luciferase Assay
  - qRT-PCR Secondary Screen (PubChem AID 743180, 743177, 743176)
  - Viability Assays (PubChem AID: 743188, 743189, 743190, 1053139, 1053140, 1053141)
  - qRT-PCR Screen Confirmation and DOS Analog Library (SYBR)
  - Chemical Synthesis of DOS Analog Library
  - Nuclear Isolation
  - Cell Lysis
  - ATPase Assay
  - Immunoblot Analysis
  - Glycerol Gradients
  - Sequential Salt Extractions
  - Biotin Pull Downs
  - CETSA Protocol
  - RNA-Seq ECS with BAFi
  - RNA-Seq Arid1a f/f ESCs
  - Cell Line Models of HIV-1 Latency
  - Ex Vivo HIV Latency Model
  - Ex Vivo HIV Latency Model (Bosque-Planelles)
  - Biomarkers
  - HIV Latency Reversal from Patient Samples
  - Activation Markers, Apoptosis and Viability of Primary CD4+ T Cells
  - FAIRE
- QUANTIFICATION AND STATISTICAL ANALYSIS
- DATA AND SOFTWARE AVAILABILITY
- ADDITIONAL RESOURCES

## SUPPLEMENTAL INFORMATION

Supplemental Information includes five figures and two tables and can be found with this article online at <https://doi.org/10.1016/j.chembiol.2018.08.004>.

## ACKNOWLEDGMENTS

We would like to thank: Nicola Tolliday and Stuart Schreiber at the Broad Institute for their continued support, Helen Bodmer for technical assistance, Naoki



Hosen for assistance with the Bmi1-luciferase knockin cell line, and Emma Chory for helpful discussion. *Arid1a<sup>fl/fl</sup>* mice were a gift from Terry Magnuson (University of North Carolina School of Medicine). HIV-1 molecular clone pNL4.3.Luc.R-E-, HIV-1 HXB2-Env expression vector, saquinavir mesylate, and raltegravir were provided by the Centre for AIDS Reagents, National Institute for Biological Standards and Control. HIV-1 molecular clone pNL4.3.Luc.R-E- and HIV-1 HXB2-Env expression vector were donated by Dr. Nathaniel Landau and Drs Kathleen Page and Dan Littman, respectively. This work was directly supported by NIH grant DA032469 to G.R.C. and E.C.D., American Cancer Society ACS 121535-PF-11-145-01-DMC to E.C.D., and the Showalter Trust to E.C.D. E.C.D. is supported by The V Foundation for Cancer Research (V2014-004 and D2016-030) the NIH (CA207532), and the Department of Defense (W81XWH-17-1-0267). Opinions, interpretations, conclusions, and recommendations are those of the author and are not necessarily endorsed by the Department of Defense. G.R.C. is supported by NIH grants (CA163915, NS046789), CIRM RB4-05886, SFARI, and the Howard Hughes Medical Institute. T.M. is supported by the European Research Council (ERC) Programme (FP/2007-2013)/ERC STG 337116 Trxn-PURGE, Dutch AIDS Fonds grant 2014021, and Erasmus MC mRACE.

## AUTHOR CONTRIBUTIONS

Conceptualization: E.C.D., G.R.C., T.M. Methodology: E.C.D., G.R.C., T.M., J.R.D., L.W., D.C.H. Software: B.C. and B.C.C. Formal Analysis: E.C.D., L.W. Investigation: E.C.D., C.A. Marian, C.A. Masciot, T.M., L.W., M.W.L., E.d.C., J.G. Resources: E.C.D., G.R.C., T.M. Data Curation: L.W. Writing – Original Draft Preparation: E.C.D., C.A. Marian, M.S., T.M., G.R.C. Writing – Review & Editing Preparation: E.C.D., C.A. Marian, M.S., T.M., G.R.C., E.d.C., J.G., D.C.H. Visualization: E.C.D. Supervision: E.C.D., T.M., G.R.C., D.C.H., J.R.D. Project Administration: E.C.D., T.M., G.R.C. Funding Acquisition: E.C.D., G.R.C., T.M.

## DECLARATION OF INTERESTS

G.R.C. is a co-founder of Foghorn Therapeutics.

Received: November 10, 2017

Revised: May 24, 2018

Accepted: August 6, 2018

Published: September 6, 2018

## REFERENCES

Agbottah, E., Deng, L., Dannenberg, L.O., Pumfery, A., and Kashanchi, F. (2006). Effect of SWI/SNF chromatin remodeling complex on HIV-1 Tat activated transcription. *Retrovirology* 3, 48.

Anders, S., and Huber, W. (2010). Differential expression analysis for sequence count data. *Genome Biol.* 11, R106.

Archin, N.M., Liberty, A.L., Kashuba, A.D., Choudhary, S.K., Kuruc, J.D., Crooks, A.M., Parker, D.C., Anderson, E.M., Kearney, M.F., Strain, M.C., et al. (2012). Administration of vorinostat disrupts HIV-1 latency in patients on antiretroviral therapy. *Nature* 487, 482–485.

Archin, N.M., Bateson, R., Tripathy, M.K., Crooks, A.M., Yang, K.H., Dahl, N.P., Kearney, M.F., Anderson, E.M., Coffin, J.M., Strain, M.C., et al. (2014). HIV-1 expression within resting CD4+ T cells after multiple doses of vorinostat. *J. Infect. Dis.* 210, 728–735.

Auld, D.S., Thorne, N., Nguyen, D.-T., and Inglese, J. (2008). A specific mechanism for nonspecific activation in reporter-gene assays. *ACS Chem. Biol.* 3, 463–470.

Baell, J.B., and Holloway, G.A. (2010). New substructure filters for removal of pan assay interference compounds (PAINS) from screening libraries and for their exclusion in bioassays. *J. Med. Chem.* 53, 2719–2740.

Barouch, D.H., and Deeks, S.G. (2014). Immunologic strategies for HIV-1 remission and eradication. *Science* 345, 169–174.

Barré-Sinoussi, F., Chermann, J.C., Rey, F., Nugeyre, M.T., Chamaret, S., Gruest, J., Dautquet, C., Axler-Blin, C., Vézinet-Brun, F., Rouzioux, C., et al.

(1983). Isolation of a T-lymphotropic retrovirus from a patient at risk for acquired immune deficiency syndrome (AIDS). *Science* 220, 868–871.

Bliss, C.I. (1939). The toxicity of poisons applied jointly. *Ann. Appl. Biol.* 26, 585–615.

Boese, A., Sommer, P., Holzer, D., Maier, R., and Nehrbass, U. (2009). Integrase interactor 1 (Ini1/hSNF5) is a repressor of basal human immunodeficiency virus type 1 promoter activity. *J. Gen. Virol.* 90, 2503–2512.

Bosque, A., and Planelles, V. (2009). Induction of HIV-1 latency and reactivation in primary memory CD4+ T cells. *Blood* 113, 58–65.

Brockman, M.A., Jones, R.B., and Brumme, Z.L. (2015). Challenges and opportunities for T-cell-mediated strategies to eliminate HIV reservoirs. *Front. Immunol.* 6, 692.

Bultman, S., Gebuhr, T., and Magnuson, T. (2005). A Brg1 mutation that uncouples ATPase activity from chromatin remodeling reveals an essential role for SWI/SNF-related complexes in beta-globin expression and erythroid development. *Gene Dev.* 19, 2849–2861.

Chandler, R.L., Damrauer, J.S., Raab, J.R., Schisler, J.C., Wilkerson, M.D., Didion, J.P., Starmer, J., Serber, D., Yee, D., Xiong, J., et al. (2015). Coexistent ARID1A-PIK3CA mutations promote ovarian clear-cell tumorigenesis through pro-tumorigenic inflammatory cytokine signalling. *Nat. Commun.* 6, 6118.

Cheng, S.W.G., Davies, K.P., Yung, E., Beltran, R.J., Yu, J., and Kalpana, G.V. (1999). c-MYC interacts with INI1/hSNF5 and requires the SWI/SNF complex for transactivation function. *Nat. Genet.* 22, 102–105.

Chun, T.-W., Carruth, L., Finzi, D., Shen, X., DiGiuseppe, J.A., Taylor, H., Hermankova, M., Chadwick, K., Margolick, J., Quinn, T.C., et al. (1997). Quantification of latent tissue reservoirs and total body viral load in HIV-1 infection. *Nature* 387, 183–188.

Chun, T.-W., Justement, J.S., Murray, D., Hallahan, C.W., Maenza, J., Collier, A.C., Sheth, P.M., Kaul, R., Ostrowski, M., Moir, S., et al. (2010). Rebound of plasma viremia following cessation of antiretroviral therapy despite profoundly low levels of HIV reservoir: implications for eradication. *AIDS* 24, 2803–2808.

Churchill, M.J., Deeks, S.G., Margolis, D.M., Siliciano, R.F., and Swanstrom, R. (2016). HIV reservoirs: what, where and how to target them. *Nat. Rev. Microbiol.* 14, 55–60.

Cillo, A.R., and Mellors, J.W. (2016). Which therapeutic strategy will achieve a cure for HIV-1? *Curr. Opin. Virol.* 18, 14–19.

Conrad, R.J., and Ott, M. (2016). Therapeutics targeting protein acetylation perturb latency of human viruses. *ACS Chem. Biol.* 11, 669–680.

Conrad, R.J., Fozouni, P., Thomas, S., Sy, H., Zhang, Q., Zhou, M.-M., and Ott, M. (2017). The short isoform of BRD4 promotes HIV-1 latency by engaging repressive SWI/SNF chromatin-remodeling complexes. *Mol. Cell* 67, 1001–1012.e6.

De Crignis, E., and Mahmoudi, T. (2017). The multifaceted contributions of chromatin to HIV-1 integration, transcription, and latency. *Int. Rev. Cell Mol. Biol.* 328, 197–252.

Dahabieh, M., Battivelli, E., and Verdin, E. (2015). Understanding HIV latency: the road to an HIV cure. *Annu. Rev. Med.* 66, 407–421.

DeChristopher, B.A., Loy, B.A., Marsden, M.D., Schrier, A.J., Zack, J.A., and Wender, P.A. (2012). Designed, synthetically accessible bryostatins analogues potentially induce activation of latent HIV reservoirs in vitro. *Nat. Chem.* 4, 705–710.

Deeks, S.G. (2012). HIV: shock and kill. *Nature* 487, 439–440.

Deeks, S.G., Lewin, S.R., and Havlir, D.V. (2013). The end of AIDS: HIV infection as a chronic disease. *Lancet* 382, 1525–1533.

Delagrèverie, H.M., Delaunay, C., Lewin, S.R., Deeks, S.G., and Li, J.Z. (2016). Ongoing clinical trials of human immunodeficiency virus latency-reversing and immunomodulatory agents. *Open Forum Infect. Dis.* 3, ofw189.

Van Duyn, R., Guendel, I., Shafagati, N., Kehn-Hall, K., Easley, R., Klase, Z., Nekhai, S., Tyagi, M., and Kashanchi, F. (2011). Varying modulation of HTLV-1 LTR activity by BAF complexes. *Retrovirology* 8, A180.

Dykhuizen, E.C., Carmody, L.C., Tolliday, N., Crabtree, G.R., and Palmer, M.A.J. (2012). Screening for inhibitors of an essential chromatin remodeler in

- mouse embryonic stem cells by monitoring transcriptional regulation. *J. Biomol. Screen.* 17, 1221–1230.
- Dykhuizen, E.C., Hargreaves, D.C., Miller, E.L., Cui, K., Korshunov, A., Kool, M., Pfister, S., Cho, Y.-J., Zhao, K., and Crabtree, G.R. (2013). BAF complexes facilitate decatenation of DNA by topoisomerase II $\alpha$ . *Nature* 497, 624–627.
- Easley, R., Carpio, L., Dannenberg, L., Choi, S., Alani, D., Van Duyne, R., Guendel, I., Klase, Z., Agbottah, E., Kehn-Hall, K., et al. (2010). Transcription through the HIV-1 nucleosomes: effects of the PBAF complex in Tat activated transcription. *Virology* 405, 322–333.
- Elliott, J.H., Wightman, F., Solomon, A., Ghneim, K., Ahlers, J., Cameron, M.J., Smith, M.Z., Spelman, T., McMahon, J., Velayudham, P., et al. (2014). Activation of HIV transcription with short-course vorinostat in HIV-infected patients on suppressive antiretroviral therapy. *PLoS Pathog.* 10, e1004473.
- Finzi, D., Hermankova, M., Pierson, T., Carruth, L.M., Buck, C., Chaisson, R.E., Quinn, T.C., Chadwick, K., Margolick, J., Brookmeyer, R., et al. (1997). Identification of a reservoir for HIV-1 in patients on highly active antiretroviral therapy. *Science* 278, 1295–1300.
- Finzi, D., Blankson, J., Siliciano, J.D., Margolick, J.B., Chadwick, K., Pierson, T., Smith, K., Lisiewicz, J., Lori, F., Flexner, C., et al. (1999). Latent infection of CD4<sup>+</sup> T cells provides a mechanism for lifelong persistence of HIV-1, even in patients on effective combination therapy. *Nat. Med.* 5, 512–517.
- Fitzgerald, M.E., Mulrooney, C.A., Duvall, J.R., Wei, J., Suh, B.-C., Akella, L.B., Vrcic, A., and Marcaurelle, L.A. (2012). Build/couple/pair strategy for the synthesis of stereochemically diverse macrolactams via head-to-tail cyclization. *ACS Comb. Sci.* 14, 89–96.
- Gao, X., Tate, P., Hu, P., Tjian, R., Skarnes, W.C., and Wang, Z. (2008). ES cell pluripotency and germ-layer formation require the SWI/SNF chromatin remodeling component BAF250a. *Proc. Natl. Acad. Sci. USA* 105, 6656–6661.
- Giresi, P.G., Kim, J., McDaniel, R.M., Iyer, V.R., and Lieb, J.D. (2007). FAIRE (formaldehyde-assisted isolation of regulatory elements) isolates active regulatory elements from human chromatin. *Genome Res.* 17, 877–885.
- Guan, B., Wang, T.-L., and Shih, I.-M. (2011). ARID1A, a factor that promotes formation of SWI/SNF-mediated chromatin remodeling, is a tumor suppressor in gynecologic cancers. *Cancer Res.* 71, 6718–6727.
- Hargreaves, D.C., and Crabtree, G.R. (2011). ATP-dependent chromatin remodeling: genetics, genomics and mechanisms. *Cell Res.* 21, 396–420.
- Ho, L., and Crabtree, G.R. (2010). Chromatin remodelling during development. *Nature* 463, 474–484.
- Ho, L., Jothi, R., Ronan, J.L., Cui, K., Zhao, K., and Crabtree, G.R. (2009). An embryonic stem cell chromatin remodeling complex, esBAF, is an essential component of the core pluripotency transcriptional network. *Proc. Natl. Acad. Sci. USA* 106, 5187–5191.
- Ho, L., Miller, E.L., Ronan, J.L., Ho, W.Q., Jothi, R., and Crabtree, G.R. (2011). esBAF facilitates pluripotency by conditioning the genome for LIF/STAT3 signalling and by regulating polycomb function. *Nat. Cell Biol.* 13, 903–913.
- Hodges, C., Kirkland, J.G., and Crabtree, G.R. (2016). The many roles of BAF (mSWI/SNF) and PBAF complexes in cancer. *Cold Spring Harb. Perspect. Med.* 6, a026930.
- Hohmann, A.F., and Vakoc, C.R. (2014). A rationale to target the SWI/SNF complex for cancer therapy. *Trends Genet.* 30, 356–363.
- Jafari, R., Almqvist, H., Axelsson, H., Ignatushchenko, M., Lundbäck, T., Nordlund, P., and Molina, D.M. (2014). The cellular thermal shift assay for evaluating drug target interactions in cells. *Nat. Protoc.* 9, 2100–2122.
- Jordan, A., Defechereux, P., and Verdin, E. (2001). The site of HIV-1 integration in the human genome determines basal transcriptional activity and response to Tat transactivation. *EMBO J.* 20, 1726–1738.
- Jordan, A., Bisgrove, D., and Verdin, E. (2003). HIV reproducibly establishes a latent infection after acute infection of T cells in vitro. *EMBO J.* 22, 1868–1877.
- Kadoch, C., Williams, R.T., Calarco, J.P., Miller, E.L., Weber, C.M., Braun, S.M.G., Pulice, J.L., Chory, E.J., and Crabtree, G.R. (2017). Dynamics of BAF-Polycomb complex opposition on heterochromatin in normal and oncogenic states. *Nat. Genet.* 49, 213–222.
- King, H.W., and Klose, R.J. (2017). The pioneer factor OCT4 requires the chromatin remodeller BRG1 to support gene regulatory element function in mouse embryonic stem cells. *Elife* 6, 380.
- Korin, Y.D., Brooks, D.G., Brown, S., Korotzer, A., and Zack, J.A. (2002). Effects of prostratin on T-cell activation and human immunodeficiency virus latency. *J. Virol.* 76, 8118–8123.
- Kumar, A., Darcis, G., Van Lint, C., and Herbein, G. (2015). Epigenetic control of HIV-1 post integration latency: implications for therapy. *Clin. Epigenetics* 7, 103.
- Laird, G.M., Bullen, C.K., Rosenbloom, D.I.S., Martin, A.R., Hill, A.L., Durand, C.M., Siliciano, J.D., and Siliciano, R.F. (2015). Ex vivo analysis identifies effective HIV-1 latency-reversing drug combinations. *J. Clin. Invest.* 125, 1901–1912.
- Lassen, K.G., Hebbeler, A.M., Bhattacharyya, D., Lobritz, M.A., and Greene, W.C. (2012). A flexible model of HIV-1 latency permitting evaluation of many primary CD4 T-cell reservoirs. *PLoS One* 7, e30176.
- Van Lint, C., Emiliani, S., Ott, M., and Verdin, E. (1996). Transcriptional activation and chromatin remodeling of the HIV-1 promoter in response to histone acetylation. *EMBO J.* 15, 1112–1120.
- Van Lint, C., Bouchat, S., and Marcello, A. (2013). HIV-1 transcription and latency: an update. *Retrovirology* 10, 67.
- Livak, K.J., and Schmittgen, T.D. (2001). Analysis of relative gene expression data using real-time quantitative PCR and the 2(-Delta Delta C(T)) method. *Methods* 25, 402–408.
- Maartens, G., Celum, C., and Lewin, S.R. (2014). HIV infection: epidemiology, pathogenesis, treatment, and prevention. *Lancet* 384, 258–271.
- Mahmoudi, T., Parra, M., Vries, R.G.J., Kauder, S.E., Verrijzer, C.P., Ott, M., and Verdin, E. (2006). The SWI/SNF chromatin-remodeling complex is a cofactor for Tat transactivation of the HIV promoter. *J. Biol. Chem.* 281, 19960–19968.
- Margolis, D.M. (2017). Towards an HIV cure: a view of a developing field. *J. Infect. Dis.* 215, S109–S110.
- Margolis, D.M., and Archin, N.M. (2017). Proviral latency, persistent human immunodeficiency virus infection, and the development of latency reversing agents. *J. Infect. Dis.* 215, S111–S118.
- Margolis, D.M., Garcia, J.V., Hazuda, D.J., and Haynes, B.F. (2016). Latency reversal and viral clearance to cure HIV-1. *Science* 353, aaf6517.
- Martus, G., and Altfeld, M. (2016). Immunological strategies to target HIV persistence. *Curr. Opin. HIV AIDS* 11, 402–408.
- Mbonye, U., and Karn, J. (2014). Transcriptional control of HIV latency: cellular signaling pathways, epigenetics, happenstance and the hope for a cure. *Virology* 454–455, 328–339.
- Megaridis, M.R., Lu, Y., Tevorian, E.N., Junger, K.M., Moy, J.M., Bohn-Wippert, K., and Dar, R.D. (2018). Fine-tuning of noise in gene expression with nucleosome remodeling. *APL Bioeng.* 2, 026106.
- Miller, E.L., Hargreaves, D.C., Kadoch, C., Chang, C.-Y., Calarco, J.P., Hodges, C., Buenrostro, J.D., Cui, K., Greenleaf, W.J., Zhao, K., et al. (2017). TOP2 synergizes with BAF chromatin remodeling for both resolution and formation of facultative heterochromatin. *Nat. Struct. Mol. Biol.* 24, 344–352.
- Over, B., Matsson, P., Tyrchan, C., Artursson, P., Doak, B.C., Foley, M.A., Hilgendorf, C., Johnston, S.E., Lee, M.D., Lewis, R.J., et al. (2016). Structural and conformational determinants of macrocycle cell permeability. *Nat. Chem. Biol.* 12, 1065–1074.
- Perreau, M., Banga, R., and Pantaleo, G. (2017). Targeted immune interventions for an HIV-1 cure. *Trends Mol. Med.* 23, 945–961.
- Pham, L.V., Tamayo, A.T., Li, C., Bueso-Ramos, C., and Ford, R.J. (2010). An epigenetic chromatin remodeling role for NFATc1 in transcriptional regulation of growth and survival genes in diffuse large B-cell lymphomas. *Blood* 116, 3899–3906.
- Porter, E.G., and Dykhuizen, E.C. (2017). Individual bromodomains of polybromo-1 contribute to chromatin association and tumor suppression in clear cell renal carcinoma. *J. Biol. Chem.* 292, 2601–2610.



- Pulice, J.L., and Kadoch, C. (2017). Composition and function of mammalian SWI/SNF chromatin remodeling complexes in human disease. *Cold Spring Harb. Symp. Quant. Biol.* 81, 53–60.
- Rafati, H., Parra, M., Hakre, S., Moshkin, Y., Verdin, E., and Mahmoudi, T. (2011). Repressive LTR nucleosome positioning by the BAF complex is required for HIV latency. *PLoS Biol.* 9, e1001206.
- Rasmussen, T.A., Sogaard, O.S., Brinkmann, C., Wightman, F., Lewin, S.R., Melchjorsen, J., Dinarello, C., Østergaard, L., and Tolstrup, M. (2013). Comparison of HDAC inhibitors in clinical development: effect on HIV production in latently infected cells and T-cell activation. *Hum. Vaccin. Immunother.* 9, 993–1001.
- Rasmussen, T.A., Tolstrup, M., and Sogaard, O.S. (2016). Reversal of latency as part of a cure for HIV-1. *Trends Microbiol.* 24, 90–97.
- Robinson, M.D., McCarthy, D.J., and Smyth, G.K. (2010). edgeR: a Bioconductor package for differential expression analysis of digital gene expression data. *Bioinformatics* 26, 139–140.
- Ruelas, D.S., and Greene, W.C. (2013). An integrated overview of HIV-1 latency. *Cell* 155, 519–529.
- Savitski, M.M., Reinhard, F.B.M., Franken, H., Werner, T., Savitski, M.F., Eberhard, D., Molina, D.M., Jafari, R., Dovega, R.B., Klaeger, S., et al. (2014). Tracking cancer drugs in living cells by thermal profiling of the proteome. *Science* 346, 1255784.
- Schiaffino-Ortega, S., Balinas, C., Cuadros, M., and Medina, P.P. (2014). SWI/SNF proteins as targets in cancer therapy. *J. Hematol. Oncol.* 7, 81.
- Sheridan, P.L., Mayall, T.P., Verdin, E., and Jones, K.A. (1997). Histone acetyltransferases regulate HIV-1 enhancer activity in vitro. *Gene Dev.* 11, 3327–3340.
- Shi, J., Whyte, W.A., Zepeda-Mendoza, C.J., Milazzo, J.P., Shen, C., Roe, J.-S., Minder, J.L., Mercan, F., Wang, E., Eckersley-Maslin, M.A., et al. (2013). Role of SWI/SNF in acute leukemia maintenance and enhancer-mediated Myc regulation. *Gene Dev.* 27, 2648–2662.
- Siliciano, J.D., and Siliciano, R.F. (2016). Recent developments in the effort to cure HIV infection: going beyond N = 1. *J. Clin. Invest.* 126, 409–414.
- Siliciano, J.D., Kajdas, J., Finzi, D., Quinn, T.C., Chadwick, K., Margolick, J.B., Kovacs, C., Gange, S.J., and Siliciano, R.F. (2003). Long-term follow-up studies confirm the stability of the latent reservoir for HIV-1 in resting CD4+ T cells. *Nat. Med.* 9, 727–728.
- Sogaard, O.S., Graversen, M.E., Leth, S., Olesen, R., Brinkmann, C.R., Nissen, S.K., Kjaer, A.S., Schleimann, M.H., Denton, P.W., Hey-Cunningham, W.J., et al. (2015). The depsipeptide romidepsin reverses HIV-1 latency in vivo. *PLoS Pathog.* 11, e1005142.
- Spivak, A.M., and Planelles, V. (2016). HIV-1 eradication: early trials (and tribulations). *Trends Mol. Med.* 22, 10–27.
- Stanton, B.Z., Hodges, C., Calarco, J.P., Braun, S.M.G., Ku, W.L., Kadoch, C., Zhao, K., and Crabtree, G.R. (2017). Smarca4 ATPase mutations disrupt direct eviction of PRC1 from chromatin. *Nat. Genet.* 49, 282–288.
- Stoszko, M., De Crignis, E., Rokx, C., Khalid, M.M., Lungu, C., Palstra, R.-J., Kan, T.W., Boucher, C., Verbon, A., Dykhuizen, E.C., et al. (2016). Small molecule inhibitors of BAF; a promising family of compounds in HIV-1 latency reversal. *EBioMedicine* 3, 108–121.
- Trautmann, L. (2016). Kill: boosting HIV-specific immune responses. *Curr. Opin. HIV AIDS* 11, 409–416.
- Tréand, C., du Chéné, I., Brès, V., Kiernan, R., Benarous, R., Benkirane, M., and Emiliani, S. (2006). Requirement for SWI/SNF chromatin-remodeling complex in Tat-mediated activation of the HIV-1 promoter. *EMBO J.* 25, 1690–1699.
- Turner, A.W., and Margolis, D.M. (2017). Chromatin regulation and the histone code in HIV latency. *Yale J. Biol. Med.* 90, 229–243.
- Verdin, E. (1991). DNase I-hypersensitive sites are associated with both long terminal repeats and with the intragenic enhancer of integrated human immunodeficiency virus type 1. *J. Virol.* 65, 6790–6799.
- Verdin, E., Paras, P., and Van Lint, C. (1993). Chromatin disruption in the promoter of human immunodeficiency virus type 1 during transcriptional activation. *EMBO J.* 12, 3249–3259.
- Wei, D.G., Chiang, V., Fyne, E., Balakrishnan, M., Barnes, T., Graupe, M., Hesselgesser, J., Irrinki, A., Murry, J.P., Stepan, G., et al. (2014). Histone deacetylase inhibitor romidepsin induces HIV expression in CD4 T cells from patients on suppressive antiretroviral therapy at concentrations achieved by clinical dosing. *PLoS Pathog.* 10, e1004071.
- Wightman, F., Lu, H.K., Solomon, A.E., Saleh, S., Harman, A.N., Cunningham, A.L., Gray, L., Churchill, M., Cameron, P.U., Dear, A.E., et al. (2013). Entinostat is a histone deacetylase inhibitor selective for class 1 histone deacetylases and activates HIV production from latently infected primary T cells. *AIDS* 27, 2853–2862.
- Wu, J.I., Lessard, J., and Crabtree, G.R. (2009). Understanding the words of chromatin regulation. *Cell* 136, 200–206.

## STAR★METHODS

### KEY RESOURCES TABLE

REAGENT or RESOURCE	SOURCE	IDENTIFIER
<b>Antibodies</b>		
Mouse monoclonal anti-ARID1A	Santa Cruz	Cat# Sc-32761; RRID: AB_673396
Mouse monoclonal anti-BAF155	Santa Cruz	Cat# Sc-32763; RRID: AB_671095
Mouse monoclonal anti-BAF47	Santa Cruz	Cat# Sc-166165; RRID: AB_2270651
Mouse monoclonal anti-LAMIN1B	Santa Cruz	Cat# Sc-377000
Rabbit polyclonal anti-PBRM1	Bethyl	Cat# A301-591A; RRID: AB_1078808
$\alpha$ -CD25-APC	eBioscience	Cat# 17-0259-42; RRID: AB_1582219
$\alpha$ -CD69-FITC	eBioscience	Cat# 11-0699-42; RRID: AB_10853975
anti-AnnexinV-PE	BD Biosciences	Cat# 556454
<b>Biological Samples</b>		
Healthy adult T cells	Sanquin blood bank, Rotterdam, The Netherlands	NVT0080
HIV-1 infected patient T cells	Erasmus Medical Center, approved by The Netherlands Medical Ethics Committee	(MEC-2012-583)
<b>Chemicals, Peptides, and Recombinant Proteins</b>		
SAHA	Bioconnect	Cat# S1047
VPA	Sigma	Cat# P4543-10G
PMA/Iono	Sigma	Cat# P1585-10MG/I9657
Prostatin	Sigma	Cat# P0077-1MG
Bryostatin	Santa Cruz	Cat# sc-201407
Romidepsin	Sigma	Cat# SML1175-1MG
Saquinavir Mesylate	Centre for AIDS Reagents, Euripred	Cat# ARP983
Raltegravir	Centre for AIDS Reagents, Euripred	Cat# ARP980
Compound 68	<a href="#">Dykhuizen et al., 2012</a>	N/A
<b>Critical Commercial Assays</b>		
Steady Glo®	Promega	Cat# <b>E2510</b>
Cell-titer Glo®	Promega	Cat# <b>G7570</b>
Dual Glo®	Promega	Cat# <b>E2920</b>
Cells to Ct™	Thermo Fisher	Cat# 4399002
<b>Deposited Data</b>		
Raw and analyzed RNA-Seq data Arid1a KO	This paper	GEO: GSE113872
Raw and analyzed RNA-Seq data Compound treated cells	This paper	GEO: GSE113627
<b>Experimental Models: Cell Lines</b>		
E14ES cells	ATCC	Cat# CRL-1821 RRID: CVCL_C320
Bmi-luc reporter ES cell line	This paper	N/A
HEK293T	ATCC	Cat# CRL-3216
A549 lung adenocarcinoma cell line	ATCC	Cat# CCL-185
HepG2 hepatocarcinoma cell line	ATCC	Cat# HB-8065
JLat Tat-GFP Cells (A2)	NIH AIDS Reagent Program	Cat# 9854
JLAT11.1	Kind gift from Dr Eric Verdin <a href="#">Jordan et al., 2003</a>	N/A

(Continued on next page)

**Continued**

REAGENT or RESOURCE	SOURCE	IDENTIFIER
<b>Oligonucleotides</b>		
Southern probes (see Table S2)	This paper	N/A
Primers for qRT-PCR (see Table S2)	Dykhuizen et al., 2012	N/A
Primers for FAIRE (see Table S2)	This paper	N/A
Taqman Probe mouse Bmi1-FAM	Applied Biosystem	Cat# Mm00776122_gH
Taqman Probe mouse Ring1a-FAM	Applied Biosystem	Cat# Mm01278940_m1/4331182
Taqman Probe mouse Fgf4-FAM	Applied Biosystem	Cat# Mm00438916_g1/4351372
Taqman Probe mouse actin-VIC	Applied Biosystem	Cat# 4352341E
<b>Recombinant DNA</b>		
Bmi1-Luciferase knock-in targeting construct	This paper	N/A
pNL4.3.Luc.R-E	Centre for AIDS Reagents	Cat# 3418
HIV-1 HXB2-Env expression vector	Centre for AIDS Reagents	Cat# 1069
PLKO.1 lentiviral vector containing shRNA to mouse Brg1: hairpin sequence: CCGGCG-CCCGACACATTATTGAGAACTCGAGTTCT-CAATAATGTGTCGGGCGTTTTTG targeted to CGCCCGACACATTATTGAGAA	Dharmacon	Clone ID: TRCN0000071386 Cat# RMM3981-201797880
<b>Software and Algorithms</b>		
DESeq	Anders and Huber 2010	<a href="http://bioconductor.org/packages/release/bioc/html/DESeq.html">http://bioconductor.org/packages/release/bioc/html/DESeq.html</a>
EdgeR	Robinson et al., 2010	<a href="http://bioconductor.org/packages/release/bioc/html/edgeR.html">http://bioconductor.org/packages/release/bioc/html/edgeR.html</a>
<b>Other</b>		
PubChem Assay ID	This paper	AID 602436

**CONTACT FOR REAGENT AND RESOURCE SHARING**

Further information and requests for resources and reagents should be directed to and will be fulfilled by the Lead Contact, Emily Dykhuizen ([edykhui@purdue.edu](mailto:edykhui@purdue.edu)).

**EXPERIMENTAL MODEL AND SUBJECT DETAILS****Cell Line Authentication**

Cell lines were obtained directly from ATCC or NIH AIDS reagent program and used at less than 15 passages.

**Cell Culture Conditions****E14 ESC and Bmi-luc ESC Culture**

Mouse male ESCs were cultured in ESC media: (DMEM (Gibco), 15% ES tested FBS (Applied Stem Cell), 1% HEPES (Gibco), 1% Sodium pyruvate (Gibco), 1% Pen/Strep (Invitrogen), 1% Glutamine (Invitrogen), 1% non-essential amino acids (Gibco) and 0.1% Lif-condition media from Cos-Lif cells. Media was changed daily. After 72 h, the cells were split with 0.25% Trypsin-EDTA (Gibco) and plated at the same density on tissue culture plates that had been treated with 0.1% gelatin in water (Millipore) for 30 minutes and removed.

**Arid1a<sup>fl/f</sup>:CreERT2 ESCs**

Mouse ESCs were cultured in Knockout™ DMEM (Thermo Fisher Sci #10829018) supplemented with 15% ESC-Sure FBS serum (Applied Stem Cell #ASM-5007) and Knockout™ Serum Replacement (Thermo Fisher Sci #10828028), 2 mM L-glutamine (Gibco #35050061), 10 mM HEPES (Gibco #15630080), 1 mM sodium pyruvate (Gibco #11360070), 100 U/mL penicillin/streptomycin (Gibco #15140122), 0.1 mM non-essential amino acids (Gibco #11140050), 0.1 mM beta-mercaptoethanol (Gibco 21985023) and leukemia inhibitory factor (LIF). ESCs were maintained on gamma-irradiated mouse embryonic fibroblast (MEF) feeders at 37°C, 5% CO<sub>2</sub> with daily media changes and passaged every other day.

### **HEK293T Cell Culture**

Human female HEK293T cells were cultured in (DMEM (Gibco), 10% FBS (Omega), 1% Sodium pyruvate (Gibco), 1% Pen/Strep (Invitrogen). After 72 h, the cells were split 1:4 with 0.25% Trypsin-EDTA (Gibco).

### **A549 Cell Culture**

Human male A549 cells were cultured in (DMEM (Gibco), 10% FBS (Omega), 1% Sodium pyruvate (Gibco), 1% Pen/Strep (Invitrogen). After 72 h, the cells were split 1:4 with 0.25% Trypsin-EDTA (Gibco).

### **HepG2 Cell Culture**

Human male HepG2 cells were cultured in (DMEM (Gibco), 10% FBS (Omega), 1% Sodium pyruvate (Gibco), 1% Pen/Strep (Invitrogen). After 72 h, the cells were split 1:4 with 0.25% Trypsin-EDTA (Gibco) and replated.

### **Jurkat Cell Culture**

Human male J-Lat A2 and J-Lat 11.1 cells were cultured in RPMI-1640 medium (Sigma Aldrich) supplemented with 10% FBS and 100 µg/ml penicillin-streptomycin (Sigma Aldrich) at 37°C in a humidified 95% air-5% CO<sub>2</sub> atmosphere. After 72 h, the cells were diluted to a concentration of  $2 \times 10^5$  cells/mL with fresh media.

### **Primary Human CD4+ T Cells**

Primary human CD4+ T cells from either healthy donors or HIV+ patients were obtained via either blood donations (buffy coats) or leukapheresis respectively. PBMCs were isolated by Ficoll gradient followed by isolation (negative selection) of CD4+ T cells by RosseteSep kit (Stem Cell Technologies) or by negative selection with EasySep (Stem Cell Technologies) from healthy donors or HIV+ patients respectively. CD4+ T cells were cultured at a density of  $1-1.5 \times 10^6$ /ml in RPMI-1640 medium supplemented with 7% FBS and 100 µg/ml penicillin-streptomycin at 37°C in a humidified 95% air-5% CO<sub>2</sub> atmosphere before treatment with compounds or incubation in presence of  $\alpha$ CD3/ $\alpha$ CD28 beads.

### **Subject Details**

This study was conducted in accordance with the ethical principles of the Declaration of Helsinki. The patients involved in the study provided signed informed consent and the study protocol was approved by The Netherlands Medical Ethics Committee (MEC-2012-583).

Three otherwise healthy adult HIV-1 infected patients on stable c-ART with effective viral suppression <50 c/mL were recruited at the Erasmus MC HIV outpatient clinic. Patient Inclusion criteria: 1. Age >18 years, 2. Confirmed HIV-1 infection. 3. Plasma HIV RNA viral load <50 copies per ml. 4. on cART. Patient Exclusion criteria: 1. Inability to place 2.5 cm venous catheter, 2. Previous use of any known latency reversal agents. 3. Pregnancy 4. Major comorbidities including anemia, defined as a hemoglobin level of <6.0 mmol/L (women) or <6.5 mmol/L (men), cardiovascular disease, hepatitis B/C co-infection, severe psychiatric disorder, active drug use.

## **METHOD DETAILS**

### **Bmi1-Luciferase Reporter Cell Line**

Low passage mESCs derived from 129 mice (20 million, p10) were electroporated with 40 µg of a linearized construct consisting of 2 kb homology upstream of the *Bmi1* locus, firefly luciferase at exon 1 of *Bmi1* followed by loxP neo and a 6 kb 3' homology arm with thymidine kinase outside the homology arms. The cells were plated on 10 gelatin treated plates (60 mm) of irradiated neo resistant MEFs and selected with G418 and ganciclovir for 5 days. 384 colonies were selected, trypsinized and replated in gelatin treated 24-well plates for expansion. The cells were split and DNA was isolated for digestions with EcoRI or BamHI. We confirmed the successful homologous recombination in 7 out 384 colonies using Southern blot analysis at both the 5' (EcoRI) and 3' (BamHI) end (see Table S2 for probe and primer sequences). We deleted the neomycin cassette using transfected Cre recombinase and confirmed the excision at all clones using a second round of Southern blot analysis at the 3' end (BamHI).

### **Lentiviral Infection**

HEK293T cells were transfected with lentiviral constructs along with lentiviral packaging vectors pMD2.G and psPAX2. After 48 h, supernatants were collected and virus isolated using ultracentrifugation at 20,000 r.p.m. for 2 h. Viral pellets were re-suspended in PBS and used to infect cell lines. Cells were selected with puromycin and harvested 72 h after infection.

### **Compound Treatment**

10,000 cells in 30 µL ESC media were plated in white 384 well CellBind plates. The cells were cultured in a 37°C, 5% CO<sub>2</sub> incubator for 24 h and 100nL/well of 0.75mM of positive control (Pubchem SID: 85814977) or 100 nL/well of 3.75 mM compound library (primary screen) was added via pin transfer into plates. There was no effect on assay readout at DMSO concentrations up to 0.5%. The cells were cultured in a 37°C, 5% CO<sub>2</sub> incubator for 24 h for luciferase reporter assay and 18 h for qRT-PCR assay.

### Luciferase Assay

(PubChem AID 602393 primary, PubChem AID 651717 confirmatory.) The assay plates were removed from the incubator and equilibrated for 10 minutes to room temperature. Promega SteadyGlo® solution (10 µL/well) was added to each well of the assay plates. The assay plates were mixed at 1000 rpm for 15 seconds and then incubated for 10 minutes at room temperature. The luciferase levels were read on a Perkin Elmer Envision in Ultra Sensitive Luminescence mode. Signals remained stable up to 2 hours.

### qRT-PCR Secondary Screen (PubChem AID 743180, 743177, 743176)

The qRT-PCR screen was performed as published (Dykhuizen et al., 2012). In brief, 5,000 ES cells were plated on gelatin-coated 384-well tissue culture plates and cultured in a 37°C, 5% CO<sub>2</sub> incubator. 24 h later, hit compounds in 100 nL DMSO were treated at eight different doses. 18h after compound treatment cells were washed two times with 100 µL PBS and all excess PBS was removed by centrifuging the plates upside down at 1000 rpm. The Ambion® Cells-to-Ct kit was used to generate cDNA. In brief, the cells were lysed in the plate in 10 µL lysis buffer containing DNase for 10 minutes and quenched with 1 µL lysis stop buffer. The lysate (2 µL) was added to 5 µL RT reaction buffer (2X), 2.5 µL nuclease-free water and 0.5 µL Reverse transcriptase (20X) and incubated at 37°C for 60 minutes and 95°C for 1 minute to generate 10 µL of cDNA. cDNA (1 µL) was used in each 5 µL qPCR reaction with Roche master mix and TaqMan probes (Applied Biosystems) for Bmi1-FAM (Mm00776122\_gH), Ring1a-FAM (Mm01278940\_m1/4331182), or Fgf4-FAM (Mm00438916\_g1/4351372) alongside actin-VIC (4352341E) for a loading control. The qPCR was run accordingly: 95°C for 10 minutes Then 55 cycles of: 95°C for 10 seconds followed by 60°C for 30 seconds. The fold increase in transcription was calculated using the  $\Delta\Delta C_T$  method (Livak and Schmittgen, 2001).

### Viability Assays (PubChem AID: 743188, 743189, 743190, 1053139, 1053140, 1053141)

Cell culture: HepG2, A549 and HEK293 cells were propagated to 95% confluence in DMEM containing 10% FBS 1% Pen/Strep, 1% L-Glutamine. Cells were plated at 2000 per well in 40 µL media in white tissue culture treated 384-well plates and incubated at 5% CO<sub>2</sub>; 95% humidity, 37°C for 24 hours. Compound (100 nL) was added to wells using a pin tool (CyBi Well) alongside 100 nL cytotoxic compounds, mitoxantrone (final concentration of 10 µM) as a positive control. The cells were incubated for 72 hours at 37°C, 95% humidity 5% CO<sub>2</sub>. Plates were removed from the incubator, equilibrated for 15 minutes to room temperature; and 20 µL 50% Promega CellTiterGlo (diluted 1:1 with PBS, pH 7.4) was added. The plates were read on Perkin-Elmer EnVision with standard luminescence settings for 0.1 sec per well.

### qRT-PCR Screen Confirmation and DOS Analog Library (SYBR)

50,000 mESCs were plated on gelatin coated 24-well plates. After 24 hours, the cells were treated with 30 µM of compound and incubated at 5% CO<sub>2</sub>; 95% humidity, 37°C for 18 hours. RNA was isolated using Trizol® and cDNA was synthesized from 1 µg RNA using Superscript III Reverse Transcriptase with Oligo(dT)12–18 primers (Thermo) and diluted 10x with water. 1 µL of this cDNA mixture was used for qPCR with 2x SYBR (Roche) and the following primers: *Bmi1*: Forward: TACCATGAATGGAACCAGCA; reverse: AAAGGAAGCAAACCTGGACGA, *Ring1a*: Forward: CCTGGACATGCTGAAGAACA; reverse: TCCCGGCTAGGGTAGATTTT, *FGF4*: Forward: GGGTGTGGTGAGCATCTTCGGA; reverse: GGTATGCGTAGGACTCGTAGGGC, *Gapdh*: Forward: TGCACCACCAACTGCTTAG; reverse: GGATGCAGGGATGATGTTT.

### Chemical Synthesis of DOS Analog Library

The synthesis of the original DOS library was performed according to the Head-to-Tail strategy for combinatorial synthesis of multiple scaffold simultaneously (Fitzgerald et al., 2012). For the synthesis of the 30 macrolactam library members in solution the backbone (compound **2141-017**) was synthesized according to published procedures in the scheme in (Figure S3). The synthesis of the six representative compounds used in HIV latency experiments (Figures 4 and S3) from this backbone are outlined below:



### Nitro Reduction (2141-018b)

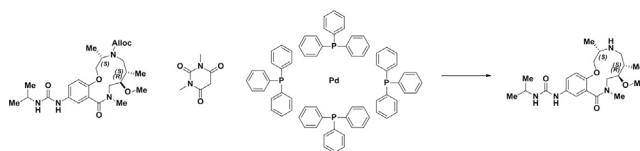
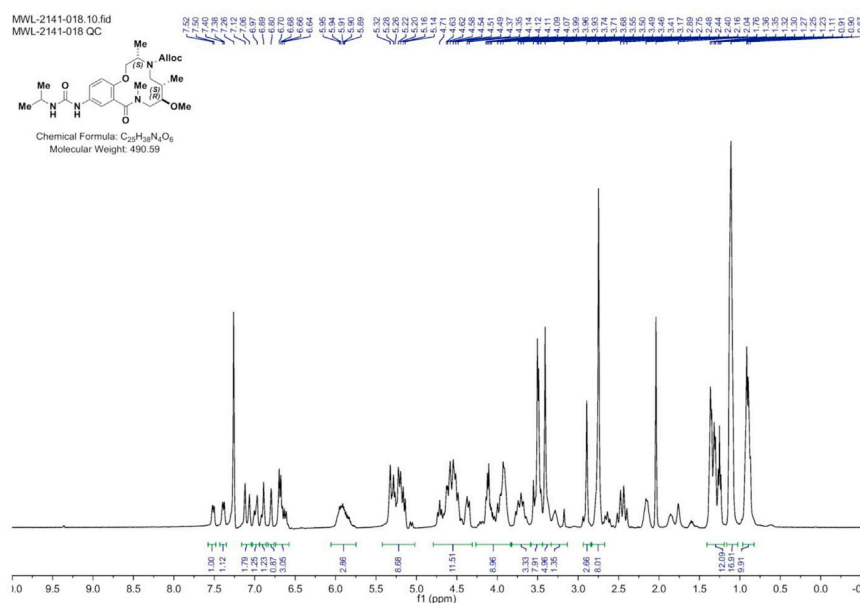
To macrocycle (**2141-017**) (675 g, 1.550 mmol) dissolved in MeOH (Volume: 15.50 ml) was added tin(II) chloride dihydrate (3.50 g, 15.50 mmol). The reaction mixture was stirred at room temperature for 2 days or until LC/MS indicates complete conversion. The residue was dissolved in EtOAc and washed with 2 M aq. KOH (2x). The combined aqueous layers were washed with EtOAc (2x) and the resulting organic layers were washed with brine, dried over MgSO<sub>4</sub>, filtered, and concentrated. The crude aniline (**2141-018b**) was used without purification. Note: The workup as described above produces a lot of precipitate/emulsion. This

can be overcome by extensive washing or by quenching with 1 volume 1 M NaOH and filtration over celite prior to workup. (M+H)<sup>+</sup> calculated = 406.24 (M+H)<sup>+</sup> measured (LC/MS) = 405.98



### ***Acylation of the Aniline (2141-018)***

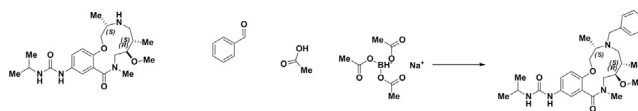
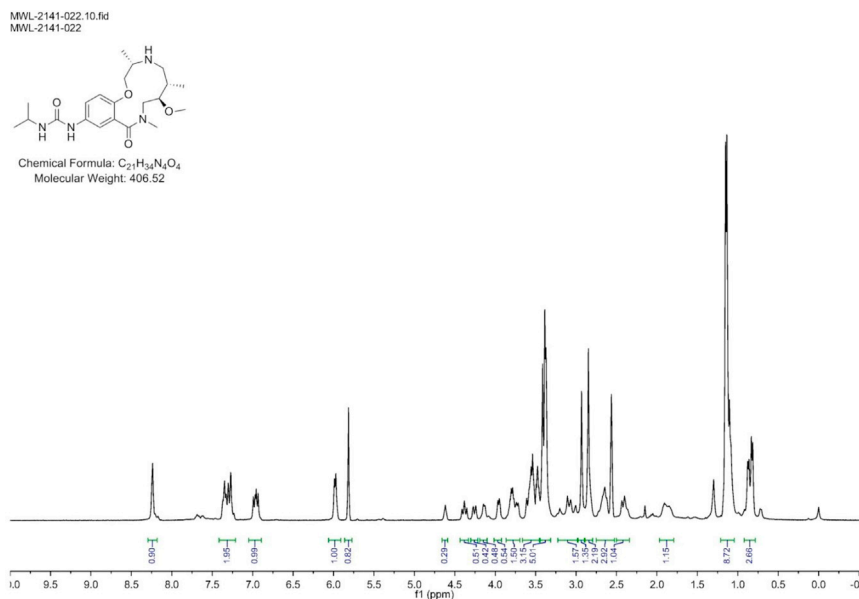
Isopropyl isocyanate (0.174 ml, 1.767 mmol) was added dropwise to a stirring solution of crude aniline (**2141-018b**) (.597g, 1.472 mmol) in  $\text{CH}_2\text{Cl}_2$  (Volume: 7.36 ml) and reaction was stirred at rt overnight. LC/MS showed conversion into the desired product. The solvent was evaporated and the residue was purified via ISCO (0.5-9% MeOH in  $\text{CH}_2\text{Cl}_2$ , 18 min); Collected fractions 40-52 to afford the product as a white solid foam. 644 mg (89% over 2 steps)  $(\text{M}+\text{H})^+$  calculated = 491.29  $(\text{M}+\text{H})^+$  measured (LC/MS) = 492.73



## Alloc Deprotection (2141-022)

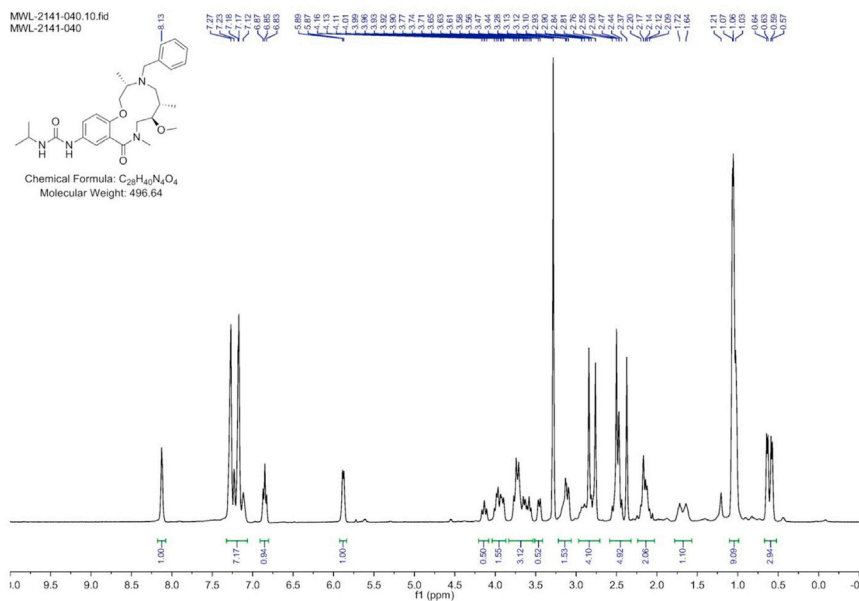
A 100 mL round-bottomed flask was charged with a solution of Urea (**2141-018**) (.625g, 1.274 mmol) in EtOH/CH<sub>2</sub>Cl<sub>2</sub> (2:1). 1,3-Dimethylbarbituric acid (0.298 g, 1.911 mmol) was added in one portion at room temperature, followed by Tetrakis(triphenylphosphine) palladium(0) (0.147 g, 0.127 mmol). The mixture was stirred at 40°C for ~16 h (overnight) or until LC/MS demonstrated conversion into a product with the same mass. The solvents were removed in vacuo, and the crude residue was dissolved in CH<sub>2</sub>Cl<sub>2</sub> and passed through a plug of acidic resin (5 equiv relative to SM) rinsing with CH<sub>2</sub>Cl<sub>2</sub> (~3 column volumes). The amine was then eluted

with 1M NH<sub>3</sub> in MeOH to afford sufficiently clean material from next step. (M+H)<sup>+</sup> calculated = 407.27 (M+H)<sup>+</sup> measured (LC/MS) = 407.56

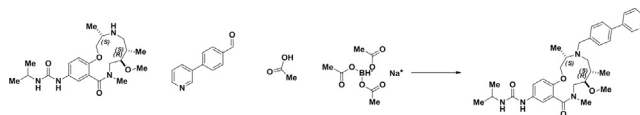


### BRD-K13648511

Benzaldehyde (0.090 ml, 0.886 mmol) was added to a DMF (Volume: 2.95 ml) solution of crude amine (**2141-022**) (.12g, 0.295 mmol) at rt. Acetic acid (0.017 ml, 0.295 mmol) was added and the mixture was stirred for 30 min before sodium triacetoxyhydroborate (0.250 g, 1.181 mmol) was added. The resulting mixture was stirred at rt overnight. LCMS indicates complete SM consumption. Saturated aqueous sodium bicarbonate solution was slowly added until gas evolution ceased. The reaction mixture was diluted with EtOAc and the layers were separated. The organic layer was washed with brine, dried with MgSO<sub>4</sub>, filtered, and concentrated. The residue was purified via ISCO (SiO<sub>2</sub>, 1-12% MeOH in CH<sub>2</sub>Cl<sub>2</sub>, 20 min, 254 nm); Collected fractions 47-54 to afford the product as a white solid in 23% yield (34 mg) over 2 steps. (M+H)<sup>+</sup> calculated = 497.3123, (M+H)<sup>+</sup> average (3 ESI replicates) = 497.3131 ± 1.81

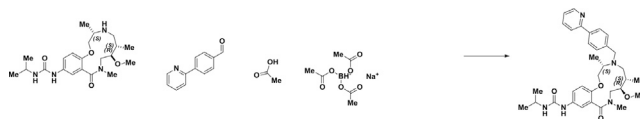
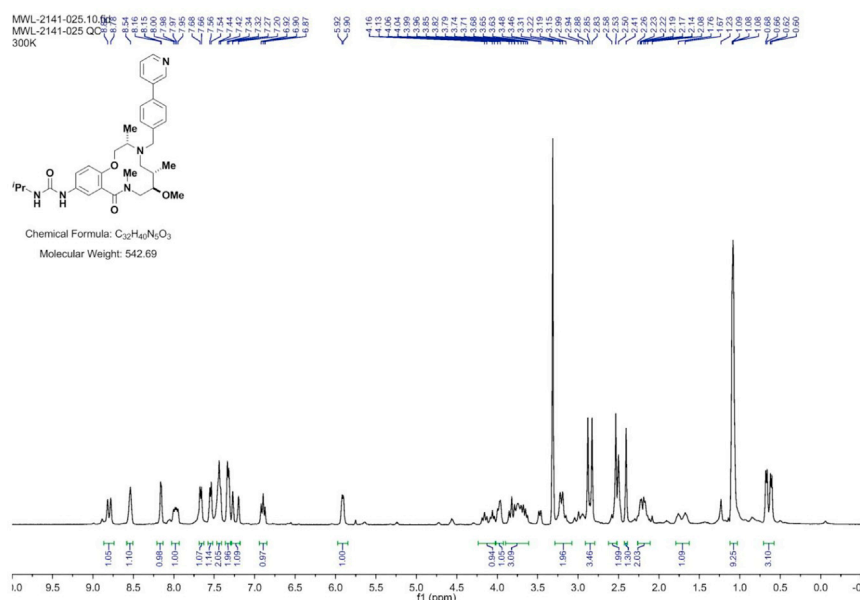






### BRD-K17257309

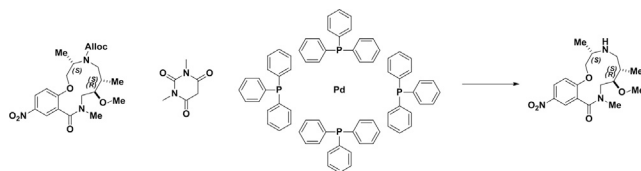
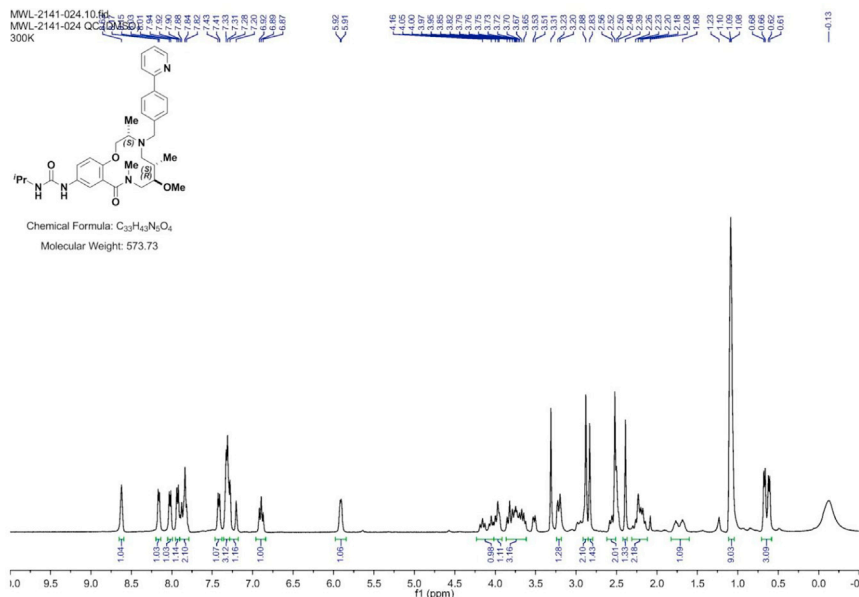
4-(pyridin-3-yl)benzaldehyde (151 mg, 0.827 mmol) was added to a DMF (Volume: 1378  $\mu$ l, Density: 0.944 g/ml) solution of Crude amine (**2141-022**) (112mg, 0.276 mmol) at rt. Acetic acid (15.77  $\mu$ l, 0.276 mmol) was added and the mixture was stirred for 30 min before sodium triacetoxyhydroborate (234 mg, 1.102 mmol) was added and the mixture was stirred at rt overnight or until LC/MS indicates conversion into product. Saturated aq sodium bicarbonate solution was slowly added until gas evolution ceased. The reaction mixture was diluted with EtOAc and the layers were separated. The aqueous phase was extracted with EtOAc (3x). The combined organic layers were washed with brine, dried with  $\text{MgSO}_4$ , filtered, and concentrated. The residue was purified via ISCO (0.5-7% MeOH in  $\text{CH}_2\text{Cl}_2$ , 13 min) to afford the product as a yellow solid in 24% yield (38 mg) over 2 steps.  $(\text{M}+\text{H})^+$  calculated = 574.3388  $(\text{M}+\text{H})^+$  average (3 ESI replicates) =  $5.74.3394 \pm 0.85$



### BRD-K98645985

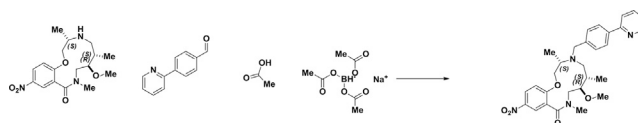
4-(Pyridin-2-yl)benzaldehyde (199 mg, 1.085 mmol) was added to a DMF (Volume: 1808  $\mu$ l) solution of crude amine (**2141-022**) (147mg, 0.362 mmol) at room temperature. Acetic acid (21.72 mg, 0.362 mmol) was added and the mixture was stirred for 30 min before  $\text{NaBH}(\text{OAc})_3$  (307 mg, 1.446 mmol) was added and the mixture was stirred at rt overnight. LC/MS indicated conversion into the desired product. Saturated aqueous sodium bicarbonate solution was slowly added until gas evolution ceased. The reaction mixture was diluted with EtOAc and the layers were separated. The aqueous phase was extracted with EtOAc (3x). The combined organic layers were washed with brine, dried with  $\text{MgSO}_4$ , filtered, and concentrated. The residue was purified via ISCO (0.5-7%

MeOH in CH<sub>2</sub>Cl<sub>2</sub>, 13 min); Collected fractions 66-73 to afford the product as a brown solid in 26% yield (54 mg) over 2 steps. (M+H)<sup>+</sup> calculated = 574.3388 (M+H)<sup>+</sup> average (3 ESI replicates) = 574.3395 ± 1.36.



### Alloc Deprotection (2141-039a)

A round-bottomed flask was charged with a solution of macrocycle (**2141-017**) (.675 g, 1.550 mmol) in EtOH/ CH<sub>2</sub>Cl<sub>2</sub> (2:1). 1,3-Dimethylbarbituric acid (0.363 g, 2.325 mmol) was added in one portion at room temperature, followed by Pd(PPh<sub>3</sub>)<sub>4</sub> (0.179 g, 0.155 mmol). The mixture was stirred under ambient conditions for ~16 h (overnight). The reaction was monitored by LC/MS and demonstrated complete starting material consumption and the presence of the desired mass. The reaction mixture was then passed over a silica plug eluting with 15% MeOH in CH<sub>2</sub>Cl<sub>2</sub> (with 2% triethylamine). The filtrate was concentrated and used in the next step without purification (used theoretical yield). (M+H)<sup>+</sup> calculated = 352.19 (M+H)<sup>+</sup> measured (LC/MS) = 351.90



### Reductive Amination (2141-039b)

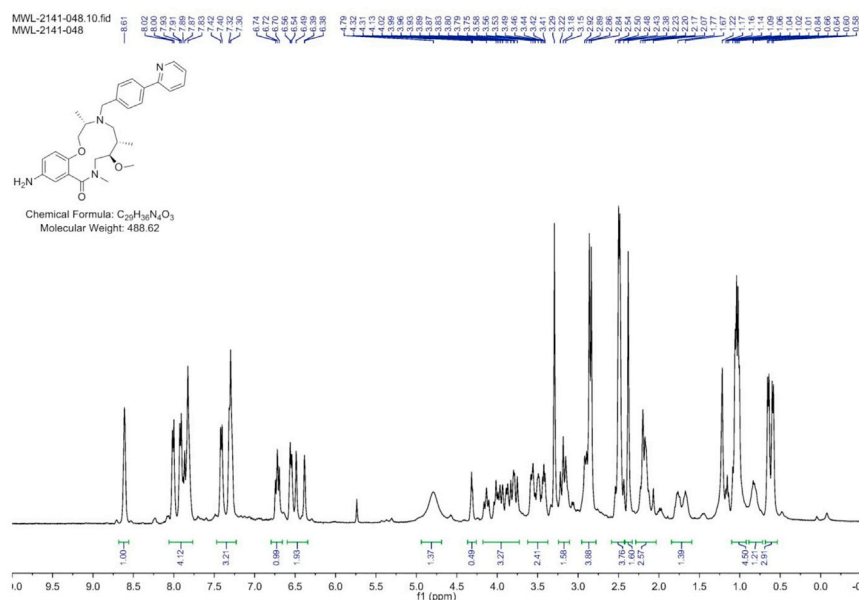
4-(2-Pyridinyl)-benzaldehyde (852 mg, 4.65 mmol, 3 eq) was added to a DMF (Volume: 7755  $\mu$ l) solution of crude amine (**2141-039a**) (545 mg, 1.551 mmol, 1 eq) at room temperature. Acetic acid (89  $\mu$ l, 1.551 mmol, 1 eq) was added and the mixture was stirred for 30 min before sodium triacetoxyhydroborate (1315 mg, 6.20 mmol, 4 eq) was added. The mixture was stirred at room temperature for 2 days when LC/MS indicated complete conversion into product (presence of SM by LCMS). Saturated aqueous sodium bicarbonate solution was slowly added until gas evolution ceased. The reaction mixture was diluted with EtOAc and the layers were separated. The aqueous layer was extracted with EtOAc (3x). The organic layer was washed with brine, dried with  $\text{MgSO}_4$ , filtered, and concentrated. Material was taken forward without further purification attempts.  $(\text{M}+\text{H})^+$  calculated = 519.29  $(\text{M}+\text{H})^+$  measured (LC/MS) = 518.91.

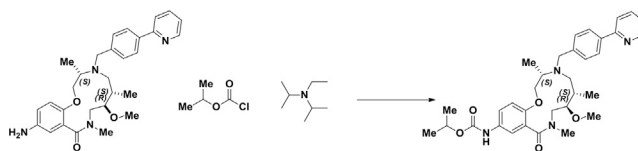


### BRD-K25923209

To Macrocycle **2141-039b** (.804g, 1.550 mmol) dissolved in MeOH (Volume: 15.50 ml) was added tin(II) chloride dihydrate (3.50 g, 15.50 mmol). The reaction mixture was stirred at 40°C for 24h until LC/MS indicated complete consumption of starting material (nitro) and presence of desired mass. Upon completion, the reaction mixture was concentrated and the resulting residue was dissolved in EtOAc and washed with 2 M aq. KOH (2x). The combined aqueous layers were washed with EtOAc (4x). The resulting organic layers were washed with brine, saturated aqueous  $\text{NaHCO}_3$ , water, and brine, dried over  $\text{MgSO}_4$ , filtered, and concentrated. The crude aniline was sufficiently pure to use in the capping step and therefore was used without purification.

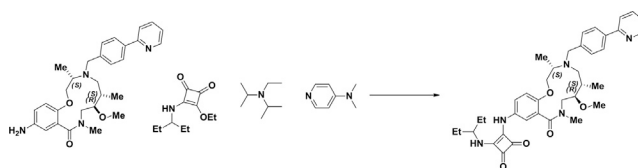
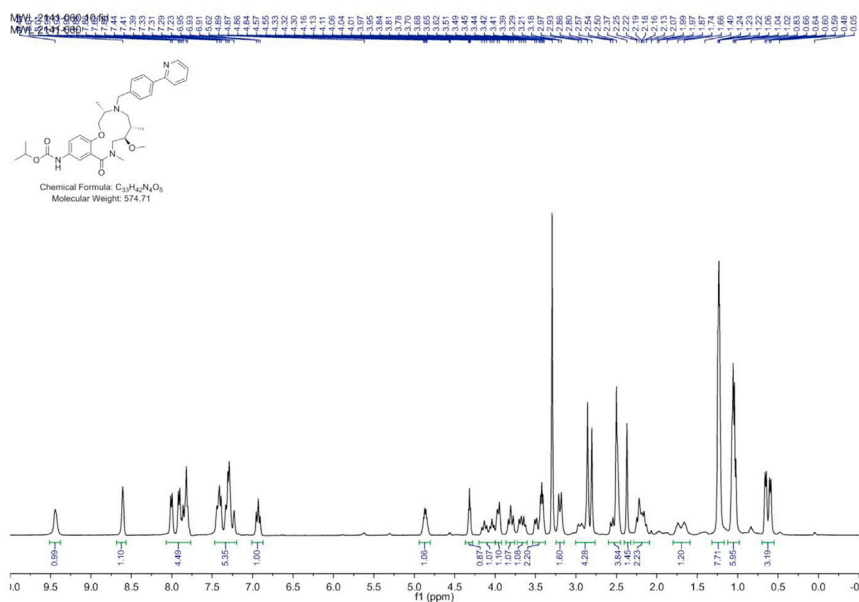
*Note:* The workup as described above produces a lot of precipitate/emulsion. This can be overcome by extensive washing or alternatively, the reaction can be quenched with 1 volume of 1 M NaOH, stirred with celite for 10 minutes, and filtered prior to workup to yield 33.8% (17.2 mg) over 3 steps.  $(\text{M}+\text{H})^+$  calculated = 489.286  $(\text{M}+\text{H})^+$  average (3 ESI replicates) =  $489.2866 \pm 0.92$ .





### BRD-K80443127

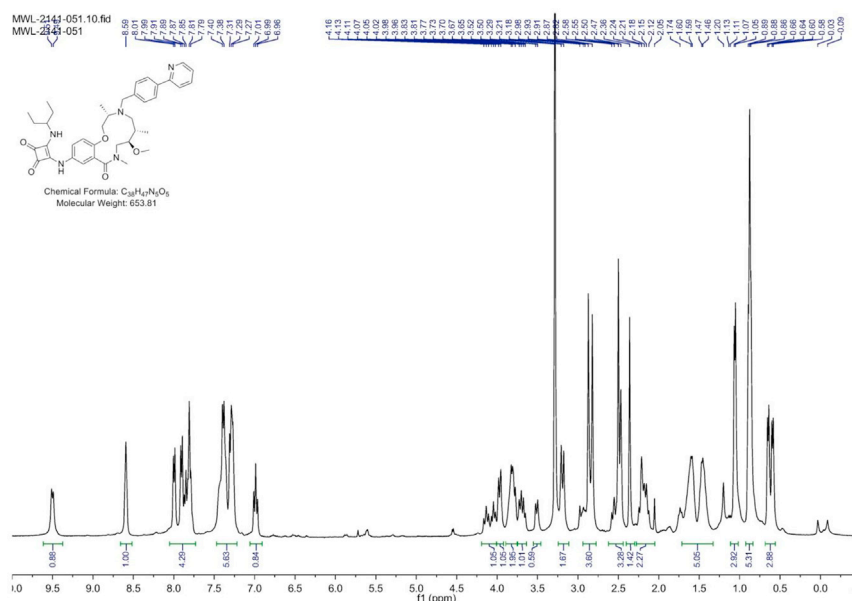
A screwtop vial was charged with aniline (**BRD-K25923209**) (43.3mg, 0.089 mmol) and  $\text{CH}_2\text{Cl}_2$  (Volume: 886  $\mu\text{l}$ , Density: 1.325 g/ml). Isopropyl chloroformate (115  $\mu\text{l}$ , 0.115 mmol) and DIEA (46.4  $\mu\text{l}$ , 0.266 mmol) were added dropwise and reaction stirred under ambient conditions for 1 h. LC/MS showed complete sm consumption. The reaction mixture was loaded directly onto  $\text{SiO}_2$  and purified via ISCO (1-12% MeOH in  $\text{CH}_2\text{Cl}_2$ , 20 min); Collected fractions 40-44 to afford the product as a yellow oil in 33.8% (17.2 mg) yield.  $(\text{M}+\text{H})^+$  calculated = 575.3228  $(\text{M}+\text{H})^+$  average (3 ESI replicates) =  $575.3235 \pm 1.32$ .



### BRD-K04244835

A 2.5mL microwave vial was charged with aniline (**BRD-K25923209**) (40 mg, 0.082 mmol) and EtOH (Volume: 819  $\mu\text{l}$ , Density: 0.81 g/ml). Squaramide (CRE-III-001) (20.75 mg, 0.098 mmol), DIEA (42.8  $\mu\text{l}$ , 0.246 mmol), and DMAP (2.000 mg, 0.016 mmol) were added in sequence and the vial was sealed. The resulting solution was stirred at  $85^\circ\text{C}$  overnight or until LC/MS indicated complete starting material consumption. The reaction mixture was loaded directly onto  $\text{SiO}_2$  and purified via ISCO (1-12% MeOH in

CH<sub>2</sub>Cl<sub>2</sub>, 20 min); fractions 50-56 were collected to afford the product as a yellow solid in 48.6% (26 mg) yield. (M+H)<sup>+</sup> calculated = 654.365 (M+H)<sup>+</sup> average (3 ESI replicates) = 654.3661 ± 1.64.



### Nuclear Isolation

Cells were trypsinized and washed 1x with PBS. Cells were suspended in Buffer A (25 mM HEPES pH 7.6, 5 mM MgCl<sub>2</sub>, 25 mM KCl, 0.05 mM EDTA, 10% glycerol, 0.1% NP-40) and cell membranes were lysed by passing cells through a 22-gauge needle 10 times and incubation on ice for 5 minutes. Nuclei were pelleted by centrifugation at 400 x g for 5 minutes.

### Cell Lysis

Pellets of whole cells or isolated nuclei were lysed with lysis buffer (50 mM Tris-HCl pH 8.0, 300 mM NaCl, 0.1% NP-40, protease inhibitors) by rotating at 4°C for 30 minutes. The lysate was cleared by centrifugation (20,000 x g) for 5 minutes and transferred to a fresh tube.

### ATPase Assay

Adapted from (Bultman et al., 2005). Each sample utilized 70 µg nuclear ESC lysates in 50 µL cell lysis buffer. The nuclear lysates were incubated with 1 µL anti-Brg1 antibody (ab110641) and 5 µL protein A dynabeads (Thermo) for 4 h and washed 1 x with lysis buffer and 1 x with wash buffer (10 mM Tris-HCl pH 7.5, 50 mM NaCl, 5 mM MgCl<sub>2</sub>, protease inhibitor). After washing, 20 µL reaction buffer (10 mM Tris pH 7.5, 50 mM mM NaCl, 5 mM MgCl<sub>2</sub>, 20% glycerol, 1 mg/ml BSA, 20 µM ATP, 20 nM plasmid DNA, 1 µCi gamma-<sup>32</sup>P ATP, protease inhibitors, 1 µL DMSO or compound to 250 µM final concentration) was added to the beads. The reaction was incubated with shaking (900 rpm) at 37°C. After 30 minutes the reaction mixture (1 µL) was spotted on PEI cellulose TLC plates (Sorbtech) and the TLC was run in 0.5M LiCl, 1M formic acid. The plates were dried and developed using phosphorimager technology. The percent conversion from starting material to product was determined using Image J software and normalized to the no enzyme control.

### Immunoblot Analysis

Total protein was denatured for 10 min at 95°C, separated on a 4–12% SDS-polyacrylamide gel, and transferred to a PVDF membrane (Immobilon FL, EMD Millipore, Billerica, MA). The membrane was blocked with 5% bovine serum albumin (VWR, Batavia, IL) in PBS containing 0.1% Tween-20 (PBST) for 30 mins at room temperature and then incubated in primary antibodies overnight at 4°C. The primary antibodies used were directed against ARID1A (Santa Cruz Biotechnology Inc., Dallas, TX; sc-32761), PBRM1 (Bethyl Laboratories, Montgomery, TX; A301-591A), BAF155 (Santa Cruz Biotechnology Inc., Dallas, TX; Sc-32763), BAF47 (Santa Cruz Biotechnology Inc., Dallas, TX; Sc-166165), LAMIN B1 (Santa Cruz Biotechnology Inc., Dallas, TX; Sc-377000). The primary antibodies were detected by incubating the membranes in goat-anti-rabbit or goat-anti-mouse secondary antibodies (LI-COR Biotechnology, Lincoln, NE) conjugated to IRDye 800CW or IRDye 680 respectively for 1 h at room temperature, and the signals were visualized using Odyssey Clx imager (LI-COR Biotechnology, Lincoln, NE).

### Glycerol Gradients

20 million mESCs were plated on gelatin coated 150 mm tissue culture plates and incubated for 24 h. Cells were treated with 30  $\mu$ M BRD-K25923209 or DMSO for 24 h. Nuclear lysate from ~50 million cells (~0.6–1 mg nuclear protein) was layered on top of a 10–30% glycerol gradient (10 mL) in HEMG buffer (25 mM Hepes 7.6, 0.1 mM EDTA, 12.5 mM  $MgCl_2$ , 100 mM KCl). The protein was separated by the gradients through ultracentrifugation in Beckman rotor SW41 at 40,000 RPM for 16 h. Twenty 500  $\mu$ L fractions were removed sequentially from the top of the gradients and 50  $\mu$ L of each fraction was used for immunoblot analysis.

### Sequential Salt Extractions

Sequential salt extractions were performed as published<sup>80</sup>, with the following modifications: mESCs were treated for 2 h with 30  $\mu$ M BRD-K25923209 or DMSO. Nuclei were isolated into two tubes (5 million each) and the salt extractions were performed with 30  $\mu$ M of BRD-K25923209 or DMSO in each salt wash.

### Biotin Pull Downs

Compound 2-57 (200  $\mu$ M in 200  $\mu$ L PBS) was pre-bound to 20  $\mu$ L high capacity streptavidin beads (Solulink) for 30 minutes. The beads were washed 1x with lysis buffer and incubated with cell lysates preincubated with DMSO or 200  $\mu$ M of BRD-K25923209 for 2 h. The beads were washed once with 1 mL lysis buffer and boiled in SDS loading buffer for immunoblot analysis.

### CETSA Protocol

CETSA was performed as published (Jafari et al., 2014) with the following modifications: mESCs were treated with 50  $\mu$ M of compound BRD-K25923209 or DMSO for 1 hour. The cells were trypsinized, washed 1 x with PBS and 2 million cells of each condition were resuspended in 1 mL PBS. Cells (100  $\mu$ L) were transferred into eight wells of a strip tube and put in a temperature gradient PCR block for 3 minutes, followed by incubation at room temperature for 3 minutes. The cells were lysed with 2 x freeze-thaw cycles on a 25°C heat block and the cell lysis was transferred to microcentrifuge tubes and centrifuged at 15,000 x g for 20 minutes at 4°C. The soluble protein (90  $\mu$ L) was removed from pellets and added to SDS loading buffer for immunoblot analysis.

### RNA-Seq ECS with BAFI

Mouse ESE14 cells were plated at a density of  $2.5 \times 10^5$  in a gelatin coated 6-well plate and in a 37°C, 5%  $CO_2$  incubator for 24 h. RNA was purified from ESCs treated with BAF inhibitor BRD-K98645985 or a DMSO mock treatment for 16h. RNA was extracted using TRIzol reagent (Life Technologies Corporation, Grand Island, NY) according to the manufacturer's instructions and cleaned up using RNeasy Mini Kit (Qiagen Inc., Valencia, CA). RNA libraries were prepared for sequencing using standard Illumina protocols. Sequencing was performed using an Illumina HiSeq 2500. Reads were 100 bp and paired-ended. Reads were trimmed using Trimmomatic and aligned to the mm10 reference genome using STAR. Gene expression levels were computed using htseq-count using default parameters. Differential expression analysis was performed with DESeq2 using default parameters (Anders and Huber, 2010). Processed and unprocessed data is deposited in GEO GSE113627.

### RNA-Seq *Arid1a*<sup>f/f</sup> ESCs

*Arid1a*<sup>f/f</sup> mice were a kind gift from Terry Magnuson (UNC School of Medicine) (Chandler et al., 2015). *Arid1a*<sup>f/f</sup> mice were bred to Actin:CreERT2 mice to obtain *Arid1a*<sup>f/+</sup>;ActinCreERT2, which were subsequently interbred with *Arid1a*<sup>f/f</sup> mice. Timed matings were set up between *Arid1a*<sup>f/f</sup>;ActinCreERT2 and *Arid1a*<sup>f/f</sup> and oviducts were flushed at day 3.5. ESCs were derived as described (Ho et al., 2011). *Arid1a*<sup>f/f</sup>;CreERT2 ESCs were treated with either ethanol or 1  $\mu$ M 4-hydroxytamoxifen for 24 hours then passaged. RNA was collected 72 hours after treatment. RNA was isolated using Quick-RNA Miniprep Kit (Zymo Research). RNA-Seq libraries were prepared using either Illumina TruSeq RNA Library Prep Kit v2 or Illumina TruSeq Stranded mRNA Kit following the manufacturer's instructions. Sequencing was performed using an Illumina HiSeq 2500. Reads were 50 bp and single-ended. Fastq files were evaluated for quality using FastQC and trimmed using Trimmomatic. Trimmed sequences were mapped to the mm10 reference genome using HISAT2 in single-end mode with default parameters. The average counts per million (cpm) was calculated for each sample condition using custom R scripts, and differentially expressed genes were identified using the edgeR package in Bioconductor (Robinson et al., 2010). A false discovery threshold of 0.05 was imposed using the toptags function of edgeR. Processed and unprocessed data is deposited in GEO GSE113872

### Cell Line Models of HIV-1 Latency

J-Lat A2 (LTR-Tat-IRES-GFP Cells) (Jordan et al., 2001) and J-Lat 11.1 (integrated full-length HIV-1 genome mutated in *env* gene and harboring GFP in place of *Nef*) (Jordan et al., 2003) cells were cultured in RPMI-1640 medium (Sigma Aldrich) supplemented with 10% FBS and 100  $\mu$ g/ml penicillin-streptomycin at 37°C in a humidified 95% air-5%  $CO_2$  atmosphere. Cells were treated with compounds or DMSO for 48 h, followed by quantitation of GFP positive cells using flow cytometry. Data was normalized as a fold increase over DMSO treated control. Data are presented as mean of at least 3 independent experiments  $\pm$  SD.

### Ex Vivo HIV Latency Model

Viral pseudotyped particles were obtained by co-transfecting HXB2 Env together with the HIV-1 backbone plasmid (pNL4.3.Luc.R-E-) into HEK 293 T cells using PEI (Polyethylenimine) transfection reagent. At 48 h and 72 h post-transfection, the



pseudovirus-containing supernatant was collected, filtered through a 0.45 µm filter, aliquoted, and stored at – 80°C. Primary CD4 + T cells were isolated from buffy coats from healthy donors by Ficoll gradient followed by density-based negative selection of CD4+ T cells with RosetteSep kit (StemCells Technologies). Twenty-four hours after isolation, cells were spin-infected as described, with minor modifications (Lassen et al., 2012; Stoszko et al., 2016). CD4+ T cells were spin-infected at 1200 g for 2 h with the HBX2 Env pseudotyped pNL4.3-Luc virus. Eighteen hours after spin-infection cells were washed and cultured in growth media supplemented with 5 µM saquinavir mesylate. After three days, latently infected cells were treated with BAFi's or left untreated for 24 h in the presence of 30 µM raltegravir, followed by luciferase assay (Promega). Data was normalized as a fold increase over untreated control. Synergy was calculated using Bliss score formula (Bliss, 1939):  $S_{exp} = [1 - (1 - A) \times (1 - B)]$ , where  $S_{exp}$  is the expected percentage of cells reactivated after combinatorial treatment in absence of synergism and A and B correspond to the percentage of cells reactivated by the single treatments. Combination was considered synergistic if the observed effect of combined treatments was significantly higher than calculated value ( $S_{exp}$ ), and is indicated with an S in the figure.

### Ex Vivo HIV Latency Model (Bosque-Planelles)

Primary CD4 + T cells were isolated from buffy coats from healthy donors by Ficoll gradient followed by density-based negative selection of CD4+ T cells with RosetteSep kit (StemCells Technologies). Twenty four hours after isolation primary CD4+ T cells were cultured in the presence of 10 ng/ml TGF-β (Sigma-Aldrich), 1 µg/ml α-IL-4 (PeproTech) and αCD3/CD28 dynabeads (Life Technologies) at the cell:bead ratio 1:1 for 3 days. αCD3/CD28 dynabeads were removed, cells washed and cultured for 4 days in growth media supplemented with 30 IU/ml rIL-2 (Roche) Then cells were washed and subjected to spininfection (90 min, 1200 g) and incubated over-night. Next day cells were washed and re-suspended in growth media supplemented with 30 IU/ml rIL-2 and Saquinavir Mesylate (5 µM). Seven days post-infection cells were treated with BRD-K80443127 in increasing concentrations or with PMA/Ionomycin in the presence of Raltegravir (30 µM). After 24 hours of stimulation cells were collected and subjected to the luciferase assay, RLU was normalized to the total protein content (Bosque and Planelles, 2009).

### Biomarkers

CD4+ T cells were isolated from three healthy donors and treated in duplicate with 3 µM BRD-K80443127 or control DMSO for 16 hours. Cells were lysed with TRIreagent (Sigma) and total RNA was isolated with Total RNA Zol-Out (A&A Biotechnology) kit and cDNA was synthesized using random primers and Superscript II Reverse Transcriptase (Life Technologies). Real-time PCR was performed using GoTaq qPCR Master Mix (Promega) on CFX Connect Real-Time PCR Detection System thermocycler (BioRad) using following conditions: 95°C for 3 min, followed by 40 cycles of 95°C for 10 sec and 60°C for 30 sec. Products quality was assessed by their melting curve analysis. Relative expression of target genes was normalized to β-2-microglobulin and calculated using Livak-Schmittgen method (Livak and Schmittgen, 2001). Primers: (p21: For-AGCAGAGGAAGACCATGTGGAC, Rev- TTT CGACCCTGAGAGTCTCCAG. cMYC: For- AAGCCACAGCATACATCC, Rev- GCACAAGAGTTCGGTAGC. B2M: For- AGCGTACTC CAAAGATTGAGGTT, Rev- ATGATGCTGCTTACATGTCTCGAT)

### HIV Latency Reversal from Patient Samples

All patients were older than 18 years, c-ART treated for at least 3 years, and their viral loads were below 50 copies/ml for more than 12 months with no blips in the past two years. CD4+ T cells from aviremic HIV+ patients were isolated as described previously (Stoszko et al., 2016) with minor modifications. Briefly, frozen PBMCs were cultured in RPMI medium over-night to recover. Then next day CD4+ T cells were isolated twice (enriched CD4+ T cells were subjected to a second round of CD4+ T cell enrichment) and left for 6hrs to recover. Three million cells were treated with DMSO, 10 µM BRD-K80443127, 200 nM Prostratin, 10 µM BRD-K80443127 and 200 nM prostratin, and αCD3/CD28 magnetic beads (at cell:bead ration 1:1) as a positive control in triplicate. After 24 hours cells were lysed in TRIreagent (Sigma), total RNA was isolated with Total RNA Zol-Out (A&A Biotechnology) kit and cDNA was synthesized using random primers and Superscript II Reverse Transcriptase (Life Technologies). Detection of cellular associated *pol* RNA was performed as described previously (Pol: For GGGTTTATTACAGGGACAGCAGAGA, Rev- ACCTGCCATCTGTTTTT CATA) (Stoszko et al., 2016). This study was conducted in accordance with the ethical principles of the Declaration of Helsinki. HIV-1 infected patient volunteers were informed and provided signed consent to participate in the study. The study protocol was approved by The Netherlands Medical Ethics Committee (MEC-2012-583). cDNA generated from control and 10 µM BRD-K80443127 treated samples was used to assess expression of BAF target genes biomarker genes– *p21* and *C-MYC*. Primers: (p21: For-AGCAGAGGAAGACCATGTGGAC, Rev- TTTCGACCCTGAGAGTCTCCAG. cMYC: For- AAGCCACAGCATACATCC, Rev- GCACAAGAGTTCGGTAGC. B2M: For- AGCGTACTCCAAAGATTGAGGTT, Rev- ATGATGCTGCTTACATGTCTCGAT)

### Activation Markers, Apoptosis and Viability of Primary CD4+ T Cells

Activation markers, namely CD25 and CD69 were analyzed as described previously (Stoszko et al., 2016). Briefly, CD4+ T cells were treated with DMSO, compound, or PMA/Ionomycin for 24 and 72 hours. Cells were collected, washed with PBS and stained for 30 min at 4°C with α-CD25-APC (17-0259-42, eBioscience) and α-CD69-FITC (11-0699-42, eBioscience). Following two washes with PBS, cells were fixed with 1% HCHO at 4°C and analyzed by flow cytometry with Becton Dickinson Fortessa instrument. To determine percent of apoptotic cells after treatment cells were stimulated for 24 and 72 hours and stained with anti-AnnexinV-PE (BD Biosciences, cat. 556454) in the presence of 2.5 mM CaCl<sub>2</sub> for 20 min at 4°C. Cells were analyzed by Becton Dickinson Fortessa



flow cytometer. Data represents the average of six experiments performed on cells from different healthy donors. Viability of ex-vivo infected primary CD4<sup>+</sup> cells was determined by flow cytometry on the basis of forward versus side scatter analysis.

### FAIRE

FAIRE experiment was performed as described, with minor modifications (Stoszko et al., 2016). Eighteen hours prior to analysis, J-Lat 11.1 cells were treated with BAFi's where indicated. Cells were fixed for 10 min by adding formaldehyde to a final concentration of 1% at room temperature. Twenty million cells were used per FAIRE experiment. The reaction was quenched with 125 mM glycine. Cross-linked cells were washed with PBS followed by washes with buffer B and buffer C. For sonication, cells were re-suspended in ChIP incubation buffer and chromatin was sheared by sonication to an apparent length of ~ 200–400 bp (corresponding to

~ 100–200 bp of free DNA) using a BioRuptor sonicator (Cosmo Bio Co., Ltd) with 20 times 60-s pulses at maximum setting at 4°C. Sonicated chromatin was once phenol:chloroform:isoamyl alcohol (24:24:1) extracted, washed with chloroform:isoamylalcohol (24:1) and ethanol precipitated. Isolated DNA was subjected to Sybergreen qPCR cycles with specific primers (Nuc-0: For-ATCTACC ACACACAAGGCTAC, rev-GTACTAACTTGAAGCACCATCC; HSS: for-AAGTTTGACAGCCTCCTAGC, rev-CACACCTCCCTGGAA AGTC; Nuc-1: for-TTTGCCTGTACTGGGTCTCTCTGG, rev-CACAACAGACGGGCACACACT) with a CFX Connect Real-Time PCR Detection System (BioRad) and GoTaq qPCR Mastermix (Promega).

### QUANTIFICATION AND STATISTICAL ANALYSIS

Statistical details can be found in the Figure legends. Bar graphs are plotted as mean ± S.D. Statistical significance was calculated using Prism 7. Asterisks indicate the level of significance using student's T test (\* p< 0.05 \*\* p< 0.01, \*\*\* p< 0.001, \*\*\*\* p< 0.0001).

### DATA AND SOFTWARE AVAILABILITY

The accession number for the RNA-Seq for *Arid1a*ff:CreERT2 ESCs reported in this paper is GEO: GSE113872. The accession number for the RNA-Seq for BRD-K98645985 treated ESCs reported in this paper is GEO: GSE113627.

### ADDITIONAL RESOURCES

A full description of the high throughput screen and associated bioassays can be found on PubChem under assay number 602436.

## **Supplemental Information**

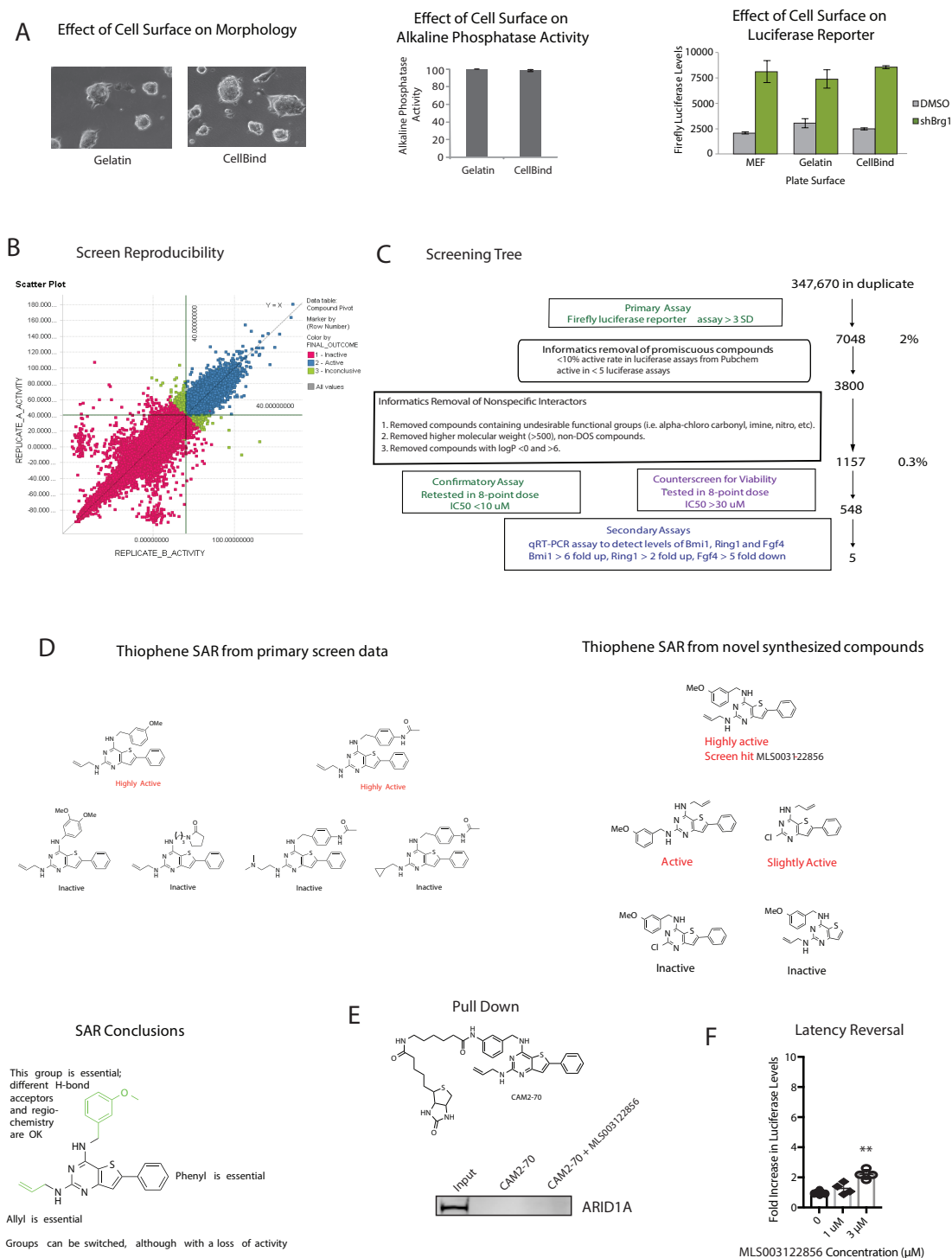
### **Small Molecule Targeting of Specific**

### **BAF (mSWI/SNF) Complexes**

### **for HIV Latency Reversal**

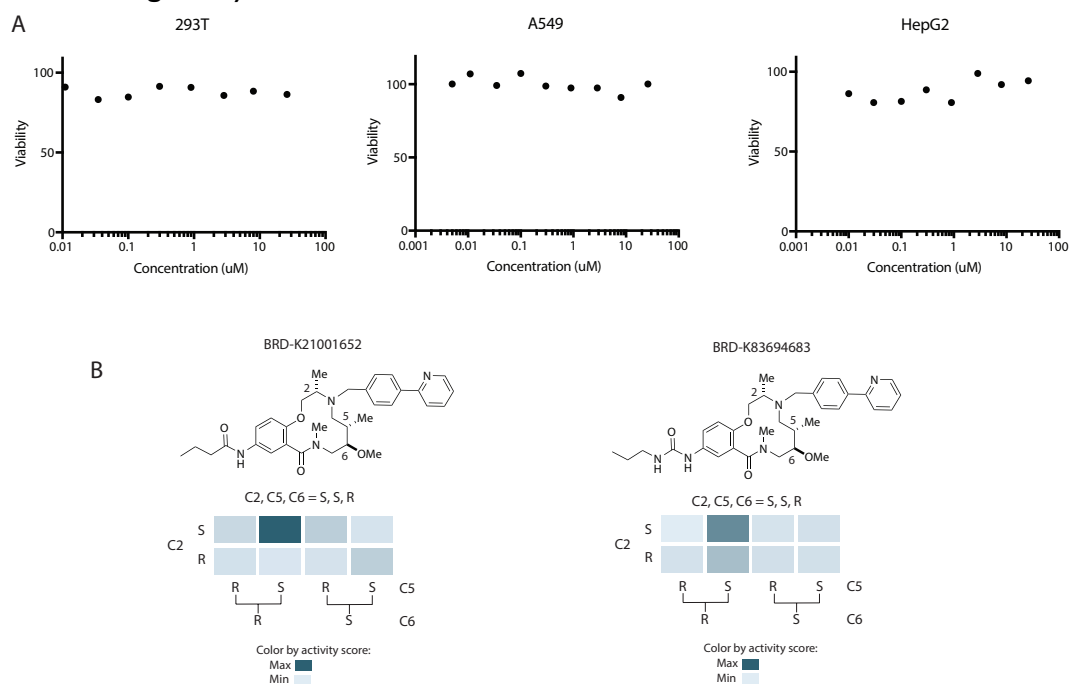
**Christine A. Marian, Mateusz Stoszko, Lili Wang, Matthew W. Leighty, Elisa de Crignis, Chad A. Maschinot, Jovylyn Gatchalian, Benjamin C. Carter, Basudev Chowdhury, Diana C. Hargreaves, Jeremy R. Duvall, Gerald R. Crabtree, Tokameh Mahmoudi, and Emily C. Dykhuizen**

**Figure S1 (related to Figure 1)**



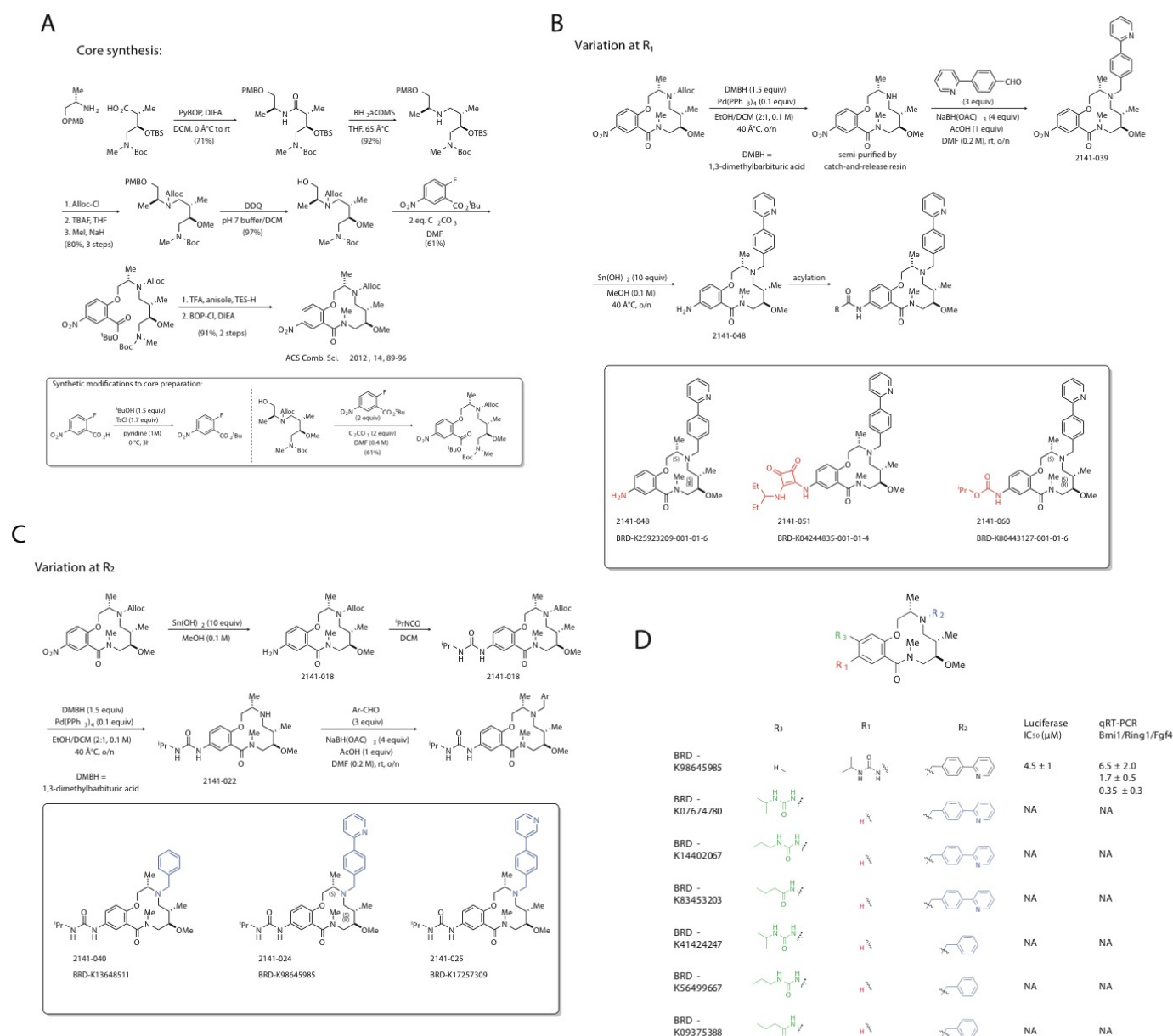
**S1: A.** The identification of Corning® CellBIND® as a commercially available tissue culture surface that supports embryonic stem cell morphology (left) and pluripotency, as defined by alkaline phosphatase activity (middle). The luciferase induction was measured after lentiviral-mediated knockdown of *Brg1* in the Bmi1-luciferase reporter ES cell line grown in various cell culture support conditions (right). **B.** Screen Reproducibility: The activity scores for each compound and its replicate from the high throughput screen were plotted. Only compounds for which both replicates displayed activity were designated as hits. **C.** Screening tree overview of compound screening steps including primary screen, cheminformatics steps, confirmatory screen, counter screen and secondary screen. **D.** The structure activity relationship of the thiophene library members based on initial luciferase induction from the primary screen and from follow-up compounds. **E.** Immunoblot staining of ARID1A after chemoprecipitation with resin conjugated with the thiophene. **F.** Latency reversal in the ex vivo model of HIV latency. n = 4. Data presented as mean ± S.D. \*\* p<0.01 using Student's T test.

**Figure S2 (related to Figure 2)**



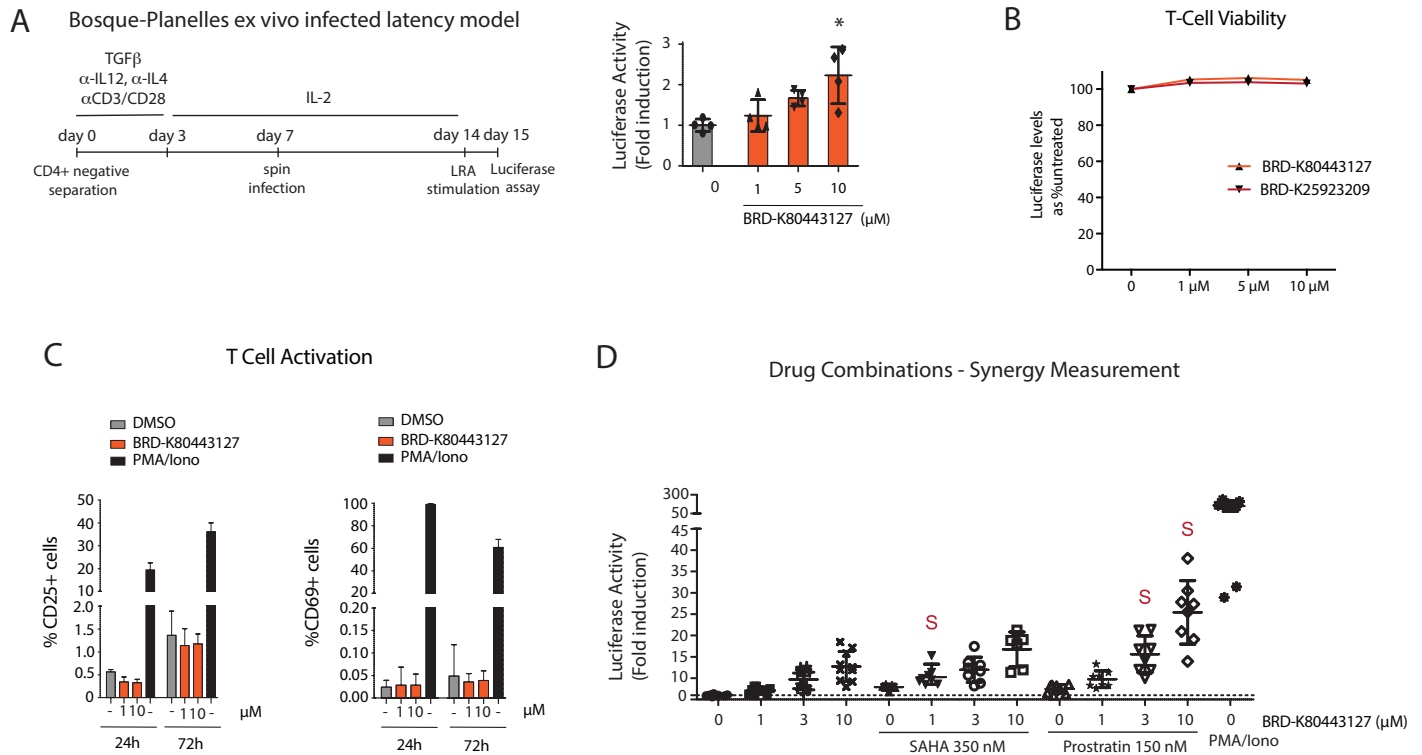
**S2: A.** Viability measurements in transformed embryonic kidney cell line HEK293T, lung cancer cell line A549, and hepatocellular carcinoma cell line HepG2 were performed after 72 h of compound or DMSO treatment using CellTiter-Glo®. **B.** The structure activity relationship of the eight stereoisomers of BRD-K21001652 and BRD-K83694683 based on initial luciferase induction from the primary screen.

**Figure S3 (related to Figure 3)**



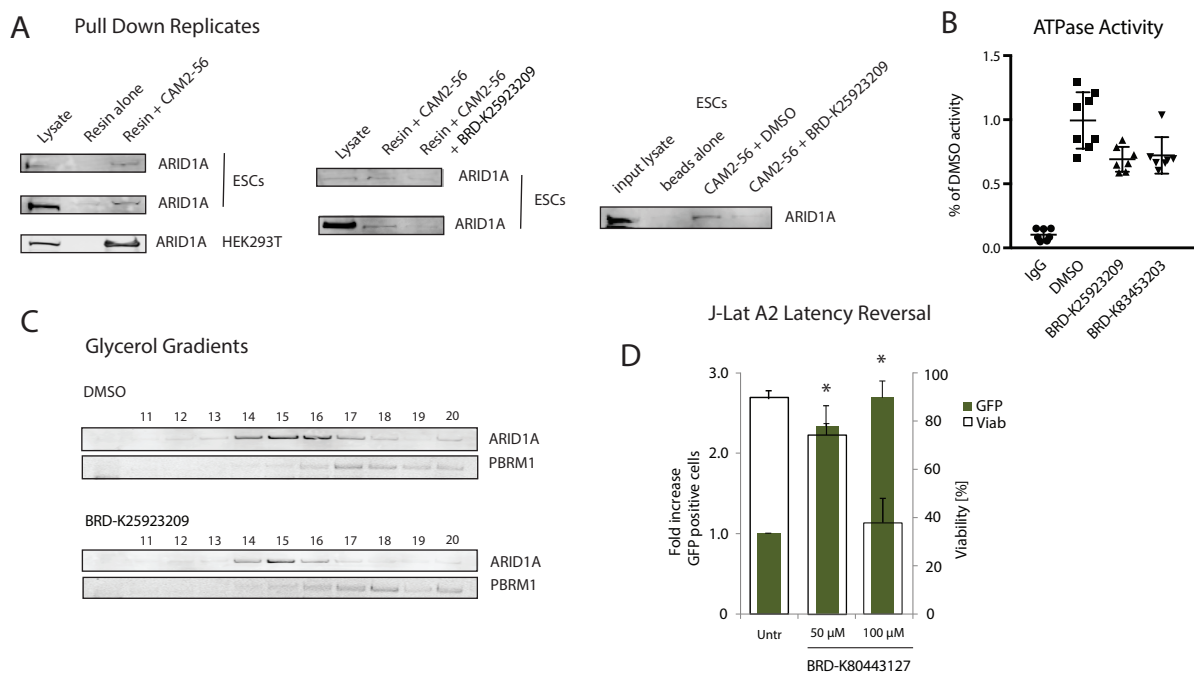
**S3: A.** Synthetic scheme for the 12-membered macrolactam core as adapted for solution phase synthesis from published procedures. **B.** Synthetic scheme for modifying the core at the aniline position, along with representative compounds included for full characterization (see full methods). **C.** Synthetic scheme for modifying the core at the or the amine position, along with representative compounds included for full characterization (see full methods). **D.** Structure activity relationship for compounds from the 30-membered solution phase library from Fig 3 with variations at the position of substituents on the aromatic ring. Activity was defined as the EC<sub>50</sub> in the luciferase reporter screen and as the fold transcriptional change of three BAF targets (*Bmi1*, *Ring1*, *Fgf4*) at a single compound concentration (30 μM) determined using qRT-PCR. n = 3. Data presented as mean ± S.D. NA = no activity.

**Figure S4 (related to Figure 4)**



**S4:** **A.** Latency reversal with BRD-K80443127 was confirmed using the Bosque-Planelles ex vivo latency model (Bosque et al. 2009). Data are presented as mean  $\pm$  S.D. Asterisks indicate the level of significance compared to untreated cells using student's T test (\*  $p < 0.05$ ). **B.** T cell viability measured using CellTiter Glo® in the presence of inhibitors. **C.** Primary CD4<sup>+</sup> T cells were stimulated for 24 and 72 hours with indicated concentrations of BRD-K80443127 or PMA/Ionomycin as a positive control. Bar plots show the percentage of cells expressing early activation marker CD69 (left) and late activation marker CD25 (right), respectively. Bars represent the average  $\pm$  SD of experiments performed on cells isolated from two healthy donors. **D.** Synergy was calculated for concentrations of BRD-K80443127 with low concentrations of SAHA (350 nM) and prostratin (150 nM) using the Lassen ex vivo HIV-1 latency model (Lassen et al. 2012).  $n = 8$ . Synergy was calculated using Bliss score formula:  $S_{exp} = [1 - (1 - A) \times (1 - B)]$ , where  $S_{exp}$  is the expected percentage of cells reactivated after combinatorial treatment in absence of synergism and A and B correspond to the percentage of cells reactivated by single treatments. Combination was considered synergistic if the observed effect of combined treatments was significantly higher than calculated value ( $S_{exp}$ ), and is indicated with an S in the figure.

**Figure S5 (related to Figure 5)**



**S5: A.** Pulldowns were performed from ES or 293T cell lysates pretreated with DMSO or 200  $\mu$ M BRD-K25923209 using CAM2-56 or biotin prebound to streptavidin resin. **B.** The DNA-stimulated ATPase activity of immobilized BAF complex was measured in the presence of DMSO or macrolactam inhibitors (250  $\mu$ M). **C.** Glycerol gradients were performed with nuclear lysates from cells treated 24 h with DMSO or BRD-K98645985 (30  $\mu$ M) and fractions were analyzed using immunoblot analysis. **D.** J-Lat A2 cells were treated with increasing concentrations of BRD-K80443127 and reactivation was quantitated at 48 h post treatment. Percent GFP positive cells (left axis, green bars) corresponding to the level of HIV-1 activation, and cell viability (right axis, transparent bars) were evaluated by flow cytometry.

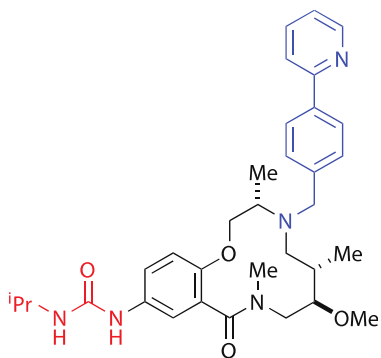


**Table S1. Solution phase macrolactam library.**

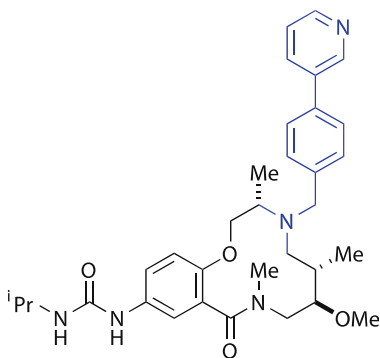
Broad ID number	Activity (Bmi-Luc IC50 $\mu$ M)	Molecular Weight	cLogP	Solubility in water ( $\mu$ M)	HepG2 Toxicity (EC50 $\mu$ M)	A549 Toxicity (EC50 $\mu$ M)	HEK293T Toxicity (EC50 $\mu$ M)
BRD-K98645985-001-02-5	4,5	573,7	4,2	30	>30	>30	>30
BRD-K17257309-001-01-8	37	573,7	4,2	26	>30	>30	>30
BRD-K13449002-001-01-5	12,6	573,7	4,2	2	>30	>30	>30
BRD-K73070754-001-01-6	NA	574,7	3,5	9	>30	>30	>30
BRD-K90159582-001-01-4	NA	587,2	3,8	89	>30	>30	>30
BRD-K79740310-001-01-5	NA	602,7	3,6	78	>30	>30	>30
BRD-K02599060-001-01-9	NA	510,6	3,2	93	>30	>30	>30
BRD-K15849455-001-02-4	NA	406,5	1,6	>100	>30	>30	>30
BRD-K13648511-001-02-4	NA	496,7	3,6	67	>30	>30	>30
BRD-K92576614-001-02-7	NA	497,6	2,6	97	>30	>30	>30
BRD-K60351210-001-01-3	NA	497,6	2,5	96	>30	>30	>30
BRD-K77628901-001-01-9	NA	497,6	2,5	86	>30	>30	>30
BRD-K81318113-001-02-3	NA	498,6	1,9	96	>30	>30	>30
BRD-K26156119-001-01-1	NA	514,6	3,7	66	>30	>30	27
BRD-K71642560-001-01-8	NA	514,6	3,7	52	>30	>30	>30

BRD-K79609051-001-01-5	NA	514,6	3,7	53	>30	>30	29
BRD-K55993513-001-01-3	NA	625,8	4,8	7	>30	>30	>30
BRD-K04244835-001-01-4	NA	653,8	5,8	2	>30	>30	>30
BRD-K09156915-001-01-8	NA	665,8	5,8	1	>30	>30	>30
BRD-K35928994-001-01-2	NA	651,8	5,3	1	>30	>30	14
BRD-K54273824-001-01-5	NA	623,8	4,5	11	>30	25	15
BRD-K51299478-001-01-2	7,6	558,7	4,6	44	>30	>30	>30
BRD-K49078264-001-01-3	4,9	566,7	4,6	21	>30	>30	25
BRD-K80443127-001-01-6	10,3	574,7	4,8	16	>30	>30	>30
BRD-K25923209-001-01-6	9,6	488,6	3,7	>100	>30	>30	>30
BRD-K07674780-001-01-4	NA	573,7	4,2	24	>30	>30	>30
BRD-K14402067-001-01-5	NA	573,7	4,3	22	>30	>30	>30
BRD-K83453203-001-01-9	NA	558,7	4,4	29	>30	>30	>30
BRD-K41424247-001-01-9	NA	496,7	3,6	57	>30	>30	>30
BRD-K56499667-001-01-4	NA	496,7	3,7	50	>30	>30	>30
BRD-K09375388-001-01-2	NA	481,6	3,8	68	>30	>30	>30

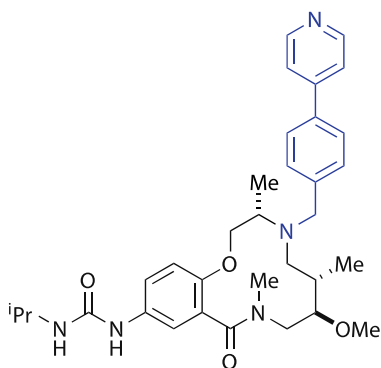
Structures of 31 solution phase library members:



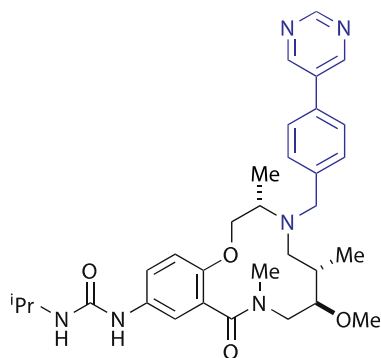
BRD-K98645985-001-02-5



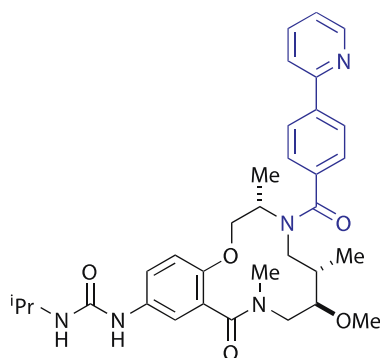
BRD-K17257309-001-01-8



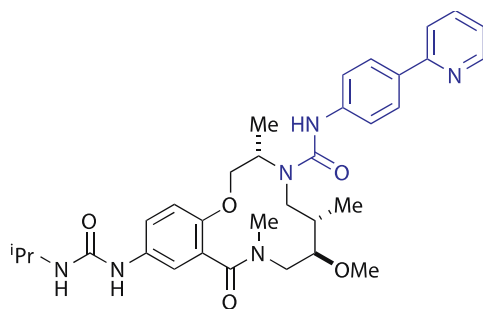
BRD-K13449002-001-01-5



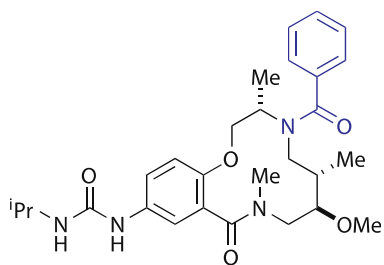
BRD-K73070754-001-01-6



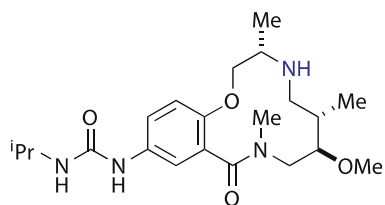
BRD-K90159582-001-01-4



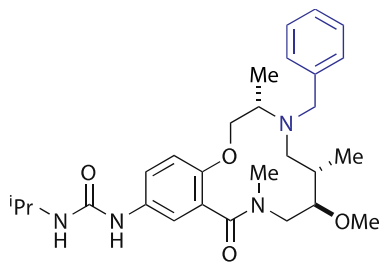
BRD-K79740310-001-01-5



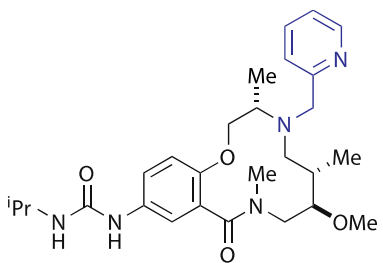
BRD-K02599060-001-01-9



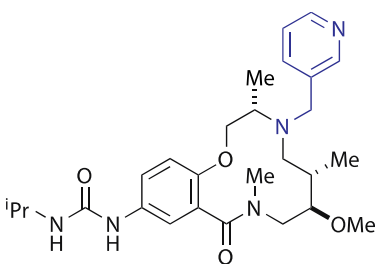
BRD-K15849455-001-02-4



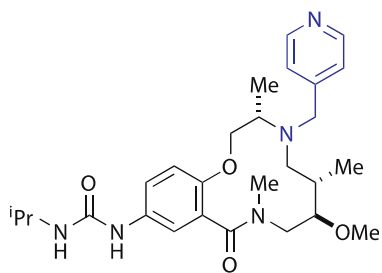
BRD-K13648511-001-02-4



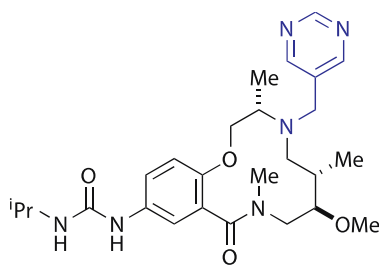
BRD-K92576614-001-02-7



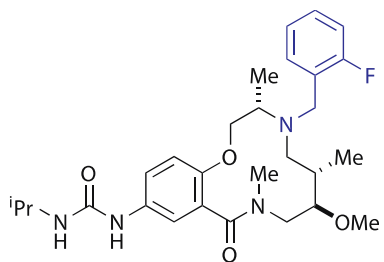
BRD-K60351210-001-01-3



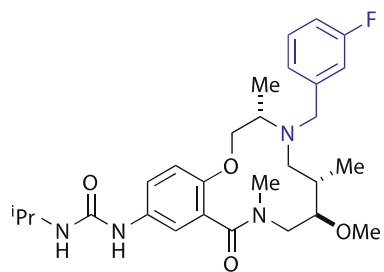
BRD-K77628901-001-01-9



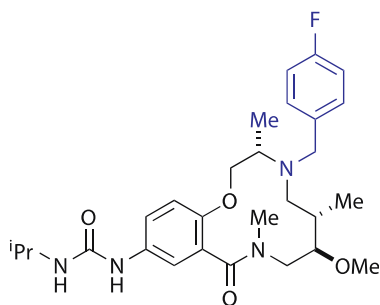
BRD-K81318113-001-02-3



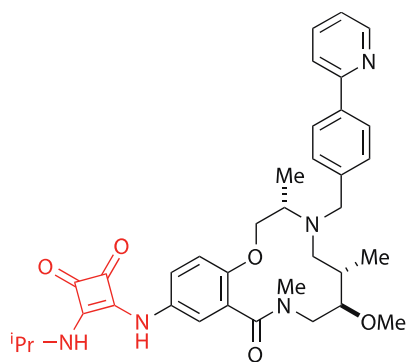
BRD-K26156119-001-01-1



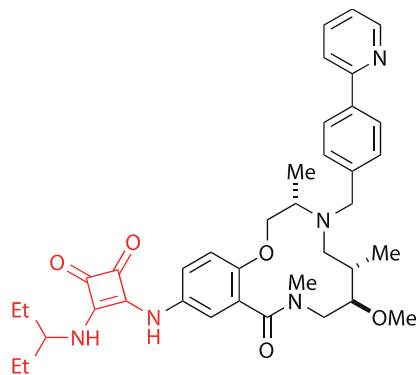
BRD-K71642560-001-01-8



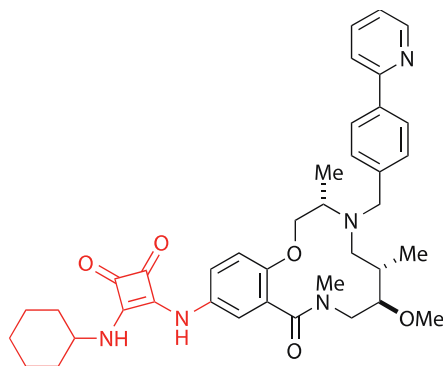
BRD-K79609051-001-01-5



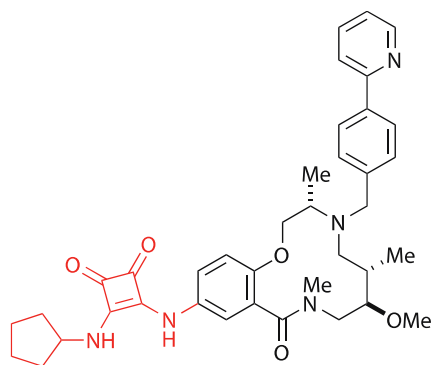
BRD-K55993513-001-01-3



BRD-K04244835-001-01-4

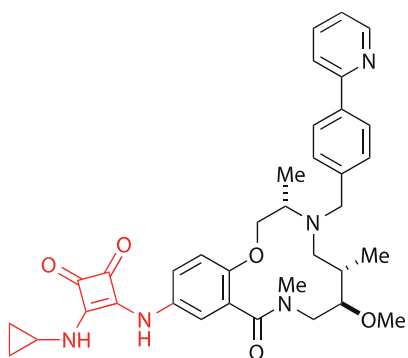


BRD-K09156915-001-01-8

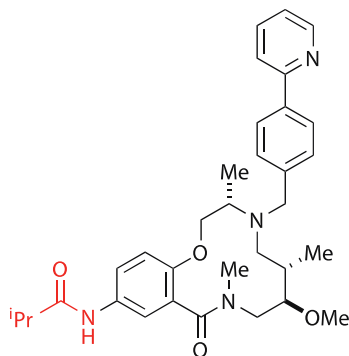


BRD-K35928994-001-01-2

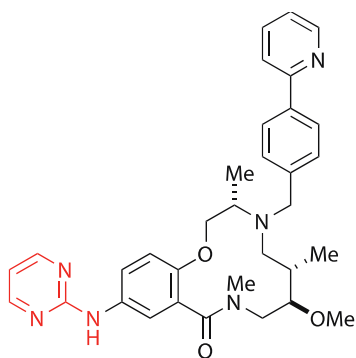




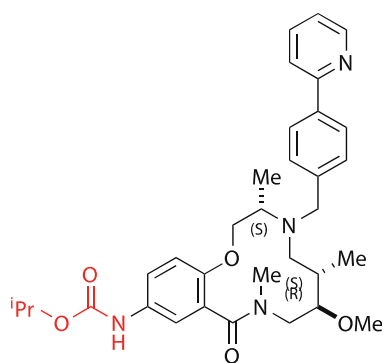
BRD-K54273824-001-01-5



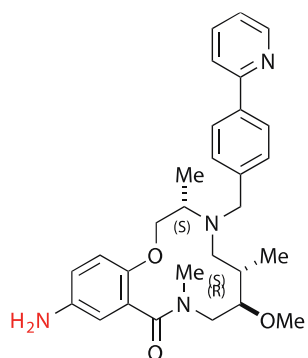
BRD-K51299478-001-01-2



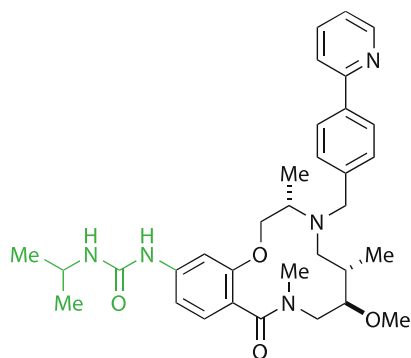
BRD-K49078264-001-01-3



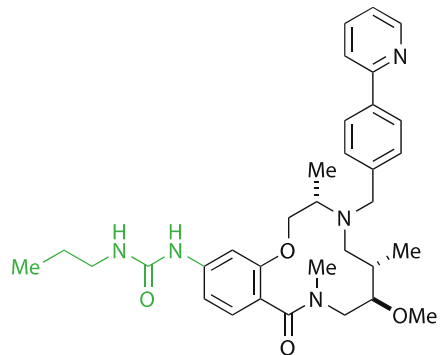
BRD-K80443127-001-01-6



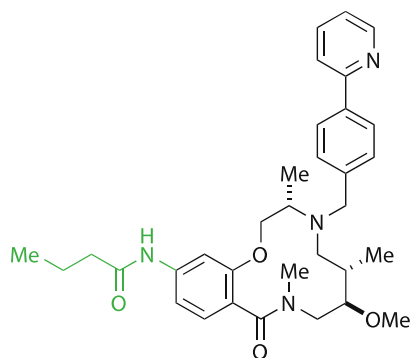
BRD-K25923209-001-01-6



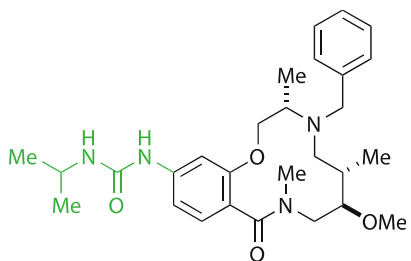
BRD-K07674780-001-01-4



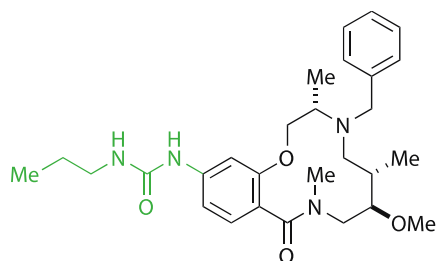
BRD-K14402067-001-01-5



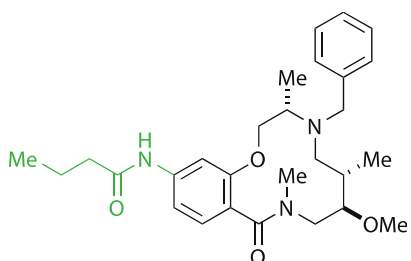
BRD-K83453203-001-01-9



BRD-K41424247-001-01-9



BRD-K56499667-001-01-4



BRD-K09375388-001-01-2

**Table S2. List of Primers for Southern Blot Probes, qRT-PCR, and FAIRE, Related to Figures 1–5.**

	Mouse		
		Forward	Reverse
<b>RT-qPCR primers</b>	Bmi1	TACCATGAATGGAACCAGCA	AAAGGAAGCAAACCTGGACGA,
	Fgf4	GGGTGTGGTGAGCATCTTCGGA	GGTATGCGTAGGACTCGTAGGGC
	Ring1	CTGGACATGCTGAAGAACA	TCCCGGCTAGGGTAGATTTT
	Gapdh	TGCACCACCAACTGCTTAG	GGATGCAGGGATGATGTTT
	Human/HIV-1		
		Forward	Reverse
	p21	AGCAGAGGAAGACCATGTGGAC	TTTCGACCCTGAGAGTCTCCAG
	cMYC	AAGCCACAGCATACATCC	GCACAAGAGTTCCGTAGC
	Pol	GGTTTATTACAGGGACAGCAGAGA	ACCTGCCATCTGTTTTCCATA
	B2M	AGCGTACTCCAAAGATTCAGGTT	ATGATGCTGCTTACATGTCTCGAT
		Forward	Reverse
<b>FAIRE primers</b>	Nuc-0	ATCTACCACACACAAGGCTAC	GTACTAACTTGAAGCACCATCC
	HSS	AAGTTTGACAGCCTCCTAGC	CACACCTCCCTGGAAAGTC
	Nuc-1	TTTGCCTGTACTGGGTCTCTCTGG	CACAACAGACGGGCACACACT
		Forward	Reverse
<b>Southern probes</b>	3' probe	Forward	TTAAGCACATTGCCTCATTTCCAT
		Reverse	CCAAGTTCCACTTCATTGGGTGTA
	5' probe	Forward	GGTCAGCAAGAAGGGAAGACACC
		Reverse	CCAGGCTTACTGGAGGCTGGAAT



# Chapter 4

## **A New Quinoline BRD4 Inhibitor Targets a Distinct Latent HIV-1 Reservoir for Reactivation from Other “Shock” Drugs**

Erik Abner<sup>a</sup>, Mateusz Stoszko<sup>b</sup>, Lei Zeng<sup>c</sup>, Heng-Chang Chene<sup>f</sup>, Andrea Izquierdo-Bouldstridge<sup>a</sup>, Tsuyoshi Konumac<sup>c</sup>, Eduard Zoritae<sup>f</sup>, Elisa Fanunza<sup>a</sup>, Qiang Zhang<sup>c</sup>, Tokameh Mahmoudi<sup>b</sup>, Ming-Ming Zhou<sup>c</sup>, Guillaume J. Filione<sup>f</sup>, Albert Jordan<sup>a</sup>.

<sup>a</sup> Molecular Biology Institute of Barcelona (IBMB-CSIC), Barcelona, Spain

<sup>b</sup> Department of Biochemistry, Erasmus University Medical Center, Rotterdam, the Netherlands

<sup>c</sup> Department of Pharmacological Sciences, Icahn School of Medicine at Mount Sinai, Icahn Medical Institute, New York, New York, USA

<sup>d</sup> First Hospital and Institute of Epigenetic Medicine, Jilin University, Changchun, China

<sup>e</sup> Gene Regulation, Stem Cells and Cancer Program, Center for Genomic Regulation (CRG), Barcelona Institute of Science and Technology (BIST), Barcelona, Spain

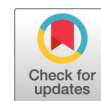
<sup>f</sup> University Pompeu Fabra (UPF), Barcelona, Spain

Published:

Journal of Virology 2018, 92:e02056-17







# A New Quinoline BRD4 Inhibitor Targets a Distinct Latent HIV-1 Reservoir for Reactivation from Other “Shock” Drugs

Erik Abner,<sup>a</sup> Mateusz Stoszko,<sup>b</sup> Lei Zeng,<sup>c,d</sup> Heng-Chang Chen,<sup>e,f</sup> Andrea Izquierdo-Bouldstridge,<sup>a</sup> Tsuyoshi Konuma,<sup>c</sup> Eduard Zorita,<sup>e,f</sup> Elisa Fanunza,<sup>a</sup> Qiang Zhang,<sup>c,d</sup> Tokameh Mahmoudi,<sup>b</sup> Ming-Ming Zhou,<sup>c</sup> Guillaume J. Filion,<sup>e,f</sup> Albert Jordan<sup>a</sup>

<sup>a</sup>Molecular Biology Institute of Barcelona (IBMB-CSIC), Barcelona, Spain

<sup>b</sup>Department of Biochemistry, Erasmus University Medical Center, Rotterdam, the Netherlands

<sup>c</sup>Department of Pharmacological Sciences, Icahn School of Medicine at Mount Sinai, Icahn Medical Institute, New York, New York, USA

<sup>d</sup>First Hospital and Institute of Epigenetic Medicine, Jilin University, Changchun, China

<sup>e</sup>Gene Regulation, Stem Cells and Cancer Program, Center for Genomic Regulation (CRG), Barcelona Institute of Science and Technology (BIST), Barcelona, Spain

<sup>f</sup>University Pompeu Fabra (UPF), Barcelona, Spain

**ABSTRACT** Upon HIV-1 infection, a reservoir of latently infected resting T cells prevents the eradication of the virus from patients. To achieve complete depletion, the existing virus-suppressing antiretroviral therapy must be combined with drugs that reactivate the dormant viruses. We previously described a novel chemical scaffold compound, MMQO (8-methoxy-6-methylquinolin-4-ol), that is able to reactivate viral transcription in several models of HIV latency, including J-Lat cells, through an unknown mechanism. MMQO potentiates the activity of known latency-reversing agents (LRAs) or “shock” drugs, such as protein kinase C (PKC) agonists or histone deacetylase (HDAC) inhibitors. Here, we demonstrate that MMQO activates HIV-1 independently of the Tat transactivator. Gene expression microarrays in Jurkat cells indicated that MMQO treatment results in robust immunosuppression, diminishes expression of c-Myc, and causes the dysregulation of acetylation-sensitive genes. These hallmarks indicated that MMQO mimics acetylated lysines of core histones and might function as a bromodomain and extraterminal domain protein family inhibitor (BETi). MMQO functionally mimics the effects of JQ1, a well-known BETi. We confirmed that MMQO interacts with the BET family protein BRD4. Utilizing MMQO and JQ1, we demonstrate how the inhibition of BRD4 targets a subset of latently integrated barcoded proviruses distinct from those targeted by HDAC inhibitors or PKC pathway agonists. Thus, the quinoline-based compound MMQO represents a new class of BET bromodomain inhibitors that, due to its minimalistic structure, holds promise for further optimization for increased affinity and specificity for distinct bromodomain family members and could potentially be of use against a variety of diseases, including HIV infection.

**IMPORTANCE** The suggested “shock and kill” therapy aims to eradicate the latent functional proportion of HIV-1 proviruses in a patient. However, to this day, clinical studies investigating the “shocking” element of this strategy have proven it to be considerably more difficult than anticipated. While the proportion of intracellular viral RNA production and general plasma viral load have been shown to increase upon a shock regimen, the global viral reservoir remains unaffected, highlighting both the inefficiency of the treatments used and the gap in our understanding of viral reactivation *in vivo*. Utilizing a new BRD4 inhibitor and barcoded HIV-1 minigenomes, we demonstrate that PKC pathway activators and HDAC and bromodomain inhibitors all target different subsets of proviral integration. Considering the

**Received** 28 November 2017 **Accepted** 10 January 2018

**Accepted manuscript posted online** 17 January 2018

**Citation** Abner E, Stoszko M, Zeng L, Chen H-C, Izquierdo-Bouldstridge A, Konuma T, Zorita E, Fanunza E, Zhang Q, Mahmoudi T, Zhou M-M, Filion GJ, Jordan A. 2018. A new quinoline BRD4 inhibitor targets a distinct latent HIV-1 reservoir for reactivation from other “shock” drugs. *J Virol* 92:e02056-17. <https://doi.org/10.1128/JVI.02056-17>.

**Editor** Frank Kirchhoff, Ulm University Medical Center

**Copyright** © 2018 American Society for Microbiology. All Rights Reserved.

Address correspondence to Albert Jordan, [albert.jordan@ibmb.csic.es](mailto:albert.jordan@ibmb.csic.es).

fundamental differences of these compounds and the synergies displayed between them, we propose that the field should concentrate on investigating the development of combinatory shock cocktail therapies for improved reservoir reactivation.

**KEYWORDS** BETi, Brd4, HIV latency, LRAs

Upon initial HIV-1 contagion, most of the afflicted CD4<sup>+</sup> T lymphocytes die rapidly in response to viral infection. A major breakthrough in controlling HIV came in 1996 with the introduction of highly active antiretroviral therapy (ART), which is able to sustain the population of T lymphocytes in patients. However, a small but significant number of latent infected cells survive the antiviral therapy, and upon cessation of treatment, the latent proviruses become capable of expression without obstruction, and the viremia reemerges.

Active CD4<sup>+</sup> T lymphocytes possess the capacity to revert to a quiescent state with minimal HIV-1 gene expression following the proviral integration and persist as long-lived central or transitional memory T lymphocytes sheltering latent HIV-1 genomes. These T lymphocyte populations harboring the latent reservoirs cannot be detected by the immune surveillance, since viral antigens are not presented to immune effector cells, and ART remains ineffective against an already integrated provirus. Unlike active T lymphocytes, which have a short half-life, in a dormant state the memory T lymphocytes possess an estimated half-life of approximately 44 months and are thus considered to be the primary reason why the disease remains a chronic affliction (reviewed in reference 1). Mathematical models predict that the eradication of a reservoir consisting of 10<sup>6</sup> cells would take 73 years *in vivo* (2). Extensive efforts have been carried out within the last 25 years to characterize these cells and to understand how HIV-1 is regulated after integration and why it can remain transcriptionally latent.

In order to cure a patient, the viral reservoir must be either completely eradicated or at least depleted to a level at which viral rebound is deemed unlikely (3). To achieve HIV eradication from infected patients, it has been suggested that ART be combined with drugs that “shock” the proviral transcription into activity and flush out the dormant viruses (4). Following the reactivation of latent proviruses, the immune system and cytopathogenicity are responsible for killing the infected cells, while the continuous ART guarantees protection against further infection.

Small-molecule inhibitors are commonly regarded as the preferred method in forcing molecular regulation. Due to technical reasons, like membrane penetration, mechanical simplicity, rapid function, cost-effectiveness, and *in vivo* stability, the “shock and kill” field is currently engaged in the identification and development of small-molecule latency-reversing agents (LRAs). It has been proposed that HIV gene expression reactivators can be grouped into two categories: direct activators and noise enhancers (5). The reasoning for this type of categorization is that the two groups of drugs possess conceptually contrasting mechanisms on the latent viral promoter, allowing them to synergize when combined (6).

Direct activators, such as protein kinase C (PKC) agonists, tumor necrosis factor alpha (TNF- $\alpha$ ), and T cell receptor agonists, are responsible for introducing stimulatory transcription factors to the promoter (such as NF- $\kappa$ B and nuclear factor of activated T cells [NFAT]) and stimulate the transcription process. Although these agents present highly efficient rates of reactivation of proviral transcription, the downside of the modulators is their aggressiveness. The highly potent compounds are incapable of discriminating between infected and uninfected cells, leading to massive T lymphocyte activation, a decrease in the patient’s immunological memory, and oftentimes a cytokine storm. On the other hand, noise enhancers are responsible for modulating the chromatin state, easing the access of transcription factors to the viral promoter, and ultimately assisting the elongation process. This class of agents includes histone deacetylase (HDAC), methyltransferase, and bromodomain inhibitors. HDAC inhibitors (HDACi) have already been approved for clinical use against T cell lymphomas; thus, due to patient safety reasons, these drugs are considered primary candidates in terms

of viral reactivation. Though the reported pilot studies utilizing HDAC inhibitors so far have proven them to be less efficient than expected, there still is potential—most of the completed clinical trials have shown an increase in intracellular viral transcription and occasionally also a higher viral load, but none of the trials have yet reported a decrease of viral reservoir size (reviewed in reference 7).

In the last 4 years, numerous studies have substantiated the notion that BET bromodomain inhibitors (BETi) can trigger HIV transcription in latently infected cells, thus activating viral replication (8–10). JQ1 was described as the first of its class as a small-molecule inhibitor of bromodomain-containing protein 4 (BRD4), displaying the highest affinity for the first bromodomain (BD1) of BRD4, and it has received much attention for its therapeutic potential against multiple myeloma and other cancer types related to the c-Myc oncogene (11–13). The effect of JQ1 in viral reactivation can be explained by tilting the competition between BRD4 and Tat for association with the P-TEFb kinase complex in Tat's favor (14). A larger pool of P-TEFb becomes vacant to associate with Tat and activate transcription elongation of the HIV genome. In line with the activator-enhancer drug type classification, bromodomain inhibition has been shown to confirm the premise of chromatin-loosening drugs synergizing with direct NF- $\kappa$ B activators to reactivate viral transcription, both in laboratory Jurkat models and under patient-derived *ex vivo* conditions (15, 16).

An excellent approach for discovering new antiretrovirus-activating small molecules is using cell lines that harbor a minimal provirus genome. An example of a viral latency model is the J-Lat A2 clone, described previously (17). A 4-kbp-long sequence consisting of various elements from the full-length HIV-1 genome and a green fluorescent protein (GFP) sequence (5' long terminal repeat [LTR]-Tat-internal ribosome entry site [IRES]-GFP-3' LTR) was integrated into an intron of the *UTX* gene of the Jurkat T cell line. In search of new LRAs, our group previously screened a library of 6,000 small molecules to identify basic agents capable of reactivating the latent HIV-1 minigenome from A2 cells (18). Virtual screening for further similar chemicals and additional substitutions of the functional groups in these compounds led to the identification of 8-methoxy-6-methylquinolin-4-ol (MMQO). While the molecular mechanism of MMQO remained elusive, it was shown that the molecule alone does not induce the transcriptional activity of minimal promoters containing binding sites for the typical HIV-1-activating transcription factors NF- $\kappa$ B, NFAT, AP-1, and Sp1. Furthermore, we observed that, in addition to inducing HIV LTR transactivation, MMQO is also able to display immunosuppressive activity by repressing CD3-induced interleukin 2 (IL-2) and TNF- $\alpha$  promoter activation (18).

Based on the previously published results with anti-CD3 ( $\alpha$ -CD3) antibody treatments, we hypothesized that MMQO functions through a pathway that exhibits immunosuppressive properties. In addition, taking into consideration that MMQO affects proviral transcription, a process that is highly dependent on cellular host factors, we assumed it to be plausible that the drug would also affect the cell transcriptome on a global scale. Therefore, we utilized gene expression microarrays to characterize and identify the cellular pathways affected by MMQO. We reconfirmed the immunosuppressive behavior of the reagent and showed it to dysregulate genes known to be sensitive to chromatin acetylation. By computational and biochemical means, we determined that MMQO reverts HIV-1 latency by inhibiting the bromodomain protein BRD4. Furthermore, utilizing the barcoded HIV ensembles (B-HIVE) methodology (19), we were able to demonstrate how the inhibition of BRD4 influences a different subset of latently integrated proviruses than does the inhibition of HDACs or the activation of PKC-dependent pathways. The present study documents a method to identify the molecular mechanisms of small molecules with unknown targets and demonstrates that a scaffold bromodomain-inhibiting compound functions on a population of HIV-1 integration sites different from those of other, more commonly used LRAs.

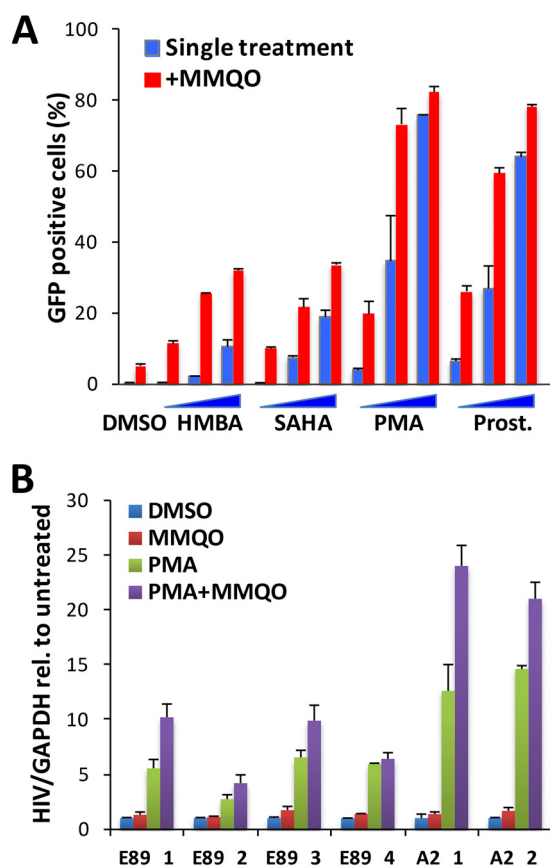


**FIG 1** MMQO reactivates latent HIV independently of Tat and potentiates other LRAs. (A) MMQO exerts its effect on the minigenome independently of viral Tat protein. Shown is flow cytometry analysis of a previously established latent Jurkat E89 clone, which was infected with a Tat-negative GFP-expressing minigenome as described previously (20). The cells were treated for 24 h with HMBA (0.5, 2.5, or 5 mM), SAHA (0.1, 0.5, or 2.5  $\mu$ M), PMA (1 to 4 or 10 nM), or prostratin (Prost.; 0.25, 0.5, or 1  $\mu$ M) in combination with MMQO (160  $\mu$ M) or an equivalent volume of vehicle (DMSO). GFP expression intensity was measured by FACS and expressed as a percentage of GFP-positive cells. Means and standard deviations (SD) from an experiment performed in triplicate are shown. (B) MMQO potentiates LRAs rapidly. RT-qPCR results show rapid activation of latent HIV by a PKC agonist and MMQO. E89 and A2 Jurkat clones were treated for 1 h with MMQO (160  $\mu$ M), PMA (10 nM), a combination of the two, or an equivalent volume of DMSO as a vehicle. *GAPDH* (glyceraldehyde-3-phosphate dehydrogenase) was measured for normalization, and the results are represented relative to results from the DMSO-treated cells. Primers to detect the 5' LTR were used. Means and SD from 4 (E89) and 2 (A2) independent experiments measured in duplicate are shown.

## RESULTS

**MMQO exerts its effect on HIV minigenome expression independently of viral Tat protein.** In order to determine the mechanism of action of MMQO, we sought to determine whether MMQO could exert its effect independently of the viral Tat protein. The discovery of MMQO was spearheaded by utilizing the latent HIV-1 J-Lat A2 clone, which contains a minimal sequence of HIV-1, encoding only GFP and the viral Tat protein (18). Although the Tat protein is considered a crucial component for efficient HIV transcription, models containing latent minigenomes lacking Tat are known to respond to external signals, albeit at lower efficiencies. Utilizing the GFP-expressing J-Lat model E89 (20), which contains a latent Tat-negative construct, we found that MMQO functioned similarly to our previous observations with Tat-expressing constructs (Fig. 1A). As a signal of viral expression, we monitored how cells expressed GFP after 24-hour treatments with four different HIV-reactivating compounds alone or in combination with MMQO via flow cytometry: the enhancer drugs hexamethylene bisacetamide (HMBA) and the HDAC inhibitor SAHA (also known as vorinostat) and the PKC pathway agonists phorbol 12-myristate 13-acetate (PMA) and prostratin. While

MMQO alone exhibited a moderate response, it nevertheless strongly potentiated the reactivating ability of the other drugs, as previously reported with Tat-expressing viruses (18). As expected, PMA and prostratin were able to induce viral reactivation at notably higher rates than the other three compounds, due to their roles as highly potent NF- $\kappa$ B-stimulatory agents and because the latent cells were originally selected as PMA responsive (20).

The effect of MMQO by itself or potentiating the effect of PKC pathway activators on HIV reactivation was also observed upon 1-h drug treatments in both Tat-negative (E89) and Tat-expressing (A2) J-Lat cells, as tested by reverse transcription-quantitative PCR (RT-qPCR) (Fig. 1B). The rapid response to these drugs suggests that they function directly on the HIV minigenome, as opposed to through a secondary wave of transcriptional products. Similar to HDAC inhibitors, MMQO may function as a noise enhancer type of drug. As expected, cells with the ability to express Tat upon initial HIV promoter activation (A2 clone) were reactivated at considerably higher rates.

**MMQO potentiates latency-reversing agents in *ex vivo* latently infected primary CD4<sup>+</sup> T cells.** We also tested the activity of MMQO in an *ex vivo* infection primary model of latency, which relies on direct spin infection of primary CD4<sup>+</sup> T cells with full-length replication-incompetent HIV driving the luciferase reporter gene. We observed a dose-dependent increase in luciferase activity after 24 h of stimulation with MMQO (Fig. 2A), confirming the data obtained in T cell line latency models. We then examined whether MMQO is capable of enhancing HIV latency reversal when used in combination with other LRA class molecules, proposed to also function via distinct mechanisms in primary latently infected cells. We costimulated latently infected primary CD4<sup>+</sup> T cells with MMQO alone or together with SAHA or prostratin, as indicated (Fig. 2B). In accordance with our results from latent T cell lines, the activities of both SAHA and prostratin were enhanced when the cells were cotreated with MMQO, with MMQO-prostratin cotreatment reaching latency reversal over 40% of that obtained with our positive-control PMA-ionomycin. Furthermore, the concentrations of MMQO used alone or in combination treatment did not result in a significant decrease in viability of primary CD4<sup>+</sup> T cells (Fig. 2C). Neither was there a significant increase in apoptosis after 24 h or 72 h of stimulation with increasing concentrations of MMQO, as determined by annexin V staining (Fig. 2D).

**Global expression profile of MMQO treatment.** Recognizing that the final output of a drug's functionality can be efficiently measured in mRNA production, we decided to follow up the characterization of MMQO by utilizing a genome-wide Agilent mRNA expression microarray platform with transcripts extracted from Jurkat cells treated or not with MMQO. We opted to use native Jurkat cells for the microarray experiment in order to identify MMQO's mechanism of action without the possibility of interference from the HIV-1 minigenome, specifically by the Tat protein, which has been reported to reprogram the cellular epigenetic landscape (21). Considering how MMQO induces minigenome expression to about an 8- to 10-fold increase after 8 h of treatment at 50% effective concentration ( $EC_{50}$ ) (18), we concluded that 8 h was an appropriate treatment time for the microarray experiments, since the specific target genes of MMQO might respond similarly to HIV-1 promoter stimulation and be differentially regulated. In addition, this relatively short treatment time should minimize excessive changes on the protein level, which could otherwise cause unwanted secondary responses in the transcriptome. The change of all transcripts between the untreated control groups and the MMQO-treated groups was considered to show differential expression if the genes presented a fold change of at least 1.5 with a *P* value lower than 0.05 after adjustment for multiple tests (22). We determined that, in total, MMQO regulated 2,193 transcripts at a fold change cutoff of 1.5 and 549 transcripts with a fold change of 2.0. As shown in the volcano plot in Fig. 3A, it can be concluded that MMQO causes substantially more potent downregulation as opposed to upregulation of genes. This trait is better illustrated in the bar graph in Fig. 3B, where the percentages of differentially expressed transcripts are sorted by fold change cutoffs. For a small collection of genes ( $n = 9$ ), we

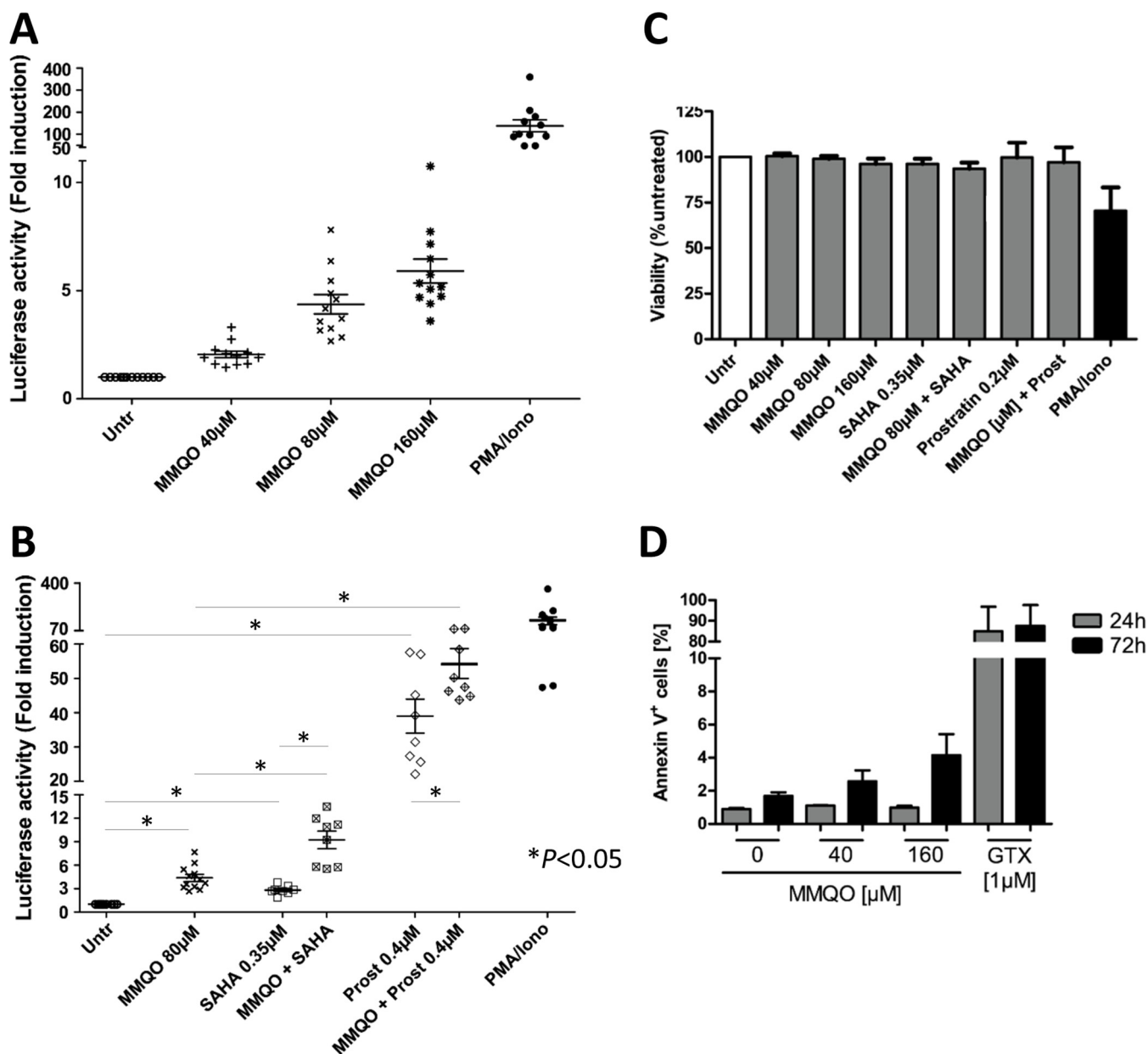


**FIG 2** MMQO potentiates LRAs in *ex vivo* latently infected primary CD4<sup>+</sup> T cells. (A and B) Dot plots showing latency reversal in *ex vivo*-infected primary CD4<sup>+</sup> T cells. The data are presented as the fold increase in luciferase activity after 24-h treatment with an MMQO concentration gradient (A) and MMQO (80  $\mu$ M) cotreatments with SAHA (350 nM) or prostratin (400 nM) (B); each point represents a single measurement. The experiments were performed in duplicate using cells isolated from 6 (A) or 4 (B) healthy blood donors. Student's *t* test was used to confirm significant differences between treatments. \*,  $P < 0.05$ . (C and D) MMQO does not reduce viability and does not induce apoptosis in primary CD4<sup>+</sup> T cells. (C) Latently infected primary cells were left untreated (Untr) or treated as indicated for 24 h, and viability was assessed by flow cytometry. (D) Uninfected primary CD4<sup>+</sup> T cells were left untreated or treated as indicated for 24 h or 72 h, followed by annexin V staining and flow cytometry analysis. The data presented are the means of at least 3 independent healthy blood donors  $\pm$  standard deviations. Gliotoxin (GTX) was used as a positive control for annexin V staining experiments.

performed an independent validation by qPCR to confirm the reproducibility of the microarray (Fig. 3C).

The global nonspecific transcriptional response was unexpected, since we initially anticipated identifying precise pathways with a low number of specifically regulated genes, allowing us to predict the factors involved. Nevertheless, the strong downregulation pattern of MMQO could partially be traced back to its immunosuppressive nature—a substantial fraction of genes from this data set are known to be direct target genes of NF- $\kappa$ B (see Table S1 in the supplemental material), while pathway analysis



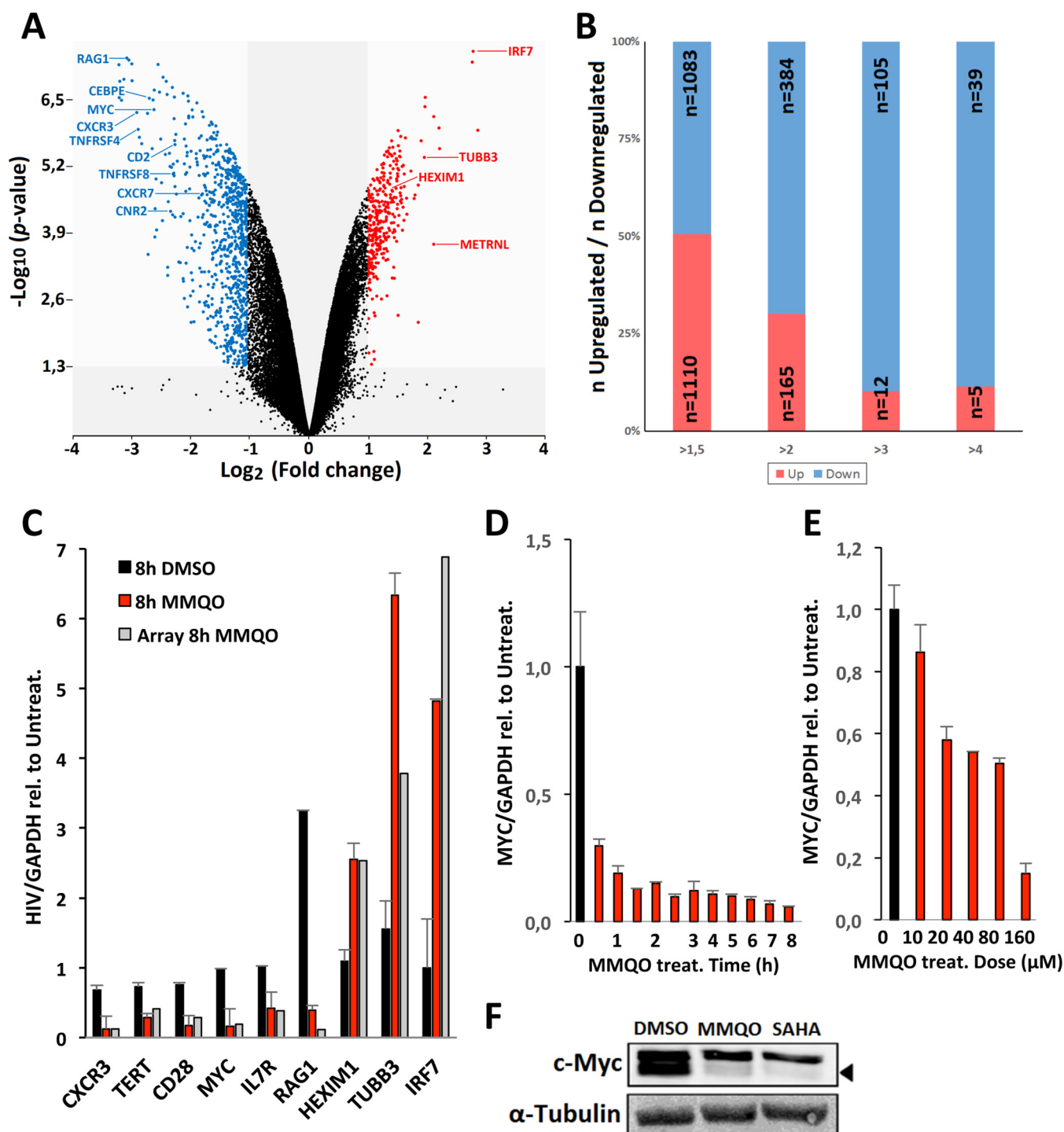


**FIG 3** Global expression profile of MMQO treatment. Expression microarray (Agilent) analysis of Jurkat cells treated or not with MMQO for 8 h was performed in duplicate. (A) Volcano plot of gene expression differences between treated and nontreated samples. The blue and red dots highlight all the statistically significant downregulated/upregulated transcripts (fold change [FC]  $\geq 1.5$ ;  $P < 0.05$ ). The Myc gene and other genes that are regulated by acetylation-dependent networks are highlighted. (B) The total number of protein-coding genes significantly up- or downregulated by 8 h MMQO were categorized into four groups based on their mean fold changes compared to the untreated samples. The number of upregulated genes was divided by the number of downregulated genes in each expression group, which is displayed as a percentage. (C) For a subset of genes, we performed an independent RT-qPCR validation of microarray results from Jurkat cells treated with MMQO (80  $\mu\text{M}$ ) or DMSO for 8 h or left untreated. GAPDH was measured for normalization, and the results are presented relative to untreated cells. The values obtained from the 8-h MMQO treatment microarray are displayed as gray bars. (D and E) Downregulation of c-Myc by MMQO in Jurkat cells. (D) RT-qPCR results depicting MYC downregulation in Jurkat cells treated with MMQO (160  $\mu\text{M}$ ) at different time points (0 to 8 h). (E) RT-qPCR results showing MYC downregulation in native Jurkat cells treated with various doses of MMQO for 1 h. GAPDH was measured for normalization, and the results are presented relative to untreated cells. The means and SD from a representative experiment measured in duplicate are shown. (F) Western blot analysis of c-Myc protein expression. Jurkat cells were incubated for 12 h with MMQO (160  $\mu\text{M}$ ) or SAHA (5  $\mu\text{M}$ ) or left untreated. Total protein was extracted with RIPA buffer and analyzed by immunoblotting against c-Myc and  $\alpha$ -tubulin as a loading control. The arrowhead indicates the specific c-Myc band.



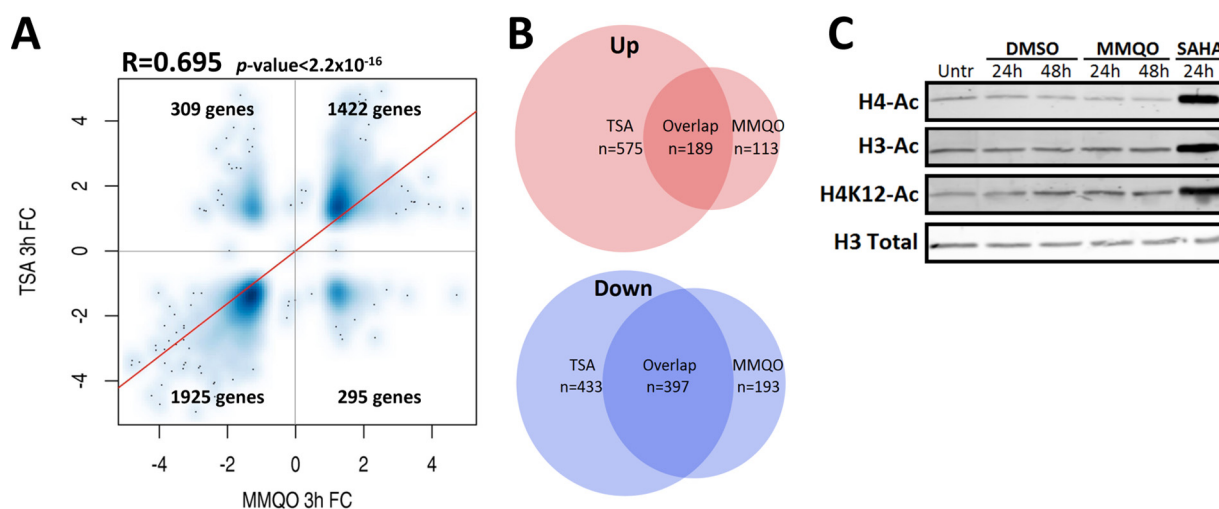


**FIG 4** MMQO targets acetylation-sensitive genes. (A and B) Microarray analysis comparing 3-h MMQO (160  $\mu$ M) and TSA (200 nM) treatments in Jurkat cells. Expression data were obtained by hybridization with an Agilent Human microarray platform. (A) Scatterplot depicting the fold changes for the 3,376 significant transcripts ( $q < 0.05$ ) from the TSA and MMQO 3-h data sets. The Pearson correlation coefficient and the number of genes in each quadrant are shown. (B) Venn diagrams of genes mutually upregulated or downregulated by MMQO or TSA ( $FC \geq 1.5$ ;  $q < 0.05$ ). The sizes of the circles are proportional to the gene numbers. (C) MMQO does not cause global hyperacetylation. Jurkat cells were incubated for 24 or 48 h with MMQO (160  $\mu$ M), SAHA (5  $\mu$ M), or DMSO or left untreated. Total protein was extracted with RIPA buffer and analyzed by immunoblotting against acetylated histone H4 (H4-Ac), H3, or H4K12 or total H3 as a loading control.

suggested that at least nine immunogenic pathways are downregulated (see Table S2 in the supplemental material).

Utilizing the Gene Set Enrichment Analysis (GSEA) toolkit, we observed the most significant MMQO-downregulated genes to be enriched in the transcription factor c-Myc-related gene sets; of the top 10 gene sets that correlated most closely with the genes downregulated by MMQO, 6 were canonically c-Myc dependent (see Table S3 in the supplemental material). In marked contrast, MMQO treatment did not significantly induce any gene set for transcription factors related to HIV-1 reactivation (e.g., NF- $\kappa$ B, STATs, IRFs, or AP-1).

**MMQO targets acetylation-sensitive genes.** Other than the dysregulation of immunosuppressive and c-Myc-dependent pathways among the GSEA results, HDAC-related gene sets were largely enriched, with nine gene sets correlating positively and three gene sets correlating negatively with MMQO treatment (see Table S4 in the supplemental material). It should be noted that these HDAC data sets contain nearly 1,000 transcripts, coinciding with the broad response produced by MMQO and suggesting the plausibility of MMQO being an HDAC inhibitor. A large proportion of the genes encompassed in the HDAC data sets are additionally related to the immune system, thus providing a possible explanation for the broad immunosuppression that has been witnessed with MMQO (18). This observation is also in agreement with previously published data showing that HDAC inhibitors have an immunosuppressive impact on both Jurkat cells and regulatory immune cells in general (23). A significant hallmark of HDAC inhibition in T cell leukemia cell lines like Jurkat is also the dysregulation of c-Myc. The downregulation of *MYC* mRNA by MMQO was confirmed to be dose dependent, extremely rapid, and persistent (Fig. 3D and E). The drastic decline of *MYC* gene expression due to MMQO further translates into the protein level (Fig. 3F), similar to the previously reported decrease caused by histone deacetylase inhibitors in Jurkat cells (24).

We performed another microarray experiment to compare the change in the gene expression profile between MMQO and the pan-HDAC inhibitor trichostatin A (TSA). While the overlap of the two compounds is significant (Fig. 4A), noteworthy divergences could also be highlighted. In total, 892 genes were differentially regulated by MMQO, while TSA treatment affected 1,594 genes (fold change cutoff,  $\pm 1.5$ ); the

overlap was 619 genes. Even though most of the MMQO-regulated genes are also dysregulated by TSA, only a minority of TSA-regulated genes are dependent on MMQO. A few of the prominent overlapping genes are highlighted in the volcano plot in Fig. 3A. The overlap between the two data sets is depicted in Venn diagrams, with up- and downregulated genes depicted separately (Fig. 4B).

Other than the differing effects of the chemicals on the transcriptome, we did not observe any global hyperacetylation of the chromatin in response to MMQO treatment (Fig. 4C). However, it is noteworthy that both MMQO and HDAC inhibitors presented potent immunosuppressive traits, hinting at coinciding mechanistic functions.

**MMQO functions as a bromodomain inhibitor.** A thorough review of the existing literature based on our experimental data led us to hypothesize that MMQO might function as a bromodomain-inhibiting protein, specifically by directly targeting the BET protein family member BRD4. The BET family proteins are responsible for recognizing acetylated chromatin via their bromodomains and for mediating transcriptional processes globally. Besides reactivating HIV transcription both Tat dependently and independently, downregulating c-Myc, and playing roles in proliferation and apoptosis, bromodomain inhibitors like JQ1 have also been reported to mimic HDAC inhibitors in their functions on the transcriptomes of cells from lymphoma lineages (25). The similarities between HDAC and bromodomain inhibition stem from their mutual protein targets. While HDAC inhibitors promote global chromatin hyperacetylation, inhibition of BET family proteins releases these proteins from the core histones, thus exposing the already acetylated lysine tails of the nucleosomes.

In addition to targeting a similar set of genes, BET family inhibitors have been shown to cause severe immunosuppression by disabling NF- $\kappa$ B's ability to mobilize to inflammatory superenhancer regions by disabling the direct interaction between BRD4 and the RelA subunit (26–29). We therefore performed another analysis comparing our microarray data with previously published data sets from microarrays performed with JQ1-treated J-Lat 10.6 HIV latency model cells (8). Even though there were crucial differences between the setups of our MMQO experiment and the published JQ1 experiments (24 h for JQ1 versus 8 h for MMQO, native Jurkat versus Tat-expressing J-Lat cells, and Agilent versus Affymetrix platforms), a significant overlap could be observed between the transcriptomes of the two drugs (Fig. 5A and B). Of note, the Pearson correlation coefficient is also higher than that for the previous comparison with TSA and MMQO (0.841 versus 0.695) (Fig. 4A).

To validate the microarray results, we compared the behaviors of MMQO and the gold standard BRD4 inhibitor, JQ1, alone or in combination, on HIV reactivation. The effects of JQ1 (1  $\mu$ M) and MMQO (160  $\mu$ M) on the latent HIV minigenome were similar in both Tat-positive (A2) and Tat-deficient (E89) minigenome-containing cells (Fig. 5C). To quantitate the interaction of JQ1 and MMQO, we treated A2 J-Lat cells with nontoxic increasing concentrations of both drugs (Fig. 5D). The ability of one drug to stimulate HIV reactivation was consistently decreased in the presence of increasing concentrations of the other drug, suggesting that the two drugs were targeting the same repressive mechanism. At high concentrations, both drugs behaved with neither a synergistic nor an additive pattern. This was further addressed using the Bliss independence model for combined drug effects. This model assumes that the stimulants act through separate mechanisms so that their effects multiply when administered in combination. A drug combination with an effect significantly exceeding the value predicted by the Bliss model can be said to exhibit synergy. We confirmed that JQ1 and MMQO cotreatments did not exhibit synergy at medium and high doses, but rather conformed to the predictions of the Bliss independence model (Fig. 5D, right) ( $>0$ , synergy;  $<0$ , antagonism). However, synergy was apparent at the lowest doses, leaving the Bliss testing partly inconclusive (see Discussion below).

Furthermore, we also examined the effect of MMQO cotreatment with JQ1 and another BET inhibitor compound, OTX-015, on *ex vivo*-infected primary CD4<sup>+</sup> T cells. Similar to what was observed in our T cell line models of latency, neither OTX-015 nor

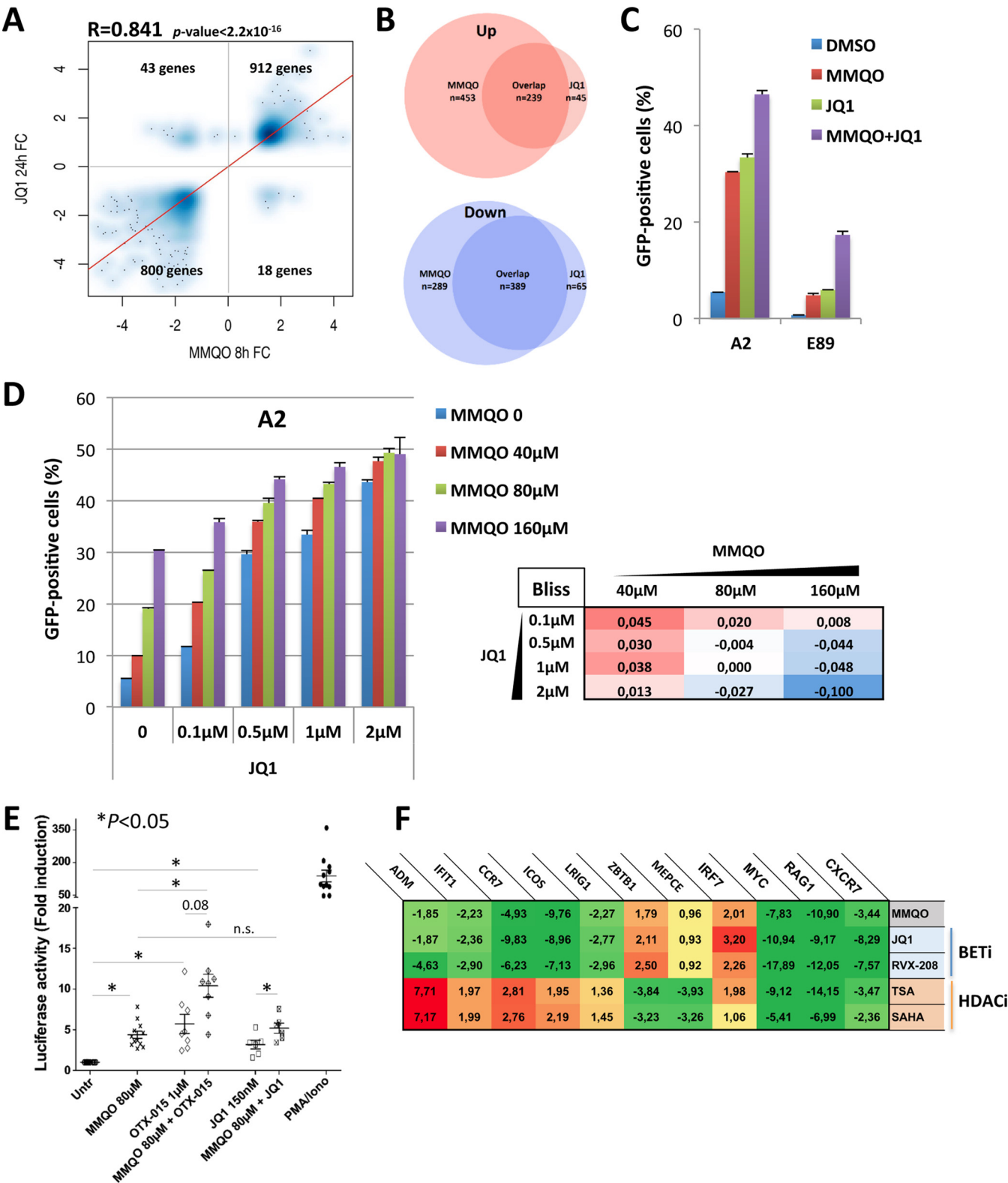


**FIG 5** MMQO functions as a bromodomain inhibitor. (A) Correlation between the transcriptome responses to MMQO and JQ1 treatments with RNA expression microarrays. Shown is a scatterplot of the fold changes for the 1,773 significant genes ( $q < 0,05$ ) from the JQ1 24-h (8) and MMQO 8-h (this work) data sets. The Pearson correlation coefficient and the number of genes in each quadrant are shown. (B) Venn diagrams of genes mutually upregulated or downregulated by MMQO or JQ1 ( $FC \geq 1.5$ ;  $q < 0.05$ ). The sizes of the circles are proportional to the gene numbers. (C) MMQO and JQ1 affect expression of the latent HIV-1 minigenome similarly. The indicated latently infected Jurkat clones were treated with MMQO (160  $\mu$ M) or JQ1 (1  $\mu$ M) for 24 h, and HIV expression was analyzed by FACS and expressed as a percentage of GFP-positive cells. The experiment was performed in triplicate. (D) MMQO and JQ1 do not synergize on HIV reactivation. J-Lat A2 latently infected cells were treated with various doses of MMQO (40 to 160  $\mu$ M) or JQ1 (0.1 to 2  $\mu$ M) for 24 h, and HIV expression was

(Continued on next page)

JQ1 was able to elicit synergistic latency reversal when used in combination with MMQO. Cotreatment resulted in a moderate additive-effect increase in luciferase activity, supporting the notion that MMQO targets the same repressive mechanism as OTX-015 and JQ1 (Fig. 5E).

To fully confirm that MMQO preferably displays BET-inhibitory behavior, we compared the effects of two known BRD4 inhibitors (JQ1 and RVX-208) and two HDAC family inhibitors (SAHA and TSA) on the MMQO-specific genes identified in the preceding microarrays. For this assay, we specifically concentrated on genes that showed opposite regulation by TSA in the 3-hour microarray (Fig. 4A, top left and bottom right quadrants). As a control for the proper functioning of the compounds, we additionally included genes universally dysregulated by both classes of drugs, like *IRF7*, *MYC*, *RAG1*, and *CXCR7*. Indeed, following a 3-h treatment with the five reagents, we witnessed MMQO displaying BET inhibitor-like behavior (Fig. 5F). As anticipated, we observed that HDAC inhibitors showed expression patterns similar to those of BET bromodomain inhibitors on the universal target genes. *IRF7* was upregulated by both classes of drugs, while *MYC*, *CXCR7*, and *RAG1* showed strong downregulation by all the drugs, further confirming the similarities between the two classes of compounds. However, MMQO-specific genes, like *ADM*, *IFIT1*, *CCR7*, *ICOS*, and *LRIG1*, were downregulated by bromodomain inhibitors but were upregulated by HDAC inhibitors. *ZBTB1* and *MEPCE* displayed potent downregulation by TSA and SAHA while being upregulated and unregulated by bromodomain inhibitors, respectively. According to this assay, all the chosen MMQO target genes displayed the expected differential regulation by the corresponding classes of drugs.

Furthermore, similar conclusions could be drawn by looking at the microarray data. Of the 295 genes upregulated with MMQO and downregulated with TSA in the scatterplot in Fig. 4A (3 h;  $q$  value  $< 0.05$ ), 55 genes were upregulated with JQ1 and none was downregulated, according to the JQ1 microarray data shown in Fig. 5A (24 h;  $q < 0.05$ ). Of the 309 genes downregulated with MMQO and upregulated with TSA, 32 genes were downregulated with JQ1 and only 3 were upregulated (see Fig. S1 in the supplemental material).

In conclusion, consistent with the hypothesis that MMQO is a BRD4 inhibitor, we observed that genes that were differentially regulated by MMQO were also specifically dysregulated by the bromodomain inhibitors JQ1 and RVX-208. Furthermore, MMQO and bromodomain inhibitors acted nonsynergistically on the reactivation of latent HIV.

**Structural basis of MMQO interactions with the bromodomains of BRD4.** To understand MMQO recognition by the bromodomains (BD1 and BD2) of BRD4, we next performed a nuclear magnetic resonance (NMR) binding study using  $^1\text{H}/^{15}\text{N}$  heteronuclear single quantum coherence (HSQC) spectra to assess MMQO binding to BD1 or BD2 of BRD4. As shown in Fig. 6A, both  $^{15}\text{N}$  HSQC spectra exhibited major chemical shift perturbation of key residues upon addition of MMQO to the protein solution, confirming that MMQO is able to bind to both BD1 and BD2. We determined the binding affinities of MMQO to BD1 and BD2 of BRD4 with a  $K_d$  (dissociation constant) of  $5.45\ \mu\text{M}$  for BD1 and a  $K_d$  of  $3.44\ \mu\text{M}$  for BD2 using isothermal titration calorimetry (ITC) (Fig. 6B).

To determine the detailed molecular basis of MMQO recognition by BRD4 bromodomains, we solved the three-dimensional structure of BRD4 BD1 bound to MMQO using heteronuclear multidimensional NMR spectroscopy (Fig. 6C). Analysis of the 20 final

#### FIG 5 Legend (Continued)

analyzed by FACS and expressed as a percentage of GFP-positive cells. Calculation of synergy for the different combinations was carried out according to the Bliss independence model (16) and is represented as a heat map on the right. The experiment was performed in triplicate. (E) *Ex vivo*-infected primary CD4<sup>+</sup> T cells were left untreated or treated with  $80\ \mu\text{M}$  MMQO alone or in combination with  $1\ \mu\text{M}$  OTX-015 or  $150\ \text{nM}$  JQ1 for 24 h, followed by luciferase assay; each point represents a single measurement. Experiments were performed in duplicate using cells isolated from at least 3 healthy blood donors. Student's  $t$  test was used to confirm significant differences between treatments. \*,  $P < 0.05$ . A  $P$  value of 0.08 is also shown. n.s., nonsignificant. (F) RT-qPCR analysis of the effects of BETi and HDACi on genes selected for their opposite expression in the 3-h MMQO/TSA arrays. Jurkat cells were treated for 3 h with MMQO ( $160\ \mu\text{M}$ ), RVX-208 ( $80\ \mu\text{M}$ ), JQ1 ( $1\ \mu\text{M}$ ), SAHA ( $5\ \mu\text{M}$ ), or TSA ( $200\ \text{nM}$ ). *GAPDH* was measured for normalization, and the results are represented relative to untreated cells. The heat map color coding represents the fold change to untreated cells. The experiment was performed in duplicate, and only genes that had reliable SD values are depicted.



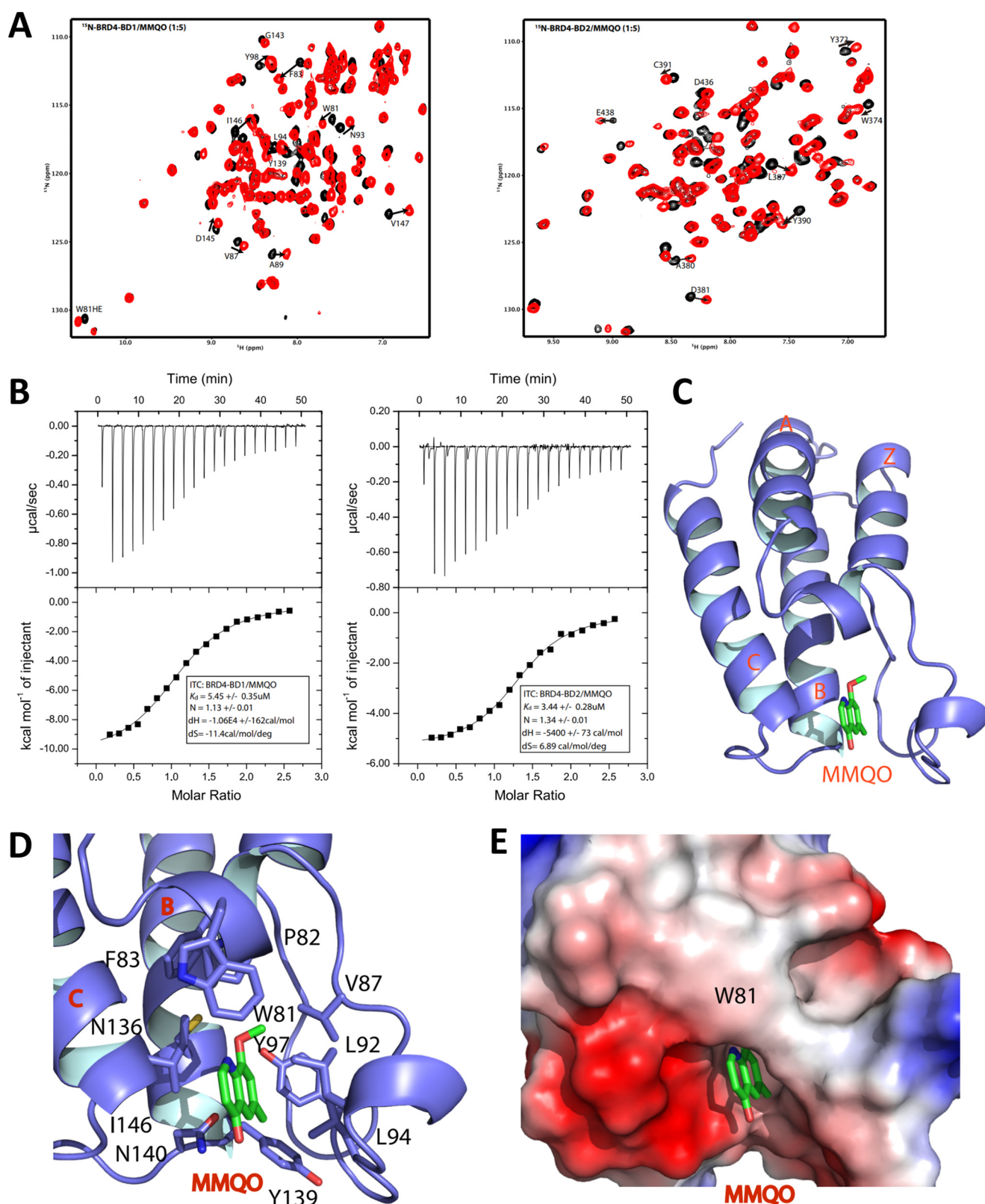


**FIG 6** Structural analysis of MMQO interaction with BRD4 bromodomains. (A) Two-dimensional (2D)  $^{15}\text{N}$ -HSQC spectrum of BRD4 BD1 (left) or BD2 (right) in the free form (black) and in complex with MMQO compound (red). The protein concentration was 0.1 mM, and the molar ratio of the protein to the compound was 1:5. (B) ITC measurement of BRD4 BD1 or BD2 binding to MMQO. (C) Ribbon depiction of the lowest-energy NMR structure of BRD4 BD1 (light blue) in complex with MMQO (green). (D) Ribbon and stick diagram of BRD4 BD1 binding pocket showing side chain interactions of protein residues in BRD4 BD1 with MMQO. BD1 residues involved in ligand binding are colored light blue, and MMQO is green. The orientation is the same as in panel C. (E) Electrostatic potential surface representation of BRD4 BD1 bound to MMQO (green). The quinoline pyridine ring is exposed to the solvent outside the pocket. The orientation is the same as in panel C.

NMR structures of the complex revealed root mean square deviations (RMSDs) of 0.16 Å and 0.50 Å for secondary backbone and heavy atoms, respectively (data not shown; see Table S5 in the supplemental material), signifying well-resolved NMR structures with highly refined conformations. Superimposing backbone atoms between the NMR structure of the BRD4 BD1-MMQO complex and the crystal structure of the BRD4 BD1-MS417 complex (Protein Data Bank [PDB] accession no. 5Z9C and 4F3I, respectively) yielded an RMSD at 0.94 Å, indicating that the protein structures are similar in different ligand-bound states (data not shown).

Although MMQO and MS417 bind similarly into the BRD4 BD1 pocket, MMQO does not form a hydrogen bond interaction with Asn140 of BD1, which is key for acetyl-lysine, as well as MS417, binding (30, 31). Nevertheless, the carbonyl group of the quinoline ring in MMQO is close to the side chain amide of Asn140. The aromatic ring with two methyl groups (ring A) intercalates into the acetyl-lysine binding pocket in BRD4 BD1, and the methyl group was observed to have nuclear Overhauser effect (NOE) signals in the NMR spectra to side chain atoms of Val87, Leu92, Leu94, Tyr139, and Ile146, indicating ligand recognition involving hydrophobic interactions (Fig. 6D and E). The methoxy group of ring A is bound in the WPF (Trp81, Pro82, and Phe83) groove and shows hydrophobic interactions with Trp81, Pro82, Val87, Leu92, and Ile146. Also, an aromatic orthoproton with respect to the methyl and methoxy groups of ring A displays hydrophobic interactions with Phe83, Val87, Cys136, Ile146, and Ala150, while the paraproton to the methoxy group interacts with Leu92, Leu94, and Ile146. The quinoline pyridine ring is exposed to the outside of the binding pocket, and protons on the pyridine ring did not show any intermolecular NOEs to the protein. Because the residues of BRD4 BD1 involved in MMQO binding are conserved in BD2, this explains why BD2 binds to MMQO with similar affinity.

Altogether, the RT-PCR, microarray, and *in vitro* experiments convincingly demonstrated that MMQO interacts with the two bromodomains of the BRD4 protein, thus forcing the dysregulation of the acetylation-sensitive transcriptome.

**BET inhibitors reactivate latent HIV-1 integrations distinct from those of HDAC inhibitors and PKC pathway agonists.** Understanding how MMQO functions allowed us to investigate its effect on the latent minigenome more adequately. Recently, a method called B-HIVE was proven to function as an effective tool to map HIV inserts across different integration loci throughout the genome and to correlate their responsiveness to LRAs (19). Utilizing this new method, we intended to characterize the specific subsets of proviral integrations capable of being reactivated by BRD4 inhibition with MMQO and JQ1. As mechanisms for comparison to bromodomain inhibition, we also included SAHA as an HDAC inhibitor and prostratin as a PKC pathway-inducing agent.

Native Jurkat cells were first infected with a barcoded library of GFP-expressing minigenomes. Four days later, the GFP-positive cells were sorted by fluorescence-activated cell sorting (FACS) and left to expand for 19 days. The GFP-negative cells were then isolated, cultured for 2 weeks, and used for treatments. Following a 24-hour treatment in duplicate with either MMQO, JQ1, SAHA, prostratin, or an equivalent volume of dimethyl sulfoxide (DMSO) as a vehicle, we extracted RNA from the treated cell pool and amplified the reverse-transcribed viral cDNA with HIV-specific primers. Each reactivated provirus produced a barcoded transcript, allowing us to distinguish it from the others. The amplified barcodes were then submitted to sequencing and bioinformatics analysis to determine specific proviruses that were activated by each treatment. Hierarchical clustering carried out on the reactivated barcodes confirmed the tight clustering of the duplicate controls (Fig. 7A). More importantly, the MMQO-treated samples clustered remarkably well with the JQ1-treated samples, confirming MMQO specificity as a bromodomain-inhibiting reagent. To our surprise, the responding barcodes from prostratin and SAHA treatments grouped together but separately from the bromodomain-inhibited samples. This result demonstrates how different subsets of HIV-1 minigenome integrations are activated by separate canonical reactivating mechanisms. The dendrogram denoting expression of all sequenced integra-

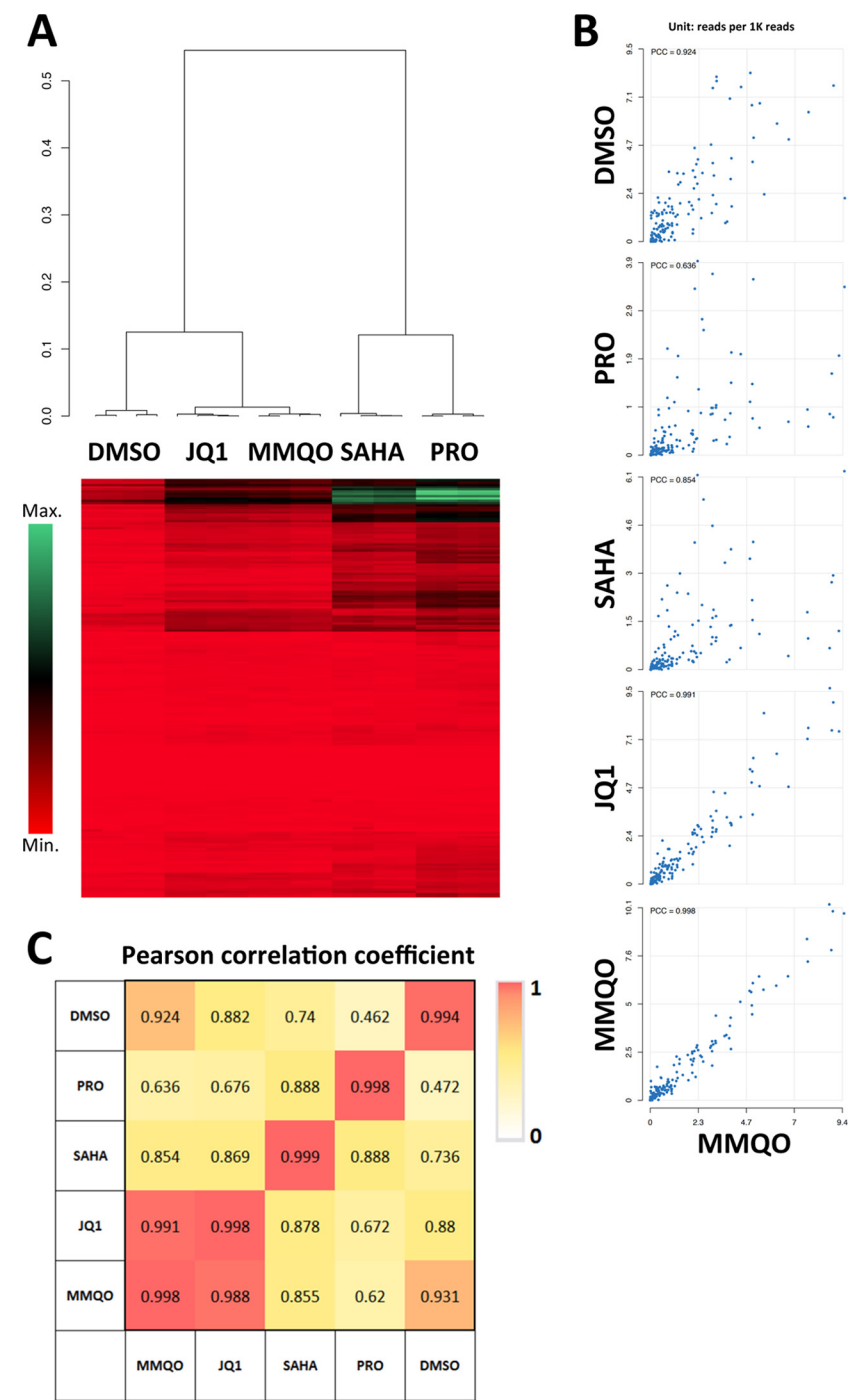


**FIG 7** Effects of bromodomain inhibitors on individual proviruses. (A) Cells infected with a barcoded library of HIV minigenomes and sorted for silenced HIV were treated with either MMQO, JQ1, SAHA, prostratin (PRO), or DMSO for 24 h. RNA was extracted and subjected to B-HIVE to determine the specific proviruses that were activated with each treatment. Shown is a heat map and its corresponding dendrogram of the mRNA tag counts of proviruses under different conditions. The experiment was performed in duplicate with each sample sequenced twice. (B) Scatterplots of the mRNA tag counts of proviruses for MMQO compared to other drugs. (C) Pearson correlation coefficients corresponding to the scatterplots of the mRNA tag counts of proviruses under different conditions.

tions shown in Fig. 7A demonstrates how prostratin activates a larger number of HIV integrations, and to a greater extent than the other drugs, in agreement with the data shown in Fig. 1. The integrants responded almost identically to MMQO and JQ1 but differently to SAHA, confirming once more the functionality of MMQO.



Next, in scatterplots, we compared the mRNA barcode tag counts of proviruses under each condition (Fig. 7B and C). Again, MMQO response was strongly correlated with JQ1, similar to the duplicates, and the lowest correlation was with prostratin. This indicated that the responses of each provirus were very similar between treatments with drugs from the same functional family and reproducible with the same drug. However, there was substantial variation in the expression of the same provirus treated with different drugs. Thus, bromodomain inhibitors stimulate different subsets of latent proviruses than HDAC inhibitors or PKC agonists. The high correlation (0.92) between the relative expression of the proviruses upon MMQO and DMSO treatment indicates that MMQO has similar effects on most of the proviruses. If MMQO acted strongly on only a subset of the proviruses, the overall distribution of expression would differ and the correlation with DMSO treatment would decline further (as in the case of prostratin).

Next, we ranked the proviral integrations as a function of their response to each drug and focused our analysis on the top 15% and 50% of responders to each drug. Most of the MMQO and JQ1 top responsive proviruses were common between the two drugs (see Fig. S2 in the supplemental material). Approximately 75% of these proviruses were inserted within active genes (the rest consisted of 6% in enhancers and 19% in intergenic regions). Among the 38 genes that hosted an HIV integration that responded to MMQO and JQ1 (from the list of the top 50% of responders), 9 were dysregulated upon MMQO treatment in our microarray experiment (4 genes were upregulated, and 5 were downregulated). All of these genes contain at least a region enriched in BRD4 according to chromatin immunoprecipitation sequencing (ChIP-seq) data in Jurkat cells published previously (GEO accession number [GSE83777](#)). In Fig. S3 in the supplemental material, we present snapshots of several of these genes. Therefore, proviruses that respond to BET inhibitors do not need to be inserted in genes that respond to the drug. This is in line with the finding that there is no correlation between the expression of the HIV provirus and its host gene (19). In fact, BRD4 is present at the promoters of a vast majority of host genes, colocalizing with the RNA polymerase (see Fig. S3 in the supplemental material; data from [GSE83777](#)). According to the MMQO and JQ1 microarrays mentioned above, only a minor proportion of genes showing BRD4 at the promoter are affected by treatment with BETi.

In conclusion, we report that MMQO, despite having a very different chemical structure, behaves like JQ1 and other BETi on HIV and global host gene expression, targeting BRD4 directly. BETi reactivate a subset of HIV proviruses with limited overlap with HDACi and PKC agonists. Although most proviruses are hosted within active genes and genes may present BRD4 at their promoters, HIV activation by BETi does not correlate with the response of the corresponding host genes to these drugs.

## DISCUSSION

In this work, we describe a workflow to characterize and determine the mechanism of a novel HIV-1-reactivating scaffold compound. Combining simple HIV-1 latency models with basic biochemical methods, RNA expression microarray technologies, and *in vitro* ligand identification methods, we demonstrate that MMQO interacts with bromodomains of BRD4 and functions as an inhibitor of the protein. BRD4 inhibition as a mechanism provides potential not only in anti-HIV settings, but also for suppression of tumorigenesis and as a regulator of immunomodulatory clinical applications. As indicated in the comparative microarrays between HDAC and bromodomain inhibition, the latter mechanism targets a more limited set of genes, which could possibly highlight the possibility that BET inhibitors have fewer side effects in clinical applications than HDAC inhibitors. Nevertheless, bearing in mind the simplistic structure of MMQO and the molecular promiscuity of BET family inhibitors in general (reviewed in reference 32), it is possible that MMQO additionally targets other bromodomains that we were not able to identify due to the constrained mRNA and protein expression detection-based methods.

**Functional evaluation of MMQO.** The quinoline scaffolds that MMQO is composed of have previously been called “privileged structures” with rich diversity in biological

properties (33). Numerous quinoline-structured chemotherapeutics are currently available on the market (e.g., lenvatinib, topotecan, and irinotecan), and they have been found to be applicable in research settings. Quinolines are applied as DNA intercalators, G quadruplex structure stabilizers, androgen receptor antagonists, metal ion chelators, and antimitotic agents. A large variety of inhibitors of tubulin polymerization, histone acetyltransferases, topoisomerases, kinesins, mTOR, PARP, proteasomes, and mitogen-activated protein kinases (MAPKs) have also been developed. Immunomodulatory effects of quinolones have been described with HDAC-, sirtuin-, STAT3-, and NF- $\kappa$ B-inhibitory chemicals (reviewed in reference 34). The 8-hydroxyquinoline structures, which served as lead compounds for designing MMQO, are specifically known to present excellent scaffold compound characteristics and have shown promise in the development of anticancer, antifungal, and antiparasitic agents and even as HIV integrase inhibitors (35). Although MMQO displays potential as a new class of bromodomain inhibitor, broader *in vitro* assays targeting the whole BET family should be carried out in order to evaluate its specificity toward their different bromodomains.

During the complex process of lead compound design, the drug-related factors that have to be taken into account are its potency, half-life in physiological settings, ease of extraction or synthesis, molecular weight (smaller molecules diffuse better), and number of reactive hydrogen bonds, among other requirements (reviewed in reference 36). Following the discovery of the first BRD4 inhibitor in 2010, various small molecules besides JQ1 have been designed. The most successful reagents are based on the triazolodiazepine structure (such as JQ1, CPI-203, OTX-015, and I-BET-762), but alternative scaffolds have also been proposed (37). Although quinoline structures have been the basis for BRD4 inhibition, as well (38), to our knowledge, none of these preliminary compounds has been developed into a final commercially available product.

MMQO provides a new minimalistic yet optimizable platform to design inhibitors of the BET family proteins, whether for clinical applications or simply as biochemical tools for research use. With the existing structure, we demonstrated that MMQO inhibits both BD1 and BD2 of BRD4 with similar potencies. To our surprise, the affinity between BRD4 and MMQO exists independently of interaction with the asparagine residues, normally a compulsory feature for bromodomain inhibitors. As a starting point for modification, improvements could be carried out on the benzene ring of MMQO to improve its affinity for the asparagine residues of bromodomains. Additionally, enhancement of MMQO could be achieved by designing additional functional groups to interact with the solvent-exposed WPF shelf of the BET family proteins, which are lacking in the existing MMQO structure but are necessary to determine the drug's higher affinity and specificity.

Along with our studies, we tested another bromodomain inhibitor for HIV reactivation, RVX-208, known to bind preferentially to BD2 domains of BET family proteins (39). Reactivation was achieved with doses  $\sim$ 20 times higher than those normally used for BD2 inhibition (data not shown), suggesting that the compound functions on the HIV-1 minigenome through nonspecific mechanisms, most probably by inhibiting the BD1 domain of BRD4. Our results suggest that inhibition of BRD4 BD2 alone is not sufficient to rescue the HIV-1 minigenome from latency. BD2 has been previously shown to bind the triple-acetylated cyclin T1 subunit of the P-TEFb complex, thus regulating its transcriptional activity (40). The lack of HIV-1 reactivation in this context suggests that the chemical inhibition of BD2 is not a sufficiently potent mechanism to increase the global free P-TEFb pool that can be hijacked by the viral Tat protein. Interestingly, our results with Tat-negative minigenomes highlight the fact that bromodomain inhibitors function independently of the Tat protein, suggesting that BRD4 could potentially harbor an alternative suppressive mechanism in HIV-1 transcription, aside from its canonical competition with the P-TEFb complex. Analogous observations were also made with similar HIV-1 minigenomes (9, 41). The exact repressive roles of BRD4 on the HIV-1 promoter remain elusive and should be further studied.

JQ1 is known to additionally inhibit the second bromodomain of BRD4 (BRD4 BD2), as well as other members of the BET family (42). If the drug can target multiple sites

simultaneously, even on the same protein, then according to the Bliss model, it can be considered to have different mechanisms. This could explain the synergism we observed between MMQO and JQ1 at low doses. Nevertheless, at higher doses, this synergy dissipates, suggesting that the effect on the latent minigenome can easily be saturated and the alternative BET-inhibitory mechanisms can be overwhelmed.

**Reimagining the shock.** CD4<sup>+</sup> T lymphocytes are known to migrate and reside in various organs besides the blood, including the brain, lymph nodes, gut, lungs, and female reproductive tract, to name a few (43). Since only 2 to 5% of the total CD4<sup>+</sup> T lymphocyte population resides in the blood, it is crucial that the proposed new LRAs possess the ability to diffuse to and function in different tissues. In addition to participating in various physiological functions, the migrated T lymphocytes might also possess diverging phenotypes, which could further interfere with drug responsiveness. The uneven outcomes due to the differences of individual compounds in the case of shock and kill therapies have already been observed: even though the HDAC inhibitors romidepsin and panobinostat increased plasma viremia and T lymphocyte activation, SAHA failed to do so (reviewed in reference 7). Furthermore, prior experiments utilizing the B-HIVE method demonstrated how SAHA targeted proviral integration sites separate from those targeted by phytohemagglutinin (PHA), primarily by reactivating minigenomes in the vicinity of gene enhancers (19). Due to the complex nature of the infected cells, a large variety of LRAs have to be identified and developed for tissue penetration, cell type, and provirus integration locus specificity.

Employing the same B-HIVE technology, we illustrated how bromodomain inhibition additionally targets separate subsets of integration events. Based on the distinct targeting mechanisms and the synergies witnessed among the tested compounds (MMQO, prostratin, and SAHA), these different agents might in the future have to be administered as cocktail regimens for an efficient shock and kill therapy. Ideally this shock cocktail should have minimal effect on T lymphocyte activation and global chromatin stability yet be able to maximally induce proviral reactivation. Even though small-molecule PKC pathway agonists like PMA, prostratin, and bryostatin 1 are known to lead to a cytokine storm in clinical trials against cancer, the doses needed for viral reactivation result in minimal cytokine release from T lymphocytes under *ex vivo* conditions (16). Additionally, the inhibitors of histone deacetylases, like valproic acid, TSA, and SAHA, have been shown to maintain the activation of resting T lymphocytes at a minimal level (reviewed in reference 44).

According to recent observations, once HIV-1 transcription passes the first phase of Tat production, HIV-1 expression can function autonomously of cellular relaxation due to the potency of the positive-feedback loop of Tat (45). This fact suggests that HIV-1 reactivation should be possible in resting CD4<sup>+</sup> T lymphocytes in a clinical setting, as well. More importantly, it implies that for an efficient therapy, activating only the first block of viral transcription (Tat protein production) should be enough to initiate the shock cascade. We propose that further assays be carried out to fully comprehend the effects of mixtures of reagents with distinct mechanisms of action in combination with the B-HIVE technology. Furthermore, these experiments should be carried out in Tat-negative models for added benefit, since in a physiological latency setting, the viral Tat protein is not sufficiently abundant. Alternatively, CD32a was recently identified as a specific marker of quiescent and latently infected HIV-harboring T lymphocytes (46). For additional clinical significance, the optimal synergies between the different classes of drugs for clinical pilot studies could be identified by utilizing quantitative viral outgrowth assays of sorted CD32a-expressing T lymphocytes isolated from HIV-positive patients. The clarification of the full potential of the synergies these compounds will generate could lead to a clinically acceptable regimen that is also capable of delivering the needed reservoir reactivation within patients.

Currently the HIV research field is still struggling with crucial unanswered questions on latency, such as the location of viral reservoirs within the patient, the cell types harboring these proviruses, and their responsiveness to LRA (reviewed in reference 47).

We think that no single compound is diverse or potent enough to qualify as a universal solution and to reactivate the whole quiescent viral reservoir; thus, a combination of optimally synergizing pharmaceuticals administered at safe doses would be needed for a maximal proviral response. As an added benefit, the cocktail compounds could theoretically be administered at lower doses than their individual components, since ideally the synergy between the reagents should exceed the potential of any single agent. With the recent development of new chemicals to reactivate latent HIV via alternate pathways, like Toll-like receptors (48, 49) and the inhibition of the SWI/SNF complex (50), a broad range of possible cocktails can be assayed for efficacy. Keeping in mind that MMQO targets a unique subset of proviral integrations, bromodomain inhibitors could play a decisive role in the design of efficient shock remedies.

## MATERIALS AND METHODS

**Cell lines, culturing conditions, and cell treatments.** Jurkat cells or latently infected derivatives carrying the pEV731 or pEV658 minigenome (LTR-Tat-IRES-GFP-LTR) were grown at 37°C with 5% CO<sub>2</sub> in RPMI 1640 medium (Sigma; R8758) supplemented with 10% fetal bovine serum (FBS) without additional antibiotics. Jurkat clones and heterogeneous Jurkat populations were described previously (17, 18). Heterogeneous HeLa cell populations were created according to a previously described protocol (17). HEK293T and HeLa cell lines were grown at 37°C with 5% CO<sub>2</sub> in Dulbecco's modified Eagle's medium and GlutaMax medium containing 10% FBS supplemented with 100 U/ml penicillin and 100 µg/ml streptomycin.

When indicated, cells were treated with reagents at the concentrations and for the durations provided in the figure legends. All the reagents were dissolved in DMSO, and when possible, the concentration of DMSO was kept at 1 µl/ml or below. DMSO, PMA, HMBA, prostratin, and TSA were purchased from Sigma and SAHA, JQ1, and RVX-208 from Selleck Chemicals. All the reagents were diluted in DMSO.

**Primary CD4<sup>+</sup> T cell isolation and infection.** Primary CD4<sup>+</sup> T cells were isolated from buffy coats from healthy donors by Ficoll gradient, followed by density-based negative selection of CD4<sup>+</sup> T cells using RosetteSep (Stem Cell Technologies, Cambridge, United Kingdom). After isolation, the cells were left for 24 h to rest, followed by infection as previously described, with minor modifications (51). Briefly, CD4<sup>+</sup> T cells were infected with the pNL4-3.Luc.R<sup>-</sup> E<sup>-</sup> virus by spinoculation at 1,200 × g for 120 min. The spin-infected cells were incubated overnight at 37°C in a humidified 95% air-5% CO<sub>2</sub> atmosphere. The next day, the cells were washed and cultured in RPMI 1640 medium (Sigma) supplemented with 10% FBS, 100 µg/ml penicillin-streptomycin, and 5 µM saquinavir mesylate. Three days after infection, the cells were left untreated or treated as indicated in the presence of 30 µM raltegravir. Cells were harvested 24 h after stimulation, and luciferase activity was measured with a luciferase assay system (Promega, Leiden, Netherlands). Viral pseudotyped particles were generated as previously described (50). The data were normalized either as the fold increase over the untreated control or as percent PMA. The following compounds were used to stimulate cells: PMA (Sigma-Aldrich), ionomycin (Sigma-Aldrich), SAHA/vorinostat (Selleck Chemicals), prostratin (Sigma-Aldrich), pyrimethamine (Sigma-Aldrich), CAPE (MP Biomedicals), OTX-015 (ApexBio), and JQ1 (Sanbio).

**Apoptosis and viability of primary CD4<sup>+</sup> T cells.** In order to determine apoptosis, primary CD4<sup>+</sup> T cells were left untreated or stimulated in duplicate for 24 and 72 h, as indicated. The cells were washed with Dulbecco's phosphate-buffered saline (DPBS) (Lonza) supplemented with 3% serum, 2.5 mM CaCl<sub>2</sub> and stained with anti-annexin V-phycoerythrin (PE) (BD Biosciences; catalog no. 556454). The viability of the *ex vivo*-infected primary CD4<sup>+</sup> T cells was measured by flow cytometry on the basis of forward versus side scatter. Samples were analyzed with a Becton Dickinson Fortessa flow cytometer. The data represent cells isolated from at least 3 independent buffy coats.

**Microarrays.** Total RNA was extracted using a High Pure RNA isolation kit (Roche) according to the manufacturer's instructions. High RNA integrity was assessed by Bioanalyzer nano-6000 assay (Agilent Technologies). Sample preparation was described previously (52). For each sample, 100 ng of total RNA was reverse transcribed into cDNA with a T7 promoter, and the cDNA was *in vitro* transcribed into cRNA in the presence of Cy3-CTP using a low-input Quick Amp kit (Agilent). Labeled samples were purified using RNeasy mini-spin columns (Qiagen). Then, 600 ng of cRNA was preblocked and fragmented in Agilent fragmentation buffer and mixed with Agilent GEx hybridization mix. The hybridization mixture was laid onto each sector of a subarray gasket slide and sandwiched against an 8 by 65,000 format oligonucleotide microarray (Human v1 Sureprint G3 Human GE 8×60K microarray; Agilent design 028004) inside a hybridization chamber, which was hybridized overnight at 65°C. Subsequently, the array chambers were disassembled, submerged in Agilent Gene Expression Buffer 1, and washed for 1 min in another dish with the same solution using a magnetic stirrer at 200 rpm at room temperature, followed by 1 min in Agilent Gene Expression Buffer 2 with a magnetic stirrer at 200 rpm at 37°C, immediate withdrawal from the solution, and air drying. The fluorescent signal was captured as TIF images with an Agilent scanner using the recommended settings with Scan Control software (Agilent). The signal intensities were extracted into a tabulated text file using Feature Extraction software (Agilent) with the appropriate array configuration and annotation files. The normalized log<sub>2</sub> intensities were obtained by the quantile method with normalized expression background correction using the Bioconductor Limma package in R.

**Microarray analysis.** Genes were sorted and organized for further analysis based on the normalized  $\log_2$  intensities obtained. Transcripts with a false-discovery rate ( $q$  value) of  $<0.05$  were considered significantly differentially expressed, and transcripts represented in multiples in several probes had their fold changes calculated to a mean value. The differentially expressed genes were then analyzed utilizing the g:Profiler toolkit (<https://biit.cs.ut.ee/gprofiler/>), GSEA software (<http://software.broadinstitute.org/gsea/index.jsp>), and R. Scatterplots and Pearson's correlation coefficients were produced using in-house R scripts.

**RNA extraction, reverse transcription, and real-time PCR.** Total RNA was extracted using a TRIzol kit (Ambion). cDNA was generated from 50 to 100 ng of RNA using a Superscript Vilo cDNA synthesis kit (Invitrogen). Gene products were analyzed by qPCR using SYBR green master mix (Invitrogen) and specific oligonucleotides in a Roche Applied Science 480 light cycler machine on 96-well plates. The primers used for qPCR are listed in Table S6 in the supplemental material.

**Protein extraction, gel electrophoresis, and immunoblotting.** Cells were washed once with PBS, and proteins were extracted in the lysis buffers indicated in the figure legends. Radioimmunoprecipitation assay (RIPA) lysis buffer was supplemented with  $1\times$  protease inhibitor cocktail (Roche), 1 mM  $\text{Na}_3\text{VO}_4$ , 5 mM NaF, 1  $\mu\text{g/ml}$  leupeptin, 0.5  $\mu\text{g/ml}$  pepstatin, 0.5  $\mu\text{g/ml}$  aprotinin, 20 mM  $\beta$ -glycerophosphate, and 1 mM phenylmethylsulfonyl fluoride (PMSF) to block product degradation. The protein concentration was determined by bicinchoninic acid (BCA) assay (Pierce), and 10 to 30  $\mu\text{g}$  of protein was boiled in Laemmli buffer and electrophoresed in 7.5 to 15% SDS-polyacrylamide gels. The separated proteins were transferred to nitrocellulose or polyvinylidene difluoride (PVDF) membranes (constant 400 mA;  $4^\circ\text{C}$ ) for 1.5 h. Blots were blocked in Tris-buffered saline (TBS) solution containing 0.1% Tween 20 (TBST) and either 5% nonfat dry milk, 3% bovine serum albumin, or 1:1 Odyssey blocking buffer for 1 h and incubated with primary antibodies at room temperature for 1 h or overnight at  $4^\circ\text{C}$ , followed by 3 10-min washes with TBST, and incubated with secondary antibodies for 1 h at room temperature. Following 3 washes of the secondary antibodies, the immunodetection of specific proteins was carried out with primary antibodies using the Odyssey infrared imaging system (Li-Cor).

**Flow cytometry.** GFP fluorescence was measured in a Cytomics FC500 MPL flow cytometer or a CytoFlex system (Beckman Coulter). A two-parameter analysis was used to distinguish viable cells (identified by forward and side scatter) containing GFP-derived fluorescence (525 nm) from the background. Fluorescence was represented in a logarithmic scale, and on average,  $>10,000$  events were observed per sample. Optical calibration was carried out using 10-nm fluorescent beads (Flow-Check fluorospheres; Beckman Coulter). Cell sorting was carried out with a FACS Aria cell sorter (BD Biosciences).

**Bliss independence model.** Lack of synergy between JQ1 and MMQO was calculated according to the Bliss independence model as described previously (16). The data are presented as the difference between the observed and predicted fractional responses relative to a 24-hour PMA (10 nM) treatment. The Bliss independence model assumes that two different drugs act through separate molecular mechanisms and therefore in an additive manner.

**Sample preparation for NMR.** The first bromodomain (BD1) of human BRD4 (residues 53 to 169) in the pNIC28 vector was expressed and purified using a procedure described previously (53). Briefly, the His-tagged BRD4 BD1 domain was overexpressed in *Escherichia coli* pRIL plasmid BL21-CodonPlus cells and induced with 0.3 mM isopropyl- $\beta$ -D-thiogalactopyranoside at  $18^\circ\text{C}$ . His-tagged BRD4 BD1 was purified by HiTrap immobilized-metal affinity chromatography (IMAC) (GE Healthcare). After removing the His tag with thrombin or tobacco etch virus (TEV) protease treatment, protein samples were further purified on a Superdex 75 or Superdex 200 column (GE Healthcare). Uniformly  $^{15}\text{N}$ - or  $^{15}\text{N}/^{13}\text{C}$ -labeled proteins were prepared as unlabeled protein by growing the bacteria in M9 minimal medium containing  $^{15}\text{NH}_4\text{Cl}$  with or without  $[^{13}\text{C}]\text{glucose}$ .

**Nuclear magnetic resonance spectroscopy.** The BRD4 BD1 domain-MMQO compound complex was used for structure determination. NMR samples of the BD1 domain (0.5 mM) in complex with 1.5 mM MMQO compound were prepared in phosphate-buffered saline (PBS) (pH 7.4) in  $\text{H}_2\text{O}$ - $\text{D}_2\text{O}$  (9/1) or  $\text{D}_2\text{O}$ . All NMR spectra were acquired at  $25^\circ\text{C}$  on Bruker 500-, 700-, 800-, and 900-MHz spectrometers equipped with z-axis gradient triple-resonance cryoprobes. The backbone  $^1\text{H}$ ,  $^{13}\text{C}$ , and  $^{15}\text{N}$  resonances were assigned using standard three-dimensional triple-resonance HNCA, HN(CO)CA, HN(CA)CB, and HN(COCA)CB experiments (54). The side chain atoms were assigned from three-dimensional HCCH-total correlation spectroscopy (TOCSY), HCCH-correlation spectroscopy (COSY), and (H)C(CO)NH-TOCSY data (55). The NOE-derived distance restraints were obtained from  $^{15}\text{N}$ - or  $^{13}\text{C}$ -edited three-dimensional nuclear Overhauser effect spectroscopy (NOESY) spectra. The MMQO was assigned from a one-dimensional  $^1\text{H}$  spectrum and two-dimensional TOCSY and NOESY and  $^{13}\text{C}/^{15}\text{N}$ -filtered TOCSY and NOESY spectra. The intermolecular NOEs used in defining the structure of the complex were detected in  $^{13}\text{C}$ -edited (F1),  $^{13}\text{C}/^{15}\text{N}$ -filtered (F3) three-dimensional NOESY spectra (unlabeled MMQO compound bound to  $^{13}\text{C}/^{15}\text{N}$ -labeled BD1 protein) (56). Spectra were processed with NMR Pipe and analyzed using NMR View (57, 58).

**Structure calculations.** The structures of the BRD4 BD1 domain/MMQO were calculated with a distance geometry simulated annealing protocol with CNS (59). Initial protein structure calculations were performed with manually assigned NOE-derived distance constraints. Hydrogen bond distance and  $\phi$  and  $\psi$  dihedral-angle restraints from the TALOS-N prediction were added at a later stage of structure calculations for residues with characteristic NOE patterns (60, 61). The converged structures were used for the iterative automated NOE assignment by ARIA refinement. Structure quality was assessed by CNS, ARIA, and PROCHECK analysis (61, 62). A total of 30 intermolecular NOE-



derived distance restraints were added in the structure determination of the BRD4 BD1-MMQO complex. A family of 200 structures was generated, and the 20 structures with the lowest energies were selected for the final analysis.

**Isothermal titration calorimetry.** Experiments were carried out on a MicroCal auto-ITC200 instrument at 25°C while stirring at 750 rpm in PBS buffer (pH 7.4). The MMQO sample (0.04 mM) in the PBS buffer was placed in the cell, whereas the microsyringe was loaded with the protein sample (0.5 mM). The titrations were conducted using 20 successive injections of 2.0  $\mu$ l (the first at 1.0  $\mu$ l and the remaining 19 at 2.0  $\mu$ l) with a duration of 4 s per injection and 150 s between injections. The collected data were processed using the Origin 7.0 software program (Origin Lab) supplied with the instrument according to the “one set of sites” fitting model.

**B-HIVE.** Native Jurkat cells were infected at a multiplicity of infection (MOI) of 0.1 with a barcoded library of GFP-expressing minigenomes described previously (19). Four days later, 10,000 GFP-positive cells were sorted by FACS and left to expand for 19 days. At that time, a sample of the cell pool was collected, the DNA was extracted, and barcodes were mapped by inverse PCR as described previously (19). The GFP-negative cells were thereafter isolated and cultured for 2 weeks. Subsequently, the cells were grown to 70% confluence, separated into 10 pools, and treated in duplicate with MMQO (160  $\mu$ M), JQ1 (1  $\mu$ M), prostratin (10  $\mu$ M), SAHA (5  $\mu$ M), or an equivalent volume of DMSO (1  $\mu$ l/ml). For each sample, two independent reverse transcription reactions were performed, each on 10  $\mu$ l purified mRNA, to which was added 1  $\mu$ l 20  $\mu$ M reverse primer (TTTCGCTTTTAATACGACTCACTAT) and 1  $\mu$ l 10 mM deoxynucleoside triphosphates (dNTPs) (Thermo Fisher Scientific; R0181). The RNA was denatured at 95°C for 1 min and incubated on ice. Then, 8  $\mu$ l master mix containing 4  $\mu$ l 5 $\times$  cDNA synthesis buffer, 1  $\mu$ l 0.1 M dithiothreitol (DTT), 1  $\mu$ l 40-U/ $\mu$ l RNase Out, 1  $\mu$ l diethyl pyrocarbonate (DEPC)-treated water, and 1  $\mu$ l 15-U/ $\mu$ l Thermo Script (reagents included in the ThermoScript RT-PCR system; Invitrogen; 11145-024) was added to the denatured RNA, and the mixture was incubated at 65°C for 1 h. The reaction mixture was heat inactivated at 85°C for 5 min, and 5  $\mu$ l RT product was used as the template in 50  $\mu$ l standard Phusion polymerase reaction mix (Thermo Fisher Scientific; F5305) in GC buffer with 1  $\mu$ M primers (AATGATACGGCGACACCGAGATCTACACTCTTCCCTACACGAGCTCTTCCGATCT and CAAGCAG AAGACGGCATACGAGAT-index-TTTTAATACGACTCACTATA, where “index” is a 4-nucleotide sequence that identifies the experiment). The cycling conditions were as follows: 98°C for 1 min; 98°C for 20 s, 60°C for 30 s, and 72°C for 1 min (27 cycles); 72°C for 5 min. The samples were sequenced as 50-bp single reads on a HiSeq 2000 sequencer (Illumina) using v3 sequencing chemistry.

HIV barcodes were extracted from paired-end reads through an inexact search of the T7 promoter sequence (TATAGTGAGTCGTA) allowing up to 3 errors (mismatches, insertions, and deletions) using Seeq v1.1.2 (<http://github.com/ezorita/seeq>). The barcodes were clustered with Starcode v1.0 (63), allowing one mismatch and using the “message passing” clustering algorithm. We considered only barcodes that had more than 1 read under at least 17 of the 20 replicate conditions. We then computed the pairwise Pearson coefficient of correlation,  $r$ , between the replicate conditions and used  $1 \times r$  as a dissimilarity metric between them. Clustering and dendrogram representations were performed with the `hclust()` function of R with default parameters.

The total number of reads per sample is fixed at pooling time, so the measurements indicate the relative expression of the provirus within a given treatment, but they cannot be compared between treatments. To that end, the number of reads was divided by the total amount of GFP fluorescence, defined as the percentage of GFP-positive cells multiplied by the average fluorescence of the GFP-positive cells. This score is a proxy for the total production of virus mRNA, establishing a baseline to compare the expression of a provirus across treatments.

**Accession number(s).** The solution structure of the BRD4 BD1-MMQO complex and the NMR spectral data are available in Protein Data Bank (PDB) under PDB code 5Z9C and BioMagResBank (BMRB) code 36163 (<http://www.bmrb.wisc.edu/search/instant.php?term=36163>), respectively.

## SUPPLEMENTAL MATERIAL

Supplemental material for this article may be found at <https://doi.org/10.1128/JVI.02056-17>.

**SUPPLEMENTAL FILE 1**, PDF file, 1.7 MB.

## ACKNOWLEDGMENTS

This work was supported by funding from the Spanish Ministry of Economy and Competitiveness (MINECO); the European Regional Development Fund (grant BFU2014-52237-P); Fundación para la Investigación y Prevención del SIDA en España (FIPSE 360946/10; to A.J.); ERC Synergy Grant 609989; Centro de Excelencia Severo Ochoa 2013-2017, SEV-2012-0208; and Plan Nacional BFU2012-37168 (to G.J.F.). The work was also supported in part by the research fund of the First Hospital of Jilin University (Changchun, China), grants from the National Institutes of Health (to M.-M.Z.) and the European Research Council under the European Union’s Seventh Framework Programme (FP/2007-2013)/ERC STG 337116 Trxn-PURGE, and Dutch AIDS Fonds grants 2014021 and an ErasmusMC research grant (to T.M.).

## REFERENCES

- Van Lint C, Bouchat S, Marcello A. 2013. HIV-1 transcription and latency: an update. *Retrovirology* 10:67. <https://doi.org/10.1186/1742-4690-10-67>.
- Persaud D, Zhou Y, Siliciano JM, Siliciano RF. 2003. Latency in human immunodeficiency virus type 1 infection: no easy answers. *J Virol* 77: 1659–1665. <https://doi.org/10.1128/JVI.77.3.1659-1665.2003>.
- Deeks SG, Lewin SR, Ross AL, Ananworanich J, Benkirane M, Cannon P, Chomont N, Douek D, Lifson JD, Lo Y-R, Kuritzkes D, Margolis D, Mellors J, Persaud D, Tucker JD, Barre-Sinoussi F, International AIDS Society Towards a Cure Working Group, Alter G, Auerbach J, Autran B, Barouch DH, Behrens G, Cavazzana M, Chen Z, Cohen EA, Corbelli GM, Eholié S, Eyal N, Fidler S, Garcia L, Grossman C, Henderson G, Henrich TJ, Jefferys R, Kiem H-P, McCune J, Moodley K, Newman PA, Nijhuis M, Nsubuga MS, Ott M, Palmer S, Richman D, Saez-Cirion A, Sharp M, Siliciano J, Silvestri G, Singh J, Spire B, Taylor J, Tolstrup M, Valente S, van Lunzen J, Walensky R, Wilson I, Zack J. 2016. International AIDS Society global scientific strategy: towards an HIV cure 2016. *Nat Med* 22:839–850. <https://doi.org/10.1038/nm.4108>.
- Hamer DH. 2004. Can HIV be cured? Mechanisms of HIV persistence and strategies to combat it. *Curr HIV Res* 2:99–111.
- Dar RD, Hosmane NN, Arkin MR, Siliciano RF, Weinberger LS. 2014. Screening for noise in gene expression identifies drug synergies. *Science* 344:1392–1396. <https://doi.org/10.1126/science.1250220>.
- Wong VC, Fong LE, Adams NM, Xue Q, Dey SS, Miller-Jensen K. 2014. Quantitative evaluation and optimization of co-drugging to improve anti-HIV latency therapy. *Cell Mol Bioeng* 7:320–333. <https://doi.org/10.1007/s12195-014-0336-9>.
- Rasmussen TA, Lewin SR. 2016. Shocking HIV out of hiding: where are we with clinical trials of latency reversing agents? *Curr Opin HIV AIDS* 11:394–401. <https://doi.org/10.1097/COH.0000000000000279>.
- Banerjee C, Archin N, Michaels D, Belkina AC, Denis GV, Bradner J, Sebastiani P, Margolis DM, Montano M. 2012. BET bromodomain inhibition as a novel strategy for reactivation of HIV-1. *J Leukoc Biol* 92: 1147–1154. <https://doi.org/10.1189/jlb.0312165>.
- Zhu J, Gaiha GD, John SP, Pertel T, Chin CR, Gao G, Qu H, Walker BD, Elledge SJ, Brass AL. 2012. Reactivation of latent HIV-1 by inhibition of BRD4. *Cell Rep* 2:807–816. <https://doi.org/10.1016/j.celrep.2012.09.008>.
- Li Z, Guo J, Wu Y, Zhou Q. 2013. The BET bromodomain inhibitor JQ1 activates HIV latency through antagonizing Brd4 inhibition of Tat-transactivation. *Nucleic Acids Res* 41:277–287. <https://doi.org/10.1093/nar/gks976>.
- Filippakopoulos P, Qi J, Picaud S, Shen Y, Smith WB, Fedorov O, Morse EM, Keates T, Hickman TT, Felletar I, Philpott M, Munro S, McKeown MR, Wang Y, Christie AL, West N, Cameron MJ, Schwartz B, Heightman TD, La Thangue N, French CA, Wiest O, Kung AL, Knapp S, Bradner JE. 2010. Selective inhibition of BET bromodomains. *Nature* 468:1067–1073. <https://doi.org/10.1038/nature09504>.
- Delmore JE, Issa GC, Lemieux ME, Rahl PB, Shi J, Jacobs HM, Kastiris E, Gilpatrick T, Paranal RM, Qi J, Chesi M, Schinzel AC, McKeown MR, Heffernan TP, Vakoc CR, Bergsagel PL, Ghobrial IM, Richardson PG, Young RA, Hahn WC, Anderson KC, Kung AL, Bradner JE, Mitsiades CS. 2011. BET bromodomain inhibition as a therapeutic strategy to target c-Myc. *Cell* 146:904–917. <https://doi.org/10.1016/j.cell.2011.08.017>.
- Zuber J, Shi J, Wang E, Rappaport AR, Herrmann H, Sison EA, Magoon D, Qi J, Blatt K, Wunderlich M, Taylor MJ, Johns C, Chicas A, Mulloy JC, Kogan SC, Brown P, Valent P, Bradner JE, Lowe SW, Vakoc CR. 2011. RNAi screen identifies Brd4 as a therapeutic target in acute myeloid leukemia. *Nature* 478:524–528. <https://doi.org/10.1038/nature10334>.
- Yang Z, Yik JHN, Chen R, He N, Jang MK, Ozato K, Zhou Q. 2005. Recruitment of P-TEFb for stimulation of transcriptional elongation by the bromodomain protein Brd4. *Mol Cell* 19:535–545. <https://doi.org/10.1016/j.molcel.2005.06.029>.
- Jiang G, Mendes EA, Kaiser P, Wong DP, Tang Y, Cai I, Fenton A, Melcher GP, Hildreth JEK, Thompson GR, Wong JK, Dandekar S. 2015. Synergistic reactivation of latent HIV expression by ingenol-3-angelate, PEP005, targeted NF- $\kappa$ B signaling in combination with JQ1 induced p-TEFb activation. *PLoS Pathog* 11:e1005066. <https://doi.org/10.1371/journal.ppat.1005066>.
- Laird GM, Bullen CK, Rosenbloom DS, Martin AR, Hill AL, Durand CM, Siliciano JD, Siliciano RF. 2015. Ex vivo analysis identifies effective HIV-1 latency-reversing drug combinations. *J Clin Invest* 125:1901–1912. <https://doi.org/10.1172/JCI80142>.
- Jordan A, Bisgrove D, Verdin E. 2003. HIV reproducibly establishes a latent infection after acute infection of T cells in vitro. *EMBO J* 22:1868–1877. <https://doi.org/10.1093/emboj/cdg188>.
- Gallastegui E, Marshall B, Vidal D, Sanchez-Duffhues G, Collado JA, Alvarez-Fernández C, Luque N, Terme J-M, Gatell JM, Sánchez-Palomino S, Muñoz E, Mestres J, Verdin E, Jordan A. 2012. Combination of biological screening in a cellular model of viral latency and virtual screening identifies novel compounds that reactivate HIV-1. *J Virol* 86:3795–3808. <https://doi.org/10.1128/JVI.05972-11>.
- Chen H-C, Martinez JP, Zorita E, Meyerhans A, Filion GJ. 2017. Position effects influence HIV latency reversal. *Nat Struct Mol Biol* 24:47–54. <https://doi.org/10.1038/nsmb.3328>.
- Jordan A, Defechereux P, Verdin E. 2001. The site of HIV-1 integration in the human genome determines basal transcriptional activity and response to Tat transactivation. *EMBO J* 20:1726–1738. <https://doi.org/10.1093/emboj/20.7.1726>.
- Reeder JE, Kwak Y-T, McNamara RP, Forst CV, D'Orso I. 2015. HIV Tat controls RNA polymerase II and the epigenetic landscape to transcriptionally reprogram target immune cells. *Elife* 4:e08955. <https://doi.org/10.7554/eLife.08955>.
- McCarthy DJ, Smyth GK. 2009. Testing significance relative to a fold-change threshold is a TREAT. *Bioinformatics* 25:765–771. <https://doi.org/10.1093/bioinformatics/btp053>.
- Kroesen M, Gielen P, Brok IC, Armandari I, Hoogerbrugge PM, Adema GJ. 2014. HDAC inhibitors and immunotherapy; a double edged sword? *Oncotarget* 5:6558–6572. <https://doi.org/10.18632/oncotarget.2289>.
- Mu Q, Ma Q, Lu S, Zhang T, Yu M, Huang X, Chen J, Jin J. 2014. 10058-F4, a c-Myc inhibitor, markedly increases valproic acid-induced cell death in Jurkat and CCRF-CEM T-lymphoblastic leukemia cells. *Oncol Lett* 8:1355–1359. <https://doi.org/10.3892/ol.2014.2277>.
- Bhadury J, Nilsson LM, Muralidharan SV, Green LC, Li Z, Gesner EM, Hansen HC, Keller UB, McLure KG, Nilsson JA. 2014. BET and HDAC inhibitors induce similar genes and biological effects and synergize to kill in Myc-induced murine lymphoma. *Proc Natl Acad Sci U S A* 111: E2721–E2730. <https://doi.org/10.1073/pnas.1406722111>.
- Nicodeme E, Jeffrey KL, Schaefer U, Beinke S, Dewell S, Chung C-W, Chandwani R, Marazzi I, Wilson P, Coste H, White J, Kirilovsky J, Rice CM, Lora JM, Priñha RK, Lee K, Tarakhovskiy A. 2010. Suppression of inflammation by a synthetic histone mimic. *Nature* 468:1119–1123. <https://doi.org/10.1038/nature09589>.
- Belkina AC, Nikolajczyk BS, Denis GV. 2013. BET protein function is required for inflammation: Brd2 genetic disruption and BET inhibitor JQ1 impair mouse macrophage inflammatory responses. *J Immunol* 190: 3670–3678. <https://doi.org/10.4049/jimmunol.1202838>.
- Brown JD, Lin CY, Duan Q, Griffin G, Federation A, Paranal RM, Bair S, Newton G, Lichtman A, Kung A, Yang T, Wang H, Lusinskas FW, Croce K, Bradner JE, Plutzky J. 2014. NF- $\kappa$ B directs dynamic super enhancer formation in inflammation and atherogenesis. *Mol Cell* 56:219–231. <https://doi.org/10.1016/j.molcel.2014.08.024>.
- Huang B, Yang X-D, Zhou M-M, Ozato K, Chen L-F. 2009. Brd4 coactivates transcriptional activation of NF- $\kappa$ B via specific binding to acetylated RelA. *Mol Cell Biol* 29:1375–1387. <https://doi.org/10.1128/MCB.01365-08>.
- Dhalluin C, Carlson JE, Zeng L, He C, Aggarwal AK, Zhou MM. 1999. Structure and ligand of a histone acetyltransferase bromodomain. *Nature* 399:491–496. <https://doi.org/10.1038/20974>.
- Zhang G, Liu R, Zhong Y, Plotnikov AN, Zhang W, Zeng L, Rusinova E, Gerona-Nevarro G, Moshkina N, Joshua J, Chuang PY, Ohlmeyer M, He JC, Zhou M-M. 2012. Down-regulation of NF- $\kappa$ B transcriptional activity in HIV-associated kidney disease by BRD4 inhibition. *J Biol Chem* 287: 28840–28851. <https://doi.org/10.1074/jbc.M112.359505>.
- Filippakopoulos P, Knapp S. 2014. Targeting bromodomains: epigenetic readers of lysine acetylation. *Nat Rev Drug Discov* 13:337–356. <https://doi.org/10.1038/nrd4286>.
- Song Y, Chen W, Kang D, Zhang Q, Zhan P, Liu X. 2014. “Old friends in new guise”: exploiting privileged structures for scaffold re-evolution/refining. *Comb Chem High Throughput Screen* 17:536–553. <https://doi.org/10.2174/1386207317666140122101631>.
- Afzal O, Kumar S, Haider MR, Ali MR, Kumar R, Jaggi M, Bawa S. 2015. A review on anticancer potential of bioactive heterocycle quinoline. *Eur J Med Chem* 97:871–910. <https://doi.org/10.1016/j.ejmech.2014.07.044>.
- Serrao E, Debnath B, Otake H, Kuang Y, Christ F, Debyser Z, Neamati N.



2013. Fragment-based discovery of 8-hydroxyquinoline inhibitors of the HIV-1 integrase-lens epithelium-derived growth factor/p75 (IN-LEDGF/p75) interaction. *J Med Chem* 56:2311–2322. <https://doi.org/10.1021/jm301632e>.
36. Zhang M-Q, Wilkinson B. 2007. Drug discovery beyond the 'rule-of-five'. *Curr Opin Biotechnol* 18:478–488. <https://doi.org/10.1016/j.copbio.2007.10.005>.
37. Vidler LR, Filippakopoulos P, Fedorov O, Picaud S, Martin S, Tomsett M, Woodward H, Brown N, Knapp S, Hoelder S. 2013. Discovery of novel small-molecule inhibitors of BRD4 using structure-based virtual screening. *J Med Chem* 56:8073–8088. <https://doi.org/10.1021/jm4011302>.
38. Chung C-W, Dean AW, Woolven JM, Bamborough P. 2012. Fragment-based discovery of bromodomain inhibitors part 1: inhibitor binding modes and implications for lead discovery. *J Med Chem* 55:576–586. <https://doi.org/10.1021/jm201320w>.
39. Picaud S, Wells C, Felletar I, Brotherton D, Martin S, Savitsky P, Diez-Dacal B, Philpott M, Bountra C, Lingard H, Fedorov O, Müller S, Brennan PE, Knapp S, Filippakopoulos P. 2013. RVX-208, an inhibitor of BET transcriptional regulators with selectivity for the second bromodomain. *Proc Natl Acad Sci U S A* 110:19754–19759. <https://doi.org/10.1073/pnas.1310658110>.
40. Schröder S, Cho S, Zeng L, Zhang Q, Kaehlcke K, Mak L, Lau J, Bisgrove D, Schnölzer M, Verdin E, Zhou M-M, Ott M. 2012. Two-pronged binding with bromodomain-containing protein 4 liberates positive transcription elongation factor b from inactive ribonucleoprotein complexes. *J Biol Chem* 287:1090–1099. <https://doi.org/10.1074/jbc.M111.282855>.
41. Boehm D, Calvanese V, Dar RD, Xing S, Schroeder S, Martins L, Aull K, Li P-C, Planelles V, Bradner JE, Zhou M-M, Siliciano RF, Weinberger L, Verdin E, Ott M. 2013. BET bromodomain-targeting compounds reactivate HIV from latency via a Tat-independent mechanism. *Cell Cycle* 12:452–462. <https://doi.org/10.4161/cc.23309>.
42. Deeney JT, Belkina AC, Shiriha OS, Corkey BE, Denis GV. 2016. BET bromodomain proteins Brd2, Brd3 and Brd4 selectively regulate metabolic pathways in the pancreatic  $\beta$ -cell. *PLoS One* 11:e0151329. <https://doi.org/10.1371/journal.pone.0151329>.
43. Sheridan BS, Lefrançois L. 2011. Regional and mucosal memory T cells. *Nat Immunol* 12:485–491. <https://doi.org/10.1038/ni.2029>.
44. Shirakawa K, Chavez L, Hakre S, Calvanese V, Verdin E. 2013. Reactivation of latent HIV by histone deacetylase inhibitors. *Trends Microbiol* 21: 277–285. <https://doi.org/10.1016/j.tim.2013.02.005>.
45. Razooky BS, Pai A, Aull K, Rouzine IM, Weinberger LS. 2015. A hardwired HIV latency program. *Cell* 160:990–1001. <https://doi.org/10.1016/j.cell.2015.02.009>.
46. Descours B, Petitjean G, López-Zaragoza J-L, Bruel T, Raffel R, Psomas C, Reynes J, Lacabaratz C, Levy Y, Schwartz O, Lelievre JD, Benkirane M. 2017. CD32a is a marker of a CD4 T-cell HIV reservoir harbouring replication-competent proviruses. *Nature* 543:564–567. <https://doi.org/10.1038/nature21710>.
47. Darcis G, Van Driessche B, Van Lint C. 2017. HIV latency: should we shock or lock? *Trends Immunol* 38:217–228. <https://doi.org/10.1016/j.it.2016.12.003>.
48. Winckelmann AA, Munk-Petersen LV, Rasmussen TA, Melchjorsen J, Hjelholt TJ, Montefiori D, Østergaard L, Søgaard OS, Tolstrup M. 2013. Administration of a Toll-like receptor 9 agonist decreases the proviral reservoir in virologically suppressed HIV-infected patients. *PLoS One* 8:e62074. <https://doi.org/10.1371/journal.pone.0062074>.
49. Novis CL, Archin NM, Buzon MJ, Verdin E, Round JL, Lichterfeld M, Margolis DM, Planelles V, Bosque A. 2013. Reactivation of latent HIV-1 in central memory CD4<sup>+</sup> T cells through TLR-1/2 stimulation. *Retrovirology* 10:119. <https://doi.org/10.1186/1742-4690-10-119>.
50. Stoszko M, De Crignis E, Rokx C, Khalid MM, Lungu C, Palstra R-J, Kan TW, Boucher C, Verbon A, Dykhuizen EC, Mahmoudi T. 2016. Small molecule inhibitors of BAF; a promising family of compounds in HIV-1 latency reversal. *EBioMedicine* 3:108–121. <https://doi.org/10.1016/j.ebiom.2015.11.047>.
51. Lassen KG, Hebbeler AM, Bhattacharyya D, Lobritz MA, Greene WC. 2012. A flexible model of HIV-1 latency permitting evaluation of many primary CD4 T-cell reservoirs. *PLoS One* 7:e30176. <https://doi.org/10.1371/journal.pone.0030176>.
52. Millán-Ariño L, Islam AB, Izquierdo-Bouldstridge A, Mayor R, Terme J-M, Luque N, Sancho M, López-Bigas N, Jordan A. 2014. Mapping of six somatic linker histone H1 variants in human breast cancer cells uncovers specific features of H1.2. *Nucleic Acids Res* 42:4474–4493. <https://doi.org/10.1093/nar/gku079>.
53. Zhang Q, Zeng L, Shen C, Ju Y, Konuma T, Zhao C, Vakoc CR, Zhou M-M. 2016. Structural mechanism of transcriptional regulator NSD3 recognition by the ET domain of BRD4. *Structure* 24:1201–1208. <https://doi.org/10.1016/j.str.2016.04.019>.
54. Clore GM, Gronenborn AM. 1994. Multidimensional heteronuclear nuclear magnetic resonance of proteins. *Methods Enzymol* 239:349–363. [https://doi.org/10.1016/S0076-6879\(94\)39013-4](https://doi.org/10.1016/S0076-6879(94)39013-4).
55. Grzesiek S, Bax A. 1992. Correlating backbone amide and side chain resonances in larger proteins by multiple relayed triple resonance NMR. *J Am Chem Soc* 114:6291–6293. <https://doi.org/10.1021/ja00042a003>.
56. Lee W, Revington MJ, Arrowsmith C, Kay LE. 1994. A pulsed field gradient isotope-filtered 3D <sup>13</sup>C HMQC-NOESY experiment for extracting intermolecular NOE contacts in molecular complexes. *FEBS Lett* 350:87–90. [https://doi.org/10.1016/0014-5793\(94\)00740-3](https://doi.org/10.1016/0014-5793(94)00740-3).
57. Johnson BA, Blevins RA. 1994. NMR View: a computer program for the visualization and analysis of NMR data. *J Biomol NMR* 4:603–614. <https://doi.org/10.1007/BF00404272>.
58. Delaglio F, Grzesiek S, Vuister GW, Zhu G, Pfeifer J, Bax A. 1995. NMRPipe: a multidimensional spectral processing system based on UNIX pipes. *J Biomol NMR* 6:277–293. <https://doi.org/10.1007/BF00197809>.
59. Brünger AT, Adams PD, Clore GM, DeLano WL, Gros P, Grosse-Kunstleve RW, Jiang JS, Kuszewski J, Nilges M, Pannu NS, Read RJ, Rice LM, Simonson T, Warren GL. 1998. Crystallography and NMR system: a new software suite for macromolecular structure determination. *Acta Crystallogr D Biol Crystallogr* 54:905–921.
60. Shen Y, Delaglio F, Cornilescu G, Bax A. 2009. TALOS+: a hybrid method for predicting protein backbone torsion angles from NMR chemical shifts. *J Biomol NMR* 44:213–223. <https://doi.org/10.1007/s10858-009-9333-z>.
61. Cornilescu G, Delaglio F, Bax A. 1999. Protein backbone angle restraints from searching a database for chemical shift and sequence homology. *J Biomol NMR* 13:289–302. <https://doi.org/10.1023/A:1008392405740>.
62. Laskowski RA, Rullmann JA, MacArthur MW, Kaptein R, Thornton JM. 1996. AQUA and PROCHECK-NMR: programs for checking the quality of protein structures solved by NMR. *J Biomol NMR* 8:477–486. <https://doi.org/10.1007/BF00228148>.
63. Zorita E, Cuscó P, Filion GJ. 2015. Starcode: sequence clustering based on all-pairs search. *Bioinformatics* 31:1913–1919. <https://doi.org/10.1093/bioinformatics/btv053>.

**Supplementary materials to**

**Chapter 4.**

**A New Quinoline BRD4 Inhibitor Targets a Distinct Latent HIV-1 Reservoir for  
Reactivation from Other “Shock” Drugs.**

## SUPPLEMENTARY MATERIAL

### Supplementary Figure Legends

**Supplementary Figure S1. Mechanistic similarity between MMQO and JQ1 on gene expression.** (A) Number of genes found up or down-regulated ( $q < 0.05$ ) in common in the microarray data sets depicted in Figure 4A (MMQO or TSA, 3h) and Figure 5A (MMQO 8h or JQ1 24h). (B) Fold-changes of genes significantly ( $q < 0.05$ ) up-regulated by MMQO and JQ1 but down-regulated by TSA (left column), or vice-versa (right column).

**Supplementary Figure S2. Distribution of the top responder proviruses to bromodomain inhibitors.** Venn diagram showing proviruses that respond to MMQO and JQ1 in the B-HIVE analysis. Top 15% or 50% responders are shown. The genomic categories of provirus integrations for the common integrants are indicated (AG, active genes; EN, enhancers; IN, intergenic). AGs that contain those integrations are listed on the side.

**Supplementary Figure S3. BRD4 localization within genes containing proviruses induced by BETi.** (A) Snapshots from the human genome browser visualized with Integrative Genomics Viewer (IGV 2.3) (64, 65), showing genes (yellow-shadowed) where HIV integrations that respond to BETi have been found in B-HIVE (among the top 15% responders). The location of the provirus identified is shown (green square), as well as ChIP-Seq tracks of BRD4 and RNA polymerase II (RP2) obtained in Jurkat cells treated or not with JQ1 (500 nM) for 4 hours (GEO accession number GSE83777). Genes dysregulated by MMQO in our microarray analysis show the fold-change with MMQO compared to untreated. Notice that RP2 is enriched or depleted upon JQ1 treatment at TSS of genes up or downregulated by MMQO, respectively. (B) Proviral integration responsive to BETi at a putative enhancer in close proximity to BRD4.

# Supplementary Figure S1\_Abner et al.

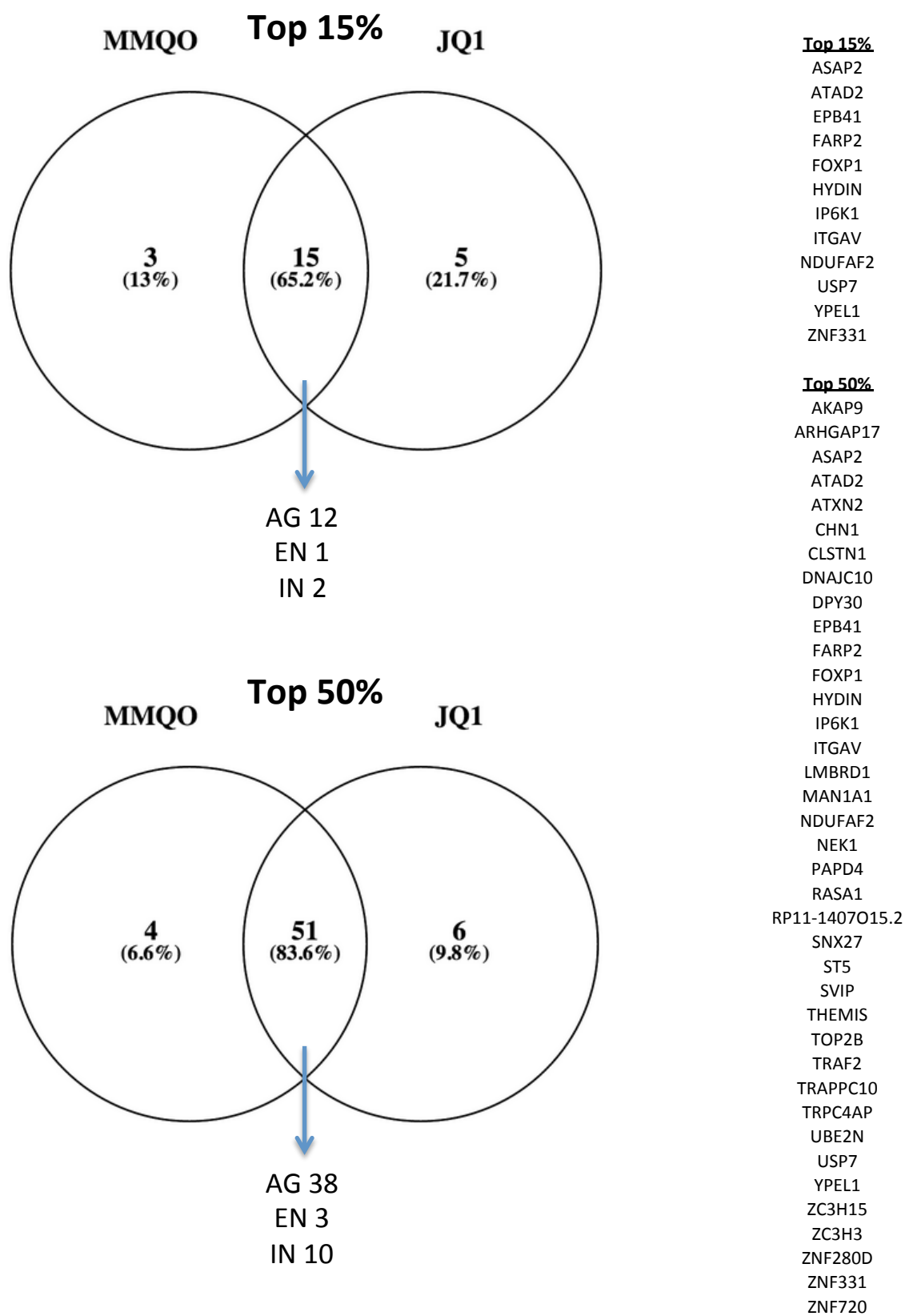
**A**

MMQO 3h	MMQO 8h	JQ1 24h	TSA 3h	number of genes
up	up	up	up	403
up	up	up	down	55
up	up	down	up	3
up	up	down	down	0
down	down	down	down	458
down	down	down	up	32
down	down	up	down	17
down	down	up	up	3

**B**

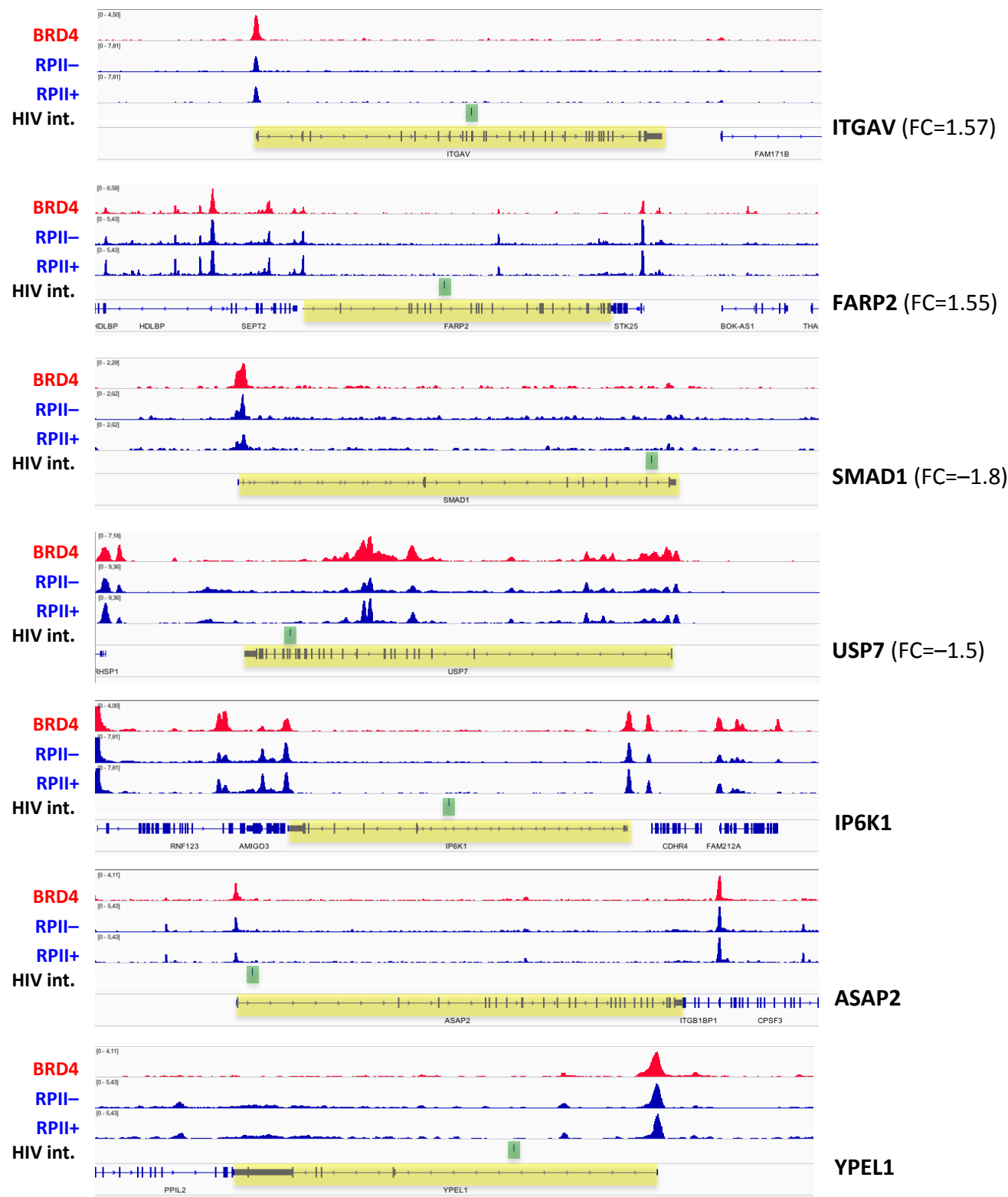
	MMQO 3h	TSA 3h	MMQO 8h	JQ1 24h		MMQO 3h	TSA 3h	MMQO 8h	JQ1 24h
ALDH16A1	1,21751	-1,37319	1,65231	1,368938	ARL4C	-2,68633	1,243787	-2,61142	-1,12218
ATF5	1,304451	-1,87954	1,564859	1,296366	BACH2	-1,25501	1,34687	-1,40965	-1,32457
BAZ2B	1,342435	-1,30728	1,504238	1,345538	BSPRY	-1,38676	1,268401	-1,63993	-1,41157
BCL2L2	1,589946	-1,30245	1,669845	1,158397	CD3EAP	-1,26494	1,449223	-1,86077	-1,1903
BRCA2	1,209909	-1,17198	1,495472	1,243074	CD69	-1,22054	1,727208	-1,5852	-1,57689
BRD2	1,623225	-1,22193	1,877205	1,426538	DCAF4	-1,30486	1,215082	-1,3803	-1,3434
C1orf144	1,142338	-1,35234	1,36439	1,074064	DCTPP1	-1,74568	1,199552	-1,56046	-1,17772
C3orf23	1,725566	-1,2551	1,990769	1,744003	FAM100A	-1,95412	2,66844	-1,71374	-1,35094
C5orf42	1,409431	-1,3196	1,703151	1,718996	FAM134B	-1,25403	1,188086	-1,4131	-1,23428
C6orf35	1,313843	-1,18579	1,756984	1,501673	GLB1L2	-1,56914	1,483876	-1,82393	-1,28062
CCNL1	1,471158	-1,2939	1,376308	1,246301	GPR56	-1,4403	1,701005	-2,59129	-2,17713
CEP63	1,145904	-1,14221	1,465393	1,185009	ICOS	-1,51099	1,663812	-1,58608	-1,1031
CEP97	1,192665	-1,22203	1,418243	1,441112	ITGB7	-1,22843	1,333847	-1,35249	-1,88851
CIRBP	4,728918	-1,35695	2,300778	2,027524	KLHL5	-1,31721	1,29034	-1,76178	-1,31761
CTNNB1	1,180813	-1,1653	1,528889	1,327482	MOCS1	-1,34624	1,224851	-1,54443	-1,49976
CYB5D2	1,291574	-1,51624	1,455566	1,565149	MYADM	-1,18146	1,301725	-1,6555	-1,78179
CYP20A1	1,408146	-1,2042	1,573494	1,625453	OSCP1	-2,16548	1,734792	-1,46066	-1,22564
CYTH2	1,183865	-1,33848	1,792931	1,519101	PTK2B	-1,29274	1,486264	-1,45087	-1,78922
D2HGDH	1,862014	-1,47727	1,908081	1,17031	PTPRU	-1,49508	1,380583	-1,81392	-1,82783
DMTF1	1,274697	-1,67181	1,380454	1,256063	RASSF2	-1,4721	1,766271	-1,91445	-2,81567
EGLN1	1,204517	-1,34594	1,888325	1,133046	SH2D3A	-1,23017	1,135995	-1,7851	-1,79434
HP1BP3	1,126468	-1,27423	1,664886	1,364213	SH2D3C	-1,40781	1,236428	-2,64371	-1,46925
KIF5B	1,223682	-1,39943	1,709089	1,193064	SLC7A5	-1,314	1,202348	-1,38142	-2,0912
LPIN2	1,223975	-1,38657	1,635012	1,375773	SRGN	-1,17801	1,682949	-1,47397	-1,30119
LUC7L	1,20003	-1,13768	1,677577	1,244231	SYNGR1	-1,24671	1,453363	-1,51082	-1,89464
MAPK1IP1	1,186491	-1,21393	1,694175	1,190719	TFAP2C	-1,90568	1,435964	-1,80571	-2,26438
MEPCE	1,371888	-2,71718	1,673168	1,105577	TMC6	-1,43904	1,572001	-1,71988	-1,74852
N6AMT2	1,240333	-1,40387	1,457646	1,276793	TMEM132A	-1,51587	1,612939	-1,83973	-1,50048
NDST2	1,723639	-1,29636	2,01939	1,97099	TMEM151E	-1,15609	2,117165	-1,43031	-1,6781
PAFAH1B1	1,170808	-1,16553	1,896661	1,230486	TRANK1	-1,34546	1,303878	-2,07651	-1,26597
PIK3R3	1,189972	-1,18975	1,621773	1,314965	TUB	-1,1258	1,173627	-1,46045	-1,53726
POPCD2	3,282821	-1,37373	1,818681	1,457158	XBP1	-1,24551	1,377723	-1,63555	-1,12351
PPAPDC1E	1,407659	-1,62487	1,374208	1,318244					
PTPRA	1,173755	-1,21163	1,674161	1,473589					
S100A13	1,699778	-1,56612	1,564789	1,524611					
SEN8	1,674847	-1,23021	1,7065	1,516763					
SGCB	1,184462	-1,56005	2,076463	1,386586					
SIRT1	1,540684	-1,45195	1,743406	1,649943					
ST3GAL3	1,478008	-1,35492	1,856716	1,249389					
STOX1	1,610875	-1,45986	1,950347	2,343925					
STRADA	1,192329	-1,19641	1,920111	1,675207					
TEP1	1,192562	-1,16285	2,12498	1,21499					
TIGD6	1,32127	-1,46382	1,356827	1,34092					
TMEM128	1,437235	-1,23977	1,735456	1,190842					
TMEM91	1,596462	-1,41534	1,711871	1,852924					
TOR2A	1,172337	-1,43914	1,484278	1,20406					
TRIOBP	1,176158	-1,2576	1,537965	1,276014					
UBE2D4	1,140518	-1,40137	1,626096	1,367481					
WIPF2	1,165755	-1,13374	1,653397	1,158392					
ZC3H6	2,242825	-1,34858	1,797969	2,005448					
ZNF333	1,603884	-1,39076	1,570463	1,762896					
ZNF397	1,776455	-1,32699	1,696358	1,36227					
ZNF565	1,167705	-1,41359	1,44877	1,562048					
ZNF713	1,263445	-1,31318	1,46089	1,818946					
ZNF837	1,850446	-1,81128	1,519034	1,281791					

Supplementary Figure S2\_Abner et al.



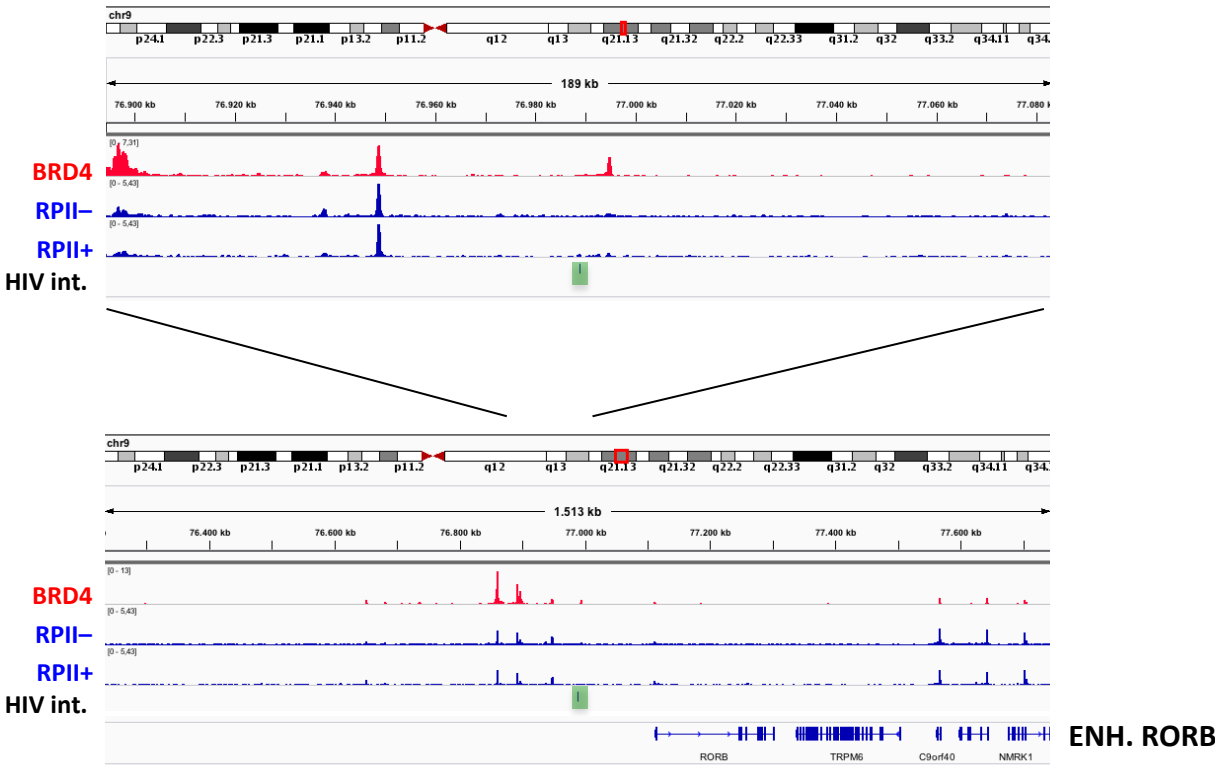
Supplementary Figure S3\_Abner et al.

A



Supplementary Figure S3\_Abner et al.

B





## Supplementary Table S1\_Abner et al.

**Supplementary Table S1. NF- $\kappa$ B target genes are oppositely dysregulated by MMQO.** Displayed is the fold change of MMQO (80 $\mu$ M, 4-hour) treatment from microarrays. 32 of the genes listed are canonically known to be upregulated by NF- $\kappa$ B, while 3 genes are known to be downregulated.

Gene	Fold Change	NF- $\kappa$ B function
GADD45A	1,839	Downregulates
ETS1	-1,373	Upregulates
TRAF3	-1,395	Upregulates
CASP4	-1,492	Upregulates
ERAP2	-1,554	Upregulates
CBR3	-1,743	Upregulates
C1R	-2,404	Upregulates
SELPLG	-4,263	Upregulates
CCR7	-1,553	Upregulates
CD86	-1,579	Upregulates
CD83	-2,475	Upregulates
BCL2	-1,457	Upregulates
FAS	-1,455	Upregulates
NFKB1	-1,951	Upregulates
CFLAR	-1,932	Upregulates
TAP2	-1,409	Upregulates
IL32	-1,434	Upregulates
CCND2	-2,028	Upregulates
ITGAL	-2,213	Upregulates
LTB	-3,363	Upregulates
MYC	-6,279	Upregulates
IRF1	-1,452	Upregulates
IL23A	-1,734	Upregulates
KIT	-1,815	Upregulates
IL7R	-2,603	Upregulates
TNFSF4	-2,595	Upregulates
IKBKE	-1,618	Upregulates
TERT	-2,609	Upregulates
CXCR3	-9,351	Upregulates
SENP1	-1,347	Upregulates
STAT5A	-3,478	Upregulates
IL15	-1,796	Upregulates
TNFSF10	-2,484	Upregulates
ICOS	-1,461	Downregulates
CFTR	-2,083	Downregulates

## Supplementary Table S2\_Abner et al.

**Supplementary Table S2. Gene Ontology (GO) and Reactome (REAC) of genes downregulated by MMQO.** Q = number of query genes. T = number of term genes. Q&T/Q denotes % of MMQO downregulated genes that belong to each particular gene set (FC<-2). Q&T/T denotes % of MMQO regulated genes that overlap with the full dataset. Data obtained with g:Profiler toolkit analysis.

NAME	TERM ID	p-Value	Q&T/Q	Q&T/T
cell activation	GO:0001775	<0,0001	0,166	0,045
antigen processing and presentation, exogenous lipid antigen via MHC class Ib	GO:0048007	0,003	0,016	0,571
mast cell activation	GO:0045576	0,017	0,028	0,130
Immunoregulatory interactions between a Lymphoid and a non-Lymphoid cell	REAC:198933	0,020	0,078	0,065
cytokine production	GO:0001816	0,020	0,091	0,037
Cell surface interactions at the vascular wall	REAC:202733	0,027	0,062	0,079
regulation of alpha-beta T cell proliferation	GO:0046640	0,027	0,020	0,217
immunoglobulin production	GO:0002377	0,035	0,032	0,096
Immune System	REAC:168256	0,041	0,305	0,025

## Supplementary Table S3\_Abner et al.

**Supplementary Table S3. Gene set enrichment analysis (GSEA) of MMQO responsive transcriptome.** Jurkat cells treated or not with MMQO for 8 hours were analyzed by expression microarrays. (Top) Gene sets enriched among genes downregulated by MMQO, highlighting the number of genes in each set (n), the normalized enrichment score (NES) and test of statistical significance (FDR *q*-value). Gene sets related to the c-Myc are highlighted in bold. (Bottom) Comparisons of top-ranking transcription factor target gene sets of known proteins needed for HIV-reactivation, enriched among the genes downregulated by MMQO.

NAME	n	NES	FDR q-val
<b>MYC_UP.V1_UP</b>	171	-2,63	< 0.0001
<b>SCHLOSSER_MYC_TARGETS_AND_SERUM_RESPONSE_DN</b>	46	-2,58	< 0.0001
<b>SCHLOSSER_MYC_TARGETS_AND_SERUM_RESPONSE_UP</b>	46	-2,53	< 0.0001
TONKS_TARGETS_OF_RUNX1_RUNX1T1_FUSION_HSC_DN	182	-2,49	< 0.0001
<b>SCHUHMACHER_MYC_TARGETS_UP</b>	79	-2,45	< 0.0001
HELLER_HDAC_TARGETS_DN	286	-2,43	< 0.0001
<b>KIM_MYC_AMPLIFICATION_TARGETS_UP</b>	197	-2,30	0,0002
HELLER_HDAC_TARGETS_SILENCED_BY_METHYLATION_DN	274	-2,27	0,0081
<b>BILD_MYC_ONCOGENIC_SIGNATURE</b>	195	-2,23	0,0012
KLEIN_PRIMARY_EFFUSION_LYMPHOMA_DN	57	-2,22	0,0013

NAME	n	NES	FDR q-val
V\$MYCMAX_01	250	-1,99	0,0029
V\$MYCMAX_02	258	-1,72	0,0202
V\$ETS_Q4	242	-1,34	0,1872
V\$AP1_04	266	-1,41	0,1879
V\$STAT5B_01	238	-1,35	0,1923
V\$STAT5A_01	243	-1,33	0,1946
V\$IRF7_01	243	-1,21	0,2501
V\$NFKB_Q6	251	-1,06	0,4095

## Supplementary Table S4\_Abner et al.

**Supplementary Table S4. Selected gene sets related to histone acetylation pathways among genes regulated by MMQO.** In total 283 gene sets correlated either positively or negatively with MMQO treatment. Gene sets are ordered according to the enrichment score. n = number of genes in each set; NES = normalized enrichment score; FDR *q*-value <0.05.

NAME	n	NES	FDR q-val
PEART HDAC PROLIFERATION CLUSTER UP	56	2,45	< 0.0001
HELLER HDAC TARGETS UP	299	2,24	< 0.0001
HELLER HDAC TARGETS SILENCED BY METHYLATION UP	446	2,09	0,003
N ACETYLTRANSFERASE ACTIVITY	21	1,94	0,013
ZHONG RESPONSE TO AZACITIDINE AND TSA UP	177	1,92	0,013
ACETYLTRANSFERASE ACTIVITY	25	1,87	0,016
PID HDAC CLASSIII PATHWAY	25	1,77	0,0324
HISTONE ACETYLTRANSFERASE ACTIVITY	16	1,73	0,0435
N ACYLTRANSFERASE ACTIVITY	24	1,71	0,0476
PEART HDAC PROLIFERATION CLUSTER DN	75	-2,07	0,0078
HELLER HDAC TARGETS SILENCED BY METHYLATION DN	274	-2,27	0,0081
HELLER HDAC TARGETS DN	286	-2,43	0,0000

## Supplementary Table S5\_Abner et al.

**Supplementary Table S5. Summary of restraints and statistics of BRD4 BD1domain in complex with MMQO compound.**

	MMQO
Protein NMR distance and dihedral constraints	
Distance constraints	
Total NOE	2703
Intra-residue	1136
Inter-residue	1567
Sequential ( $ i - j  = 1$ )	496
Medium-range ( $1 <  i - j  \leq 5$ )	537
Long-range ( $ i - j  > 5$ )	534
Inter-molecular constraints	29
Hydrogen bonds	52
Total dihedral angle restraints	
Phi angle	109
Psi angle	109
Ramachandran Map Analysis (%)	
Most favored resions	97.5
Additional allowed regions	2.5
Generally allowed regions	0.0
Disallowed regions	0.0
Structure statistics	
Violations (mean +/- s.d.)	
Distance constraints (Å)	0.062 +/- 0.0013
Dihedral angle constraints (°)	0.53 +/- 0.057
Max. dihedral angle violation (°)	0.65
Max. distance constraint violation (Å)	0.066
Deviations from idealized geometry	
Bond lengths (Å)	0.0071 +/- 0.0001
Bond angles (°)	0.79 +/- 0.0068
Impropers (°)	1.9 +/- 0.041
Average pairwise r.m.s. Deviation ** (Å)	
Heavy	0.50 +/- 0.069
Backbone	0.16 +/- 0.045

<sup>a</sup>: Procheck calculation was done for protein residues 60-68, 70-84, 88-92, 106-116, 121-139 and 140-165.

<sup>b</sup>: The residue number ranges used in full molecule pairwise root-mean-square (r.m.s.) deviation calculations consists of 60-163

<sup>c</sup>: Pairwise r.m.s. deviation was calculated among top 20/200 lowest energy structures.

## Supplementary Table S6\_Abner et al.

**Supplementary Table S6. Primer sequences used for qPCR.**

Name	Sequence
ADMfw	TGCCCAGACCCTTATTCGG
ADMrev	AGTTGTTTCATGCTCTGGCGG
CCR7fw	TGGTTTACCGCCCAGAGAG
CCR7rev	GACACAGGCATACCTGGAAA
CD28fw	CGGACCTTCTAAGCCCTTT
CD28rev	ATAGGGCTGGTAATGCTTGC
CXCR3fw	ACACCTTCCTGCTCCACCTA
CXCR3rev	GTTCAAGTAGCGGTCAAAGC
CXCR7fw	TGGGTGGTCAGTCTCGT
CXCR7rev	CCGGCAGTAGGTCTCAT
FOSfw	AACCTCATTCCACGGTCAC
FOSrev	GGCCTCCTGTCATGGTCTT
GAPDHfw	GAGTCAACGGATTTTGGTCGT
GAPDHrev	TTGATTTTGGAGGGATCTCG
HEXIM1fw	GACCTGGGAAGAGAAGAAAAAG
HEXIM1rev	GAGGAAGTGCCTGGTGTATAG
HIV_5'_fw	AGTAGTGTGTGCCCGTCTGT
HIV_5'_rev	TCGCTTTCAGGTCCCTGTTCTG
ICOSfw	GGATGTGCAGCCTTTGTTGT
ICOSrev	GGTCACATCTGTGAGTCTAGATTTT
IFIT1fw	GCCTCCTTGGGTTCTGTATATA
IFIT1rev	TCAAAGTCAGCAGCCAGTCTCA
IL7Rfw	CGCCAGGAAAAGGATGAAA
IL7Rrev	ATACATTGCTGCCGGTTGG
IRF7fw	ACAGACCCCCAGCAGGTAG
IRF7rev	CCACCTCCAGTACACCTTG
LRIG1fw	GGTGAGCCTGGCCTTATGTGAATA
LRIG1rev	CACCACCATCCTGCACCTCC
MEPCEfw	GCCAGAGCAGTTCAGTTCCT
MEPCErev	CAGGACGCTGGAAGCCTTTA
MYCfw	TCAGAGAAGCTGGCCTCCTA
MYCrev	CTGTCGTTGAGAGGGTAGGG
RAG1fw	CTGCTGAGCAAGGTACCTCAGCCAG
RAG1rev	GAGAGGGTTTCCCTCAAAGGAATC
TERTfw	TGTTTCTGGATTTCAGGTG
TERTrev	GTTCTTGGCTTTCAGGATGG
TUBB3fw	AACGAGGCCTCTCTCACAA
TUBB3rev	GGGTCTGCCATCAGAGCTT
ZBTB1fw	ATGGCCAGTGGTGAAATAGGG
ZBTB1rev	GGAAGACAGAAAAGATGGTGCC

# Chapter 5

## **Gliotoxin, identified from a screen of *Aspergillus fumigatus* metabolites, reverses HIV-1 latency via release of P-TEFb**

Mateusz Stoszko<sup>1</sup>, Abdullah M.S. Al-Hatmi<sup>2,3,4†</sup>, Anton Skriba<sup>5†</sup>, Michael Roling<sup>1†</sup>, Yvonne M. Mueller<sup>6†</sup>, Enrico Ne<sup>1†</sup>, Mohammad Javad Najafzadeh<sup>2,7†</sup>, Raquel Crespo<sup>†</sup>, Joyce Kang<sup>8</sup>, Renata Ptackova<sup>5</sup>, Alessia Bertoldi<sup>9</sup>, Tsung Wai Kan<sup>1</sup>, Elisa de Crignis<sup>1</sup>, Robert-Jan Palstra<sup>1</sup>, Miroslav Sulc<sup>5</sup>, Joyce H.G. Lebbink<sup>10</sup>, Casper Rokx<sup>11</sup>, Peter D. Katsikis<sup>6</sup>, Vladimir Havlicek<sup>5</sup>, Sybren de Hoog<sup>2,3</sup>, Tokameh Mahmoudi<sup>1\*</sup>.

<sup>1</sup> Department of Biochemistry, Erasmus MC University Medical Center Rotterdam, PO Box 2040, 3000 CA Rotterdam, The Netherlands.

<sup>2</sup> Westerdijk Fungal Biodiversity Institute, Utrecht, The Netherlands.

<sup>3</sup> Center of Expertise in Mycology of Radboud UMC/CWZ, Nijmegen, The Netherlands.

<sup>4</sup> Ministry of Health, Directorate General of Health Services, Ibri, Oman.

<sup>5</sup> Institute of Microbiology of the CAS, v.v.i., Videnska 1083, CZ 14220 Prague 4, Czech Republic.

<sup>6</sup> Department of Immunology, Erasmus MC University Medical Center Rotterdam, PO Box 2040, 3000 CA Rotterdam, The Netherlands.

<sup>7</sup> Department of Parasitology and Mycology, Faculty of Medicine, Mashhad University of Medical Sciences, Mashhad, Iran.

<sup>8</sup> Key Laboratory of Environmental Pollution Monitoring / Disease Control, Ministry of Education & Guizhou Talent Base of Microbes and Human Health, School of Basic Medicine, Guizhou Medical University, Guiyang, 550025, P. R. China.

<sup>9</sup> Microbiology Section, Department of Experimental, Diagnostic and Specialty Medicine, School of Medicine, University of Bologna, Italy.

<sup>10</sup> Department of Molecular Genetics and Department of Radiation Oncology, Erasmus University Medical Center, PO Box 2040, 3000 CA Rotterdam, The Netherlands.

<sup>11</sup> Department of Internal Medicine, Section of Infectious Diseases, Erasmus University Medical Center, PO Box 2040 3000CA, Rotterdam, The Netherlands.

† equal contribution

Submitted





# **Gliotoxin, identified from a screen of *Aspergillus fumigatus* metabolites, reverses HIV-1 latency via release of P-TEFb**

Mateusz Stoszek<sup>1</sup>, Abdullah M.S. Al-Hatmi<sup>2,3,4†</sup>, Anton Skriba<sup>5†</sup>, Michael Roling<sup>1†</sup>, Yvonne M. Mueller<sup>6†</sup>, Enrico Ne<sup>1†</sup>, Mohammad Javad Najafzadeh<sup>2,7†</sup>, Raquel Crespo<sup>†</sup>, Joyce Kang<sup>8</sup>, Renata Ptackova<sup>5</sup>, Alessia Bertoldi<sup>9</sup>, Tsung Wai Kan<sup>1</sup>, Elisa de Crignis<sup>1</sup>, Robert-Jan Palstra<sup>1</sup>, Miroslav Sulc<sup>5</sup>, Joyce H.G. Lebbink<sup>10</sup>, Casper Rokx<sup>11</sup>, Peter D. Katsikis<sup>6</sup>, Vladimir Havlicek<sup>5</sup>, Sybren de Hoog<sup>2,3</sup>, Tokameh Mahmoudi<sup>1\*</sup>.

## **Affiliations:**

<sup>1</sup> Department of Biochemistry, Erasmus MC University Medical Center Rotterdam, PO Box 2040, 3000 CA Rotterdam, The Netherlands.

<sup>2</sup> Westerdijk Fungal Biodiversity Institute, Utrecht, The Netherlands.

<sup>3</sup> Center of Expertise in Mycology of Radboud UMC/CWZ, Nijmegen, The Netherlands.

<sup>4</sup> Ministry of Health, Directorate General of Health Services, Ibri, Oman.

<sup>5</sup> Institute of Microbiology of the CAS, v.v.i., Videnska 1083, CZ 14220 Prague 4, Czech Republic.

<sup>6</sup> Department of Immunology, Erasmus MC University Medical Center Rotterdam, PO Box 2040, 3000 CA Rotterdam, The Netherlands.

<sup>7</sup> Department of Parasitology and Mycology, Faculty of Medicine, Mashhad University of Medical Sciences, Mashhad, Iran.

<sup>8</sup> Key Laboratory of Environmental Pollution Monitoring / Disease Control, Ministry of Education & Guizhou Talent Base of Microbes and Human Health, School of Basic Medicine, Guizhou Medical University, Guiyang, 550025, P. R. China.

<sup>9</sup> Microbiology Section, Department of Experimental, Diagnostic and Specialty Medicine, School of Medicine, University of Bologna, Italy.

<sup>10</sup> Department of Molecular Genetics and Department of Radiation Oncology, Erasmus University Medical Center, PO Box 2040, 3000 CA Rotterdam, The Netherlands.

<sup>11</sup> Department of Internal Medicine, Section of Infectious Diseases, Erasmus University Medical Center, PO Box 2040 3000CA, Rotterdam, The Netherlands.

\* Correspondence to: Tokameh Mahmoudi, t.mahmoudi@erasmusmc.nl.

† equal contribution

## **Summary**

A leading pharmacological strategy towards HIV cure requires “shock” or activation of expression of the HIV genome in latently infected cells with Latency Reversal Agents (LRAs) followed by their subsequent clearance. As a source of bio-active molecules we used fungal secondary metabolites (extrolites) in a screen for novel LRAs. We used orthogonal mass spectrometry (MS) coupled to latency reversal bioassays, and identified gliotoxin (GTX) to potently reverse latency. GTX significantly induced HIV-1 gene expression in latent ex vivo infected primary cells and in CD4<sup>+</sup> T cells from all aviremic HIV-1<sup>+</sup> participants. RNA sequencing identified 7SK RNA to be most significantly downregulated in independent donors upon GTX treatment of CD4<sup>+</sup> T cells. GTX disrupted the 7SK snRNP complex causing release of P-TEFb, which induced phosphorylation of RNA Pol II CTD, and increased HIV transcription. Our data highlight the power of combining low throughput bioassays, mycology and orthogonal mass spectrometry as an approach to screen for and characterize novel LRAs.

## Introduction

Combination anti-retroviral therapy (cART) causes a drastic and immediate viral decrease by targeting distinct steps in the HIV-1 life cycle effectively blocking replication and halting disease progression (Ho et al., 1995; Perelson et al., 1997; Wei et al., 1995). Unfortunately, one third of the estimated 37 million people living with HIV have no access to the costly therapy (Avert, 2017; Gupta et al., 2016; UNAIDS, 2017). Additionally, cART does not target or eliminate HIV that persists in a latent state in cellular reservoirs (Siliciano and Siliciano, 2015). Because some of the proviruses are replication competent, latent HIV infected cells inevitably rebound once c-ART is interrupted, leading to necessity for life-long therapy (Siliciano and Siliciano, 2015). Particularly in resource-limited countries, which are also disproportionately affected, this is translated into an insurmountable medical, social and financial burden. To achieve a scalable cure for HIV infection, it will be necessary to reduce or eliminate the latent HIV infected reservoir of cells and/or equip the immune system with the robustness and effectiveness necessary to prevent viral rebound such that c-ART can be safely discontinued.

An important breakthrough in HIV-1 cure was the unequivocal proof that it is possible to mobilize the latent patient HIV reservoir by treatment with agents that activate HIV gene expression (LRAs) (Archin et al., 2012). However, clinical studies thus far have shown little to no reduction in the latent reservoir in patients. This indicates a limited potency and specificity of currently tested drugs, which appear to be unable to reach a significant proportion of latently infected cells, or to induce HIV-1 expression in latent reservoir at sufficient levels to produce viral proteins for recognition by the immune system (Kim et al., 2018; Leth et al., 2016). Furthermore, transcriptional stochasticity and heterogeneity of latent HIV integrations (Battivelli et al., 2018) may pose an additional barrier to complete reactivation of the latent reservoir as a whole; sequential rounds of stimulation yielded new infectious particles (Ho et al., 2013b), while certain LRA combinations produced more efficient latency reversal when administered in intervals rather than at once (Bouchat et al., 2016a). In addition, pleiotropic functional and toxic effects of LRAs may compromise the ability of CD8<sup>+</sup> T cells to eliminate HIV protein expressing cells (Zhao et al., 2019a). Therefore, it is critical to identify and develop novel therapeutics, which strongly induce HIV-1 gene expression to effectively disrupt HIV latency without dampening the immune response.

The pharmaceutical industry is highly equipped for high throughput screens using defined synthetic libraries. While this is an effective approach, it is important to record that approximately 42% of the novel small molecules introduced to the market between 1981 and 2014 are natural or nature-derived (Newman and Cragg, 2016). Biological systems represent an invaluable source of functional molecules with high chemical diversity and biochemical specificity, evolved during millions of years of adaptation (Cary et al., 2016; Richard et al., 2018; Vo and Kim, 2010; Wang et al., 2017; Yasuhara-Bell et al., 2010). In particular, fungi represent a largely unexplored source of compounds with potential therapeutic use. Fungi secrete a gamut of extracellular

compounds and other small-molecular extrolites (Sanchez et al., 2012). While some of these compounds have been shown to have antibiotic (ex. penicillin) or carcinogenic (ex. aflatoxin) properties, little is known in general about their biological activities and possible molecular targets. In addition, a single fungal strain often produces a wide array of secondary metabolites which are not essential for its growth but are exuded as a consequence of specific environment such as nutrient-rich *versus* minimal growth conditions (Brakhage, 2013; Přichystal et al., 2016). Fungal extrolites might target various signaling pathways in mammalian cells, such as those influencing HIV-1 gene expression. Fungal supernatants are an ideal source for an expert academic setting where low and medium throughput biological screening systems, academic knowledge of evolutionary mycology, and state-of-the-art fractionation and purification techniques are routinely combined.

Studies of regulation of HIV-1 gene expression have identified distinct and diverse molecular mechanisms and cellular pathways at play, which can be targeted pharmacologically to activate expression of latent HIV (De Crignis and Mahmoudi, 2016; Mahmoudi, 2012; Ne et al., 2018). The rich diversity of fungal extrolites therefore, may prove an untapped source of new compounds that target HIV reactivation. The present paper introduces such novel, highly effective LRA of fungal origin.

## Results

### ***Aspergillus fumigatus* extrolites reverse latency.**

We screened 115 species of filamentous fungi for their ability to induce HIV-1 proviral expression; of species that appeared promising, 2-4 additional strains were tested (Table S1). Species belonged to 28 orders (43 families) of the fungal Kingdom (Figs 1A, S1A) and were chosen based on their evolutionary position, ecological trends, and known active production of extracellular compounds. The majority of fungi were of ascomycetous affinity, 4 species were of basidiomycetous affinity and two belonged to the lower fungi. Culture supernatants were screened for latency reversal activity using a Jurkat derived 11.1 and A2 cell lines model of HIV-1 latency (J-Lats) in a low-medium through-put assay set up, in which expression of GFP is controlled by the HIV-1 promoter and indicates latency reversal. We identified the supernatant of *Aspergillus fumigatus* CBS 542.75 to strongly activate the latent HIV-1 5'LTR (Fig. 1B). We also compared other *Aspergillus* species growth supernatants for the potential to induce HIV-1 expression (Fig. 1C) and observed that only strains of *A. fumigatus* (CBS 542.75, CBS 113.26 and CBS 100074) possessed latency reversal activity (Fig. 1C).

### ***Aspergillus fumigatus* secondary metabolite gliotoxin reverses HIV-1 latency.**

Due to the chemical complexity of the positive fungal supernatants, direct mass spectrometry (MS) analysis of their constituents proved to be impossible. Therefore, *A. fumigatus* CBS 100074 growth supernatant was fractionated several times by means of orthogonal MS (Fig. 2A). We selected this particular supernatant as it showed the highest potency to reverse latency in the J-Lat A2 model. After each round of fractionation, all samples/fractions were again tested in latency reversal bioassays, followed by quantitation of the GFP

expression and identification of fractions retaining latency reversal activity. As expected, originally less active fractions became more active during the fractionation/enrichment process (Fig. 2B). The most active 7B/7C fractions were further fractionated on HLB cartridge (11-samples) and components of 7B/7C and 11C fractions de-replicated by Cyclobranch software (Fig. 2B and S2B) (Novák et al., 2017). Compound matching against the annotated database of *Aspergillus* secondary metabolites revealed a set of candidate compounds further selected for latency reversal testing (Fig. S2A and Table S2). Among candidate molecules identified, Gliotoxin (GTX) was able to induce expression of the latent pro-virus in a concentration dependent manner (Fig. 2C). Of note, GTX was found in all positive fractions (Table S2). Interestingly, while GTX isolated from supernatant of CBS 100074 showed strong induction of HIV-1 transcription, supernatant of *Aspergillus flavus* (CBS 625.66), a close relative of *A. fumigatus* which was inactive in latency reversal (Fig 1C), did not contain GTX (Fig. S2C and S2D), providing further support that GTX is the main mediator of LRA activity in *A. fumigatus* supernatants.

### **Gliotoxin reverses latency in ex vivo infected primary CD4+ T cells without side effects.**

To examine the latency reversal potential of GTX in a more clinically relevant system, we employed a modified primary *ex vivo* infected latency model (Fig. S3A) (Lassen et al., 2012). Treatment of latently infected CD4+ T cells with GTX resulted in significant, concentration-dependent latency reversal at lower concentrations than necessary to achieve re-activation in latently infected cell-lines. Interestingly, GTX [20 nM] treatment resulted in an over 10% latency reversal of that observed upon maximal stimulation with PMA/Ionomycin, which translated into over 20-fold induction of HIV-1 expression (Figs 3A, S3B). At high concentrations GTX is known to be toxic to immune cells (Stanzani et al., 2005; Suen et al., 2001; Yamada et al., 2000), ascribed to its unusual disulfide bridge, responsible for pleiotropic effects on cellular and viral systems (Scharf et al., 2016). However, at lower concentrations in which strong latency reversal is induced, GTX did not show toxicity on CD4+ T cells (Fig. 3C). CD8+ T cells play a central role in eliminating HIV-infected cells (Trautmann, 2016). Therefore, it is of utmost importance to evaluate potential toxicity of newly developed drugs have on CD8+ T cells. Importantly, GTX at a low concentration of 20 nM did not reduce the viability of CD8+ T cells whether unstimulated or anti-CD3/anti-CD28-stimulated PBMCs were examined (Fig. 3E, S4B). Consistent with the literature (Hur et al., 2008; Nouri et al., 2015; Orciuolo et al., 2007; Stanzani et al., 2005; Suen et al., 2001; Sutton et al., 1995; Wichmann et al., 2002; Yamada et al., 2000; Zhou et al., 2000), treatment with higher concentrations of GTX at 100 nM and 1  $\mu$ M caused apoptosis and death of primary CD4+ and CD8+ T cells as well as B cells, NK cells and monocytes (Fig. 3C, 3E, S4B, S5A). Potential for clinical applicability of a candidate LRA also requires that it does not induce global T-cell activation, nor should it interfere with CD8+ T cell activation. Treatment of unstimulated primary CD4+ T-cells and CD8+ T cells with GTX [20 nM], which significantly reversed latency, did not induce expression of the T cell activation markers CD69 and CD25 (Fig. 3F, S5B and S5C), nor did it induce proliferation of resting CD4+ and CD8+ T cells

(Fig. 3D, 4E, 4F), while, as expected, PMA/Ionomycin treatment activated T cells (Fig. 3F). Conversely, GTX treatment of activated PBMCs also did not inhibit CD25 expression (Fig. 4E and 4F) or proliferation (Fig. 3D, S5B and S5C) of activated CD4<sup>+</sup> or CD8<sup>+</sup> T cells.

### **Gliotoxin synergizes with other known LRAs.**

To investigate possible synergies, we tested the latency reversal potential of GTX [20 nM] in combination with a panel of known LRAs in the J-Lat A2 and 11.1 models of latency as well as in *ex vivo* infected primary CD4<sup>+</sup> T cells (Fig. 4A, 4B, S3A and S4A). GTX co-treatment enhanced the latency reversal activity observed after single treatments with all compounds (Fig. 4A, 4B and S4A). Interestingly, when latent CD4<sup>+</sup> T cells were co-treated with GTX [20 nM] and either the HDAC inhibitor SAHA or BAF inhibitor CAPE, synergistic reversal of HIV-1 latency was observed (Fig. 4A, 4B and S4A). Co-treatments with BET inhibitors JQ-1 and OTX-015, as well as Prostratin resulted in an additive effect on HIV-1 pro-virus expression. Interestingly, in the primary CD4<sup>+</sup> T cell model of HIV-1 latency, GTX treatment alone showed more potent latency reversal activity than SAHA, CAPE, OTX-015, JQ-1 or Romidepsin (RMD) alone at tested concentrations (Fig. 4B). RMD treatment showed modest latency reversal (Fig. 4B) and consistent with the literature significant CD4<sup>+</sup> and CD8<sup>+</sup> T cell cytotoxicity (Fig. 4C and 4D) (Zhao et al., 2019b). With the exception of RMD, we did not observe any negative impact of these co-treatments on viability and proliferation of CD4<sup>+</sup> T cells (Fig. 4C and S5B), CD8<sup>+</sup> T cells (Fig. 4D, 4F and S5C) and other immune sub-populations including CD19<sup>+</sup> B cells, CD56<sup>+</sup> NK cells and CD14<sup>+</sup> monocytes (Fig. S5A). Moreover, none of the co-treatments altered the activation status of either resting or activated CD4<sup>+</sup> and CD8<sup>+</sup> T cells (Fig. 4E and 4F).

The definition of synergism assumes that drugs targeting similar mechanisms cannot enhance each other synergistically, as targeting same pathways with different molecules would rather result in additive effects. Collectively, our observations of co-treatments with the use of different classes of LRAs indicate that GTX should not be considered an HDAC or BAF inhibitors. Indeed, we do not see an increase in acetylation of the histones upon 4-hour treatment with GTX (Fig. S7C). Similarly, we excluded that GTX behaves as a PKC agonist, as treatments with gliotoxin did not induce cell activation, and did not induce expression of the genes targeted by PKC pathway (Fig. 3F, 6C, S3C and S6).

### **Gliotoxin reverses latency in cells of aviremic participants *in vitro*.**

Most importantly, we also examined the potential of GTX to reverse latency after *ex vivo* treatment of CD4<sup>+</sup> T cells obtained from people living with HIV-1. All five participants enrolled were treated with c-ART and maintained HIV-1 viremia below 50 copies/ml for at least last two years. Despite differences in the size of the latent pool – assessed by maximal stimulation of the cells with  $\alpha$ -CD3/CD28 beads or PMA/Ionomycin, GTX treatment significantly increased the levels of cell-associated HIV-1 *pol* RNA (CA-*pol*) in CD4<sup>+</sup> T cells obtained from aviremic HIV-1<sup>+</sup> participants (Fig. 5A and 5B). Notably, GTX effect is systematic as latency

reversal was uniformly observed in the cells of all tested participants after only 24 hours of stimulation (Fig. 2B). Additionally, we observed no increase in expression of genes related to T cell specific responses, reactive oxygen species or apoptosis, a side effects reported previously (Fig. S6). These results therefore indicate that GTX treatment at non-toxic concentrations reverses latency without inducing immune cell toxicity, activation and without affecting T cell proliferation (Fig. 5A, 5B, S3C and S6), making it a very promising candidate for further clinical investigation for HIV-1 latency reversal and inclusion in “shock and kill” strategies.

### **Gliotoxin reverses latency through P-TEFb.**

To gain more insight into the mechanism by which GTX reverses latency, we performed RNA sequencing of primary CD4<sup>+</sup> T cells isolated from healthy blood donors that were treated for 4 hours with 20 nM GTX. This short incubation time was chosen to focus on examination of primary effects of GTX on the global transcriptome, decreasing the presence of secondary transcriptional effects. We observed a very good correlation between treatments of two independent healthy blood donors (Fig. 6A top panel). Moreover, less than 700 genes showed an altered differential expression pattern (Fig. 6A bottom panel). Interestingly, small nuclear RNA 7SK was the most downregulated (more than 9-fold) transcript after GTX treatment in both donors CD4<sup>+</sup> T cells. 7SK RNA serves as a scaffold for the 7SK snRNP complex that sequesters and inhibits activity of the positive elongation factor (P-TEFb) (Quaresma et al., 2016; Nguyen et al., 2001; Uchikawa et al., 2015; Yang et al., 2001; Yik et al., 2003). Among all components of the complex and its close interactors, only the 7SK transcript was affected by treatment with GTX (Fig. 6B). Concomitant with observation in aviremic participants, we did not observe any change in expression of NF- $\kappa$ B, oxidative stress, apoptosis and T-cell effector function related genes after treatment (Fig. 6C and S6), indicating that GTX [20 nM] does not influence these pathways neither at 4 nor at 24 hours of stimulation. This data suggested that GTX treatment may lead to destabilization of the 7SK snRNP complex and the release of free P-TEFb, which would then become available for transcription elongation at the latent HIV-1 LTR, a critical step required for HIV-1 latency reversal (Jonkers and Lis, 2015; Yukl et al., 2018a). To test this, we performed glycerol gradient sedimentation experiments after treatment of resting CD4<sup>+</sup> T cells with GTX (Fig. S8). Indeed, 20 nM GTX treatment of CD4<sup>+</sup> T cells for 4 hours resulted in release of free P-TEFb, from its inhibitory higher molecular weight 7SK snRNP complex, as shown by western blotting for the P-TEFb component CDK9 (Fig. 6D and S7A). As expected, control treatment of CD4<sup>+</sup> T cell lysates with RNase A resulted in disassembly of the 7SK snRNP complex and subsequent release of free P-TEFb, which eluted at lower molecular weight fractions (Fig. 6D and S7A). Phosphorylation of serine 2 residues within C-terminal domain (CTD) of RNA Polymerase II is a prerequisite for activation of transcription elongation and is mediated by kinase activity of CDK9, a component of P-TEFb (Peterlin and Price, 2006). To examine whether GTX treatment resulted in Serine 2 RNA Pol II phosphorylation, we treated resting CD4<sup>+</sup> T cells with GTX, the CDK9 inhibitor flavopiridol (FPD), and PMA as a positive control (Fig. 7B, S7C). As expected, FPD treatment abrogated RNA Pol II phosphorylation, while



PMA stimulation led to strong Ser2 RNA Pol II phosphorylation. Importantly, treatment with GTX caused an increase in phosphorylation of the CDK9 target, RNA Polymerase II Serine 2 in three independent donors tested, confirming that the enzymatic activity of CDK9 in context of P-TEFb remains unaffected after GTX – mediated release from 7SK snRNP (Fig. 6D and S7A). Our data is consistent with a model in which GTX, disrupts the 7SK snRNP complex resulting in release of 7SK RNA and P-TEFb (Fig. 7A). In resting CD4<sup>+</sup> T cells, 7SK RNA is then degraded, and free P-TEFb is recruited to the paused RNA Polymerase II at the latent HIV LTR by the Tat-TAR axis. CDK9 then phosphorylates CTD of RNA Polymerase II, leading to activation of proviral transcription elongation (Fig. 7A).

### **LARP7 is a putative target of gliotoxin.**

To understand better which component of the 7SK snRNP complex may be targeted by GTX, we performed docking experiments *in silico* employing two independent software packages Chimera and Achilles. Unfortunately, complete crystal structure of 7SK snRNP is not yet available, therefore we modelled GTX against all essential components of the complex separately. Strikingly, we observed preferential binding of GTX into the hydrophobic pocket of LARP7, which in physiological conditions is responsible for binding stem loop 4 (SL4) of the 7SK RNA (Fig. S9). Interestingly, LARP7 is responsible for stabilization of the complex as knock down experiments show that LARP7 depletion leads to decreased levels of 7SK RNA with concomitant increase in free P-TEFb levels (Krueger et al., 2008). Moreover, LARP7 depletion also lead to increase in Tat-mediated transactivation of the HIV-1 LTR (Krueger et al., 2008). Similar effects were observed for other structural component of the complex, namely MEPCE, however to a lesser extent (Krueger et al., 2008). Similarly, Krueger et al., (2008) showed that 7SK RNA knock down resulted in release of free P-TEFb. Based on published data and our results and this modelling exercises we hypothesize that GTX interferes with the binding of SL4 of 7SK RNA into hydrophobic pocket of LARP7, which results in destabilization of the complex with subsequent release of P-TEFb. However, further studies are necessary to confirm this preliminary modeling.

### **Discussion**

So far none of the tested LRAs is able to induce strong expression of the provirus or to strongly deplete latent reservoir, which indicate limitations of single treatments. It has been shown that distinct classes of LRAs target different subpopulations of proviruses (Abner et al., 2018; Battivelli et al., 2018; Chen et al., 2017). Additionally, only a fraction of the latent, replication competent proviruses is being expressed as second round of stimulation of the aviremic participants cells with PHA still yielded infectious virions (Ho et al., 2013a). Therefore, it is being postulated that successful “shock and kill” strategies will consist of cocktails of LRAs, preferably tailored to unique latency make-up of persons living with HIV-1, so that HIV-1 latency could be

most effectively and specifically reversed (Abner and Jordan, 2019; Bouchat et al., 2016b; Darcis et al., 2015; De Crignis and Mahmoudi, 2014; Hashemi et al., 2017; Laird et al., 2015; Stoszko et al., 2019; Röling et al., 2016; Rasmussen et al., 2015; Rasmussen and Lewin, 2016). We already identified a synergy between BAF inhibitors and HDAC inhibitors (Marian et al., 2018; Stoszko et al., 2016). Here, we report that GTX also synergizes with BAFs and with HDACs, therefore we postulate that even more robust latency reversal should be observed when these three classes of LRAs would be combined. Additionally experimental evidence points to the importance of targeting of transcription elongation as a rate limiting step in strong latency reversal (Yukl et al., 2018b).

To our knowledge GTX is the first molecule described to cause direct disruption of the 7SK snRNP complex with subsequent release of the active P-TEFb. Given the significance of P-TEFb in HIV transcription elongation and the current lack of molecules able to mediate its release from the inhibitory 7SK snRNP complex, GTX may be a promising candidate – not only in context of HIV-1 latency reversal, but also in other diseases in which P-TEFb may play a prominent regulatory role (eg. cardiac hypertrophy, mixed-lineage leukemia (Kohoutek, 2009)). Interestingly, our modeling exercises provide an insight into possible mechanism where GTX competes with 7SK RNA for the hydrophobic pocket of LARP7, which explains 7SK snRNP disassembly with subsequent release of P-TEFb and degradation of 7SK RNA scaffold as observed in our experiments (Fig. 6, 7 and S7). Indeed, knock down of LARP7 via RNAi lead to degradation of 7SK RNA concomitant with elevated levels of free P-TEFb and increased Tat-mediated HIV-1 expression, pointing the importance of LARP7 for the stability of the complex (Krueger et al., 2008)

Thus far GTX has been regarded as a toxin and a virulence factor of *Aspergillus* fungi, that acts as a immunosuppressant that inhibits phagocytosis, blocks Nf-kB signaling and cytokine production, moreover it has been reported to induce ROS formation (Choi et al., 2007; Kwon-Chung and Sugui, 2009; Sakamoto et al., 2015; Scharf et al., 2016; Stanzani et al., 2005; Wichmann et al., 2002; Yamada et al., 2000). However, it is important to note that all these effects of gliotoxin were observed at concentrations higher than 100 nM, a concentration at which we see massive death of the cells. Additionally, from our practice we learnt that gliotoxin once dissolved is rather an unstable molecule and that its stability strongly depends on the solvent used. We observed very weak stability of GTX when reconstituted in DMSO, a solvent used frequently in laboratory practice, also in some of abovementioned studies. Therefore, we believe that previously reported effects of GTX should be interpreted with caution. Interestingly, lowest serum concentrations of GTX reported in patients with aspergillosis are found to be more than 10 orders of magnitude higher than concentrations effective in reversing HIV-1 latency in primary T cells and cells of aviremic participants, namely ~200nM (Lewis et al., 2005). Together, we believe that concentrations of 20 nM, that effectively reverses latency in all tested models should be safe in people, additionally these low concentrations should be physiologically achievable in a therapeutic context. Finally, our screen of fungal

extrolites provides proof-of-principle that various fungi produce plethora of chemical entities, most of which have greatly unknown biological functions, and that these can be further exploited to identify novel compounds with therapeutic potential.

## **Acknowledgement**

TM received funding from the European Research Council (ERC) under the European Union's Seventh Framework Programme (FP/2007-2013)/ERC STG 337116 Trxn-PURGE, the Dutch AIDS Fonds grant. 2014021 and Erasmus MC mRACE research grant.

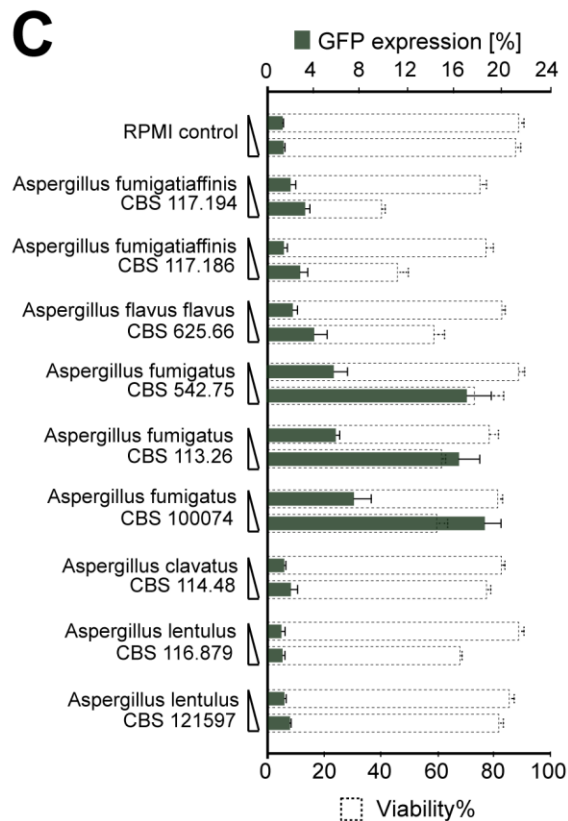
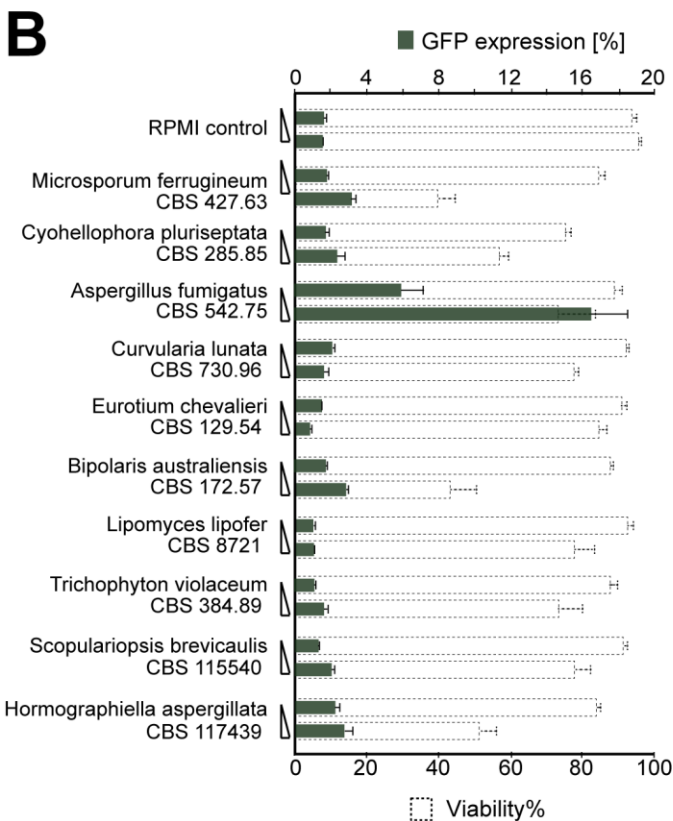
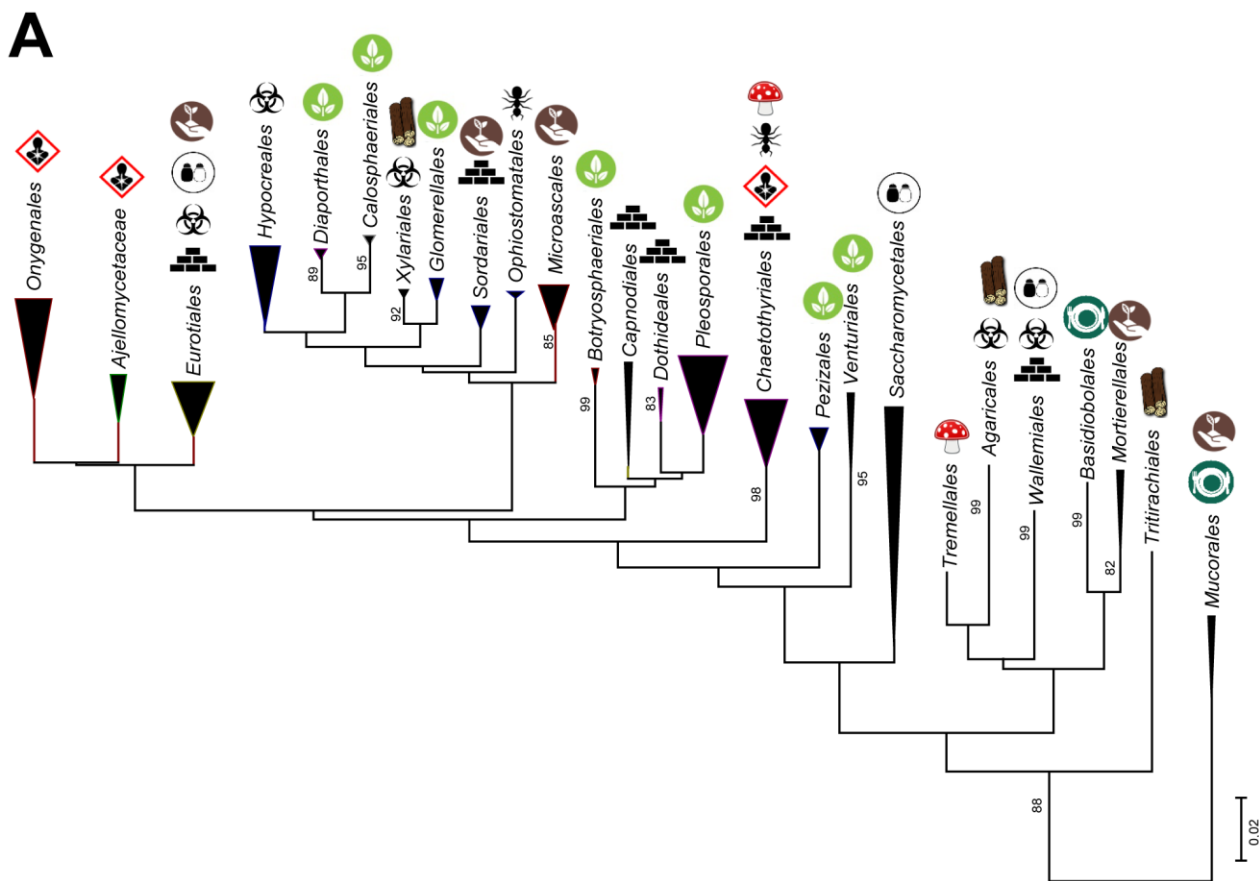
Y.K was supported by the Technology Innovation Team Project of Guiyang [20161001]005; Guiyang Science and Technology Project [2017] No.5-19.










VH was supported by the Ministry of Education, Youth and Sports of the Czech Republic (LO 1509).

JL is supported by the gravitation program CancerGenomiCs.nl from the Netherlands Organisation for Scientific Research (NWO). Supported in part by a grant awarded by Worldwide Cancer Research to PDK

**Declaration of Interests:** The authors declare no competing interests.

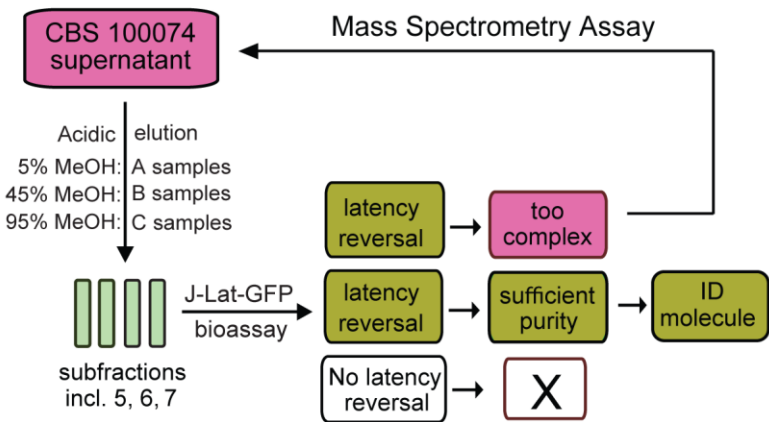
Figure 1



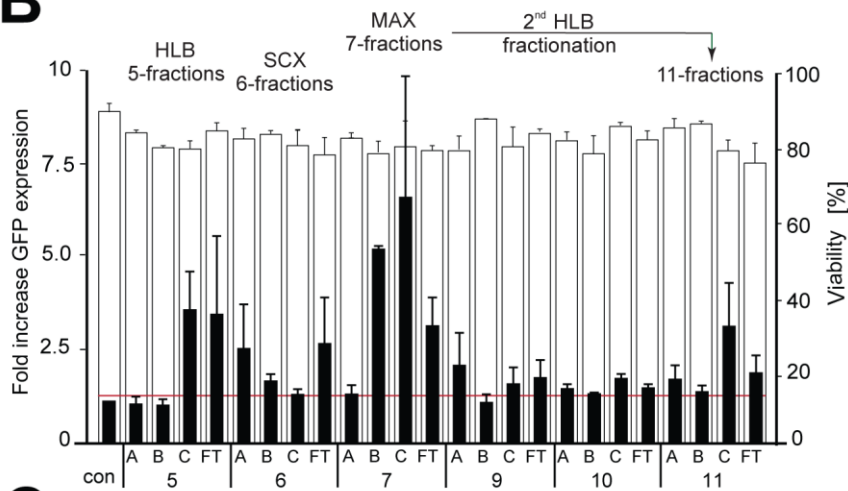
**Figure 1. Fractionation of *Aspergillus fumigatus* growth supernatant identifies GTX as a novel latency reversal agent from a screen of fungal secondary metabolites.** (A) Phylogenetic tree representing main orders of the fungal Kingdom with strains used in current study, collapsed per order. Orders selected from the tree published by Gostincar et al. (2018), with some of the lower orders included for structural reasons. Approximate ecological trends in the orders are summarized by symbols, as follows:  vertebrate pathogenicity prevalent,  climatic extremotolerance prevalent;  frequent production of extracellular metabolites or mycotoxins,  frequent osmotolerance or growth in sugary fluids,  numerous members with soilborne lifestyle,  numerous members inhabiting decaying wood rich in hydrocarbons,  frequent insect-association,  frequent mushroom decomposition or hyperparasitism on fungi or lichens,  frequent inhabitants of foodstuffs or vertebrate intestinal tracts. (B) Latency reversal bioassay performed in J-Lat A2 cells with growth supernatants obtained from selected fungal strains. (C) Latency reversal bioassay in J-Lat A2 cells with growth supernatants obtained from members of the *Aspergillus* genus. Cells were treated as in panel B.

# Figure 2

A



B



C

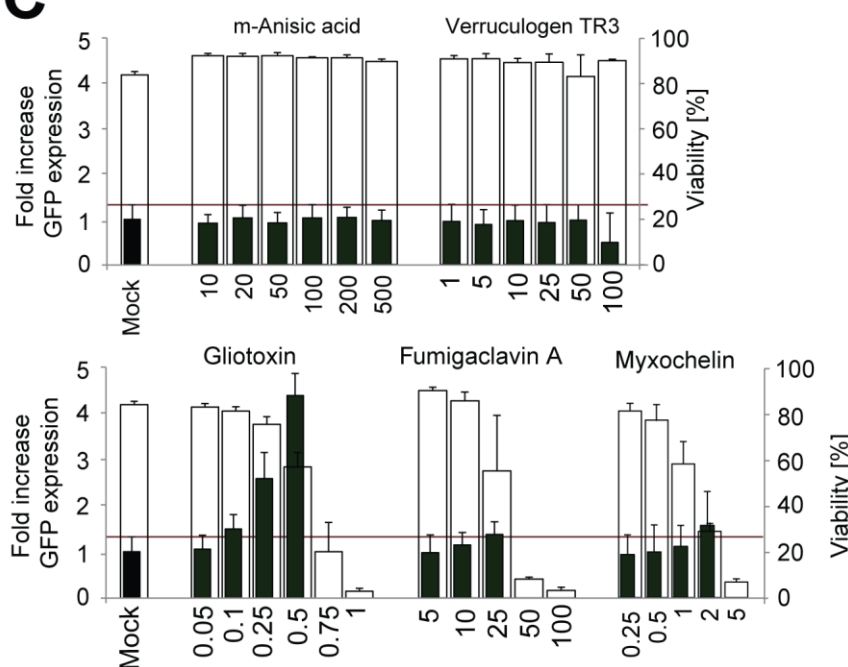


**Figure 2. Gliotoxin is the active component of growth supernatant of *Aspergillus fumigatus* and reverses latency in cell line models of HIV-1 latency.** (A) Schematic representation of the orthogonal MS strategy coupled to latency reversal bioassays used to identify putative LRA. (B) Three pre-concentration cartridges (HLC, SCX, MAX) were combined with variable content of extracting solvent. Latency reversal potential of fractionated secondary fungal metabolites was tested via treatment of J-Lat A2 cells. (C) Five molecules identified in active fractions were tested for LRA activity in J-Lat A2 cells. Data are presented as percent of GFP expression of fold increase in GFP expression as indicated,  $\pm$  SD from at least three independent experiments.

Figure 3

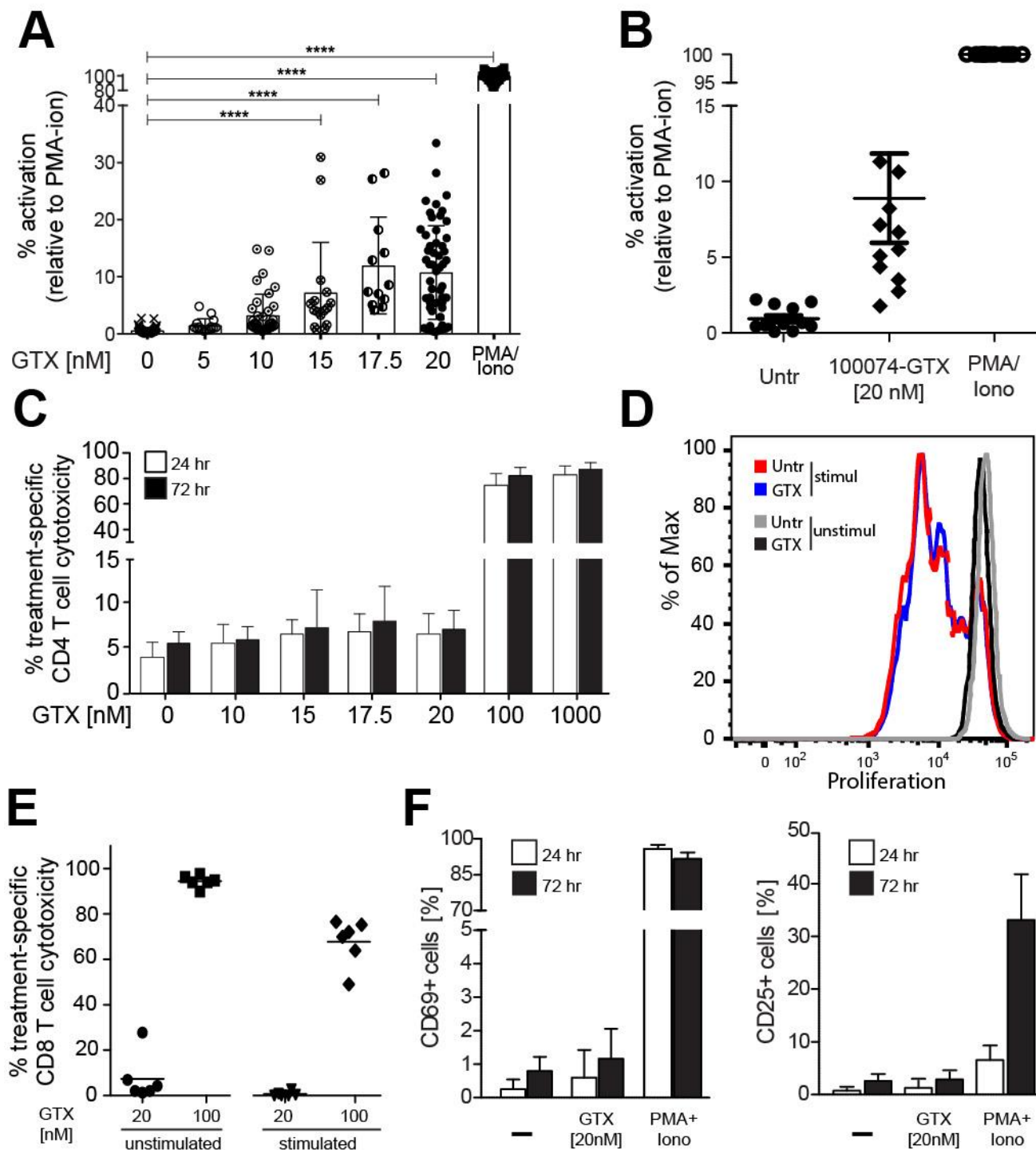


**Figure 3. GTX reverses HIV-1 latency in primary CD4+ T cells ex vivo infected without associated cytotoxicity, T cell activation, or inhibition of proliferative capacity.** (A) Latency reversal measured as luciferase activity after 24 hour treatment of latent primary CD4+ T cells with increasing concentrations of GTX as indicated, normalized to the positive control PMA/Ionomycin. (B) Latency reversal measured as luciferase activity after 24 hour treatment of latent primary CD4+ T cells with increasing concentrations of GTX isolated from growth supernatant of *Aspergillus fumigatus* CBS 100074, normalized to the positive control PMA/Ionomycin. Experiments were performed in duplicate using cells



obtained from at least 6 healthy donors. Wide horizontal lines represent average, shorter horizontal lines represent standard deviation. **(C)** Annexin V staining of primary CD4<sup>+</sup> T cells treated with increasing concentrations of GTX as indicated after 24- and 72-hours treatment. **(D)** Representative FACS plot overlay showing the division of unstimulated and  $\alpha$ CD3/CD28-stimulated CD8<sup>+</sup> T cells in the presence or absence of GTX. Averaged data from 3 experiments is presented in panel E. **(E)** Unstimulated or  $\alpha$ CD3/ $\alpha$ CD28 stimulated PBMCs were treated with GTX as indicated for 72 h followed by Annexin V staining of CD8<sup>+</sup>CD3<sup>+</sup> T cells and flow cytometry. Each symbol represents one healthy donor (n = 6 from 3 independent experiments using 2 different donors cells), horizontal line depicts mean. **(F)** Activation status of primary CD4<sup>+</sup> T cells upon GTX treatment as indicated. Averaged data of 3 independent experiments performed using 2 different donors cells in duplicate (n=6).

Figure 4

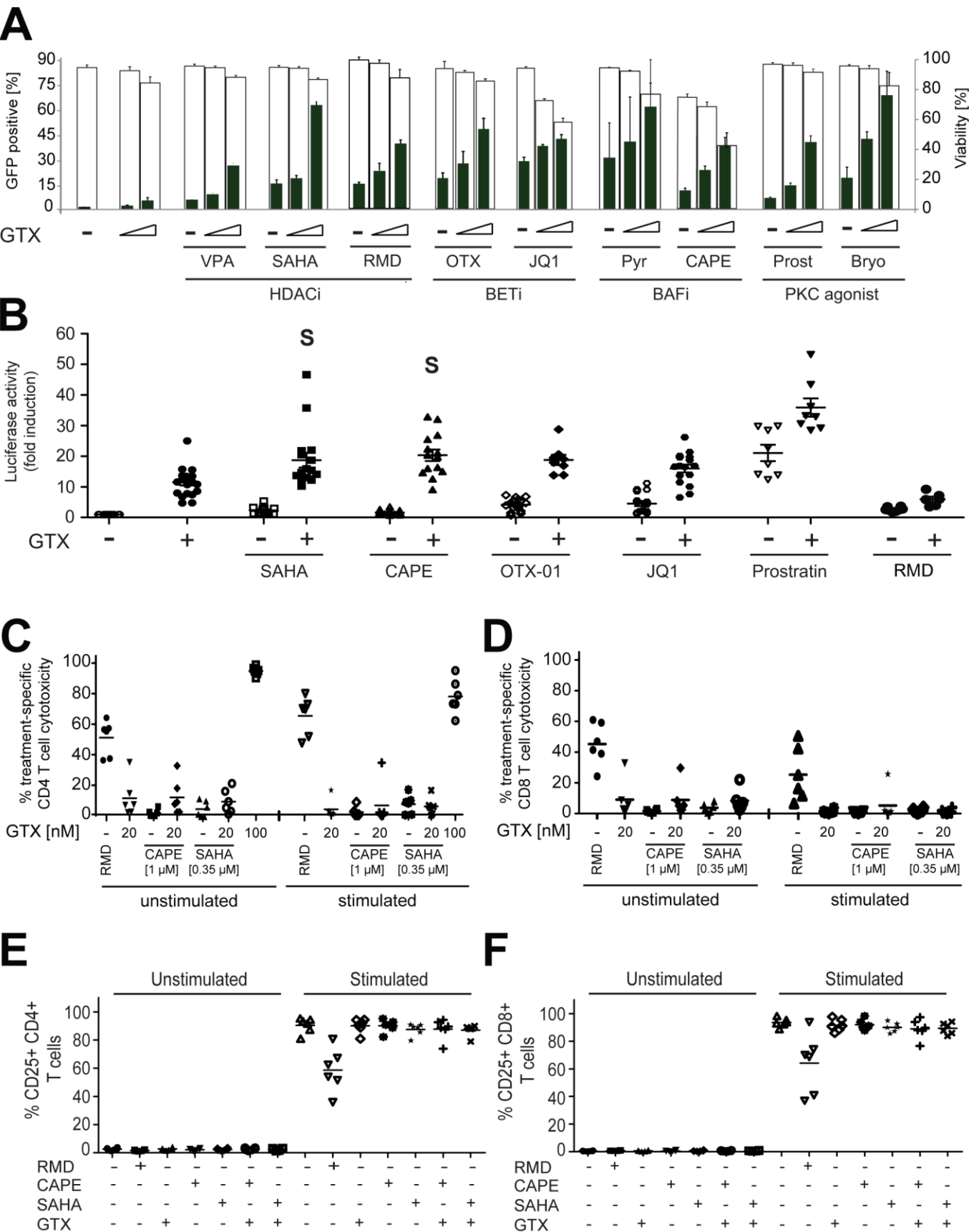
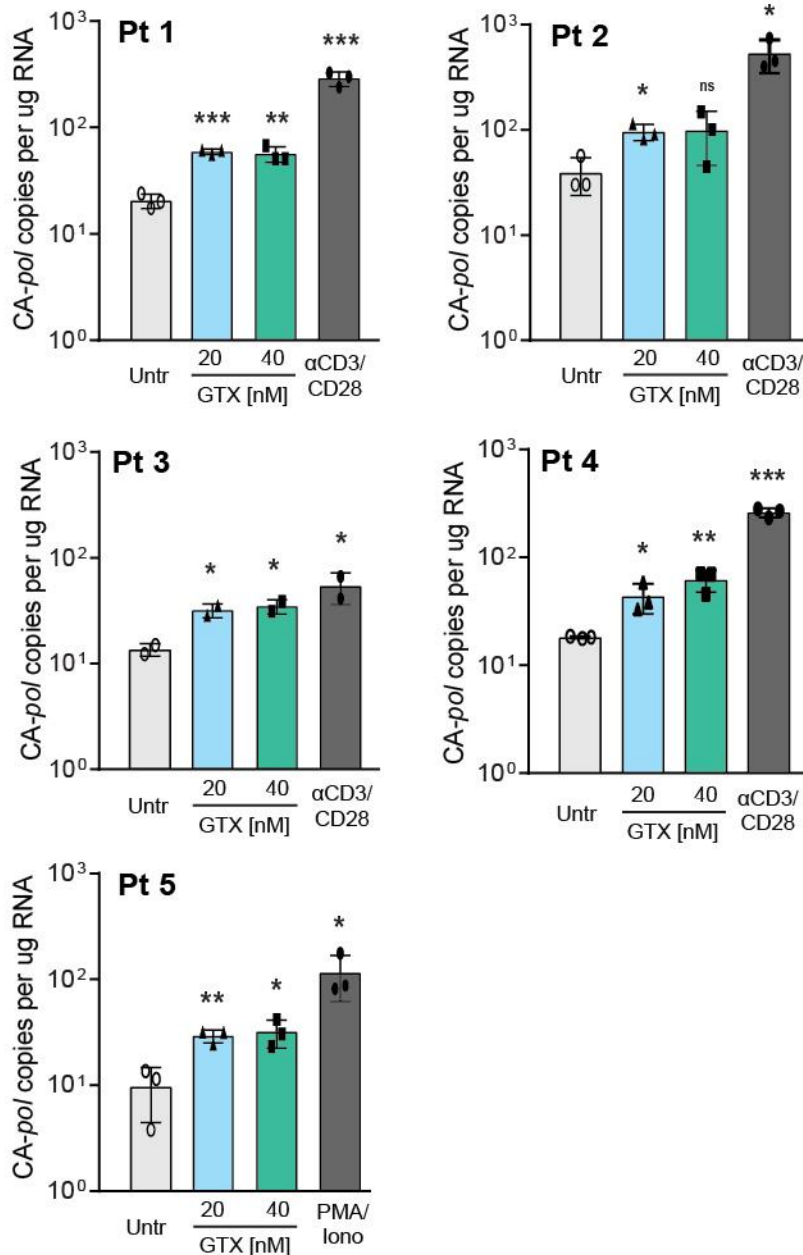


**Figure 4. GTX enhances the latency reversal activity of distinct LRA class molecules and strongly synergizes with HDAC inhibitor and BAF inhibitor family molecules.** (A) A2 J-Lat cells were left untreated or treated with increasing GTX concentrations (0.25  $\mu$ M and 0.5  $\mu$ M) alone or in combination with other known LRAs as indicated for 48 hours. Data are presented as mean GFP expression  $\pm$  SD from three independent experiments. (B) Fold induction luciferase activity after 24 hour co-treatment of ex vivo infected, latent primary CD4<sup>+</sup> T cells with 20 nM GTX and distinct LRA class compounds as indicated. S indicates compound synergism in latency reversal according to the Bliss independence score. (C & D) Unstimulated and  $\alpha$ CD3/ $\alpha$ CD28 stimulated PBMCs were co-treated as indicated for 72 h followed by Annexin V staining of (C) CD4<sup>+</sup>CD3<sup>+</sup> T cells and (D) CD8<sup>+</sup>CD3<sup>+</sup> T cells. (E and F) 20 nM GTX does not alter activation of CD4<sup>+</sup> (E) and CD8<sup>+</sup> (F) T cells. PBMC from healthy donors were incubated with the indicated LRAs for 72 hours either unstimulated or stimulated with anti-CD3/anti-CD28 antibodies. Representative FACS plots showing CD25 expression on gated CD8<sup>+</sup> T cells are shown in top panel. Bottom panels depicts pooled data showing the frequency of CD25<sup>+</sup> cells within CD4<sup>+</sup> (E) and CD8<sup>+</sup> T cells (F).

# Figure 5

**A**



**B**

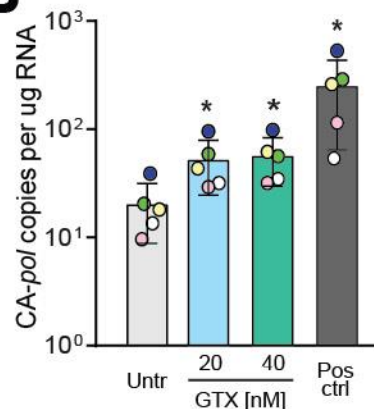


**Figure 5. Gliotoxin reverses latency in primary CD4+ T cells obtained from aviremic participants.** (A) Absolute, cell associated (CA) *pol* copy number in CD4+ T cells isolated from 5 aviremic participants that were treated in vitro for 24 hours as indicated. Statistical significance was calculated using t test, \* –  $p < 0,05$ ; \*\* –  $p < 0,005$ ; \*\*\* –  $p < 0,0005$ . (B) Data presented in panel A has been averaged and plotted together. Each symbol represents aviremic participant: green- participant 1; blue- participant 2; white- participant 3; yellow- participant 4; pink- participant 5. Statistical significance was calculated using unpaired Mann-Whitney test, \* –  $p < 0,05$ .

## Figure 6

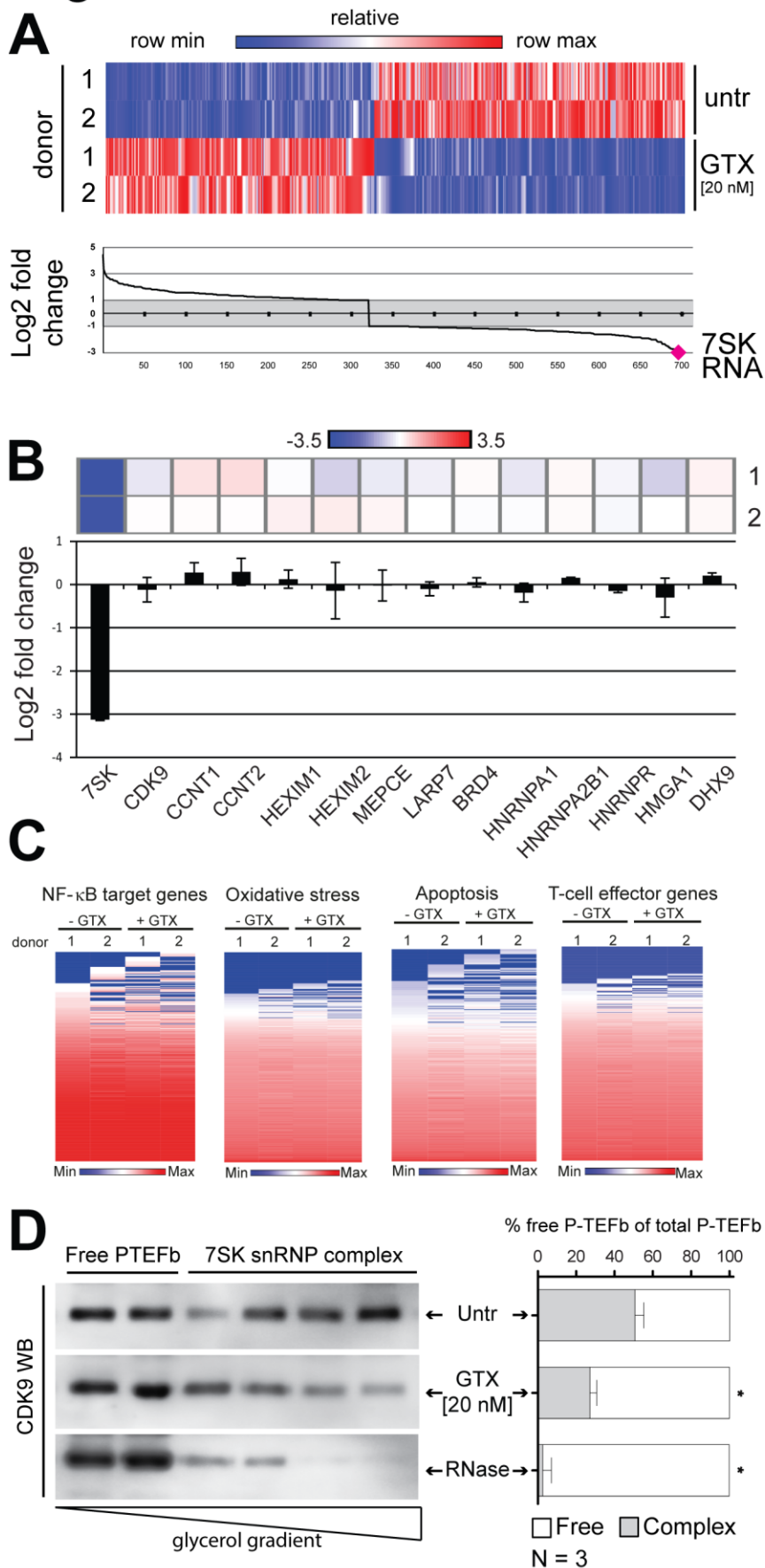
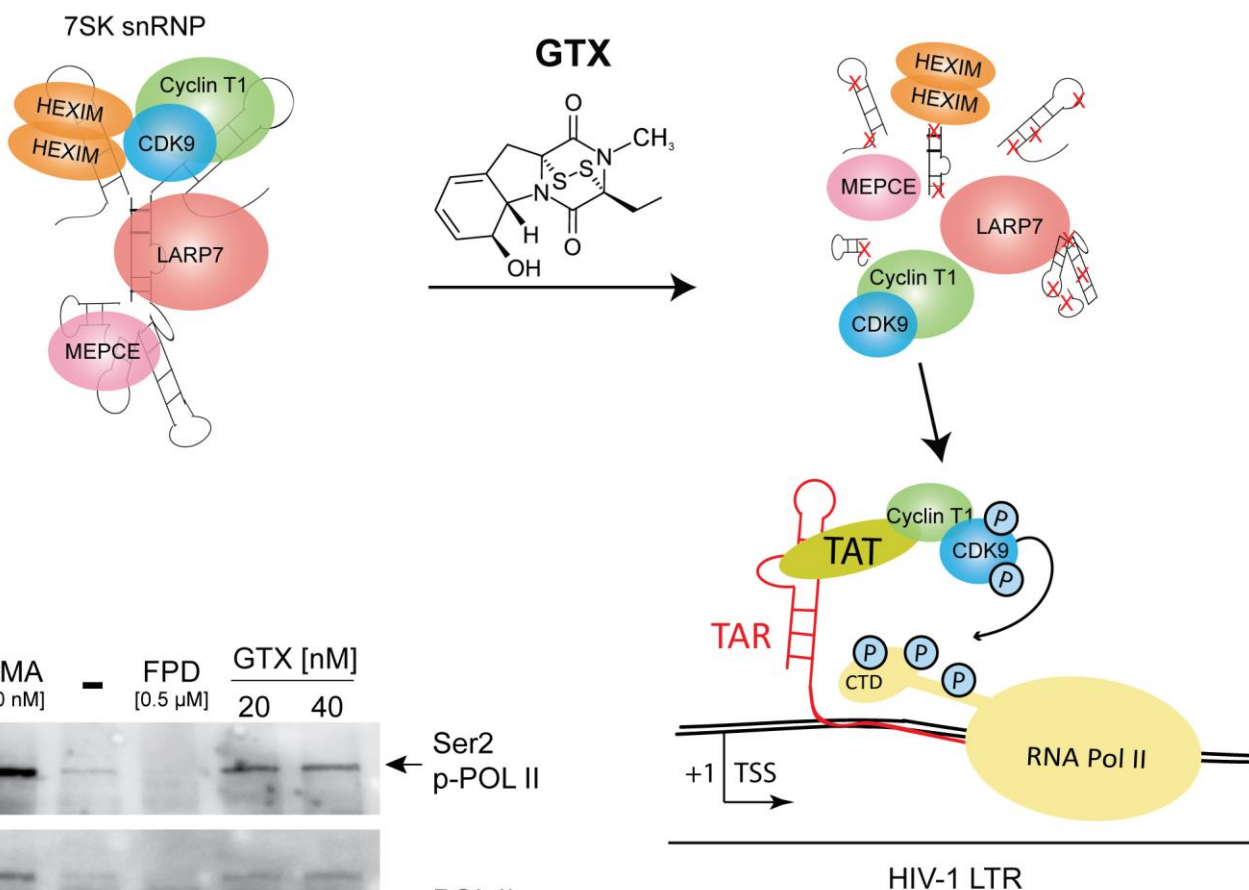


**Figure 6. GTX treatment causes massive downregulation of 7SK RNA with subsequent release of PTEF-b from its inhibitory 7SK snRNP complex.** (A) Heat map of differentially expressed genes obtained from RNA sequencing analysis of primary CD4<sup>+</sup> T cells treated as indicated for 4 h (top panel). RNA sequencing indicates 7SK RNA to be the most differentially downregulated gene in response to GTX treatment of CD4<sup>+</sup> T cells in two independent donors (bottom panel). (B) GTX treatment of primary CD4<sup>+</sup> T cells for 4 h leads to specific depletion of 7SK RNA levels and not mRNA levels of other components of the 7SK snRNP complex. (C) Heatmaps of RNA-seq data for NF-κB target genes, oxidative stress related genes, apoptosis related genes and T-cell effector genes demonstrates that 20 nM GTX does not influence these pathways. Primary CD4<sup>+</sup> T cells from two healthy blood donors were left unstimulated or stimulated with GTX [20nM] for 4 hours, RNA was isolated and processed for RNA sequencing. (D) GTX treatment causes release of pTEFb from sequestration within the 7SK snRNP complex. Representative western blot analysis of glycerol gradient sedimentation of lysates from primary CD4<sup>+</sup> T cell treated as indicated (left panel). Quantification of free versus total CDK9 in primary CD4 T cells treated as indicated, as shown in left panel from three independent donors (right panel). Statistical significance was calculated using ANOVA followed by Tukey test ( $p < 0.01$ ).

# Figure 7

**A**



**B**

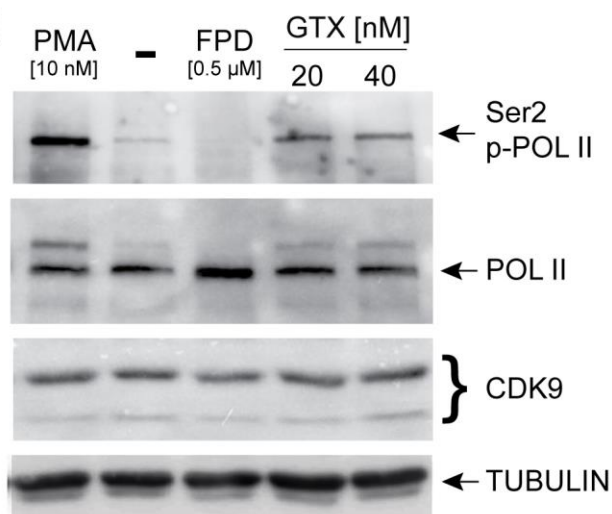


**Figure 7. GTX enhances the elongation step in HIV transcription via 7SK RNA degradation.** (A) Proposed model for GTX-mediated transcription activation of the latent HIV-1 LTR. GTX treatment leads to degradation of 7SK RNA, resulting in release of CDK9 (P-TEFb component) from the 7SK snRNP complex. Free P-TEFb is then recruited to the HIV-1 Tat-TAR axis, leading to phosphorylation of RNA polymerase II at Serine 2 and subsequent stimulation of transcription elongation. (B) Representative western blot analysis of CTD Serine 2 phosphorylation of RNA Polymerase II mediated by the CDK9 in primary CD4<sup>+</sup> T cells treated for 6h with GTX as indicated. PMA was used as a positive control, flavopiridol was used as a negative control.

# Figure S1

*A. fumigatus*  
CBS 100074

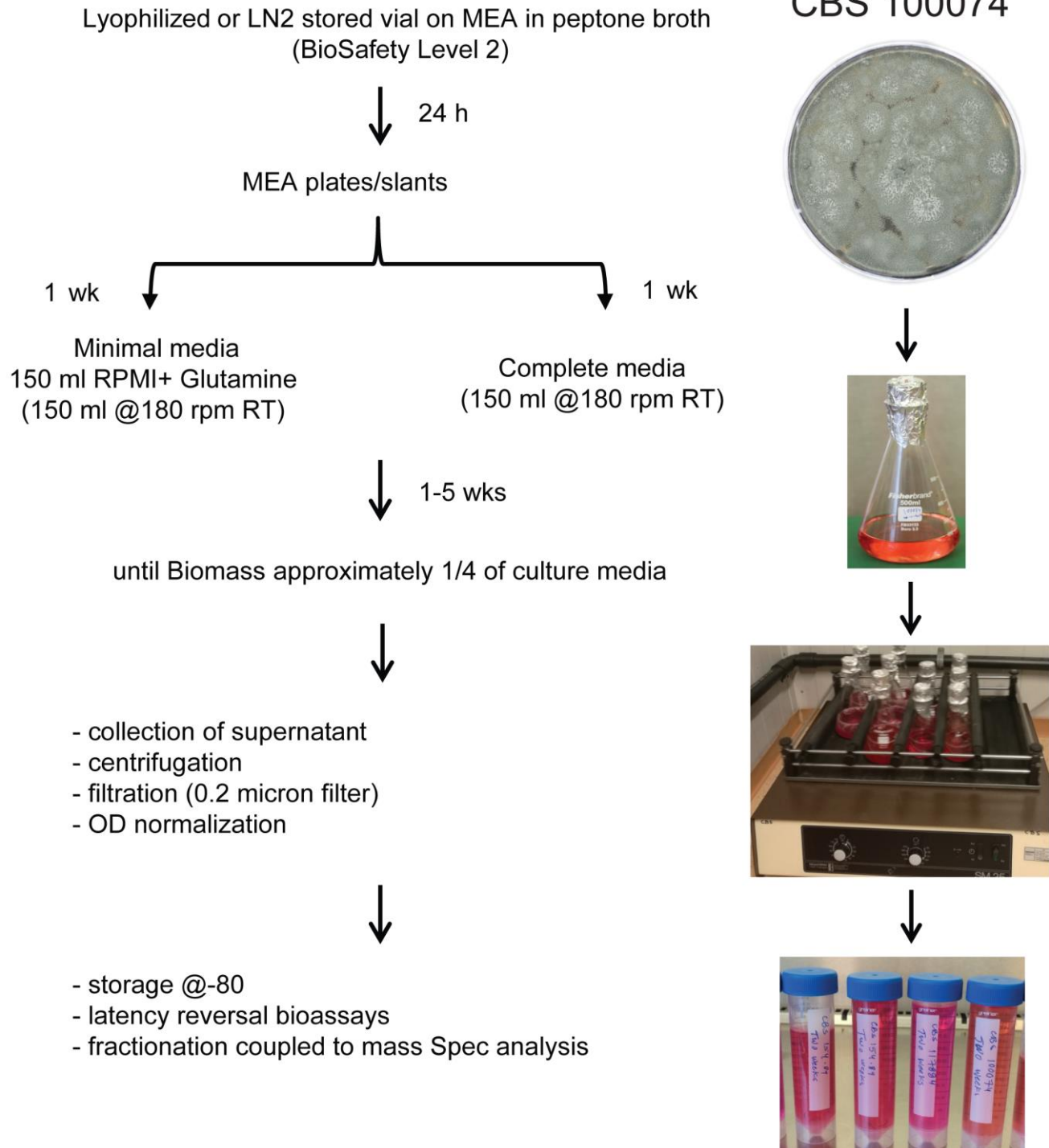


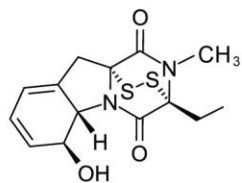
**Figure S1.** Schematic representation of the strategy used to culture fungi and prepare fungal supernatants.



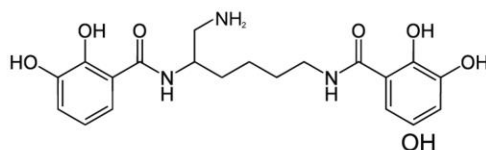
# Figure S2

**A**

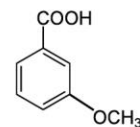
**GLIOTOXIN - GTX**



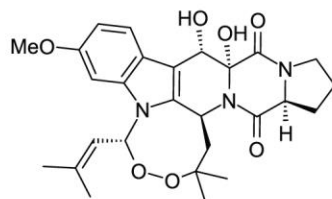
**MYXOCHELIN - MYX**



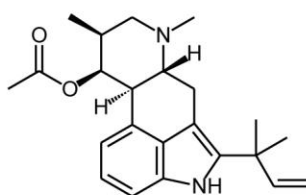
**m-ANISIC ACID - mAA**



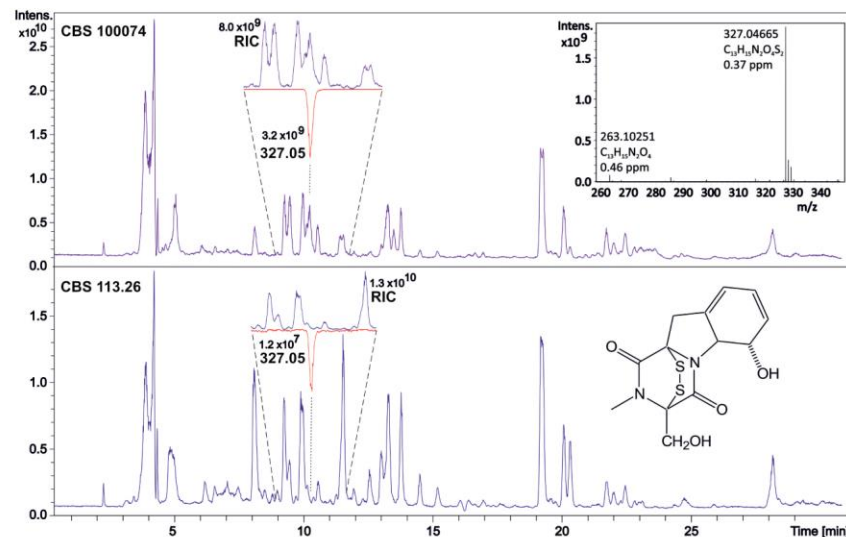
**VERRUCULOGEN - VER**



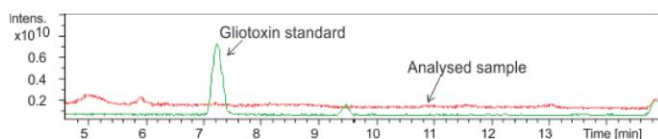
**FUMIGACLAVINE C - FCA**



**B**



**C**



**D**

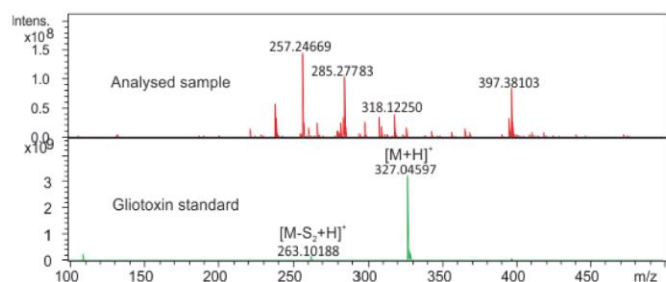


**Figure S2. Identification of constituents of fungal supernatants** (A) Commercially available, common constituents found in positive fractions that were tested for HIV-1 latency reversal. (B) HPLC-MS separation of dichloromethane extracts of *Aspergillus fumigatus* (CBS 100074 and CBS 113.26) fermentation broths. The insets indicate different gliotoxin content representing here more than 2.5 orders of magnitude (electrospray ionization). Quest for GTX in CBS 625.66 supernatant. (C) Total ion current from HPLC-MS of GTX standard (green curve) and analyzed sample (red curve). (D) MS spectrum extracted from the chromatogram (7-8 min region).

# Figure S3

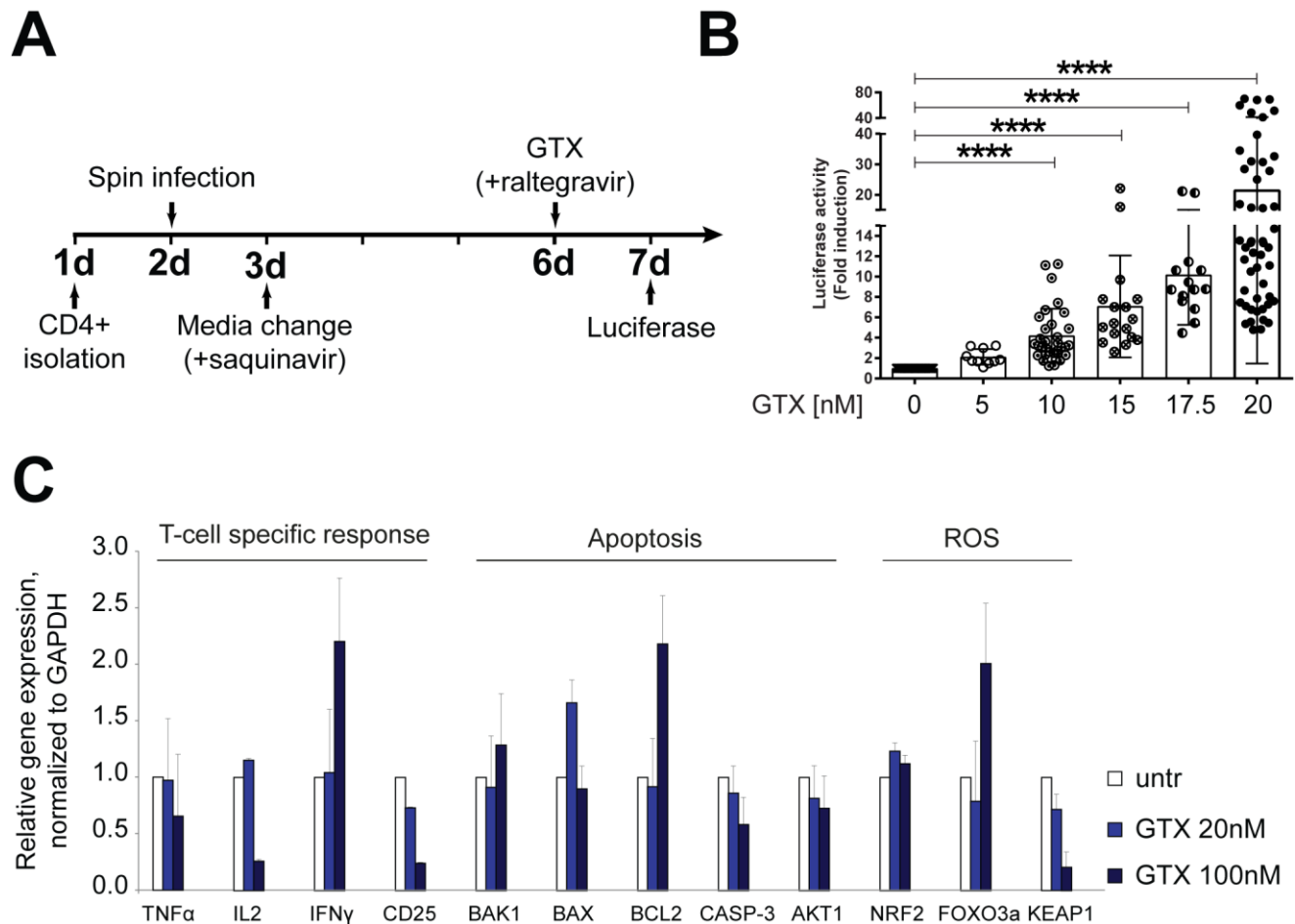
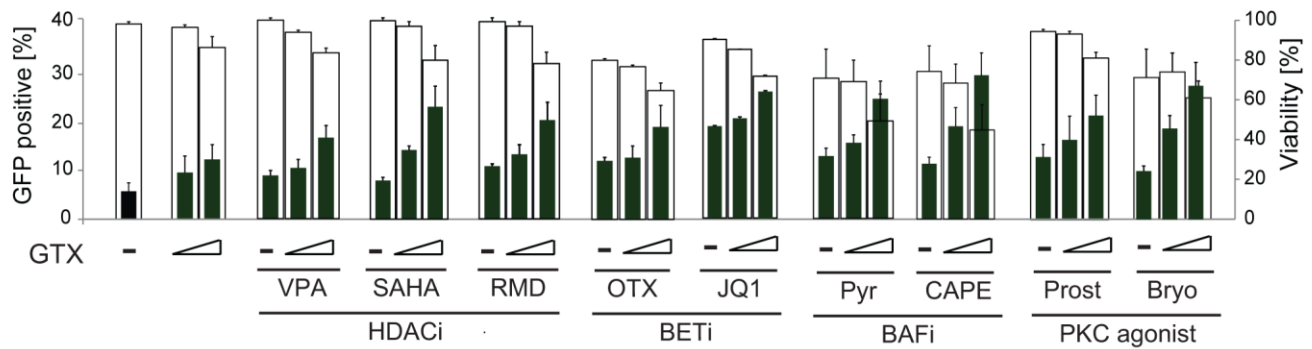


**Figure S3. GTX reverses HIV-1 latency in primary CD4<sup>+</sup> T cells *ex vivo* infected without associated cytotoxicity, T cell activation, or inhibition of proliferative capacity.** (A) Schematic of the strategy used to generate latent *ex-vivo* HIV-1 infected primary CD4<sup>+</sup> T cells. (B) Data presented in Figure 3A normalized as a fold induction over untreated control (C) GTX treatment of primary CD4<sup>+</sup> T cells at lower concentrations does not affect expression of reactive oxygen species (ROS), apoptosis or T-cell specific response related genes. Cells were isolated from 2 healthy blood donors and treated with GTX or left untreated for 4h as indicated. mRNA expression of T-cell effector functions, apoptosis and ROS related genes was assessed by real-time PCR.

# Figure S4

**A**



**B**

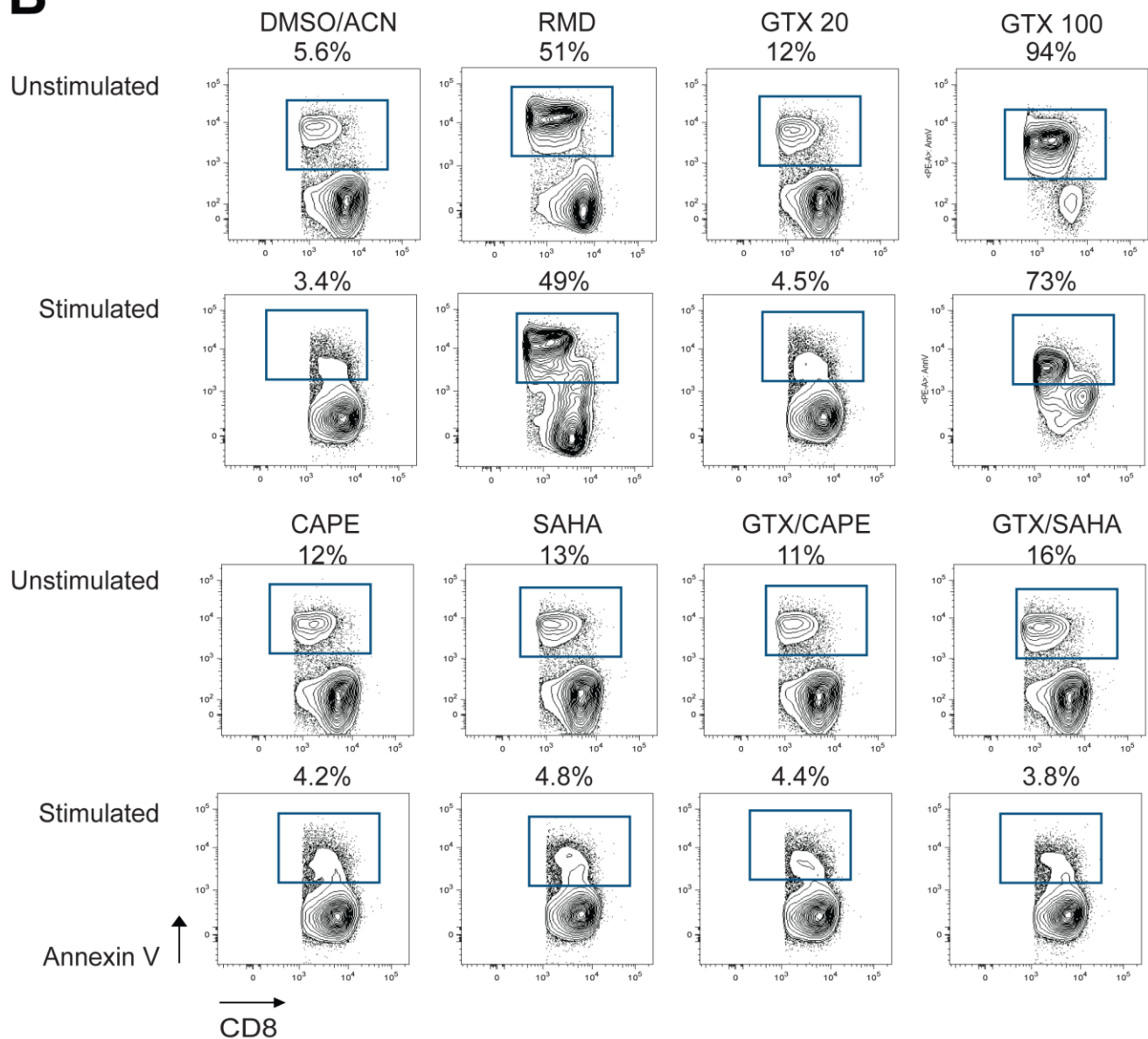


**Figure S4. GTX enhances the latency reversal activity of distinct LRA class molecules.** (A) 11.1 J-Lat cells were left untreated or treated with increasing GTX concentrations (0.25  $\mu$ M and 0.5  $\mu$ M) alone or in combination with other known LRAs as indicated for 48 hours. Latency reversal (%GFP, left axis, green bars) and cell viability (% viable, right axis, empty bars) was then assessed by flow cytometry analysis. Data are presented as mean  $\pm$  SD from three independent experiments. (B) 20 nM GTX alone or in combination with other LRA is non-toxic for CD8<sup>+</sup> T cells. PBMC from a healthy donor were incubated with the indicated concentrations of either DMSO/ACN or LRA under unstimulated or plate-bound anti-CD3/anti-CD28 antibody stimulated conditions. After 72 hours exposure, cell death of CD8<sup>+</sup>CD3<sup>+</sup> T cells was determined by Annexin V staining and flow cytometry. Representative flow cytometry plots are shown for one healthy donor. Numbers in plot depict frequency of gated Annexin V<sup>+</sup> CD8<sup>+</sup> T cells.

Figure S5

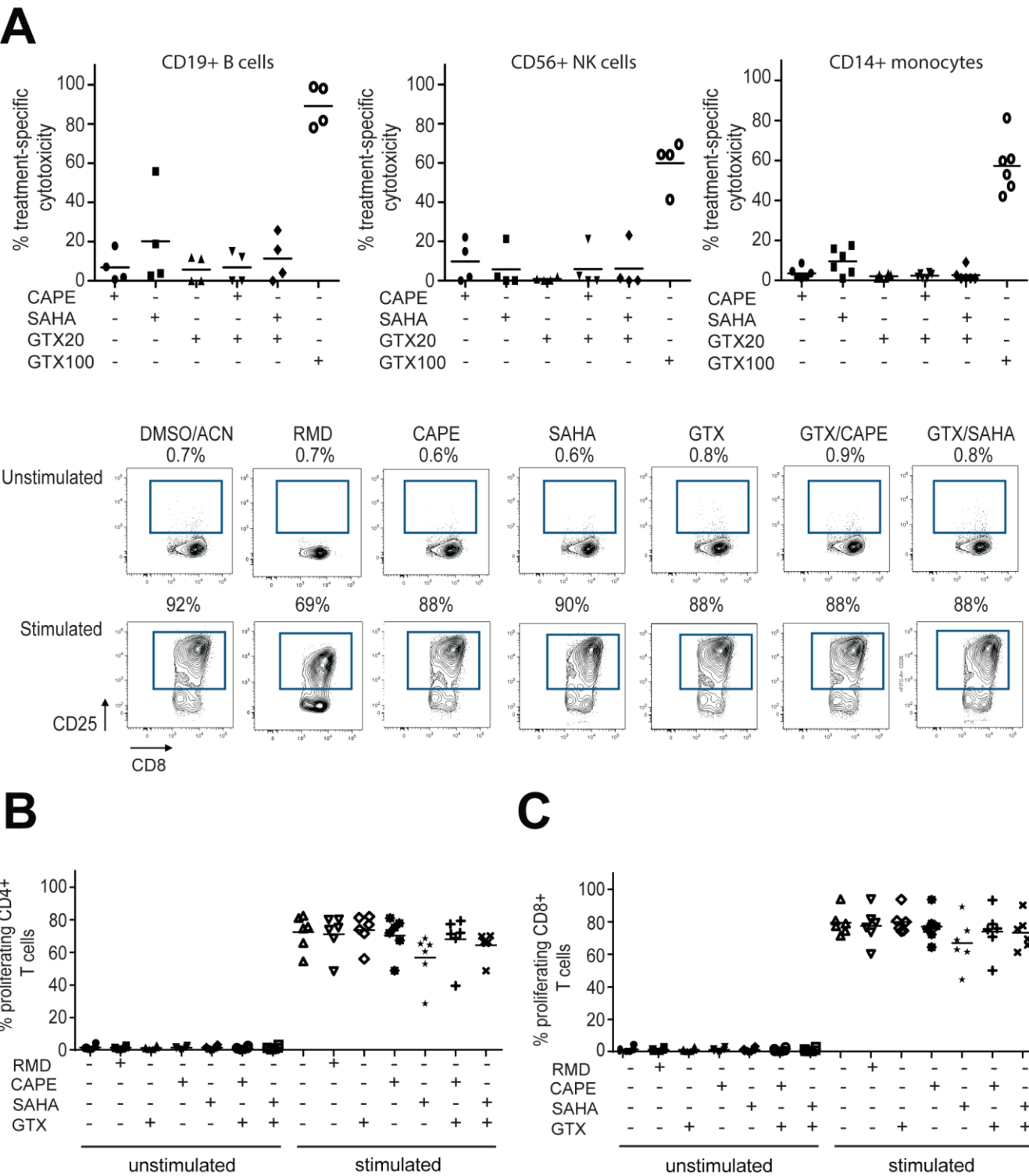


**Figure S5.** Co-treatments of GTX with other classes or LRAs are nontoxic to the primary white blood cells. (A) Low concentration of GTX is non-cytotoxic for B cells (left panel), NK cells (middle panel) and monocytes (right panel). PBMC from healthy donors were incubated with the indicated concentrations of LRA for 72 hours and the frequency of drug-specific cell cytotoxicity was calculated for CD19+ B cells, CD56+ NK cells and CD14+ monocytes. Bottom FACS

panels represent the gating strategy used for analysis. Each symbol represents one healthy donor (n = 6 from 2-3 independent experiments), horizontal line depicts mean. (B) CD4<sup>+</sup> T cells and (C) CD8<sup>+</sup> T cells were treated as indicated and the frequency of proliferating cells was assessed by flow cytometry. Each symbol represents one healthy donor (n = 6 from 2-3 independent experiments), horizontal line depicts mean.



Figure S6

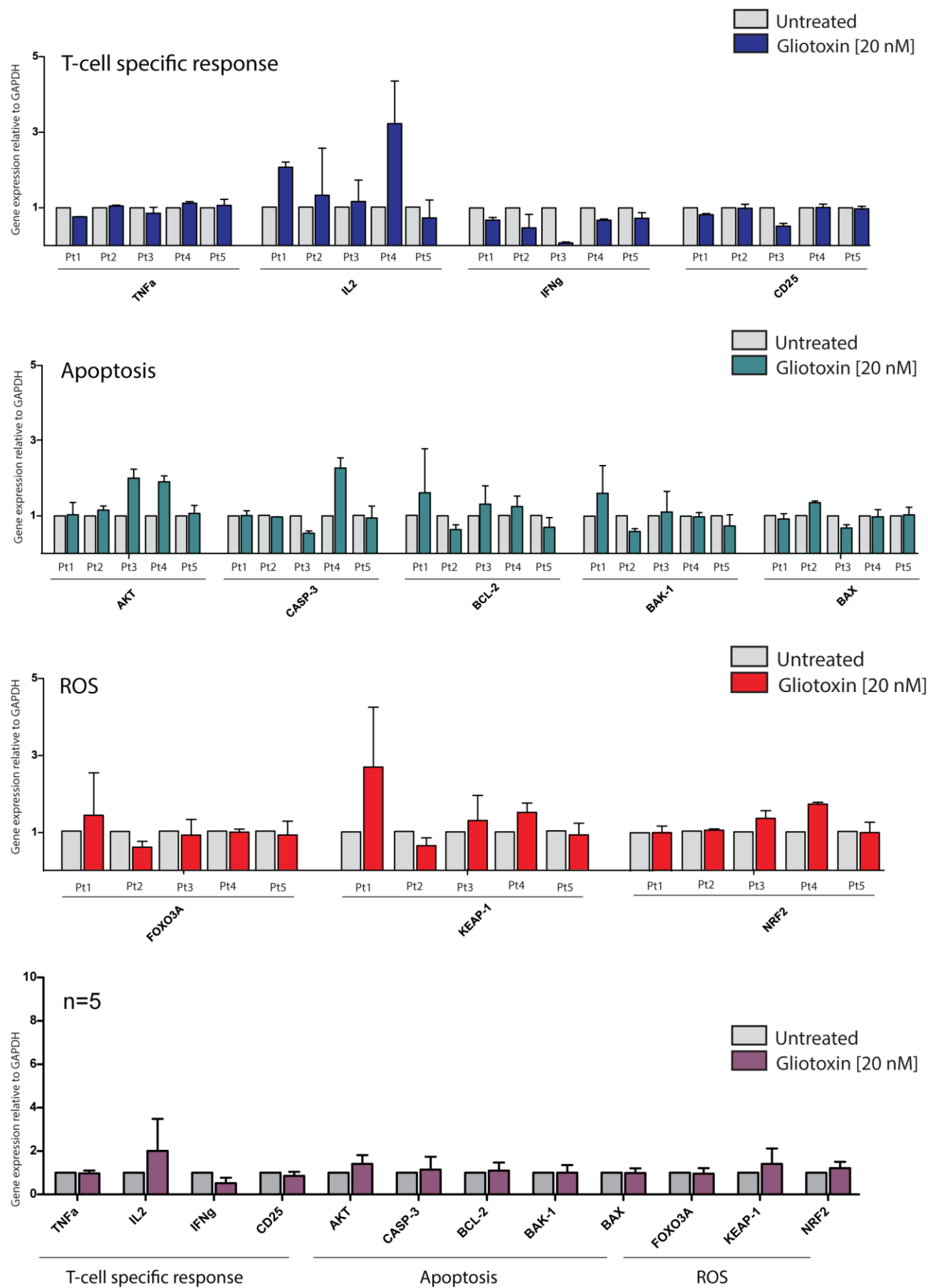
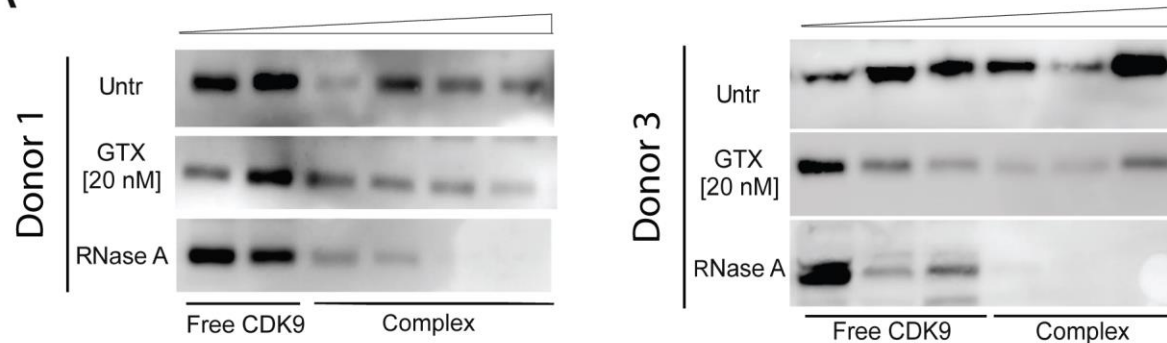


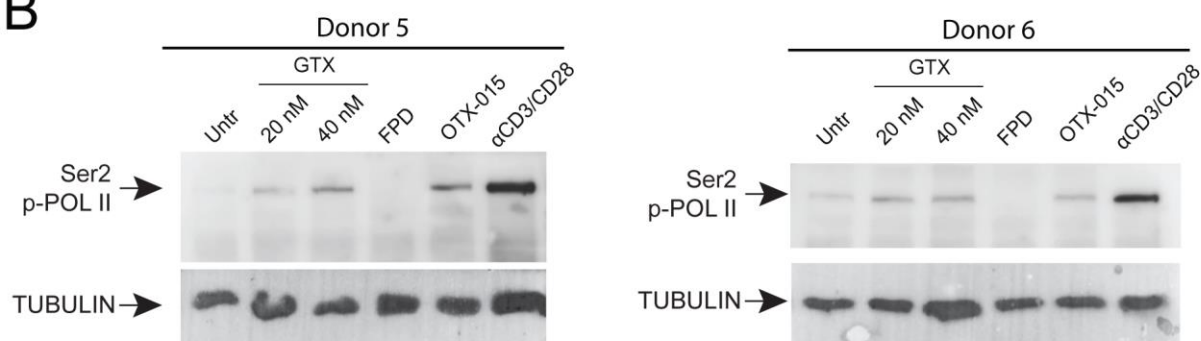
**Figure S6. GTX treatment of CD4<sup>+</sup> T cells obtained from aviremic participants does not induce ROS, apoptosis or T-cell specific responses.** (A) 20 nM GTX treatment of primary CD4<sup>+</sup> T cells isolated from 5 aviremic patients for 24 hours does not affect expression of reactive oxygen species (ROS), apoptosis or T cell effector function related genes. mRNA expression of genes was assessed by real-time PCR, expression was normalized with GAPDH. Bottom panel represents averaged data from all 5 aviremic HIV<sup>+</sup> participants.

# Figure S7

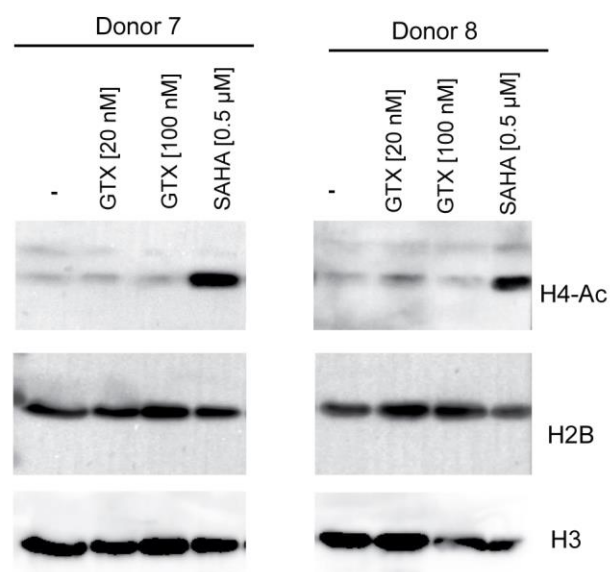
A



B



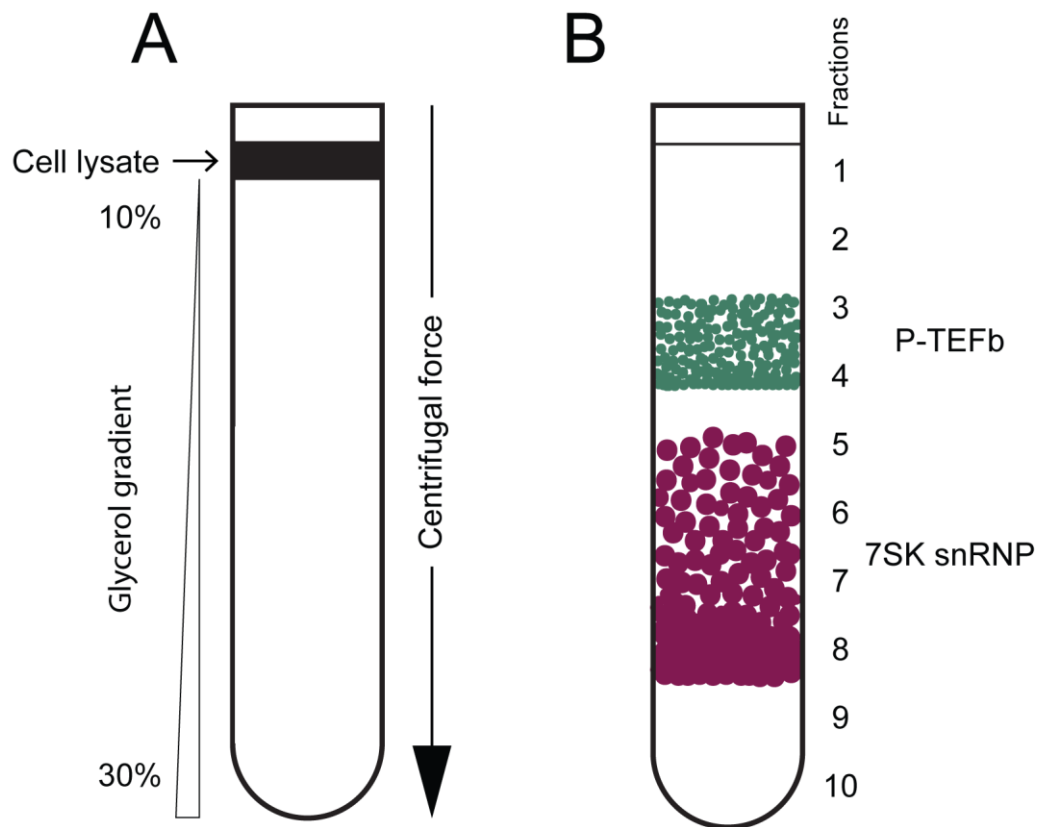
C



**Figure S7. GTX treatment causes release of active PTEF-b from its inhibitory 7SK snRNP complex.** (A) GTX treatment causes release of P-TEFb from sequestration within the inactive 7SK snRNP complex. Western blot analysis of glycerol gradient sedimentation of lysates from primary CD4<sup>+</sup> T cell (from two additional donors) either untreated or

treated with RNase [100 µg/ml] or GTX [20nM] as indicated, using antibody specifically recognizing CDK9. Release of P-TEFb complex from sequestration within the inactive 7SK RNA complex. (B) GTX treatment results in phosphorylation of RNA polymerase II at serine 2 in CD4<sup>+</sup> T cells obtained from two additional donors. Primary CD4<sup>+</sup> T cells were untreated or treated with GTX, BET inhibitor OTX-015 [1 µM], CDK9 (P-TEFb component) catalytic inhibitor flavopiridol (FPD) [500 nM] and  $\alpha$ -CD3/CD28 as a positive control for 6 h. Western blot analysis was performed using antibodies specific for Total RNA Pol II, serine 2 phosphorylated RNA Pol II, total CDK9 and tubulin as indicated. (C) GTX is not an HDAC inhibitor. Primary CD4<sup>+</sup> T cells from two healthy blood donors were left untreated or treated with GTX or SAHA as indicated for 4 h and subjected to western blot analysis of acetylated histone H4, and total histones H2B and H3.

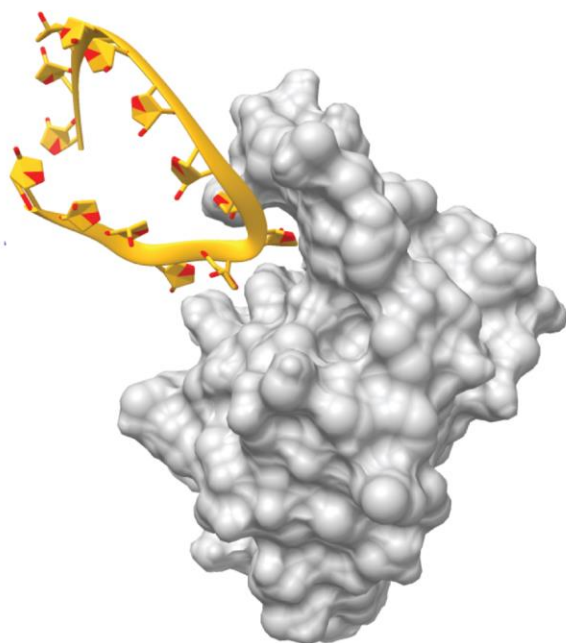
## Figure S8



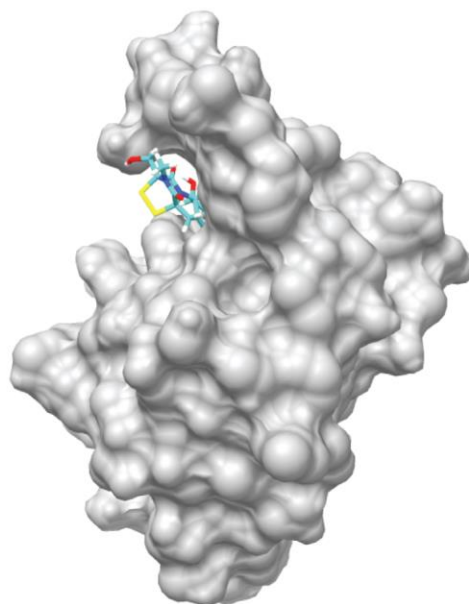
**Figure S8. Schematic of the setup of glycerol gradient experiments.** (A) Glycerol gradients are established by layering 2 ml of glycerol fractions (10, 15, 20, 25, 30 %) in buffer A into ultracentrifuge tubes. After 6 hours gradients are ready to use, cell lysate is loaded onto top of the gradients. Tubes are subjected to ultracentrifugation – 38 000 rpm for 20 hours. (B) After centrifugation 1 ml fractions are collected and subjected to Trichloroacetic acid (TCA) protein precipitation protocol with subsequent analysis by SDS-PAGE western blot.

Figure S9

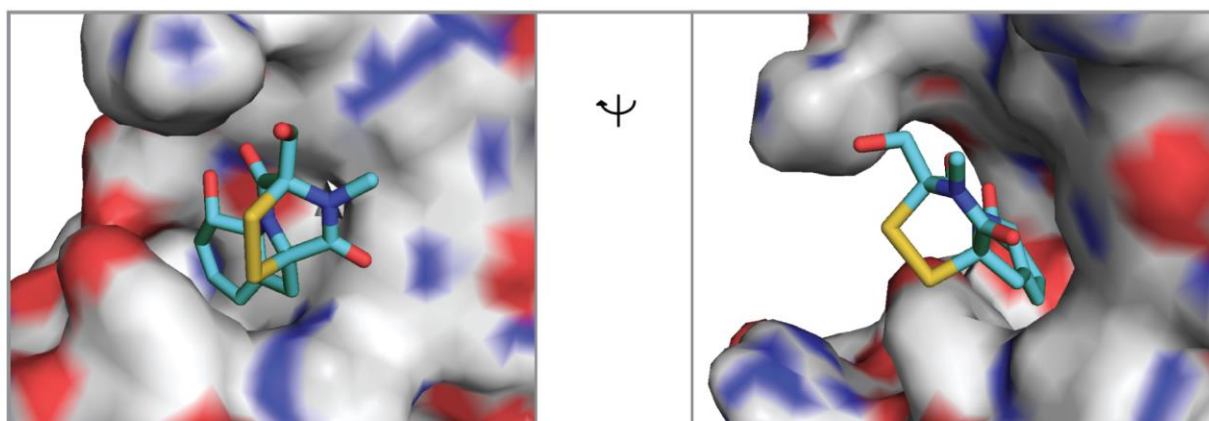
**A**



**B**



**C**



**D**

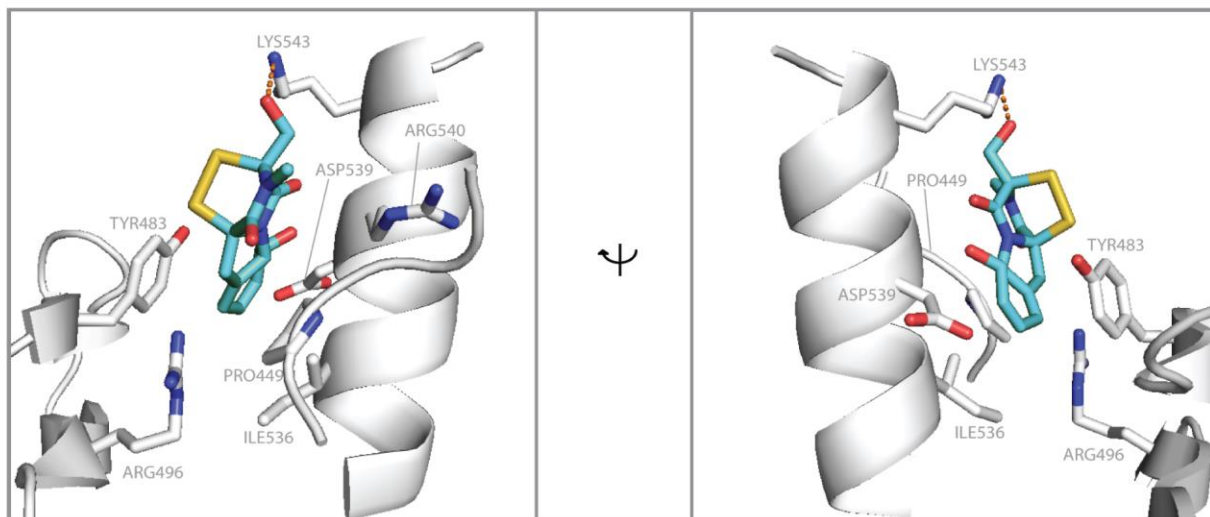


**Figure S9. Molecular docking of GTX onto LARP7.** (A) Crystal structure of human LARP7 C-terminal domain in complex with 7SK RNA SL4 (PDB ID code 6D12). LARP7 is shown in space-filling representation (grey) with bound RNA as yellow cartoon representation with bases indicated as flat rings (oxygens in red). One of the bases of 7SK RNA SL4 is bound into a deep pocket on the surface of LARP7. (B) Proposed binding mode of GTX into the deep pocket on the surface of LARP7 as predicted by Chimera's AutoDock Vina function and the Achilles Blind Docking Server. Color code for GTX is turquoise for carbon, red for oxygen, yellow for sulphur, white for hydrogen, blue for nitrogen. (C) Close up of hydrophobic pocket on the surface of LARP7 with bound GTX (highest scoring prediction from Achilles coordinates) in two orientations. LARP7 surface color code is red for oxygen, blue for nitrogen, grey for carbon (hydrophobic). Color code for GTX as in panel B. (D) Details of interactions formed between LARP7 and GTX. Color code as in panel B. The predicted hydrogen bond between GTX and Lysine 543 from LARP 7 is indicated with a dashed line. Side chain atoms of Asp539, Ile536, Pro449 and Tyr483 make favorable van der Waals contacts with GTX. All images were generated with the use of PyMol software.

## **STAR Methods**

### **EXPERIMENTAL MODEL AND SUBJECT DETAILS**

#### **Cells and culture conditions**

Jurkat latent (J-Lat) cell lines A2 and 11.1 were cultured in RPMI-1640 media supplemented with 10% FBS and 100 µg/ml penicillin-streptomycin at 37 °C in a humidified 95%-air-5%CO<sub>2</sub> incubator. Primary CD4<sup>+</sup> T cells were cultured in RPMI-1640 media supplemented with 7% FBS and 100 µg/ml penicillin-streptomycin at 37 °C in a humidified 95%-air-5%CO<sub>2</sub> incubator.

### **METHOD DETAILS**

#### **Preparation of fungal supernatants**

We screened 115 species of filamentous fungi (Table S1, Fig. S1A). Species belonged to 28 orders (43 families) of the fungal Kingdom. The majority were of ascomycetous affinity including ascomycetous yeasts (Saccharomycetales: four species), 12 were of basidiomycetous affinity including three basidiomycetous yeasts (Trichosporonales, Tremellales), and three species of lower fungi (Mucorales)(Gostinčar et al., 2018). Rationale for choice was the expected production of a wide array of metabolites, which are known to be more pronounced in fungi living in habitats with environmental stress or microbial competition. Particularly versatile nutrient scavengers in Eurotiales and Hypocreales are established metabolite and toxin producers. Onygenales are cellulose and keratin degraders, and contain a large cluster of mammal pathogens with alternating environmental life cycles. Members of Capnodiales are saprobes in environments with stressful microclimates such as rock, glass and indoor. Identity of all strains was verified by rDNA ITS (Internal Transcribed Spacer) and partial nucLSU (D1/D2 of Large SubUnit) sequencing.

Strains were derived from lyophilized storage in the reference collection of the Centraalbureau voor Schimmelcultures (housed at Westerdijk Fungal Biodiversity Institute, Utrecht, The Netherlands). After opening, contents of vials were taken up in 1 mL malt peptone and distributed on Malt Extract Agar (Oxoid) culture plates. Strains



were maintained MEA slants and subcultured regularly until use. Mycelial fragments of one-week-old colonies grown on MEA at 25°C were used as inocula for 500-mL flasks containing 150 mL RPMI (with glutamine) shaken at 180 r.p.m. and incubated at 25°C for 7 days, with one negative control. Flasks were checked daily until biomass reached 1/3 to 1/4 of the volume, then harvested by centrifugation at 14,000 g and filtered using 0.2 µm metal filters. Supernatants were transferred to falcon tubes and used for latency screens. One strain per genus was used in a first round; additional isolates, some of which were close relatives and others located at larger phylogenetic distance, were tested in case of positive response. Positive tests of strain *Aspergillus fumigatus* CBS 113.26 was thus followed by *A. fumigatus* CBS 154.89, CBS 117884, CBS 100074, *A. lentulus* CBS 117884, and *A. flavus* CBS 625.66.

### Fractionation and mass spectrometry characterization of active components

Complex fungal supernatants (3.3 mL) were twice extracted with ethylacetate (3 mL) in glass tubes (5 minute vortex) and centrifuged at 3000 rpm. Water phase was discarded and organic extract dried in vacuum concentrator. Lipids were removed by consequent hexane/water extraction (50/50, v/v, 4 mL total volume), aqueous phase was collected and dried. The dried material was reconstituted in a 50% methanol and such a solution loaded onto HLB, MCX and MAX cartridges (**Fig. 2A**) obtained from Waters Corporation (Prague, Czech Republic). The adsorbed compounds were desalted and stepwise eluted with increasing (5, 45 and 95%) organic solvent (MeOH) gradient (1% HCOOH) providing A, B and C sample variants, respectively (**Fig. 1C**). HLB was based on N-vinylpyrrolidone – divinylbenzene copolymer and provided 5-fractions. MCX was cation exchange sorbent represented the HLB material modified with SO<sub>3</sub>H<sup>-</sup> groups (6-fractions). The best performance was provided anion exchange MAX cartridge providing 7-fractions. After each round of fractionation all samples were tested in J-Lat/S-Lat latency models, followed by quantitation GFP/luciferase expression and identification of fraction retaining activating component. As expected, originally less active fractions have become positive as the active components became populated during the enrichment process. The same phenomenon was observed when working with less or more active *Aspergillus* strains (**Supplemental Fig. 2C**).

The most active 7B/7C fractions were further fractioned on HLB cartridge (11-samples) and components dereplicated by Cyclobranch software (Novák et al., 2017). Compound matching against the annotated database of *Aspergillus* secondary metabolites has revealed a set candidate compounds further selected for latency reversal testing. Gliotoxin was present in active fractions (**Figs. 2D, E**).

Detailed examination of commercial (GTX, Cayman and ApexBio) and natural gliotoxins was performed by high performance liquid chromatography (HPLC) and Fourier transform ion cyclotron resonance (FTICR) mass spectrometry. Solarix XR 12T FTICR instrument (Bruker Daltonics, Billerica, USA) was operated in positive ion mode with electrospray ionization. Separation of GTX components was performed on Acquity UPLC HSS T3 analytical column (Waters, Prague, Czech Republic) with 1.0x150 mm dimensions and 1.8 µm particle size. The analysis was carried out at 30 °C and 30 µL/min flow rate with the following A/B gradient: 0 min – 30% B; 30 min - 95% B; 40 min - 95% B; 50 min - 30% B; 60 min - 30% B. The gradient components A and B were represented by 0.1% formic acid in water or acetonitrile, respectively. One minute time windows around S2 and S3/S4 gliotoxins were used for fraction isolation. The preparative chromatography was performed both with commercial gliotoxin as well as with *A. fumigatus* 100074 strain.

### **Flow cytometry and annexin V staining**

GFP expression of cell lines J-Lat A2 and 11.1 and phenotype of spin infected primary CD4<sup>+</sup> T cells at the moment of reactivation were analyzed by FACS (fluorescence-activated cell sorting) as described previously (Stoszko et al. 2015). For Annexin V staining 10<sup>6</sup> cells were washed with PBS supplemented with 3% FBS and 2.5mM CaCl<sub>2</sub> and stained with Annexin V-PE (Becton and Dickinson) for 20 min at 4 °C in dark in the presence of 2.5mM CaCl<sub>2</sub>. Stained cells were washed with PBS/FBS/CaCl<sub>2</sub>, fixed with 1% formaldehyde and analyzed by FACS.

### **Primary CD4<sup>+</sup> T cell isolation and infection**

Primary CD4<sup>+</sup> T cells were isolated from buffy coats from healthy donors by Ficoll gradient (GE Healthcare) followed by negative selection with RosetteSep Human CD4<sup>+</sup> T Cell Enrichment Cocktail (StemCells Technologies). Isolated cells were left overnight for recovery and used for spin-infection according to Lassen and Greene method as described previously (Spina et al. 2013, Stoszko et al. 2015). Briefly, CD4<sup>+</sup>T cells were infected with the PNL4.3.LUC.R-E- virus by spinoculation (120 min at 1200 g) and cultured for three days in RPMI 10% FBS and 100 µg/ml penicillin-streptomycin in presence of Saquinavir Mesylate (5 µM). Three days after infection cells were treated as indicated in presence of Raltegravir (30 µM). Cells were harvested 24 h after treatment and luciferase activity was measured using Luciferase Assay System (Promega, Leiden, The Netherlands). Infections were performed using pseudotyped particles obtained by co-transfecting HXB2 Env with pNL4.3.Luc.R-E- plasmid into HEK 293t cells using PEI, 48 and 72 h post transfection, supernatants containing pseudotyped virus were collected, filtered with 0.45µm filter and stored at -80 °C. Molecular clones pNL4.3.Luc.R-E- and HIV-1 HXB2-Env, and antiretroviral drugs Saquinavir Mesylate and Raltegravir were kindly provided by the Centre for AIDS Reagents, NIBSC. HIV-1 molecular clone pNL4.3.Luc.R-E- and HIV-1 HXB2-Env expression vector were donated by Dr. Nathaniel Landau and Drs Kathleen Page and Dan Littman, respectively.

### **HIV-1 latency reversal in primary CD4<sup>+</sup> T cells isolated from aviremic patients**

Primary CD4<sup>+</sup> T cells were isolated as described previously (Stoszko et al., 2015). Three million CD4<sup>+</sup> T cells were plated in triplicate at the cell density of 10<sup>6</sup>/ml and treated as indicated. After 24 hours cells were lysed and total RNA was isolated as described below. Written informed consent was obtained from all patients involved in the study. The study was conducted in accordance with ethical principles of the Declaration of Helsinki. The study protocol and any amendment were approved by The Netherlands Medical Ethics Committee (MEC-2012-583).

### **Total RNA isolation and quantitative RT-PCR**

Cells were lysed in TRI reagent and RNA was isolated with Total RNA Zol-out kit (A&A Biotechnology), cDNA synthesis and qPCR was performed as described previously (Stoszko et al., 2016). Gene expression was calculated using 2<sup>-ΔΔCt</sup> method by Livak/Schmittgen (Schmittgen and Livak, 2008), expression of GAPDH was used for normalization. Absolute quantification of cell-associated *pol* RNA was performed as described previously (Stoszko et al., 2016). Briefly, qPCR was performed in a final volume of 25 µl using 4 µl of cDNA, 2.5 µl of 10× PCR buffer (Life Technologies), 1.75 µl of 50mM MgCl<sub>2</sub> (Life Technologies), 1 µl of 10 mM dNTPs (Life Technologies), 0.125 µl of 100 µM Pol Forward primer (HXB2 genome 4901 → 4924), 0.125 of 100 µM Pol Reverse primer (HXB2 genome 5060 → 5040), 0.075 µl of

50  $\mu$ M of Pol Probe, and 0.2  $\mu$ l Platinum Taq polymerase (Life Technologies). The lower limit of detection of this method was of 20 copies of HIV-1 RNA in 1  $\mu$ g of total RNA. The absolute number of polcopies in PCR was calculated using a standard curves ranging from 7 to 480 copies of a plasmid containing the full-length HIV-1 genome (pNL4.3.Luc.R-E-). The amount of HIV-1 cellular associated RNA was expressed as number of copies/ $\mu$ g of input RNA in reverse transcription. Preparations of cell-associated RNA were tested for potential contamination with HIV-1 DNA and-or host DNA by performing the PCR amplification in the presence and absence of reverse transcriptase. List of all primers used can be found in Table S3.

### **Glycerol gradient sedimentation (Fig. S8)**

Glycerol gradients were prepared as described previously (Contreras et al., 2007). Briefly, around  $40 \times 10^6$  primary CD4<sup>+</sup> T cells isolated from healthy donors were either untreated or treated with GTX [20 nM] for 4 h, for RNase A treatment. Cells were lysed for 30 min in buffer A supplemented with either 100U/ml RNasin (Promega) for untreated and GTX conditions, or with 100  $\mu$ g/ml RNase A. RNase supplemented lysates were incubated for 10 min at room temperature to ensure efficient degradation of RNA. Lysates were fractionated by centrifugation in a SW41 Ti rotor at 38000rpm for 20h. 1mL fractions were collected in 2 ml tubes and subjected to Trichloroacetic Acid precipitation of proteins as described previously (Link and LaBaer, 2011). Briefly, to each 1 ml fraction 110  $\mu$ l of ice-cold 100% trichloroacetic acid (TCA) was added and incubated on ice for 10 min. Then, 500  $\mu$ l of ice-cold 10% TCA was added to each sample and incubated on ice for 20 min, followed by centrifugation at 20 000g for 30min. Supernatants were carefully removed and precipitates were gently washed with 500  $\mu$ l of ice-cold acetone followed by centrifugation at 20 000g for 10 min. Supernatants were gently removed and dried at room temperature for about 10 min. Protein precipitates were then re-suspended in 50  $\mu$ L of Laemmli loading buffer and subjected to 10% SDS-PAGE separation and detection of CDK9 (C-20, sc-484, Santa Cruz Biotechnology).

### **RNA Polymerase II phosphorylation**

Ten million primary CD4<sup>+</sup> T cells were either untreated or treated with GTX, OTX-015 [1  $\mu$ M], flavopiridol [500 nM], PMA [10 nM] or  $\alpha$ CD3/CD28 beads (cell: bead ratio 1:1) for 6 h. Cell were lysed for 30min on ice with IP buffer (Stoszko et al., 2015) and subjected to western blot analysis using following antibodies: total RNAPII (N-20, sc-899 Santa Cruz Biotechnology), phospho-Ser2 RNAPII (H5, ab-24758, Abcam), CDK9 (C-20, sc-484, Santa Cruz Biotechnology),  $\alpha$ -tubulin (ab6160, Abcam).

### **Histone acetylation**

Ten million primary CD4<sup>+</sup> T cells were treated with gliotoxin concentration gradient, SAHA or left untreated for 4 h and then washed twice in PBS. Cells were lysed for 10 min at 4  $^{\circ}$ C in TEB buffer (PBS, 0.5 % triton X-100 (v/v), 2 mM phenylomethylsulfonyl fluoride (PMSF), 0.02 % (w/v) NaN<sub>3</sub>) at a density of  $10^7$  cells per 1 ml of the buffer. Samples were centrifuged at 425 g for 10 min at 4  $^{\circ}$ C. Supernatants were discarded and cell pellets were washed in half the volume of TEB buffer used for lysis and centrifuged as before. Supernatants were discarded and pellets were resuspended in 0.2N HCl at a density of  $4 \times 10^7$  cells per ml. Histones were extracted overnight at 4  $^{\circ}$ C and then centrifuged at 425 g for 10 min at 4  $^{\circ}$ C. Supernatants were collected, protein concentration was determined by the Bradford assay and samples

were subjected to SDS-PAGE western blot. Following antibodies were used in western blot analysis: anti-acetyl-histone H4 (06-598, Milipore) and anti-histone H2B (ab52484, Abcam).

### **RNA sequencing and data analysis**

Ten million primary CD4<sup>+</sup> T cells were stimulated with 20 nM gliotoxin or left unstimulated for 4 h. Experiment was performed in duplicate on cells isolated from two buffy coats from healthy donors as described above. RNA was isolated as described above. cDNA libraries were generated using Illumina TruSeq Stranded mRNA Library Prep kit (Illumina). The resulting DNA libraries were sequenced according to the Illumina TruSeq Rapid v2 protocol on an Illumina HiSeq2500 sequencer. Reads were generated of 50 base-pairs in length. Reads were mapped against the GRCh38 human reference using HiSat2 (version 2.0.4). We called gene expression values using htseq-count (version 0.6.1), using Ensembl transcript annotation.

### **Toxicity assay**

Peripheral blood mononuclear cells (PBMC) were isolated by density gradient centrifugation (Ficoll-Hypaque, GE Healthcare life sciences) from buffy coats from healthy donors (Sanquin Amsterdam) and either used immediately or frozen in freezing media (90% FBS/10% DMSO) and stored short term at -80°C. For cytotoxicity testing, cells were cultivated in culture media RPMI 1640 (Life Technologies) supplemented with 10% FBS, 2 mM L-glutamine, 100 U/ml penicillin, and 100g/ml streptomycin-sulfate at a concentration of 1x10<sup>6</sup> cells/ml in 24-well plates (Thermo Scientific) that were either uncoated (unstimulated cells) or coated with anti-human CD3 (1µg/ml, clone UCHT1, no azide/low endotoxin, BD Bioscience) and anti-CD28 (10µg/ml, clone CD28.2, no azide/low endotoxin, BD Bioscience) monoclonal antibodies (stimulated cells). The following LRA were added at the concentrations indicated in figures: Gliotoxin (GTX, ApexBio), SAHA-Vorinostat (Selleck Chemicals), caffeic acid phenethyl ester (CAPE, MP Biomedicals), and Romidepsin (RMD, Sigma Aldrich). LRA at indicated concentrations were added to the cultures and cells were continuously exposed for 72 hours. Since GTX was reconstituted in acetonitrile (ACN), and all other LRA in dimethyl sulfoxide (DMSO), both solvents were added to the DMSO/ACN control culture (ACN 1:10000, DMSO 1:2500) to control for the effect these solvents may have on cell viability.

### **Flow cytometric for cytotoxicity assay**

To examine the effect the LRA have on immune cell subpopulations, cell viability, activation and proliferation was analyzed by flow cytometry. Surface antigens were detected by incubating 0.8-1.0x10<sup>6</sup> cells with pre-determined optimal concentrations of monoclonal antibody mixes in FACS wash (FW, Hanks buffered saline solution (HBSS, Life Technologies)), 3% fetal bovine serum (FBS, Life Technologies), 0.02% NaN<sub>3</sub>, 2.5 mM CaCl<sub>2</sub>) for 20 min at 4° C, washed one times with FW and fixed with 1% paraformaldehyde. To determine proliferation, cells were stained with 0.07 µM CellTrace Far Red Cell Proliferation dye according to manufacturer's protocol (ThermoFisher Scientific) before cultivating for 72 hours with either unstimulated or stimulated conditions in the presence of LRA.

The following directly conjugated monoclonal anti-human antibodies were used to analyze CD8<sup>+</sup> T cells (CD3+CD8<sup>+</sup>), CD4<sup>+</sup> T cells (CD3+CD4<sup>+</sup>), B cells (CD3-CD19<sup>+</sup>), monocytes (CD14<sup>+</sup>) and NK cells (CD3-CD56<sup>+</sup>): CD3-BV421 (clone UCHT1), CD4-BV650 (SK3), CD8-BV786 (RPA-T8), CD14-PE-Cy7 (61D3, eBioscience), CD19-

PerCP-Cy5.5(HIB19, eBioscience), CD56-PE-Cy5.5(CMSSB, eBioscience), Annexin V-PE, CD25- Super Bright 600 (BC96, eBioscience). All antibodies were purchased from BD Biosciences unless otherwise indicated. Between 2 - 4x10<sup>5</sup> events were collected per sample within 24 hours after staining on a LSRFortessa (BD Biosciences, 4 lasers, 18 parameters) and analyzed using FlowJo software (version 9.7.4, Tree Star). Data are represented as frequency within a defined population. Drug-specific cell death was calculated using the following formula:

$$[(\% \text{ Drug-induced cell death} - \% \text{ cell death in DMSO/ACN only}) / (100 - \% \text{ cell death in DMSO/ACN only})] * 100$$

### **Molecular docking**

Molecular docking was used to predict the most likely binding mode of gliotoxin to LARP7 C-terminal domain. The crystal structure of human LARP7 C-terminal domain in complex with 7SK RNA stem loop 4 (PDB ID code 6D12) was optimized using PDB-REDO (Joosten et al., 2014) and used as a template to define the receptor for the docking simulation. The resulting pdb file was manually adapted for input into the docking procedure by elimination of protein chain B and RNA domain C and replacement of Selenium atoms (present as selenomethionin, incorporated for phasing purposes; (Eichhorn et al., 2018)) by sulfur. GTX ligand structure was built and energy minimized using the program Chimera (Pettersen et al., 2004). Molecular docking of GTX to LARP7 C-terminal domain was performed using Achilles Blind Docking server (<https://bio-hpc.ucam.edu/achilles/>) and Chimera's AutoDock Vina function (Trott and Olson, 2010). The resulting solutions were ranked based on highest binding affinity (or lowest binding energy). Figures were created using PyMol software (Schrödinger, LLC, 2015).

## **QUANTIFICATION AND STATISTICAL ANALYSIS**

### **Western blot quantification**

Differential band density was quantified by ImageQuant TL software using area and profile-based toolbox. For glycerol gradient western blot quantification an area frame was defined for all bands (total CDK9 protein content in all fractions), complex-bound CDK9 bands (heavy fractions) or free CDK9 bands (light fractions) were defined. The three area frames were measured for total density after background subtraction (local average). Relative complex-bound CDK9 or free CDK9 percentage was calculated regarding the untreated control (total CDK9 abundance). For immunoprecipitation western blot quantification an area for each LARP7 and CDK9 band was defined and total density was measured after background subtraction (local average). LARP7 abundance was first normalized to CDK9 abundance for each lane and relative abundance was calculated regarding untreated control. Statistical significance was calculated using ANOVA followed by Tukey's test (p<0.01).

### **Statistical significance**

Statistical significance was calculated as indicated in figure legends. Analyses were performed using Prism version 7.03 (GraphPad software).

## References:

- Abner, E., Jordan, A., 2019. HIV “shock and kill” therapy: In need of revision. *Antiviral Res.* 166, 19–34. <https://doi.org/10.1016/J.ANTIVIRAL.2019.03.008>
- Abner, E., Stoszko, M., Zeng, L., Chen, H.-C., Izquierdo-Bouldstridge, A., Konuma, T., Zorita, E., Fanunza, E., Zhang, Q., Mahmoudi, T., Zhou, M.-M., Filion, G.J., Jordan, A., 2018. A New Quinoline BRD4 Inhibitor Targets a Distinct Latent HIV-1 Reservoir for Reactivation from Other “Shock” Drugs. *J. Virol.* 92, e02056-17. <https://doi.org/10.1128/JVI.02056-17>
- Archin, N.M., Liberty, A.L., Kashuba, A.D., Choudhary, S.K., Kuruc, J.D., Crooks, A.M., Parker, D.C., Anderson, E.M., Kearney, M.F., Strain, M.C., Richman, D.D., Hudgens, M.G., Bosch, R.J., Coffin, J.M., Eron, J.J., Hazuda, D.J., Margolis, D.M., 2012. Administration of vorinostat disrupts HIV-1 latency in patients on antiretroviral therapy. *Nature* 487, 482–485. <https://doi.org/10.1038/nature11286>
- Avert, 2017. Funding for HIV and AIDS [WWW Document]. Avert. URL <https://www.avert.org/professionals/hiv-around-world/global-response/funding> (accessed 4.4.19).
- Battivelli, E., Dahabieh, M.S., Abdel-Mohsen, M., Svensson, J.P., Tojal Da Silva, I., Cohn, L.B., Gramatica, A., Deeks, S., Greene, W.C., Pillai, S.K., Verdin, E., 2018. Distinct chromatin functional states correlate with HIV latency reactivation in infected primary CD4+ T cells. *Elife* 7. <https://doi.org/10.7554/eLife.34655>
- Bioinformatics and High Performance Computing (BIO-HPC) Research group. *Achilles Blind Docking Server*, <https://bio-hpc.ucam.edu/achilles/> (2019).
- Bouchat, S., Delacourt, N., Kula, A., Darcis, G., Van Driessche, B., Corazza, F., Gatot, J.-S., Melard, A., Vanhulle, C., Kabeya, K., Pardons, M., Avettand-Fenoel, V., Clumeck, N., De Wit, S., Rohr, O., Rouzioux, C., Van Lint, C., 2016a. Sequential treatment with 5-aza-2'-deoxycytidine and deacetylase inhibitors reactivates HIV-1. *EMBO Mol. Med.* 8, 117–38. <https://doi.org/10.15252/emmm.201505557>
- Bouchat, S., Delacourt, N., Kula, A., Darcis, G., Van Driessche, B., Corazza, F., Gatot, J.-S., Melard, A., Vanhulle, C., Kabeya, K., Pardons, M., Avettand-Fenoel, V., Clumeck, N., De Wit, S., Rohr, O., Rouzioux, C., Van Lint, C., 2016b. Sequential treatment with 5-aza-2'-deoxycytidine and deacetylase inhibitors reactivates HIV-1. *EMBO Mol. Med.* 8, 117–38. <https://doi.org/10.15252/emmm.201505557>
- Brakhage, A.A., 2013. Regulation of fungal secondary metabolism. *Nat. Rev. Microbiol.* 11, 21–32. <https://doi.org/10.1038/nrmicro2916>
- C. Quaresma, A.J., Bugai, A., Barboric, M., 2016. Cracking the control of RNA polymerase II elongation by 7SK snRNP and P-TEFb. *Nucleic Acids Res.* 44, 7527–7539. <https://doi.org/10.1093/nar/gkw585>
- Cary, D.C., Fujinaga, K., Peterlin, B.M., 2016. Euphorbia Kansui Reactivates Latent HIV. *PLoS One* 11, e0168027. <https://doi.org/10.1371/journal.pone.0168027>
- Chen, H.-C., Martinez, J.P., Zorita, E., Meyerhans, A., Filion, G.J., 2017. Position effects influence HIV latency reversal. *Nat. Struct. Mol. Biol.* 24, 47–54. <https://doi.org/10.1038/nsmb.3328>

- Choi, H.S., Shim, J.S., Kim, J.-A., Kang, S.W., Kwon, H.J., 2007. Discovery of gliotoxin as a new small molecule targeting thioredoxin redox system. *Biochem. Biophys. Res. Commun.* 359, 523–528. <https://doi.org/10.1016/J.BBRC.2007.05.139>
- Contreras, X., Barboric, M., Lenasi, T., Peterlin, B.M., 2007. HMBA Releases P-TEFb from HEXIM1 and 7SK snRNA via PI3K/Akt and Activates HIV Transcription. *PLoS Pathog.* 3, e146. <https://doi.org/10.1371/journal.ppat.0030146>
- Darcis, G., Kula, A., Bouchat, S., Fujinaga, K., Corazza, F., Ait-Ammar, A., Delacourt, N., Melard, A., Kabeya, K., Vanhulle, C., Van Driessche, B., Gatot, J.-S., Cherrier, T., Pianowski, L.F., Gama, L., Schwartz, C., Vila, J., Burny, A., Clumeck, N., Moutschen, M., De Wit, S., Peterlin, B.M., Rouzioux, C., Rohr, O., Van Lint, C., 2015. An In-Depth Comparison of Latency-Reversing Agent Combinations in Various In Vitro and Ex Vivo HIV-1 Latency Models Identified Bryostatin-1+JQ1 and Ingenol-B+JQ1 to Potently Reactivate Viral Gene Expression. *PLOS Pathog.* 11, e1005063. <https://doi.org/10.1371/journal.ppat.1005063>
- De Crignis, E., Mahmoudi, T., 2016. The Multifaceted Contributions of Chromatin to HIV-1 Integration, Transcription, and Latency, *International Review of Cell and Molecular Biology* International Review of Cell and Molecular Biology. Elsevier Inc. <https://doi.org/10.1016/bs.ircmb.2016.08.006>
- De Crignis, E., Mahmoudi, T., 2014. HIV eradication: combinatorial approaches to activate latent viruses. *Viruses* 6, 4581–608. <https://doi.org/10.3390/v6114581>
- Eichhorn, C.D., Yang, Y., Repeta, L., Feigon, J., 2018. Structural basis for recognition of human 7SK long noncoding RNA by the La-related protein Larp7. *Proc. Natl. Acad. Sci. U. S. A.* 115, E6457–E6466. <https://doi.org/10.1073/pnas.1806276115>
- Gostinčar, C., Zajc, J., Lenassi, M., Plemenitaš, A., de Hoog, S., Al-Hatmi, A.M.S., Gunde-Cimerman, N., 2018. Fungi between extremotolerance and opportunistic pathogenicity on humans. *Fungal Divers.* 93, 195–213. <https://doi.org/10.1007/s13225-018-0414-8>
- Gupta, A., Juneja, S., Vitoria, M., Habiyambere, V., Nguimfack, B.D., Doherty, M., Low-Beer, D., 2016. Projected Uptake of New Antiretroviral (ARV) Medicines in Adults in Low- and Middle-Income Countries: A Forecast Analysis 2015-2025. *PLoS One* 11, e0164619. <https://doi.org/10.1371/journal.pone.0164619>
- Hashemi, P., Barreto, K., Bernhard, W., Lomness, A., Honson, N., Pfeifer, T.A., Harrigan, P.R., Sadowski, I., 2017. Compounds producing an effective combinatorial regimen for disruption of HIV-1 latency. *EMBO Mol. Med.* e201708193. <https://doi.org/10.15252/emmm.201708193>
- Ho, D.D., Neumann, A.U., Perelson, A.S., Chen, W., Leonard, J.M., Markowitz, M., 1995. Rapid turnover of plasma virions and CD4 lymphocytes in HIV-1 infection. *Nature* 373, 123–126. <https://doi.org/10.1038/373123a0>
- Ho, Y.-C., Shan, L., Hosmane, N.N., Wang, J., Laskey, S.B., Rosenbloom, D.I.S., Lai, J., Blankson, J.N.,

- Siliciano, J.D., Siliciano, R.F., 2013a. Replication-Competent Noninduced Proviruses in the Latent Reservoir Increase Barrier to HIV-1 Cure. *Cell* 155, 540–551. <https://doi.org/10.1016/J.CELL.2013.09.020>
- Ho, Y.-C., Shan, L., Hosmane, N.N.N., Wang, J., Laskey, S.B.B., Rosenbloom, D.I.S.I.S., Lai, J., Blankson, J.N.N., Siliciano, J.D.D., Siliciano, R.F.F., 2013b. Replication-competent noninduced proviruses in the latent reservoir increase barrier to HIV-1 cure. *Cell* 155, 540–51. <https://doi.org/10.1016/j.cell.2013.09.020>
- Hur, J.-M., Yun, H.-J., Yang, S.-H., Lee, W.-Y., Joe, M., Kim, D., 2008. Gliotoxin enhances radiotherapy via inhibition of radiation-induced GADD45a, p38, and NFκB activation. *J. Cell. Biochem.* 104, 2174–2184. <https://doi.org/10.1002/jcb.21776>
- Jonkers, I., Lis, J.T., 2015. Getting up to speed with transcription elongation by RNA polymerase II. *Nat. Rev. Mol. Cell Biol.* 16, 167–177. <https://doi.org/10.1038/nrm3953>
- Joosten, R.P., Long, F., Murshudov, G.N., Perrakis, A., 2014. The *PDB\_REDO* server for macromolecular structure model optimization. *IUCrJ* 1, 213–220. <https://doi.org/10.1107/S2052252514009324>
- Kim, Y., Anderson, J.L., Lewin, S.R., 2018. Getting the “Kill” into “Shock and Kill: Strategies to Eliminate Latent HIV. *Cell Host Microbe* 23, 14–26. <https://doi.org/10.1016/j.chom.2017.12.004>
- Kohoutek, J., 2009. P-TEFb- the final frontier. *Cell Div.* 4, 19. <https://doi.org/10.1186/1747-1028-4-19>
- Krueger, B.J., Jeronimo, C., Roy, B.B., Bouchard, A., Barrandon, C., Byers, S.A., Searcey, C.E., Cooper, J.J., Bensaude, O., Cohen, E.A., Coulombe, B., Price, D.H., 2008. LARP7 is a stable component of the 7SK snRNP while P-TEFb, HEXIM1 and hnRNP A1 are reversibly associated. *Nucleic Acids Res.* 36, 2219–29. <https://doi.org/10.1093/nar/gkn061>
- Kwon-Chung, K.J., Sugui, J.A., 2009. What do we know about the role of gliotoxin in the pathobiology of *Aspergillus fumigatus*? *Med. Mycol.* 47 Suppl 1, S97-103. <https://doi.org/10.1080/13693780802056012>
- Laird, G.M., Bullen, C.K., Rosenbloom, D.I.S., Martin, A.R., Hill, A.L., Durand, C.M., Siliciano, J.D., Siliciano, R.F., 2015. Ex vivo analysis identifies effective HIV-1 latency-reversing drug combinations. *J. Clin. Invest.* 125, 1901–1912. <https://doi.org/10.1172/JCI80142>
- Lassen, K.G., Hebbeler, A.M., Bhattacharyya, D., Lobritz, M.A., Greene, W.C., 2012. A Flexible Model of HIV-1 Latency Permitting Evaluation of Many Primary CD4 T-Cell Reservoirs. *PLoS One* 7, e30176. <https://doi.org/10.1371/journal.pone.0030176>
- Leth, S., Schleimann, M.H., Nissen, S.K., Højten, J.F., Olesen, R., Graversen, M.E., Jørgensen, S., Kjær, A.S., Denton, P.W., Mørk, A., Sommerfelt, M.A., Krogsgaard, K., Østergaard, L., Rasmussen, T.A., Tolstrup, M., Søgaaard, O.S., 2016. Combined effect of Vacc-4x, recombinant human granulocyte macrophage colony-stimulating factor vaccination, and romidepsin on the HIV-1 reservoir (REDUC): a single-arm, phase 1B/2A trial. *Lancet HIV* 3, e463–e472. [https://doi.org/10.1016/S2352-3018\(16\)30055-8](https://doi.org/10.1016/S2352-3018(16)30055-8)



- Lewis, R.E., Wiederhold, N.P., Chi, J., Han, X.Y., Komanduri, K. V, Kontoyiannis, D.P., Prince, R.A., 2005. Detection of gliotoxin in experimental and human aspergillosis. *Infect. Immun.* 73, 635–7. <https://doi.org/10.1128/IAI.73.1.635-637.2005>
- Link, A.J., LaBaer, J., 2011. Trichloroacetic acid (TCA) precipitation of proteins. *Cold Spring Harb. Protoc.* 2011, 993–4. <https://doi.org/10.1101/pdb.prot5651>
- Mahmoudi, T., 2012. The BAF complex and HIV latency. *Transcription* 3, 171–6. <https://doi.org/10.4161/trns.20541>
- Marian, C.A., Stoszko, M., Wang, L., Leighty, M.W., de Crignis, E., Maschinot, C.A., Gatchalian, J., Carter, B.C., Chowdhury, B., Hargreaves, D.C., Duvall, J.R., Crabtree, G.R., Mahmoudi, T., Dykhuizen, E.C., 2018. Small Molecule Targeting of Specific BAF (mSWI/SNF) Complexes for HIV Latency Reversal. *Cell Chem. Biol.* 25, 1443-1455.e14. <https://doi.org/10.1016/j.chembiol.2018.08.004>
- Michael D. Röling, M.S. and T.M., 2016. Advances in Molecular Retrovirology.
- Ne, E., Palstra, R.-J., Mahmoudi, T., 2018. Transcription: Insights From the HIV-1 Promoter, in: *International Review of Cell and Molecular Biology.* pp. 191–243. <https://doi.org/10.1016/bs.ircmb.2017.07.011>
- Newman, D.J., Cragg, G.M., 2016. Natural Products as Sources of New Drugs from 1981 to 2014. *J. Nat. Prod.* 79, 629–661. <https://doi.org/10.1021/acs.jnatprod.5b01055>
- Nguyen, V.T., Kiss, T., Michels, A.A., Bensaude, O., 2001. 7SK small nuclear RNA binds to and inhibits the activity of CDK9/cyclin T complexes. *Nature* 414, 322–325. <https://doi.org/10.1038/35104581>
- Nouri, M.A., Al-Halbosiy, M.M.F., Dheeb, B.I., Hashim, A.J., 2015. Cytotoxicity and genotoxicity of gliotoxin on human lymphocytes in vitro. *J. King Saud Univ. - Sci.* 27, 193–197. <https://doi.org/10.1016/j.jksus.2014.12.005>
- Novák, J., Sokolová, L., Lemr, K., Pluháček, T., Palyzová, A., Havlíček, V., 2017. Batch-processing of imaging or liquid-chromatography mass spectrometry datasets and De Novo sequencing of polyketide siderophores. *Biochim. Biophys. Acta - Proteins Proteomics* 1865, 768–775. <https://doi.org/10.1016/j.bbapap.2016.12.003>
- Orciuolo, E., Stanzani, M., Canestraro, M., Galimberti, S., Carulli, G., Lewis, R., Petrini, M., Komanduri, K. V., 2007. Effects of *Aspergillus fumigatus* gliotoxin and methylprednisolone on human neutrophils: implications for the pathogenesis of invasive aspergillosis. *J. Leukoc. Biol.* 82, 839–848. <https://doi.org/10.1189/jlb.0207090>
- Perelson, A.S., Essunger, P., Cao, Y., Vesanen, M., Hurley, A., Saksela, K., Markowitz, M., Ho, D.D., 1997. Decay characteristics of HIV-1-infected compartments during combination therapy. *Nature* 387, 188–191. <https://doi.org/10.1038/387188a0>
- Peterlin, B.M., Price, D.H., 2006. Controlling the Elongation Phase of Transcription with P-TEFb. *Mol. Cell* 23, 297–305. <https://doi.org/10.1016/J.MOLCEL.2006.06.014>

- Pettersen, E.F., Goddard, T.D., Huang, C.C., Couch, G.S., Greenblatt, D.M., Meng, E.C., Ferrin, T.E., 2004. UCSF Chimera?A visualization system for exploratory research and analysis. *J. Comput. Chem.* 25, 1605–1612. <https://doi.org/10.1002/jcc.20084>
- Přichystal, J., Schug, K.A., Lemr, K., Novák, J., Havlíček, V., 2016. Structural Analysis of Natural Products. *Anal. Chem.* 88, 10338–10346. <https://doi.org/10.1021/acs.analchem.6b02386>
- Rasmussen, T.A., Lewin, S.R., 2016. Shocking HIV out of hiding. *Curr. Opin. HIV AIDS* 11, 394–401. <https://doi.org/10.1097/COH.0000000000000279>
- Rasmussen, T.A., Tolstrup, M., Søgaaard, O.S., 2015. Reversal of Latency as Part of a Cure for HIV-1. *Trends Microbiol.* <https://doi.org/10.1016/j.tim.2015.11.003>
- Richard, K., Williams, D., de Silva, E., Brockman, M., Brumme, Z., Andersen, R., Tietjen, I., Richard, K., Williams, D.E., de Silva, E.D., Brockman, M.A., Brumme, Z.L., Andersen, R.J., Tietjen, I., 2018. Identification of Novel HIV-1 Latency-Reversing Agents from a Library of Marine Natural Products. *Viruses* 10, 348. <https://doi.org/10.3390/v10070348>
- Sakamoto, H., Egashira, S., Saito, N., Kirisako, T., Miller, S., Sasaki, Y., Matsumoto, T., Shimonishi, M., Komatsu, T., Terai, T., Ueno, T., Hanaoka, K., Kojima, H., Okabe, T., Wakatsuki, S., Iwai, K., Nagano, T., 2015. Gliotoxin Suppresses NF-κB Activation by Selectively Inhibiting Linear Ubiquitin Chain Assembly Complex (LUBAC). *ACS Chem. Biol.* 10, 675–681. <https://doi.org/10.1021/cb500653y>
- Sanchez, J.F., Somoza, A.D., Keller, N.P., Wang, C.C.C., 2012. Advances in Aspergillus secondary metabolite research in the post-genomic era. *Nat. Prod. Rep.* 29, 351. <https://doi.org/10.1039/c2np00084a>
- Scharf, D.H., Brakhage, A.A., Mukherjee, P.K., 2016. Gliotoxin - bane or boon? *Environ. Microbiol.* 18, 1096–1109. <https://doi.org/10.1111/1462-2920.13080>
- Schmittgen, T.D., Livak, K.J., 2008. Analyzing real-time PCR data by the comparative CT method. *Nat. Protoc.* 3, 1101–1108. <https://doi.org/10.1038/nprot.2008.73>
- Schrödinger, LLC, 2015. The {PyMOL} Molecular Graphics System, Version~1.8.
- Siliciano, J.M., Siliciano, R.F., 2015. The Remarkable Stability of the Latent Reservoir for HIV-1 in Resting Memory CD4<sup>+</sup> T Cells. *J. Infect. Dis.* 212, 1345–1347. <https://doi.org/10.1093/infdis/jiv219>
- Stanzani, M., Orciuolo, E., Lewis, R., Kontoyiannis, D.P., Martins, S.L.R., St. John, L.S., Komanduri, K. V., 2005. Aspergillus fumigatus suppresses the human cellular immune response via gliotoxin-mediated apoptosis of monocytes. *Blood* 105.
- Stoszko, M., De Crignis, E., Rokx, C., Khalid, M.M., Lungu, C., Palstra, R.J., Kan, T.W., Boucher, C., Verbon, A., Dykhuizen, E.C., Mahmoudi, T., 2016. Small Molecule Inhibitors of BAF; A Promising Family of Compounds in HIV-1 Latency Reversal. *EBioMedicine* 3, 108–121. <https://doi.org/10.1016/j.ebiom.2015.11.047>
- Stoszko, M., Ne, E., Abner, E., Mahmoudi, T., 2019. A broad drug arsenal to attack a strenuous latent HIV

- reservoir. *Curr. Opin. Virol.* 38, 37–53. <https://doi.org/10.1016/J.COVIRO.2019.06.001>
- Suen, Y.K., Fung, K.P., Lee, C.Y., Kong, S.K., 2001. Gliotoxin induces apoptosis in cultured macrophages via production of reactive oxygen species and cytochrome c release without mitochondrial depolarization. *Free Radic. Res.* 35, 1–10. <https://doi.org/10.1080/10715760100300541>
- Sutton, P., Beaver, J., Waring, P., 1995. Evidence that gliotoxin enhances lymphocyte activation and induces apoptosis by effects on cyclic AMP levels. *Biochem. Pharmacol.* 50, 2009–2014. [https://doi.org/10.1016/0006-2952\(95\)02101-9](https://doi.org/10.1016/0006-2952(95)02101-9)
- Trautmann, L., 2016. Kill: boosting HIV-specific immune responses. *Curr. Opin. HIV AIDS* 11, 409–16. <https://doi.org/10.1097/COH.0000000000000286>
- Trott, O., Olson, A.J., 2010. AutoDock Vina: improving the speed and accuracy of docking with a new scoring function, efficient optimization, and multithreading. *J. Comput. Chem.* 31, 455–61. <https://doi.org/10.1002/jcc.21334>
- Uchikawa, E., Natchiar, K.S., Han, X., Proux, F., Roblin, P., Zhang, E., Durand, A., Klaholz, B.P., Dock-Bregeon, A.-C., 2015. Structural insight into the mechanism of stabilization of the 7SK small nuclear RNA by LARP7. *Nucleic Acids Res.* 43, 3373–3388. <https://doi.org/10.1093/nar/gkv173>
- UNAIDS, 2017. UNAIDS DATA 2017 | UNAIDS [WWW Document]. URL [http://www.unaids.org/en/resources/documents/2017/2017\\_data\\_book](http://www.unaids.org/en/resources/documents/2017/2017_data_book) (accessed 4.4.19).
- Vo, T.-S., Kim, S.-K., 2010. Potential Anti-HIV Agents from Marine Resources: An Overview. *Mar. Drugs* 8, 2871. <https://doi.org/10.3390/MD8122871>
- Wang, P., Lu, P., Qu, X., Shen, Y., Zeng, H., Zhu, X., Zhu, Y., Li, X., Wu, H., Xu, J., Lu, H., Ma, Z., Zhu, H., 2017. Reactivation of HIV-1 from Latency by an Ingenol Derivative from *Euphorbia Kansui*. *Sci. Rep.* 7, 9451. <https://doi.org/10.1038/s41598-017-07157-0>
- Wei, X., Ghosh, S.K., Taylor, M.E., Johnson, V.A., Emmini, E.A., Deutsch, P., Lifson, J.D., Bonhoeffer, S., Nowak, M.A., Hahn, B.H., Saag, M.S., Shaw, G.M., 1995. Viral dynamics in human immunodeficiency virus type 1 infection. *Nature* 373, 117–122. <https://doi.org/10.1038/373117a0>
- Wichmann, G., Herbarth, O., Lehmann, I., 2002. The mycotoxins citrinin, gliotoxin, and patulin affect interferon-g rather than interleukin-4 production in human blood cells. *Environ. Toxicol.* 17, 211–218. <https://doi.org/10.1002/tox.10050>
- Yamada, A., Kataoka, T., Nagai, K., 2000. The fungal metabolite gliotoxin: immunosuppressive activity on CTL-mediated cytotoxicity, *Immunology Letters*. [https://doi.org/10.1016/S0165-2478\(99\)00155-8](https://doi.org/10.1016/S0165-2478(99)00155-8)
- Yang, Z., Zhu, Q., Luo, K., Zhou, Q., 2001. The 7SK small nuclear RNA inhibits the CDK9/cyclin T1 kinase to control transcription. *Nature* 414, 317–322. <https://doi.org/10.1038/35104575>
- Yasuhara-Bell, J., Yang, Y., Barlow, R., Trapido-Rosenthal, H., Lu, Y., 2010. In vitro evaluation of marine-microorganism extracts for anti-viral activity. *Virol. J.* 7, 182. <https://doi.org/10.1186/1743-422X-7-182>
- Yik, J.H., Chen, R., Nishimura, R., Jennings, J.L., Link, A.J., Zhou, Q., 2003. Inhibition of P-TEFb

- (CDK9/Cyclin T) Kinase and RNA Polymerase II Transcription by the Coordinated Actions of HEXIM1 and 7SK snRNA. *Mol. Cell* 12, 971–982. [https://doi.org/10.1016/S1097-2765\(03\)00388-5](https://doi.org/10.1016/S1097-2765(03)00388-5)
- Yukl, S.A., Kaiser, P., Kim, P., Telwatte, S., Joshi, S.K., Vu, M., Lampiris, H., Wong, J.K., 2018a. HIV latency in isolated patient CD4<sup>+</sup> T cells may be due to blocks in HIV transcriptional elongation, completion, and splicing. *Sci. Transl. Med.* 10, eaap9927. <https://doi.org/10.1126/scitranslmed.aap9927>
- Yukl, S.A., Kaiser, P., Kim, P., Telwatte, S., Joshi, S.K., Vu, M., Lampiris, H., Wong, J.K., 2018b. HIV latency in isolated patient CD4<sup>+</sup> T cells may be due to blocks in HIV transcriptional elongation, completion, and splicing. *Sci. Transl. Med.* 10, eaap9927. <https://doi.org/10.1126/scitranslmed.aap9927>
- Zhao, M., De Crignis, E., Rokx, C., Verbon, A., van Gelder, T., Mahmoudi, T., Katsikis, P.D., Mueller, Y.M., 2019a. T cell toxicity of HIV latency reversing agents. *Pharmacol. Res.* 139, 524–534. <https://doi.org/10.1016/J.PHRS.2018.10.023>
- Zhao, M., De Crignis, E., Rokx, C., Verbon, A., van Gelder, T., Mahmoudi, T., Katsikis, P.D., Mueller, Y.M., 2019b. T cell toxicity of HIV latency reversing agents. *Pharmacol. Res.* 139, 524–534. <https://doi.org/10.1016/J.PHRS.2018.10.023>
- Zhou, X., Zhao, A., Goping, G., Hirszel, P., 2000. Gliotoxin-induced cytotoxicity proceeds via apoptosis and is mediated by caspases and reactive oxygen species in LLC-PK1 cells. *Toxicol. Sci.* 54, 194–202. <https://doi.org/10.1093/TOXSCI/54.1.194>

**Table S1. Strains analyzed for their ability to induce HIV-1 proviral expression.**

<b>CBS</b>	<b>Name</b>	<b>Order</b>	<b>Family</b>
220,84	<i>Acremonium recifei</i>	Hypocreales	Hypocreaceae
603,78	<i>Alternaria alternata</i>	Pleosporales	Pleosporaceae
177,80	<i>Alternaria caespitosa</i>	Pleosporales	Pleosporaceae
210,86	<i>Alternaria infectoria</i>	Pleosporales	Pleosporaceae
163,74	<i>Ascodesmis nigricans</i>	Pezizales	Ascodesmidaceae
114,48	<i>Aspergillus clavatus</i>	Eurotiales	Aspergillaceae
625,66	<i>Aspergillus flavus</i>	Eurotiales	Aspergillaceae
113,26	<i>Aspergillus fumigatus</i>	Eurotiales	Aspergillaceae
416,68	<i>Acremonium potronii</i>	Eurotiales	Aspergillaceae
117884	<i>Aspergillus lentulus</i>	Eurotiales	Aspergillaceae
589,65	<i>Aspergillus nidulans</i>	Eurotiales	Aspergillaceae
769,97	<i>Aspergillus niger</i>	Eurotiales	Aspergillaceae
245,65	<i>Aspergillus versicolor</i>	Eurotiales	Aspergillaceae
116686	<i>Aspergillus terreus</i>	Eurotiales	Aspergillaceae
584,75	<i>Aureobasidium pullulans</i>	Dothideales	Aureobasidiaceae
172,57	<i>Bipolaris australiensis</i>	Pleosporales	Pleosporaceae
173,57	<i>Bipolaris hawaiiensis</i>	Pleosporales	Pleosporaceae
586,80	<i>Bipolaris spicifera</i>	Pleosporales	Pleosporaceae
113191	<i>Botryosphaeria dothidea</i>	Botryosphaeriales	Botryosphaeriaceae
567.78A	<i>Botrytis cinerea</i>	Helotiales	Sclerotiniaceae
545,83	<i>Chaetomium globosum</i>	Sordariales	Chaetomiaceae
104,62	<i>Chrysosporium keratinophilum</i>	Onygenales	Onygenaceae
173,52	<i>Cladophialophora bantiana</i>	Chaetothyriales	Herpotrichiellaceae
316,56	<i>Cladophialophora boppii</i>	Chaetothyriales	Herpotrichiellaceae
166,54	<i>Cladophialophora carrionii</i>	Chaetothyriales	Herpotrichiellaceae
109501	<i>Cladosporium cladosporioides</i>	Capnodiales	Cladosporiaceae
399,80	<i>Cladosporium bruhnei</i>	Capnodiales	Cladosporiaceae
108,85	<i>Cladosporium herbarum</i>	Capnodiales	Cladosporiaceae
113856	<i>Coccidioides immitis</i>	Onygenales	Onygenaceae
113859	<i>Coccidioides posadasii</i>	Onygenales	Onygenaceae
117439	<i>Coprinopsis cinereus</i>	Agaricales	Psathyrellaceae
220,52	<i>Curvularia geniculata</i>	Pleosporales	Pleosporaceae
730,96	<i>Curvularia lunata</i>	Pleosporales	Pleosporaceae
637,82	<i>Cylindrocarpon cyanescens</i>	Hypocreales	Hypocreaceae
116632	<i>Cyphellophora europaea</i>	Chaetothyriales	Cyphellophoraceae
190,61	<i>Cyphellophora laciniata</i>	Chaetothyriales	Cyphellophoraceae
286,85	<i>Cyphellophora pluriseptata</i>	Chaetothyriales	Cyphellophoraceae

443,88	<i>Dissitimurus exedrus</i>	Pleosporales	Pleosporaceae
177.60	<i>Emmonsia crescens</i>	Onygenales	Ajellomycetaceae
102456	<i>Emergomyces pasteurianus</i>	Onygenales	Ajellomycetaceae
214,63	<i>Epidermophyton floccosum</i>	Onygenales	Arthrodermataceae
129,54	<i>Eurotium chevalieri</i>	Eurotiales	Aspergillaceae
207,35	<i>Exophiala dermatitidis</i>	Chaetothyriales	Herpotrichiellaceae
537,76	<i>Exophiala jeanselmei</i>	Chaetothyriales	Herpotrichiellaceae
899,68	<i>Exophiala spinifera</i>	Chaetothyriales	Herpotrichiellaceae
102455	<i>Exophiala xenobiotica</i>	Chaetothyriales	Herpotrichiellaceae
196,79	<i>Falciformispora senegalensis</i>	Pleosporales	Leptosphaeriaceae
102237	<i>Fonsecaea pedrosoi</i>	Chaetothyriales	Herpotrichiellaceae
840,88	<i>Fusarium oxysporum</i>	Hypocreales	Hypocreaceae
120996	<i>Fusarium proliferatum</i>	Hypocreales	Hypocreaceae
181,29	<i>Fusarium solani</i>	Hypocreales	Hypocreaceae
539,79	<i>Fusarium verticillioides</i>	Hypocreales	Hypocreaceae
109689	<i>Ganoderma lucidum</i>	Polyporales	Polyporaceae
224,48	<i>Geotrichum candidum</i>	Saccharomycetales	Dipodascaceae
136,72	<i>Histoplasma capsulatum</i>	Onygenales	Ajellomycetaceae
410,51	<i>Hortaea werneckii</i>	Capnodiales	Capnodiaceae
118183	<i>Hypoxylon investiens</i>	Xylariales	Hypoxylaceae
467,74	<i>Lomentospora prolificans</i>	Microascales	Microascaceae
331.50	<i>Madurella grisea</i>	Sordariales	Chaetomiaceae
110087	<i>Madurella mycetomatis</i>	Sordariales	Chaetomiaceae
119449	<i>Microsporum audouinii</i>	Onygenales	Arthrodermataceae
114329	<i>Microsporum canis</i>	Onygenales	Arthrodermataceae
427,63	<i>Microsporum ferrugineum</i>	Onygenales	Arthrodermataceae
246,89	<i>Monascus ruber</i>	Eurotiales	Monascaceae
157,58	<i>Moniliella suaveolens</i>	Moniliellales	Moniliellaceae
616,63	<i>Mucor racemosus</i>	Mucorales	Mucoraceae
120675	<i>Nannizzia gypsea</i>	Onygenales	Arthrodermataceae
116672	<i>Nannizziopsis vriesii</i>	Onygenales	Nannizziopsidaceae
204,33	<i>Neoscytalidium dimidiatum</i>	Dothideales	Dothioraceae
113,64	<i>Neosartorya fischeri</i>	Eurotiales	Aspergillaceae
331,78	<i>Neotestudina rosatii</i>	Sordariales	Neotestudinaceae
116660	<i>Ochroconis gallopava</i>	Venturiales	Sympoventuriaceae
109438	<i>Onychocola canadensis</i>	Arachnomycetales	Arachnomycetaceae
339,51	<i>Paecilomyces variotii</i>	Eurotiales	Aspergillaceae
272,86	<i>Penicillium funiculosum</i>	Eurotiales	Aspergillaceae
120336	<i>Penicillium chrysogenum</i>	Eurotiales	Aspergillaceae

119375	<i>Penicillium brevicompactum</i>	Eurotiales	Aspergillaceae
190,67	<i>Penicillium camemberti</i>	Eurotiales	Aspergillaceae
113273	<i>Phaeoacremonium inflatipes</i>	Diaporthales	Togniniaceae
108946	<i>Phaeoacremonium parasiticum</i>	Diaporthales	Togniniaceae
121222	<i>Phialemonium curvatum</i>	Sordariales	Cephalothecaceae
225,97	<i>Phialophora verrucosa</i>	Chaetothyriales	Herpotrichiellaceae
281,83	<i>Phoma glomerata</i>	Pleosporales	Didymellaceae
271,31	<i>Piedraia hortae</i>	Dothideales	Piedraiaceae
483,80	<i>Pleurostomophora richardsiae</i>	Calosphaeriales	Pleurostomataceae
113566	<i>Pochonia chlamydosporia</i>	Clavicipitales	Clavicipitaceae
430,87	<i>Purpureocillium lilacinus</i>	Clavicipitales	Ophiocordycipitaceae
650,93	<i>Rhinocladiella mackenziei</i>	Chaetothyriales	Herpotrichiellaceae
109135	<i>Rhinocladiella similis</i>	Chaetothyriales	Herpotrichiellaceae
112,07	<i>Rhizopus arrhizus</i>	Mucorales	Rhizopodaceae
117419	<i>Scedosporium apiospermum</i>	Microascales	Microascaceae
118934	<i>Scedosporium aurantiacum</i>	Microascales	Microascaceae
254,66	<i>Scedosporium boydii</i>	Microascales	Microascaceae
103,20	<i>Schizophyllum commune</i>	Schizophyllales	Schizophyllaceae
115540	<i>Scopulariopsis brevicaulis</i>	Microascales	Microascaceae
345,58	<i>Scopulariopsis brumptii</i>	Microascales	Microascaceae
119145	<i>Sporothrix schenckii</i>	Ophiostomatales	Ophiostomataceae
119370	<i>Stachybotrys chartarum</i>	Hypocreales	Stachybotryaceae
568,91	<i>Syncephalastrum racemosum</i>	Mucorales	Syncephalastraceae
107,89	<i>Talaromyces marneffeii</i>	Eurotiales	Trichocomaceae
642,68	<i>Talaromyces minioluteum</i>	Eurotiales	Trichocomaceae
112095	<i>Talaromyces pinophilum</i>	Eurotiales	Trichocomaceae
123071	<i>Trichoderma harzianum</i>	Hypocreales	Hypocreaceae
121805	<i>Trichophyton interdigitale</i>	Onygenales	Arthrodermataceae
511,73	<i>Trichophyton erinacei</i>	Onygenales	Arthrodermataceae
303,38	<i>Trichophyton rubrum</i>	Onygenales	Arthrodermataceae
564,94	<i>Trichophyton schoenleinii</i>	Onygenales	Arthrodermataceae
417,65	<i>Trichophyton simii</i>	Onygenales	Arthrodermataceae
384,89	<i>Trichophyton violaceum</i>	Onygenales	Arthrodermataceae
496,48	<i>Trichophyton tonsurans</i>	Onygenales	Arthrodermataceae
319,31	<i>Trichophyton violaceum</i>	Onygenales	Arthrodermataceae
116300	<i>Tritirachium oryzae</i>	Tritirachiales	Tritirachiaceae
123286	<i>Ulocladium chartarum</i>	Pleosporales	Pleosporaceae
102593	<i>Veronaea botryosa</i>	Chaetothyriales	Herpotrichiellaceae
196,56	<i>Wallemia sebi</i>	Wallemiales	Wallemiaceae

154,31	<i>Alternaria alternata</i>			
916,96	<i>Alternaria alternata</i>			
109455	<i>Alternaria alternata</i>			
120829	<i>Alternaria alternata</i>			
199,67	<i>Ulocladium chartarum</i>			
200,67	<i>Ulocladium chartarum</i>			
117137	<i>Ulocladium chartarum</i>			
121494	<i>Ulocladium chartarum</i>			
192,65	<i>Aspergillus fumigatus</i>			
475,75	<i>Aspergillus fumigatus</i>			
287,95	<i>Aspergillus fumigatus</i>			
175,97	<i>Aspergillus fumigatus</i>			
100074	<i>Aspergillus fumigatus</i>			
117884	<i>Aspergillus lentulus</i>			
121597	<i>Aspergillus lentulus</i>			
116879	<i>Aspergillus lentulus</i>			
117186	<i>Aspergillus fumigatiaffinis</i>			
117194	<i>Aspergillus fumigatiaffinis</i>			
144,34	<i>Coccidioides immitis</i>			
146,56	<i>Coccidioides immitis</i>			
711,73	<i>Coccidioides immitis</i>			
113851	<i>Coccidioides immitis</i>			
113853	<i>Coccidioides immitis</i>			
113859	<i>Coccidioides posadasii</i>			
113848	<i>Coccidioides posadasii</i>			
113850	<i>Coccidioides posadasii</i>			
113858	<i>Coccidioides posadasii</i>			
113839	<i>Coccidioides posadasii</i>			
113840	<i>Coccidioides posadasii</i>			
113841	<i>Coccidioides posadasii</i>			
113844	<i>Coccidioides posadasii</i>			
120,77	<i>Uncinocarpus reesii</i>			
668,78	<i>Uncinocarpus reesii</i>			
113679	<i>Uncinocarpus reesii</i>			
491,72	<i>Alternaria chlamydospora</i>			
120987	<i>Alternaria chlamydospora</i>			
240,70	<i>Alternaria phragmospora</i>			
481,81	<i>Alternaria limaciformis</i>			
548,81	<i>Alternaria molesta</i>			



239,73	<i>Alternaria brassicae</i>			
116531	<i>Alternaria brassicae</i>			
113,44	<i>Alternaria japonica</i>			
118390	<i>Alternaria japonica</i>			
106,41	<i>Alternaria brassicicola</i>			
121335	<i>Alternaria brassicicola</i>			

\*Strains of *Alternaria alternata*, *Aspergillus fumigatus*, and *Coccidioides immitis* showed response above baseline. Additional isolates are therefore in Eurotiales, Pleosporales and Onygenales, respectively. Responses were variable within species.

Note: GTX is known to be produced by species of *Aspergillus* (Eurotiales) and *Gliocladium* (Hypocreales).

**Table S2. List of constituents of positive fractions annotated by MALDI-TOF mass spectrometry.**

	Constituent	Molecular mass	Chemical formula
<b>Fraction 7B</b>	Gliotoxin	365.0027	C13H14N2O4S2(K)(H-1)
	Bis-N-norgliovictin	365.0390	C14H18N2O3S2(K)(H-1)
	Pseudomonine	316.1292	C16H17N3O4
	Vanchrobactin	436.1229	C16H23N5O7(K)(H-1)
	Endocrocin	337.0319	C16H10O7(Na)(H-1)
	3-hydroxymugeneic acid	337.1242	C12H20N2O9
	Fumigaclavine A	337.1313	C18H22N2O2(K)(H-1)
	Pacifarinic acid	426.1007	C16H21N1O11(Na)(H-1)
	Salmoachelin SX	426.1007	C16H21N1O11(Na)(H-1)
	Benarthin	412.1827	C17H25N5O7
	Myxochelin B	426.1636	C20H25N3O6(Na)(H-1)
	Pistillarin	426.1636	C20H25N3O6(Na)(H-1)
	12,13-dihydroxy fumitremorgin C	412.1867	C22H25N3O5
	Cyclotryprostatine A	412.1867	C22H25N3O5
	Verruculogen TR 3	412.1867	C22H25N3O5
	Cyclotryprostatine B	426.2023	C23H27N3O5
	Sphingofungin B	412.2670	C20H39NO6(Na)(H-1)
<b>Fraction 7C</b>	Gliotoxin E	381.0008	C13H14N2O4S3(Na)(H-1)
	Pseudomonine	316.1292	C16H17N3O4
	Vanchrobactin	436.1229	C16H23N5O7(K)(H-1)
	Fumiquinazolines F	381.1322	C21H18N4O2(Na)(H-1)
	Fumiquinazolines G	381.1322	C21H18N4O2(Na)(H-1)
	Endocrocin	337.0319	C16H10O7(Na)(H-1)
	3-hydroxymugeneic acid	337.1242	C12H20N2O9
	Fumigaclavine A	337.1313	C18H22N2O2(K)(H-1)
	Gliotoxin	365.0027	C13H14N2O4S2(K)(H-1)
	Bisdechlorogeodin	369.0371	C17H14O7(K)(H-1)
	Bis-N-norgliovictin	365.0390	C14H18N2O3S2(K)(H-1)
	m-Anisic acid	369.0945	C18H18O7(Na)(H-1)
	Acinetobactin	369.1169	C16H18N4O5(Na)(H-1)
<b>Fraction 11C</b>	Dimerumic acid	523.2165	C22H36N4O8(K)(H-1)
	Pseudomonine	316.1292	C16H17N3O4
	Gliotoxin	365.0027	C13H14N2O4S2(K)(H-1)
	Pyrocatechin violet	409.0352	C19H14O7S(Na)(H-1)
	Spirotryprostatin A	396.1918	C22H25N3O4
	Bis-N-norgliovictin	365.0390	C14H18N2O3S2(K)(H-1)
	2-chloro-1,3,8-trihydroxy-6-methyl-(8Cl); 2-Chloro-1,3,8-trihydroxy-6-methylanthrone	313.0238	C15H11ClO4(Na)(H-1)

2-chloro-1,3,8-trihydroxy-6-methyl-(8CI); 2-Chloro-1,3,8-trihydroxy-6-methylanthrone	328.9977	C15H11ClO4(K)(H-1)
9(10H)-Anthracenone, 2-chloro-1,3,8-trihydroxy-6-(hydroxymethyl)-	329.0187	C15H11ClO5(Na)(H-1)
Orlandin	411.1074	C22H18O8
Bisdechlorogeodin	369.0371	C17H14O7(K)(H-1)
Didehydrobisdethiobis(methylthio)gliotoxin	393.0340	C15H18N2O4S2(K)(H-1)
Myxochelin	427.1476	C20H24N2O7(Na)(H-1)
Putrebactin	411.1640	C16H28N4O6(K)(H-1)
Enantio-pyochelin	347.0495	C14H16N2O3S2(Na)(H-1)
Ent-pyochelin	347.0495	C14H16N2O3S2(Na)(H-1)
Pyochelin	347.0495	C14H16N2O3S2(Na)(H-1)
Serratiochelin	438.1272	C20H21N3O7(Na)(H-1)
m-Anisic acid	369.0945	C18H18O7(Na)(H-1)
Sterigmatocystine	347.0526	C18H12O6(Na)(H-1)
Alcaligin	427.1799	C16H28N4O8(Na)(H-1)
Deoxyschizokinen	427.1799	C16H28N4O8(Na)(H-1)
Benarthin	412.1827	C17H25N5O7
12,13-dihydroxy fumitremorgin C	412.1867	C22H25N3O5
Cyclotryprostatine A	412.1867	C22H25N3O5
Verruculogen TR 3	412.1867	C22H25N3O5
Emericellin	409.2010	C25H28O5
Acinetobactin	369.1169	C16H18N4O5(Na)(H-1)
Fusarin Y	438.1523	C22H25NO7(Na)(H-1)
Trypacidin	367.0788	C18H16O7(Na)(H-1)
m-Anisic acid	347.1125	C18H18O7
Heterobactin B	438.1983	C19H27N5O7
Acinetobactin	347.1350	C16H18N4O5
Sphingofungin B	412.2670	C20H39NO6(Na)(H-1)
Terezine D	364.1422	C19H23N3O2(K)(H-1)
6-methoxyspirotryprostatin B	394.1761	C22H23N3O4
Rhodotorulic acid	367.1588	C14H24N4O6(Na)(H-1)
Spirotryprostatin B	364.1656	C21H21N3O3

**Table S3.** Primers used for RT-qPCR

<i>pol</i> forward	GGTTTATTACAGGGACAGCAGAGA
<i>pol</i> reverse	ACCTGCCATCTGTTTTCCATA
<i>pol</i> probe	[6FAM] AAA ATT CGG TTA AGG CCA GGG GGA AAG AA[BHQ1]
<i>TNF<math>\alpha</math></i> forward	AACCCCGAGTGACAAGCCTGTAGC
<i>TNF<math>\alpha</math></i> reverse	CACCACCAGCTGGTTATCTCTCAGCTC
<i>IL-2</i> forward	GAATGGAATTAATAATTACAAGAATC
<i>IL-2</i> reverse	ATGTTGTTTCAGATCCCTTTAGTTCCAGA
<i>INF<math>\gamma</math></i> forward	TTCAGCTCTGCATCGTTTTG
<i>INF<math>\gamma</math></i> reverse	CTCTTT TGGATGCTCTGGTC
<i>CD25</i> forward	ATCAGTGCGTCCAGGGATAC
<i>CD25</i> reverse	GACGAGGCAGGAAGTCTCAC
<i>BAK1</i> forward	GGTTTTCCGCAGCTACGTTTTT
<i>BAK1</i> reverse	GCAGAGGTAAGGTGACCATCTC
<i>BAX</i> forward	CCCGAGAGGTCTTTTTCCGAG
<i>BAX</i> reverse	CCAGCCCATGATGGTTCTGAT
<i>BCL2</i> forward	GGTGGGGTCATGTGTGTGG
<i>BCL2</i> reverse	CGGTTCAAGTACTCAGTCATCC
<i>CASP-3</i> forward	CATGGAAGCGAATCAATGGACT
<i>CASP-3</i> reverse	CTGTACCAGACCGAGATGTCA
<i>AKT1</i> forward	AGCGACGTGGCTATTGTGAAG
<i>AKT1</i> reverse	GCCATCATTCTTGAGGAGGAAGT
<i>NRF2</i> forward	TCAGCGACGGAAAGAGTATGA
<i>NRF2</i> reverse	CCACTGGTTTCTGACTGGATGT
<i>FOXO3a</i> forward	CGGACAAACGGCTCACTCT
<i>FOXO3a</i> reverse	GGACCCGCATGAATCGACTAT
<i>KEAP1</i> forward	GAGTGGCGAATGATCACAGCA
<i>KEAP1</i> reverse	TAGCCTCCAAGGACGTAGATTCTC

## Summary and general discussion

It is estimated that currently around 36.9 million people worldwide are living with HIV/AIDS. Only 59% of these individuals receive some form of antiretroviral therapy. Additionally, it is estimated that only 75% of people living with HIV globally are aware of their HIV status, meaning that around 9 million people are unknowingly living with the virus (as of 2017). Modern antiretroviral therapies, termed combinatorial antiretroviral treatment (cART) while being extremely efficient in suppressing the virus, pose immense financial burden. According to the Centers for Disease Control and Prevention (CDC) life-long treatment of person living with HIV in United States of America costs \$ 379 668. So far, there is one well documented case of HIV-1 eradication. Timothy Brown underwent two bone marrow transplants from donors with HIV-1 resistance. Additionally, recently two more such cases were reported (Hütter *et al.*, 2009; Symons *et al.*, 2014). However, bone marrow transplantation, aside from being a very invasive costly procedure poses a substantial risk of approximately 20-30% death (Martin *et al.*, 2010), and is the last resort for cancer patients. Bone marrow transplantation is thus not a viable general strategy for cure for the millions of people living with HIV. Therefore, it is of great importance to explore new pharmacological avenues for HIV cure.

The main barrier to eradication is the latent reservoir, a very small pool of long-lived cells, mostly composed of resting memory CD4<sup>+</sup> T cells that do not express the virus, even though they contain replication competent provirus integrated within their genome (Siliciano and Siliciano, 2015). Since cART targets viral proteins, it cannot deplete virus in the latent reservoir. Several approaches for HIV cure have been proposed (Stoszko *et al.*, 2019). Currently the most sought after is so called “shock and kill”. It is believed that strong and specific latency reversal will make latent cells vulnerable to the immune clearance, which could be further enforced by HIV-targeted immunotherapies. Spread of the infection would be prevented by the presence of cART. Such approach would result in eradication of the HIV-1, where no replication competent virus remains in the body, so called sterilizing cure. Another approach that is recently gaining attention is so called “block and lock”, where deep state of latency could be achieved so that people living with HIV will not need daily cART, concomitant with undetectable viremia. This approach would result

in a functional cure, where the pro-virus still lingers in the body but its low levels are controlled by the host. Additionally, some researchers propose combining these two strategies. First, “shock and kill” could be employed to eradicate cells in which latency is easily reverted, second “block and lock” could potentiate deep latency, rendering remaining replication competent proviruses non-activatable. This thesis investigates novel small molecules for inclusion in “shock and kill” approach.

**Chapter 1** presents broad and in-depth spectrum of molecular mechanisms that are governing HIV-1 latency. We introduce HIV-1 latency phenomenon and clinical picture of HIV epidemic. First chapter also describes available model systems to study HIV-1 latency, as well as intensely investigated pathways regulating HIV-1 latency. We introduce most of the important and interesting latency reversing agents. In the second part of the chapter we present recent advances in HIV-1 latency reversal field. We introduce a list of all known latency reversal agents with highlight of those which were or are currently under clinical investigation. We also discuss kill strategies for the eradication of HIV-1. Lastly, we hypothesize which approaches should be combined in order to achieve HIV-1 cure.

**Chapter 2** characterizes newly identified BAF inhibitors – CAPE and PYR as potent inducers of HIV-1 transcription. We tested a panel of 18 small molecules that were shown in murine stem cells to regulate the expression of BAF target genes. We showed that 3 of them reversed latency in cell lines model systems with limited cytotoxicity. Moreover, we showed that BAFis induced expression of the virus in ex-vivo infected primary CD4<sup>+</sup> T cells and more importantly we observed same treatment outcome in primary CD4<sup>+</sup> T cells isolated from aviremic persons living with HIV-1, the gold standard for assessing HIV-1 latency reversal potential of new drugs. We also showed that HIV-1 latency reversal was enhanced when those BAFis were combined with other classes of LRAs, such as Vorinostat (HDAC inhibitor) and Prostratin (PKC agonist). Additionally, we showed that BAFis prevent establishment of latency, pointing the importance of BAF complex in this process. Furthermore, we showed that BAFis do not activate the immune system, a toxic side effect of some small molecules, suggesting the possibility of a safe therapeutic toxicity profile for these drugs.

Interestingly, Megaridis et al., showed that, consistent with our data showing their mechanism of action as inhibitors of the HIV-repressive BAF complex, the BAFis CAPE and PYR behave as HIV transcriptional noise enhancers. Transcriptional noise is defined as fluctuations around the mean gene-expression level (Dar *et al.*, 2014). Therefore, mechanistically BAFis do not activate HIV-1 transcription per se. They rather either increase mean abundance while conserving noise levels (CAPE) or increase transcriptional noise initiation frequency (PYR). This explains why we observed rather modest enhancement of HIV-1 expression in single treatments with CAPE or PYR, while when combined with a transcriptional activator (eg. Prostratin) we observed strong expression of the virus, including in HIV infected patient cells treated ex vivo. These results point out the importance of combinatorial use of various classes of LRAs in pursuit of robust reversal of the HIV-1 latency towards eradication.

**Chapter 3** describes novel and more specific BAFis based on macrolactam structure. These molecules were identified by screening of nearly 350 000 compounds and were further optimized to improve their potency, solubility and toxicity profile. These macrolactams reversed latency not only in cell lines and ex vivo infected primary CD4<sup>+</sup> T cells models of latency but more importantly in primary CD4<sup>+</sup> T cells isolated from aviremic persons living with HIV-1. Target identification experiments showed ARID1A subunit (specific component of BAF complex) to be the main target of these small molecules. The exact epitope of the target protein is yet to be unraveled, possibly with employment of protein-ligand modelling experiments *in silico* followed by more precise pull-down assays. Mechanistically, we showed that these macrolactams reverse HIV-1 latency by reducing repressive nucleosome occupancy at the 5'LTR, which is governed by BAF complex. Importantly, macrolactams also belong to the class of transcriptional noise enhancers that greatly boost activity of transcriptional activators such as prostratin or TNF $\alpha$ . Due to known protein target of these molecules, ARID1A, and specific mode of action, macrolactams have high potential as more clinically relevant; ARID1A targeting BAF inhibitors will likely have fewer pleiotropic side effects than inhibitors that target the catalytic domain of BAF, BRG-1, as not all BRG-1 containing BAF complexes contain ARID1A. Therefore, it is very compelling to further investigate and compare the mechanism by which BAF inhibitors modulate

transcriptional noise, activate HIV transcription, examining also their potential pleiotropic and toxic side-effects.

**Chapter 4** investigates molecular mechanism of HIV-1 latency reversal mediated by the small molecule MMQO (8-methoxy-6-methylquinolin-4-ol). We found that MMQO does not require viral transcription factor Tat for latency reversal, which makes it a very interesting candidate for inclusion in “shock and kill” therapies. Furthermore, by comparing transcriptomes of the cells treated with MMQO, JQ1 (BET inhibitor), RVX-208 (BET inhibitor), TSA (HDAC inhibitor) and SAHA (HDAC inhibitor) we concluded that MMQO effect mimics behavior of BET inhibitors. Moreover, when cells were co-treated with MMQO and SAHA we observed synergistic latency reversal, while MMQO co-treatment with JQ1 or OTX-015 (BET inhibitors) resulted in additive effect, suggesting that indeed MMQO belongs to the BET inhibitors class of LRAs. Further, utilizing nuclear magnetic resonance (NMR) binding studies we showed that MMQO binds directly to BRD4. Interestingly, using bar-coded viruses we showed that BETis, HDACis and PKC agonists reverse latency in different populations of cells, indicating that depending on integration site pro-viral latency is governed by different mechanisms. This further suggest the importance of combining different classes of LRAs for efficient and robust latency reversal.

Given all above results it would be also very interesting to investigate if MMQO, similarly to JQ1 inhibits short isoform of BRD4 (BRD4S). Since BRD4S is responsible for recruitment of BAF complex to the HIV-1s promoter (Conrad *et al.*, 2017), it would be interesting to investigate whether MMQO exerts dual role in latency reversal – via BRD4 inhibition and inhibition of BAF complex recruitment via BRD4S. In this light it would be very compelling to investigate the effect of cocktail of BAF inhibitors and MMQO. Mechanistically, it seems that these two classes of molecules would not synergize. However, since MMQO behaves as noise enhancer, cocktail of it with one of the BAFi (ie. Macrolactam) could boost activity of transcriptional activators (eg. prostratin, IAPs) much more than double treatment with BAFi + activator or BETi + activator. These experiments are highly compelling for further investigation.

**Chapter 5** identifies and characterizes GTX as a novel LRA that aids in transcription elongation, a crucial step in latency reversal (Yukl *et al.*, 2018). GTX was identified in a screen of fungal growth supernatants containing plethora of secondary metabolites that were subjected



to orthogonal mass spectrometry coupled to latency reversal bioassays. We found that GTX potently reversed latency in models of latency, and more importantly in cells from aviremic HIV-1+ participants. Moreover, we showed that combination of GTX with SAHA or CAPE (BAFi) exerts synergistic latency reversal in cell lines and ex-vivo infected primary CD4+ T cells models of latency. RNA sequencing unraveled that 4-hour treatment with GTX results in massive downregulation of 7SK RNA, a scaffold for 7SK snRNP complex that sequesters P-TEFb. Of note, sequencing also showed that treatment with GTX has relatively few primary gene targets, as less than 700 genes showed differential expression pattern. Furthermore, glycerol gradient sedimentation experiments showed that 4-hour treatment with GTX results in disassembly of the complex with subsequent release of P-TEFb. Importantly, we confirmed that newly released P-TEFb retains its kinase activity and phosphorylates RNA Polymerase II. Interestingly, our *in silico* modelling exercises revealed that GTX most likely targets hydrophobic pocket of LARP7 (structural component of the 7SK snRNP complex), which normally is responsible for binding of the 7SK RNA.

Interestingly, to our best knowledge GTX seems to be one of very few molecules able to specifically release P-TEFb. It would be interesting to test whether GTX has also impact on other diseases linked to levels of this transcription factor such as cardiac hypertrophy or mixed-lineage leukemia. Since P-TEFb plays crucial role in general transcription, we hypothesize that GTX could be a useful tool in modulating transcription in artificial cellular systems. It's also compelling to investigate role of GTX in transcription modulation.

In light of noise enhancement, it is very interesting to see that two noise enhancers – BAFis and HDAC inhibitor SAHA when combined exert synergy in inducing transcription of HIV-1. It is very compelling to test whether addition of activator would result in even greater expression of the virus with possible significant therapeutic outcome in shock and kill therapy.

We believe that combinations of noise enhancers with an activator could lead to great improvement of “shock” step of the eradication strategies. It is of high interest to yet test combinations of: BAFis and SAHA; BAFis and GTX; BAFis and MMQO; GTX and MMQO with a strong activator such as prostratin, IAPs or double TLR agonists (i.e. TLR2 and TLR7). Especially combinations with IAPs inhibitors and dual TLR agonists seems very compelling as these two

classes or drugs seems to be very specific and effective towards activation of transcription of HIV-1 (Pache *et al.*, 2015; Hattori *et al.*, 2018). Combining multiple classes of LRAs seems inevitable as it has been shown by us and others that different integration sites of the virus dictate different mechanisms governing latency. Therefore, in order to broadly target pro-virus, we must employ broad arsenal of drugs. One must not forget that timing of co-treatments is of high importance as well, it has been shown by Bouchat *et al.*, that timing between co-treatments has strong impact on the treatment outcome (Bouchat *et al.*, 2016). Therefore, not only triple (or more) LRAs cocktail should be tested for inclusion in effective “shock” but also timing between dosing and order or co-treatments.

Lastly, we believe that we have delivered broad panel of novel LRAs, with known mechanisms of action that should be tested in combinations also with other, already known LRAs (eg, HDACis, BETis, IAPis, dual TLR agonists, etc) so that we could achieve satisfactory outcome of “shocking” the pro-virus from hiding. It is also highly interesting to go further and test whether latent cells were “shocked” enough for recognition by CD8+ T cells and/or NK cells followed by killing of infected cells. Theoretically, it is also possible to circumvent the need of specific/strong immune response towards latent cells that have been “shocked” by for example addition of inhibitors of IAPs to so called “shocktails” could result in latency reversal with subsequent apoptosis of infected cells. All of these approaches seem promising and as such should be explored in a more thorough fashion.

## Samenvatting en algemene discussie

Er wordt geschat dat er op het moment wereldwijd ongeveer 36.9 miljoen mensen met HIV/AIDS leven. Slechts 59% van deze individuen ontvangt enige vorm van antivirale therapie. Daarbovenop wordt er geschat dat slechts 75% van de mensen die wereldwijd HIV hebben zich bewust zijn van hun HIV status wat betekent dat ongeveer 9 miljoen mensen geïnfecteerd zijn met het virus (cijfers van 2017). Moderne antiretrovirale therapieën, combinatorial antiretroviral treatment (cART) genoemd vormen, alhoewel ze het virus zeer efficiënt onderdrukken, een behoorlijke financiële belasting. Volgens de Centers for Disease Control and Prevention (CDC) kost een levenslange behandeling van een persoon die met HIV leeft \$379668. Tot nu toe is er een goed beschreven geval van HIV-1 genezing. Timothy Brown onderging twee beenmergtransplantaties van donors die HIV-1 resistent zijn. Daar bovenop zijn recent twee verdere gevallen gerapporteerd (Hütter *et al.*, 2009; Symons *et al.*, 2014). Beenmerg transplantatie brengt echter, los van het feit dat het een zeer invasieve en dure procedure is, een substantieel risico van 20-30% op de dood met zich mee (Martin *et al.*, 2010), en is de laatste behandeling voor kanker patiënten. Beenmergtransplantatie is dus niet een reële algemene strategie voor de genezing van miljoenen personen die met HIV leven. Daarom het van groot belang om nieuwe farmacologische wegen voor HIV-1 genezing te onderzoeken.

De belangrijkste barrière voor het uitroeien van het HIV virus is het latente reservoir, een kleine groep van lang levende cellen, die voornamelijk uit rustende geheugen CD4+ T-cellen die het virus niet tot expressie brengen des ondanks het feit dat ze replicatie competent pro-virus in hun genoom geïntegreerd hebben (Siliciano and Siliciano, 2015). Omdat cART virale eiwitten als doel heeft kan het niet het virus in het latente reservoir verminderen. Verschillende aanpakken om een HIV genezing te bewerkstelligen zijn voorgesteld (Stoszko *et al.*, 2019). Op het moment is de methode die het meest nagestreefd wordt de zogenaamde “shock and kill” aanpak. Er wordt gedacht dat een sterke en specifieke latentie omkeer latent geïnfecteerde cellen vatbaar maakt voor opruiming door het immuunsysteem wat verder gestimuleerd kan worden door doelgerichte HIV-immuuntherapieën. Verspreiding van de infectie wordt dan bewerkstelligd door de aanwezigheid van cART. Zo een aanpak zou resulteren in de verwijdering van HIV-1, waarbij geen replicatie competent virus in het lichaam aanwezig blijft, een zogenaamde steriliserende genezing. Een alternatieve aanpak die recent de aandacht krijgt

wordt “lock and block” genoemd. Hierbij wordt een diepe staat van latentie bewerkstelligd wat samenhangt met on detecteerbare viremia zodat personen die met HIV leven geen dagelijkse cART behandeling nodig hebben. Deze aanpak zou leiden tot een functionele genezing waarbij het pro-virus nog steeds in het lichaam sluimert maar de lage hoeveelheid gecontroleerd wordt door de gastheer. Tenslotte stellen sommige wetenschappers voor om beide strategieën te combineren. Eerst zou “shock and kill” worden toegepast om de cellen waarin de latentie gemakkelijk omgekeerd zou worden op te ruimen waarna “block and lock” diepe latentie in de overige cellen zou bewerkstelligen zodat de overgebleven replicatie competente pro-virussen niet meer te activeren zijn. Dit proefschrift onderzoekt nieuwe kleine moleculen om op te nemen in een “shock and kill” aanpak.

**Hoofdstuk 1** beschrijft een breed en diepgaand spectrum van moleculaire mechanismen die HIV-1 latentie induceren. We introduceren het fenomeen latentie en het klinische beeld van de HIV-epidemie. Het eerste hoofdstuk beschrijft ook de beschikbare model systemen om HIV-1 latentie te bestuderen als mede de intens bestudeerde routes die HIV-1 latentie reguleren. We introduceren de meest belangrijke en interessante latentie omkeer middelen. In het tweede deel van het hoofdstuk presenteren we recente vooruitgang in het HIV-1 latentie omkeer veld. We beschrijven een lijst van alle bekende latentie omkeer middelen waarbij aangegeven wordt welke op het moment onderzocht worden voor een klinische toepassing. We bespreken tevens de “kill” strategieën voor de uitroeiing van HIV-1. Tenslotte beargumenteren we welke strategieën gecombineerd zouden moeten worden om tot een HIV-1 genezing te komen.

**Hoofdstuk 2** beschrijft de karakterisatie van de nieuw geïdentificeerde BAF-remmers – CAPE en PYR als potente induceerders van HIV-1 transcriptie. We hebben een paneel van 18 kleine moleculen getest die in muizen stamcellen de expressie van BAF gereguleerde genen beïnvloede. We laten zien dat drie van hen latentie omkeert in cellijn modelsystemen met een beperkte cytotoxiciteit. Daarnaast laten we zien dat BAF-remmers de expressie van het virus induceert in ex-vivo geïnfecteerde primaire CD4+ T-cellen en nog belangrijker namen we hetzelfde behandelingsresultaat in primaire CD4+ T-cellen geïsoleerd uit aviremische personen die met HIV-1 leven wat de gouden standaard is om de HIV-1 latentie omkeer potentie van nieuwe middelen te bepalen. We laten ook zien dat HIV-1latentie omkering verhoogd wordt als deze BAF-remmers gecombineerd worden met andere klassen van LRAs zoals Vorinostat (HDAC-remmer) en Prostratin (PKC-agonist). Daarnaast laten we zien dat BAF-remmers het

ontstaan van latentie voorkomt wat het belang van het BAF-complex in dit proces aangeeft. Verder laten we zien dat BAF-remmers het immuunsysteem niet activeren, wat een toxisch bij effect is van sommige kleine moleculen, wat een veilig therapeutisch profiel suggereert voor deze middelen.

Interessant genoeg hebben Megaridis et al. laten zien dat overeenkomstig onze data het mechanisme als remmers van het HIV onderdrukkende BAF-complex, de BAF-remmers CAPE en PYR zich gedragen als HIV-transcriptie ruis versterkers. Transcriptie ruis wordt gedefinieerd als fluctuaties rond het gemiddelde genexpressie niveau (Dar *et al.*, 2014). BAF-remmers activeren daarom niet HIV-1 transcriptie per se maar ze verhogen of de gemiddelde hoeveelheid terwijl het ruis niveau gehandhaafd blijft (CAPE) of de transcriptie ruis initiatie frequentie (PYR). Dit verklaart waarom we een slechts geringe verhoging van HIV-1 expressie waarnemen in behandeling met enkel CAPE of PYR terwijl in combinatie met een transcriptionele activator (bv. Prostratin) we een hoge expressie van het virus zien inclusief in HIV geïnfecteerde patiënt cellen die ex vivo behandeld zijn. Deze resultaten geven het belang aan om gebruik te maken van een combinatie van verschillende klassen LRAs in het najagen van een robuuste omkering van HIV-1 latentie.

**Hoofdstuk 3** beschrijft nieuwe en meer specifieke BAF-remmers die gebaseerd zijn op de macrolactam structuur. Deze moleculen werden geïdentificeerd door bijna 350000 moleculen te screenen en werden verder geoptimaliseerd om hun te potentie, oplosbaarheid en hun toxologische profiel te verbeteren. Deze macrolactams keerden latentie niet alleen om in cellijn en ex vivo geïnfecteerde primaire CD4<sup>+</sup> T-cel modellen maar van meer belang ook in primaire CD4<sup>+</sup> T-cellen geïsoleerd uit aviremische personen die met HIV-1 leven. Experimenten gericht op het identificeren van de doelwitten toonden aan dat de ARID1A sub unit (een specifieke component van het BAF-complex) het belangrijkste doel van deze kleine moleculen is. Het exacte epitoom van het doel eiwit moet nog ontrafeld worden, mogelijk via het toepassen van in silico eiwit-ligand modelleer experimenten gevolgd door meer precieze pull-down experimenten. Mechanistisch laten we zien dat deze macrolactams HIV-1 latentie omkeren door repressieve nucleosoom bezetting op de 5' LTR te verminderen dat door het BAF-complex in stand gehouden wordt. Van belang is dat macrolactams ook behoren tot de klasse van transcriptionele ruis verhogers die de activiteit van transcriptionele activators zoals Prostratin of TNF $\alpha$  aanzienlijk verhogen. Door het eiwit doel van deze moleculen, ARID1A, en het specifieke mechanisme hebben macrolactams een groot potentie om klinisch relevant te

zijn; BAF-remmer die ARID1A als doel hebben, hebben waarschijnlijk minder pleiotrofe neven effecten dan remmers die het katalytische domein van BAF, BRG-1, als doel hebben omdat niet alle BRG-1 bevattende BAF-complexen ARID1A bevatten. Daarom is het aanlokkelijk het mechanisme waarmee BAF-remmers transcriptionele ruis moduleren en HIV-transcriptie activeren verder te bestuderen en vergelijken waarbij ook hun pleiotrofe en toxische neven effecten bekeken worden.

**Hoofdstuk 4** bestudeert het moleculaire mechanisme van HIV-1 omkering zoals dat door het kleine molecuul MMQO (8-methoxy-6-methylquinolin-4-ol) gemedieerd wordt. We vonden dat MMQO niet de virale transcriptie factor Tat nodig heeft voor latentie omkering, wat het een zeer interessante kandidaat maakt om in “shock and kill” therapieën opgenomen te worden. Daar bovenop concludeerden wij, door het transcriptome van cellen behandeld met MMQO, JQ1 (BET-remmer), RVX-208 (BET-remmer), TSA (HDAC -remmer) en SAHA (HDAC-remmer), dat het effect van MMQO hetzelfde gedrag als BET-remmers vertoont. Bovendien als cellen met zowel MMQO als SAHA behandeld werden observeerden we een synergistische latentie omkering terwijl MMQO-behandeling samen met JQ-1 of OTX-1 (BET-remmers) een additief effect opleverde wat suggereert dat MMQO inderdaad behoort tot de BET-remmer klasse van LRAs. Door gebruik te maken van nucleaire magnetische resonantie (NMR) bindingsstudies konden we verder laten zien dat MMQO direct aan BRD4 bindt. Interessant genoeg konden we door gebruik te maken van ge-barcode virussen aantonen dat BET-remmers, HDAC-remmers en PKC-agonisten latentie omkeren in verschillende populaties van cellen wat suggereert dat afhankelijk van de plaats van integratie van het pro-virus latentie bepaald wordt door verschillende mechanismen. Dit suggereert nog meer het belang van het combineren van diverse klassen van LRAs voor een efficiënte en robuuste omkering van latentie.

Gegeven de bovenstaande resultaten zou het zeer interessant zijn om te onderzoeken of MMQO, net zoals JQ1, de korte vorm van BRD4 (BRD4S) remt. Aangezien BRD4S verantwoordelijk is voor het rekruten van het BAF-complex naar de HIV-1 promoter (Conrad *et al.*, 2017), zou het interessant zijn om te onderzoeken of MMQO een duale rol in latentie omkeer heeft -via BRD4-remming en via het tegengaan van het rekruteren van het BAF-complex via BRD4S. In dit licht wordt het ook zeer aanlokkelijk om het effect van een cocktail van BAF-remmers en MMQO te testen. Mechanistisch gezien lijkt het erop dat deze twee klassen van moleculen geen synergistisch effect zouden hebben. Echter, omdat MMQO zich

gedraagt als een ruis versterker, zou een cocktail of dit gecombineerd met een van de BAF-remmers (bv Macrolactam) de activiteit van transcriptionele activators (bv Prostratin, IAPs) veel meer dan verdubbelen ten opzichte van behandeling met BAF-remmer + activator of BET-remmer + activator. Deze experimenten zijn zeer aantrekkelijk voor verder onderzoek.

**Hoofdstuk 5** identificeert en karakteriseert GTX als een nieuwe LRA dat help bij transcriptionele elongatie, een cruciale stap in latentie omkering (Yukl *et al.*, 2018). Wij identificeerden GTX door het testen media waarin schimmels gegroeid hebben die een uitgebreid scala aan secundaire metabolieten bevatten die gekoppeld werden aan orthogonale massa spectrofotometrie gekoppeld aan latentie omkeringstesten. Wij vonden dat GTX de latentie zeer potent omkeert in latentie modellen en nog belangrijker in cellen van aviremische HIV-1+ deelnemers. Daarbovenop laten we zien dat een combinatie van GTX met SAHA of CAPE (BAF-remmers) een synergistisch effect heeft in cellijnen en ex-vivo geïnfecteerde primaire CD4+ T-cel modellen van latentie. RNA-sequenzen liet zien dat een 4 uur behandeling met GTX leidde tot een immense afname van het 7SK RNA, een geraamte voor het 7SK snRNP complex dat P-TEFb bindt. Noot waardig is dat behandeling relatief weinig primaire gen doelen heeft omdat minder dan 700 genen een afwijkend expressie patroon hadden. Bovendien toonden glycerol gradiënt sedimentatie experimenten aan dat een 4 uur behandeling met GTX resulteert in het uiteenvallen van het complex en een daar op volgende bevrijding van P-TEFb. Van belang is dat we bevestigen dat het vrijgelaten p-TEFb zijn kinase activiteit behoud en RNA II polymerase fosforileert. Interessant is dat onze in-silico modellering aantonen dat GTX zeer waarschijnlijk bindt aan de hydrofobe holte van LARP7 (een structurele component van het 7SK complex), welke normalerwijze verantwoordelijk is voor het binden van het 7SK RNA.

Interessant is dat, naar ons beste weten, GTX een van de weinige moleculen is die specifiek p-TEFb uit het complex kunnen vrijmaken. Het zou interessant zijn om te testen of GTX ook een effect heeft op andere ziekten die in verband worden gebracht met de hoeveelheid van deze transcriptiefactor zoals cardiac hypertrophy of mixed-lineage leukemia. Omdat P-TEFb een cruciale rol speelt in algemene transcriptie, veronderstellen wij dat GTX een handig stuk gereedschap kan zijn om transcriptie te moduleren in artificiële cel systemen. Het is ook aanlokkelijk om de rol van GTX in transcriptie modulatie te onderzoeken.

Wat betreft ruis versterking is het erg interessant om te zien dat twee ruis versterkers – BAF-remmers en de HDAC-remmer SAHA als ze gecombineerd worden een synergistisch effect op de inductie van HIV-1 transcriptie hebben. Het is zeer aanlokkelijk om te testen of

toevoeging van een activator zou resulteren in een nog grotere expressie van het virus met een potentieel significante therapeutische rol in “shock and kill” therapie.

Wij geloven dat combinaties van ruis versterkers met een activator kan leiden tot een grote verbetering in de “shock” stap van de HIV uitroei strategieën. Het is zeer interessant om de volgende combinaties te testen: BAF-remmers en SAHA; BAF-remmers en GTX; BAF-remmers en MMQO; GTX en MMQO samen met een sterke activator zoals Prostratin, IAPs of dubbele TLR-agonisten (bv TLR2 en TLR7). Vooral combinaties van IAPs-remmers en duale TLR-agonisten zijn zeer aantrekkelijk omdat deze twee klassen erg specifiek en effectief lijken te zijn met betrekking tot de activatie van HIV-1 transcriptie (Pache *et al.*, 2015; Hattori *et al.*, 2018). Het combineren van meerdere klassen LRAs lijkt onontkoombaar omdat zowel wij als anderen hebben aangetoond dat verschillende integratie plekken van het virus een verschillend mechanismen hebben dat latentie bepaald. Daarom om het pro-virus breed aan te pakken hebben we een breed scala aan medicijnen nodig. Men moet niet vergeten dat de timing van gecombineerde behandelingen ook van groot belang is, Bouchat *et al.* hebben laten zien dat de timing van gecombineerde behandelingen een sterke impact heeft op het resultaat van de behandeling (Bouchat *et al.*, 2016). Daarom moeten niet alleen drievoudige (of meer) LRAs cocktails getest worden om in een effectieve “shock” maar ook de timing tussen de doseringen en de volgorde van de gecombineerde behandelingen.

Tot slot, geloven we dat we een breed paneel van nieuwe LRAs aangeleverd hebben die bekende mechanismen van werking hebben die getest moeten worden in combinatie met andere bekende LRAs (bv HDAC-remmers, BET-remmers, IAP-remmers, duale TLR-agonisten etc) zodat we een bevredigend resultaat verkrijgen om het pro-virus uit zijn schuilplaats te “shocken”. Het is ook zeer interessant om verder te gaan en om te testen of latente cellen genoeg “geshocked” zijn om door CD8+ T-cellen en/of NK-cellen herkend en gedood te worden. Theoretisch is het mogelijk om de noodzaak van een specifieke/sterke immuunrespons tegen de “geshockte” latente cellen te omzeilen door bijvoorbeeld remmers van IAPs toe te voegen aan zogenaamde “Shocktails” wat zou kunnen resulteren in latentie omkering met vervolgens de inductie van celdood dmv apoptose van de geïnfecteerde cellen. Elk van deze aanpakken lijken veel belovend en zouden daarom verder uitgebreid onderzocht moeten worden.



# Acknowledgements

This rollercoaster of an adventure called Ph.D. would not be possible without you **Tokameh**. I owe you a lot for granting me your trust and believing in me. Since I was a high school student, I wanted to research transcription, translation, and viruses to help those in need. The projects you gave me were all about it, and it's so awesome! Moreover, you were always there to answer my indefinite questions with great patience. Aside from creating such a great research environment, you have also created a safe space, where I could be myself without the fear of judgment. Because of all these things, I learned a lot, not only about HIV or how to execute good experiments but also about myself. All this experience is simply invaluable. Thank you!

**Elisa**, you have been one of the most demanding teachers, yet it was fun! I learned from you so much, from simple cell culture through infection experiments and patient material handling to intricate details of HIV biology. Without you, none of my projects would succeed. Hope you enjoy the new place and wish you all the best!

**Robert-Jan**, RJ, a fellow lion (born on the same day, how crazy is that?!), it was a pleasure to work around you. Even though we worked together rarely, I learned from you a lot. Without you my ChIP, FAIR or cloning would never work! You're a great expert on chromatin, yet I felt like I could ask the dumbest question and you would patiently explain all the details, over and over again. Thank you and I wish you many climbed walls!

**Michael**, working with you required putting aside so many differences, yet we managed amazingly! I admire your intelligence and eye for detail. I will always be grateful for explaining to me what the Dutch culture is about, how to ask difficult questions or how to improve my English. Good luck with your thesis!

**Enrico**, it was very nice to work with you. I appreciate every hint on how to polish (haha, pun intended) my ChIP and IP experiments, you're such an expert! I also admire your eye for detail - analysing other people's research was quite a learning process, and you helped me to improve my skills. It was also great to go for parties together, sometimes above the sky, and sometimes to complain how hard it is to be a Ph.D. student at EMC ;). Good luck with your thesis!

**Shringrar**, it's such a pity you started your post-doc with us so late, I would love to work with you more! Despite that, I enjoyed your warmth and puns. Your drive to do good science is such a motivation! And despite this short time, I have learned a lot from you, FISH-flow rocks! I look forward to working together sometime in the future.

**Shalla**, you're such a great person. Always ready to help, asking smart questions and always smiling. Your attitude is something I need to learn. You have such a peaceful charm that working around you was always a great pleasure.

**Tsung Wai**, without your technical help none of my projects would work out so smoothly and fast. Without your knowledge of the lab and Erasmus, I'd be simply a lost child in a maze of wonder. Thank you for helping me to find reagents, people, my way around and for solving all the issues with buffie coats. Working with you was also a great learning experience so thank you very much for that.

**Haleh**, without you paving the way, BAF projects would be so much more difficult, if not impossible to accomplish. I wish you all the best!

Dear students, **Raquel, Pritha, Helen, Adacia, Marloes, Cynthia, Lan Ahn** working with all of you was something I have never done before - supervising others, beginners. Your countless and difficult questions taught me how to be even more critical and meticulous. You're all from such different backgrounds I could learn first-hand all about your foreign cultures, and I loved it! Some of you are pursuing scientific careers, go girls! All the best to you all!

This thesis would not come to light without the whole **biochemistry group** led by **Peter**. From finding antibodies, chemicals, and sonication probes to getting lots of questions about my experiments during meetings, this thesis came to its shape because of all of you. I would like to thank especially **Gill** and **Jan** for your friendly attitude and readiness to help me out either with experiments or with finding reagents and/or equipment. **Ayestha** and **Lennart** thanks for great research questions and sharing burdens of Ph.D. life with a positive attitude.

**Yvonne**, your enormous knowledge of immunology, strong research drive and cheerful personality are so motivating and inspiring. Working with you was such a great learning experience and I had so much fun too. Thank you!

**Casper**, working with you was a great pleasure. You're a skilled student with very clever questions, that also let me grow. Last days at Erasmus working with you made me realize that I can be a decent teacher, and I had quite some fun too. That was very motivating and very much needed so thank you very much. I hope to work together sometime in the future.

I would also like to thank the **EHEG group: Henrieke, Peter, Annelies, Charles, Rob, Jeroen** and **Cynthia**, and others for all the interesting questions and fruitful meetings.

**Kasia Nowek**, your friendship helped me survive the last laps of my Ph.D. with laughter and understanding. It was so great to go out for lunch or to dance on the pole and shake the stress off. A good pole is a pole dancer (yes Adrian, it's your quote and I love it!), we keep standards high ;). I hope we will stay partners in crime because you're such a beautiful and creative person inside out!

**Lena**, without you I would never discover my passion - exotic pole dance. It is such a revelation to me, big thank you! You're such an inspiring dancer, so beautiful, sexy and charming! Also, your friendship and kind words of support helped me survive the last laps of this journey. Looking forward to dancing to your amazing choreos <3

My pole family, meeting all of you means a world to me. I'm not sure if I'd survived my Ph.D. without your cheer, support and a never-ending drive to polish those sick moves ("point your toes and smile"). **Tiffany**, I love your choreos and your attitude, keep it going! **Ruslana**, you've been such a great cheerleader, I find your drive to be a better pole dancer so inspiring! **Isaac**, it's so great to pole dance with another boy at the class, someday we have to slay at Milkshake ;). **Paaldans Academy** girls: **Sophia, Marilin, Imara, Kirsten, Dyonne, Iva, Jill, Carolina, Renske, Crystal, Alexandra, Clelia, Leonie, Annemarie** it's always so good when you're around and we can shake the stress off, cheer each other, and laugh like crazy over our fails.

**Iza** and **Rafał**, your **Iron Convent** camp gave me such a strong blow in my wings! The support, hard training, fun, and amazing people. All of it was so missing in my life until now! Many thanks! Shout out to my fellow polish pole dancers the queen, one and only **Martyna, Magda, Ola, Ala, Ewa, Klaudia, Piotrek, Ania, Gosia, Janek**, and the others, you guys are amazing, just keep poling, because like it's said before a good pole is a pole-dancer!

**Kuba**, your friendship means the world to me. Thank you for being there, when I needed it the most. You're an amazing person, like no one else, I hope we will stay great friends forever. Much love <3

**Kasia Lipińska**, I have known you for most of my life and coincidentally we ended up in Rotterdam, life is such a crazy journey, eh?! You saved my life multiple times during my Ph.D. Either by serving a meal when I was broke or lending me your credit card when I lost mine while traveling overseas. It means the world to me to be always able to turn to you. Also

complaining about the hardships of living in a foreign country like the Netherlands would not be as much fun as it was with you. Thank you!

**Judyta** And **Kinga** it's so amazing that we know each other most of our lives and we still keep in touch and have a proper laugh, I know I can always count on you. Thank you :\*  
**Gosia**, I will always remember that day in the cell culture room when you spoke to me in polish leaving me completely shocked and speechless. I would like to thank you for all those long "chit-chats" about everything and nothing. Much love to you, your wonderful husband Niels and your baby!

Crazy **bisons**, **Adrian**, **Keane**, **Onno**, **Alicja** (we did masters together and now we rave together <3), **Ian**, **Jana** (girl-boss you go!), **Rodrigo**, **Pablo**, **Isabella**, **Irini**, **Tania**, **Alex**, **Livia**, **Daniel** and the rest of the gang. There would be no thesis and the defense at all if not for all the crazy fun parties, concerts, and festivals with you. I feel so privileged to know you all, from all corners of the globe. It's so wonderful to feel accepted the way I am by so many, much love <3.

**Jeremy**, you're such a great person. A model, a date for a genderbending party or as a Dutch teacher, I can always rely on you. Feels like we became friends, and it's not easy for me to make friends. You have a beautiful soul that gave me strength and comfort when I needed it, thank you for it all :\*

During this time at Erasmus MC I have met many people, it's simply impossible to thank you all. But every person though me something and aided in my growing experience, for which I thank you all.

I would never start my Ph.D. if not for the great people I worked with before, I stand on the shoulders of amazing people. Dr. **Marek Szklarczyk**, you taught me all the basics of molecular biology, and no one will convince me that sugar beet is boring. Dr. **Agnieszka Jaźwa**, you taught me so much of molecular medicine, and I will be forever grateful for your guidance and patience. **Mateusz**, you though me most of the lab skills I know. On top of that you're such a good friend, thank you!

Last but not least I want to thank my **parents and family**, without them none of it would be possible at all. Drodzy rodzice oraz rodzino, zwłaszcza wy łobuzy jedne Michał, Filip i Miłosz, super jest wiedzieć, że we mnie wierzycie. Dzięki waszemu poświęceniu i wierze we mnie udało mi się osiągnąć tak wiele, bez znajomości, pieniędzy czy nieuczciwym zagraniami. Nauczyliście mnie ciężkiej pracy, która zaowocowała tak wspaniałą pracą naukową. Jestem

przeszczęśliwy, że mogłem dołożyć swoją małą cegiełkę do wiedzy o wirusie HIV, która być może przyniesie w przyszłości prawdziwą ulgę ludziom w potrzebie. Także wiedza, że zawsze mogę na was liczyć uskrzydla, dziękuję.



# CURRICULUM VITAE

**MATEUSZ STOSZKO**

Born 14-08-1988, Kowary, Poland

mateusz.stoszek@gmail.com

## Education:

2014 – 2019 **PhD candidate**, Erasmus Medical Center, Rotterdam, The Netherlands  
Department of Biochemistry

2012 – 2013 **Master of Science** in Biotechnology Analytics, Biotechnology  
Interdepartmental Studies, University of Agriculture in Kraków, Poland

2008 – 2012 **Bachelor of Science** in Applied Biotechnology, Biotechnology  
Interdepartmental Studies, University of Agriculture in Kraków, Poland

## Research experience:

2014 – 2019 **PhD candidate. Thesis:** “Solving a BAF’ling problem. Pharmacological quest to revert HIV-1 latency for eradication of the virus.”  
Tokameh Mahmoudi PhD, Dept. of Biochemistry, Erasmus Medical Center, Rotterdam, The Netherlands

2013 – 2014 **Research assistant:** “Functional TALEN enzymes generation against FKTN and ERCC2 genes.”  
Prof. Józef Dulak MD. PhD, Dep. of Medical Biotechnology, Faculty of Biochemistry, Biophysics and Biotechnology, Jagiellonian University, Kraków, Poland

2012 – 2013 **Master thesis:** “Pre-emptive, multiple, hypoxia-regulated gene therapy for ischemic tissue protection: an innovative approach for regenerative biomedicine.”  
Agnieszka Jaźwa PhD, Dep. of Medical Biotechnology, Faculty of Biochemistry, Biophysics and Biotechnology, Jagiellonian University, Kraków, Poland

2008 – 2012 **Bachelor thesis:** “Analysis of genetic factors associated with fertility restoration in sugar beet plants with the Owen’s sterilizing cytoplasm.”  
Marek Szklarczyk PhD, Dept. of Genetics, Plant Breeding and Seed Science, University of Agriculture in Kraków, Poland

## Publications:

1. **Stoszko M**, Ne E, Abner E, Mahmoudi T. A broad drug arsenal to attack a strenuous latent HIV reservoir. *Current opinion in virology*. 2019
2. Marian C, **Stoszko M**, Leighty MW, Wang L, de Crignis E, Gatchalian J, Chowdhury B, Carter BC, Hargreaves DC, Duvall JR, Dandapani S, Mahmoudi T, Crabtree GR, Dykhuizen EC. Small Molecule Targeting of Specific BAF complexes for HIV Latency Reversal. *Cell Chemical Biology*. 2018.
3. Abner E, **Stoszko M**, Zeng L, Chen HC, Izquierdo-Bouldstridge A, Konuma T, Zorita E, Fanunza E, Zhang Q, Mahmoudi T, Zhou MM, Filion G, Jordan A. A new quinoline BRD4 inhibitor targets a distinct latent HIV-1 reservoir for re-activation from other 'shock' drugs. *Journal of Virology*. 2018.
4. Röling M, **Stoszko M** and Mahmoudi T. Molecular Mechanisms Controlling HIV Transcription and Latency – Implications for Therapeutic Viral Reactivation in *Advances in Molecular Retrovirology*. InTech; 2016.
5. **Stoszko M**, De Crignis E, Rokx C, Khalid MM, Lungu C, Palstra R-J, Kan TW, Boucher C, Verbon A, Dykhuizen EC and Mahmoudi T. Small Molecule Inhibitors of BAF; A Promising Family of Compounds in HIV-1 Latency Reversal. *EBioMedicine*. 2016.
6. Jazwa A, **Stoszko M**, Tomczyk M, Bukowska-Strakova K, Pichon C, Jozkowicz A and Dulak J. HIF-regulated HO-1 gene transfer improves the post-ischemic limb recovery and diminishes TLR-triggered immune responses - Effects modified by concomitant VEGF overexpression. *Vascular pharmacology*. 2015.
7. Jazwa A, Tomczyk M, Taha HM, Hytonen E, **Stoszko M**, Zentilin L, Giacca M, Yla-Herttuala S, Emanuelli C, Jozkowicz A and Dulak J. Arteriogenic therapy based on simultaneous delivery of VEGF-A and FGF4 genes improves the recovery from acute limb ischemia. *Vascular cell*. 2013.

## Conferences:

1. **Stoszko M**, Röling M, De Crignis E, Kan TW, Al-Hatmi AMS, Sulc M, Bourne A, LeMasters E, Funa NE, Kang J, Müller Y, Katsikis P, de Hoog S, Havlíček V, Mahmoudi T – Validation of an unbiased screen method for the identification of secondary fungal metabolites reversing HIV-1 latency. **Poster** presented at HIV Persistence During Therapy workshop, Miami 12-15 December 2017.
2. De Crignis E, **Stoszko M**, Mir Mubashir K, Lungu C, Palstra RJ, Kan TW, Rokx C, Verbon A, Dykhuizen EC, Mahmoudi T – Small molecule inhibitors of BAF; a new family of compounds in HIV-1 latency reversal, **Poster** presented at IAS 2016 Towards an HIV Cure Symposium, Durban 16-17 July 2016.
3. **Stoszko M**, De Crignis E, Rokx C, Khalid MM, Lungu C, Palstra R-J, et al. Small Molecule Inhibitors of BAF; Novel Family of Compounds in HIV-1 Latency Reversal, **oral presentation** at 9th Netherlands Conference on HIV Pathogenesis, Epidemiology, Prevention and Treatment, Amsterdam 18th November 2015.
4. **Stoszko M**, De Crignis E, Rokx C, Khalid MM, Lungu C, Palstra R-J, et al. Small Molecule Inhibitors of BAF for HIV-1 Latency Reversal, **Poster** presented at 22nd MGC PhD Workshop, Maastricht 15-18 June 2015.
5. Tomczyk M, **Stoszko M**, Bukowska-Strakova K, Józkowicz A, Dulak J, Jaźwa A – Myocardial infarction in mice – model of endothelial cell injury”. **Oral presentation** 21st Kraków Conference on Endothelium, 13-16 June 2013, Kościelisko.



**Awards/grants:**

2017 Conference Travel Grant – The Erasmus Trustfund

2017 Young Investigator Grant – HIV Persistence During Therapy

2012 One-Year Master of Science Scholarship – Homing Plus project from the Foundation for Polish Science.

**Teaching/supervising:**

2019 – Raquel Crespo Galvan, master thesis: PTEF-b is released from the 7SK complex after gliotoxin treatment and suggests a potential mechanism for HIV-1 latency reversal

2018 – Pritha Biswas, master internship: Maraviroc, BAF inhibitors and Gliotoxin; A Potentially Potent Combination in HIV-1 Latency Reversal.

2017 – Helen Bodmer, bachelor thesis: The Haploid Genetic Screen technology, a tool to defy HIV latency?

2016 – Adacia T. Bourne, master thesis: Journey towards HIV-1 cure: Identification and evaluation of putative latency reversing agents.

2016 – Marloes Arts, bachelor thesis: Is RFX3 an inhibiting factor for HIV transcription?

2015 – Cynthia Lungu, master thesis: BAF Complex Inhibitors in Reactivation of Latent HIV-1.

2014 – Lan A. Dúóg, bachelor thesis: Screening of small molecule BAF inhibitors in reactivating latent HIV-1.



## Portfolio

Mateusz Łukasz Stoszek

Erasmus Medical Center: department of Biochemistry

PhD period: February 2014 – June 2019

Promotor: Prof. dr. C.P. Verrijzer

Supervisor: Dr. Tokameh Mahmoudi

### PhD training:

#### Courses:

Genetics	2014
Biochemistry and Biophysics	2014
Cell and developmental biology	2014
Partek course on Microarray and NGS	2014
The ins and outs of CRISPR-Cas	2017
Biomedical English writing	2017

#### Seminars, conferences, symposia:

Biochemistry department weekly work discussion	2014-2019
Cell biology, reproduction and development and biochemistry groups weekly work discussion	2014-2018
Annual MGC PhD workshops	2014-2018
PhD-students work weekly meeting	2017-2019
AIDS 2018	2018
HIV Persistence During Therapy workshop	2017
9th Netherlands Conference on HIV Pathogenesis, Epidemiology, Prevention and Treatment	2015

#### Supervision:

Raquel Crespo Galvan, master thesis	2019
Pritha Biswas, master internship	2018
Helen Bodmer, bachelor thesis	2017
Adacia T. Bourne, master thesis	2016
Marloes Arts, bachelor thesis	2016
Cynthia Lungu, master thesis	2015
Lan A. Dúong, bachelor thesis	2014